

Novel quantitative push gravity/field theory poised for verification

Gerasimos D Danilatos

(Version 1: 1 January 2020)

Version 29: 29 January, 2026

DOI [10.5281/zenodo.3596184](https://doi.org/10.5281/zenodo.3596184)

ESEM Research Laboratory
28 Wallis Parade
North Bondi, NSW 2026
Australia
gerry@danilatos.com
gerry.danilatos@gmail.com

*In memory of my father,
who inspired me with truth and honesty,
the science ethics,
I dedicate this to all independent science workers.*

Abstract

[Note: The edits of this version_29 are typed in blue color font]

This work develops a quantitative formulation of Push Gravity (PG), a physical framework in which gravitation arises from momentum transfer by an omnipresent flux of discrete particles, rather than from action at a distance or from spacetime curvature. Building on a small set of primary principles, the theory recovers the classical inverse-square law of gravity for stationary bodies in the steady state, while extending gravitational behavior beyond the weak-absorption regime assumed in earlier push-based models.

A central result is that gravitational interaction depends not only on total mass but on an absorption-controlled effective mass, which may differ from the real (substantial) mass of a body due to self-shielding effects. The gravitational constant emerges as a derived quantity linked to a mass-attenuation coefficient, allowing the inverse-square law to be locally preserved even when effective mass varies with internal structure and compactness. The theory predicts a universal maximum gravitational acceleration associated with saturation of momentum transfer, beyond which additional mass accretion does not increase surface acceleration, but increases the range of the gravitational field.

The framework provides explicit treatments of internal and external gravitational fields of layered spherical bodies, reformulates gravitational superposition, and clarifies the operational meaning of the equivalence principle. Matter, inertia, and mass acquire well-defined physical interpretations rooted in momentum exchange and geometry. Extensions to moving bodies suggest that many empirical relations of special and general relativity may continue to operate as effective descriptions within a broader PG ontology, without being foundational to it.

Push Gravity further admits analogous momentum-transfer descriptions for electromagnetic and nuclear interactions, indicating a potential route toward unification of fundamental forces through a common absorption-driven mechanism. Applications developed in this work range from particle structure to astrophysical compact objects and cosmology. In particular, the theory predicts that gravitational redshift can become extremely large for sufficiently compact systems without invoking event horizons or spacetime singularities. This leads to a novel redshift-distance relation and to the existence of a minimum mass threshold for a true black hole, defined operationally by complete suppression of electromagnetic escape.

Taken together, these results suggest that gravitational redshift may play a far more significant role in astrophysics and cosmology than conventionally assumed, challenging the necessity of universal expansion as the sole origin of observed cosmological redshifts. The theory is presented as a self-contained physical framework poised for further analytical development and experimental interrogation.

Beyond gravitation, the push principle has been extended to other interaction fields within the broader body of work. These developments indicate that a unified push-based description of fundamental forces may be achievable in principle, forming the basis for a prospective quantum push field theory (QPFT).

Foreword

To assist returning readers, edits introduced in successive versions of this work are indicated using different font colors. This convention allows the chronological development of ideas to be followed without requiring repeated reading of unchanged material. More importantly, it enables readers to track how the author’s understanding has evolved over time and to see why certain corrections, extensions, or reinterpretations have become necessary.

At the present stage, it has not yet been possible to consolidate all material into a single, fully harmonized and internally optimized version. Achieving this would require a substantial revision effort at a time when several foundational aspects of the theory remain actively under development. Attempting a comprehensive unification prematurely would be counterproductive, particularly while new concepts, symbols, and models continue to be introduced. Readers are therefore encouraged to follow the chronological sequence of versions rather than relying solely on the spatial organization of the current report. In this work, temporal progression has become an essential aid to proper understanding.

Inevitably, some results proposed in earlier versions have required partial or complete revision as the theory has developed. When encountering conclusions that later prove untenable or incomplete, readers are encouraged not to abandon the discussion at that point, but to continue through subsequent developments, where revisions and clarifications are often provided. While this mode of presentation reflects an evolving and exploratory process, confidence in the internal consistency and explanatory scope of the framework has grown steadily with continued analysis.

A salient recent example of this evolutionary process is a separate study entitled “The Massive Black Hole Bias: A Potential Origin for the Cosmological Redshift–Distance Relation without Universal Expansion” (Danilatos, 2025), and now added in Section 18.4. That work introduces a novel gravitational redshift–distance relation within the Push Gravity framework and derives a finite minimum mass requirement for a true black hole to form. In earlier parts of the present report, written chronologically prior to these results, the term black hole was applied more broadly to bodies achieving maximal absorptivity, $A_R = 1$. This earlier usage has been left unmodified in the interim to preserve the developmental record. Readers should therefore be aware that a comprehensive terminological and structural revision will ultimately be required to fully integrate these later findings, without detracting from their significance or validity within the evolving framework.

Readers who wish to consult referee commentary, publication history, or related evaluative material concerning this work are directed to Section 35.

1 Introduction

Scientific theories are built upon earlier concepts and discoveries and are refined as new insights and empirical constraints emerge. The theory of gravitation is no exception. While the predictive success of Newtonian gravity and, later, General Relativity is well established, persistent conceptual and observational challenges motivate continued scrutiny of their underlying physical interpretation. In this context, re-examining historically sidelined approaches may prove useful, not as replacements of successful theories, but as complementary frameworks capable of revealing overlooked structure.

This work revisits push gravity (PG), also known historically as shadow gravity. Although the basic idea dates back to the seventeenth century, PG has largely remained outside the mainstream of gravitational physics and is rarely discussed in modern curricula, even critically. The reasons for this marginalization have been discussed and include serious objections raised in earlier mechanical formulations. Nonetheless, the present study argues that several of these objections are not intrinsic to the push-gravity concept itself but rather to specific historical implementations. Here, PG is reformulated on a new basis, intended to overcome many of the traditional difficulties. In fact, after several years of development, the theory has now produced compelling evidence for push gravity to be included as a legitimate contender in official physics research endeavors for understanding the cosmos.

To avoid a premature return to longstanding debates, the present work proceeds by first developing the mathematical and physical consequences of a clearly stated set of PG principles. The results and conclusions produced are important in their own right. The emphasis is placed on newly derived quantitative relations and their internal consistency. Critical discussion of classical objections is deferred until after the core structure of the theory has been established, allowing the results to be assessed on their own merits rather than through inherited critiques. Triggering a protracted series of arguments and counter-arguments from the outset could be counter-productive for the ordinary reader to proceed and appreciate the main findings and purpose of this report.

Based on these principles, Newton’s law of gravity is recovered as a limiting case corresponding to

weak absorption of the push carriers; moreover, a new understanding of the universal constant of gravity is obtained. More generally, a universal acceleration law is derived that exposes the underlying physical quantities governing gravitational interaction. The gravitational field of a material sphere and the force between two bodies are obtained within the same framework, followed by discussion of possible experimental tests and observational consequences. In this way, the theory provides an independent route to several classical results while also extending beyond the Newtonian regime.

The overall aim is to develop a self-contained physical theory. This approach then, overall, will further assist towards invalidating most of the objections and at least neutralizing the others, or placing them on a rational speculation for an interim period. This will allow experts in the areas of particle physics, theoretical physics, astrophysics and mathematics to find new and fruitful ground for further progress to both use and advance the presented theory to its logical conclusions.

A comprehensive review of the literature is not attempted, while the emphasis is on original development. Where work is attempted beyond the author's primary reach, an invitation is extended for further scrutiny and refinement by specialists in related fields.

The methodological stance adopted here follows the spirit articulated by Feyerabend (2010): *"No theory ever agrees with all the facts in its domain, yet it is not always the theory that is to blame. Facts are constituted by older ideologies, and a clash between facts and theories may be proof of progress. It is also a first step in our attempt to find the principles implicit in familiar observational notions"*.

As an illustrative analogy, early atomic theory was originally speculative and inaccessible to direct observation, yet capable of coherently explaining macroscopic phenomena. More than two millennia later, those hypothetical entities have become experimentally observable. There was nothing fundamentally flawed in the speculative method of the ancients; its validation simply awaited appropriate tools. In a similar spirit, the present work posits gravions as sub-photon constituents whose collective behavior gives rise to observable gravitational effects. If the observed structure of matter and the cosmos can be consistently derived from such entities, the theory remains viable irrespective of the present lack of direct access to this underlying level.

Special Relativity and General Relativity begin with empirically accessible observables, while the Standard Model emerges from a sustained synthesis of experimental scattering data and phenomenological symmetries; all three ultimately build upward toward increasingly abstract descriptions. The approach pursued here instead reverses the usual direction of inference, proceeding from hypothesized microscopic structure toward emergent macroscopic phenomena. While the properties of the smallest-scale entities are necessarily uncertain, this direction of inference—from the microscopic to the macroscopic—has proven physically legitimate and historically productive. Ultimately, the value of the theory will be judged by its ability to reproduce established results and to suggest new, testable consequences.

Beyond the initial formulation of push gravity, subsequent work has explored the possible extension of the push principle to other fundamental interactions. This line of investigation motivates a broader framework tentatively referred to as a *quantum push field theory* (QPFT), in which multiple force fields are modeled as arising from distinct but related flux-mediated mechanisms. At the most fundamental level, this framework suggests the existence of a deeper organizing field—provisionally termed the *Planck field*—mediated by corresponding elementary push entities. Within this perspective, gravitation emerges as a derived interaction rather than a primary one. These ideas remain exploratory and are introduced here only to indicate potential directions of development beyond the initial scope of explaining gravity.

What began as an attempt to re-express gravity through alternative physical mechanisms thus opens the possibility of a broader and unified description of fundamental interactions. Whether such a program can ultimately be sustained remains to be determined, but its provisional structure suggests a novel ontology worthy of examination.

Inevitably, some heuristic reasoning and speculation are involved and are clearly separated from the core derivations. For this purpose, the report is divided into four parts. Part 1 presents the fundamental mathematical formulation of PG. Part 2 explores applications and tentative interpretations. Part 3 addresses more speculative models and open problems. Part 4 provides a general discussion and outlook.

Structure and scope. Readers primarily interested in the foundational formulation of push gravity may proceed directly to Part 1, where all assumptions, definitions, and derivations required to reproduce the principal results are presented in a self-contained manner. More speculative developments, including extensions beyond gravity and tentative unification schemes, are explicitly confined to Part 3. These later sections are logically downstream of the core theory and are not required for understanding or assessing the validity of the results derived in Parts 1 and 2.

Reader’s guide for skeptics. Readers skeptical of push-gravity mechanisms or of sub-photonic models in general are encouraged to treat the present work as an exercise in constrained physical modeling rather than as a proposal requiring prior philosophical commitment. In particular, the mathematical development of Part 1 may be read independently of its broader interpretive context: if the stated axioms are accepted provisionally, the resulting derivations either reproduce known gravitational behavior or they do not. Agreement or disagreement with later interpretive extensions is therefore not required for evaluating the internal consistency, empirical adequacy, or potential falsifiability of the foundational results.

Part One (1)

2 Early push gravity theory

Nicolas Fatio de Duillier (de Duillier, 1929; Gagnebin, 1949) is generally credited with the first attempt to explain gravitation as a mechanical effect rather than an inherent attraction. Working contemporaneously with Newton, Fatio’s theory is “*based on minute particles streaming through space and pushing upon gross bodies...*” via collisions between ordinary matter and ethereal corpuscles, which was thought to be his greatest work. This idea was later reformulated and popularized by Georges-Louis Le Sage (Wikipedia contributors, 2018).

Fatio’s original writings are not easily accessible in modern journals but are discussed extensively in secondary sources and historical reviews along with Le Sage writings. In essence, this theory envisioned a flux of ultramundane corpuscles whose partial absorption by matter leads to an anisotropic momentum transfer, producing an effective attractive force between bodies.

Despite its conceptual originality, classical push gravity faced serious objections. Most notably, no observable drag on planetary motion was detected, and the required energy flux appeared incompatible with thermal constraints. By the early twentieth century, these difficulties—together with the emergence of Special and General Relativity—led to the near abandonment of mechanical gravity models.

Nevertheless, periodic attempts to revive push gravity have appeared in the literature. While these efforts have generally failed to gain traction, they demonstrate sustained interest (albeit sporadic and limited) in the possibility that gravitation might emerge from underlying transport processes rather than from spacetime geometry alone. The present work builds on this tradition but departs from earlier models in key respects, particularly in its treatment of absorption, re-emission, and the statistical properties of the gravion flux.

The aim here is not to rehabilitate historical formulations, but to develop a modernized and internally consistent version of push gravity that can be confronted directly with established gravitational laws and observational constraints.

The layered presentation reflects a methodological separation between foundational derivation and speculative extension, consistent with the historical development of successful physical theories.

3 Push Gravity (PG) principles

The fundamental assumption of push gravity (PG), as developed in this report, is that the forces ordinarily attributed to an effective gravitational field associated with material bodies arise from the flow and absorption of radiant energy. This radiation consists of elementary entities —particles or waves, or both— propagating randomly yet statistically homogeneously in all directions through interstellar and interplanetary space, at least on length scales comparable to planetary systems, in the absence of matter.

This radiation field constitutes a radiant flux whose detailed nature need not be specified at the outset. For convenience, it is provisionally modeled as a flux of elementary particles termed **gravions** (gravity + ion —from ancient Greek “ἰόν” meaning “going” or “that which goes”). Gravions are postulated to possess the following properties:

1. Gravions interact negligibly among themselves, resulting in mean free paths that are large compared with planetary orbital scales and allowing gravion transport to be treated as effectively collisionless on such or larger scales wherever appropriate.
2. Gravions interact with material bodies at a rate proportional to the local material density encountered along their paths.
3. During interaction with matter, gravions are absorbed but subsequently re-emitted in transformed forms of energy or particles possessing much shorter mean free paths. These re-emitted products do

not mediate further gravitational interaction. Elastically and isotropically reflected gravions, if they exist, cannot generate a gravitational field. For anisotropic elastic scattering, if it exists, see Section 28.

4. Conservation of momentum holds during gravion–matter interaction: absorbed gravions transfer momentum to material bodies, producing a macroscopic force.

Two provisional assumptions were initially introduced to facilitate compliance with existing theories. These are retained here only for reference and completeness:

- 5 Gravions are relativistic. However, this assumption is not required at the present level of development and is not used in the derivations that follow. It may ultimately prove to be redundant.
- 6 The propagation speed of gravions is constant. Where identification with the speed of light is assumed, it is stated explicitly.

Notes: The third principle (#3) is analyzed and discussed in considerable detail in Part 2 and in much greater depth in Part 3.

The cumulative absorption of gravions by a material body produces a surrounding depletion of flux, which manifests as a gravitational field acting on other bodies immersed within it.

Initially, neither the intrinsic nature of gravions nor the detailed mechanisms of their interaction with matter or among themselves are specified. The terms “particle” and “matter” are therefore used operationally and may refer to energy or mass in particulate or wave-like form. Their precise interpretation is clarified progressively as the theory develops.

Some readers may object that special relativity is not applied at the gravion level from the outset. This is deliberate. Relativity is based on photon-mediated observations and the spacetime description of observable events. In contrast, PG is formulated at a pre-photon level, where observables emerge only indirectly. An observer in PG need not rely on photons but may instead measure forces directly using local instruments such as gravimeters. For the present development, attention is restricted to steady-state configurations involving stationary or slowly moving bodies; time-dependent phenomena are minimally examined or deferred to later work. This stance represents a difference of foundational ordering, not a rejection of established relativistic phenomenology.

Possible extensions of these principles beyond the gravitational interaction, including collective and field-theoretic effects, are developed separately in Part III and play no role in the derivations presented in Part I.

The above principles of PG will be better conceived as they are applied in the ensuing theory to be initially pursued, before we can return to them and attach a strict mathematical, physical and philosophical meaning. We employ a “trial-and-error” approach. The ultimate aim is to make PG a self-contained and self-consistent theory without reliance on prevailing theories, which might contain errors or might be approximations of PG.

Regarding our choice for the term “gravion”, we opted to use a fresh term for good reasons, such as to dissociate, though not critically, the presented theory here from previous ones on this subject.

For example, Dibrov (2011) introduced the term *fations* in connection with a pulsating electron model, while other names also appear in the literature. Although gravions may ultimately relate to *gravitons* proposed elsewhere, a distinct term is adopted here to avoid importing assumptions not required by the present formulation.

The principles stated above are intended as operational starting points rather than final ontological claims.

3.1 Formulation of **core** principle

Let Φ_0 denote the radiant gravion energy flux, defined as the total gravion energy crossing a closed surface per unit time (in watts). Individual gravions carry finite energy and momentum.

The radiance L_0 is defined as the radiant flux received per unit projected area S_\perp (normal to the direction of propagation) per unit solid angle Ω ,

$$L_0 = \frac{\partial^2 \Phi_0}{\partial \Omega \partial S_\perp} \quad (1)$$

At any point in space, we will need to find and use the flux density J_0 (also called intensity), namely, the flux per unit area received within a solid angle $\Delta\Omega$

$$J_{0\Delta\Omega} = L_0 \Delta\Omega \quad (2)$$

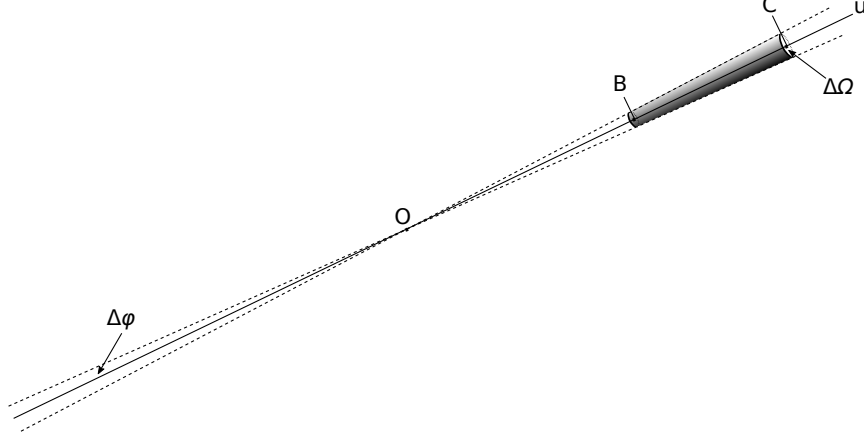


Figure 1: *Schematic illustration of the core Push Gravity (PG) principle. An observation point O is immersed in an otherwise isotropic and homogeneous graviton flux. In free space, equal flux densities arrive from all directions, yielding zero net momentum transfer. The presence of matter within a small solid angle $\Delta\Omega$, defined at O and subtending a cone of semi-angle $\Delta\varphi$, introduces partial absorption of gravitons along the path segment $BC = \ell$. This absorption produces a directional deficit in the flux arriving from direction u and a corresponding imbalance with the opposite direction at point O .*

If within this solid angle there is a finite material body, the received flux will be diminished due to absorption. Referring to Fig. 1, the radiance and the flux density at any point in free space is initially the same from all directions resulting in zero force, except when at a point O the flux density is affected by the presence of matter in the direction u within a cone with small semi-angle $\Delta\varphi$ subtending a small solid angle $\Delta\Omega$. Due to the absorption of gravitons by matter contained in the distance BC , there is a deficiency from that direction and hence an excess flux from the opposite direction within the same angle.

We can treat the problem as we use the general case of any radiation absorption by matter and write the well known equations of absorption. In the general case, the flux density (also called *directional intensity in radiative-transfer terminology*) $J_{\Delta\Omega}(u)$ at any point u along the line u diminishes in proportion to the product $J_{\Delta\Omega}(u)du$

$$dJ_{\Delta\Omega}(u) = -kJ_{\Delta\Omega}(u)du \quad (3)$$

where the constant of proportionality k is the coefficient of absorption for gravitons (or attenuation coefficient in the Beer-Lambert law). Upon integration, we obtain the classical exponential transmission equation

$$J_{\Delta\Omega}(u) = J_{0\Delta\Omega} \exp(-ku) \quad (4)$$

where $J_{0\Delta\Omega}$ is the incident (initial) intensity per above. The absorbed intensity $J_{a\Delta\Omega}$ is simply the difference

$$J_{a\Delta\Omega}(u) = J_{0\Delta\Omega} - J_{\Delta\Omega}(u) \quad (5)$$

and the corresponding absorption fraction $f_{a\Delta\Omega}$ in the small solid angle $\Delta\Omega$ is:

$$f_{a\Delta\Omega}(u) = \frac{J_{0\Delta\Omega} - J_{\Delta\Omega}(u)}{J_{0\Delta\Omega}} = 1 - \exp(-ku) \quad (6)$$

For the case in Fig. 1, by setting $BC = \ell$ we simply write

$$f_{a\Delta\Omega}(\ell) = 1 - \exp(-k\ell) \quad (7)$$

where k is constant if the density is uniform.

We note that for very small values of $k \ll 1$ (or better, for $k\ell \ll 1$), Eq. 4 reduces to

$$J_{\Delta\Omega}(\ell) \approx J_{0\Delta\Omega}(1 - k\ell) \quad (8)$$

and

$$J_{a\Delta\Omega}(\ell) = J_{0\Delta\Omega} - J_{\Delta\Omega}(\ell) \approx J_{0\Delta\Omega}k\ell \quad (9)$$

so that

$$f_{a\Delta\Omega}(\ell) \approx k\ell \quad (10)$$

The above equation is the basic assumption of Fatio's theory and all subsequent theories of push gravity, i.e. the absorption of gravions by a planet is very weak and linear, [because only then could Newton's equation of gravity be recovered](#).

In all of the above and subsequent notations, we use the subscript "a" to denote the presence of absorption so that f_a is a shorthand notation for the absorption fraction of gravions per unit area inside a finite solid angle Ω , where absorption by a given body takes place:

$$f_a = \int_{\Omega} f_{a\Delta\Omega} d\Omega \equiv f_{a\Omega} \quad (11)$$

and f_a is a simplified expression of $f_{a\Omega}$ by identity. [In other words, we denote by \$f_{a\Omega}\$ the total absorption fraction integrated over the relevant solid angle \$\Omega\$. When the context is unambiguous, we write \$f_a \equiv f_{a\Omega}\$.](#)

This fraction will be used later for finding the total energy absorbed by a sphere.

Clarifications: There is a significant variety of expressions relating to the spatial and temporal flow of energy, so that we have slightly adapted the terms in order to best fit our purposes in this development. Also, we use spherical bodies with constant (fixed) density so as to avoid the need of complex mathematical expressions, like tensor analysis, etc, without compromising the [essential physical content of the](#) derivations. Our initial aim is to familiarize ourselves with novel quantities and physical systems in the simplest way leaving a complete mathematical analysis of the most general cases for future work. For our immediate needs, we make [some further](#) clarifications in application of the above PG principles.

We have opted to use the quantity of flux density J_0 (or flux intensity) for our needs in the derivation of PG equations. This quantity bears a direct relationship to the radiance L_0 , which is often encountered in related physics topics. This relationship is evident from Eq. 2 to be:

$$J_{0-total} = \int_{4\Omega} L_0 d\Omega = 4\pi L_0 \quad (12)$$

However, for practical purposes in formulating the equations of force, we use half of the above flux density from one direction and subtract it from the other opposing half of flux density in the corresponding two hemispheres on either side of a receiving surface element. Thus, we define J_0 for this report by:

$$J_0 = \int_{2\Omega} L_0 d\Omega = 2\pi L_0 \quad (13)$$

which should be used in correlating this work with other references. In "free" space (absence of an absorbing body, the total force at the surface element is zero [\(if the surface had absorptive capacity\)](#), because the flux intensities from the opposite directions cancel each other by :

$$J_0 - J_0 = 0 \quad (14)$$

However, the total energy arriving from both directions adds up to the total of:

$$J_{0-total} = J_0 + J_0 = 2J_0 \quad (15)$$

The energy density u_0 of space, [correspondingly](#) also referred to in the literature as "vacuum" energy density, is given by:

$$u_0 = \frac{4\pi L_0}{c} = \frac{2J_0}{c} \quad (16)$$

where [here](#) c is the gravion velocity.

We further clarify and stress the starting tenets of PG: [In contrast to formulations that rely on photon-based observation](#) (like special relativity), where an observer experiences (uses) and measures outcomes from observing the behavior of light (photons), our theory requires that an observer need not use photons, in lieu of which the observer needs only a counter (like a gravimeter, or spring) to measure all the gravions arriving from all directions. For our purposes, he/she may be blind and need not see the presence or not of nearby or faraway material bodies and need not measure the distance, size, or time between various events, like absorption of gravions. He/she only measures the incoming gravions [locally](#), feels impulses from each gravion and experiences the total force exerted. We then propose a theory, with which we can predict the

effect measured by the observer [in the presence of various bodies](#). We initially assume Euclidean geometry of a space filled with gravions traveling in all directions with equal intensity (density).

[In the present work, we restrict attention to regimes in which gravion-gravion interactions may be neglected, so that gravion transport may be treated as effectively collisionless on planetary and stellar scales. However, the theory does not a priori require gravion-gravion mean free paths to exceed all astrophysical length scales. Should the gravion mean free path become comparable to galactic dimensions \(for example\), collective transport effects may arise. Such effects lie beyond the scope of the present development and will be examined separately, once the local foundations of push gravity have been fully established.](#)

4 Newton's gravity law

Based on the outlined PG principles, we can first derive Newton's equation of gravitational force in a direct way as follows:

For simplicity, we start with a spherical material body as shown in Fig. 2 in Euclidean geometry. Let us consider a point O (observer) at distance r from the center of a sphere at point P with radius R . We draw a straight line u from point O traversing the sphere along the chord AB, the length $\ell(\varphi)$ of which is given by:

$$AB = 2(AM) = 2\sqrt{R^2 - r^2 \sin^2 \varphi} = 2r\sqrt{a^2 - \sin^2 \varphi} \equiv \ell(\varphi) \quad (17)$$

since

$$PM = r \sin \varphi \quad (18)$$

[Note: In versions v1-v28, a typographical error appeared in this equation, where OM should read PM. The correction is purely notational and does not affect any derivation or result.] and

$$a = \frac{R}{r} = \sin \varphi_0 \quad (19)$$

while we want these quantities expressed as a function of the angle φ in the range

$$0 \leq \varphi \leq \varphi_0 \quad (20)$$

We also need the initial $u_1 = OA$ and final $u_2 = OB$ lengths on the line OAB along u corresponding to points A and B

$$u_1(\varphi) = r \cos \varphi - \sqrt{R^2 - r^2 \sin^2 \varphi} = r \left(\cos \varphi - \sqrt{a^2 - \sin^2 \varphi} \right) \quad (21)$$

and

$$u_2(\varphi) = r \cos \varphi + \sqrt{R^2 - r^2 \sin^2 \varphi} = r \left(\cos \varphi + \sqrt{a^2 - \sin^2 \varphi} \right) \quad (22)$$

We note that the above equations describe the given circle in polar coordinates, when the origin O lies away from the circle, which then it is simplified to just the chord length, when the origin lies on the surface ($r = R$) by the well known cosine equation:

$$\ell(\varphi) = 2r \cos \varphi \quad (23)$$

The small solid angle $\Delta\Omega$ used to define the intensity flux $J_{\Delta\Omega}$ along the length of the corresponding cone in equation 3 is now first integrated around the axis OP yielding the elementary annular solid angle $d\Omega$ between angle φ and $d\varphi$ around the axis OP as

$$d\Omega = 2\pi \sin \varphi d\varphi \quad (24)$$

Gravions arrive at point O from all directions uniformly in the absence of any mass around. However, if the sphere contains a uniform mass we can initially assume that some gravions are absorbed by the mass in direct proportion to the elementary solid angle and the length of the chord AB at angle φ . This creates a depletion of gravions from that direction, from which the total depletion (fractional absorption) of gravions is found by the double integral

$$f_a = \int_0^{\varphi_0} \int_{u_1}^{u_2} 2\pi \sin \varphi d\varphi du \quad (25)$$

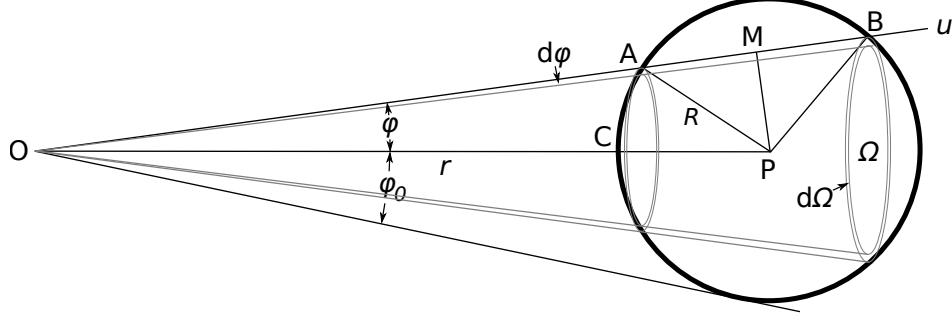


Figure 2: *Derivation of general push gravity around a sphere. Upon integration over azimuth, only the component of gravion momentum projected along OP survives; transverse components cancel by symmetry. This geometric result underlies the inverse-square law and remains valid independently of the gravion absorption regime.*

where we use the previously defined absorption coefficient being $k \ll 1$ along the length $\ell(\varphi)$. Integrating with u along the $\ell(\varphi)$, we get

$$f_a = \int_0^{\varphi_0} 2\pi \sin \varphi d\varphi \cdot k(u_2 - u_1) = 2\pi \int_0^{\varphi_0} \sin \varphi k \ell(\varphi) d\varphi \quad (26)$$

or

$$f_a = 4\pi k r \int_0^{\varphi_0} \sin \varphi \sqrt{a^2 - \sin^2 \varphi} d\varphi \quad (27)$$

Now, since the flux of gravions is a directional quantity (vector) at the test point O, the components normal to direction OP cancel out and only the components along OP add to a total directional flux for the generation of an acceleration of gravity g . The latter components are integrated by multiplying the above integrand by $\cos \varphi$:

$$f_g = 4\pi k r \int_0^{\varphi_0} \sin \varphi \cos \varphi \sqrt{a^2 - \sin^2 \varphi} d\varphi \quad (28)$$

to find the total component of accelerating fraction f_g below:

$$f_g = \left[-\frac{4\pi k r}{3} (a^2 - \sin^2 \varphi)^{3/2} \right]_0^{\varphi_0} \quad (29)$$

By substituting the integration limits on account of the above relationships, we finally get:

$$f_g = \frac{4\pi k r}{3} a^3 = \frac{4\pi k R^3}{3r^2} \quad (30)$$

By introducing an average density ρ of the spherical mass, the last result becomes :

$$f_g = \frac{k}{\rho} \frac{4\pi \rho R^3}{3r^2} = \frac{k}{\rho} \frac{M}{r^2} \quad (31)$$

where M is the total mass of the sphere. This is essentially Newton's law of gravity subject to a proportionality constant to yield the force of the gravions on a test unitary mass, which is the acceleration at point O.

In the above and subsequent notation, we use the subscript "g" to mean the component of absorption responsible for the generation of acceleration g .

It should be noted that the ratio $\Lambda = \frac{k}{\rho}$ is the mass attenuation coefficient of the Beer-Lambert law in any absorption situation written in alternative form as a function of the area density (or mass thickness) $\lambda = \rho \ell$, that applies also in flux density attenuation in PG, i.e.

$$J = J_0 \exp \left(-\frac{k}{\rho} \rho \ell \right) \equiv J_0 \exp (-\Lambda \lambda) \quad (32)$$

The fraction f_g as initially derived above is a pure (dimensionless) parameter involving geometrical parameters (Euclidean geometry) that appears to be a fundamental property of nature. The inverse square of distance law appears from the outset together with the sphere diameter and the absorption co-efficient k , which implies an absorbing entity like the mass, or density of the mass to appear in the next step.

This fraction was obtained by integrating over all absorption possible around the axis of symmetry defined by points O and P and yielding the simplest solution for a sphere. However, for any other shape, we should integrate around three normal independent axes (x,y,z) and add the corresponding acceleration fractions vectorially, as is shown in Appendix B.

5 Beyond Newton

Next, we obtain the expected acceleration from the previous derivation, as a consequence of the push gravity principle. We first complete the case for Newton, which corresponds to very low values of gravion absorption and then we pioneer the case beyond Newton for significant values of gravion absorption all the way up to their total absorption. Our derivation of Newton's gravitational law below already goes beyond the original law being obtained by empirical observation alone. That is, we now derive the same law exclusively (only) from the principles of PG.

5.1 Universal gravitational constant in weak absorption regime

The simple derivations above can already lead to a better understanding of the universal constant G (or bigG).

From the absorption and acceleration fractions f_a and f_g introduced in the previous section, we convert to the corresponding fractions of absorption and acceleration for the flux density J_a and J_g below:

$$J_a = J_0 f_a \quad (33)$$

$$J_g = J_0 f_g \quad (34)$$

where J_a is the flux density absorbed by the presence of a mass (here spherical uniform mass) and J_g is the component of J_a in the direction of the axis of symmetry responsible for the generation of acceleration.

We now proceed to find the constant of proportionality to reproduce Newton's gravitational law from Eq. 31 by

$$J_g = J_0 \frac{k M}{\rho r^2} = J_0 \Lambda \frac{M}{r^2} \quad (35)$$

using the newly introduced constant Λ .

The physical meaning of this constant is the number of absorption events per unit density of matter in units of inverse mass-thickness (m^2/kg). In other words, it is the number of absorption events per kilogram per square meter. [Λ plays the role of a universal mass–attenuation constant for gravions.](#) The inverse ($1/\Lambda$) is the mass-thickness (or area density) per absorption event. This is a new cosmic constant the magnitude of which remains to be found.

It is generally known in flow problems that the product of pressure times the velocity of the flow yields the flux intensity. Thus, if we divide J_g by the velocity c of the radiant flux (gravions), we obtain the pressure p_g exerted by the gravions at O:

$$p_g = \frac{J_g}{c} \quad (36)$$

An elementary test mass dm is located at point O with a surface area dS and thickness x having a density ρ' with corresponding absorption coefficient k' . The force dF on this test mass is then given by:

$$dF = p_g dS \cdot k' x = \frac{J_g}{c} dS \cdot k' x \quad (37)$$

where we multiply by $k' x$ to allow only for the fraction of gravions absorbed by the test mass, considering that k' , in general, is the number of absorption events per unit length. The force per unit mass, i.e. the acceleration g is then

$$g = \frac{dF}{dm} = \frac{\frac{J_g}{c} dS \cdot k' x}{\rho' dS \cdot x} = \frac{J_0 k M k'}{c \rho r^2} = \frac{J_0}{c} \Lambda^2 \frac{M}{r^2} \quad (38)$$

The above equation is exactly Newton's law, where the factors of proportionality between g and M/r^2 must correspond to the universal constant G :

$$G = \frac{J_0}{c} \Lambda^2 \quad (39)$$

The above is already an important derivation for the universal gravitational constant in terms of other constants, namely, the graviton speed and intensity of the neighboring universe, and the mass attenuation coefficient (new universal constant). Eqs. 38 and 39 are thought to be new fundamental derivations beyond Newton even within the realm of Newtonian mechanics for weak absorption. [We may say that Newton's constant is not fundamental—it is environmental. Furthermore, Eq. 38 directly explains equivalence of inertial and gravitational mass without postulating it. This applies within a gravitational field, but later the equivalence principle is re-appraised when considering forces across \(between\) different fields.](#)

5.2 General gravitation law in any absorption regime

Having considered the case of weak absorption, we now proceed to investigate what happens if absorption is strong, or to any arbitrary degree, i.e. the absorption coefficient can take any value. This actually means that we allow gravitational shielding inside a material body and between bodies. We may also refer to this condition as self-shadowing within the bulk of a massive body. In other words, we allow “gravitational shielding” as a core condition of a general push gravity theory, as opposed to considering it a case for rejecting PG, as has been done by the hitherto critics. This ushers a novel approach to push gravity.

In the general case, where self-shadowing (shielding) is caused by a significant k , we follow the same initial procedure as previously with reference to Fig. 2; [this diagram shows the geometric projection underpinning push gravity, from which both the Newtonian and general PG force laws follow](#): The force is proportional again to the elementary annular solid angle $2\pi \sin \varphi$, but now multiplied by the absorption fraction of the flux intensity along the length AB provided by Eq. 6; we also multiply by $\cos \varphi$ to allow, as previously, only for the component of force along the direction OP, so that we only need to integrate with respect to angle as follows:

$$f_g = \int_0^{\varphi_0} 2\pi \sin \varphi \cos \varphi d\varphi \cdot [1 - \exp(-k\ell(\varphi))] \quad (40)$$

and

$$f_g = 2\pi \int_0^{\varphi_0} \sin \varphi \cos \varphi \left[1 - \exp\left(-2kr\sqrt{a^2 - \sin^2 \varphi}\right) \right] d\varphi \quad (41)$$

The final integration of the above expression in the given subtended angle φ_0 by the sphere is fortunately an analytical expression of the form:

$$f_g = 2\pi \left[\frac{\sin^2 \varphi}{2} - \frac{\exp\left(-2kr\sqrt{a^2 - \sin^2 \varphi}\right) \left(2kr\sqrt{a^2 - \sin^2 \varphi} + 1\right)}{4k^2 r^2} \right]_0^{\varphi_0} \quad (42)$$

and with the given values of integration from 0 to φ_0 , we finally obtain

$$f_g = \pi \left[R^2 - \frac{1}{2k^2} + \frac{\exp(-2kR)(2kR + 1)}{2k^2} \right] \frac{1}{r^2} \equiv \frac{\pi A}{r^2} \quad (43)$$

where we have now a new parameter A , which is a function of k and R only (i.e. independent of r):

$$A = \left[R^2 - \frac{1}{2k^2} + \frac{\exp(-2kR)(2kR + 1)}{2k^2} \right] \quad (44)$$

Like in Eq. 30, we find that the fraction f_g derived in the general case of strong absorption is again a dimensionless parameter (quantity) that appears to be a fundamental property of nature and that the inverse square of distance law is preserved. This law is a consequence of the geometry alone (Euclidean) by any uniform flux propagated and absorbed in space. It is the law in the steady state around any absorbing medium (mass), whilst the time dependence remains to be introduced at a later stage of PG development.

Now, we follow the same procedure, as previously, to obtain the acceleration: For the test mass acted upon by a pressure p_g , Eq. 34 now becomes

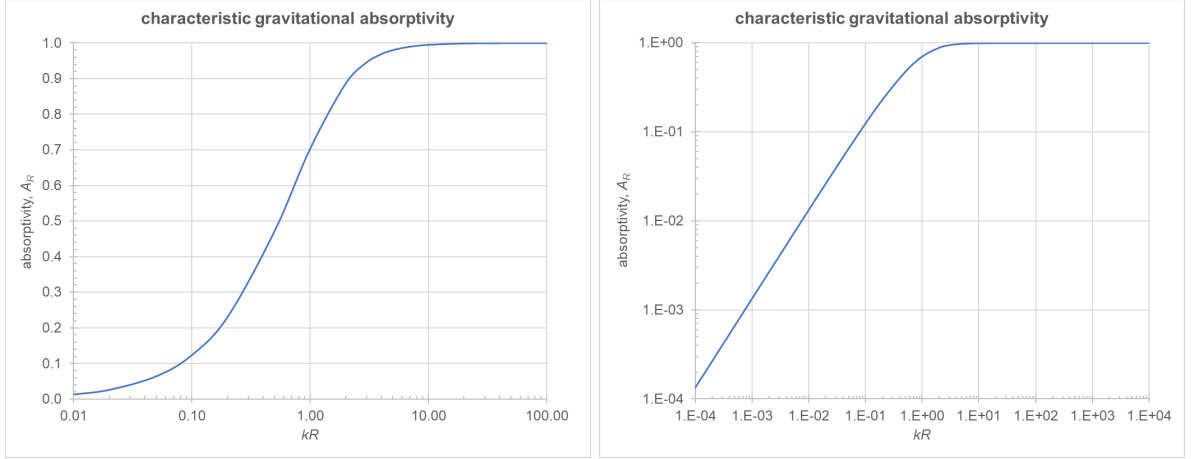


Figure 3: *Characteristic gravitational absorptivity A_R as a function of the dimensionless absorption parameter kR on linear-log axes (left) and log-log axes (right); absorptivity approaches zero at low values of kR while it increases monotonically and saturates for large kR , demonstrating the intrinsic shielding limit of a spherical body in push gravity.*

$$J_g = J_0 \frac{\pi A}{r^2} \quad (45)$$

In view of above, Eq. 38 is modified to become:

$$g = \frac{dF}{dm} = \frac{\frac{J_g}{c} dS \cdot k'x}{\rho' dS \cdot x} = \frac{J_0 k' \pi A}{c \rho' r^2} = \frac{J_0}{c} \Lambda \frac{\pi A}{r^2} \quad (46)$$

The above provides the equation of acceleration in PG, which again preserves the inverse square of distance law. However, the factor(s) of proportionality between g and $1/r^2$ is different from the corresponding PG derivation in Newton's equation. **This is the mechanism by which universality breaks in strong fields, not geometry.** Although the spatial dependence of gravity remains inverse-square, the effective coupling between matter and gravion flux is no longer linear in mass once self-shadowing becomes significant. **Newton fails in coupling, not geometry.** The deeper significance of this finding will be described later. To understand the difference from prevailing physics, we need to first investigate the properties of the newly derived parameter A .

6 Investigation, consequences and new physics with parameter A

The extension of PG theory to include gravion absorption for material bodies of any density and size, i.e. covering all absorption regimes, is found to have far-reaching consequences across many areas of physics. In effect, PG ushers in new physics. Established notions of mass—particularly intrinsic and rest mass—together with the universal gravitational constant G , are superseded by more fundamental parameters from which both mass and G can be derived. Newton's law is replaced by a more general equation, itself derivable from PG principles. An entirely new framework for practicing physics progressively emerges in the subsequent Sections and Parts of this work, the study of which is best undertaken in chronological order via the versions uploaded from time to time.

6.1 PG versus Newton

Dependence of characteristic gravitational absorptivity A_R on kR :

From Eqs. 30 and 43, we observe that the quantity f_g (and therefore g , or force) remains proportional to $1/r^2$ for all values of k and R . The long-standing assumption in earlier PG formulations—that gravion absorption must be extremely weak just because it reproduces Newton's law—is therefore unnecessary. Likewise, the commonly cited objection that gravitational shielding invalidates PG, because it has not been observed yet, is unfounded. On the contrary, shielding is revealed to be a fundamental mechanism intrinsic to PG requiring observation at the right place in astrophysics under the right framework. This is already a significant new finding.

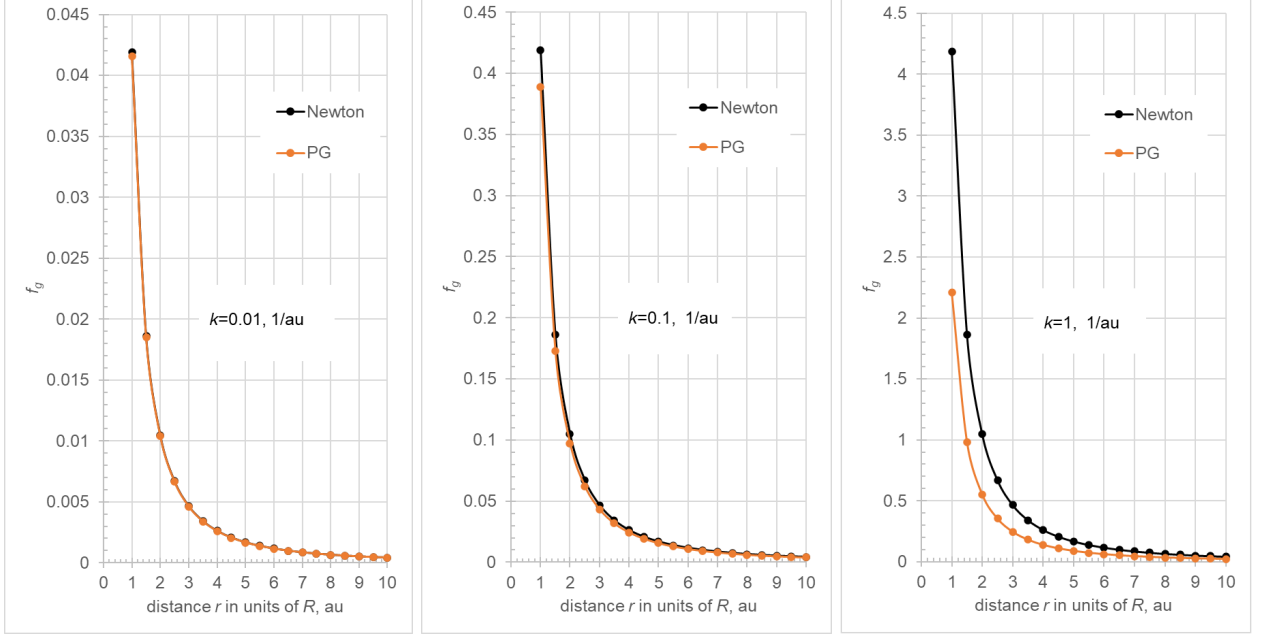


Figure 4: Gravity acceleration factor f_g vs. distance r in units of radius R for three different absorption coefficients k using linear (Newton) and exponential (PG) absorption.

It is helpful to normalize the distance r by the sphere radius R , defining:

$$n_R = \frac{r}{R} \quad (47)$$

whereby the expression for f_g may be rewritten as

$$\frac{f_g}{\pi} = \left[1^2 - \frac{1}{2k^2 R^2} + \frac{\exp(-2kR) \cdot (2kR + 1)}{2k^2 R^2} \right] \frac{1}{n_R^2} = \frac{A_R}{n_R^2} \quad (48)$$

upon introducing the **characteristic gravitational absorptivity**:

$$A_R = 1 - \frac{1}{2k^2 R^2} + \frac{\exp(-2kR) \cdot (2kR + 1)}{2k^2 R^2} \quad (49)$$

That is, A_R equals the shadowing parameter f_g/π at $n_R = 1$, i.e. at the surface of the sphere. The parameter A_R depends solely on the product kR and it is plotted in Fig. 3. It increases monotonically and approaches a saturation limit at large kR , as expected. For convenience, one may fix either $R = 1$ m and plot against k , or set $k = 1$ m⁻¹ and plot against R , both yielding the same curve.

A key observation is that most of the variation in A_R occurs over roughly four orders of magnitude in k , or R , or kR . Overall, A_R spans values from near zero to near unity. Consequently, increasing the radius of a sphere causes the surface acceleration to approach a finite saturation value, rather than diverging to infinity as predicted by Newton. Likewise, increasing the absorptive capacity (density, or k) of a sphere of fixed radius also produces saturation rather than divergence. The parameter A_R therefore characterizes the *intrinsic gravitational absorptivity* (**absorptivity**, for short) of a spherical body —planet, star, etc. This saturation is a direct manifestation of gravitational self-shadowing and represents a qualitative departure from Newtonian gravity, where no internal attenuation mechanism exists.

Dependence of the ratios $f_{gPG}/f_{gNewton}$ and q_ℓ on k :

For a direct comparison, we plot simultaneously f_g against normalized distance r_R for $n_R > 1$, i.e. by setting $R = 1$ au (arbitrary unit) in Eqs. 30 and 43 as shown in Fig. 4 for three fixed values of k in a range spanning three orders of magnitude. Initially, we may avoid the involvement of mass M and density ρ by investigating only the quantity f_g . For very low values of k , the pair of curves are indistinguishable. We note that as we increase k , the shadowing derived from PG is increased **absolutely** (see actual values), as it should, because more absorption by the gravitating mass means more **net** push by gravions. However, the curve lies below the corresponding expected Newtonian force, as it should. This is to be expected from the general absorption Eqs. 6 and 10, whereby the second equation is a straight line tangent to the first near (or at) the origin (at very short distance, or very low k), always yielding a higher value above the concave

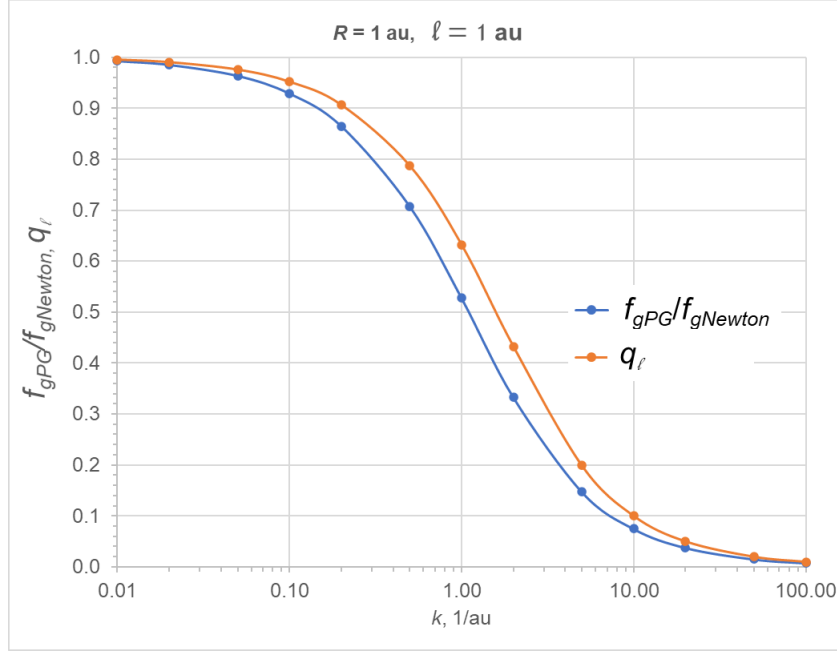


Figure 5: *Ratio of push-gravity to Newtonian gravitational response as a function of the absorption coefficient k for a fixed sphere radius. The global contraction factor $f_{gPG}/f_{gNewton}$ and the local length-contraction factor q_ℓ are shown. Newtonian gravity is recovered in the weak-absorption limit $k \rightarrow 0$, while for strong absorption PG predicts saturation rather than divergence, reflecting self-shadowing (gravitational shielding)*

line of PG absorption. The latter is a consequence of the self-shadowing (gravitational shielding) effectively creating a hidden mass, which, if it could exert an “attractive” force (per Newton), it would be greater than the corresponding PG force found.

The above analysis is also consistent with a comparison between Newton and PG as provided in Fig. 5 by plotting the ratio of $f_{gPG}/f_{gNewton}$ from (Eq. 43)/(Eq. 30) vs. k for a constant sphere radius $R = 1$ au. The absorption ratios by PG/Newton approaches unity for very small values of k ($k < 0.01$), as it should, but vanishes for very large values of k , which means that f_g becomes infinity in Newton, whilst it reaches a saturation value in PG. This is reasonable and helpful in understanding the mechanism of shielding. Noted that the horizontal axis is logarithmic tending to uplift (concave up) the initial straight line (Newtonian) but eventually tending to reach a saturation value asymptotically (concave down). PG is the overriding physics in all cases, whilst Newtonian physics is an approximation in the limiting case of very low values of k . The above ratios are given by:

$$q = \frac{f_{gPG}}{f_{gNewton}} = \frac{g_{PG}}{g_{Newton}} = \frac{3A_R}{4kR} \quad (50)$$

which will be referred to as contraction factor, or factor q . The significance and use of this factor will become apparent in further development of PG theory.

If we also take the ratio from the integrands of Eqs. 28 and 41, i.e. the ratio of the differential accelerations (or factors df_g) inside an elementary solid angle $d\Omega$, we obtain another factor q_ℓ , to be referred to as length contraction factor:

$$q_\ell = \frac{df_{gPG}}{df_{gNewton}} = \frac{1 - \exp\left(-2kr\sqrt{a^2 - \sin^2\varphi}\right)}{2kr\sqrt{a^2 - \sin^2\varphi}} = \frac{1 - \exp(-k\ell)}{k\ell} \quad (51)$$

and is plotted on the same Fig. 5.

This is the ratio of an effective length $\ell_e(\varphi)$ in PG divided by the real length in Eq. 17 of the chord traversing the sphere at angle φ from the origin O in Fig. 2:

$$\ell_e(\varphi) = \frac{1}{k} \left[1 - \exp\left(-2kr\sqrt{a^2 - \sin^2\varphi}\right) \right] \quad (52)$$

It is a contracted or compressed length, with which we may construct a virtual volume (body) by replacing the points defined by Eq. 22 with new ones defined by

$$u_{e2} = u_1 + \ell_e \quad (53)$$

or correspondingly replacing the points by Eq. 21 with new ones defined by

$$u_{e1} = u_2 - \ell_e \quad (54)$$

We may refer to these shapes as *gravitoids*, which are helpful for our theoretical understanding of the underlying workings of PG. Further details and analysis are provided in Appendix A.

Note 1: The current practice to find the mass of a planet is to place an artificial satellite around it and measure the period and radius of orbit. However, we now find that the actual mass still remains unknown by such measurements. This is not a trivial finding.

Note 2: For small values of k or R , we revert to Newtonian mechanics, which can also be seen by expanding the exponential to a Taylor series $e^x = 1 + x + \frac{x^2}{2} + \frac{x^3}{6}$.

$$A_{R_{kR \rightarrow 0}} = \frac{4}{3}kR(1 - kR)_{kR \rightarrow 0} \approx \frac{4}{3}kR \quad (55)$$

$$\text{i.e. for very small } kR: \pi A_R = \frac{4}{3}\pi kR = f_{g\text{Newton}} \quad (56)$$

the latter reproducing Eq. 30 for f_g in Newton derivation at $r = R$.

Note 3: The full ramifications of the findings in this section become evident in Part 2, where the ontological meaning of mass and inertia is consolidated.

6.2 Universal gravitational “constant” in any absorption regime vs. a new cosmic constant

We note that in Eq. 30 the multiplier preceding the factor $1/r^2$ divided by k provides the volume V of the gravitating sphere. Likewise, in Eq. 43, the multiplier preceding $1/r^2$ divided by k also provides an *effective* sphere volume V_e with the same center:

$$V_e \equiv \frac{\pi A}{k} \quad (57)$$

The real volume, real density and real mass are designated by V , ρ , and M . The measured (effective, measured, or apparent) density ρ_e is the effective mass M_e divided by the real volume

$$\rho_e = \frac{M_e}{V} = \frac{\rho V_e}{V} \quad (58)$$

and

$$\rho_e V = \rho V_e = M_e \quad (59)$$

also

$$\frac{\rho}{\rho_e} = \frac{V}{V_e} = \frac{M}{M_e} \quad (60)$$

We can now continue from Eq. 43 by multiplying with $V\rho_e$ both numerator and denominator as follows:

$$f_g = \frac{\pi A}{V\rho_e} \frac{V\rho_e}{r^2} = \frac{kV_e}{V\rho_e} \frac{M_e}{r^2} = \frac{kV_e}{V_e\rho} \frac{M_e}{r^2} = \frac{k}{\rho} \frac{M_e}{r^2} \quad (61)$$

which is identical to Eq. 31, except that we use the real density and not the effective (fictitious) one used (or implied) in Newton’s equation. Based on this, we can repeat the same steps to establish the force on a testing mass and derive an identical form of equation as in 38

$$g = \frac{dF}{dm} = \frac{\frac{J_g}{c} dS \cdot k'x}{\rho' dS \cdot x} = \frac{J_0}{c} \frac{k}{\rho} \frac{M_e}{r^2} \frac{k'}{\rho'} = \frac{J_0}{c} \Lambda^2 \frac{M_e}{r^2} \quad (62)$$

but where again we use the real density of the gravitating body in Λ . We repeat the same equations in order to stress that they are different in the meaning of ρ and A , whereby we derive the same expression for the universal gravitational constant:

$$G = \frac{J_0}{c} \Lambda^2 \quad (63)$$

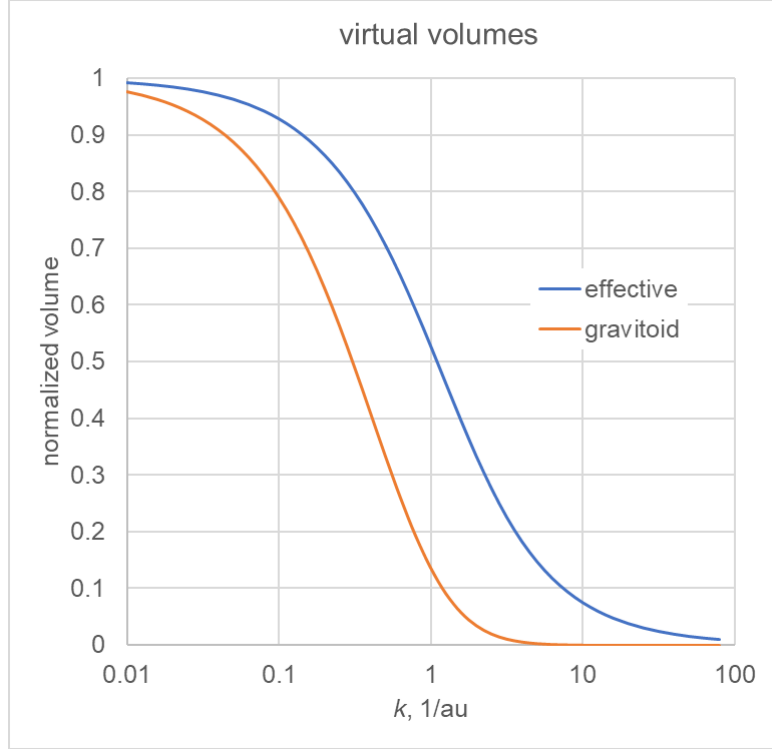


Figure 6: *Virtual volumes, gravitoid and effective, normalized over the real spherical volume.*

This is the same equation arrived at for weak graviton absorption, so that Λ is the new universal constant for the cosmos. From this and the known density of a given mass, we derive the absorption coefficient k . The universal constant G is proportional to the ratio of k/ρ squared, where ρ is the real density. For very low values of k the real density becomes very close to or is indistinguishable from the measured (effective) density. From this, we learn that G is constant only to the extent that J_0/c is constant in the neighboring universe. As pointed out earlier, Λ expresses the number of scattering events per unit length per unit mass density anywhere and provides a more tangible constant parameter to have. Thus, G may be found to be relatively more variable than previously suspected, according to further investigations by PG.

The effective volume introduced above is plotted in Fig. 6 against k after it is normalized over the real volume. As expected, it coincides with the real volume (at very low k), but then monotonically decreases to a vanishing value at very large k .

Note: The real mass dm in the denominator for g in the above Eq. 62 is equal to the effective mass dm_e . This is because for any given real density ρ' there is a corresponding absorption coefficient k' , and the thickness x' of the test body can be taken exceedingly small, so that the product $k'x'$ can be exceedingly small. For the latter product, the absorptivity is also exceedingly small according to Fig. 3 meaning that we operate in Newtonian regime. The two masses are then indistinguishable and $dm = dm_e$. This means that the acceleration g in the above Eq. 62 is the same as the measured Newtonian acceleration. The thickness x' could be written as a differential dx' , which was originally omitted only for simplicity of expression. In a differential thickness, there is no shadowing effect.

6.3 Maximum universal acceleration

We can try to use known values of planet parameters to derive the Λ , k , ρ and J_0 . Basically, we need to know the flux intensity J_0 , or the absorption coefficient k , on which all other parameters depend. Conversely, from the known physical parameters of a planet, we may assume values for J_0 in any given range and derive the other new parameters of Λ , k and ρ as a function of J_0 . In practice, we may proceed as follows:

The acceleration of gravity g_R at the surface of a sphere, i.e. at $r = R$, is given by Eq. 46 as:

$$g_R = \frac{J_0}{c} \Lambda \frac{\pi A}{R^2} = \frac{\pi J_0}{c} \Lambda A_R = \frac{\pi G}{\Lambda} A_R \quad (64)$$

From Eqs. 46, 49 and Fig. 3, there is a maximum possible acceleration $g_{maximum} \equiv g_0$ in the surrounding universe to be manifested on the surface of a star (sphere) with sufficiently large product kR , i.e. with $A_R = 1$, given by any of the following equations:

$$g_0 = \pi \frac{J_0}{c} \Lambda = \frac{\pi G}{\Lambda} = \frac{\pi \rho G}{k} \quad (65)$$

In subsequent work, we will be using values of g_0 in a tentative range to obtain an idea of the expected magnitude of various parameters and anticipated measurements. That is, until we establish the actual value of g_0 , we may obtain the new constant Λ and hence k from the known density of a mass, for any given value g_0 .

It is useful to write Eqs. 62 and 64 correspondingly as:

$$g = G \frac{M_e}{r^2} = \frac{G \pi A}{\Lambda r^2} = g_0 \frac{A}{r^2} \quad (66)$$

$$g_R = g_0 A_R \quad (67)$$

Now, given the measured acceleration g_R on the surface of a spherical body, we can find k by solving the equation below:

$$g_0 A_R - g_R = g_0 \left[1 - \frac{1}{2k^2 R^2} + \frac{\exp(-2kR)(2kR + 1)}{2k^2 R^2} \right] - g_R = 0 \quad (68)$$

as a function of g_0 . Then, for any given g_0 , we can find in turn ρ , Λ and J_0 from Eq. 65. We will return to the question of g_0 in a subsequent section.

6.4 Commonality and departure between Newton and PG

It is not fortuitous that both Newtonian and PG mechanics share a common limiting case but depart thereafter. Let us start from the derivation of the volume of the sphere as seen from point O in Fig. 2. For the elementary volume we have

$$dV = d\Omega u^2 du \quad (69)$$

which multiplied by the density ρ gives the elementary mass and, divided by the inverse square distance, yields the Newtonian acceleration:

$$dg_{Newton} = \frac{d\Omega u^2 du}{u^2} \rho \quad (70)$$

In PG, we use the factor f_g from which we obtain the same elementary acceleration by :

$$dg_{PG} = \frac{g_0}{\pi} d\Omega k du \quad (71)$$

which is identical to Newton above except for the proportionality constants. This initial similarity is not trivial, because it explains the fundamental difference at the root of the two theories (approaches), as we increase the absorption coefficient: In Newton, it is given that the acceleration is inversely proportional to the square of distance, whilst in PG this is a consequence of the solid angle (geometry) incorporating the inverse square distance relationship. In Newton, this is the result of an assumed radiance (of gravity) emanating from the elementary mass, whilst in PG the same field emanates from the radiance of the surrounding universe. Whilst the analogy might seem trivial simply shifting the problem of origin of the elusive gravity from the inside to the outside of a given mass, the consequences diverge from the two approaches as we increase the absorption coefficient to any level. That is, when considering very large masses or densities, Newton and PG provide very different solutions and outcomes: Newton provides a linear cumulative radiance of gravity by simple summation of all the constituent masses/volumes, whilst PG allows for shadowing (shielding) of the universal radiance traversing the mass, which, in turn, results in an asymptotic limit to the total shielding and hence to the total acceleration or force. We may think of this limit as effectively integrating the Newtonian law linearly but within contracting upper limits of a volume per Eq. 71, which defines the said gravitoid. This shape would produce the same Newtonian force with a mass having the actual (real) density. The above integration has been performed numerically and potted against k in Fig. 6 after it is normalized by dividing by the sphere volume, as was done for the effective spherical volume defined by Eq. 57. For comparison, this is also plotted against k in Fig. 6. We note that it is generally lying above the

gravitoid, as it should, because it is further away from the gravitoid. They both have the same real density and both yield the correct value of acceleration for the real gravitating sphere.

Hence, these are important findings for cosmological considerations in relation to what happens as we keep adding mass (accretion) to a star (dwarfs, black holes, etc.). We will discuss this again later.

An important conclusion here is that there is more mass in the universe than Newton's Law measures. This is a form of dark matter but not exactly in the sense considered by existing theories to date, in accounting for the observed celestial motions. We now find weaker forces, not greater. However, the greater forces, if needed, may be accounted for by forces originating from the outside now predicted from PG theory, not from the inside anticipated by Newton. At very large distances, forces are exerted by the gravions in the universe, so there is no need to attribute them to an attraction by dark matter. However, dark matter should assume a different meaning now by the shadowing effect (gravitational shielding) in PG. Thus, breaking up a planet to dust would appear to create new matter (out of shadow - see redistribution of density in later Section 10), which gives a kind of credence to the creationist theory of matter, except that no new matter actually is created other than new matter coming out of the shadows (literally). All this and more creates new understanding and new physics that will become clearer as we develop and prove the novel PG presented in this work. As we investigate next, the bigG is a function of the gravion density in the universe, which should vary between regions inside a galaxy and in intergalactic regions. So, if we need extra forces, these may arise from the variation of bigG alone. The sum total of the effects caused by hidden masses and the variation of bigG might explain or replace the hypothesized dark matter and dark energy of current theories. PG may offer the new physics needed.

6.5 Summary of new parameters and relationships

We have already expressed various relationships in alternative forms, which we may further re-arrange for easy reference in later derivations here or elsewhere as follows: By combining Eqs. 46 and 62 we derive:

$$\pi A = \Lambda M_e \quad (72)$$

and

$$\Lambda = \frac{\pi A}{M_e} = \frac{\pi}{M_e} \left[R^2 - \frac{1}{2k^2} + \frac{\exp(-2kR)(2kR + 1)}{2k^2} \right] = \frac{\pi R^2 A_R}{M_e} \quad (73)$$

We obtain a further insight of the above parameters by re-writing the above as

$$A_R = \Lambda \frac{M_e}{\pi R^2} = \Lambda \lambda_e \quad (74)$$

by defining an effective mass-thickness λ_e (or area-density) with

$$\lambda_e = \frac{M_e}{\pi R^2} \quad (75)$$

The neighborhood prevailing gravion pressure p_g should be handy to have (per Eq. 63) as

$$p_g = \frac{J_0}{c} = \frac{G}{\Lambda^2} \quad (76)$$

If two spheres (planets) 1 and 2 have equal surface acceleration g_R , it follows from Eq. 64 that the product kR for both spheres is the same

$$k_1 R_1 = k_2 R_2 \quad (77)$$

Also we have the universal (cosmic) constancy for Λ giving:

$$\Lambda = \frac{k_1}{\rho_1} = \frac{k_2}{\rho_2} = \frac{\pi G}{g_0} = \frac{cg_0}{\pi J_0} = \text{constant} \quad (78)$$

so that we obtain

$$\rho_1 R_1 = \rho_2 R_2 \quad (79)$$

The above equations apply in PG theory with real densities ρ_1 and ρ_2 . In Newtonian mechanics, we similarly obtain for the effective (apparent) densities ρ_{e1} and ρ_{e2} , i.e. if the g_R is equal for both spheres (at their surface):

$$g_R = \frac{4}{3}GR_1\rho_{e1} = \frac{4}{3}GR_2\rho_{e2} \quad (80)$$

$$\rho_{e1}R_1 = \rho_{e2}R_2 \quad (81)$$

We obtain the ratios of real to effective densities as

$$\frac{\rho_1}{\rho_{e1}} = \frac{\rho_2}{\rho_{e2}} \quad (82)$$

From a given value for g_0 , we find the corresponding k from Eq. 68 and then ρ from Eqs. 65:

$$\rho = g_0 \frac{k}{\pi G} \quad (83)$$

and then the ratio ρ/ρ_e from the known effective (measured) density. This ratio is also provided directly from:

$$\frac{\rho}{\rho_e} = \frac{4}{3}kR \frac{g_0}{g_R} \quad (84)$$

We also derive relationships including the frequently encountered factor A_R :

$$M_e = \frac{\pi\rho R^2}{k}A_R = \frac{3A_R}{4kR}M = \frac{g_0}{G}R^2A_R \quad (85)$$

$$V_e = \frac{\pi R^2}{k}A_R \quad (86)$$

Finally, it is important to note that the parameter g_0 or the factor f_g yield the acceleration g , via Eqs. 48, 65 and 66 in a simple form by a summary of equations:

$$g = f_g \frac{g_0}{\pi} = f_g \frac{J_0}{c} \Lambda = f_g \frac{G}{\Lambda} = g_0 \frac{A}{r^2} = g_0 \frac{A_R}{n_R^2} \quad (87)$$

The maximum (or limiting) universal constant g_0 now takes on a tangible significance in establishing the quantitative relationships in PG, and it may substitute the constant G accordingly. We should stress that new universal constant of the cosmos Λ is given by Eq. 73, which in words states that the hitherto universal constant G is proportional to the new universal constant (maximum acceleration) g_0 both with reference to a region of the universe, so that together they yield the cosmic (overall universal) constant Λ . It should be noted that we attempt to distinguish the term “universal” from the term “cosmic” with reference to the neighboring universe or to the “entire” universe (=cosmos).

With the new parameters now introduced, it is useful to re-write Eq. 50 of the ratio of accelerations as a function of tentative values for g_0 :

$$q = \frac{g_{PG}}{g_{Newton}} = \frac{3A_R}{4kR} = \frac{3A_R}{4\pi G\rho R}g_0 \quad (88)$$

This factor characterizes a multitude of parameters, not only the acceleration, with reference to PG and Newton. For example we can write

$$q = \frac{\rho_e}{\rho} = \frac{M_e}{M} = \frac{V_e}{V} \quad (89)$$

7 Force between two spherical bodies

For the force between two spherical masses, we can formulate the problem entirely from gravion absorption considerations, carry out four integrations and produce the force law, as we did for the acceleration at a point for a single sphere. This would be an independent way, from first principles, to derive the required relationship. However, we can still arrive at the same desired result in a much simpler way as follows:

Since we already have established the relationships between all the parameters needed for the PG force equations, we can apply a “reverse engineering” approach. Now, in the knowledge that Newton is correct except for the masses used, we can start with the Newtonian law of force by using the effective masses provided by PG theory together with preceding equations between various parameters:

$$F = G \frac{M_{e1} M_{e2}}{r^2} = G \frac{\pi A_1}{\Lambda} \frac{\pi A_2}{\Lambda} \frac{1}{r^2} = \frac{J_0}{c} \frac{\pi A_1 \pi A_2}{r^2} = \frac{g_0}{\Lambda} \frac{\pi A_1 A_2}{r^2} \quad (90)$$

This is consistent with our hitherto understanding of the meaning of the parameters involved. The importance is that Newton's law now involves the effective masses M_{e1} and M_{e2} , not the real masses assumed, but not used, in prior mechanics. The above equations is a far reaching conclusion. Now we can write, or start with the PG force law as

$$F = \pi \frac{g_0}{\Lambda} \frac{A_1 A_2}{r^2} \quad (91)$$

where we do not need the masses, but equivalently we need the more intrinsic parameter of absorption coefficients (relating to mass), the radii (geometry), the new cosmic constant Λ and the prevailing maximum acceleration g_0 in the neighboring universe, or equivalently the pressure J_0/c exerted by the radiant energy in our neighborhood. We may further rearrange the above to provide a more tangible idea of how the force is derived by

$$F = p A_{R1} A_{R2} \frac{\pi R_1^2 \pi R_2^2}{r^2} \quad (92)$$

which states that the force is proportional to a pressure $p = \frac{J_0}{c}$ exerted by the gravions times the absorptivities times the cross-sections of the spheres while still being inversely proportional to the square of the distance. It seems like we can separate one group of factors pertaining to geometry alone and another group of factors pertaining to matter (energy) and its interactions involving the local system of two masses interacting with the universal pressure of gravions. The two masses do nothing by themselves except for the mediating flow of gravions.

Therefore, the above equations provide variant expressions of the law of gravitational force in the new physics of PG. They are particularly appealing by their consistency and symmetry of parameters beyond Newtonian physics.

The mathematical derivation from first principles of the radiant intensity absorption involving multiple integrations involves a number of simplifications and cancellation of terms by appropriate choice of a reference system of co-ordinates. The multiple integrations may also be done by numerical means via relatively simple Python codes run in parallel to shorten the computation times. Integrals involving absorption along lines crossing a single sphere cancel out leaving only integrals crossing both spheres simultaneously. This work has been omitted from this Section to avoid needless congestion that could potentially distract from the important finding above and beyond. This section may be expanded to form a self contained chapter with sufficient detail to qualify for publication, which, however, can await at least for an initial response by the established scientific community on the current report as is. In the meantime, we have added more details by presenting the constitutional equations of the interaction of two material spheres in Appendix C, etc. Numerical integration of those equations has lead to important results and conclusions.

Some concern might arise by a later proposal in Section 14.5, namely, that the effective mass being involved in the generation of force may be variable with its distance from another mass due to the perturbation of the surrounding gravion flux. However, these concerns have been eased by finding that the above presented fundamental equation is still valid. The envisaged variation of mass is coordinated by the mathematics of absorption in a way that the inverse square of distance law is always preserved at any absorption regime. We have tested ordinary solar system bodies (near Newtonian) as well as "artificial" ones with extremely dense and massive bodies. These outcomes are better presented together with a new analysis of effective mass generation and variation with distance in Sections 15.7 and 16.

IMPORTANT: The new gravitational law in PG expressed by Eq. 92 has far more repercussions than being a simple substitution of old parameters with new. It states that the force between two masses is not simply proportional to the effective masses but proportional to the associated absorptivities of the masses. This means that non-spherical masses exert a different force for different relative orientation of the same masses (bodies). If, as they move towards or away from each other they change orientation, they also change gravitational absorptivity and hence the trajectories would not be as expected from Newtonian mechanics. The dependence of acceleration on the density distribution will become more clear in Section 10. Further analysis is presented under the Equivalence Principle in Section 14.3.

8 Internal spherical field

So far, we have examined the field generated externally to a spherical body, but we now proceed to find the field also inside the sphere. With reference to Fig. 7, the acceleration at any point X inside a sphere with

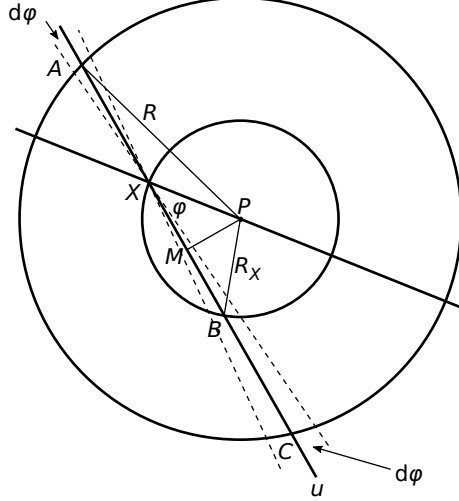


Figure 7: *Derivation of the internal field of a uniform density sphere.*

radius $AP = R$ is provided by integrating the absorption along the lengths of mass inside the differential solid angles indicated on either side of the point X along any direction of the line u . We note that the absorption length $XA = BC$ leaving only the length XB to yield a net force absorption, which is the same as that of the sphere with radius R_X crossing the point X . Therefore, we have the same situation as that experienced by Newtonian mechanics, in that a hollow sphere would exert zero force inside its cavity. Now, the acceleration at this internal point is given by (see Eq. 87)

$$g_X = g_{0X} \left(1 - \frac{1}{2k_X^2 R_X^2} + \frac{\exp(-2k_X R_X) \cdot (2k_X R_X + 1)}{2k_X^2 R_X^2} \right) \equiv g_{0X} A_{R_X} \quad (93)$$

where A_{R_X} is the familiar A_R factor at the surface of the internal sphere with radius $PB = R_X$ and $g_{0X} < g_0$ due to the shielding of the outer layer from X (more on this can be found in Section 24).

We can find g_{0X} by resorting to the usual absorption factor f_{gX} at point X by the following steps:

The exponential absorption factor in the direction XBC is

$$1 - \exp(-k \cdot XB(\varphi) - k \cdot BC(\varphi))$$

and in the direction XA is

$$1 - \exp(-k \cdot XA(\varphi))$$

so that we take their difference in the integral:

$$f_{gX} = \int_0^{\pi/2} 2\pi \sin \varphi \cos \varphi d\varphi \cdot [\exp(-k \cdot XA(\varphi)) - \exp(-k \cdot XB(\varphi) - k \cdot BC(\varphi))] \quad (94)$$

and integrate with respect to angle φ from 0 to $\pi/2$ as can be seen in the referenced diagram.

From the geometry shown and M being the mid-point of the chord AC , we find and replace the lengths accordingly with:

$$XB(\varphi) = 2R_X \cos \varphi$$

$$XA(\varphi) = BC(\varphi) = \sqrt{R^2 - (R_X \sin \varphi)^2} - R_X \cos \varphi$$

to obtain the integral formula:

$$f_{gX} = \int_0^{\pi/2} 2\pi \sin \varphi \cos \varphi d\varphi \cdot \left[\exp\left(-k\sqrt{R^2 - (R_X \sin \varphi)^2} + kR_X \cos \varphi\right) - \exp\left(-k\sqrt{R^2 - (R_X \sin \varphi)^2} - kR_X \cos \varphi\right) \right] \quad (95)$$

$depth=$	2500	5000	7500	10000	12500
$g_N=$	9.816404	9.812551	9.808697	9.804844	9.800990
g_0	Δg_X	Δg_X	Δg_X	Δg_X	Δg_X
300	7.29E-05	1.45E-04	2.18E-04	2.90E-04	3.61E-04
500	4.32E-05	8.62E-05	1.29E-04	1.72E-04	2.14E-04
1000	2.14E-05	4.27E-05	6.39E-05	8.50E-05	1.06E-04
2000	1.07E-05	2.13E-05	3.18E-05	4.23E-05	5.28E-05
5000	4.25E-06	8.48E-06	1.27E-05	1.69E-05	2.11E-05
10000	2.12E-06	4.24E-06	6.34E-06	8.43E-06	1.05E-05
20000	1.06E-06	2.12E-06	3.17E-06	4.21E-06	5.26E-06
30000	7.08E-07	1.41E-06	2.11E-06	2.81E-06	3.50E-06
50000	4.24E-07	8.47E-07	1.27E-06	1.69E-06	2.10E-06

Table 1: *Difference of acceleration Δg between Newton and PG at various depths in Earth.*

From this found, we can derive the acceleration at X by the factor g_0/π and equate it to its value given above by Eq. 93:

$$g_X = \frac{g_0}{\pi} f_{gX} = g_{0X} A_{R_X} \quad (96)$$

from which we can find the relationship between the internal g_{0X} and external g_0 .

$$g_{0X} = \frac{g_0 f_{gX}}{\pi A_{R_X}} \quad (97)$$

The expected Newtonian acceleration at X is given by:

$$g_{XN} = \frac{4}{3} \pi G \rho_e R_X \quad (98)$$

No analytical relationship was found for f_{gX} , so that we may resort to numerical means for this parameter. For practical application, we also need to see the difference of PG from Newton acceleration against various depths from the surface of the Earth by replacing the internal radius as a function of depth.

$$R_X = R - depth \quad (99)$$

We present some values as in Table 1 for Earth by using average values for density and absorption coefficient taken from the Table 3 as used for various planets in the following section. Tentatively, we initially use the value $g_0 = 1000 \text{ m/s}^2$. The results provide the expected deviation of measurements from Newtonian physics at various depths, if the Earth's crust had uniform density and a spherical shape. We can do measurements in a very deep mine or in a deep ocean, however, we would need to re-calculate the local

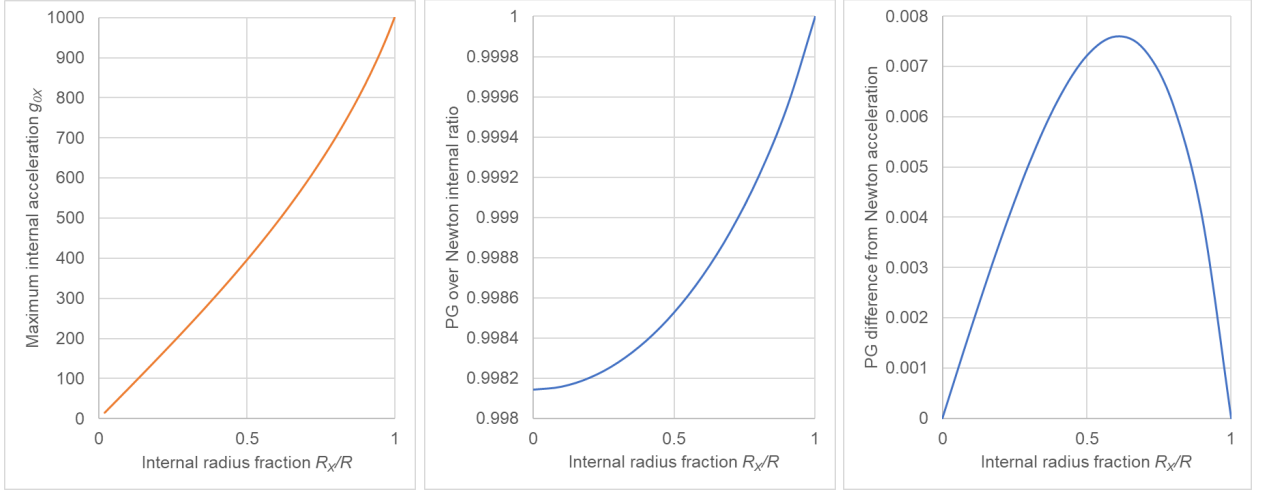


Figure 8: *Internal maximum acceleration g_{0X} , internal ratio of PG over Newton accelerations and internal difference of PG from Newton acceleration in Earth.*

acceleration in both Newton and PG cases. In practice, measurements of this kind would be complicated by influences of the local variations of density and time dependent fluctuations of the local acceleration, but the given table provides a first idea of the order of magnitude of expected deviation from Newton for a prospective careful experiment. It seems that these deviations should be measurable by a sensitive gravimeter with sufficient confidence if g_0 has a sufficiently low value. In turn, by establishing true measurements of the acceleration at various depths, we can deduce the unknown parameter g_0 .

For theoretical considerations, we can also see the variation of maximum internal acceleration g_{0X} , the ratio of g_X/g_{NX} (PG/Newton) and the difference of PG from Newton acceleration in Fig. 8 at any depth (fractional radius) again for a tentative external $g_0 = 1000 \text{ m/s}^2$ in the case of planet Earth using the same parameters. For further analysis, reference should be made to Section 24, especially noting that the internal Newton-acceleration is derived from the actual Newton-acceleration at the surface of the sphere.

Establishing the variation of the maximum acceleration factor g_0 inside a planet, it also suggests that this parameter may not be so constant even in our relatively “small” area of the universe even inside the heliosphere, since there is a significant mass within the heliosphere itself, whilst our planets are just internal points within this sphere. This might explain the Pioneer anomaly for the deviation of gravity measurements from expected values from Newtonian mechanics. This then points also to the alternative possibility of purposefully sending a spacecraft to more accurately measure the same effect while eliminating (preventing) other already proposed causes and explanations.

8.1 The Greenland experiment anomaly

Shortly before publication of the manuscript of this work, it has been accidentally found a report on “*The Greenland Gravitational Constant Experiment*” Zumberge *et al.* (1990) dealing exactly with the measurement of gravity in a bore hole in the ice-sheet. A deviation (shortfall) from Newton has been found in the range of between 1-4 mGal. This report appears particularly comprehensive in dealing with all possible sources of error and still found to establish a gravitational anomaly that cannot be explained by known theory stating in the abstract that: “*An anomalous variation in gravity totaling 3.87 mGal ($3.87 \times 10^{-5} \text{ m/s}^2$) in a depth interval of 1460 m was observed. This may be attributed either to a breakdown of Newtonian gravity or to unexpected density variations in the rock below the ice*”. Although these measurements cannot be used “as is” to do any quantitative connection to the PG predictions in this Section, we do note that the order of magnitudes match well with those of Table 8. This is particularly encouraging to organize a similar experiment, perhaps, best suited in an ocean, where the local variations of gravity may be less or more easily predictable and the depth measurements about one order of magnitude greater.

However, variant reports by Zumberge and coworkers have failed to reproduce this anomaly at various oceanic depths, which might be attributed to either (a) the experimental error involved overwhelms the anticipated effect, which is of the order of magnitude tentatively deduced from the Allais effect per Section 12.4 of prior version v16 (or before) of this report, or (b) the mathematical treatment used for the Newtonian derivation may need reworking, else the direct method used in PG computations needs to be applied for the specific mass distribution at the location tested and integrated with the whole planet.

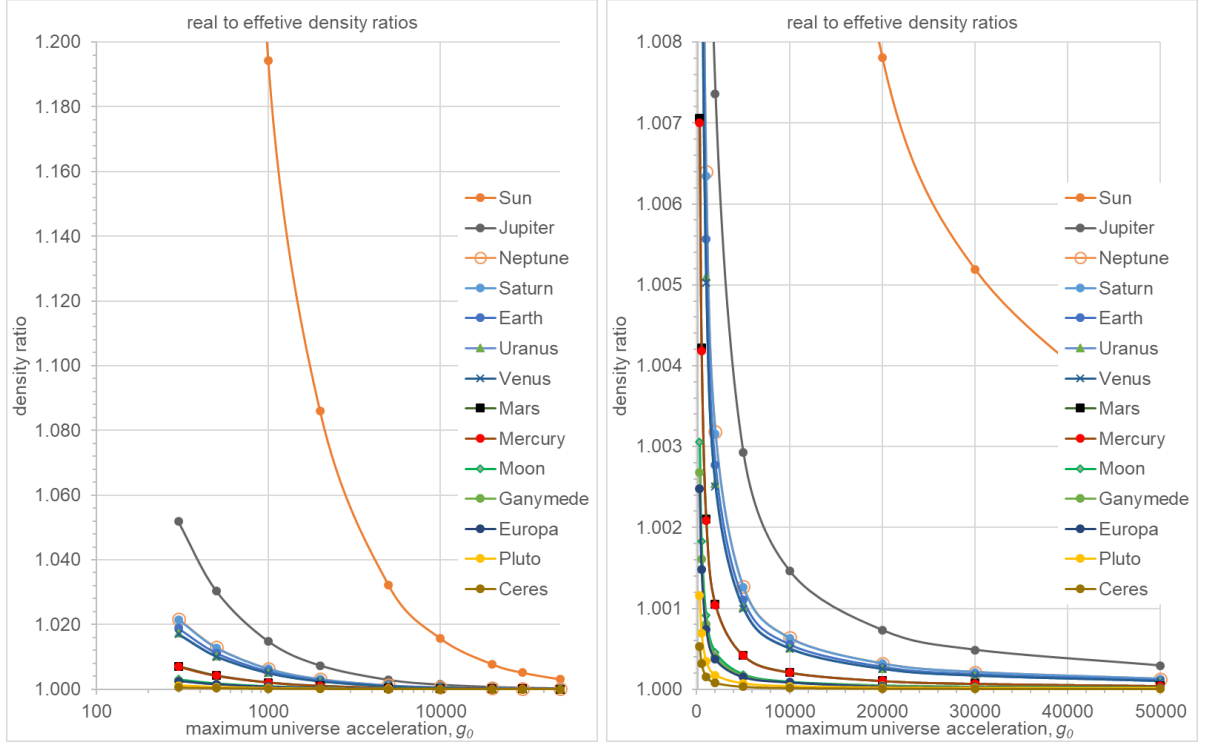


Figure 9: *Ratio of real to effective (measured) densities for planets, moons and the Sun.*

9 Application to the solar system

We can tentatively apply the equations of PG so far, like in Sections 6.3 and 6.5, to the solar system by assuming values of the maximum prevailing acceleration g_0 in our area of the universe.

We first plot the density ratios for many bodies of the solar system in Fig. 9 in the given hypothetical range of values for g_0 between 300-50000 m/s^2 . These graphs show that we get practically identical curves for Mercury and Mars having close to same surface accelerations, whilst all else are proportionally separated in accordance to their surface gravity. The graphs indicate the degree of departure from real densities depending on the chosen value of g_0 .

For better appreciation of the magnitudes involved, numerical results are also presented, as example, for three bodies (Sun, Earth and Moon) in Table 2 in the same range of g_0 . Some typical values of Λ for the same range of g_0 are also given being universal for all bodies per Eq. 78.

For any given set of mass and radius of each planet, we have derived the corresponding surface acceleration and effective density rather than using random (published) values from different sources. This is necessitated by the need to be consistent and accurate in these calculations and avoid discrepancies. These parameters are sensitive to very small changes of the input data. Small bodies are even more sensitive and round-off errors in the calculations are significant. Excel sheets were used for formatting the plotted figures, which initially necessitated the use of an “Add-in” (xlPrecision) to increase accuracy beyond 15 decimal places. Likewise, in a later use of Python code to reproduce the same output, we had to use increased computational precision to avoid serious round-off errors. In Table 3, we provide the initial data used for various bodies here and in all calculations elsewhere in this report. We also quote in parenthesis some variant values of the surface acceleration that were found from different sources for comparison, but not applied.

In all above, the derived and used parameters are based on the average density of the chosen bodies, which strictly speaking cannot produce the correct (actual) PG result, unless we knew in advance the radial density distribution for any given body. However, we obtain some first order of magnitude idea of the new important parameters introduced in this work. It should be noted that the density ratios approach unity as we increase g_0 .

9.1 Further analysis

To better understand the meaning of the real density expected for a planet, we can plot what the acceleration on the surface would be if the measured (effective) density were used as the real density. Let’s use the data for the Sun given by Table 3 and plot g_R against g_0 in Fig. 10 using Eqs. 64 and 65. We note that the Sun’s

	Sun		Earth		Moon		
g_0 , m/s ²	k, 1/m,	ρ/ρ_e	k, 1/m	ρ/ρ_e	k, 1/m	ρ/ρ_e	Λ , m ² /kg
300	3.4245E-09	3.4640	3.9262E-09	1.01886	2.3464E-09	1.003060	6.99E-13
500	9.1141E-10	1.5366	2.3380E-09	1.01121	1.4061E-09	1.001833	4.19E-13
1000	3.5419E-10	1.1943	1.1625E-09	1.00556	7.0242E-10	1.000915	2.10E-13
2000	1.6103E-10	1.0860	5.7963E-10	1.00277	3.5105E-10	1.000457	1.05E-13
5000	6.1225E-11	1.0322	2.3146E-10	1.00111	1.4038E-10	1.000183	4.19E-14
10000	3.0125E-11	1.0158	1.1567E-10	1.00055	7.0185E-11	1.000091	2.10E-14
20000	1.4944E-11	1.0078	5.7818E-11	1.00028	3.5091E-11	1.000046	1.05E-14
30000	9.9371E-12	1.0052	3.8542E-11	1.00018	2.3393E-11	1.000030	6.99E-15
50000	5.9499E-12	1.0031	2.3123E-11	1.00011	1.4036E-11	1.000018	4.19E-15

Table 2: *Calculated absorption coefficient k and ratio of real ρ over effective ρ_e density for the Sun, Earth and Moon in an assumed range of g_0 values.*

planet	radius R	mass M_e	density ρ_e	g_R (other)
Sun	6.95E+08	1.989E+30	1.41446E03	274.825 (273.7)
Jupiter	6.9911E7	1.8982E27	1.326E3	25.9204 (24.79)
Neptune	2.4622E7	1.02413E26	1.6379344E3	11.27456624 (11.15)
Saturn	5.8232E7	5.6834E26	6.87123E2	11.1860(10.44)
Earth	6.371E6	5.97237E24	5.5136E03	9.82026 (9.807)
Uranus	2.5362E7	8.6810E25	1.27037E3	9.00729 (8.69)
Venus	6.0518E6	4.8675E24	5.243E3	8.87009 (8.87)
Mars	3.3895E6	6.4171E23	3.93408E03	3.727854(3.720)
Mercury	2.4397E6	3.3011E23	5.42701E3	3.70150 (3.7)
Moon	1.73700E06	7.34767E22	3.34705E03	1.62533 (1.625)
Ganymede	2.634E6	1.4819E23	1.93590E3	1.42554 (1.428)
Europa	1.560E6	4.799844E22	3.01832E03	1.316343805 (1.315)
Pluto	1.1883E6	1.303E22	1.85386E03	0.615862 (0.62)
Ceres	4.730E05	9.393E20	2.161E3	0.280203 (0.28)
Callisto	2.4103E6	1.075938E23	1.8344	1.235

Table 3: *Numerical constants of planets, moons, and the Sun used in calculations of preceding tables and graphs.*

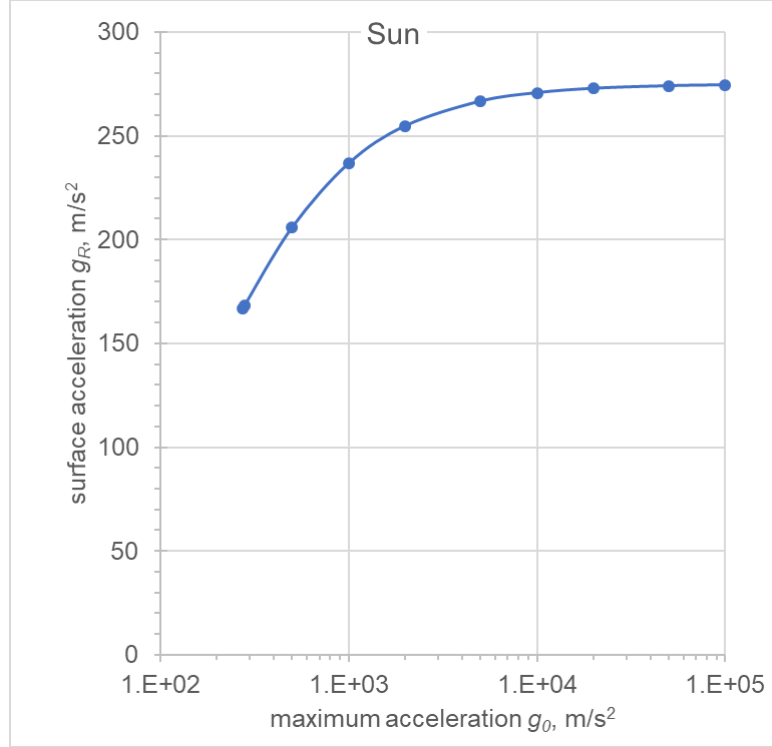


Figure 10: *Expected surface acceleration on the surface of the Sun against maximum g_0 using the measured density as real density.*

real acceleration is approached asymptotically at very high values of g_0 . The latter is as expected, because increasing g_0 decreases k , which makes the PG value to become Newtonian, i.e. to reduce to $g_R = 274.825$ m/s² as given in Table 3. The same can be deduced by taking the limit of Eq. 64 as $k \rightarrow 0$.

We have already found that by increasing the radius of a planet by adding mass at constant density, the surface acceleration reaches a saturation limiting value, namely, g_0 , i.e. when A_R becomes unity. This is at variance with Newtonian prediction of infinity by Eq. 80.

Likewise, with increasing the density by keeping the radius constant, the Newtonian prediction is infinity. However, in PG the factor A_R being a function of the product kR becomes a product also of $\Lambda\rho R$ meaning that $A_R \rightarrow 1$ by increasing ρ with constant R and Λ . Similarly, by shrinking a star (sphere) with constant mass, we obtain unity for A_R as the density becomes fast very large (the density being inversely proportional to the third power of radius). In other words, the eventual surface acceleration reaches the saturation value of g_0 in clear distinction from Newtonian mechanics.

Last in this connection, we should also consider what happens at a fixed point in space away from a sphere (star), when the sphere shrinks with constant mass. By Newton, the acceleration remains constant at that point, but by PG this is not the case: The acceleration monotonically becomes smaller, due to self shadowing (k increases much faster than the radius) by

$$g_{fixed_r} = g_0 \frac{\pi A}{r^2} \quad (100)$$

noting that A varies as:

$$A = R^2 \left[1 - \frac{R^4}{2C^2} + \frac{R^4}{2C^2} \exp(-2C/R^2) \cdot (2C/R^2 + 1) \right] \quad (101)$$

where the constant C is defined during the k substitution below:

$$k = \frac{3GM}{4g_0 R^3} \equiv \frac{C}{R^3} \quad (102)$$

Noted also that the PG equation of acceleration reduces to Newton's equation, as expected, for very small values of k :

$$g_A = g_0 A_{k \rightarrow 0} = g_0 \frac{4}{3} k R = \frac{4}{3} \pi G \rho R = G \frac{M}{R^2} \quad (103)$$

Furthermore, we can substitute k accordingly and find g_A for a white dwarf and a neutron star. The extreme accelerations reported for these bodies pose for now a serious question on whether PG could ever be directly measurable or detectable if g_0 needs to be too high. This would constitute a new serious challenge for PG by not being able to detect it experimentally, unless those extremely high values of acceleration are generated by yet another type of push particle. We will discuss this issue again in Part 2 of this report.

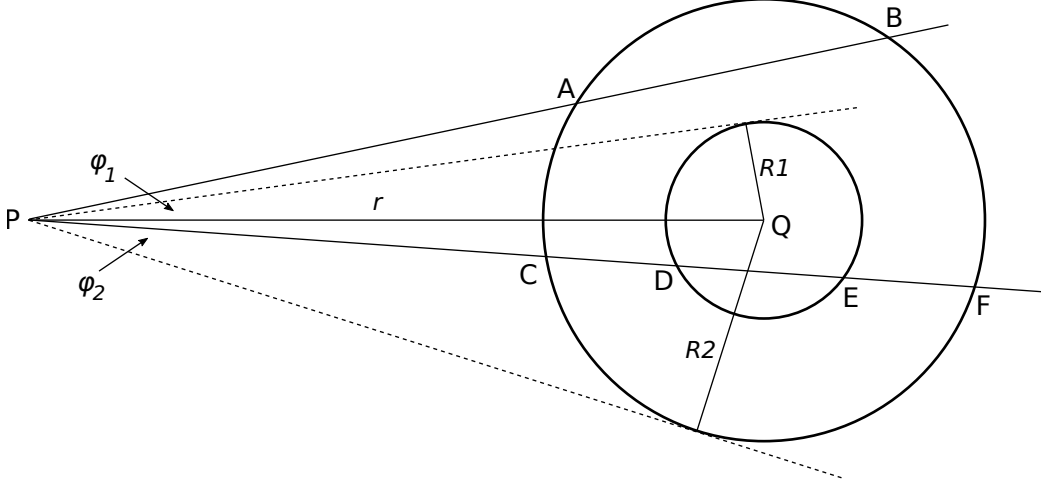


Figure 11: *Derivation of acceleration from concentric spheres with different densities.*

10 Concentric spheres with different densities

We now consider the case of two concentric spheres of different density as depicted in Fig. 11. The inner sphere has a radius R_1 with density ρ_1 , mass M_1 and absorption coefficient k_1 , and the outer sphere has a radius R_2 with density ρ_2 , mass M_2 , and absorption coefficient k_2 . There are two cases of PG absorption, namely, one along a typical chord AB traversing only the outer sphere, and another traversing segment CD of the outer sphere then a chord DE of the inner sphere and then segment EF of the outer sphere again.

To find the acceleration at point P being at a distance $r = PQ$, we follow the integration steps as in the first place for PG (Eq. 42), but for the two parts described above:

Part one involves integration in the angle between φ_1 and φ_2 for the outer spherical layer.

$$f_{g2} = 2\pi \left[\frac{\sin^2 \varphi}{2} - \frac{\exp\left(-2kr\sqrt{a^2 - \sin^2 \varphi}\right) \left(2kr\sqrt{a^2 - \sin^2 \varphi} + 1\right)}{4k_2^2 r^2} \right]_{\varphi_1}^{\varphi_2} \quad (104)$$

where

$$a = \frac{R_2}{r} = \sin \varphi_2 \quad (105)$$

After substituting the integration limits, we get a familiar relationship as follows:

$$f_{g2} = \pi \left[R_2^2 - R_1^2 - \frac{1}{2k_2^2} + \frac{\exp\left(-2k_2\sqrt{R_2^2 - R_1^2}\right) \left(2k_2\sqrt{R_2^2 - R_1^2} + 1\right)}{2k_2^2} \right] \frac{1}{r^2} \quad (106)$$

Part two then involves the following steps starting with the general PG Eq. 42, where we have for the inner sphere

$$a = \frac{R_1}{r} = \sin \varphi_1 \quad (107)$$

and need to replace the exponential having length ℓ in the exponent with three exponential factors corresponding to the three consecutive absorption layers (lengths) in EF, DE and CD:

$$f_{g1} = \int_0^{\varphi_0} 2\pi \sin \varphi \cos \varphi d\varphi \cdot [1 - \exp(-k_2 \cdot EF(\varphi)) \cdot \exp(-k_1 \cdot DE(\varphi)) \cdot \exp(-k_2 \cdot CD(\varphi))] \quad (108)$$

That is

$$f_{g1} = \int_0^{\varphi_0} 2\pi \sin \varphi \cos \varphi d\varphi \cdot [1 - \exp(-2k_2 \cdot EF(\varphi) - k_1 \cdot DE(\varphi))] \quad (109)$$

Because

$$2EF = CF - DE \quad (110)$$

and using Eq. 17 for each of the spheres, we can easily replace with:

$$f_{g1} = \int_0^{\varphi_0} 2\pi \sin \varphi \cos \varphi d\varphi \cdot \left[1 - \exp \left(-2k_2 r \sqrt{a_2^2 - \sin^2 \varphi} - 2(k_1 - k_2) r \sqrt{a_1^2 - \sin^2 \varphi} \right) \right] \quad (111)$$

for which unfortunately the anti-derivative could not be found analytically. The total acceleration is given by the usual factor as:

$$g = g_0(f_{g1} + f_{g2})/\pi \quad (112)$$

As usual, we equate $r = R_2$, when we need to find the acceleration g_R at the surface of a sphere.

We may appreciate the relative magnitudes involved, if we were to take, for example, Jupiter as consisting of two concentric spheres with the tentative (arbitrary) parameters provided in Table 4. Jupiter's core constitution is uncertain, so that the values are only indicative for the present purposes and chosen among various values in the literature (<https://sciencing.com/jupiters-core-vs-earths-core-21848.html>). The Jupiter mass is actually layered with variable densities, but the best we can demonstrate at this stage is to start with a uniform mass equal to the total one actually measured (M_e) from its corresponding acceleration $g_R = 25.92 \text{ m/s}^2$ (already used here). We then find the real mass M , as we did for various planets before, by first solving the equation of the parameter A_R for k with any given g_0 , from which we establish the real density ρ and density ratio ρ/ρ_e . Next, we redistribute this mass in the two spheres in the same proportion as initially provided in this table, namely 0.2259599008534 fraction of the total is compressed inside the inner sphere (core) and the remainder fraction is contained by the outer spherical layer. The real densities ρ_1 and ρ_2 in the two layers are readily found, from which the corresponding parameters k_1 and k_2 are calculated and used in Eq. 11. The results for the acceleration on the surface of the planet are given in numerical form in Table 4 again as a function in the typical range of g_0 .

In Newtonian mechanics, the redistribution would have no effect on the surface acceleration g_R , but in PG the surface acceleration g_{RPG} is very different, as we can see it is significant. The lower values obtained from PG indicate that the final actual densities should be increased in order to yield the real measured surface acceleration. In other words, there is a significant amount of hidden mass by the mere fact of having a dense core over and above (in addition to) the hidden mass also present in a uniform distribution. This is important, which means that any attempt to redistribute the mass of Jupiter along the radius should take into account the new physics revealed by PG. This also means that all previous calculations assuming an average constant density for the planets produces only approximate results. The difference becomes more important with the increase of the planet or star size. Noted also that the main (dominant) component of the PG acceleration comes from the diluted outer layer mass for the chosen mass redistribution - if the two components are considered separately. Hence in general, all prior attempts dealing with assumed mass and mass distributions should be re-appraised accordingly. In fact, artificial satellites orbiting Jupiter have reported anomalous orbits with a noticeable wobble, which may be attributed to Moons of Jupiter being shadowed by a different core density from the outer planet. We now have a new basis to re-evaluate and explain many phenomena already on record.

We may generalize and conclude that the radial distribution of density in a spherical body is critical in the generation of acceleration at the surface of the sphere and beyond according to PG, whereas this distribution makes no difference in the Newtonian acceleration lumping the mass at the center of gravity (i.e. center of the sphere). In an arbitrary shape with an arbitrary density distribution then, the only correct way is to derive the acceleration and force by integration of the graviton absorption around three coordinate axes yielding the three components of the vector of acceleration.

Jupiter	radius R	mass M_e	density ρ_e
whole planet	6.9911E7	1.8982E27	1326
core	1.6E7	4.289E26	25000
outer	6.9911E7	1.4693E27	1039
g_0	g_{RPG}	$g_R - g_{RPG}$	ρ/ρ_e
300	18.97555828	6.944841717	1.051873063
500	18.87716456	7.043235439	1.030304147
1000	18.80444874	7.115951257	1.014860051
2000	18.76839103	7.152008972	1.007359332
5000	18.74684295	7.17355705	1.002927051
10000	18.73967389	7.180726112	1.001460768
20000	18.73609184	7.184308161	1.000729697
30000	18.73489819	7.185501814	1.000486312
50000	18.73394339	7.186456606	1.000291714

Table 4: *A two-layered sphere model of Jupiter with same real mass redistributed to the corresponding radii provided; Surface accelerations with PG and difference from Newton in a range of g_0 values.*

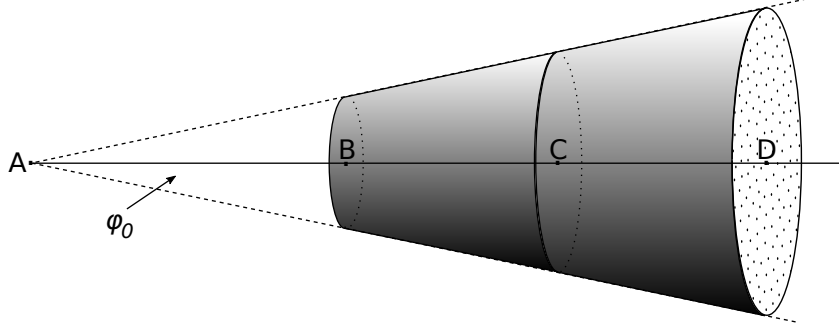


Figure 12: *Coaxial truncated spherical cones (sections) with fixed and equal height.*

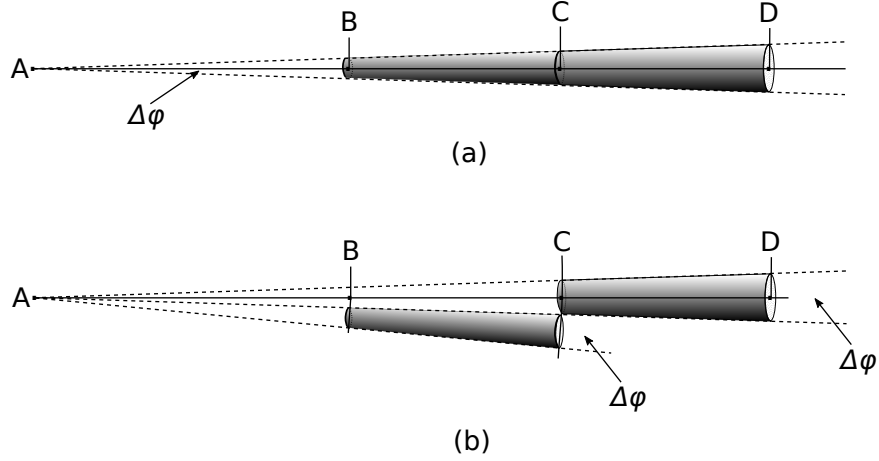


Figure 13: *Elementary truncated cones of equal height in series (a) and in parallel (b).*

11 The superposition principle revisited and revised

The superposition principle, also known as superposition property, states that, for all linear systems, the net response caused by two or more stimuli is the sum of the responses that would have been caused by each stimulus individually. This applies to Newtonian gravity. However, this is not valid in general PG, unless the absorption coefficient k is relatively small. This will be illustrated with a two-body and a three-body general outline of the PG case next.

11.1 Two-body superposition

Let us now consider Fig. 12, where we draw two co-axial truncated cones subtending the same solid angle at point A with semi-angle φ_0 and with equal height, namely, $BC = CD = \ell$. Each material cone creates the same amount of gravion shadowing, if considered separately, i.e. without the presence of the other. In other words, PG provides an insight first with an immediate result that all truncated cones of constant angle and equal height will produce the same acceleration of gravity regardless of their distance from a common convergence point; this result can be derived without any computation or integration of the elementary masses constituting these shapes.

However, when they act in series as depicted, the inner (nearest to A) cone is shadowed by the outer one and absorbs a lesser amount from the decreased output of gravion intensity by the outer cone. In the special case where the absorption is linear, which is the case when k is sufficiently small, then we can superpose their separate absorption like in Newtonian superposition of gravity.

Now, we consider the general case of PG again in Fig. 13(a), which is essentially the same as the previous figure but the truncated cones subtend a very small angle $\Delta\varphi$, which allows the shifting of the inner cone as in 13(b) by the same small angle without practically changing the direction of the vector of shadowing (acceleration), i.e. both are considered to retain the same direction at point A. By this, we get a simplified derivation in the case of exponential absorption of gravions (i.e. general PG) below.

Each truncated cone constitutes a material layer with thickness ℓ and absorption coefficient k , so that the

transmitted intensity is given by Eq. 6. When the layers are in series as shown in (a), the total absorption through the double thickness is

$$\Delta J_{series} = \Delta J_0 (1 - \exp(-k2\ell))$$

However, if the inner cone is shifted as in (b) with the vectors of acceleration practically lined up, we can add them numerically for the total absorption according to Eq. 6 as

$$\Delta J_{parallel} = \Delta J_0 2 (1 - \exp(-k\ell))$$

The difference between these cases then becomes

$$\Delta J_{parallel} - \Delta J_{series} = \Delta J_0 (1 + \exp(-k2\ell) - 2\exp(-k\ell))$$

which is a positive number and indicates that the total shadowing (acceleration) by the two layers is stronger when they are in parallel than when in series by one shielding the other.

The same can be expressed also in terms of absorption fractions:

$$f_{parallel} - f_{series} = 1 + \exp(-k2\ell) - 2\exp(-k\ell) \quad (113)$$

and in terms of acceleration:

$$\Delta g = g_{parallel} - g_{series} = g_0 (1 + \exp(-k2\ell) - 2\exp(-k\ell))$$

Note: Care is needed when using the above factors $f_{parallel}$ and f_{series} in comparison with the factors f_a and f_g already introduced and used in the derivation of acceleration. At the outset, we defined the factor $f_{a\Delta\Omega}$ by Eq. 7 and f_a by Eq. 11, so that the former is the derivative of the latter with respect to solid angle:

$$f_{a\Delta\Omega} = \frac{df_a}{d\Omega} \quad (114)$$

which is the radiance by Eq. 1 we started with. We were compelled to introduce the factor $f_{a\Delta\Omega}$, because we needed to multiply by the absorption coefficient k at the foundation of PG theory. This was followed by an integration yielding the absorption factor f_a , from which we derived the force (acceleration) along a particular direction (e.g. towards the center of a sphere) via the factor f_g . Therefore, the factors $f_{parallel}$ and f_{series} are the derivatives of f_a

$f_{parallel} = f'_{a-parallel}$ and $f_{series} = f'_{a-series}$ yielding the corresponding accelerations g by multiplication with g_0 in the elementary solid angle shown in Fig. 13.

11.2 Three-body superposition equations

The superposition principle in PG applies to any number of bodies. A demonstration of the formulation is also provided for a three-body case, as it can assist in various applications later.

The diagrams (a) and (b) in Fig. 14 describe the generation of gravitational field at point A in space at the apex of an elementary solid angle $\Delta\Omega$ (with cone angle $\Delta\varphi$) that is filled with matter (hyle) over the specified lengths AE , BC and CD with corresponding absorption coefficients k_{AE} , k_{BC} , k_{CD} . We adopt the same terminology and symbols as before. Thus, we have for (a) that

$$\Delta J_{series} = \Delta J_0 [\exp(-k_{AE}AE) - \exp(-k_{BC}BC - k_{CD}CD)]$$

For (b) we get that

$$\Delta J_{parallel} = \Delta J_0 [2 \cdot \exp(-k_{AE}AE) - \exp(-k_{BC}BC) - \exp(-k_{CD}CD)]$$

The difference between these cases then becomes

$$\Delta J_{parallel} - \Delta J_{series} = \Delta J_0 [\exp(-k_{AE}AE) + \exp(-k_{BC}BC - k_{CD}CD) - \exp(-k_{BC}BC) - \exp(-k_{CD}CD)]$$

In terms of acceleration factors f , we have:

$$f_{parallel} - f_{series} = \exp(-k_{AE}AE) + \exp(-k_{BC}BC - k_{CD}CD) - \exp(-k_{BC}BC) - \exp(-k_{CD}CD) \quad (115)$$

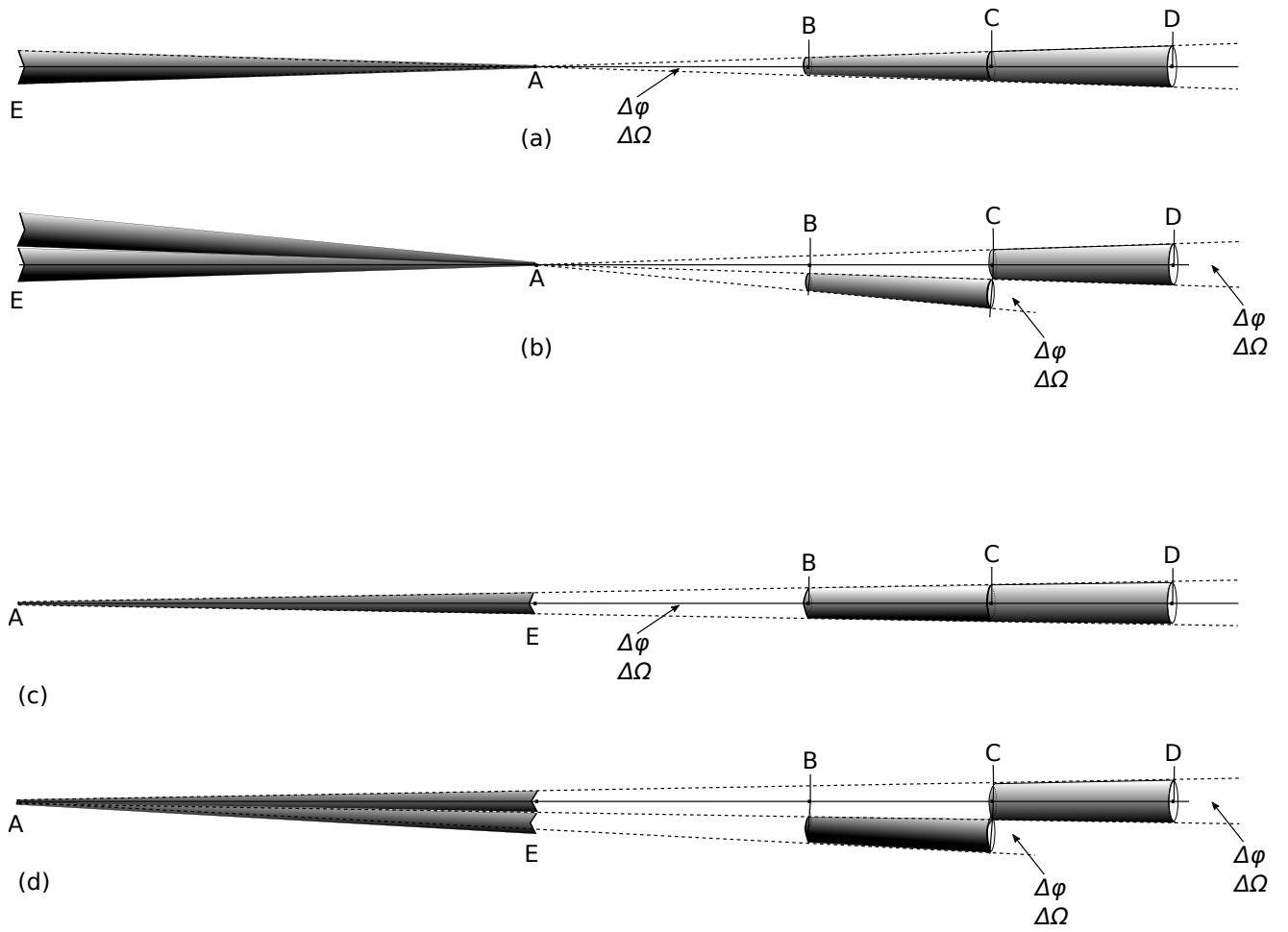


Figure 14: *Superposition principle with three absorbing bodies.*

If we set $k_{AE} = 0$, i.e. there is no absorption or no body to absorb, then the term $\exp(-k_{AE}AE) = 1$ and we recover Eq. 113. The positive sense of acceleration has been set (arbitrarily) towards the right, but we usually set it in the direction of the prevailing acceleration.

The diagrams (c) and (d) in Fig. 14 describe the case where we interchange previous points A and E and wish to find the acceleration field at A with all three bodies being to the right of point A. Thus, we have for case (c)

$$\Delta J_{series} = \Delta J_0 [(1 - \exp(-k_{AE}AE - k_{BC}BC - k_{CD}CD))]$$

while for case (d) we have

$$\Delta J_{parallel} = \Delta J_0 [(1 - \exp(-k_{AE}AE - k_{BC}BC)) + (1 - \exp(-k_{AE}AE - k_{CD}CD))]$$

The difference between these cases then is found to be:

$$\Delta J_{parallel} - \Delta J_{series} = \Delta J_0 \{1 - \exp(-k_{AE}AE) [\exp(-k_{BC}BC) + \exp(-k_{CD}CD) - \exp(-k_{BC}BC - k_{CD}CD)]\}$$

In terms of acceleration factors f , we have :

$$f_{parallel} - f_{series} = 1 - \exp(-k_{AE}AE) [\exp(-k_{BC}BC) + \exp(-k_{CD}CD) - \exp(-k_{BC}BC - k_{CD}CD)] \quad (116)$$

Again, setting $\exp(-k_{AE}AE) = 1$ we recover the above Eq. 115, while the acceleration g is obtained by multiplying the above factors f by g_0 as noted previously.

12 On PG measurements and verification

General outline

We have already proposed measurements of the internal field of Earth's crust, variation of gravity in the heliosphere and other methods above. Another test may be by using very sensitive gravimeters to measure the variation of gravity on Earth during a 24 hour rotation preferably during a new Moon (or better before, during and after a solar (better total) eclipse), whereby the Earth is shadowing the Sun+Moon system overnight. The deviation from predicted values using Newtonian mechanics should provide an indication and perhaps an evaluation of the PG parameters.

Alternatively, a similar to the previous observation could be made by the variation of the orbit of an Earth satellite during a new Moon (or better before, during and after a solar (better total) eclipse), whereby the Earth is shadowing the Sun and Moon systems during the night passage of the satellite, presuming that the effect on the orbit could be measurable. Could then such a variation explain the variations (wobble) observed by Juno during orbiting Jupiter?

Perhaps, minimal experimental and logistical requirements are involved if well planned experiments are conducted on Earth. The simplest of them might be to select an appropriate location on the equator and measure the variation of gravity over a 24-hour period with the most sensitive gravimeter available. This would require minimal field work preceded by a significant amount of office work for a thorough theoretical preparation. The latter would involve the calculation of all possible effects that can be had like on a straightforward calculation of Newtonian acceleration, tidal and local density variation. Actually, theoretical work for a similar purpose has been presented in order to measure the screen effect of the Earth in the "*electro-thermo-dynamical theory of gravitation*" by Adămuți (1982). If a difference can be established between the expected acceleration by all known factors and the measured one, then we can attribute it to an external source of radiation, such as we propose for gravions. For that purpose, we should couple corresponding computations with an expected PG value taking into account all known factors again (like eccentricity, etc.). The big unknown would be the radial density distribution of Earth, which does not enter (not needed) in the Newtonian calculation. This is a critical difference between the two derivations. Recent studies have revealed a much denser core, which could have an even greater effect on PG calculations. It might indicate the presence of PG effects even in a more pronounced manner, if we record the variation of acceleration in the entire 24-hour rotation period. The latter might reveal an anomalous variation around the midnight hour if the core presents a pronounced density difference from the mantle.

An alternative experiment would be to conduct the measurements at the poles of the Earth for a period of six months, which presumably averages out several anomalies (effects). The accuracy and precision would be increased if the measurements could be conducted concurrently at both poles over an entire year, presumably to even out most (if not all) extraneous effects.

The so called “Allais effect” was proposed in previous versions (v16 or before) of this work as a potential test for PG verification. However, in a preliminary investigation by Lahres (2023, private communication), there seems to appear no measurable variation of gravity on the Earth’s surface during solar eclipses that could be attributed to a PG effect. That is, there is no variation at least of the order of a few nm/s^2 , but a variation smaller than that should exist according to PG. The intensity of the expected variation is as yet unknown subject to the value of prevailing g_0 and the ultimate accuracy of the employed gravimeters, or whatever methods are used to measure gravity. That means that the previously used average value of gravity variation $g_{Allais} = 3.5E-7 \text{ m/s}^2$ during eclipses taken from Lorenzen (2017) cannot be relied upon either as a source for determining g_0 , or even as an explanation of the reported Allais effect by PG. The Allais effect may be some chance measurement and, therefore, possible explanation for this effect (if real) based on PG is now withdrawn. In addition, Lorenzen attributed it to an “*Anisotropic Dark Flow Acceleration*” from a particular direction of the sky, in which PG has taken no part. Based on preliminary findings by Lahres, we project that g_0 should be $g_0 > 10^7 \text{ m/s}^2$, while any references to the previously tentative (speculative) value of around $g_0 = 4 \times 10^4 \text{ m/s}^2$ should be accordingly adjusted.

Alternatively, it may be that similar measurements taken from the Moon during a solar eclipse by the Earth could provide more reliable values; clearly, in that case, we should derive another equation taking into account the actual solid angles subtended by Earth and the Sun at the Moon (which were assumed to be equal in the previous evaluation for an Allais effect).

In the following subsections, we start by applying PG computations directly to a given body of known real density, which is compared with the expected Newtonian acceleration for the same density. For example, if we start with a small size (less than one meter) steel sphere, PG and Newton accelerations around it are practically equal, while the measured (effective) density is practically equal to the real density. By gradually increasing the size of the body, the PG effect should start appearing as a deviation of the measured acceleration g_{PG} from the calculated Newtonian one g_N . The difference $\Delta g = g_N - g_{PG}$, if verified, could be also used to find the unknown maximum universal acceleration g_0 . However, those measurements involve sizes of bodies, which for all practical purposes would yield very minute differences that might not be easily detected. This may be overcome by involving large bodies, the immediate of which are the Earth, Moon and Sun. The problem is that their densities are unknown for our PG purposes. This problem can be obviated by using various combinations of these three bodies in a shadowing configuration interaction, that should reveal, hopefully, a measurable outcome.

For completeness, we go through the method of “direct” measurement of PG effect first with a single body of known density, followed by the detection of a PG effect involving the Earth, Moon and Sun albeit of unknown real density. Overall, such tests should amount for a relatively minuscule budget and effort in comparison to other ongoing experiments on deciphering gravity.

12.1 Sphere

We can inquire about the difference of acceleration derived by Newton and PG on the surface of a sphere of known density to determine if it is practically possible to detect and measure the new PG parameters directly. If the Newton acceleration on the surface is g_{RN} and the PG acceleration g_R , their difference is given by

$$\Delta g = g_{RN} - g_R = \frac{4}{3}\pi G\rho R - g_0 A_R \quad (117)$$

for which we need k in A_R given from Eq. 65 as

$$k = \frac{\pi G\rho}{g_0} \quad (118)$$

from assumed values of g_0 and the real density of the sphere. We can plot the difference like we plotted the ratio of accelerations in Fig. 5, but we prefer to see directly some numerical outputs in Table 5 by choosing, say steel with $\rho = 7500 \text{ kg/m}^3$.

We may also further work on the equation above to produce:

$$\Delta g = g_0 \left(\frac{4}{3}kR - A_R \right) \quad (119)$$

which is a function of the product kR .

For very high kR , the difference is very high, but for very small kR the difference is very small but finite. By expanding the exponential to a Taylor series $e^x = 1 + x + \frac{x^2}{2!} + \frac{x^3}{3!} + \frac{x^4}{4!}$ and taking the limit for small kR , we obtain for the difference of accelerations

$R=$	10	100	1000	10000	100000
$g_N=$	2.097E-05	2.097E-04	2.097E-03	2.097E-02	2.097E-01
g_0	Δg	Δg	Δg	Δg	Δg
300	8.243E-13	8.243E-11	8.243E-09	8.243E-07	8.243E-05
500	4.946E-13	4.946E-11	4.946E-09	4.946E-07	4.946E-05
1000	2.473E-13	2.473E-11	2.473E-09	2.473E-07	2.473E-05
2000	1.236E-13	1.236E-11	1.236E-09	1.236E-07	1.236E-05
5000	4.946E-14	4.946E-12	4.946E-10	4.946E-08	4.946E-06
10000	2.473E-14	2.473E-12	2.473E-10	2.473E-08	2.473E-06
20000	1.236E-14	1.236E-12	1.236E-10	1.236E-08	1.236E-06
30000	8.243E-15	8.243E-13	8.243E-11	8.243E-09	8.243E-07
50000	4.946E-15	4.946E-13	4.946E-11	4.946E-09	4.946E-07

Table 5: *Difference of acceleration between Newton and PG on the surface of an iron sphere with density 7500 kg/m³ [All units used are in the SI system].*

$$A_{R_{kR \rightarrow 0}} = \frac{1}{6}kR(8 - 6kR + 4k^2R^2) \quad (120)$$

$$\Delta g_{kR \rightarrow 0} = \frac{1}{3}g_0k^2R^2(3 - 2kR)_{kR \rightarrow 0} = g_0k^2R^2 \quad (121)$$

For the numerical example of the table, we see that we could have used Eq. 121 for small kR , which provides that the difference is proportional to g_0 and to the square of the radius of the sphere. The practical outcome is that, for the smallest sphere, we would need an extremely sensitive gravimeter with an accuracy up to 10 orders of magnitude smaller than the expected Newtonian value. The situation improves fast as we increase the sphere diameter, except that such spheres are out of any practical use. The situation improves with decrease of g_0 .

12.2 Cone

We have further investigated whether the same reference spherical masses used above, if reshaped properly, they could yield any improved (i.e. greater) difference between Newton and PG for a possible measurement from a known density mass. This has been investigated for truncated and spherical cones with negative results (i.e. no improvement). However, interestingly enough it was found that there is an optimum cone angle yielding maximum acceleration difference at their apex, but still very close to, (but less than) the spherical shape. There is no need to present these results at present in order to give priority to more mundane issues below.

12.3 Cube

Perhaps, a large steel (or other heavy material) cube shape might be more feasible to construct by bricks, which would reduce cost by later disassembling and re-use of the steel material. The Newtonian gravitational fields has already been provided analytically by Chappel *et al.* (2012). Measurements of some gravity contour (or point) around the cube may be done with the most sensitive gravimeter to investigate possible "anomaly". With a positive outcome, we can then calculate the corresponding PG gravity contour (or point)

by integrating the shading of gravions per established theory. From the known density, we will then be able to directly derive all other PG parameters.

12.4 PG effect: Earth-Moon-Sun interactions

Whereas the preceding investigations concern direct measurements of PG differences (effects) from Newtonian mechanics involving bodies of known real density, below we are considering the use of the three largest bodies nearest to us, namely, the Earth (E), Moon (M) and Sun (S) to achieve the same aim. The direct method of the preceding sections suffers from the difficulty of extremely low values needed to be detected. This is aggravated by the unknown g_0 , which can assume very large values with concomitant even much lower detectable PG effect on the acceleration of those relatively small bodies. This problem could be overcome by involving configurations (combinations) between E, M and S in pairs, or all together. We examine all these possibilities below in order to establish an optimum strategy for detecting the maximum expected PG effect.

However, the initial problem is that their real density is unknown. Nevertheless, we can assume a range of values for g_0 , from which we deduce the corresponding absorption coefficients k that reproduces the given acceleration at the surface of each of the said bodies by Eq. 68. The latter procedure reproduces Newtonian acceleration but by itself makes no progress with any single body towards our objective, unless the said bodies are combined in a way that produce a shadowing of gravions through one or two of them. Then, the strategy is to compute the expected PG acceleration g_{PG} , which subtracted from the corresponding Newton acceleration g_N provides an expected difference $\Delta g = g_N - g_{PG}$ as a function of g_0 . If we can experimentally observe some difference Δg , then we have a first indication of a verification of PG theory, while if we can measure the same with adequate accuracy and precision, we can finally establish the universal maximum acceleration g_0 , and all else follows.

The formulation of PG equations for two spherical bodies has been presented for a general case in the Appendices. They start with integration around some given axis other than the axis joining two spheres. To initially reduce the complexity, we use the common axis when possible. Shapes with other than spherical geometry are left for future investigations until we can first verify PG by the simplest of means. For this purpose, we consider E, M and S to be spherical and uniform with radii and masses (or accelerations) given in Table 3. While in reality they are not exactly spherical, we assume that the deviation applied to both theories would have a second order difference.

We apply the two and three body superposition equations previously developed. Care must be taken to involve the correct chords along which the gravions are absorbed, as they pass through each body. During solar and lunar eclipses we have gravion shadowing, but we also have it at all times as the Earth rotates around its axis relative to the Sun and/or Moon.

With reference to Fig. 14, the elementary cone of the left hand side may belong to Earth, followed by the Moon and Sun to right hand side. The Earth absorption factor $\exp(-k_{AE}AE)$ plays a critical role in the expected outcomes. It depends on the actual path that the gravions traverse as the Earth rotates. The altitude of the Sun (or eclipse) and the rotation of the Earth result in a variable chord position and length, along which the gravions pass. This means that, in reality, they experience also a variable absorption coefficient k_{AE} . The gravion traces along changing chords through the Earth can contribute to the anomalous variations of g measurements with sensitive gravimeters (after known variations are subtracted). These variations can be exaggerated, if the chord trace moves between significant density changes from the core to the crust. By way of notation, the absorption coefficient k_{AE_S} is in relation to the Sun and is a function of the Earth chord AE_S in the direction of the Sun given by its altitude α_S and azimuth γ_S . At the same time, it is a function of the location of the gravimeter on the Earth surface given by its latitude ϕ and longitude λ . Thus, the absorption function is a complex function like:

$$k_{AE_S} = k_{AE_S} (AE_S (\alpha_S, \gamma_S, \phi, \lambda))$$

where the subscript S indicates variables in connection with the Sun's direction. The corresponding absorption function in relation to the Moon's direction is then given by:

$$k_{AE_M} = k_{AE_M} (AE_M (\alpha_M, \gamma_M, \phi, \lambda))$$

The form of each of the above functions depends on the material density distribution along the Earth chord. Therefore, we expect a variable value of each absorption coefficient during the apparent motion of the Sun, Moon and rotation of the Earth. The gravions may be thought of as a ray, like an X-ray penetrating a given material. With appropriate analysis and experimental arrangements, we might be able in the future to diagnose the materials along any given chord of the Earth that can be aligned with the Sun, or the Moon. The convolution/deconvolution of the combined variations due to length and material density would require

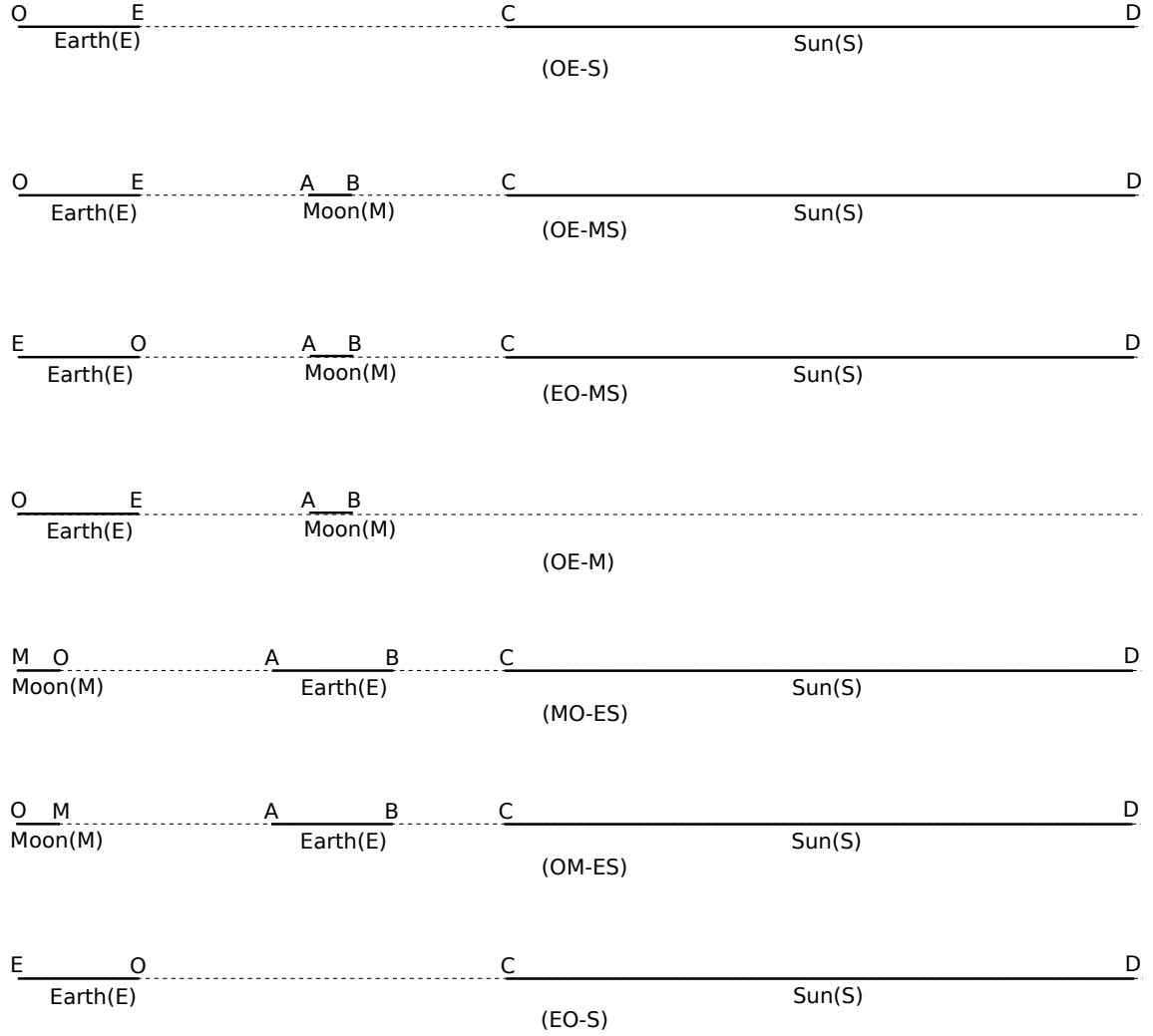


Figure 15: *PG effect: Relative positions of Earth, Moon and Sun providing various cases for investigation*

an appropriate analysis. This is not practical or desirable to achieve at this early stage, before we have even confirmed the principle of PG theory. However, we can assume a uniform density, on which we can base our equations for a hopefully initial verification work. This would be a first order effect, albeit small, at which we first aim, while variations are of second order intensity and might be the object of high resolution recordings.

Now, the immediate task is not to write down the complete PG equations governing the motion of the three bodies but to give priority to an easiest test that can presumably reveal a PG effect at its best. The latter would appear as an “anomaly” to the Newtonian solutions in a test that maximizes the anomaly. The maximum graviton absorption occurs along the diameter of the Earth, hence it would be best to carry out measurements at some appropriate location, like on the equator at midnight during an equinox. Equivalent measurements may also be achieved with an overhead Sun at midnight/midday twice a year at locations with latitudes less than 23.4 degrees. This approach will become clear in the following Sections, whereby we have found significant outcomes being sufficient to plan and organize a strategy for testing.

The superposition principle diagrams of Figs. 13 and 14 are now shown by simpler sketches in Fig. 15. It is not practical to draw the sizes and distances of these specific cases on a linear scale, but we only represent the elementary solid angle to be integrated over by a dotted line and the chords (or diameters) by solid line segments: The line segment $OE = \ell_E$ for Earth, $CD = \ell_S$ for the Sun and $AB = MO = \ell_m$ for the Moon together with the distances among them are all drawn out of proportion. We prefer that the line segments include also the diameters of the respective bodies, even if this is not likely (frequent, or possible?) to occur with every configuration provided, like a solar eclipse at the equator during an equinox at midnight/midday. The idea is to consider theoretically all these configurations that will enable us to discard the unnecessary or rare cases in order to determine the best strategy for the purpose of PG verification.

12.4.1 Midnight Earth-Sun interaction (OE-S)

This case is depicted in Fig. 15(OE-S), where the point of measurement is at the antipode O of Earth (E) relative to the Sun (S), while the presence of the Moon is ignored.

We set up one (first) differential equation to be integrated in the range $0 \leq \varphi \leq \varphi_S$, where $\sin \varphi_S = \frac{R_S}{r_S} = a_S$ with R_S and r_S being the radius and the distance of the Sun from the point of measurement. The usual acceleration factor f_{g1n} in this first range is:

$$f_{g1n} = \int_0^{\varphi_S} 2\pi \sin \varphi \cos \varphi d\varphi \cdot [1 - \exp(-k_E \ell_E(\varphi) - k_S \ell_S(\varphi))]$$

where we have added the combined contribution of the Earth and Sun in the sum of the exponent. The corresponding absorption coefficients are k_E and k_S . The chord lengths are found from the radius and distance by equations given at the outset, and the above becomes:

$$f_{g1n} = \int_0^{\varphi_S} 2\pi \sin \varphi \cos \varphi d\varphi \cdot \left[1 - \exp \left(-2k_E r_E \sqrt{a_E^2 - \sin^2 \varphi} - 2k_S r_S \sqrt{a_S^2 - \sin^2 \varphi} \right) \right]$$

Care is taken to set the Sun's distance as $r_S = r_{S-tabled} + R_E$, where we use values provided in Table 3. With $a_E = \sin \varphi_E = \frac{R_E}{r_E} = 1$, since the distance $r_E = R_E$ on the surface of Earth, the above becomes:

$$f_{g1n} = \int_0^{\varphi_S} 2\pi \sin \varphi \cos \varphi d\varphi \cdot \left[1 - \exp \left(-2k_E R_E \sqrt{1 - \sin^2 \varphi} - 2k_S r_S \sqrt{a_S^2 - \sin^2 \varphi} \right) \right]$$

We continue the integration for the contribution from Earth without the Sun in the remaining angle range $\varphi_S \leq \varphi \leq \pi/2$ radians by adding the factor:

$$f_{g2n} = \int_{\varphi_S}^{\pi/2} 2\pi \sin \varphi \cos \varphi d\varphi \cdot \left[1 - \exp \left(-2k_E R_E \sqrt{1 - \sin^2 \varphi} \right) \right]$$

which is given by an analytical expression:

$$f_{g2d}/\pi = 1 - \frac{1}{2k_E^2 R_E^2} - \sin^2 \varphi_S + \frac{\exp \left(-2k_E R_E \sqrt{1 - \sin^2 \varphi_S} \right) \left(2k_E R_E \sqrt{1 - \sin^2 \varphi_S} + 1 \right)}{2k_E^2 R_E^2} \quad (122)$$

We use numerical means to integrate for f_{g1n} , which is added to the result by the analytical expression for the second term f_{g2n} . The analytical expressions, where available, provide unlimited precision by the Python program used, whereas the numerical integration precision is limited by the provided integrator script in the program.

In terms of acceleration, we have a PG acceleration g_{PG} for the combined interaction between Earth-Sun:

$$g_{PG} = g_0 (f_{g1n} + f_{g2n}) / \pi$$

The Newtonian acceleration g_N at the same location is found by adding the Sun's g_{Nr_S} to the Earth's g_{NR_E} acceleration:

$$g_N = g_{NR_E} + g_{Nr_S} = g_{NR_E} + g_{NR_S} \frac{R_S^2}{r_S^2}$$

where g_{NR_S} is a given acceleration on the surface of the Sun from Table 3 (or computed from its mass provided).

We finally compute the PG effect by the difference of accelerations between the two theories:

$$\Delta g = g_N - g_{PG}$$

as a function of g_0 in an arbitrary range of values, as was similarly done in prior examples. We follow the rule that the positive sense is in the direction towards the center of the Earth. For this case, the above effect (difference) is positive. We plot the result in Fig. 16($1 * Me, 1 * Ms$) on logarithmic scales. The effect of

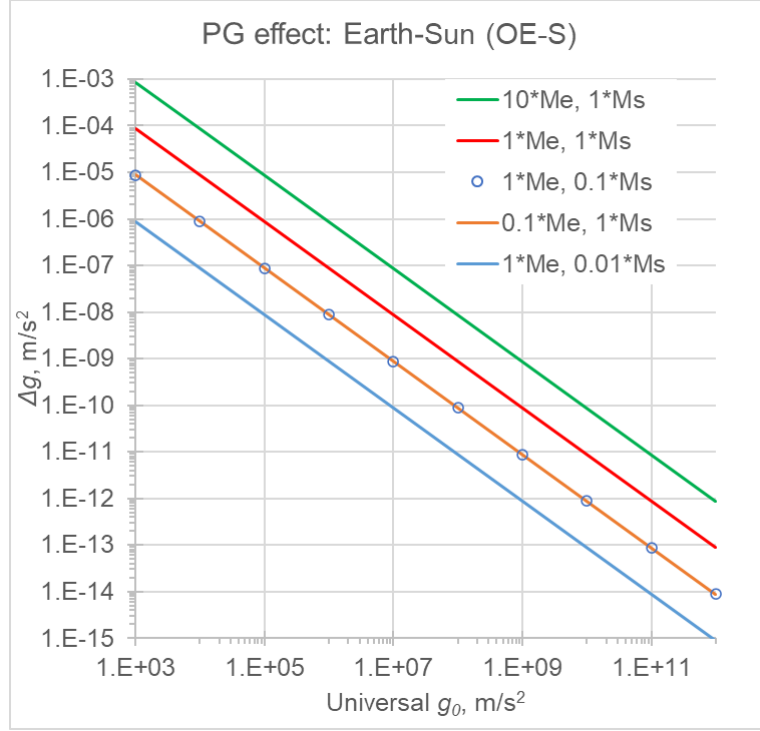


Figure 16: *PG effect: Earth-Sun (OE-S) with different densities*

Δg is practically inversely proportional to g_0 on these scales, but the relationship is not exactly hyperbolic as will be analyzed later. There are subtle changes in the exponential terms of the equations, which are not immediately obvious, while the effects may often appear counter-intuitive. It is helpful to use graphical means to obtain some immediate impressions. In the same figure, we vary the density of the Earth and the Sun by some orders of magnitude keeping all other parameters constant, in order to theorize the trend of the change in the outcome. The initial unitary masses of M and S are multiplied by factors of 10, 0.1 and 0.01 as shown with the plotted lines. We note that the PG effect changes by about the same factor in all cases. This information will assist us in selecting an appropriate configuration among those presented.

12.4.2 Midnight Earth-new_Moon interaction without Sun (OE-M)

For purposes of comparison, we consider a hypothetical case involving the Moon alone (without the Sun) at the same location and time as the preceding case involving the Sun. This is to quickly establish the theoretical order of magnitude between the two cases. With reference to Fig. 15(OE-M), we apply the same equations as previously, by simply replacing the Sun's parameters with those of the Moon:

$$f_{g1n} = \int_0^{\varphi_S} 2\pi \sin \varphi \cos \varphi d\varphi \cdot \left[1 - \exp \left(-2k_E R_E \sqrt{1 - \sin^2 \varphi} - 2k_M r_M \sqrt{a_M^2 - \sin^2 \varphi} \right) \right] \quad (123)$$

where the Moon's distance is $r_M = r_{M-tabled} + R_E$ and $\sin \varphi_M = \frac{R_M}{r_M} = a_M$.

We continue again the integration for the contribution from Earth without the Moon in the remaining angle range $\varphi_M \leq \varphi \leq \pi/2$ radians by adding the factor:

$$f_{g2n} = \int_{\varphi_M}^{\pi/2} 2\pi \sin \varphi \cos \varphi d\varphi \cdot \left[1 - \exp \left(-2k_E R_E \sqrt{1 - \sin^2 \varphi} \right) \right] \quad (124)$$

In the same way, we finally plot the effect Δg in Fig. 17(OE-M). We juxtapose this with the previous one (OE-S) transferred in the same figure, where we also add the outcomes from other following configurations.

We note that the difference of the effect between Sun and Moon taken separately is more than two orders of magnitude. In both cases, the effect should appear as a lowering of the acceleration below the level of Newton acceleration. If all Newtonian effects (due to tides, etc.) are subtracted from recorded data to

establish a zero reference level, then PG effect should appear as a broad trough (negative) between sunset and sunrise over a 24 hour recording of acceleration.

Note: The integration for the second factor f_{g2n} results in an analytical expression (as previously), which was used in plotting the line (OE-M). Instead, when we use the available Python integrator in the second range, we gradually lose precision with increasing g_0 , becoming quite significant as seen by the points of curve (OE-M integrator); the deviation becomes visible for $g_0 > 10^{11}$ m/s². We can set arbitrary precision with all other mathematical functions, except for the provided integrator, which seems to create a “bottleneck” in our precision. In future work, a special integrator can be developed to cater for higher precision when needed.

12.4.3 Earth-Moon-Sun, solar eclipse at midnight (OE-MS)

We follow with the configuration of Fig. 15(OE-MS) denoting a solar eclipse on the equator during an equinox at midnight. This configuration may be hypothetical, or extremely unusual to take place, but it provides a useful comparison in our study. The three bodies (E, M, S) are aligned all on the same side of the measuring station at O. With the Moon added to the preceding case of OE-S, we follow the usual sequence of equations in three ranges of integration. By adopting the values for the Moon and Sun again from Table 3, the Moon subtends a slightly smaller solid angle than the Sun resulting in a small intermediate range of integration $\varphi_M \leq \varphi \leq \varphi_S$. Thus we have:

$$f_{g1n} = \int_0^{\varphi_M} 2\pi \sin \varphi \cos \varphi d\varphi \cdot \left[1 - \exp \left(-2k_E R_E \sqrt{1 - \sin^2 \varphi} - 2k_M r_M \sqrt{a_M^2 - \sin^2 \varphi} - 2k_S r_S \sqrt{a_S^2 - \sin^2 \varphi} \right) \right]$$

$$f_{g2n} = \int_{\varphi_M}^{\varphi_S} 2\pi \sin \varphi \cos \varphi d\varphi \cdot \left[1 - \exp \left(-2k_E R_E \sqrt{1 - \sin^2 \varphi} - 2k_S r_S \sqrt{a_S^2 - \sin^2 \varphi} \right) \right]$$

For the last (third) range of integration $\varphi_S \leq \varphi \leq \pi/2$ radians, the Earth alone adds the factor:

$$f_{g3n} = \int_{\varphi_S}^{\pi/2} 2\pi \sin \varphi \cos \varphi d\varphi \cdot \left[1 - \exp \left(-2k_E R_E \sqrt{1 - \sin^2 \varphi} \right) \right]$$

The total PG acceleration is:

$$g_{PG} = g_0 (f_{g1n} + f_{g2n} + f_{g3n}) / \pi$$

Newton acceleration is:

$$g_N = g_{NR_E} + g_{Nr_M} + g_{Nr_S} = g_{NR_E} + g_{NR_M} \frac{R_M^2}{r_M^2} + g_{NR_S} \frac{R_S^2}{r_S^2}$$

The effect $\Delta g = g_N - g_{PG}$ is plotted in Fig. 17(OE-MS). The graph lies slightly but clearly above that of (OE-S).

12.4.4 Solar eclipse at midday (EO-MS)

This is a complementary calculation of the same event as the previous one, except that we measure at the antipode during midday. Albeit a theoretical case, it is useful again for comparison of magnitudes of PG effect. The corresponding equations then become:

$$f_{g1n} = \int_0^{\varphi_M} 2\pi \sin \varphi \cos \varphi d\varphi \cdot \left[\exp \left(-2k_M r_M \sqrt{a_M^2 - \sin^2 \varphi} - 2k_S r_S \sqrt{a_S^2 - \sin^2 \varphi} \right) - \exp \left(-2k_E R_E \sqrt{1 - \sin^2 \varphi} \right) \right]$$

with the Moon still subtending a smaller angle than the Sun. For the middle range, we get the second factor:

$$f_{g2n} = \int_{\varphi_M}^{\varphi_S} 2\pi \sin \varphi \cos \varphi d\varphi \cdot \left[\exp \left(-2k_S r_S \sqrt{a_S^2 - \sin^2 \varphi} \right) - \exp \left(-2k_E R_E \sqrt{1 - \sin^2 \varphi} \right) \right]$$

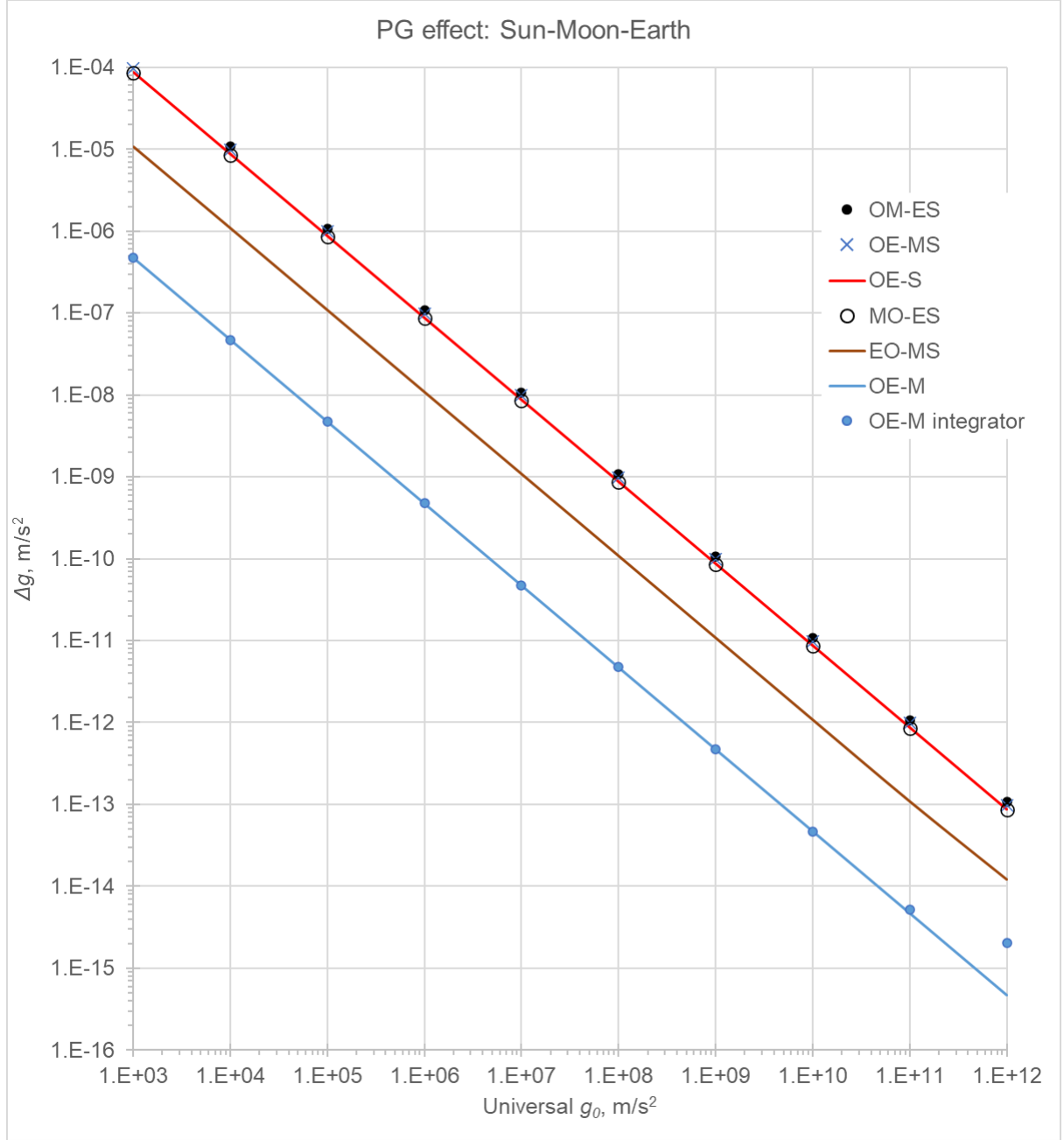


Figure 17: *PG effect by various combinations of Earth (S), Moon (M) and Sun (S) by plotting the Δg deviation from Newton vs. assumed universal acceleration g_0*

and for the third range:

$$f_{g3n} = \int_{\varphi_S}^{\pi/2} 2\pi \sin \varphi \cos \varphi d\varphi \cdot \left[1 - \exp \left(-2k_E R_E \sqrt{1 - \sin^2 \varphi} \right) \right]$$

The PG acceleration is the sum:

$$g_{PG} = g_0 (f_{g1n} + f_{g2n} + f_{g3n}) / \pi$$

The Newtonian acceleration g_N :

$$g_N = g_{NR_E} - g_{Nr_M} - g_{Nr_S} = g_{NR_E} - g_{NR_M} \frac{R_M^2}{r_M^2} - g_{NR_S} \frac{R_S^2}{r_S^2}$$

Now, the difference of accelerations $\Delta g = g_N - g_{PG}$ is found to be negative. This means that Newtonian pull by the combined M+S in series during the eclipse is greater than their PG pull. This is also what the superposition principle in Fig. 13 leads us to expect. If the total Newtonian acceleration recording is used as base line (zero reference), then we should see a peak of acceleration during a solar eclipse at daytime, appearing as an unexpected anomaly by conventional physics. For comparison purposes here, we are interested in the absolute difference of this PG effect ($|\Delta g|$), which we plot in Fig. 17(EO-MS). The graph is clearly one order of magnitude below the preceding graph of the same event at the antipode of the Earth (midnight).

12.4.5 Solar eclipse interaction on the Moon day side (MO-ES)

The previous outcomes have prompted us to consider also what would be the measurements on the surface of the Moon during a solar eclipse caused by a transiting Earth between Sun and Moon. First, we consider the case of this event being measured on the day-side (visible) of the Moon according to the sketch in Fig. 15(MO-ES). We follow the same sequence as in the preceding case simply changing the corresponding parameters and ranges of integration. Thus we have::

$$f_{g1d} = \int_0^{\varphi_S} 2\pi \sin \varphi \cos \varphi d\varphi \cdot \left[\exp \left(-2k_E r_E \sqrt{a_E^2 - \sin^2 \varphi} - 2k_S r_S \sqrt{a_S^2 - \sin^2 \varphi} \right) - \exp \left(-2k_M R_M \sqrt{1 - \sin^2 \varphi} \right) \right]$$

in the first angle. We continue in the angle $\varphi_S \rightarrow \varphi_E$

$$f_{g2d} = \int_{\varphi_S}^{\varphi_E} 2\pi \sin \varphi \cos \varphi d\varphi \cdot \left[\exp \left(-2k_E r_E \sqrt{a_E^2 - \sin^2 \varphi} \right) - \exp \left(-2k_M R_M \sqrt{1 - \sin^2 \varphi} \right) \right]$$

and finally the third factor being the contribution by the Moon alone in the remaining angle:

$$f_{g3d} = \int_{\varphi_E}^{\pi/2} 2\pi \sin \varphi \cos \varphi d\varphi \cdot \left[1 - \exp \left(-2k_M R_M \sqrt{1 - \sin^2 \varphi} \right) \right]$$

The PG acceleration is as usually:

$$g_{PG} = g_0 (f_{g1d} + f_{g2d} + f_{g3d}) / \pi$$

The Newtonian acceleration g_N :

$$g_N = g_{NR_M} - g_{Nr_E} - g_{Nr_S} = g_{NR_M} - g_{NR_E} \frac{R_E^2}{r_E^2} - g_{NR_S} \frac{R_S^2}{r_S^2}$$

and the absolute value of the difference Δg is plotted in Fig. 17(MO-ES). Here again, the difference is negative for the same reason as on Earth daytime, but we plot the logarithm of the absolute value $|\Delta g|$ for comparison.

12.4.6 Moon Earth Sun, solar eclipse on invisible side (OM-ES)

Our investigation continues by monitoring the previous solar eclipse on the other (antipode) invisible side of the Moon, as shown by the diagram in Fig. 15(OM-ES). As all three bodies (M, E, S) are practically aligned on the same side of the measuring station at O, we sum their contribution in the exponent of the first range:

$$f_{g1n} = \int_0^{\varphi_S} 2\pi \sin \varphi \cos \varphi d\varphi \cdot \left[1 - \exp \left(-2k_M R_M \sqrt{1 - \sin^2 \varphi} - 2k_E r_E \sqrt{a_E^2 - \sin^2 \varphi} - 2k_S r_S \sqrt{a_S^2 - \sin^2 \varphi} \right) \right]$$

leaving out the Sun in the second range $\varphi_S \leq \varphi \leq \varphi_E$:

$$f_{g2n} = \int_{\varphi_S}^{\varphi_E} 2\pi \sin \varphi \cos \varphi d\varphi \cdot \left[1 - \exp \left(-2k_M R_M \sqrt{1 - \sin^2 \varphi} - 2k_E r_E \sqrt{a_E^2 - \sin^2 \varphi} \right) \right]$$

with the Moon acting alone in the third range:

$$f_{g3n} = \int_{\varphi_E}^{\pi/2} 2\pi \sin \varphi \cos \varphi d\varphi \cdot \left[1 - \exp \left(-2k_M R_M \sqrt{1 - \sin^2 \varphi} \right) \right]$$

and finally

$$g_{PG} = g_0 (f_{g1n} + f_{g2n} + f_{g3n}) / \pi$$

$$g_N = g_{NR_M} + g_{Nr_E} + g_{Nr_S} = g_{NR_M} + g_{NR_E} \frac{R_E^2}{r_E^2} + g_{NR_S} \frac{R_S^2}{r_S^2}$$

The effect of Δg is plotted in Fig. 17(OM-ES) and is located above all other graphs.

12.4.7 Earth-Sun midday equations (EO-S)

The last configuration in Fig. 15(EO-S) is also considered below. We set up the first integration in the range $0 \leq \varphi \leq \varphi_S$ to find f_{g1d} :

$$f_{g1d} = \int_0^{\varphi_S} 2\pi \sin \varphi \cos \varphi d\varphi \cdot \left[\exp \left(-2k_S r_S \sqrt{a_S^2 - \sin^2 \varphi} \right) - \exp \left(-2k_E R_E \sqrt{1 - \sin^2 \varphi} \right) \right]$$

That is followed by the second integration in the remaining angle:

$$f_{g2d} = \int_{\varphi_S}^{\pi/2} 2\pi \sin \varphi \cos \varphi d\varphi \cdot \left[1 - \exp \left(-2k_E R_E \sqrt{1 - \sin^2 \varphi} \right) \right]$$

Both of the above factors result in analytical expressions and after cancellations we obtain (also adding $-1 + 1$ in the first):

$$\begin{aligned} f_{g1d} &= \int_0^{\varphi_S} 2\pi \sin \varphi \cos \varphi d\varphi \cdot \left[\exp \left(-2k_S r_S \sqrt{a_S^2 - \sin^2 \varphi} \right) - 1 + 1 - \exp \left(-2k_E r_E \sqrt{a_E^2 - \sin^2 \varphi} \right) \right] \\ &= -\frac{\pi A_S}{r_S^2} + \int_0^{\varphi_S} 2\pi \sin \varphi \cos \varphi d\varphi \cdot \left[1 - \exp \left(-2k_E r_E \sqrt{a_E^2 - \sin^2 \varphi} \right) \right] \\ f_{g1d} + f_{g2d} &= -\frac{\pi A_S}{r_S^2} + \int_0^{\pi/2} 2\pi \sin \varphi \cos \varphi d\varphi \cdot \left[1 - \exp \left(-2k_E r_E \sqrt{a_E^2 - \sin^2 \varphi} \right) \right] \\ f_{g1d} + f_{g2d} &= -\frac{\pi A_S}{r_S^2} + \frac{\pi A_E}{r_E^2} \end{aligned}$$

m/s^2	$\Delta g, m/s^2$					
g_0	OE-M	EO-MS	MO-ES	OE-S	OE-MS	OM-ES
1.E+03	4.7218E-07	1.0585E-05	8.5380E-05	8.7206E-05	9.7682E-05	1.0654E-04
1.E+04	4.7296E-08	1.0709E-06	8.5550E-06	8.7352E-06	9.8105E-06	1.0691E-05
1.E+05	4.7304E-09	1.0720E-07	8.5566E-07	8.7366E-07	9.8146E-07	1.0695E-06
1.E+06	4.7305E-10	1.0721E-08	8.5568E-08	8.7367E-08	9.8150E-08	1.0695E-07
1.E+07	4.7305E-11	1.0721E-09	8.5568E-09	8.7368E-09	9.8151E-09	1.0695E-08
1.E+08	4.7305E-12	1.0721E-10	8.5568E-10	8.7368E-10	9.8151E-10	1.0695E-09
1.E+09	4.7305E-13	1.0722E-11	8.5568E-11	8.7368E-11	9.8150E-11	1.0695E-10
1.E+10	4.7305E-14	1.0717E-12	8.5565E-12	8.7368E-12	9.8153E-12	1.0695E-11
1.E+11	4.7306E-15	1.0800E-13	8.5562E-13	8.7368E-13	9.8098E-13	1.0701E-12
1.E+12	4.7310E-16	1.2032E-14	8.5347E-14	8.7369E-14	9.7902E-14	1.0727E-13

Table 6: *Comparative PG effect*

In terms of acceleration, we have a PG acceleration g_{PG} for the combined interaction between Earth-Sun:

$$g_{PG} = g_0 (f_{g1d} + f_{g2d}) / \pi$$

We can readily recognize that the above reverts back to the Newtonian acceleration according to Eqs. 44 and 66:

$$g_0 \left(\frac{\pi A_E}{r_E^2} - \frac{\pi A_S}{r_S^2} \right) = g_{NR_E} - g_{NR_S} = g_N$$

That is, the PG effect is zero by $g_N - g_{PG} = \Delta g = 0$. This may appear a tautology or trivial, but it is important. We should expect a mutual shadowing by each of the two bodies and the null outcome is not obvious or intuitive. This is further analyzed by integrating over the entire bulk of the two bodies as is done later in Section 16. The problem lies in understanding the meaning of mass as it is used by Newton. To avoid duplication, the reader is referred to the subsequent development of the theory through to the mass-matter relationships in Section 24. For the present purposes, it is sufficient to know that this configuration does not produce the desired PG effect for measurement. Actually, it would and should produce a clear PG effect, if we knew and used the actual (real) densities for E, M and S in Newton acceleration. In the latter case, the Newtonian acceleration would be clearly above the PG acceleration (as we have shown in Table 5); the null result here is artificially forced in matching the surface acceleration with PG derivation as long as g_0 remains unknown.

The other cases are further analyzed and discussed below.

12.4.8 Analysis

From the summary of results in Fig. 17, we can immediately discard for our purposes the component of Moon effect acting alone (OE-M), or in combination during the day solar eclipse (EO-MS), both being well below the other graphs; the latter is also an unlikely (rare, if possible?) event happening on the equator during an equinox. Even the same solar eclipse at midnight (OE-MS) is only a little above the Sun acting alone. Therefore, the simple configuration (OE-S) of Sun alone seems the best practical (sufficient for now) option for terrestrial measurements of the PG effect.

These results can be viewed also numerically in Table 6. The simple configuration of OE-S is typed in bold-face font for reference and comparison. We see the small improvement with OE-MS, at least for theoretical purposes, over the simpler case of OE-S. More importantly, lunar measurements (i.e. on the Moon) are comparable with OE-S: They show a little lower value on the visible side with an improved (higher) and promising value on the invisible side of the Moon.

Our strategy then can be to organize and setup first terrestrial measurements at the equator on a 24 hour (or more) basis around equinoxes. We may like to increase the amount of data by setting up a series of measuring stations along the equator to obtain an average over, say, 2-3 days. The preferred equator

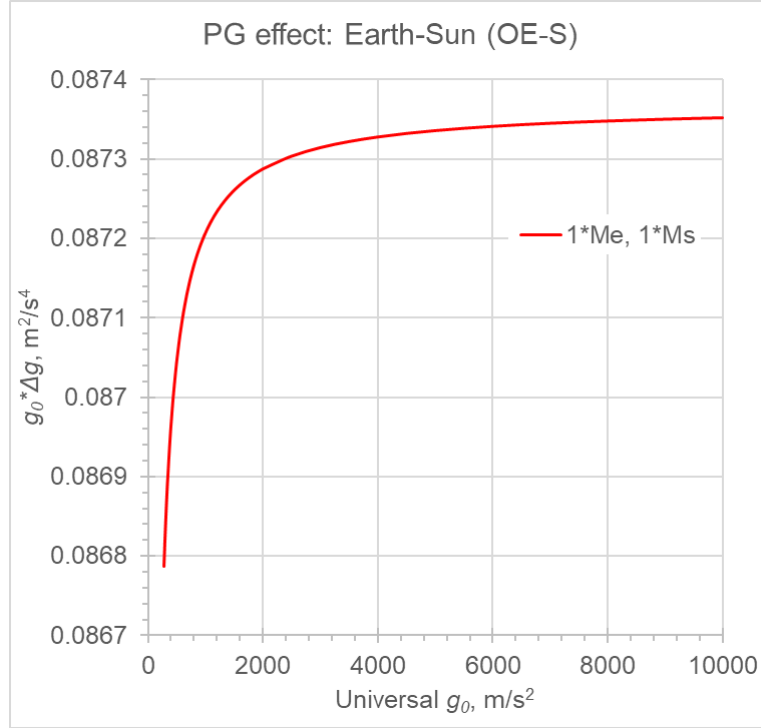


Figure 18: *Product $g_0 \cdot \Delta g$*

m/s^2	$g_0 \cdot \Delta g, m^2/s^4$					
g_0	OE-M	EO-MS	MO-ES	OE-S	OE-MS	OM-ES
1.E+03	4.721781E-04	1.058540E-02	8.537969E-02	8.720626E-02	9.768211E-02	1.065446E-01
1.E+04	4.729648E-04	1.070948E-02	8.554967E-02	8.735156E-02	9.810549E-02	1.069100E-01
1.E+05	4.730432E-04	1.072027E-02	8.556619E-02	8.736604E-02	9.814613E-02	1.069461E-01
1.E+06	4.730511E-04	1.072133E-02	8.556784E-02	8.736749E-02	9.815018E-02	1.069497E-01
1.E+07	4.730519E-04	1.072142E-02	8.556801E-02	8.736764E-02	9.815059E-02	1.069500E-01
1.E+08	4.730519E-04	1.072139E-02	8.556800E-02	8.736765E-02	9.815054E-02	1.069500E-01
1.E+09	4.730521E-04	1.072197E-02	8.556803E-02	8.736765E-02	9.815030E-02	1.069499E-01
1.E+10	4.730506E-04	1.071663E-02	8.556476E-02	8.736769E-02	9.815271E-02	1.069495E-01
1.E+11	4.730556E-04	1.079979E-02	8.556185E-02	8.736761E-02	9.809818E-02	1.070122E-01
1.E+12	4.731044E-04	1.203205E-02	8.534696E-02	8.736914E-02	9.790189E-02	1.072729E-01

Table 7: *Comparative product $g_0 \cdot \Delta g$*

location may be chosen to have minimal local anomalies of acceleration due to nearby mountains, uneven crust density and mineral deposits distribution, tides, etc., as much as it is possible to know in advance or by a specialized study. Perhaps, a location in the middle of an ocean might present optimum or predictable results, but all these factors can be considered in advance of a carefully planned experiment. Furthermore, we may need to reconsider lesser Newtonian corrections already applied to compensate for atmospheric pressure, temperature variations and other local (suspected or real) variations that might compete against a consistent PG effect. Those corrections may allow adjustments, should they have been exaggerated by Newtonian considerations for some reason (e.g. to incorrectly compensate for an anomaly, like a PG effect).

With a single station (or preferably more), we may also collect data at the equator during an entire year with a variable Sun altitude between two consecutive equinoxes. That would be useful if we aim at obtaining more precise determination of g_0 , which would also require to include the variable altitude of the Sun in the corresponding PG derivations. That is, the factors f_{g1n} can be found by integrating in the first range $0 \leq \varphi \leq \varphi_S$, where φ_S and zenith angle ($\theta - \text{altitude}$) are functionally interconnected in the formulation. The latter formulation has been presented for a general case in Appendix B (see Fig. 114). In the meantime, we should first ascertain the presence of a PG effect by the simpler approach of equatorial equinox observations of the Sun.

Equivalent measurements can also be taken at locations with latitudes less than 23.4 degrees with an overhead Sun at midnight/midday occurring twice a year. The restriction of “equator during equinoxes” is used only for a more accurate theoretical description of the required events that may include (or not) the likelihood of eclipses; also the equator position might facilitate by symmetry better averages throughout the year in both PG measurements and Newtonian corrections. In any event and for practical purposes, the strategy should include also all stations within latitudes of $\pm 23.4^\circ$ already in operation that can contribute to our requirements.

Several of the above difficulties may be overcome by corresponding measurements on the Moon. Atmospheric pressure is eliminated, whilst temperature and Moon “tidal” (deformation) effects are minimized, if not practically ignored; Earth’s tides should have a second order effect from a distance. Concurrent measurements on both the visible and invisible side of the Moon could provide useful data for subsequent analysis.

For further theoretical interest, we also analyze the graphs of Fig. 17: The lines appear to be straight on logarithmic scales, but this is not exactly so. If we plot the product $g_0 \cdot \Delta g$, we find it to be a nearly constant but with a small variation per Fig. 18 in the range of g_0 provided. Thus the relationship between g_0 and Δg is nearly hyperbolic, but with a slightly increasing “constant” as a function of g_0 . This “constant” changes sharply when g_0 approaches very close to the surface acceleration of the Sun (274.8252 m/s^2), which is the maximum acceleration in the two body system of Earth-Sun. That means that the Sun becomes a black hole as the assumed g_0 approaches the highest (Sun) acceleration of this two-body system. This is noted for later theoretical considerations, because this is what we should expect to happen in the case of actual black holes being present.

In the meantime, we understand the situation for near-Newtonian bodies (E, M, S) used to establish an expected PG effect. For practical effect, we provide the product $g_0 \cdot \Delta g$ also in numerical form in Table 7 in the same range as the graphs. The values tend to a constant at the highest g_0 as the bodies become more Newtonian. The exception in the last few rows of the table where the deviation from the constant seems to be an artifact of the precision allowed by the Python integrator used, as was shown in Fig. 17(OE-M integrator); this does not affect the substance of our findings, while the issue can be addressed later as needed by an improved computational integrator.

For understanding the PG effect and its possible significance, it is distinct from other gravitational effects. For example, the Moon gravitational effect on Earth may be significant in some aspects like tidal effects, but the Moon-PG effect can be overshadowed by the Sun-PG effect, as we have seen. The specific PG effect analyzed here is a novel concept that may present itself as an “anomaly” to current theories of gravity. There are other examples of known “anomalies” that may be possible to explain via PG, as mentioned elsewhere in this report.

12.4.9 Planets

It is found useful to extend the preceding analysis by considering also the intensity of PG effect that we should experience on the surface of other planets, for comparison. For now, we only need to see the trend of this effect; we choose Jupiter as being massive, Venus being similar to Earth but closer to the Sun, and Mercury being closest to the Sun and with a high eccentricity. For each one of them, we only take the case of measuring the effect on the “midnight” side relative to the Sun (only) and utilize the same convention for notation of each configuration. Thus, we use OX-S for each case, where X is the initial letter of the planet. For now only, we replace the Roman name of Mercury with the Greek one being Hermes, like OH-S in order

m/s^2	$\Delta g, m/s^2$						
g_0	OJ-S	OV-S	OH1-S	OH2-S	OJs-S	OEs-S	<OEs-S
1.E+03	8.4838E-06	1.5057E-04	3.3337E-04	1.5030E-04	9.7230E-05	8.7206E-05	6.3552E-05
1.E+04	8.5214E-07	1.5080E-05	3.3358E-05	1.5039E-05	1.0355E-05	8.7351E-06	6.4266E-06
1.E+05	8.5251E-08	1.5082E-06	3.3360E-06	1.5040E-06	1.0411E-06	8.7366E-07	6.4329E-07
1.E+06	8.5255E-09	1.5082E-07	3.3361E-07	1.5040E-07	1.0417E-07	8.7367E-08	6.4335E-08
1.E+07	8.5255E-10	1.5082E-08	3.3361E-08	1.5040E-08	1.0417E-08	8.7367E-09	6.4336E-09
1.E+08	8.5256E-11	1.5082E-09	3.3361E-09	1.5040E-09	1.0417E-09	8.7366E-10	6.4336E-10
1.E+09	8.5256E-12	1.5082E-10	3.3361E-10	1.5040E-10	1.0416E-10	8.7371E-11	6.4336E-11
1.E+10	8.5256E-13	1.5082E-11	3.3361E-11	1.5040E-11	1.0402E-11	8.7334E-12	6.4336E-12
1.E+11	8.5255E-14	1.5082E-12	3.3361E-12	1.5041E-12	1.0510E-12	8.6178E-13	6.4337E-13
1.E+12	8.5256E-15	1.5082E-13	3.3357E-13	1.5034E-13	9.5264E-14	9.0824E-14	6.4334E-14

Table 8: *Comparative PG effect for planets and satellites*

to avoid mixing it with Moon(M). In addition, we investigate separately the shortest distance of Hermes by setting $r_S \equiv r_{H1S} = 47000000000.0$ m at its perihelion and the longest distance $r_S \equiv r_{H2S} = 70000000000.0$ m at the aphelion. The results for Δg are presented in Table 8 and for the product $g_0 \cdot \Delta g$ in Table 9.

We note that Jupiter yields one order of magnitude less Δg than Earth, despite being very massive. This is understood to be due to it having a lower overall density being gaseous for its most part, while having a dense core with much smaller radius. We have already attempted to see the PG change in acceleration of Jupiter with a two phase density model in Section 10. Similarly, we can see what happens to the PG effect, if all its mass were to be concentrated in its core in the next section. Here, we note that Δg is much greater for Venus than for Earth, although it is about the same size and mass as Earth; The fact of being closer to the Sun imparts a significant increase to the effect that would help in its measurement by a satellite around it. The situation is more striking with Mercury (Hermes). The PG effect is about two orders of magnitude greater than with Earth. Furthermore, the orbital position has a significant effect too.

The above differentials in PG effect among all cases are also important: First, there is a differential of this effect between antipodes on every planet. This means that there is a differential acceleration, albeit very small, imparting both a deformation on the planet and a deviation from the predicted Newtonian orbit that should be seen as an anomaly. The first should be compounded with the tidal effects and the second with the planet's precession. Both effects are maximized with the innermost planets and in particular with Mercury. We therefore propose to keep an open mind about PG taking part in (contributing to) those long discussed, analyzed and debated physical phenomena of Mercury.

12.4.10 Satellites

As suggested in the outline, it is pertinent to add some information about PG effect that should be experienced by artificial satellites orbiting Earth, or a particular planet. For demonstration, we consider a satellite around the Earth at a typical altitude $h_s = 200000$ m on an orbit overhead at midnight with the Sun at the antipode, or an orbital radius $r_{Es} = R_E + h_s = 6571000.0$ m (we use lower case s index for satellite and upper case S for Sun). That means that we should adjust the integration angles from the satellite apex

position: For f_{g1n} this is $0 \leq \varphi \leq \varphi_S$, where $\sin \varphi_S = a_S = \frac{R_S}{r_S}$ with $r_S = r_{Es} + r_{S-tabled}$. For the second

term f_{g2n} , we integrate in the range $\varphi_S \leq \varphi \leq \varphi_E$, where $\sin \varphi_E = a_E = \frac{R_E}{r_{Es}}$. The Δg is given in the column entitled OEs-S of Table 8. The corresponding product $g_0 \cdot \Delta g$ is given in Table 9. We note that the PG effect at that altitude is practically the same as on the surface of the Earth. As a result, if Δg is measurable, there should also be a measurable deviation from the predicted Newtonian orbit of the satellite given enough transit time overnight (in the Earth shadow). Ranging measurements might reveal this effect. Last, we see what happens if the satellite is far enough so that both Earth and Sun subtend equal solid angle at the satellite. This point is at the apex of the Earth's umbra at a distance $h = 1384037027$ m (using our nominal tabled parameters). The result is shown in the same Tables under the symbolic title <OEs-S with

m/s^2	$g_0 \cdot \Delta g, m^2/s^4$						
g_0	OJ-S	OV-S	OH1-S	OH2-S	OJs-S	OE-S	<OE-S
1.E+03	8.4838E-03	1.5057E-01	3.3337E-01	1.5030E-01	9.7230E-02	8.7206E-02	6.3552E-02
1.E+04	8.5214E-03	1.5080E-01	3.3358E-01	1.5039E-01	1.0355E-01	8.7351E-02	6.4266E-02
1.E+05	8.5251E-03	1.5082E-01	3.3360E-01	1.5040E-01	1.0411E-01	8.7366E-02	6.4329E-02
1.E+06	8.5255E-03	1.5082E-01	3.3361E-01	1.5040E-01	1.0417E-01	8.7367E-02	6.4335E-02
1.E+07	8.5255E-03	1.5082E-01	3.3361E-01	1.5040E-01	1.0417E-01	8.7367E-02	6.4336E-02
1.E+08	8.5256E-03	1.5082E-01	3.3361E-01	1.5040E-01	1.0417E-01	8.7366E-02	6.4336E-02
1.E+09	8.5256E-03	1.5082E-01	3.3361E-01	1.5040E-01	1.0416E-01	8.7371E-02	6.4336E-02
1.E+10	8.5256E-03	1.5082E-01	3.3361E-01	1.5040E-01	1.0402E-01	8.7334E-02	6.4336E-02
1.E+11	8.5255E-03	1.5082E-01	3.3361E-01	1.5041E-01	1.0510E-01	8.6178E-02	6.4337E-02
1.E+12	8.5256E-03	1.5082E-01	3.3357E-01	1.5034E-01	9.5264E-02	9.0824E-02	6.4334E-02

Table 9: *Comparative product $g_0 \cdot \Delta g$ for planets and satellites*

values showing a little less but of the same order of magnitude as on the surface of Earth. This indicates that the effect relates to the amount of shading by Earth that varies little with distance just as dictated by the geometry of the corresponding chords at the set distances. We do not expect an orbital variation of a satellite at this point without “much time to fall” during its night transit, but we learn that Δg varies little inside the entire Earth’s umbra. This point is a “little” closer than the L2 Lagrange point and requires more attention. The relatively small variation of Δg may be used in planning or calculating satellite trajectories, if they can travel a considerable length and time inside the umbra.

Last, given the low value of PG effect for Jupiter as discussed, we can check what the effect would be at the same point (on the “surface”), if hypothetically the entire planet contracted to a much smaller radius, say, to $R_J = 2.0E7$ m, from its actual (used before) $R_J = 6.9911E7$ m. The equations are the same as the ones used above for a satellite around Earth. The results for Δg in this case are given in the column entitled OJs-S of Table 8. The corresponding products $g_0 \cdot \Delta g$ are given in Table 9. We note that the effect is about one order of magnitude greater than before (i.e. on the surface with the tabled radius of Jupiter).

12.5 Discussion on PG effect

The preceding work attempts to establish the condition, which would allow both verification of PG by indication of an anomaly in the correct direction and measurement of g_0 . Neither of these outcomes may be possible to achieve easily, if g_0 is equal to the highest value of acceleration for black holes reported in the literature. The latter is said to be in the order of magnitude of 10^{12} m/s², which would require a lowest value for $\Delta g \approx 10^{-15}$ m/s² in the configuration examples we considered. We have “wished” that the latter Δg could be of a much higher order of magnitude and in the range of existing gravimeters. However, lack of immediate evidence for this outcome should by no means lead to any disappointment about PG and rejection of it by the scientific community. The early speculation by the present author that the strong fields of white dwarfs, neutron stars and black holes may be generated by different types of push particle, it may also be dis-proven. This should not impact on PG theory at all. On the contrary, should g_0 coincide with the highest field of black holes, then we could even have an easier way to gradate the other fields downwards simply by the smaller density of all other bodies (black holes \rightarrow neutron stars \rightarrow white dwarfs \rightarrow stars \rightarrow planets, \rightarrow etc.). This would also help in the unification of various fields by simpler PG means than resorting to different types of push particles. Even so, we could consider that different push particles degenerate from one type to the next, but the point here is that the absence of a detectable PG anomaly should await judgment until we can reach the expected limits of detection arising from maximum field forces, if necessary. Until then, PG should remain on the table as an alternate theory to address outstanding issues in physics. In the meantime, the search for a PG effect should start with terrestrial tests, lunar tests, followed by interplanetary spacecraft tests. Later or concurrently, astrophysicists should also reappraise phenomena of interaction of dense bodies or specifically they should search for ones that are expected to present pronounced PG effects. This approach is supported by the trend of density variation indicated in Fig. 16.

It is interesting to note that the early PG theory relying simply on mechanical corpuscles could not

reproduce Newtonian physics unless the corpuscles could attain superluminal speeds. The higher their speed the better approximation. In lieu of these speeds, our PG theory relies on a sufficiently high value of a universal acceleration g_0 associated with a flux density J_0 , or radiance L_0 of gravions in conjunction with an absorption coefficient for each body density. Our principles do not contravene established observations (physics).

The space test of the equivalence principle (STEP) with an orbiting satellite by Touboul *et al.* (2019) failed to establish any deviation from the Equivalence Principle. However, this negative outcome is consistent with the null PG effect we demonstrated for the midday Sun-Earth explanation. This is further corroborated by our later theory on falling body acceleration in Sections 14.3, 23.2 and 23.2.4. The Equivalence Principle should be tested where PG expects differences from Newton, like a Δg effect. We have proposed various situations, where we can look and test for possible deviations from conventional mechanics throughout this report.

By way of a “gedanken” experiment, the PG effect would be maximized if we consider that the Sun and Earth are stationary and measure the final velocity or time of a falling body from a highest point at midnight. The absolutely highest point is at the apex of Earth’s umbra. For practical outcomes, it is up to spacecraft trajectory engineers to maneuver a spacecraft to maximize a fall inside the shadow in reality, i.e. while the Earth moves along a complex orbit around the Sun. In general, the equivalence principle should be tested under conditions where PG appears to be an anomaly to conventional physics, but such an expected anomaly should not be reason for rejecting PG, for example, as is incorrectly done by Wikipedia article (Wikipedia contributors, 2018).

The PG effect and theory should be included in next-generation laser ranging (Williams *et al.*, 2022), like in the research list of physics topics referenced in the following excerpt from a paper on characteristics of differential lunar laser ranging: “*With more than 50 yr of tracking the Moon from Earth, LLR contributes to many scientific research fields related to the Earth-Moon system. ... For gravitational physics, LLR can test many parts of Einstein’s theory of relativity, including the change of the gravitational constant, G , with time, the geodetic precession, the equivalence principle (EP) for the Earth and Moon in the gravitational field of the Sun, and of the galactic dark matter as well as the parametrized post-Newtonian (PPN) parameters, etc.*” (Zhang *et al.*, 2022).

Experimental measurements of g_0 , or other equivalent parameters like k , J_0 , n_0 , Λ etc., would greatly facilitate the theoretical endeavors to establish the same elsewhere in this report. In fact, some tentative theoretical values for g_0 are considered in Sections 31.1 and 31.4.3, so that experimental work becomes imperative in the hope that we may obtain a value of one of the said interdependent PG parameters.

13 Discussion on gravitational law

The finding that the gravitational force is inversely proportional to distance constitutes a universal relationship now derived from the principles of static PG theory. It is unlikely that this is a fortuitous derivation, although we must wait to find the same consistency with dynamic PG. It is likely that PG can provide a genuine platform to re-work many other relationships with new physics.

We have derived some fundamental but novel relationships yielding the classical acceleration and force but revealing a different relationship with the actual mass. The classical (Newtonian) mass is now understood to be only an apparent or effective manifestation of the real mass. The inverse square of distance law is preserved, whilst the classical gravitational constant G is itself a function of another constant like Λ , J_0 or g_0 , all of which are characteristic of any given region of space. It is important that these relationships are not merely empirical, but are based on a simple principle or premise of particles uniformly traveling in all directions, while they are absorbed by matter at a rate in proportion to the density of the matter. This provides a more “tangible” explanation of gravity, which, however, shifts the problem to the understanding of the nature of these particles, not less mysterious than the elusive gravity to date. Nevertheless, it looks like we can narrow down the fundamental problem of gravity to a “lesser” entity bringing us closer to the goal of a unification theory. After all, forces are already attributed to the exchange of different kind of particles: Gluons for the strong nuclear force, photons for the electromagnetic force, the bosons for the weak nuclear force and speculated gravitons for gravity. Quantum chromodynamics aims to find the smallest building block of nature and the forces that hold them together. PG may not be seen in conflict but rather it may offer a general platform to remold and hopefully unify current quantum gravity and graviton, superstring theory, loop quantum gravity and blending quantum gravity with quantum mechanics for a theory of everything.

The validity of the gravitational law derived is further subject to ensuring that the involved gravitating bodies exist in “free space”, otherwise the space itself is filled with matter albeit of extremely low density. For in the latter case, we deal effectively with an internal field as found in Section 8 and further elaborated later in Section 24.1. Then, g_0 is *internally* variable and a function of distance r from some center of mass,

while the overall gravitational law ceases to be strictly inversely proportional to the square of distance. Later work has found that internal $G(r)$ is invariable and equal to the external big G . That means that the gravitational constant $G(r)$ can be a weak function of distance from the said center of mass. In the latter case, the force will be slightly weaker than Newton's law resulting in precession for an orbiting planet. No attempt is made here to evaluate the magnitude (significant or negligible for an elliptical orbit) of possible variation of $G(r)$, before we can establish the theory PG itself. Eventually, relativistic effects may also have to be included in addition to the classical derivation of precession under PG, but this is subject to further PG analysis and development.

In one aspect, the form of Newton's gravitational law could be considered correct with regard to $1/r^2$ (being universal), but if the mass becomes effective mass as revealed by PG, then such a law is incorrect. This is further analyzed under Section 16 establishing the variation of effective mass m_{er} with distance (in vacuum). Over and above this variation, there is also another variation due to internal effects as revealed in Section 24.1. Hence, it is this extra mass variation (not $G(r)$ variation) that may provide an alternative explanation for the missing planet "Vulcan" hypothesized in 19th century in order to account for the peculiarities in Mercury's orbit. It remains to derive its precession based on PG theory and see if a satisfactory explanation can be found. In fact, we may not need to travel very far to realize that its value varies significantly within the heliosphere and more so as we approach the neighborhood of the Sun. Close enough to the Sun, there may be a lot of mass emitted to a significant level, which makes the closest planets effectively experiencing an "internal" gravitational field per Section 8. Mercury may be significantly affected by the variation of $G(r)$ during its orbit. Conversely, we could introduce a "fudge" factor for the variation of $g_0(r)$ or $G(r)$ to match Mercury's precession and thus indirectly work out the unknown g_0 , but such an approach would be counter-productive for the acceptance of PG theory. The PG effect now quantified in the preceding sections must play an important role on top of the inverse-square-distance gravitational law discussed here. We have established that there is a difference in the intensity of this effect across the antipodes of a planet, where the antipodes are located in the direction of the Sun. There is a self-shadowing effect resulting in a differential acceleration across the antipodes contributing to some deformation. Furthermore, there is an overall Δg , which is superimposed to the conventional Newtonian force and may contribute to the observed precession. We already saw that this effect is maximum for Mercury, which is consistent with observation. Therefore, it remains to work out the mathematical relationship of PG effect to the overall gravitational law, but we need to know g_0 . Alternatively, we might be able to "fit" a value to match the observation, per usual practice elsewhere in physics.

This discussion applies to gravity around stars and planets, but can we still call *gravity* the field around dwarfs, neutron stars and black holes, if it is caused by the different proposed types of push particles, according to a subsequent proposal? Each of these fields would have its own mass attenuation coefficient Λ with a different value from that corresponding to gravions. Beyond white dwarfs, a neutron star would have a variable Λ by superposition of two types of push particles, whilst black holes by superposition of more types of push particles. We may then have to introduce other terms (semantics) to differentiate the fields around these massive bodies from our familiar gravity field. In fact, we should expect to have a mixed or variable effective Λ parameter, which we might wish to denote or index with a different subscript. In those fields then the inverse square of distance law may break down again, but the math remains to be worked out. Correct terminology is important, because, when we say that the gravitational law is preserved in the cosmos, we mean that it applies to gravity due to gravions under the postulates at the outset, which is correct only regionally in the cosmos.

Last but not least is to discuss the mean free path (mfp) of gravions postulated at the outset of PG. Whereas the mfp is assumed to be much greater than the size of the gravitating bodies, no further qualifications were made. How much greater is it in reality? We have no knowledge of this yet, so we can only discuss the various main possibilities: (a) the mfp is infinite, i.e. gravions never interact between themselves, (b) the mfp is of intergalactic order and (c) the mfp is of intra-galactic order. These orders of magnitude are not the only possibilities, but are sufficient for a general discussion in Part 2 of this report. These ranges of mfp define corresponding regions of space, where the gravitational law varies. As soon as the postulated mfp ceases to apply, push gravity behaves differently and is governed by different relationships and laws. It is of great importance to know also the forces (fields) at the transition from one region to the next and beyond. Part 1 has not dealt with such regions yet. Pending such work, we can only speculate at this stage what happens. The inadequacy of PG theory of Part 1 for those regions may correspond to the inadequacy of GR (general relativity) also at long distances, except that PG can be readily expanded and advanced in ways discussed further in the next part of this report.

Part Two (2)

The following presentation is an integral part of the whole report, but it is separated out because it contains a significant amount of speculative theory, which may have to be revised or rejected without affecting the preceding Part One (1). Part 1 should remain valid at least as a mathematical development of PG based on a set of postulates, barring inadvertent but rectifiable errors. In Part Two (2) specifically, it is proposed that the theory can be extended to a general push gravity (GPG) by borrowing some mathematical tools of general relativity (if and to the extent needed), astrophysics and other cosmological theories, or that all theories may complement one another. However, no analytical steps have been undertaken in all cases presented yet, whilst it is hoped that this would be achieved better by experts in the corresponding science fields. It is only initially attempted to introduce PG in astrophysics in the case of white dwarfs, neutron stars and black holes, but again it is hoped that this task would be best undertaken by others. The application of PG in particle physics and cosmology is barely but humbly mentioned, or discussed, in the hope that it might also spark further discussion and research for a unified field theory and a theory of everything: It makes sense to assume that all fields are created by particles, now by push particles, i.e. all with a common denominator as the only way to achieve unity.

As more material is added, re-organization of this report and its parts may become due. As a consequence, there may be some conflicting statements left unchanged, that can be better understood via a historical reading of ascending versions. It seems that some of the material of the second part can be safely included in the first part. Until this is done, it is hoped that no misunderstanding arises from the way it is currently presented. In any case, the overall spirit of the entire report remains a “what if” approach. What if the push principles do create gravity? The conventional approach has been not to proceed in considering PG, because e.g. of an alleged violation of the second law of thermodynamics. As a result, the exploration and development of PG presented in this report has been previously unknown, which has prevented science to consider new possibilities. The latter only now lay bare to see and think if they can help physics to cross through existing barriers. The only prerequisite for this to happen is to be free of preconceptions about sacred notions, like “inertia”, “mass”, “force”, “energy” and “equivalence principle”.

14 Towards a dynamic push gravity

The introduction of time in PG for moving bodies should constitute another chapter of PG dynamics still to be developed. However, an attempt to introduce some elements and ideas of it here is thought to help prepare towards a proper dynamics theory, but also address possible questions arising from the static PG of Part 1.

Since we already established that Newton’s gravitational law can actually be derived from first principles of PG, we may wonder, if we should accept the other laws of Newton by way of principle (granted), or they may also be derived wholly or in part. For clarity, we understand that Newton’s first law states that “*an object either remains at rest or continues to move at a constant velocity, unless acted upon by a force*”, in other words, material bodies have “*inertia*”. The second law states that “*the force F on an object is equal to the mass ‘ m ’ of that object multiplied by the acceleration ‘ a ’ of the object, i.e. $F=ma$* ”. The third law states that “*action = reaction, i.e. when a body exerts a force on a second body, the second body simultaneously exerts a force equal and opposite in direction on the first body*”.

Regarding a fourth law stating that “*forces exerted by different bodies add up (superimpose) like vectors, i.e. the forces obey the principle of superposition.*”, we already found that it does not apply in PG per Section 11.

Now, it is not clear, if we can mix and match the above first three laws with PG, or we should strive to derive them also from the first principles already adopted at the outset in Part 1. For example, is it legitimate to inquire as to the intrinsic meaning of inertia? Is it an a priori physical attribute for all material bodies or just a convenient empirical entity to express an experience mathematically per second law of gravity? Connected to this question is also, why “action-reaction” takes place.

Furthermore, it would be unwise to rely entirely on Newton’s laws alone without regard to subsequent revolutionary developments in many fields of physics, and in particular relativity. We already assume, at least provisionally, the existence of moving particles, the gravions, at the speed of light as an added principle of PG, hence we have to take into account at least the special theory of relativity (SR). By no means do we imply exclusion of the general theory of relativity (GR), but we can try to determine how far we can reach initially without it. We may also mix and match various attempts with all theories of gravity, by trial and error, iteratively, in order to arrive at some understanding as to how things pan out under the framework of PG. In this course, we may need to use much of the existing tools (math) and insights of other theories

without prejudice or fear. The subsequent part of this section serves only as a beginning along these lines.

Important: By the current PG development (version 22), no use of relativity has been necessary. The indication is that PG may remain self-contained and self-consistent relying only on the least number and simplest of principles. By no means does this imply an opposition or intention to oppose relativity, as the preceding (above) text testifies. In fact, we anticipate that the photon behavior and relativity will be derivable from PG theory. The hitherto mainstream physics may be reduced to a subset of PG physics.

14.1 Relative and absolute reference frames

Throughout Part 1, we considered only stationary material bodies relative to each other but implicitly also relative to the gravions as a whole. We already discussed the possibility of gravions with different mean free paths defining different regions of the universe. Gravions then may be treated like a gas or an aether. Such an aether, though, is not a passive medium for the propagation of light like the classical (conventional) aether in prior physics. It is an absolutely energetic medium interacting with material bodies. This medium “fills”, or better forms the space, which acts on material bodies, while at the same time this space is acted upon by the material bodies. Based on this primary interaction between space and matter, in turn, there arises interaction between matter and matter giving rise to displacement of matter (bodies) relative to it (i.e. relative to each other body) and relative to space (aether). In this way, the gravions, or space (aether) is now endowed with a privileged rest frame of reference, against which all other movements can be measured. While each body is stationary in its own reference frame and moves relative to the reference frame of other moving bodies, they all interconnect via the primary or privileged reference frame of the aether. Distance and time are now interconnected via the reference frame of the aether. If aether inflates or streams in the universe, so is its frame of reference. The analogy is the same as with the motion of an expanding (better, inflating) universe carrying with it its clocks and length-measuring-sticks, and operating under the presumably tested laws of relativity. If we can continue using some tools and concepts of relativity, we can now also flesh it out with a material (energy) content, namely, that of the gravions incessantly moving in all directions while defining an absolute frame of reference for time and distance. The aether of gravions is a source of energy, from which all other forms of energy emanate and to which they return in a perpetual cycle of cosmos.

In such an absolute reference system of a cosmic aether, we may have a better understanding of the effects on a rotating material body. PG provides an opportunity to have a fresh examination and re-think about the “Mach’s principle”.

It is important to note that the “aether of gravions” can co-exist with a host of other types of particles as proposed in Section 18.

“Statics” in physics is the branch of mechanics concerned with bodies at rest and forces in equilibrium. We may provisionally use this term in PG too, but with the qualification that there is continuous action by the relativistic moving gravions underlying the emerging forces. Until we may coin another term (if needed), we use “static PG” to describe the theory as in Part 1. Furthermore, to avoid possible confusion between the terms of “kinematics” and “kinetics”, let’s use the existing term of “dynamics” to describe the motion of bodies including its causes or not. So “dynamic PG” refers to the theory including both kinetics and kinematics. If there are disagreements with such a terminology, we may defer a possible resolution for later. After all, there may not be any need to distinguish “statics” from “dynamics” in PG.

14.2 The Equivalence Principle

We can easily reproduce Newton’s attraction force by push gravity and hopefully all other observed relationships (a task by later work). Furthermore, under the understanding of PG, we can now say that the well known equivalence principle (EP) is not violated. In fact, it is better explained as an identical process in the two systems being referred to, namely, one in a gravitational field and another accelerated by an equal force in space outside the gravitational field. That is, whether a mass is pushed “by hand” (or pulled via a rope in an elevator in free space), or the same mass is pushed by gravions by an equal force, then the outcome should be the same, namely, the mass will travel distances proportional to the square of time (t^2). Push gravity creates a force by streaming gravions through the entire mass dragging every mass element concurrently, the sum total being a force no different from a push (pull) force acting by a spring with measurable deformation on a solid mass (or an imaginary accelerating force experienced inside an elevator in space). The gravitational push force is distributed throughout the mass, whilst the spring force acts on the external surface of a **rigid** (for argument’s sake) mass and indirectly transmitted and distributed to all body elements producing an identical outcome. Then the same mass being acted by an equal force would accelerate by the same amount, i.e. we would measure distances proportional to the square of time, from the moment the mass is set free to travel (in free space or in the neighborhood of the gravitating body). If the mass is held stationary by some stationary “wall”, then the mass experiences the force (by the gravions or

the spring) without moving (like pushing on or pushed by a stationary wall). The gravion force appears as a mysterious attraction force by Newton, which necessitated the adoption an “equivalence principle” to explain the observable equal outcomes by the same mass acted upon by the Earth’s gravity, or by “ the rope on an enclosed elevator encompassing the same total mass”. With the insight readily provided by PG (streaming gravions), the "equivalence principle" need not be a "principle" at all any more; it is just an identity as seen by PG, **it is** the same thing.

The Equivalence Principle (EP) is a mere and easily understood consequence of the hidden reality of the PG gravity principle, hence there is no need to postulate the EP any longer. The self-shadowing (shielding) causing an underestimation of the real mass does not refute the above understanding: To the extent that part of the mass is shielded from the action of gravions, if we push it “by hand” by the same force, as Newton would have us to use, then we would correspondingly measure the same distances. The actual mass (bigger than the apparent one) would be acted upon with an equal force, in both cases, of a falling body due to gravity or moving in space outside gravity. In both systems (cases) the same force acts on the same mass being real or effective, producing the same outcome.

Summary: PG does not require an equivalence principle, since everything exists in a real “elevator” being pushed by streaming gravions, not requiring a fictitious (gedanken) second elevator as theorized to date.

The above arguments are upgraded with an updated Section 16.

14.3 Falling bodies and Flyby anomaly

From the above description and understanding of the EP and if there is no distinction between effective and real mass (as per PG), then it follows that the gravitational and inertial mass are equivalent, actually equal. The latter equality then forms an alternative form of the Principle. In other words, the ratio of gravitational to inertial mass of any object is equal to some constant C, if and only if all objects fall at the same rate in a given gravitational field, so that C=1. The latter form of the Principle must be distinguished from its original “gedanken” description stating that “*the gravitational force we experience on Earth is identical to the force we would experience were we sitting in a spaceship accelerating at 1g*”.

However such an equality of masses is clearly at variance with PG: As understood and described above, the effective mass corresponds to the gravitational mass, the force from which is transmitted to the real (entire) mass of the body, i.e. to the inertial mass of the body.

Thus, applying the PG parameters as developed so far, let us designate by M_e the mass of a large gravitating body (sphere), so that it is considered stationary, when other much smaller bodies with effective mass m_e fall to it. We consider only the case, where the falling trajectory is radial, so that the assumed steady state of PG is thought to be practically retained. A uniform (parallel) gravitational field allows the use of the static force during fall without time effects. We can use the effective mass as in Newtonian mechanics for the potential energy $GM_e m_e / r$ of the system of both masses each with an equal share of energy. We obtain the potential energy by integrating the corresponding acting force times the elementary path lengths of the falling body. Likewise, we integrate for the work done by the **same** force on the total (real/inertial) mass m to obtain the additional kinetic energy as the body falls from point (radius) r_1 to r_2 and apply the conservation of energy equation:

$$\frac{1}{2} m u_{PG}^2 = \frac{1}{2} \frac{GM_e}{r_1} m_e - \frac{1}{2} \frac{GM_e}{r_2} m_e \quad (125)$$

from which the final velocity u_{PG} is given by

$$u_{PG} = \sqrt{GM_e \left(\frac{1}{r_1} - \frac{1}{r_2} \right) \frac{m_e}{m}} \quad (126)$$

It there is no distinction between the two masses above, then, by Newtonian mechanics, the corresponding final velocity u_N would be

$$u_N = \sqrt{GM_e \left(\frac{1}{r_1} - \frac{1}{r_2} \right)} \quad (127)$$

The ratio between the above two velocities is then immediately obtained as

$$\frac{u_{PG}}{u_N} = \sqrt{\frac{m_e}{m}} \quad (128)$$

g_0	PG over Newton velocity ratios
300	0.999999980343
500	0.999999988206
1000	0.999999994103
2000	0.999999997051
5000	0.999999998821
10000	0.999999999410
20000	0.999999999705
30000	0.999999999803
50000	0.999999999882

Table 10: *Ratio of falling velocities by PG over Newton.*

From Section 6.5, we substitute the ratio of masses to obtain:

$$\frac{u_{PG}}{u_N} = \sqrt{\frac{3A_R g_0}{4\pi G \rho R}} = \sqrt{q} \quad (129)$$

as a function of the unknown parameter g_0 . The ratio of masses in Eq. 128 is independent of the gravitating center (body) and it is equal to the accelerations ratio given by Eq. 88 on the moving (gravitated) sphere (the contraction factor q). We already listed the difference of the two velocities in Table 5 for steel spheres. We repeat the same, but for the above ratios of a steel sphere with radius $R = 10$ m and density $\rho = 7500$ kg/m³ in the typical range of g_0 in Table 10.

We can apply the above figures for reported flyby velocities (at perigee) and find that the difference between velocities is of the order of mm/s. This is consistent with observed flyby anomalies and it might help further explain them, i.e. in addition to or in lieu of various other proposed explanations. The Oumuamua anomaly (Bialy & Loeb, 2018) might be another candidate to re-examine as a flyby effect.

Theoretically, a spacecraft on an elliptical orbit could experience a greater force on its inbound direction than on its outbound one by changing direction of its disk-like (for example) shape thus exhibiting a greater effective mass in one part of the orbit than in the other. This would result in incremental accretion of energy until it can reach escape velocity and then repeat the same process around a bigger planet (e.g. Jupiter), or the Sun. This explained in more detail in a later Section 23.2.4. Similarly, mass distribution in a fan-like configuration might optimize the flyby effect by opening and closing the fan accordingly. In Section 12.2, we report that there is an optimum angle for spherical and truncated cone shape, whilst other shapes may be further investigated later. This might have little practical application, but it remains to be seen, if there is some benefit in furthering such an investigation. For an elliptical orbit, time effects on the shadow (push force) of relativistic gravions become important in PG, a problem not yet formulated.

In general, this effect says that a steel ball and a feather do not fall at the same speed inside a vacuum chamber: Let us consider a flat feather falling with its plane parallel or vertical to the direction of the gravitational field. In both cases it has the same real mass but different effective mass. When it falls with its plane vector parallel to the field, the effective mass is greater than when it falls with its plane vector normal to the field. In both cases, we have the same object (mass) and the same inertial mass. However, it will fall faster in the first case than in the second. The maximum speed (and acceleration) will be when the effective mass is practically equal to the real mass, i.e. when the feather can be spread out as much as possible (e.g. by further thinning it down). Let us then consider a steel sphere and a very thin steel disk of the same mass; we can achieve this by first using the sphere and then the same object is flattened out to a very thin disk. Like with the feather, the steel sphere will achieve a slower final velocity than the same mass in the shape of disk. Now, the fine steel disk and the fine feather will fall at the same speed if they are both thin enough to expose their real mass to the field, and will fall in accordance with Newtonian mechanics, because they both use the real (total) mass. However, the steel sphere will be slower than the feather, because the sphere displays an effective mass further away from its real mass than the feather does. The effect of orientation of a falling body is thus a new finding by PG, an extremely small effect to measure in the laboratory, but it may become cumulative and observable during a fall towards a planet or star from a significant distance.

Corollary: All bodies fall at equal rates inside a uniform gravitational field, if and only if they all expose their real mass to gravions, or if they expose the same ratio of effective-to-real-mass, i.e. if and only if they have the same contraction factor q . (This is further confirmed in a later Section 23.2.4).

The flyby difference (referred to as an anomaly to date) might be used purposefully for the measurement of the unknown value g_0 in our solar system. Furthermore, the presented perceptions on EP itself from the perspective of PG theory might help us better understand the Principle itself and its implications in past and future physics.

It must be stressed that the above derivations of velocities were used for “falling bodies” acted upon by forces generated in the steady state of gravion flow, so that the time effect is presumably small and the validity of equations is tacitly assumed.

As a further approximation in this section, we have been tempted to include the flyby anomaly, but for which the time effects must be ultimately included, as it is also discussed in following sections.

IMPORTANT: The above derivations are based on conventional equations of a body in motion in combination with some PG equations based only on the stationary body situation. However, in subsequent sections, we gradually establish the meaning of mass in various forms. Furthermore, we need to consider also the concurrent role of the electric field inside a falling body, and the total balance among all forms of mass and energy. We will need to derive the equations of mass, energy and contraction factors both for a stationary and a falling (moving) body based entirely on PG principles and computations similar to work presented in the Appendix. Pure PG quantitative considerations would provide consistent outcomes. We further examine the falling body situation later in Section 23.2 and it seems that there are some exciting prospects ahead.

14.4 Advance theoretical solution

If we use the above reasoning in a similar fashion for an orbiting body in circular motion (for simplicity), we equate the inertial and gravitational force (initially) in PG:

$$m \frac{u_{PG}^2}{r} = G \frac{m_e M_e}{r^2} \quad (130)$$

where again m_e and m are the effective and real masses moving around a large (hence stationary) effective mass M_e , yielding

$$u_{PG} = \sqrt{G \frac{M_e}{r} \frac{m_e}{m}} \quad (131)$$

In Newton we have:

$$u_N = \sqrt{G \frac{M_e}{r}} \quad (132)$$

so that we again get for the ratio of velocities:

$$\frac{u_{PG}}{u_N} = \sqrt{\frac{3A_R g_0}{4\pi G \rho R}} = \sqrt{q} \quad (133)$$

Now, if we apply this to the Sun-Earth system for simplicity assuming circular orbit, there is a significant slower than experience velocity component. We find this from the density ratio values in previous Table 2 and list them again together with the ratios and differences between PG and Newton in Table 11.

We have used the Earth’s average speed of 29.78 km/s. The tabulated outcome is clearly incompatible with experience: With $g_0 = 50000 \text{ m/s}^2$,² the orbit length would be by 51.876 km shorter in one year. We have the option of increasing g_0 until we bring the difference to an acceptable level, but first we have to modify the above equations to include time effects. The equations used above assume instantaneous transmission of the push force, which is incorrect. After we derive the correct equations for orbital motion, we can find the required value of g_0 to bring the velocity u_{PG} to an acceptable level and consistent with experience. This would constitute an advance theoretical solution to the problem of finding the prevailing maximum acceleration g_0 in our solar system, over and above the proposed experiments throughout this report. This work has not been done yet, whilst it is not clear how it will pan out. At present, this objective falls outside the scope of the present report and beyond the resources available to this author.

We have reached a critical point in the development of a general PG theory for moving bodies. In the following Section 15.3, we discuss the possibility of using the tools of general relativity (GR) to develop a

g_0	velocity ratios of PG over Newton	velocity difference, m/s
300	0.990700461	-276.9402851
500	0.994442855	-165.4917729
1000	0.997229786	-82.49698282
2000	0.998616965	-41.18677725
5000	0.999447281	-16.45996439
10000	0.999723723	-8.227530833
20000	0.999861882	-4.113155718
30000	0.999907926	-2.741968791
50000	0.999944759	-1.645082695

Table 11: *Earth velocity ratios and differences by PG and Newton.*

dynamic PG, or further develop GR in the framework of PG. Now, this might appear to be inconsistent with GR from the outset, because PG breaches the equivalence principle, if stated as equality between inertial and gravitational mass, which is a cornerstone of GR. To reconcile this contradiction, we may inquire that the postulated equation:

$$m_{\text{gravitational}} = m_{\text{inertial}} \quad (134)$$

be replaced with the equation:

$$m_{\text{gravitational}} = qm_{\text{inertial}} \quad (135)$$

which is prompted from the corresponding relationship between effective (gravitational) and real mass (inertial) in PG:

$$m_e = qm \quad (136)$$

In other words, can we introduce the contraction factor q to redefine (or replace) the EP and carry on with a modified GR? This is where the subtle differences in the understanding of EP become important. This leaves the inquiry open on how to integrate relativity with PG. Gravions are assumed relativistic and we need to develop a relativistic theory of PG. Then, we could also address the objection listed in the following Section 15.6. Time effects must also include the almost helical Earth trajectory, as the Sun moves around the center of galaxy, which makes the overall formulation more complex.

The breakdown of the EP expressed in terms of differing inertial and gravitational mass seems to be necessitated also in new quantum theory (Kajari *et al.*, 2010), so that our finding here is not alone or alarming. In fact, coming to the same conclusion from an entirely different perspective, namely, from quantum mechanics, provides a strong reason to correlate the corresponding theories in an effort to unify quantum mechanics and gravitational field.

Should any further difficulties appear or remain in the development of a general PG theory, then we may have to look for some other counteracting (compensating) mechanism for the shortfall in orbital motion, before we can confidently abandon PG. For example, in Sections 15.7 and 15.8, an attempt is made to account for the postulated exiting forms of the absorbed gravions, not yet knowing if they have some second order perturbation on the gravitational field. Other compensating mechanisms may also be present.

At any rate, we can always resort to high enough g_0 in order to establish compatibility between theory and measurements, i.e. by bringing the fraction q much closer to unity. This alternative solution always remains on the table for consideration, except that it would make the prospect of measurements more difficult. In this case then, all the referenced gravitational anomalies (Allais effect, Greenland gravity anomaly, Pioneer anomaly, flyby anomaly, etc.) must be re-visited and conclusively discounted as been anomalies of gravity, namely, deviations from Newton and/or GR. This strengthens our proposal of the need to undertake some decisive experimental tests in the event that static PG theory (for stationary bodies) can be confirmed and measured.

The case of very high g_0 values, if needed, must also be considered in the spirit of discussion in Section 18 dealing with white dwarfs, neutron stars and black holes. Increasing g_0 only resolves the problem for our nearby solar system, but it shifts the importance of distinction between effective and real mass for much larger, or denser bodies and systems, like binary systems, black holes, etc, whereby compatibility of PG with such systems must be established. The difference between real and effective masses must be very high for such bodies, which also means that the EP would be grossly violated in terms of great inequality between gravitational and inertial mass. The proposal of establishing momentum or push gravity as the universal and unifying cause of all types of acceleration in Section 17 provides a reasonable platform to relate to the new quantum theory mentioned above (Kajari *et al.*, 2010).

14.5 Matter, inertia and mass

In continuation to the previous analysis, we can bring it to its logical conclusion below.

We intuitively identified the real mass $m \equiv m_{real}$ with the inertial mass $m_{inertial}$ and the gravitational mass $m_{gravitational}$ with the effective mass $m_{effective}$. However, this need not be necessarily so. It may be that, after all, the inertial mass is equal with the gravitational mass making the equivalence principle absolutely inviolable in all its expressions. Such a finding could lead to either of two outcomes:

(a) The PG becomes unsustainable, unless:

(b) Both PG as advanced in this report and the EP are true, even if EP includes equality of masses.

Then we have to accept some inexorable conclusions, even if they are counter-intuitive at first.

To avoid possible confusion, we write the subscripts of various masses explicitly by a full word. In case (b), it is not the entire m_{real} responsible for the phenomenon of inertia, i.e. a resistance to change in kinetic state (to move faster or slower). In reality then, it should be only the $m_{effective}$ that manifests inertia. At the same time, we can continue identifying $m_{effective} \equiv m_{gravitational}$. This implies that there is a fraction of the real mass, namely, the difference

$$m_{passive} = m_{real} - m_{effective} \quad (137)$$

being passive, oblivious and not resisting to the application of the gravitational force on the effective fraction of the total mass. If this were to be true, it would revolutionize our understanding and perceptions about the hitherto meanings of matter and mass. Newton defined (or identified) mass as the amount of matter:

$$mass_{Newton} \equiv matter = m_{inertial} \quad (138)$$

which would need to be re-appraised, if case (b) is true.

In fact, upon further considering this idea, we may also bring some intuition one way or another. In one way, we could think of the gravions constituting a sort of a “lattice” that activates the effective part of the mass. In doing so, it is this lattice that resists in changing the kinetic state, or inertia of the body. The passive part of the mass is ineffective and does not care (does not resist) moving along with the active part ($m_{effective}$) of the mass without actually offering any resistance. We could then safely identify the total mass of a body with its matter:

$$matter \equiv m_{real} \neq m_{inertial} \quad (139)$$

Yet, by further iterative thinking, we can make the inventive step that, instead of the gravion-lattice **activating** the effective mass to resist, it is the lattice itself that resists the movement of the body (matter) by engaging via the effective (active) part of the mass. The effective mass is passive by itself, except that it is somehow tied to the activating gravions. In consequence then, we can safely state that the entire mass is actually passive and hence it has no inertia; what appears as inertia of the mass (or part thereof), it is actually the resistance of the gravions opposing the mass to change its kinetic state.

The concept of gravion-lattice may take on various embodiments and conceptualizations: Gravions continuously penetrating and being absorbed through a mass could be likened to rolling ropes (albeit very inefficient way) constraining the mass from changing momentum. By whatever means and ways to describe the gravion-mass interaction, we can generally state that it is the gravions that are responsible for what appears as inertia of matter. When we try hard to move a sledge on slippery ice, it is the gravions, which resist invisibly to us, but we only experience the force on the tangible sledge. By such thinking, we may have ultimately deciphered the mystery of controversial inertia. We may know why bodies resist, now saying that bodies actually do not resist, but it is the energetic gravions that want to “push back” on us via the mass ($m_{effective}$). There remains to better conceptualize how they do this and why they only do it when

we accelerate or decelerate a body. For the time being, we can summarize our possibly new understanding as follows:

$$m_{inertial} = m_{gravitational} = m_{effective} = qm_{real} \equiv q \cdot matter \quad (140)$$

We note that the above equation is similar to Eq. 135 except for the semantics on masses, i.e. which mass is which and what they do. If the above is true, the consequences would be immense. For example, the inertial mass of a very dense body, like a neutron particle, or a white dwarf, or a neutron star, or a black hole is much-much smaller than it could be if the same body is expanded (diluted) to produce an effective mass close to its real mass. The *dynamics* of an exploding star would be far different from what we would derive by allowing for a constant mass. Mass, inertia and matter now (in PG) mean different and variable entities. As another example, the flyby gravitational anomaly still applies, so that if we are able to vary the effective mass by a large factor minimizing it during the outbound trajectory, we could hurdle a body into space at huge velocities.

In all above, we made no mention of relativity implying that we considered only low speeds. When we go to relativistic speeds, then we have to expand on additional notions of masses, namely, that of rest mass m_{rest} and that of relativistic mass $m_{relativistic}$. In doing so, we may not be in conflict with GR and we may just carry on with established relativistic theory. Actually, it seems that we may even have a better understanding of the meaning of relativistic mass, which has been often misconstrued by many GR proponents for over a century. Relativistic mass has been so confusing even among notables in relativity, that it has been called “the pedagogical virus” (Okun, 2006). For consistency with our introduced terminology and semantics, we should set for the rest mass:

$$m_{rest} \equiv m_{effective} \quad (141)$$

so that the relativistic mass can be given by:

$$m_{relativistic} = \gamma m_{effective} \quad (142)$$

with the usual relativistic factor

$$\gamma = \frac{1}{\sqrt{1 - v^2/c^2}} \quad (143)$$

There remains now only to conceptualize and formulate how exactly the relativistic mass comes into being. Nevertheless, the important conclusion must be that the gravions remain responsible for this mass too, which is not a “mass” per se, i.e. it is not matter (stuff), but only an inertial mass. Such a conceptualization is then closely consistent with the “orthodox” and rigorous teachings of the theory of relativity, namely, that the relativistic mass is not a “mass”. However, this is a close agreement with GR but not a total agreement, because GR teaches that the “*only true mass is the rest mass*”. We may now have found that even the rest mass is not true mass, because it is only an effective mass, which can vary with density and orientation for any given body. The only true mass is actually the real mass as has been established by the present PG theory, which is non other than the matter of the body. In any case, none of all these masses has an inertia (a will to resist), but the energetic gravions are responsible for the quantity (parameter) of mass that enters our equations in physics. Therefore, gravions create both gravitational fields and apparent masses. This should be in happy agreement with GR originating from an “opposite” direction.

From the preceding analysis, it seems that PG reaches a critical point as soon as we apply the concept of effective and real mass to moving bodies. This could be either the end of PG, or a long awaited breakthrough in physics. The latter might occur in one sense, if we are prepared to review and re-appraise the notion of “inertia”. It is interesting to note that the dictionary synonyms of “inert” are “dormant, immobile, impotent, inactive, listless, motionless, paralyzed, passive, powerless”. However, in physics, we associate inertia with a resistance or refusal of a body to change its kinetic status, which is not passivity or inactivity. A resistance to the change of movement implies a power, or will, or action to resist, i.e. a reaction. Where does this power for objection to an action come from? It might have been a misnomer to use the word “inertia” to describe our experience, when we try to change the kinetic state of a body. A more appropriate word might have been “reactivity”. In chemistry, it is more appropriate to call an inert element so, because the element does nothing by way of (chemical) reaction; it is action-neutral. However, in physics, all bodies are not action-neutral, when prompted to move or stop or change velocity. They all present reactivity and not “inertia” per the outside-of-physics use of the word. “Inertia” means inaction, the same as in other languages, e.g. in Greek inertia $\iff \alpha\delta\rho\acute{\alpha}\nu\epsilon\iota\alpha \iff$ inaction. Of course, word-play does not make physics, except that

we may have fortuitously come to use the word “inertia” for what it actually means for the real mass. As a result, the word “effective” mass may now assume the role of the formerly “inertial” mass.

In the preceding analysis, we reached the dilemma of either abandoning PG, or abandoning the classical inertia meaning. We also used the word “passive” for a passive mass $m_{passive}$ of a material body.

We can better appreciate why, the EP stated as per “gedanken elevator”, is a different thing than stated as equality of masses. We may provisionally use the equality of masses in PG to learn that the “effective” mass plays the role of both the “inertial” and the “gravitational” mass of prior physics. If we can establish such a finding by other means, then there is no distinction between those two prior masses, and the EP becomes redundant again. A good way to this end is to start by experimentally verifying the static PG, namely, the existence of effective mass as already proposed, or by some other experimental means. Theoretical means are also welcome, but practice is the ultimate criterion of truth.

14.6 Mass, energy and black holes

As a result of the previous potential discovery of possible properties of the effective and real mass, we further investigate the consequences on mass and energy of bodies with increasing density all the way to the creation of black holes. We have already considered the effect of increasing density, but we also need to account for the distribution of effective mass inside a given material sphere at very high density.

14.6.1 Material sphere

We need first to clarify and summarize some previous findings to help us make an important step without laborious cross referencing: If the real density ρ is known in advance, we can find the absorption factor k directly from $k = \pi\rho G/g_0$, which substituted in Eq. 49 yields the contraction factor

$$q = \frac{3A_R}{4kR} = \frac{3}{4kR} \left(1 - \frac{1}{2k^2R^2} + \frac{\exp(-2kR) \cdot (2kR + 1)}{2k^2R^2} \right) = \frac{\rho_e}{\rho} = \frac{m_e}{m} \quad (144)$$

From the above, we obtain the effective mass and effective density:

$$m_e = \frac{3A_R}{4kR} m = \frac{\pi R^2 A_R}{k} \rho = \frac{\pi R^2}{\Lambda} A_R = \frac{g_0}{G} R^2 A_R \quad (145)$$

$$\rho_e = \frac{3A_R}{4kR} \rho = \frac{3A_R}{4\Lambda R} = \frac{3g_0 A_R}{4\pi G R} \quad (146)$$

The above equations state that, we as increase the real mass arbitrarily inside any fixed radius sphere, the corresponding effective mass increases monotonically to an asymptotic value as the absorptivity A_R approaches unity. At the same time, the contraction factor vanishes to a zero value but never reached.

We can also arrive at the same equations by starting with a given (known from Newtonian mechanics) effective mass, or effective density. Then, we find the coefficient k directly by solving Eq. 68 written as:

$$g_0 A_R - g_R = g_0 \left[1 - \frac{1}{2k^2 R^2} + \frac{\exp(-2kR)(2kR + 1)}{2k^2 R^2} \right] - G \frac{m_e}{R^2} = 0 \quad (147)$$

from which we immediately obtain again (as from Eq. 85):

$$m_e = \frac{g_0}{G} R^2 A_R = \frac{\pi R^2}{\Lambda} A_R \quad (148)$$

The above findings state that we cannot pack any arbitrary Newtonian mass (i.e. effective mass) inside a given radius sphere for a given universal constant Λ , or a combination of constants G with g_0 ; there is a limit approached asymptotically as A_R approaches unity. That limit is given by

$$m_{emax} = \frac{g_0}{G} R^2 = \frac{\pi R^2}{\Lambda} \quad (149)$$

and

$$\rho_{emax} = \frac{3g_0}{4\pi G R} = \frac{3}{4\Lambda R} \quad (150)$$

By way of example and comparison, we use a sphere with the radius of Earth ($R = 6.37 \times 10^6$ m) and $g_0 = 1000$ m/s², and find the maximum possible effective M_{emax}

$$M_{emax} = \frac{g_0}{G} R^2 = \frac{1000}{G} \cdot (6.37E + 06)^2 = 6.08 \times 10^{26} \text{ kg} \quad (151)$$

That limit would be achieved, if a near infinite amount of real mass could be accreted. For the particular example here, the ratio of that limiting value over the Earth's effective (Newtonian) mass is $M_{emax}/M_e = 101.8303172467580$.

Even risking of becoming pedantic, we need some further clarifications, because there is a bigger risk from misusing the two densities in the new situation of PG. The contraction factor q was defined for a condition outside a sphere. Thus, initially we assumed that the density is known and real, so that, if we use it in both PG and Newton, we arrive at different outcomes correspondingly, the ratio of which is provided by $q(\rho)$ being a function of real density. Subsequently, we introduced the effective density to match Newton with PG. If we use the two densities at the same time in the contraction factor, we obtain unity:

$$q(\rho, \rho_e) = \frac{g_{PG}(\rho)}{g_N(\rho_e)} = \frac{g_0 A_R}{\frac{4}{3} \pi G R \rho_e} = 1 \quad (152)$$

after substituting ρ_e from Eq. 146. This is useful background to correctly understand the internal accelerations ratio used in Section 8 for a low (typical) density-of-the-Earth example. There, we found the internal parameters of g_{0X} , $q_X = g_X/g_{XN}$ and the difference $\Delta g_X = g_{XN} - g_X$ at any point X inside a sphere per Fig. 7 defining the internal radius R_X and the fractional radius R_X/R of the sphere with radius R . Explicitly, we have:

$$q_X(\rho, \rho_e) = \frac{g_X}{g_{XN}} = \frac{3g_{0X} A_{R_X}}{4\pi G \rho_e R_X} \quad (153)$$

where we use both the real and effective densities already established for the material sphere from the outside, whilst they do not change once found.

With q_X known per process in Section 8, we can find the corresponding density ρ_{eX} at point X required to balance the PG acceleration at that internal point for the internal sphere, for which we have:

$$q_X = \frac{\rho_{eX}}{\rho_e} \quad (154)$$

This finds the effective density for any internal sphere with radius R_X , which, in effect, provides also the desired overall distribution of the total effective mass for the entire sphere as a function of R_X . Thus, we can verify that for $R_X = R$, we get $q_X = q = \rho_e/\rho_e = 1$ as expected. Therefore, q_X provides solution to our inquiry.

Now, we are ready to plot the same internal parameters as per Fig. 8, but close to (i.e. a little under) the limiting value of M_{emax} found above. This is done in Fig. 19 using $M_{e-test} = 101.83M_e$, for which the corresponding densities are $\rho_{e-test} = 561449.92$ kg/m³ and $\rho_{test} = 299899725.44$ kg/m³ with a contraction factor $q_{test} = 0.01829587874417$. The latter factor indicates that the total effective mass is only $\approx 1.83\%$ of the total mass, i.e. relatively low but over $100\times$ the Earth's mass. The graph of the same factor internally decreases extremely fast from the surface to the center of the sphere. The effective mass is practically concentrated in the top 1% of the radius forming a very thin active layer very close to the surface. It should be noted that to reproduce the graphed numerical example, one needs to apply high precision computations. The distribution of the same and other internal parameters is further explored for the general case in Section 24, whereby the g_{0X} has been theoretically corrected and now redrawn with red circles in Fig. 19; the correction is hardly distinguishable on the graph in this range of fractional radius (approaching unity). The contraction factor is renamed as “*normalized contraction factor*” q_{Xnorm} in the figure. We used corresponding $k = 0.0000628806972857207$ m⁻¹.

If the hypothesis that the real mass is inactive and passive (i.e. without classical inertia), whilst the only bearer of active (reactive) mass is the effective mass, it might provide us with what looks like a black hole. There are generally different ideas about what happens inside a black hole. Especially from our reference frame, it is generally unknown what happens, other than a singularity to in-falling material. Some say nothing happens at all, not even a vacuum, it has no properties and it is not even a hole; whilst matter approaches the black hole, it slows down and finally stops at the event horizon. They also say that all mass becomes concentrated at the two-dimensional surface of the event horizon. The latter is very close to what we also find in Fig. 19. They also say that it seems that a black hole destroys energy, which is again similar

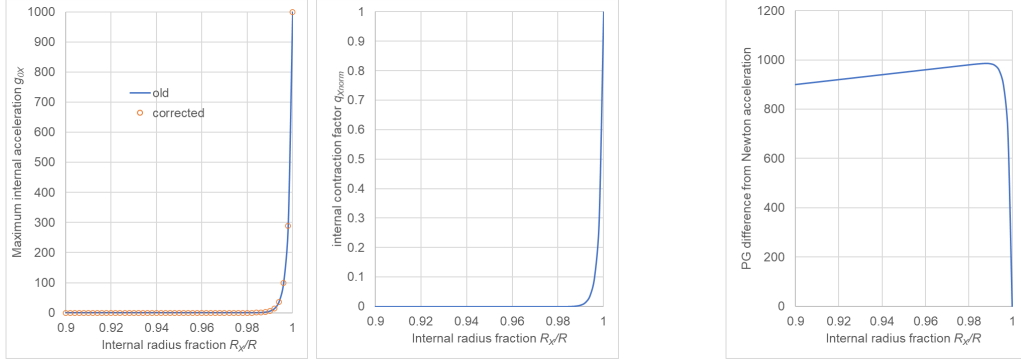


Figure 19: *Internal maximum acceleration g_{0X} , normalized contraction factor q_{Xnorm} and difference $g_{NX} - g_{0X}$ near maximum effective mass limit $M_{e-test} = 101.83M_e$ using Earth's diameter and $g_0 = 1000 \text{ m/s}^2$.*

to what we say, i.e. that the real mass has no energy, but also no inertia (new finding). Actually, with our approach, there is no paradox, except that we might have been misguided about the meaning of our experienced inertia. The Schwarzschild envelope or boundary and the Schwarzschild radius may be exactly, what we find for the limiting case by Eq. 149.

Actually, a close examination of Eqs. 148 and 149 may be full of meaning: The effective mass is proportional to the surface area of the sphere (πR^2) over the universal constant Λ and how close the absorptivity A_R is to unity. It is a simple equation and, hopefully, it is also true.

We further understand that: By increasing g_0 , say by a factor of $10\times$ or $100\times$ with all other parameters constant, the distribution of the effective mass is pushed inward toward the center of the sphere. However, if we also increase the effective mass by the same factor, then we recover the same distribution, i.e. resembling the event horizon. So far, it is arbitrary to keep the sphere radius constant while mass is accreted, unless we can find or propose a mechanism to achieve exactly that. For this, we need to consider what happens in the formation of high surface acceleration on white dwarfs, neutron stars and black holes together with an interim presentation of some other issues below. We continue with more on mass, energy and black holes in Section 18.1

14.6.2 Material line segment

Based on what appears to be an important development for a high density material sphere, we need to repeat a similar formulation for a material line segment; all this will help us derive a possible relationship between the contraction factors in PG with the Lorentz contraction factor in GR. We could take a similar approach for a material thin rod, but we greatly simplify the mathematical formulation required by using the shape of Fig. 1, within a very small (differential) solid angle $d\Omega$, length $\ell = BC$, absorption coefficient k and real density ρ . All corresponding referenced parameters for this case will have the subscript ℓ font. The contraction factor q_ℓ for a material line segment was given by Eq. 51 actually written for chord lengths of a sphere. However, it is better to repeat and review all needed PG parameters with a fast-track derivation below.

We should point out that the material body in Fig. 1 is traversed by gravions in all possible directions interacting with it, but all such interactions are not transmitted to an observer at point O. Point O is affected by all gravions arriving from all possible directions in a full 4π solid angle at that point; they all have a null effect except for those inside the bi-directional elementary solid angle subtended by the material object in the drawing.

Axial external points of line segment: We aim to find the (external) contraction factor along the axis at any distance up to and including the end points of the line length together with other parameters needed for further work and analysis.

The elementary absorption factor df_a (no need for f_g here) is given by Eq. 7 in PG:

$$df_{aPG} = [1 - \exp(-k\ell)] d\Omega \equiv f_{\ell PG} \quad (155)$$

where, for convenience, we abbreviate the differential absorption factor within the differential solid angle $d\Omega$ by $f_{\ell PG}$; the above equation also defines the corresponding absorptivity A_ℓ of the line body with

$$A_\ell = 1 - \exp(-k\ell) \quad (156)$$

It is worth noticing that the ratio A_ℓ/k now is an effective length ℓ_e as opposed to the spherical parameter ratio A/k producing an effective volume V_e per Eq. 57.

The corresponding absorption factor for Newton (i.e. with extremely small k) is:

$$df_{\ell N} = k\ell d\Omega \equiv f_{\ell N} \quad (157)$$

The length contraction factor is the ratio of the two accelerations:

$$q_\ell(\rho) = \frac{f_{\ell PG}}{f_{\ell N}} = \frac{1 - \exp(-k\ell)}{k\ell} = \frac{\ell_e}{\ell} \quad (158)$$

which is the same as for the length contraction found for the chords of the sphere in Eq. 51.

Next, we need to introduce the relationship of effective to real density ratio. For this, we follow the same steps as for a sphere by introducing a small test mass to find the accelerations, and easily obtain the corresponding equations:

$$g_{\ell PG}(\rho) = \frac{J_0}{c} \Lambda A_\ell = \frac{G}{\Lambda} A_\ell = G\rho \frac{A_\ell}{k} = G\rho \ell_e \quad (159)$$

$$g_{\ell N}(\rho) = G\rho \ell \quad (160)$$

Thus

$$q_\ell = \frac{g_{\ell PG}(\rho)}{g_{\ell N}(\rho)} = \frac{\ell_e}{\ell} \quad (161)$$

By introducing an effective density for Newton equation to produce the same acceleration as with PG:

$$g_{\ell N}(\rho_e) = \frac{J_0}{c} \Lambda^2 \rho_e \ell = G\rho_e \ell \quad (162)$$

we obtain the ratio of accelerations being unity:

$$\frac{g_{\ell PG}}{g_{\ell N}} = \frac{\rho \ell_e}{\rho_e \ell} = \frac{\ell_e}{\ell} \frac{\rho_e}{\rho} = 1 \quad (163)$$

and the absorptivity and ratio of densities given by

$$A_\ell = \Lambda \rho_e \ell \quad (164)$$

$$\frac{\rho_e}{\rho} = \frac{\ell_e}{\ell} = \frac{A_\ell}{k\ell} = q_\ell \quad (165)$$

This tells us that the ratio of densities for an elongated shape, like the thin truncated cone of Fig. 1, is different from a sphere. A material line body has different PG effects, whilst all other shapes should have PG effects between the extreme cases of a line segment and a sphere.

With sufficiently large $k\ell$, we get $A_\ell = 1$, so that there is a maximum acceleration $g_{\ell max}$ at the end of the length, or at any distance away from it on the axis, $g_{\ell max} \equiv g_{\ell 0} = g_0$

$$g_0 = \frac{G}{\Lambda} = \frac{G\rho}{k} \quad (166)$$

which corresponds to Eq. 65 without the factor π . From any given k , we obtain the real density for a material line segment:

$$\rho = \frac{g_0}{G} k \quad (167)$$

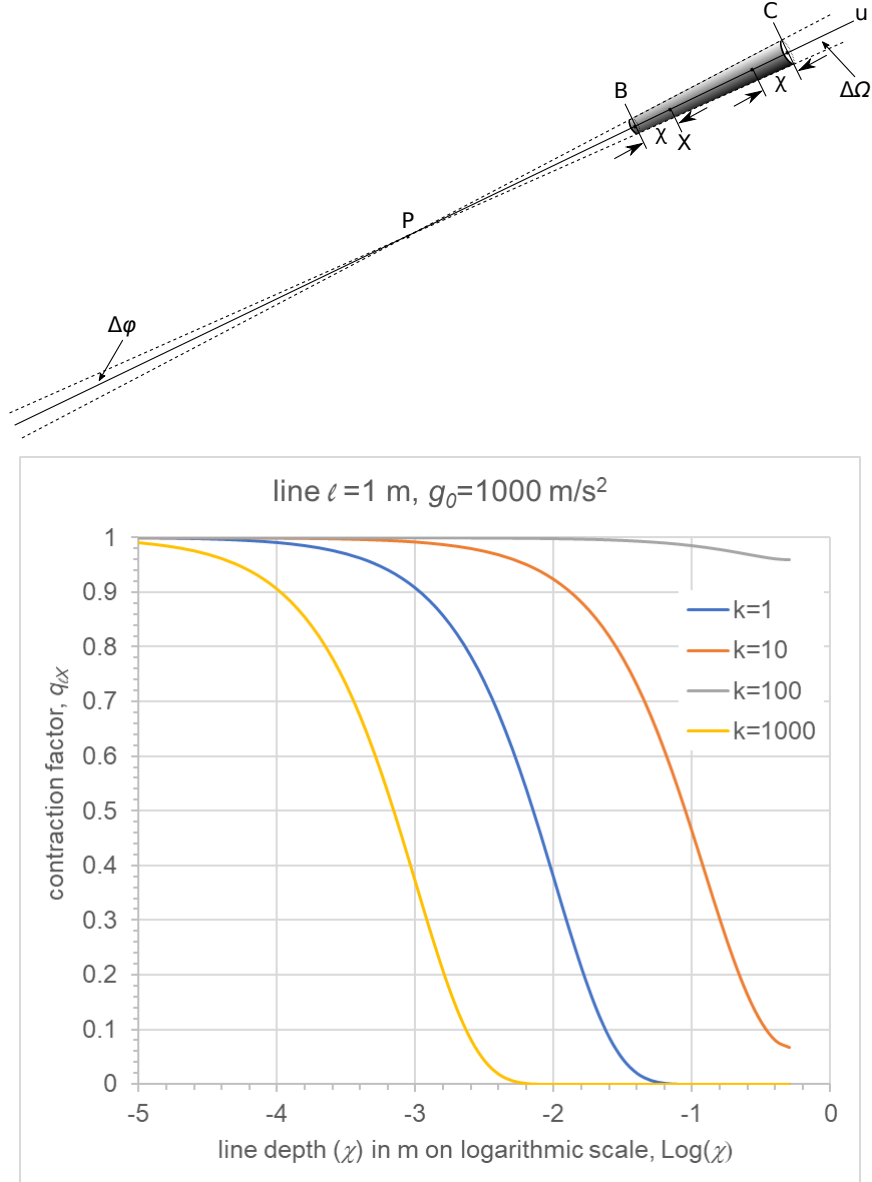


Figure 20: *Line segment geometry (upper) and internal contraction factor $q_{\ell\chi}$ against depth χ (lower), for line length ℓ , maximum acceleration g_0 and fixed absorption factors k indicated*

and for the effective density:

$$\rho_e = q_\ell \rho = \frac{A_\ell}{k\ell} \rho = \frac{1 - \exp(-k\ell)}{k\ell} \rho = \frac{g_0 [1 - \exp(-k\ell)]}{G\ell} \quad (168)$$

Finally, the distribution of the effective mass along the line segment is the derivative of $f_{\ell PG}$ in Eq. 155 with respect to fractional distance $h = \chi/\ell$ from the end of the line segment in the range $0 \leq h \leq 1$

$$\frac{df_{\ell PG}}{dh} = k\ell \exp(-k\ell h) \quad (169)$$

from which the normalized over $k\ell$ distribution is

$$\frac{1}{k\ell} \frac{df_{\ell PG}}{dh} = \exp(-k\ell h) \quad (170)$$

Axial internal points of line segment: We aim also to find the internal contraction factor at any point inside the line length together with other important parameters needed for further work and analysis.

The upper drawing in Fig. 20 is the same material line object: At any point X inside at a distance (depth) χ from either end point, there is a net length $\ell_X = \ell - 2\chi$ responsible for the net absorption at that point, because the absorption by the two outer layers χ cancel out. Thus, at point X, we have:

$$g_{\ell X PG} = g_{0X} [1 - \exp(-k\ell_X)] \equiv g_{0X} A_{\ell_X} \quad (171)$$

where A_{ℓ_X} is the familiar A_ℓ factor but at the end point of the internal line length ℓ_X , and $g_{0X} < g_0$ due to the shielding of the outer layer length from X.

$$A_{\ell_X} = 1 - \exp(-k\ell_X) = 1 - \exp(-k(\ell - 2\chi)) \quad (172)$$

We can find g_{0X} by resorting to the usual absorption factor $f_{\ell X PG}$ at point X simply by

$$f_{\ell X PG} = [\exp(-k\chi) - \exp(-k\ell + k\chi)] d\Omega \quad (173)$$

without the need to integrate over the sphere as previously.

From this found, we can derive the acceleration $g_{\ell X}$ at X by the product with the factor g_0 and equate it to its value given above by Eq. 171:

$$g_{\ell X PG} = g_0 f_{\ell X PG} = g_{0X} A_{\ell_X} \quad (174)$$

from which we can find the relationship between the internal g_{0X} and external g_0 .

$$g_{0X} = \frac{g_0 f_{\ell X PG}}{A_{\ell_X}} \quad (175)$$

The expected Newtonian acceleration at X per Eq. 162 is given by:

$$g_{\ell X N} = G\rho_e \ell_X = G\rho_e (\ell - 2\chi) \quad (176)$$

The ratio of PG over Newton accelerations at point X per above provides the corresponding internal contraction factor for the line length:

$$q_{\ell X} = \frac{g_{\ell X PG}}{g_{\ell X N}} = \frac{g_0 [\exp(-k\chi) - \exp(-k\ell + k\chi)]}{G\rho_e (\ell - 2\chi)} \quad (177)$$

With $q_{\ell X}$ known per above, we can find the corresponding effective density ρ_{eX} at point X required to balance the PG acceleration at that internal point for the internal line length ℓ_X , namely:

$$g_{\ell X PG} = g_{\ell X N}(\rho_{eX}) = G\rho_{eX} (\ell - 2\chi) \quad (178)$$

from which we have:

$$q_{\ell X} = \frac{\rho_{eX}}{\rho_e} \quad (179)$$

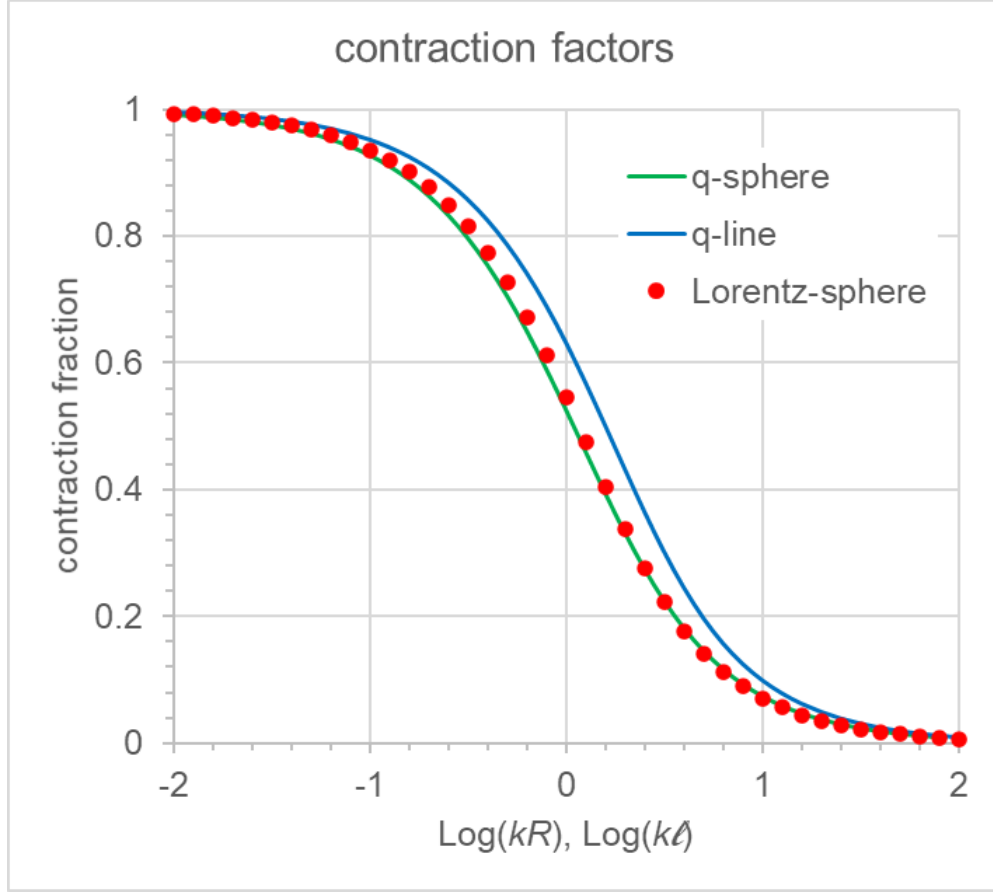


Figure 21: *Comparison of PG contraction factors with Lorentz factor fitted with A_R .*

This finds the effective density for any internal line length ℓ_X , which, in effect, provides also the desired overall distribution of the total effective mass for the entire length as a function of ℓ_X , or the depth χ with $0 \leq \chi \leq \ell/2$; we can verify that for $\ell_X = \ell$, we get $q_{\ell X} = q_\ell = \rho_e/\rho_e = 1$, as expected. We plot the internal contraction factor for a line length $\ell = 1$ m and $g_0 = 1000$ m/s² as a demonstration in Fig. 20 with some fixed values of the absorption coefficient k . This is a monotonically decreasing function of χ , which decreases extremely fast at very high values of the absorption coefficient k (or the real density ρ). This means that there is a look-like “event horizon” at the two ends of the material line segment, like with the sphere found before. Of course, this is only a theoretical outcome, because any “rod”-like structure would collapse to a spherical geometry at high accretion of mass. Nevertheless, it is useful to consider this contraction too in the following presentation.

14.7 PG contraction factors versus Lorentz factor

The previous suggestion that we may have already discovered an alternative explanation for the Schwarzschild event horizon in black holes prompts us to have a closer investigation of the meaning of the contraction factors given by Eqs. 50 and 51. We further attempt to establish a possible relationship with the Lorentz contraction factor. These attempts are made in a kind of round-about-way, not strictly building the dynamics of PG theory from ground up yet. Trialing such attempts involves a mix-and-match of prior principles and understandings. We already acted like that in arriving at the proposal that the effective mass could be the same as the prior “inertial” mass. This potential conclusion was based on the use of the EP despite its possible redundancy in PG. We are fully aware about this on/off relationship with the principle. Redundant does not mean invalid. Valid or invalid will be determined as we develop the theory and practice of PG. With this proviso, we should be entitled to continue trialing various novel possibilities now open with PG, which are not yet well understood or finally accepted. We aim at eventually using as fewer postulates or “principles” as possible, which entails or presupposes better knowledge of the physical processes behind the principles.

Let us rehash some of the things already learned from Part 1, as a prelude to make an important next step towards a dynamic PG theory. The presumably event horizon in PG was deduced by observing the sphere's internal mass distribution at an ever increasing density. However, for an observer (or small test mass) on the surface or away from the sphere, the experience would be described differently. As we increase the mass of the sphere, the observer would feel an increased attraction from the direction of the sphere in proportion to the factor f_g . If the observer was trained only in Newtonian mechanics, he/she would report that the sphere was increasing its mass to an amount equal to what we now call effective mass. However, if the observer could view and count all the gravions arriving at the test particle, then he/she would report no change in all directions but from those in the solid angle subtended by the sphere. In more detail, it would be reported that a maximum variation (depletion) comes from the center of the sphere. In the case of observation from a point at 100 radii from the gravitating sphere, the directional depletion of gravions would correspond to the gravitoid shapes calculated by PG theory in Fig. 113. A PG observer would report that a net push is experienced from the opposite direction of depletion. The Newtonian observer would report only an attraction by the visible spherical geometry (real one) with an apparent mass coming from the entire sphere, although it could be pointed out (with PG hindsight) that an equal effect could result from the real mass contained in the said gravitoid (unknown to the Newtonian observer).

Since we introduced the possibility of the effective mass playing the role of “inertial” mass in Section 14.5, which was not anticipated when the concept was first introduced in Part 1, it is helpful to review and clarify the following (even with some repetition): The effective mass and density are initially distributed uniformly over the real volume of a sphere and produce the measured (Newtonian) acceleration (or force F) at any external point. However, there exist a greater real mass and density also distributed uniformly but with a part of it being shielded from gravion action and without inertia; this part is probably the “stuff” of black holes, but possibly also ever present along with “ordinary” effective mass. We have also devised an effective spherical volume (smaller than the real volume), which, filled with real mass, produces the same Newtonian force F . Furthermore, we have devised gravitoids, which, filled also with real mass, produce the same force F . Since we attached a special interest to the effective mass, we have also become interested in finding its actual distribution inside a sphere (or line segment). Effective mass is created, where a gravion is absorbed. The outer layers are the most active with diminishing effect towards the center of the sphere. We have found the internal distribution for a stationary sphere relative to an observer (or small test mass) inside the sphere. However, for an external observer, the distribution of effective mass starts with highest concentration at the opposite end of the chord relative to the observer. Eq. 170 was derived for this purpose. Plotting the latter distribution (no need to be shown here) yields corresponding curves as in Fig. 20 but for the full line (chord) length. It is this distribution, which directly describes an important physical process, whilst other parameters are only mathematical tools and notions helping in the development of PG. We also note that we introduce a kind of relativity with respect to the observer's location: At a point outside the sphere, only the interactions of gravions inside the subtended solid angle by the gravitating body enter in making the force F , whereas at a point inside the sphere all gravions from all directions are involved in finding the internal force F . With all these clarifications, we realize that increasing the density of a material sphere produces a Moon-like meniscus of effective mass towards the outer surface away from the observer, or correspondingly, a gravitoid (imaginary) meniscus of real mass towards the near side of the sphere to the observer. For an observer inside the sphere, we report a maximum concentration of effective mass towards an envelop close to the surface of the sphere (probably the “event horizon”). In all cases, the geometrical integrity of the sphere remains invariant, whilst it is only the amount and distribution of effective mass that varies by Eq. 145 towards some extreme state (and effective shape), which might correspond to certain mathematical outcomes by GR.

The above is according to PG theory about the effects of increasing the mass (and acceleration) to very high levels, which is an analog to the paradigm of relativity, but without establishing any relationship between the two theories yet. We only establish a concept of contraction in PG, more precisely a concentration of effective mass, possibly corresponding to a contraction of length in relativity. Clearly, these two kinds of contraction are two different things, but they may share a common underlying process, which GR is not telling us about, but which PG is being built on. It is said(?) that in GR time dilation and length contraction near a massive body are not the same as time dilation and length contraction at relativistic speeds. Correspondingly in PG, we may not say from the outset that the contraction factors derived for a stationary body are the same for a moving body at relativistic speeds. However, it is reasonable to envisage that as we increase the speed of a moving sphere, the amount of gravion intensity traversing and interacting with the sphere increases with concomitant increase of the effective mass and variation of its distribution (see Eq. 145). That means that there is a correlation and possibly a relationship between speed v and kR . It is the task of PG to establish such a relationship, if it exists. Pending such rigorous development though, it can be helpful to attempt and try some intuitive steps as a kind of advance scouting exercise.

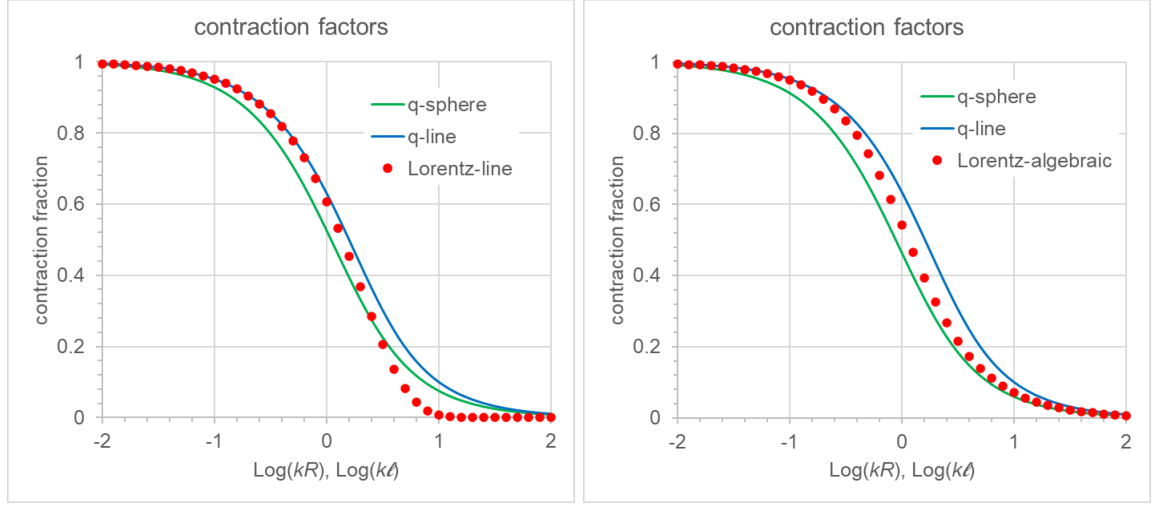


Figure 22: Comparison of PG contraction factors q -sphere (q) and q -line (q_ℓ) with Lorentz factor fitted with A_ℓ from line segment (left) and algebraic sigmoid (right)

For a possible connection between PG and relativity, we can initially try to express the PG contraction factor as a function of velocity, or the velocity as a function of kR , since we already have the function of $q(kR)$ (per Eq. 50). We try the latter by proposing some impromptu functions for the ratio of velocities v^2/c^2 in the Lorentz contraction factor $L(v^2/c^2)$

$$L = \gamma^{-1} = \sqrt{1 - \frac{v^2}{c^2}} \quad (180)$$

We note that both types of contraction (in PG and relativity) are functions of the same form (sigmoids) varying between 1 and 0. We inquire, if v^2/c^2 can be expressed as a function of kR preferably without a “fudge” coefficient to bring both $q(kR)$ and $L(kR)$ to agreement. Fudge coefficients are often detested and preferably avoided. We further note that the absorptivity factor A_R has a sigmoid form without any arbitrary constant to “fudge” with, which conveniently prompts us to try first by simply setting:

$$\frac{v^2}{c^2} = A_R = 1 - \frac{1}{2(kR)^2} + \frac{\exp(-2kR) \cdot (2kR + 1)}{2(kR)^2} \quad (181)$$

The result is plotted in Fig. 21 with curve points (in red) labeled “*Lorentz-sphere*” along with the two PG contraction factors for sphere $q(kR)$ and line segment $q_\ell(k\ell)$. There is an immediate very good-to-excellent agreement between “*Lorentz-sphere*” and “*q-sphere*”. This is very encouraging and may be used as guidance to proceed further with PG.

We can also try to replace the Lorentz velocities ratio with the absorptivity factor of line length per Eq. 156:

$$\frac{v^2}{c^2} = A_\ell = 1 - \exp(-k\ell) \quad (182)$$

and plot the outcome (*Lorentz – line*) together with q – line and q – sphere as before in Fig. 22 (left). We now see a significant deviation from both q – sphere and q – line. Actually, there is good agreement with about the first half of the q – line curve. The deviation is surprising at first, but considering that distribution of mass and shape in a body are important in PG, the outcome may be justified. It could be that both q – line and q – sphere are correct, whilst all other body shapes may be characterized by curves lying in-between those two. In that case, if PG can express the correct contraction for any shape, then the Lorentz contraction may be a good approximation of reality, either for sphere or line segment, but not an exact one. The shape of the accelerating body does not appear in relativity(?).

For good measure, we have also tried several other sigmoid fitting forms, like the so called “generalized logistic”, “hyperbolic” and “algebraic” sigmoid functions. All failed to produce any reasonable or better fit, except for the algebraic function:

$$\frac{v^2}{c^2} = f(z) = \frac{z}{\sqrt{1+z^2}} \quad (183)$$

where z is the product of some characteristic *length* times the absorption coefficient: $z = k \cdot \text{length}$. The outcome is provided in Fig. 22 (right). Interestingly, the Lorentz factor fits well with $q - \text{line}$ at low values of z and well with $q - \text{sphere}$ at high values of z , with transition values in-between.

If the “*Lorentz-sphere*” fitting curve in Fig. 21 is the correct one, then we could write that:

$$q = \frac{3A_R}{4kR} \approx \sqrt{\left(1 - \frac{v^2}{c^2}\right)} \quad (184)$$

which could herald an initial (tentative) expression of the PG contraction factor as a function of velocity. If in any way it can be shown that the PG contraction is equivalent or near equivalent to the relativistic contraction, then it could have enormous consequences in physics. It is impractical to exhaustively mention and discuss all those consequences here. A lot of work should follow. In the meantime, we may provide some tentative thoughts about the significance of the above findings.

First, some serious questions arise, which can have critical repercussions not only for PG but probably also for GR. The discussion of these questions will determine if PG and GR can coexist and complement each other, or one of them has to give way to the other.

In one aspect and by way of Eq. 184, it follows that an increased speed is accompanied by an increase of the absorption coefficient k for a fixed body radius, or length. This means an increase in mass or density. This means that the relativistic mass is not simply a mathematical intervention to enforce the light speed limit. The relativistic mass can be an effective mass increasing with the speed of the body.

It may be argued that no such new mass is consistent with experiment. For example, in the Large Hadron Collider at CERN, both Xe and Pb ions are accelerated to energies of about 2–4 TeV and nothing seems to happen to the ions. However, we may wonder, if all is taken correctly into account in arriving at such a conclusion. By no means do we challenge that conclusion here, except to draw attention to the possibility of other parameters playing a role too. For example, it is said that two “up/down quarks” are found in “ordinary” matter, but another four “other types of quarks” are found only in accelerator collisions. It is not clear why this happens (at least to the present author). Could then accretion of mass take place in nuclear and sub-nuclear structures that do not alter the macroscopic appearance of matter? If the PG “real mass” contains one active fraction (effective mass) and one inactive fraction without classical inertia, could we then allow and account for mass accretion in an accelerated ion beam in the LHC experiments?

Therefore, it seems that accelerating a body to relativistic speeds is equivalent to increasing its mass to an asymptotic upper limit, but not to infinity. We may initially surmise that the effective mass is gradually created and redistributed preferentially in the direction of motion. The increase of effective mass could only come about by a concomitant increase of the total real mass at fixed g_0 . The length itself in the direction of motion does not actually contract, but the amount of effective mass is compressed close to the head of the moving body and away from its tail. This is a point of fundamental departure from GR preaching that the actual mass does not increase, since there is only one mass, namely, the rest mass, whilst the physical length contracts. Theorists insist that relativistic mass per se has been thoroughly deprecated from the outset of GR, whilst it was introduced mathematically only to make the limit of speed of light look natural. However, PG can accommodate, literally, an actual increase of mass, namely, real mass, part of which constitutes an increasing amount of effective in lieu of relativistic mass. There is a balance between the rate of accreted and the rate of re-emitted mass according to a forthcoming Eq. 199. This novel finding of PG could resolve a persisting debate (or misunderstanding) and revolutionize the understanding of relativity.

There is no doubt that the problem of mass is one of the key problems of modern physics, whilst one wonders why the “debate” or corrective steps on the meaning of relativistic mass has continued since the inception of GR. Even notables like Penrose and Hawking did not come clear on this issue for whatever reasons (Okun, 2006). The relativistic mass may not be a “pedagogical virus”, after all, it might be a common sense reality. More about the concepts of mass and force have been worked out in Section 16 with a possible explanation on how new matter could be generated in particle accelerators. That is, the particle mass can acquire an effective mass over and above the maximum permitted outside the accelerator. The latter creates an artificially increased value of g_0 , so that when the particle decelerates at the end of its journey, it has to shed the extra mass in the form of new particles inside the accelerator. This re-adjustment of particle mass continues as long as it violates the PG law of maximum effective mass. ~~The artificially increased value of g_0 is understood to originate during acceleration via a mechanism not yet described at this point.~~ The extra effective mass accrues during acceleration but more details are now presented in Section 23 after we also consider the electric field under “push electricity” (PE) in Section 21 and other developments.

In another aspect and by way of Eq. 184, we may have another more serious conflict between PG and GR: The Lorentz factor necessitates an arbitrary increase of the relativistic mass, as we approach the speed of light. That would require PG to be able to also increase the effective mass to infinity, correspondingly. However, PG anticipates an upper acceleration limit g_0 for a stationary body. If accelerating a body by motion is equivalent to accelerating it by a nearby massive body, then either PG, or GR, or both should be adapted to produce equivalent outcomes. It is unclear if this is possible at this stage of development, especially if GR rules out(?) relativistic-speed and nearby-massive-body equivalence. May be this equivalence breaks down at relativistic speed extremely close to the speed of light. May be GR cannot be verified too close to the speed of light. May be GR needs to modify its prediction from an infinite relativistic mass to some maximum (limiting) value relativistic mass corresponding to a PG upper limit of acceleration and effective mass. The alternative for PG is to think of a way (formulation or whatever) that increases the amount of absorbed gravions to infinity as we get too close to the speed of light, something waiting to be worked out. As a last resort for PG would be to apply superluminal speeds of the body absorbing an arbitrarily increasing amount of gravions, but not likely. After all these combinations of possibilities, it is also quite possible that all three curves in Fig. 21 are valid considering that contraction factors may not be the same for a moving body at relativistic speeds and for a nearby massive body! This means that the Lorentz contraction factor for a moving body remains to be found in PG.

In summary of above ideas, PG may anticipate that all gravions swept at the head of the moving body are (near) totally absorbed, whilst (nearly) no gravions are absorbed at the tail, when motion is very close to the speed of light. Total absorption occurs at the limit of maximum acceleration g_0 , at some maximum effective mass $m_{\text{max-moving}}$, or density $\rho_{\text{max-moving}}$ and provided that the real geometric integrity of the body is preserved, i.e. the radius for a sphere remains constant; otherwise, the situation becomes more complex. The details for such outcomes remain to be worked out.

Whilst GR has been verified on many occasions, it is not known (at least to the present author), if it has been verified at speeds somewhere sufficiently close to the speed of light. Could it be that the Lorentz factor is an approximate manifestation of another “contraction” process as now described by PG? It may be that one of the two theories is the true one, whilst the other is an approximation. They both appear to converge (agree) at low enough speeds (whilst disagreeing on the meaning of relativistic mass), but they are in conflict too close to the speed of light. For a proper answer, we have to wait until PG is put to the test for verification or not, while we also continue to develop it theoretically.

We are aware that we did not derive the Lorentz contraction factor above from PG principles, except to demonstrate the possibility that the PG contraction factors may already describe what the Lorentz factor exists for and much more. We have derived, hopefully, equivalent contraction factors and the Schwarzschild envelope without even resorting to relativity yet. At the outset, we have added the postulates (or principles) #5 and #6 provisionally on the assumption that PG may be built as an expansion of relativity taken for granted. Furthermore, a significant discussion on postulate #3 is presented and proposed in the following sections of Part 2, which could make this principle redundant too. Part 2 of this report is an open-ended discussion towards elaboration of a fully fledged, self contained PG theory and practice.

We are pioneering a totally new ground with PG necessitating a re-examination of a large number of problems in physics. For another example, the new concept of PG contraction factors could provide another understanding of the Michelson-Morley experiment. There is a need to re-trace the founding steps of relativity in order to juxtapose them with those of PG and explain why the two theories result in similar but also mutually exclusive outcomes in an increasing number of cases. There is both commonality and departure between the two, like between PG and Newton, and like GR and Newton. Which one is the bigger one? There is a lot of work (rework) to be done by re-visiting a lot of outstanding or seemingly established topics in physics. For one thing, though, so far PG demonstrates a lot of promise with fresh ideas and outcomes.

In the preceding analysis, we advanced some bold assumptions and assertions not necessarily exhausting the gamut of possibilities under PG. That means that we may continue to try and reconcile the aspects of PG with prior prevailing theories on the nature of matter, mass, energy and inertia. For example, see some additional aspects possible in Section 19. All options remain on the table. For this reason, it should be appreciated that the current single-author advancement of PG ideas has its limits, which can be overcome by the participation of the broader scientific community.

15 Response to criticisms

As mentioned at the outset of this report, there have been numerous objections to the idea of push gravity since the original proposal by Fatio. This has applied to all hitherto variants of PG, but it is hoped that all these objections may be overcome in part by the preceding findings and in part by some new arguments and models presented in this Part 2. Most of the objections may be overcome without further ado, but the

main problem of energy absorption and mass accretion can only be tackled speculatively at this point, if we have to face the dilemma of abandoning the preceding findings, or advancing forward on those findings. The best known objections, as outlined in this referenced version of Wikipedia contributors (2018), are discussed next.

15.1 Weak absorption, range and gravitational shielding

Whilst early conceptions of push gravity maintained that it was mandatory to assume very minimal absorption of gravions in order to avoid the objectionable gravitational shielding, it is exactly the opposite consideration that frees push gravity and explains some of its intrinsic workings. Gravitational shielding or self-shadowing by mass is now at the core of the workings and understanding of PG. This is not something to object to, because via and by its presence we can actually derive the gravitational law, in fact, in a new form that can account for a lot of missing information in Newtonian mechanics including singularities.

By the same token, gravitational shielding leads to a distinction between real and effective mass, which, in turn, may lead to a re-appraisal or re-think of the notion of inertia and mass per Section 14. When we can faithfully describe the observed motion of bodies with a theory of the dynamics of PG, we will finally put this objection to rest, unless we better achieve verification of PG by experimental means first.

15.2 Equivalence Principle

The allegation that PG would violate the Equivalence Principle must have been a misconception in view of our previous explanation. PG actually frees us from having to resort to the Equivalence Principle, which arose out of the need to understand the nature of force initially perceived as arising either from a gravitational field or from a moving mass under acceleration by an applied external force. PG finds no distinction between these two kinds of force, as the flow of gravions produces the same force in both situations (systems). For the first time, we have a tangible explanation of the **phenomenon** of equivalence of force. The gravitational force experienced by a body as attraction (pull) is actually a push force, namely, the sum total of all elementary push forces distributed in the bulk of the mass and arising from absorbed gravions. The latter force is of the same nature as the push force applied to a hypothetical elevator in free space, inside which we would experience an equivalent force. This equivalent force need not be such (equivalent) axiomatically, because it is “prima-facie” push in nature. Hence the Equivalence Principle per se vanishes without ever being in conflict with PG.

Nevertheless, if the Principle emanates from (or is based upon) the equality of the gravitating mass to the inertial mass, then PG is clearly at variance. However, PG quantifies the variance as being extremely small to easily detect in the human laboratory, but, hopefully, big enough to measure in flyby experiments and planetary orbits. If the EP is described as equality of masses (gravitational and inertial) then PG clearly violates it. Conversely, if PG provides the true relationship between the two masses via $m_e = qm$, then EP violates nature and becomes redundant under PG. Expressed differently, if “equivalence” means true proportionality but not equality, then PG provides exactly this proportionality in a tangible, physical and explanatory form.

The above ideas summarize the analysis of Section 14.2, but we should also stress that the EP seems to be only an arbitrary approximation for scales of our immediate experience. This approximation breaks down at very large masses, or densities. Large densities occur in white dwarfs, neutron stars and black holes (large scales), but they also occur at nuclear and sub-nuclear particles (small scales). Thus, the finding that EP clearly breaks down at quantum levels (Kajari *et al.*, 2010) may not be a mere coincidence, but a great consistency with our independent findings on EP. The inertial and gravitational masses are not equal, whilst the original “gedanken” conception of the EP is now redundant needlessly locking down further development of physics for over a century.

Finally, in view of the possibility to decipher the meanings of matter, inertia and mass per Sections 14.5 and 16, PG appears to be on strong ground but not necessarily consistent with the EP, or with the theory of relativity in every respect.

15.3 Theory of relativity

The prior text of this section is retained for historical completeness but has been crossed out in the present version. It was written at an early stage of the development of Push Gravity (PG), when it was reasonably anticipated that PG might ultimately need to be embedded within, reconciled with, or derived from General Relativity (GR), or that both theories might represent complementary descriptions of the same underlying physics.

Subsequent years of extensive analytical development and application of PG—culminating in the present version (v28)—have demonstrated that this presumption is no longer necessary. Push Gravity has emerged as a self-contained and internally consistent physical framework, founded on a small number of clearly stated principles, capable of accounting for gravitational phenomena from the particle scale to cosmological distances without reliance on relativistic postulates or spacetime geometry. An example of an application to cosmology can be found in a separate article by Danilatos (2025).

This reassessment was prompted in particular by subsequent theoretical developments and exploratory applications of PG to extreme compactness regimes and cosmology, where PG admits very large but finite gravitational redshifts, a finite minimum mass for a true black hole to form, and an emergent redshift-distance relation without invoking spacetime expansion. These results arise within a self-contained PG framework and would be difficult to accommodate naturally if PG were treated as subordinate to, or derived from, GR.

While GR has historically been invoked as a basis for criticizing or dismissing push-gravity-type theories, the results developed in this work now allow such criticisms to be addressed directly and constructively within the PG framework itself. The reader is therefore advised to regard the crossed-out text below as an expression of the author's earlier intent to seek harmony with relativity, rather than as a reflection of the present theoretical position. Full appreciation of this evolution requires consideration of the work as a whole.

It has been argued that PG is incompatible with the established theories of relativity. It is often argued that since the general theory of relativity (GR) is continually verified by contemporary measurements with great accuracy, PG not emanating from within GR must be wrong. However, the counter-argument may be that PG is a re-appraisal of classical Newtonian mechanics, upon which to build and extend the current relational developments of relativity. PG explains the generation of a gravitational field around a mass that presumably can be observed and measured identically with existing data. We would suggest that it is prejudicial to think that PG has to arise out of (or fit in) GR, whilst the opposite might be true. Therefore, the two theories may not have to be in conflict upon closer examination.

If gravions travel with the speed of light, then in the steady state, they establish a pushing field that fictitiously appears as an attractive field around the shadowing (gravitating) mass. This field is being established at the speed of light without emanating from the mass, but rather emanating from the surrounding universe. If the mass starts moving at speeds comparable to the speed of gravions (and light), then there will be a disturbance of the surrounding shadowing or warped space (field) due to a time lag that propagates at the gravion speed. This disturbance would be consistent with the gravitational waves scientists are trying to detect.

An analogy may be found in solid state physics near a PN-junction, where “holes” are formed from the absence of electrons on one side of the junction with an equal amount of excess electrons on the other side. These holes are treated, or behave, like a positive current of charge moving in the opposite direction to electrons with negative current. GR then is like it is treating gravity as gravion-holes apparently emanating from (or associated with) the mass, whilst in reality it is the real gravions (particles) moving in the opposite direction towards the gravitating mass that should be considered, or equivalently considered. The end result (force and acceleration) appears to be the same by both approaches. Both ways of creating a field around a mass presumably create identical apparent outcomes.

We propose then that the gravitational field described by PG and the field described by GR are quantitatively identical at every point around a stationary material body. The difference is that PG tells us how/why this is formed (i.e. its origins), whilst GR remains mute about the origin of the same field, but it yields verifiable measurements, anyway. The latter is sometimes described like “GR generates correct results for the wrong reasons”. However, knowing the origins of gravity is a fundamental difference between GR and PG that could get us over the existing barriers in physics.

When we start applying PG to moving bodies with significant speed relative to the speed of gravions, then we may be able to borrow the mathematical tools already developed for relativity, special and general, to describe the same resulting effects and measurements. There is probably no restriction to the importation of Special Relativity as is. The mathematical derivations and achievements of GR may also be transferred and used in PG, in particular as they relate space and time. This transfer might be particularly useful where GR actually succeeds and discarded where GR fails (e.g. at very long distances, etc). The present work has only dealt with PG in the steady state without ever involving time effects yet. Therefore, it might be premature to argue that the two theories are in conflict.

Arguments of the type, for example, that because the Mercurial precession can be explained by GR is proof and manifestation of the success of GR should by no means be used to oppose PG. The same fields being established also by PG should arrive at the same outcomes. In fact, PG provides a new framework to

re-appraise the contributions of other planets on Mercury's precession by expanding classical mechanics with PG, which may produce a further refinement of the same calculations taking into account the real density and mass distributions of all the planets contributing to this precession. The other argument that the Sun bends the star light is not the privilege of GR only, because PG can do the same thing on photons by the pushing gravions presumably at the same (correct) deflection angle.

If at first sight the above assertions might seem simplistic, it is because there is a large volume of phenomena to be understood under PG, before we make further assertions. For example, could the temporal part of the metric in relativity, which determines the rate at which clocks tick and is responsible for Newtonian gravity, relate to the rate of gravion flux intensity? Could the increase of mass (relativistic mass) of a moving body as it approaches the speed of light be tied and explained in the new terms of real and effective mass? Should we, perhaps, re-appraise the meaning of inertial mass in conjunction with the meaning of matter and "stuff"? In general, could the theoretical concepts of relativity achieve an embodiment in PG theory?

The above important questions together with issues raised in Section 14 may now be better understood in the hope to further an inquiry into the novel PG theory. We may be faced with any of the following outcomes: (a) PG and GR may complement each other, (b) GR may be expanded to incorporate PG ideas, (c) PG may replace GR as an all inclusive description of experience, or (d) PG becomes unsustainable. The examination of these possibilities is the next challenge that we face for building a dynamic PG. The preceding trials may serve to provide some indication of what may come next. Clearly, such a task is huge and falls outside the capacity and resources of a single author. Hopefully, the learned adherents of GR can make a critical contribution.

In summary to the related objections, relativity may not be presented as reason for rejection of PG. Even if it appears that PG is not consistent with certain established ideas of GR, the "jury remains out" until sufficient experimental evidence is gathered in support or not of PG. It may ultimately be that there is a substantial overlap or correspondence of ideas and conclusions between PG and GR, but also with a fundamental departure between the two theories from some point onward (see Section 16).

Important (as of version 22, 2024): During the development of PG up to the current stage, no use of special or general relativity has been made. For a static PG, we only need a stationary observer to report on the sum-total impulses recorded from all directions by the arriving gravions. The measurement of force is the starting premise of the theory, while no use of transformations between reference frames is required. This does not mean that we oppose relativity, other than PG being possible to develop consistently without resorting to the founding principles of relativity. Early attempts to initiate a dynamic PG seem promising. It may be possible that relativity can be deduced from PG theory.

15.4 Drag

It has been argued that push particles (original ultramundane corpuscles) would introduce a drag force on the orbiting Earth, eventually slowing down the planet to ever closer orbits around the Sun. This would indeed be a consequence, if the particles were acting like classical mechanical balls. However, the gravions are relativistic with no difference in speed relative to the planet motion. Gravions are not expected to make a difference over any effects already experienced with photons over the broadest spectrum of wavelengths originating from outer space.

In view of the attempted explanations on the nature of matter, mass, energy and inertia in Section 14, it is implied that the gravions have no drag on the effective mass being energized (generated) by the very same gravions. This is an assumption pending further investigation on the nature of gravions and their interactions with real mass and with themselves.

Further work on PG (see later versions of it) has now advanced an even better understanding of mass and matter (hyle). Attempts have been made to find a relationship between absorptivity and speed, a relationship between mass and speed, and a relationship between mass and hyle. It seems that we may be able to derive some relativistic relationships from the premises of PG theory. We have found that while gravions (and hyle) are being absorbed, hyle is also concurrently emitted by a moving body with a steady state established at constant speed. The net variation of hyle (and mass) takes place only during acceleration (deceleration) of the moving body. It seems that PG may be self sufficient in explaining away the "drag problem" without even having to resort to the special theory of relativity. It should be appreciated that this work remains incomplete needing contributions by many other workers (and time) before uninterested parties rush to dismiss it out of hand on this or that account from the perspective of prior theories.

An alternative explanation of the presumed "drag problem" is now presented in Section 30.6.

Drag is predicted by existing theories, i.e. an object at a constant velocity will eventually come to a halt, albeit extremely slowly (see <https://www.youtube.com/watch?v=lcjdwSY2AzM>). This prediction then may be due to, and account for the small drag "feared" for gravions and used to criticize or oppose PG.

15.5 Superluminal speed

During the early stages of push gravity theories, the hypothetical corpuscles were required to have some superluminal speed to reduce the expected drag to a practically ineffective minimum. However, this is not required in the light of the present arguments against the perceived problem of drag.

15.6 Orbital aberration

It has been further argued that PG would introduce orbital aberration due to the finite speed of gravity created by gravions. This aberration would tend to accelerate an orbiting body away from the other, unless gravity propagates much faster than the speed of light, or must not be a purely central force. It has been further argued that the same finite speed of gravity problem is almost exactly canceled by the mathematics in GR. Now, it is not clear why PG cannot overcome this problem in the same way, if GR can. It is proposed that we may continue to use and adapt aspects and derivations of GR, or postulate an equivalence between GR and PG (at least in part), until it can be finally clarified if this is at all appropriate, or under what conditions.

Nevertheless, recent measurements report that planetary orbits are widening faster than if this were solely through the Sun losing mass by radiating energy. This results in an anomalous increase of the astronomical unit, which might then be explained by the above PG criticism pending further analysis of the situation.

As discussed in Section 14.4, and until we can quantify time effects, PG theory remains incomplete. Any verdict can be postponed, until at least some tests are done to possibly verify the principle of PG.

15.7 Energy and mass considerations

15.7.1 Single sphere absorption

Basically, the most serious criticism arises from the need that the gravions must be absorbed in order to produce a force, but the amount of energy absorption would then be so high as to be unsustainable by the gravitating body. This is the main reason, for which notables like Kelvin, Maxwell and Poincaré (Wikipedia contributors, 2018; Poincaré, 1908), after initial consideration, moved away from PG. There is no obvious or immediate solution to this major problem haunting any PG theory. For this reason, we based the entire development of PG on the assumption that the absorbed energy is somehow re-emitted. However, until some experiments provide encouragement at least, we are entitled to speculate with some improved models in continuation to previous attempts to overcome this hurdle. Let's first formulate the energy absorption problem based on derivations in Part 1.

We find the total energy passing per unit surface area of a sphere and absorbed by the bulk in the sphere: We start with the absorbed gravions (energy) inside the solid angle subtended by the sphere at point O (see Fig. 2), which is given by the previously defined J_a (not J_g):

$$J_a = J_0 f_a = J_0 \int_0^{\varphi_0} 2\pi \sin \varphi d\varphi \cdot [1 - \exp(-k\ell(\varphi))] \quad (185)$$

$$J_a = 2\pi J_0 \int_0^{\varphi_0} \sin \varphi \left[1 - \exp \left(-2kr \sqrt{a^2 - \sin^2 \varphi} \right) \right] d\varphi \quad (186)$$

The above provides the per unit area absorption at each gravion trace direction (not the per unit area of the surface of the sphere). However, at the surface of the sphere (with $r = R$ and $a = 1$), for the absorbed flux density per unit area of the sphere, we must apply the cosine law for oblique incidence and multiply by $\cos \varphi$ yielding the parameter J_{aR} :

$$J_{aR} = 2\pi J_0 \int_0^{\varphi_0} [1 - \exp(-2kR \cos \varphi)] \sin \varphi \cos \varphi d\varphi \quad (187)$$

which can be integrated analytically as per Eq. 41 including the established absorptivity A_R :

$$J_{aR} = \pi J_0 A_R \quad (188)$$

The above provides the absorbed density flux per unit area of the sphere from all directions inside a hemispherical solid angle, i.e. by integrating from 0 to $\pi/2$. Thus, we multiply by the surface area of the sphere to obtain the total absorbed density flux, i.e. the total energy per unit time, or power W as:

$$W = 4\pi^2 J_0 A_R R^2 \quad (189)$$

By replacing J_0 from Eqs. 73 and 78:

$$J_0 = \frac{cg_0}{\pi\Lambda} = \frac{cg_0 M_e}{\pi^2 R^2 A_R} \quad (190)$$

we finally obtain

$$W = 4cg_0 M_e \quad (191)$$

from which we have an energy absorption rate per unit effective mass W_{M_e}

$$W_{M_e} = \frac{W}{M_e} = 4cg_0 \quad (192)$$

If we want to use the equation $E = mc^2$, the above energy is equivalent to a mass accretion rate per unit mass:

$$mass_accretion_rate = \frac{4g_0}{c} \quad (193)$$

from which, depending on the prevailing g_0 , we find the absorbed energy. With a moderate level of $g_0 = 10^4$ m/s², we would get about 1.3×10^{-4} kg for every kg of the sphere (say, Earth) every second. This is clearly an enormous amount of energy (mass) that cannot be accounted for by our experience on the planet. An early criticism leveled against PG claimed that the absorbing mass would be doubling every second. This criticism is generally valid even with our much lower accretion rate found here, which we can formulate as follows:

If we again borrow the “ $E = mc^2$ ” equation, we use Eq. 191 to find this accretion or decay as a function of time:

$$W = \frac{dE}{dt} = c^2 \frac{dM_e}{dt} = \pm 4cg_0 M_e \quad (194)$$

$$\frac{dM_e}{M_e} = \pm \frac{4g_0}{c} dt$$

$$\ln M_e = \pm \frac{4g_0}{c} t + constant$$

$$M_e(t) = M_{e0} \exp\left(\pm \frac{4g_0}{c} t\right) \quad (195)$$

where $M_{e0} = 4\pi^2 J_0 A_R R^2 / 4cg_0$ is the initial effective mass at $t = 0$ s, when we imagine a cessation of mass emission or a cessation of the gravion field (mass accretion). This “initial” mass is the effective mass we have introduced up to now, which, for the record, can be expressed also by:

$$M_{e0} \equiv M_e = \frac{\pi^2 J_0 A_R R^2}{cg_0} = \frac{\pi R^2 A_R}{\Lambda} = \frac{S_{xsection} A_R}{\Lambda} = \frac{S_{a-xsection}}{\Lambda} \quad (196)$$

where $S_{xsection}$ is the geometric cross-section of the sphere and $S_{a-xsection}$ is the absorption cross-section.

Eq. 195 provides a time constant $t_0 = c/4g_0$, in which the mass increases by $e = 2.718$ times the initial value or decays to $1/e = 0.368$ of its initial value M_{e0} . Equivalently, the mass doubles or halves in time $t_{double} = t_0 \ln 2 = t_{half} = -t_0 \ln(1/2)$. Caution is drawn to the possibility that these rates of absorption and decay may characterize the process only around the equilibrium point of the steady-state condition; the entire process of effective mass emergence from real mass, or the decay of effective mass back to real mass may be a multi-staged process, a topic for further study.

The characteristic time constants t_0 , or t_{half} , or t_{double} are additional fundamental constants along with g_0 , J_0 and Λ all directly relating with each other.

To continue with numerical examples, we may use the tentative value of $g_0 = 30000$ ms⁻² (say, from a “claimed” Allais effect measurement) and with $c = 3 \times 10^8$ ms⁻¹, we get $t_0 = 2.5 \times 10^3$ s (i.e. 41.7 min) and $t_{half} = t_{double} = 1732.87$ s, i.e. 28.9 min. This is akin to radioactivity, the theories of which may also be better understood on the basis of PG. [Curiously, the decay time of free neutrons falls within the range of the given numerical example. The mean lifetime of a neutron is 879.6 s, which curiously is about half of the preceding halftime]. Incidentally, we have considered only the energy-rates, but not the number-rate of absorbed gravions and the number-rate of emitted particles. These two number-rates are thought to be very different from each

other, presumably by many orders of magnitude. The mechanism for possible re-emission is discussed under considerations of the second law of thermodynamics in the next section. This issue will be the subject also of a quantum push gravity (QPG) theory later.

The above derivations about an absorbed energy (mass) that allegedly cannot not be re-emitted at a steady-state point are the most telling reason for the rejection of PG, as has been the case with mainstream physics to date. Therefore, this constitutes a critical point whether to continue with this theory or come to an end of this investigation once more. The present author is of the opinion to persist in finding some way(s) to push through this barrier, literally. That is because the preceding findings have produced a system of consistent outcomes with Newtonian mechanics as the limiting case, and because it promises to resolve many other cosmological problems on a new basis. At any rate, we investigate the “what if” case, the outcomes of which may be compatible with experience. We may recall an analog situation early in the 20th century, when the orbiting electrons should be emitting electromagnetic radiation, the lack of which did not deter the then visionary scientists to introduce and accept the orbital model of the atom. Thus, instead of rejecting the PG theory, we may have to accept that the dissipated energy by gravions manages somehow to escape out of the absorbing mass in a different form of radiating particles. A new motto could then be “*what goes in must come out*”, but catchphrases don’t make science on their own, unless they are confirmed without leading to another impasse: The above demand allegedly leads to another violation, namely, of the second law of thermodynamics, an objection discussed separately next.

Equivalent alternative formulations to derive the gravion absorption rate by a single (lone) material sphere are provided in Appendix D.2.1, etc.

15.7.2 Planetary absorption

The preceding analysis of energy absorption by a single sphere is further expanded for the case of two spheres in section 16, whereby we also find a relationship between force and mass. This finding goes beyond the criticism based on the alleged catastrophic energy absorption. It constitutes a novel understanding that can be used for the multi-body interaction, of which the planetary absorption is just one aspect of PG theory and should be treated in its own right.

15.8 Second law of thermodynamics

It has been argued that the gravions, if re-emitted as different particles to carry away the dissipated energy, would violate the second law of thermodynamics, which was the reason for rejecting the re-emission of particles/energy as initially (tentatively) proposed but abandoned by notables such as Kelvin, Poincaré, Lorentz and Thomson (Wikipedia contributors, 2018). However, if we look closer at the intrinsic meaning of this law, it may not necessarily be violated overall. This arises from the fact that the law relates to the most probable state of a closed system having the maximum entropy. The entropy S relates with the number of accessible states Ω via

$$\Omega = \exp(S/k) \quad (197)$$

(k here is the Boltzmann constant) and the probability P of finding the system in that state is

$$P \sim \Omega = \exp(S/k) \quad (198)$$

Now, when the system has a relatively small number of accessible states, the fluctuations can be very frequent, wide and repeatable, i.e. recurrence of unstable states may be quite feasible within the time scale of gravion frequency absorption. The consequence of this is that the system can often be found “momentarily” in a state of decreased entropy favoring the emission of some augmented (with accreted mass) particle out of the system. This happens when by random redistribution of mass and energy within the subsystem generates a sub-particle capable of overcoming the constraints that keep the subsystem together. When enough quantitative material and energy accumulation has occurred (accreted), the subsystem bounces emitting a new particle, all of this on an extremely short time-scale (appearing to us). The particles of the subsystem co-operate to get rid of and push out one of their own members every-now-and-then, often or not in the time scale of the subsystem. In other words, the second law of thermodynamics does not prevent us from accepting that matter/energy can be re-emitted after a number of trial fluctuations following a certain number of gravion absorption inside a proton, electron, neutron or any other nuclear, sub-nuclear, or elementary particle (subsystem). Thus, what was initially conceived by the critics as thermal dissipation inside matter in general, it will not appear as known chemical (molecular) heat that would melt and evaporate the planet. It would only appear as internal energy of a particle that is not thermally coupled with an atom or

molecule via some sort of recoil action during the said re-emission. The re-coil produced by the proposed re-emission is taken up and averaged out by the subsystem behaving under the established quantum mechanical laws. In fact, it might be that the underlying mechanism of quantum mechanical randomness may be caused exactly by such re-coil of the subsystems of particles. Electrons and nuclear particles move about randomly per quantum mechanics. This model further assumes that the re-emitted particles are also penetrating the surrounding matter out of the planet with a long enough mean free path as not to heat the planet catastrophically but not long enough as to act like gravions in generating gravity (i.e. canceling out gravity). It is only the very long mean free paths of gravions that generate gravity among planets and stars, while the second generation emitted particles, as proposed here, behave like a diffusing gas out of the planet, perhaps, with some but not catastrophic heat dissipation. It may be that part of, if not all, the heat in the core of planets is generated by this mechanism in an analogous way, in addition to, or in lieu of, the heat being produced by radioactivity per prevailing theories.

We need not at this point specify the exact nature of the particles being re-emitted, other than for them to be able to carry away the absorbed gravion energy, or a critical part thereof. It is left for further investigation by particle and nuclear physics to establish if any of the known particles qualifies to play this role, as for example, neutrinos might (or might not) serve this purpose. Alternatively, we may build on a new model to describe the properties and consequences of this second generation of particles emanating from the primary gravion flow.

In support of the above general proposal, we may cite a similar situation that explains radioactivity. Particles can rearrange in the nucleus, or change from one type to another statistically over time. Random quantum fluctuations can promote relaxation to a lower energy state and decay via quantum tunneling. Radioactive decay half-life varies over many orders of magnitude on a timescale down to 10^{-23} seconds (Wikipedia contributors, 2019e). In our proposed analog, we may envisage all sub-nuclear particles including protons, electrons, positrons, etc. to undergo such statistical fluctuations inside themselves at even extremely smaller time scales beyond the range of our measuring instruments, in effect, appearing like providing a continuous absorption of gravions and re-emission of secondary type-II particles diffusing in the surrounding material space without causing further gravitation or catastrophic heat. This continuous absorption then is tantamount to a continuous push without the feared catastrophic melting down.

The above proposed model should not be less plausible than the latest quantum fluctuation theories (Wikipedia contributors, 2019d). It is in accord with the fluctuation theorem and the ongoing discussion, research and experiments relating to Maxwell's demon.

Thus, the present framework in understanding gravity should not be inconsistent with modern theories. Quantum field theory is about very small stuff, small particles (the standard model). Gluons bind quarks together. Quantum gravity considers loops of gravitational force, then we get knots, loop quantum gravity and time disappears (problem of frozen time). These quantum states of space fluctuate, fluctuations in the quantum states of space create the appearance of time. These loops exist on the scale of Plank length. A proton contains 10^{65} quantum volumes, whilst gravitons is said to carry the force of gravity by exchanging them, (the photon carries the electromagnetic force, so the graviton carries the gravitational force), but gravitons are thought to be pseudo-force particles according to loop theory. The quantum nature of space does not allow singularities, whilst the universe did not come about with a bang but with a big bounce [Jim Baggott: <https://www.youtube.com/watch?v=dW7J49UTns8>]. All these latest conceptions might be further adjusted and advanced by the new understanding of PG, so that our approach should not be less plausible than all these other modern models and proposals. In fact, PG seems to be consistent with the above theories so that PG may act as a resolution by binding together of the best of elements in those theories.

Finally, if the main concern of PG theory has been the huge amount of energy or mass required to be absorbed in order to result in the measured acceleration on a planet, the likely revelation in Section 14.5 may help. In view of the idea of the creation of effective mass (Newtonian mass) by gravion absorption, the absorption becomes a blessing rather than a curse: The large absorption is consistent with a large presence of planet mass, however, subject to a balancing rate of outflow of the same energy. We proposed a mechanism for such an outflow via the fluctuation theorem above. In the steady state, the outflow must be proportional to the steady state effective mass m_e as in the general formulation found by Eq. 194:

$$\frac{dE}{dt}(\text{inflow}) = \frac{dE}{dt}(\text{outflow}) = \text{constant} \cdot M_e \quad (199)$$

Our "method" outlined in the Introduction accommodates macroscopic thermodynamics very well: At most elementary level of the cosmos, there is no friction, absorption, emission, etc. and no distinction between various forms of energy like thermal, potential, kinetic, mass-energy equivalence or whatever is said by prevailing theories. There are only invariable gravions (see Section) flowing around randomly. The so

called “thermodynamic death of the universe” has already happened at that lowest level. The density of gravions is on “average” steady, but there are at small and large scales. The average relates to scale. The fluctuations at the smallest scale do not violate the second thermodynamics law, but they complement it. Out of these fluctuations there occurs bigger fluctuations naturally, resulting in the lowest forms of hyle (matter) organization. The percentage of organized forms of hyle can be extremely low. The prevailing view is that only 5% of the cosmos is observed, while 95% is not. We may say that we do not actually know the true percentage of the observable universe. It can be much less than that, it can be less than 1%, or it can be less than 0.00001%. The latter percentage would not constitute any contradiction or inconsistency between our theories, in general, and reality, simply because no theory can be relied upon to tell us the ultimate constitution of the cosmos. The overall conclusion, herewith, is that we cannot invoke the second law of thermodynamics to oppose PG. This is more true without first developing PG; unless, in the process, we find compelling evidence disallowing further work.

16 Two-sphere variation of mass and force

In continuation to and based on preceding analysis, we can derive some important relationships between mass or energy and force for two material spheres. The energy absorption rate given for a single sphere by Eq. 189 is derived by the universal gravion intensity J_0 times a factor S_a . For a single (lone) sphere and according to Eq. 189 the latter factor is:

$$S_a = 4\pi^2 R^2 A_R \quad (200)$$

and is involved in the known relationships:

$$S_a J_0 = 4cg_0 M_e \quad (201)$$

$$S_a \frac{cg_0^2}{\pi^2 G} = 4cg_0 M_e \quad (202)$$

$$S_a = 4\pi^2 G \frac{M_e}{g_0} \quad (203)$$

The S_a is a characteristic surface area pertaining to the omnidirectional absorption of gravions from all directions around the sphere with radius R and can be also computed directly from the constitutional equations of gravion absorption provided in the Appendix. We will later see that this relates via a factor 4π to an effective cross-section for a classical unidirectional absorption of a beam of particles.

With S_a derived (or computed), we can then find the corresponding effective mass as:

$$M_e = \frac{g_0}{4\pi^2 G} S_a = \frac{S_a}{4\pi\Lambda} \quad (204)$$

We can readily ascertain that, S_a being an effective absorption area and the universal constant Λ being an area per unit mass, correctly yields a mass M_e . It is an important finding and understanding that the effective mass is the ratio of these two parameters. Note: $S_a = 4\pi S_{a-xsection}$ from Eq. 196.

Up this point, we have considered a single (or lone) material sphere, but this begs the question what happens in the presence of another material sphere at a distance r in the neighborhood. The answer is found by considering the constitutional equations of absorption simultaneously for the two spheres. This is done in considerable detail in the Appendix. We apply those methods here to three representative cases with a brief description of the approach. To discuss and understand what happens, we have computed in one case, by way of example, the Earth-Moon interaction as we vary the distance. In a second case, we repeat the same for two very dense spheres, one of which is very small. In the third case, we use two very dense sphere with both being also extensive (large).

We have developed and used two equivalent methods in the Appendix, namely, one integrating through the bulk of each sphere, the other around the surface of the sphere. This is possible by noting that for every internal point (in the bulk), all possible gravion traces must cross the surface. Conversely, all gravion traces through every point on the surface account for the entire bulk points twice (note that in Eq. 189, we used only one direction of flow at each point, so that we summed over the entire surface without dividing by 2).

With reference to the Appendix and related figures, we compute various fractions of gravion absorption pertaining to two kinds or classes of gravion traces or paths through each sphere. There is one class of traces crossing only one sphere, to which we refer with the term “single”, or “lone” trace. The other class of traces belongs to (i.e. they cross) both spheres, to which we refer with the term “joint” trace. Gravions along single

paths produce no net force as they travel in opposite directions in equal numbers. Nevertheless, they are absorbed by a certain amount in each direction along the chord length of a sphere, the total amount of which relates to certain effective mass. Gravions along joint paths produce a net force along the trace due to the unequal amount of gravions entering from the two ends of the chord. In addition, they are also absorbed by a certain amount in each direction, the total of which again relates to a certain effective mass. The task is to find both the net force exerted on one of the spheres by the other and at the same time the total effective mass of the sphere “created” by (or related to) the absorbed gravions.

At the outset, we need to choose one of the two spheres for investigation of force and total absorption. Let this be sphere_2 and let's apply the “surface” method of investigation to find the total gravions absorbed (we investigate the force afterwards). We consider what happens at every point O on the surface of this sphere and integrate over the entire surface for the total result of absorption relating to force or effective mass. A chord OC traversed by “single” traces yields an absorption factor $2(1 - \exp(-k_2 OC))$. However, if chord OC is traversed by “joint” gravion traces, the absorption factor becomes $(1 - \exp(-k_2 OC))(1 + \exp(-k_1 AB))$, where A_1B_1 is the jointly traced chord of the other sphere_1, with corresponding absorption coefficients k_2 and k_1 . We integrate at point O separately all single and all joint traces with respect to the azimuth and zenith angles around the axis normal to the surface of the sphere at point O:

$$M_{ar-single} = \int_{\varphi_1}^{\varphi_2} \int_{\theta_1}^{\theta_2} (2(1 - \exp(-k_2 OC))) \sin \varphi_z \cos \varphi_z d\theta_z d\varphi_z \quad (205)$$

The above outcome is the same for all points on an elementary surface annulus by rotation around the axis joining the two spheres at angle ω . This elementary surface is $2\pi \sin \omega R_2^2 d\omega$, so that by a final integration over this angle, we obtain the end result:

$$S_{ar-single} = \int_0^\pi M_{ar-single} \cdot 2\pi \sin \omega R_2^2 d\omega \quad (206)$$

We follow the same steps for the “joint” traces of sphere_2:

$$M_{ar-joint} = \int_{\varphi_1}^{\varphi_2} \int_{\theta_1}^{\theta_2} (1 - \exp(-k_2 OC))(1 + \exp(-k_1 AB)) \sin \varphi_z \cos \varphi_z d\theta_z d\varphi_z \quad (207)$$

$$S_{ar-joint} = \int_0^\pi M_{ar-joint} \cdot 2\pi \sin \omega R_2^2 d\omega \quad (208)$$

The total characteristic absorption surface is:

$$S_{ar-total} = S_{ar-single} + S_{ar-joint} \quad (209)$$

The notation “ $_{ar}$ ” in the subscripts above stands for “absorption” at distance “ r ”. Now, there is an important new quantity to consider. That is the difference between the total absorption of sphere_2 being at distance r from sphere_1 and the absorption that sphere_2 has when it is at infinite distance from the other, in other words, when it is away from the influence of any other bodies. We have already found the latter by Eq. 200. It is instructive to write the corresponding equations for this quantity starting with the corresponding factor for a chord OC. The “single” contributions cancel out leaving only the difference of the “joint” terms between the two situations. This is easily found to be $(1 - \exp(-k_2 OC))(1 - \exp(-k_1 AB))$, with which we can write the corresponding integrations:

$$M_{ar-netloss} = \int_{\varphi_1}^{\varphi_2} \int_{\theta_1}^{\theta_2} (1 - \exp(-k_2 OC))(1 - \exp(-k_1 AB)) \sin \varphi_z \cos \varphi_z d\theta_z d\varphi_z \quad (210)$$

$$S_{ar-netloss} = \int_0^\pi M_{ar-netloss} \cdot 2\pi \sin \omega R_2^2 d\omega \quad (211)$$

We use the term “net loss” to refer to this absorption in an effort to distinguish it from present (current) absorption taking place at distance r , because it does not exist, i.e. it is not current, but was present when the sphere was “lone” but now this amount of gravion absorption has gone missing. This is caused by the

r , m	$M_{er-single}$, kg	$M_{er-joint}$, kg	$M_{er-loss}$, kg	M_{e-sum} , kg	<i>Asymptotic loss</i>
12742000	5.9134E+24	5.8939E+22	$4.7876E+19$	5.9724E+24	$4.5098E+19$
25484000	5.9583E+24	1.4058E+22	$1.1431E+19$	5.9724E+24	$1.1274E+19$
50968000	5.9689E+24	3.4775E+21	$2.8281E+18$	5.9724E+24	$2.8186E+18$
101936000	5.9715E+24	8.6712E+20	$7.0524E+17$	5.9724E+24	$7.0465E+17$
203872000	5.9722E+24	2.1664E+20	$1.7620E+17$	5.9724E+24	$1.7616E+17$
407744000	5.9723E+24	5.4152E+19	$4.4043E+16$	5.9724E+24	$4.4041E+16$
815488000	5.9724E+24	1.3537E+19	$1.1010E+16$	5.9724E+24	$1.1010E+16$

Table 12: *Variation of various fractions of the Earth effective mass versus distance using $R = 6371000$ m, $k = 1.16248157479707E - 09$ m⁻¹ and $g_0 = 1000$ ms⁻² (CASE_1)*

r , m	$M_{er-single}$, kg	$M_{er-joint}$, kg	$M_{er-loss}$, kg	M_{e-sum} , kg	<i>Asymptotic loss</i>
12742000	6.3579E+22	9.8495E+21	$4.7876E+19$	7.3477E+22	$4.5098E+19$
25484000	7.1141E+22	2.3241E+21	$1.1431E+19$	7.3477E+22	$1.1274E+19$
50968000	7.2900E+22	5.7361E+20	$2.8281E+18$	7.3477E+22	$2.8186E+18$
101936000	7.3333E+22	1.4295E+20	$7.0524E+17$	7.3477E+22	$7.0465E+17$
203872000	7.3441E+22	3.5710E+19	$1.7620E+17$	7.3477E+22	$1.7616E+17$
407744000	7.3468E+22	8.9259E+18	$4.4043E+16$	7.3477E+22	$4.4041E+16$
815488000	7.3474E+22	2.2314E+18	$1.1010E+16$	7.3477E+22	$1.1010E+16$

Table 13: *Variation of various fractions of the Moon effective mass versus distance using $R = 1737000$ m, $k = 7.02425385602087E - 10$ m⁻¹ and $g_0 = 1000$ ms⁻² (CASE_1)*

perturbation of the universal graviton flux by the other sphere. We can then write the more general equation with these parameters as:

$$S_a \equiv S_{a-sum} = S_{ar-total} + S_{ar-netloss} = S_{ar-single} + S_{ar-joint} + S_{ar-netloss} \quad (212)$$

All this will be better understood and discussed looking at the results of the following three cases.

CASE_1 (Earth-Moon). The masses and radii used are taken from Table 3 together with their absorption coefficients from Table 2. We performed the above integrations separately for the Earth and Moon, each one being the sphere of investigation with regards to its own graviton absorption. The numerical results of the above integrals are better shown first in table form for all three factors for Earth and Moon in Tables 12 and 13. The distance is varied in multiples of Earth radius from 2 to 128 radii doubling each distance. Actually, we have converted the S_- parameters to an effective mass via the conversion Eq. 204, in order to make it more tangible with our familiar (perhaps) “mass” concept. These masses $M_{er-single}$, $M_{er-joint}$, $M_{er-loss}$ and $M_e = M_{e-sum}$ correspond to the terms of above Eq. 212.

We note that the variation of mass is small but significant within a few radii distance, but it approaches fast and asymptotically the “lone” mass, as we increase the distance; the sum of the three fractions of mass is constant with distance and equal to the lone mass, as it should. The “single” component increases, whilst the “joint” component decreases as we increase the distance, so that their sum is always much closer to the “lone” mass. We can see this by the variation of mass loss being 5 orders of magnitude for the Earth and 3 orders for the Moon at the shortest distance below the “lone” mass, whilst it becomes 8 and 6 orders of magnitude at 128 Earth radii. We further note that the net loss is the same for the Moon and Earth, as should be expected on account of the symmetry in the chords of the net loss factor. We investigate the mass loss also in graph form in Fig. 23 but by plotting the net loss of absorption factor $S_{a-netloss}$ on logarithmic scales for both axes. We have also added an extra four point up to 2048 radii distance to assist the look of a trendline. The fitted straight line ($y = -2.0048x + 22.33$) is indistinguishable from the computed curve indicating a strong inverse square distance relationship. We suspected that this overlap may be only due to a Newtonian approximation for this case; the absorptivity for Earth being $A_{R-earth} = 0.00982$ and for

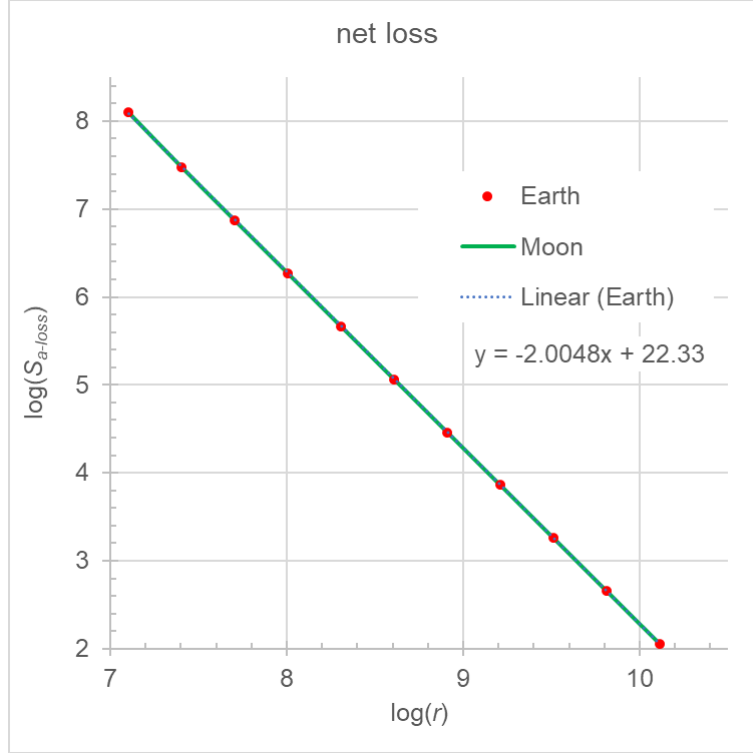


Figure 23: Absorption loss of Earth and Moon versus distance (CASE_1)

Moon $A_{R-moon} = 0.00162$ with $g_0 = 1000 \text{ ms}^{-2}$ clearly place the case very early on the A_R graph in Fig. 3. This prompted us to repeat the same investigation for other denser and/or more extensive spheres below.

CASE_2 (Small-and-large-dense-spheres). An extreme case at the other end of Newtonian regime is to use $A_R = 0.99$ (near saturation absorption). We can do this using the Earth radius R_2 and corresponding $k_2 = 1.10987744324188E - 06 \text{ m}^{-1}$. We can pack a large amount of effective mass inside the given radius depending on the g_0 that we can choose according to Eq. 204. Let's choose $g_0 = 10^5 \text{ ms}^{-2}$. For the second interacting sphere, we chose a very small one with radius $R_1 = 1 \text{ m}$ but with the same $A_R = 0.99$ corresponding to $k_1 = 7.07102919089469E + 00 \text{ m}^{-1}$. The results for each sphere are given in Tables 14 and 15. Then likewise, we plot the net loss factor $S_{a-netloss}$ in Fig. 24.

Now, we can make the following observations: The mass losses for the large gravitating sphere are practically (relatively) negligible being 14 orders of magnitude below that of the lone mass, as is also the “joint” fraction of mass, whilst the “single” fraction is practically equal to the lone (not enough decimal places are provided in the limited width of the table). However, the joint and net loss masses of the small sphere are of the same order of magnitude as the lone, whilst the single mass is a few orders of magnitude less. This was to be expected, since the small sphere, when brought only 2 m above the surface of the large sphere, is practically shielded from about half the gravions from the direction of the large sphere. The unforeseen behavior is that of the net loss, which is better shown in graph form in the provided figure. The curve looks for the most part close to a straight line especially at long distance, but it significantly deviates from the straight line at close range. Further and most importantly, we have now found that the curve becomes asymptotic with a special straight line (on log-log scales) given by:

$$S_{F0} \equiv \frac{\pi A_1 \pi A_2}{r^2} = \frac{\pi^2 A_{R_1} A_{R_2} R_1^2 R_2^2}{r^2} \quad (213)$$

which is identical with the factor in deriving the force between the two spheres in Eq. 90. This is an extraordinary novel finding in PG, which we discuss and analyze after we tabulate the corresponding results of an additional extreme case below.

CASE_3 (Two-large-and-dense-spheres). We again choose a near saturation regime with $A_R = 0.99$, but with both spheres being extensive, i.e. with $R_1 = 1000000 \text{ m}$, $R_2 = 6371000 \text{ m}$ and corresponding $k_1 = 7.07102919089467E - 06 \text{ m}^{-1}$, $k_2 = 1.10987744324188E - 06 \text{ m}^{-1}$. The results are given in Tables 16 and 17. Also, the net loss is plotted in Fig. 25.

Due to the chosen radii, we can't have the situation of a very close range equivalent to that of case_2, so that the asymptotic in case_3 is hardly distinguishable on the plot. However, we can compare at the same

r, m	$M_{er-single}, kg$	$M_{er-joint}, kg$	$M_{er-loss}, kg$	M_{e-sum}, kg	<i>Asymptotic loss</i>
6371002.0	6.0209E+28	7.0314E+14	$6.8921E+14$	6.0209E+28	$3.6713E+14$
6.3711E+06	6.0209E+28	7.0065E+14	$6.8887E+14$	6.0209E+28	$3.6712E+14$
6.3716E+06	6.0209E+28	6.8829E+14	$6.8678E+14$	6.0209E+28	$3.6706E+14$
6377371.0	6.0209E+28	6.3098E+14	$6.7466E+14$	6.0209E+28	$3.6640E+14$
7008100.0	6.0209E+28	4.3435E+14	$4.2575E+14$	6.0209E+28	$3.0341E+14$
7645200.0	6.0209E+28	3.3379E+14	$3.2718E+14$	6.0209E+28	$2.5495E+14$
8919400.0	6.0209E+28	2.2439E+14	$2.1995E+14$	6.0209E+28	$1.8731E+14$
12742000.0	6.0209E+28	1.0029E+14	$9.8300E+13$	6.0209E+28	$9.1782E+13$
25484000.0	6.0209E+28	2.3783E+13	$2.3312E+13$	6.0209E+28	$2.2946E+13$
50968000.0	6.0209E+28	5.8751E+12	$5.7588E+12$	6.0209E+28	$5.7364E+12$
101936000.0	6.0209E+28	1.4645E+12	$1.4355E+12$	6.0209E+28	$1.4341E+12$
203872000.0	6.0209E+28	3.6586E+11	$3.5861E+11$	6.0209E+28	$3.5852E+11$
407744000.0	6.0209E+28	9.1447E+10	$8.9637E+10$	6.0209E+28	$8.9631E+10$
815488000.0	6.0209E+28	2.2861E+10	$2.2408E+10$	6.0209E+28	$2.2408E+10$

Table 14: Variation of various fractions of the effective mass of the large dense sphere versus distance, i.e with $R_2 = 6371000 \text{ m}$ and $k_2 = 1.10987744324188E-06 \text{ m}^{-1}$ (CASE_2)

r, m	$M_{er-single}, kg$	$M_{er-joint}, kg$	$M_{er-loss}, kg$	M_{e-sum}, kg	<i>Asymptotic loss</i>
6371002.0	1.1659E+12	7.9297E+14	$6.8921E+14$	1.4834E+15	$3.6713E+14$
6371063.7	6.6336E+12	7.8784E+14	$6.8887E+14$	1.4834E+15	$3.6712E+14$
6371637.1	2.0976E+13	7.7560E+14	$6.8678E+14$	1.4834E+15	$3.6706E+14$
6377371.0	6.6288E+13	7.4240E+14	$6.7466E+14$	1.4834E+15	$3.6640E+14$
6434710.0	2.0822E+14	6.5665E+14	$6.1848E+14$	1.4834E+15	$3.5990E+14$
7008100.0	6.1796E+14	4.3964E+14	$4.2575E+14$	1.4834E+15	$3.0341E+14$
7645200.0	8.1995E+14	3.3622E+14	$3.2718E+14$	1.4834E+15	$2.5495E+14$
8919400.0	1.0381E+15	2.2527E+14	$2.1995E+14$	1.4834E+15	$1.8731E+14$
9556500.0	1.1056E+15	1.9105E+14	$1.8668E+14$	1.4834E+15	$1.6317E+14$
12742000.0	1.2846E+15	1.0043E+14	$9.8300E+13$	1.4834E+15	$9.1782E+13$
25484000.0	1.4362E+15	2.3790E+13	$2.3312E+13$	1.4834E+15	$2.2946E+13$
50968000.0	1.4717E+15	5.8755E+12	$5.7588E+12$	1.4834E+15	$5.7364E+12$
101936000.0	1.4805E+15	1.4645E+12	$1.4355E+12$	1.4834E+15	$1.4341E+12$
203872000.0	1.4826E+15	3.6586E+11	$3.5861E+11$	1.4834E+15	$3.5852E+11$
407744000.0	1.4832E+15	9.1448E+10	$8.9637E+10$	1.4834E+15	$8.9631E+10$
815488000.0	1.4833E+15	2.2861E+10	$2.2408E+10$	1.4834E+15	$2.2408E+10$

Table 15: Variation of various fractions of the effective mass of the small dense sphere versus distance, i.e with $R_1 = 1 \text{ m}$ and $k_1 = 7.07102919089469E+00 \text{ m}^{-1}$ (CASE_2)

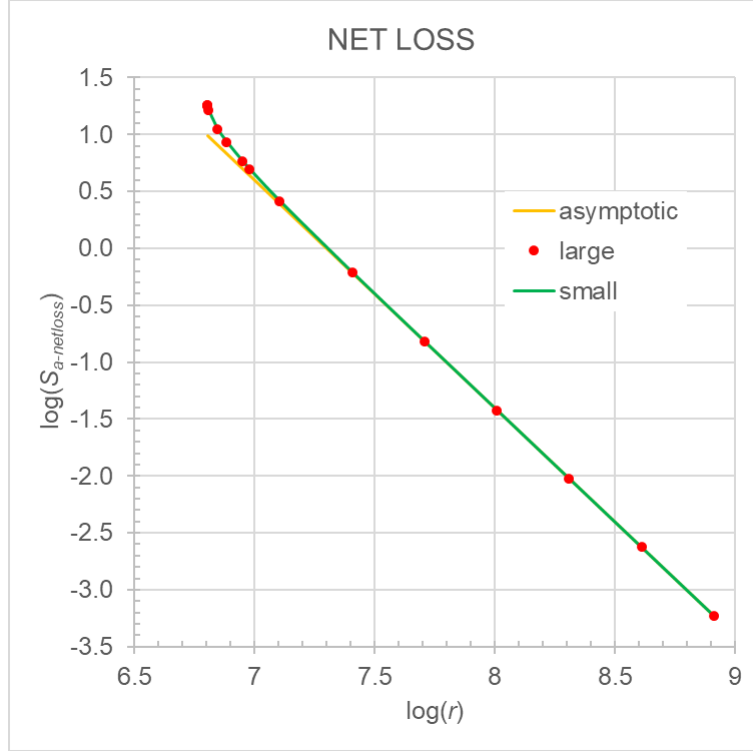


Figure 24: *Net loss of small and large dense spheres with asymptotic loss versus distance (CASE_2)*

short distance of $r = 2R_2$. We note that the deviation of the mass loss from the asymptotic line at $r = 2R_2$ distance is about the same in all three cases, namely, the ratio of $M_{e-loss}/M_{e-asymptotic}$ is 1.062, 1.070 and 1.073 as can be found from the corresponding tables. That is, the variation of mass loss is nearly inversely proportional to the square of distance almost regardless of density, whilst it is the distance, or better the geometry that is the main controlling parameter.

We recall that the gravitational force in Eq. 90 was derived by a simple “reverse engineering approach” from the associated single (or lone) effective masses of each sphere, to which we attached their characteristic absorptivity. We then confirmed the same outcome from the integration of equations constituted from first PG principles (see “bulk method” in the Appendix). We have now further confirmed the same outcome with an alternative approach involving three integrations (the “surface” method), which allowed much improved precision with much shorter computation times including the cases of high absorption with A_R values close to unity. Thus, if we normalize the computed force factor S_F over the theoretical (reverse engineering) force factor denoted by S_{F0} , we invariably find unity as a function of distance, as can be seen by some representative results now shown in Table 18. The deviation from unity beyond 9 decimal places is caused by the set relative integration tolerance of errors, namely, of $eps_{rel} = E - 06$, $E - 05$ and $E - 04$ for the

r , m	$M_{er-single}$, kg	$M_{er-joint}$, kg	$M_{er-loss}$, kg	M_{e-sum} , kg	Asymptotic loss
12742000	6.0010E+28	1.0051E+26	$9.8516E+25$	6.0209E+28	$9.1782E+25$
25484000	6.0162E+28	2.3793E+25	$2.3322E+25$	6.0209E+28	$2.2946E+25$
50968000	6.0197E+28	5.8757E+24	$5.7593E+24$	6.0209E+28	$5.7364E+24$
101936000	6.0206E+28	1.4645E+24	$1.4355E+24$	6.0209E+28	$1.4341E+24$
203872000	6.0208E+28	3.6586E+23	$3.5861E+23$	6.0209E+28	$3.5852E+23$
407744000	6.0208E+28	9.1448E+22	$8.9637E+22$	6.0209E+28	$8.9631E+22$
815488000	6.0209E+28	2.2861E+22	$2.2408E+22$	6.0209E+28	$2.2408E+22$

Table 16: *Variation of various fractions of the effective mass of the bigger dense sphere versus distance with $R_2 = 6371000$ m and $k_2 = 1.10987744324188E - 06$ m⁻¹ (CASE_3)*

$r, \text{ m}$	$M_{er-single}, \text{ kg}$	$M_{er-joint}, \text{ kg}$	$M_{er-loss}, \text{ kg}$	$M_{e-sum}, \text{ kg}$	$Asymptotic \text{ loss}$
1.2742E+07	1.2842E+27	1.0065E+26	$9.8516E+25$	1.4834E+27	$9.1782E+25$
2.5484E+07	1.4362E+27	2.3800E+25	$2.3322E+25$	1.4834E+27	$2.2946E+25$
5.0968E+07	1.4717E+27	5.8761E+24	$5.7593E+24$	1.4834E+27	$5.7364E+24$
1.0194E+08	1.4805E+27	1.4646E+24	$1.4355E+24$	1.4834E+27	$1.4341E+24$
2.0387E+08	1.4826E+27	3.6586E+23	$3.5861E+23$	1.4834E+27	$3.5852E+23$
4.0774E+08	1.4832E+27	9.1448E+22	$8.9637E+22$	1.4834E+27	$8.9631E+22$
8.1549E+08	1.4833E+27	2.2861E+22	$2.2408E+22$	1.4834E+27	$2.2408E+22$

Table 17: Variation of various fractions of the effective mass of the smaller dense sphere versus distance with $R_1 = 1000000 \text{ m}$ and $k_1 = 7.07102919089467E-06 \text{ m}^{-1}$ (CASE_3)

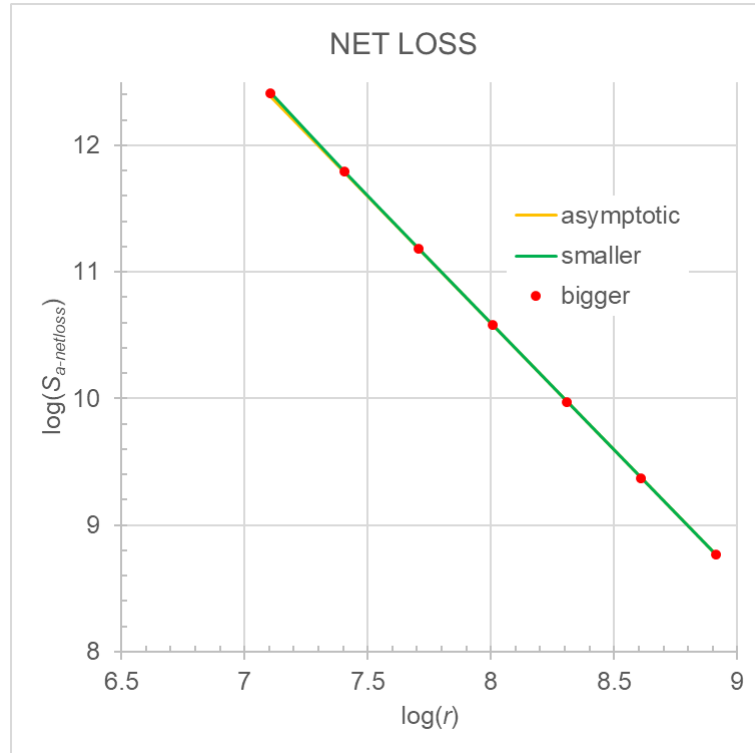


Figure 25: Net loss of two large (smaller, bigger) and dense spheres with asymptotic loss versus distance (CASE_3).

	CASE_2	CASE_3
r	S_F/S_{F0}	S_F/S_{F0}
6371002.0	0.9999999942	
6377373.0	1.0000000084	
6434712.0	1.0000000068	
7008102.2	1.0000000035	
8919402.8	1.0000000030	
9556500.0	1.0000000029	
12742000.0	0.9999999747	0.9999999726 0.9999999999990
31855000.0	1.0000000023	
63710000.0	1.0000000021	1.0000000021
318550000.0	1.0000000020	1.0000000020
637100000.0	1.0000000020	1.0000000020

Table 18: *Computed S_F over theoretical S_{F0} force factor ratio versus distance for CASE_2 and CASE_3; second value with decreased tolerance at $r = 12742000.0$ m*

first, second and third integral. By decreasing the tolerance by four orders of magnitude in each integral, we obtain $S_F/S_{F0} = 0.9999999999990$ (at $r = 12742000.0$, see table).

Now, the variation of effective mass with distance, i.e. a decrease of mass with decrease of distance, means that Newton’s gravitational law, if applied using the effective masses, yields a smaller value of force than if the masses were independent of distance as is assumed by Newton. PG finds exactly the latter, i.e. the force behaves as if the masses were invariant without actually being so! This is a novel understanding, unexpected by Newton. It is a consequence of the underlying mathematical (better physical) relationship among the PG parameters involved via the graviton absorption.

The above difference between PG and Newton gravitational laws is fundamental, although they can be both written by a similar equation. They differ in the concept of mass, which is not trivial. Newton does not distinguish the “lone” mass from the mass acted upon by another mass. Thus, we can now distinguish between the two laws as follows:

If we use the actual masses (i.e. acting or effective) then Newton’s force should be:

$$F_{Newton} = G \frac{M_{e1r} M_{e2r}}{r^2} = G \frac{(M_{e1r-single} + M_{e1r-joint})(M_{e2r-single} + M_{e2r-joint})}{r^2} \quad (214)$$

whereas PG law using the far away lone masses (see also 90) is:

$$F_{PG} = G \frac{M_{e1} M_{e2}}{r^2} \quad (215)$$

The ratio of the above forces can be written also as a ratio involving the S_- parameters via the proportionality Eq. 203:

$$\frac{F_{Newton}}{F_{PG}} = \frac{S_{a1r} S_{a2r}}{S_{a1} S_{a2}} = \frac{(S_{a1r-single} + S_{a1r-joint})(S_{a2r-single} + S_{a2r-joint})}{S_{a1} S_{a2}} \quad (216)$$

We illustrate the difference between Newton and PG in Fig. 26 by plotting the above ratio (normalizing) as a function of distance for the same three cases. The importance of this difference can now be better appreciated by considering the involvement of the mathematical derivations dictated by PG and presented in the Appendix. The coincidence in mathematical form is uncanny, except that Newton’s gravitational law is both empirical and approximate, whereas PG gravitational law is derivable and precise.

We see that case_1 (Earth-Moon) is very close to Newtonian behavior, but not so when the absorptivity A_R increases. Has conventional physics found how very dense bodies interact at close range, or only now PG reveals exactly that behavior? The present findings can afford us a deeper understanding of the notions of mass and force. We note that the initial integrand during the derivation of force and net loss have an

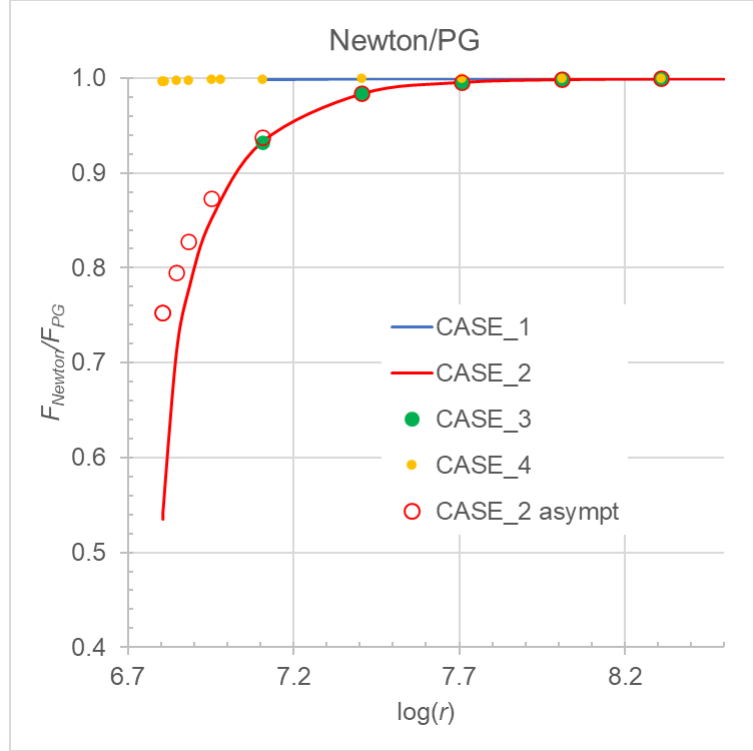


Figure 26: *Ratio of Newton/PG forces against distance for four cases of density and size of spherical masses*

identical factor apart from the trigonometric factors used to calculate the directional (projection of) flow of gravions. This applies with both methods, bulk or surface (see Appendix). There is clearly a common denominator under the idea of force and mass. The common denominator is the push gravions. Whereas the effective mass is made from gravions being absorbed from all possible directions, force is made from the net directional absorption of gravions between the centers of spheres, or presumably between the “centers of gravity” of any two bodies in a general case (to be shown in later PG development). In other words, effective mass and force have a common cause, namely, the rate of gravion absorption. Mass is the omnidirectional gravion absorption resulting in a scalar quantity, whilst force is the component of gravion absorption in a particular direction defined by two bodies at a distance apart, resulting to a vector quantity.

16.1 Discussion

If PG can be experimentally confirmed and if Fig. 26 correctly reveals the deviation of Newtonian mechanics from actual physical processes, then EP, the equivalence principle emanating from Newtonian experience and carried over to GR, ceases to apply. That means that EP is not only redundant as previously suggested, but it may be an invalid one. We may have to reassess our own stance vis-a-vis EP (see Section 15.2), i.e. we may have to go from a defensive argument to a critical one against it. Here, it is important to clarify that the critics of PG citing the equivalence principle as reason for rejection of PG have presumably done so for different reasons, because they did not have our development of PG in front of them. In the light of the present findings, we have to say that PG seems to contradict the EP, but this is no reason to oppose PG. Conversely, it may be a reason to reassess the theories based on EP. It may be the reason why current theories have unsolved fundamental problems. Then, use of EP as basis for rejection of PG would be arbitrary. It may eventually be that EP is the pivot point between GR and PG, i.e. which direction to take. This can only be arbitrated by a proper experimental assessment of PG, whilst all hitherto tests of EP may have been simply inadequate.

Should we then realign the conventional meaning of “intrinsic” mass? Should this be the effective mass of a body away from other material bodies, because the effective mass varies with the distance from other bodies, albeit imperceptibly in Newtonian mechanics? This is clearly explained under the platform of PG. We distinguish the three components of effective mass, namely, “joint”, “single” and “loss” mass. The sum of these three components is a constant (at the prevailing J_0 , or g_0 or Λ) equal to the isolated lone body’s mass, which we may now call “intrinsic” mass, or use another term to describe the new understanding (sooner or later, we will have to deal with the question of terminology in a more consistent and comprehensive way, but

we can await for more results, especially a confirmation of PG). The finding that the force is derived from the product of such intrinsic masses, whilst they are actually smaller at a given distance, could be the key for explaining why the equivalence principle has imposed itself for such a long time. It provides a fortuitous condition that yields correct answers for things that don't really exist. It assumes masses that don't exist, but their assumed value yields correct outputs such as the gravitational law. It may be that PG for the first time deciphers a trick that nature has played on science.

It should be appreciated that throughout this report we have loosely used the notions of mass, force and energy, which is an unavoidable situation, if we have to evolve from our standard education in physics; not only pedagogical but fundamental errors may creep in science for these and other concepts. Like GR redefines these concepts in terms of space-time, etc., PG now also seems to afford us an alternative understanding of the same concepts, as they evolve from an assumed universal graviton absorption. Only by persistence in developing and evolving PG theory backed by purposeful experiments, may we ultimately understand and re-define the concepts of energy, mass and force. We have started with a set of principles, which themselves will evolve dialectically (back-and-forth) as we move forward and the pig picture of cosmos unravels more clearly.

The new understanding of mass and force can further lead to an ultimate understanding of energy in the form of work ($force \times distance$), potential and kinetic energy and the $E = mc^2$ relationship. An initial check does not equate the potential energy with the mass-energy equivalence conversion, but this should be of no concern. We should bear in mind that a system of bodies acted upon by their associated gravitational fields does not constitute a closed system. The bodies are inside an "aether" of gravitons coupled with them. They constitute an open thermodynamic system that exchanges gravitons with the surrounding universal reservoir of gravitons. The bodies must always be seen together with the surrounding universe acting from both short and long range. This universe is intimately connected with any system of bodies, small or big, at any moment of time and space, "here and now" (whatever this may mean!). The interconnection is such that the body resists any change of its steady-state status. This resistance is the conventional "inertia". Therefore, when the gravitational "pulling" force is doing "work" by displacing a body between two points, the interchange between work and gravitational energy must be computed as a balance of graviton exchange with the surrounding universe. An analogous system in physics is an electronics signal (current or power) amplifier, whereby a given signal input is amplified in conjunction with an external supply circuit of electrons (energy).

Actually, the new notion of mass variation inside the gravitational field of interacting bodies is not limited to dense and massive bodies in astrophysics, but it must apply also to very small but dense particles. This seems to be consistent with particle physics phenomena. Let's recall that within a given radius, there is an upper limit of effective mass that we can pack. This upper limit is determined by the surrounding maximum J_0 (or g_0 , see also Eqs. 200 and 203). If we can think of a particle in an accelerator that it absorbs more push particles at more speed, it is like creating an artificially increased g_0 enabling the particle to pack more effective mass over and above the maximum it might have prior to its entry in the accelerator. When the particle "stops", it cannot retain the extra mass above the limit it acquired during its acceleration. Then, it has to shed this "unnatural" load of mass in the form of new particles inside the accelerator. Those new particles themselves usually have very short lives, if they still have to readjust and obey the PG law of an upper limit of effective mass. As it was also theorized in Section 14.7, the approach to an upper speed limit is not because the mass becomes mathematically infinite, but because the real mass becomes saturated with graviton absorption as A_R approaches the upper value of unity.

If the above understanding could prove correct, it would have enormous consequences. While more cases have been studied with the formulations of PG in the Appendix, they and many more can be the subject of continuing work by the scientific community under the new physics of PG. The case of three or more interacting spheres can be investigated by expanding the work presented in the Appendix; then, we can study the eclipses of Moon and Sun over and above the simplified study outlined in Section 12.4. All this requires more resources, but also makes it ever more imperative that PG should be verified by the relevant organizations.

To summarize and avoid possible contradiction of terms (words), let's clarify (again) the following: The effective mass is a different quantity from the real mass, whilst they are expressed in the same units. The first is the active part (fraction) of the second and relates to an experienced force. We generally experience an object as "stuff", which we can safely identify with the real mass. The force acts on the object via its effective mass, i.e. it does not directly act on the entire object, because part of it (no matter how small or big) is shielded from the action of gravitons. The effective mass of the object is different when the object is alone from that when it is in the neighborhood of other objects. For convenience of description, let's call the lone effective mass "intrinsic" mass (same as rest mass) as opposed to the "current" mass being the effective mass in any case. The force between two objects can be found from the intrinsic mass of the objects even

though the force is acted upon each other via their current masses. With these clarifications, we can return to the equivalence principle as it originally started and as it can be now explained under PG theory. This principle has been described in the following way(s):

An object under its weight by the Earth's gravity travels the same distance over time as when the same object is under the same force in space outside a gravitational field. By the same token, this principle says that the object's mass is the same in both cases, i.e. its gravitational mass is equal to its inertial mass, where the two types of mass are simply the constant of proportionality between force and acceleration and this proportionality is the same in both cases.

Now, under PG we find that the proportionality between force and mass applies only when we use the intrinsic mass of the object, but not when we use its current mass. The use of intrinsic mass necessitates that we operate away from other objects, so that when we bring the object inside the gravity of another object, then its current mass is smaller. However, our experience of the falling object inside the gravity of the second object is as if it has a mass equal to its intrinsic mass. This explains exactly the equivalence principle, but the equivalence principle does not explain the nature of mass, because it fails to distinguish the current effective mass from the lone effective mass. In other words, the expression of "gravitational mass" being the same as the "inertial mass" bypasses the physics about force and real mass (stuff), it overlooks the underlying mechanism resulting in what we experience as force and stuff, as force and object. This omission is not trivial, but it explains why we get the correct result for the wrong reason. PG is about revealing the reason operating behind our experience of an object and force, and much more. In doing so, it frees the ground to unravel some discrepancies and impasses of conventional physics. Furthermore, real mass as revealed by PG bears no compatibility with EP, which makes it even more fundamental to be able to decipher and decouple the various notions of mass from the stuff an object actually has.

Based on the above clarification, we can see again why EP is at least redundant (not needed for PG by way of a "space elevator"), or even invalid (by way of mass equivalence) under the terminology and concepts of mass in PG. This is another or better re-affirmation of our stance in previous sections. The bottom line is that EP can by no means be used against PG, whilst EP stands on precarious grounds itself.

On the previously asked question whether conventional physics has found how very dense bodies interact at close range, the implication was if such findings correspond to reality. More specifically, the question is if general relativity (GR) correctly describes the interaction of very dense objects based on parameters of bodies that may be incorrectly measured. The latter possibility exists and is better explained according to the ideas expounded in Section 18.2.

16.2 Ramifications and importance of mass variation

Having said all of the above about effective mass variation with distance between two spheres and what it means under PG so far, we must stress that we have considered only the static steady-state situation. However, it is important to clarify what the "static" condition means in an actual situation by explaining what it is not, i.e. not yet before we investigate the following cases:

(a) It is not the situation whereby the two spheres are held at a fixed distance by some other medium, such as a rod between them. In the latter case, the rod would exert a force opposing the gravitational force begging the question about the underlying mechanism of this opposing force. We may know that this is an electric force created by compression at the atomic scale. This then necessitates that we explain the electric force too, which for consistency we have proposed that it be also a push particle force. This may influence the prevailing effective mass via another mechanism. That is the subject of a following Section 21 that expands the push particle principle to a "push electricity (PE)" theory.

Therefore, the way to imagine what we described and quantified in the present section is what happens moments just after we remove the holding rod and before the spheres acquire any significant velocity by "falling". In other words, the spheres are both stationary and in a steady state situation with regard to absorption of gravions and re-emission of their energy into something else (let's say electrions) and are free in space without influence by anything else like a rod.

(b) It is not the situation whereby the two spheres are held at a fixed distance while moving at an orbit with respect to each other, like in a binary system, or one very small (light) sphere orbiting around another large (heavy) sphere. Also, it is not the situation whereby the two spheres are falling to each other having acquired a significant velocity. For a falling body, we have not yet established what happens to the current effective mass (at time t) and how (if) the gravion flux varies and differs from the postulated static situation. This problem could be solved under Section 14 for the development of a dynamic PG theory. The prospects are very interesting and important, if we can only speculate thus now: A sphere orbiting around or falling towards another "stationary" sphere may have yet another current effective mass, quantitatively different from the stationary one.

(c) It is not the situation whereby one sphere (with or without the presence of the other sphere) is pushed by some medium like a rocket. We can imagine this happening in different ways. While the two spheres are held apart with a fixing rod, one sphere disappears or is let loose while the rod-rocket continues to act on the other sphere. We have not examined these two cases yet. In other words, moment(s) after the disappearance or letting loose of one sphere, the other sphere exists at practically the same (prior fixed) distance before it acquires a significant velocity being propelled by the rod-rocket. It would be a mistake to apply our derived equations in this section for the prevailing effective mass of the sphere. This is because we have to consider the mechanism of the rocket force, which we again expect it to be an electrical force. Therefore, we should examine these cases also after we first develop and understand push electricity. Later work has now been done in Section 23.

From the above clarifications, we can see the reasons why the effective mass may be different depending on the prevailing conditions. If we postulate that the “mass” is the same (equivalent) in all situations, which is exactly what the Equivalence Principle has demanded from the mainstream physics, then we have not seen the above described fundamental differences. Current theories have overlooked the above analysis, exactly because they have adopted a problematic EP. In other words, EP has imposed a severe constraint limiting further developments in physics, in fact leading to impasses. For if we let the mass vary and/or transfer under static and dynamic situations, we can free ourselves for much better explanations of experiments, phenomena and the cosmos. Now, we understand that “mass” is an objective entity in various forms like “stuff” = matter = real mass, with subsets of effective mass and black mass. Mass is not a mere mathematical multiplier factor to an invariable conventional rest mass.

16.3 Supplementary study of two sphere interaction cases

Due to the need for better understanding of the positional variation of two spherical masses, we undertook the study of many more cases. The relationship of geometry (radii and distance) with nature of material (absorptivity) is the main purpose of the study. This work has revealed some important patterns of behavior that is necessary to know in further studies, development and applications of the theory of PG. The salient aspects of this behavior are described by some representative cases presented below.

CASE_4 involves the Earth and a small sphere with $R_1 = 1$ m having Earth-like density, for which we used $k_1 = 1.15604978409807E - 09 \text{ m}^{-1}$, at $g_0 = 1000 \text{ ms}^{-2}$. [Note: Throughout this report, we often provide numerals with the same many decimal places used to allow other workers to reproduce the same numerical results]. This is a Newtonian (or close to it) case where the small diameter of one sphere allows to bring it down to 2 m above the Earth surface (i.e. at $r = 6371002$ m). We plot the net loss of mass against distance in Fig. 27a along with the corresponding asymptotic line given by Eq. 213. The difference

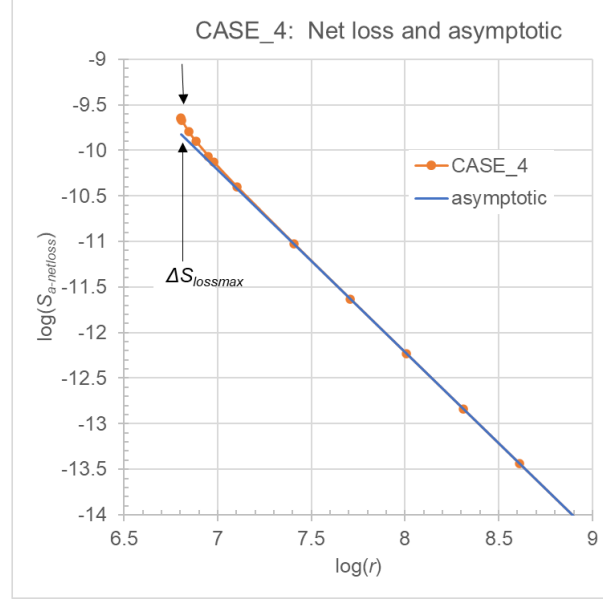
$$\Delta S_{loss}(r) = S_{a-netloss}(r) - S_{F0}(r) \quad (217)$$

and ratio

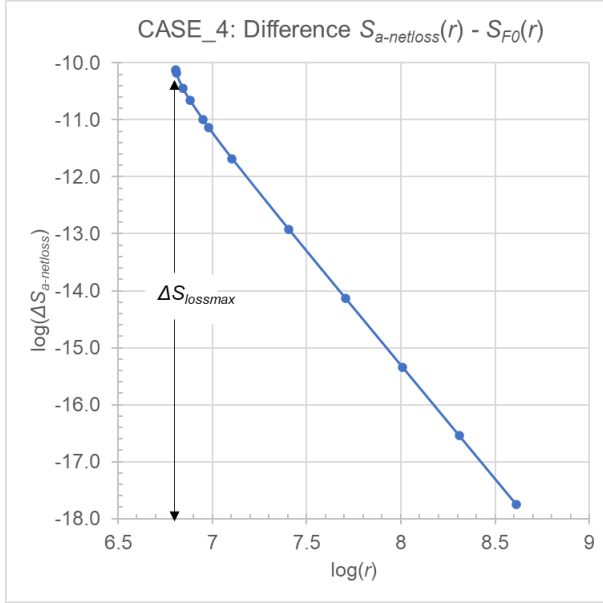
$$\Re(r) = \frac{S_{a-netloss}(r)}{S_{F0}(r)} \quad (218)$$

between actual and asymptotic values are also plotted against distance in Fig. 27b&c. We note that the deviation from the asymptotic is as significant as in Fig. 24 done for the very dense (non-Newtonian) spheres with identical geometry. This knowledge is needed for studies involving the $S_{a-netloss}(r)$ function in other parameters describing the behavior of bodies with different density (absorptivity). One such parameter is the ratio of Newton/PG forces given by Fig. 26, to which we now add CASE_4 and note that the points remain close to unity even at close range.

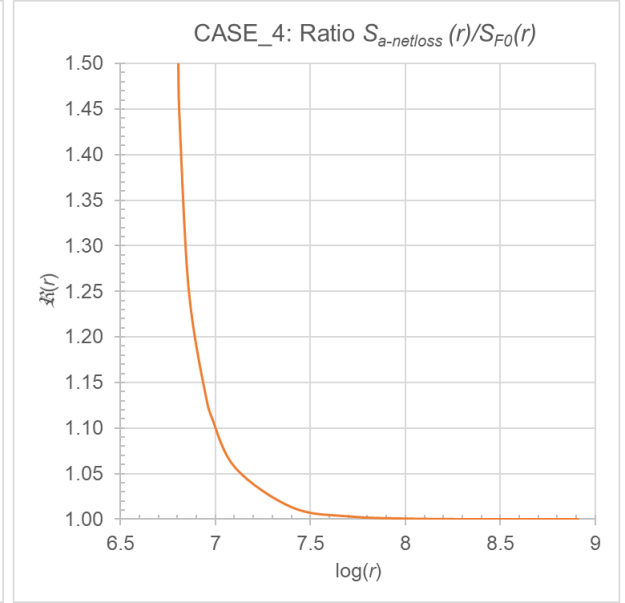
The approach (or deviation) of the net loss function to (from) the asymptotic straight line is an important consideration. If we use the asymptotic function of CASE_4 instead of the actual values of the net loss function in the same Fig. 26, the difference is not visible on the graph. However, if we apply the asymptotic function for CASE_2, the deviation from the actual function becomes quite obvious (red circle points now added in the same figure). From this, we may conclude that use of the asymptotic function is a good approximation in the Newtonian regime, which may be allowed for some parameters, like the one plotted in Fig. 26. However, this may also provide erroneous outcomes for other parameters, like the falling speed between bodies. The speed that results from the action of force at various points is a cumulative parameter that can result in significant deviation between using the asymptotic or the actual function of net loss of mass. We have already suggested (per Section 14.3) that the falling speed is a function of the contraction factor, so that later studies should take into account even the smallest deviation, even in the Newtonian regime. (Note that we do not need to use a subscript ($_1$ or $_2$) to designate the net loss of mass for either sphere 1 or 2, because they share the same mass loss).



a

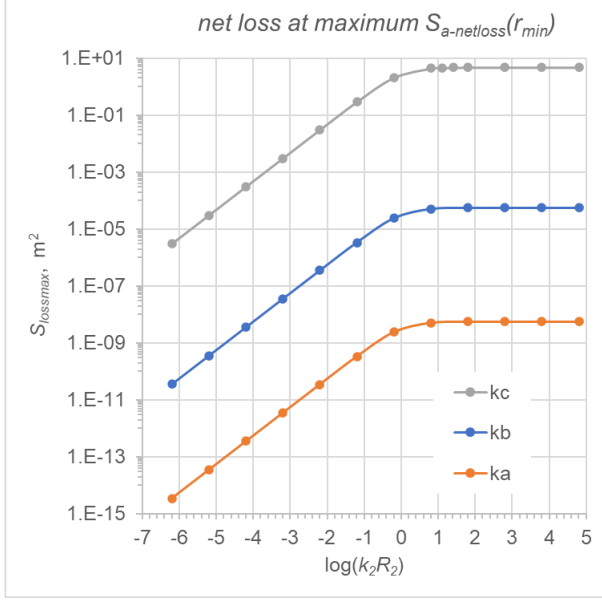


b

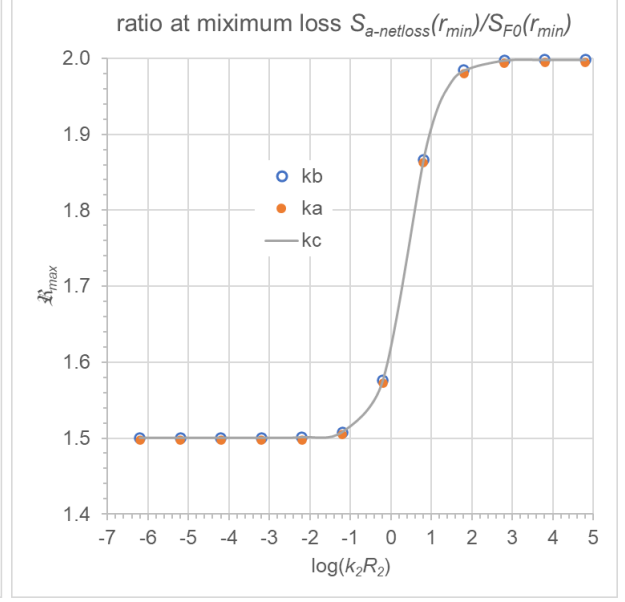


c

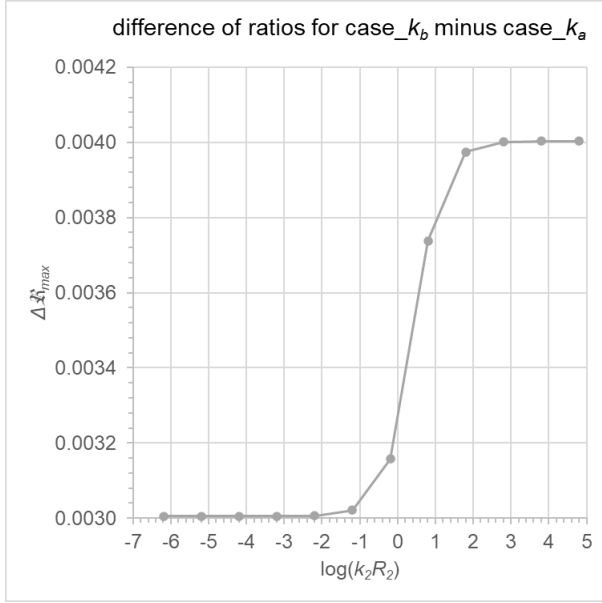
Figure 27: *CASE_4* using a small sphere with $R_1 = 1 \text{ m}$, $k_1 = 1.15604978409807E - 09 \text{ m}^{-1}$ and Earth with $R_2 = 6371000 \text{ m}$, $k_2 = 1.16248157479707E - 09 \text{ m}^{-1}$, and $g_0 = 1000 \text{ ms}^{-2}$; (a) *net_loss_function* and asymptotic, (b) difference between net loss and asymptotic and (c) ratio of net_loss_function over asymptotic, all plotted against distance between spheres



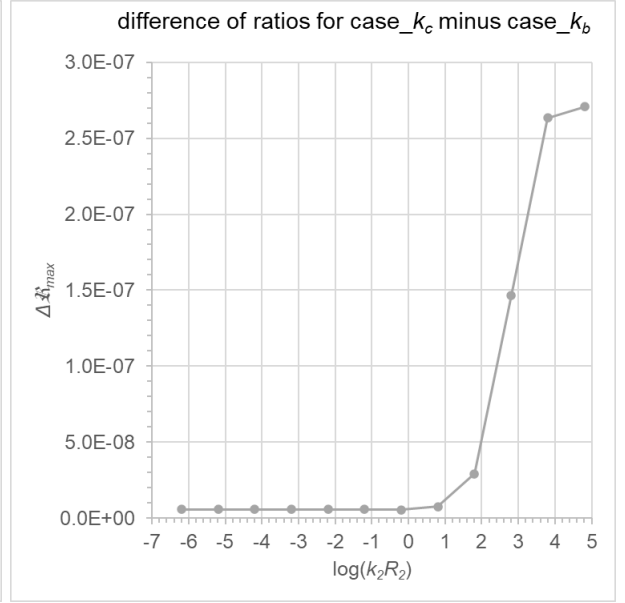
a



b



c



d

Figure 28: Variation of the small sphere parameters against $k_2 R_2$ of the large sphere for three fixed values k_1 of the small sphere: (a) Absolute values of the net loss function, (b) ratio of max net_loss over max asymptotic_loss, (c) difference of ratios corresponding to case_ k_b minus case_ k_a and (d) difference of ratios corresponding to case_ k_c minus case_ k_b .

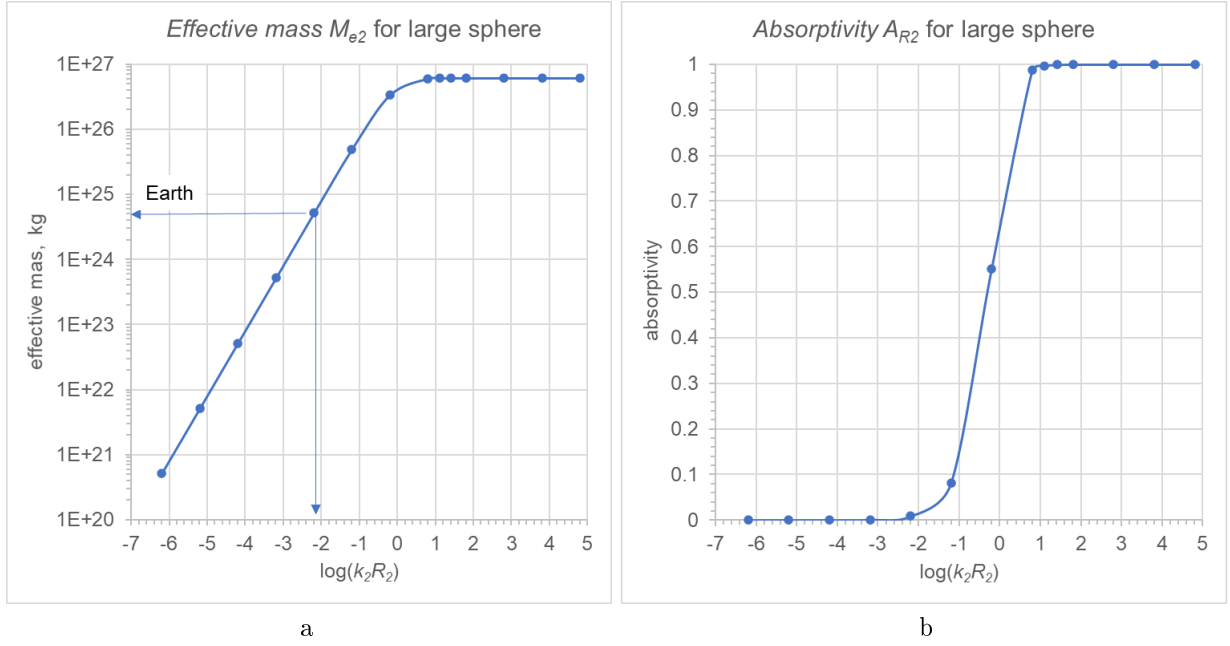


Figure 29: (a) *Effective mass and (b) absorptivity for the large (Earth size) sphere against $k_2 R_2$*

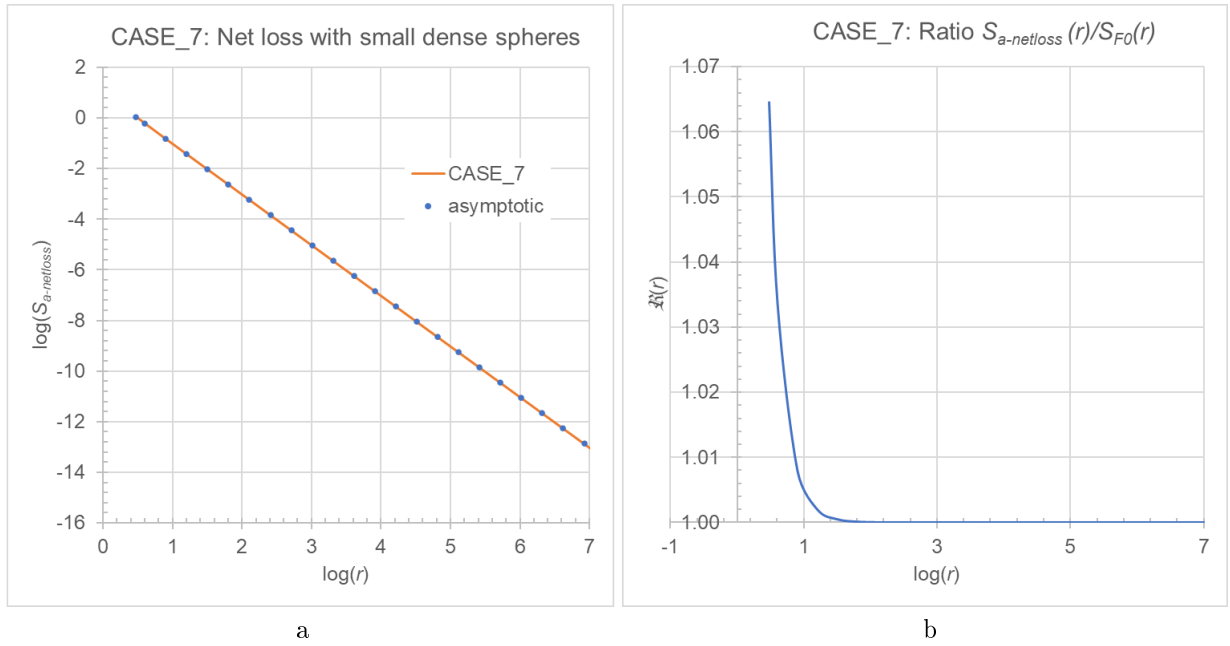


Figure 30: *CASE_7: Two identical small and dense spheres with $R = 1$ m and $k = 7.07102919089469$ m $^{-1}$*

The above findings prompted us to study further cases in an effort to establish some patterns or “rules” about the behavior of the $S_{a-netloss}(r)$ function. This behavior is not obvious directly from the integrals involved for computing the net loss for a set of two spherical masses with different absorptivities by use of the method in Appendix E. Closer to practical application for our study, we fix the gravitating “large” sphere_2 to the Earth radius and the “small” sphere to the radius of $R_1 = 1$ m. We vary the absorptivity (or k_2 factor) of the large sphere over a wide range of values in conjunction with some fixed absorptivities (or k_1 factors) for the small sphere between extreme densities; we found that three fixed values, namely, $k_{1a} = 2.09672407007571E - 10 \text{ m}^{-1}$ (case_ka), $k_{1b} = 2.09672407007571E - 06 \text{ m}^{-1}$ (case_kb) and $k_{1c} = 2.09672407007571E - 01 \text{ m}^{-1}$ (case_kc), chosen arbitrarily, are sufficient for the current purposes. We generalize the presentation by plotting the results against the usual product of $k_2 R_2$. To minimize the work and reporting, we computed only the maximum value $S_{lossmax} \equiv S_{a-netloss}(r_{min})$ at the closest distance $r_{min} = 6371002$ m, where the deviation from the asymptotic function $S_{F0}(r_{min})$ is maximum. Then the ratio \mathfrak{R}_{max} of these quantities at the minimum distance:

$$\mathfrak{R}_{max} = \frac{S_{a-netloss}(r_{min})}{S_{F0}(r_{min})} \quad (219)$$

has been found to be a good indicator of the regime behavior for the given k factors (absorptivities) of any set of sphere densities. The corresponding difference $\Delta S_{lossmax}$ of the same values:

$$\Delta S_{lossmax} = S_{a-netloss}(r_{min}) - S_{F0}(r_{min}) \quad (220)$$

is more cumbersome to use because it provides absolute values varying over many orders of magnitude, which cancel out in the ratio \mathfrak{R}_{max} . We can see the variation of net loss $S_{a-netloss}(r_{min})$ in absolute values plotted in Fig. 28a. However, plotting the ratio by Eq. 219 results in grouping all three cases very close together, but not exactly overlapping, as can be seen in Fig. 28b. The latter closeness may simplify some engineering problems, but the subtle difference may be important in further development and understanding of PG application. For good measure, the difference between the closely presenting graphs are given in the same Fig. 28c&d. Therefore, the multiplier factor $\mathfrak{R}(r)$ is itself also a function of the absorptivity of both spheres, so that we can write an overall general function for $S_{a-netloss}$ as:

$$S_{a-netloss}(A_{R_1}, A_{R_2}, r) = \frac{\pi^2 A_{R_1} A_{R_2} R_1^2 R_2^2}{r^2} \mathfrak{R}(A_{R_1}, A_{R_2}, r) \quad (221)$$

Recalling that the absorptivity itself is a function of the radius R (geometry) and absorption factor k (nature of material), namely, of the product kR at a given universal acceleration g_0 , the net_loss of mass is function of the geometry, determined by the radii of spheres and distance between them, as well as the nature of the materials for each sphere. Therefore, the system of two spherical masses is always described by a peculiar function above including the Newtonian regime, whereby we may or may not reduce it to the asymptotic function depending on the associated parameter under examination.

As for a rule, we may say that cases involving the interaction of two bodies differing greatly by size and/or density, it is the larger body that imposes its dominance and a characteristic pattern like the one we see in Fig. 28. The smaller sphere appears to be overwhelmed by the large one throughout the entire range of $k_2 R_2$ variation of the large sphere; that is, when the small sphere is “immersed” in, or “engulfed” by the gravitational field of the large sphere. The small sphere appears to play a secondary role with second order significance from a “practical” point of view, but nonetheless its role is ever present and non-trivial for an overall theoretical examination and in problems involving a cumulative effect of what appears as a secondary role at first. It is striking that the factor \mathfrak{R}_{max} varies very closely only between 1.5 and 2.0 for a large number of cases. Planet Earth seems to be around the onset of an abrupt transition from $\log(k_2 R_2) > 2$ according to Fig. 29a providing the variation of effective mass; the corresponding variation of absorptivity is given in (b).

A deviation from the above rule and the effect of geometry alone can be readily seen if use a case with comparable size spheres, as we present CASE_7 in Fig. 30 involving two identical small-and-dense spheres with 1 m radius (identical with the small sphere of CASE_2). Neither sphere exerts a dominance, and one is not “engulfed” by the field of the other; they interact on an “equal footing” at all distances possible. This geometry brings closer together the net_loss function with its asymptotic as seen in (a) but there is a difference, albeit much smaller, as can be seen by plotting the $\mathfrak{R}(r)$ factor in (b) of the same figure.

Important: This entire Section 16 is fundamental for the development of PG and should be moved to Part 1 in continuation of Section 7 during a later revision of the report.

16.3.1 Energy considerations

It is further instructive to table the variation of energy forms with distance for CASE_4. This case appears graphically to be close to Newtonian regime in Fig. 26. Based also on the preceding presentation of this case, we may wonder how close to Newtonian regime actually it is. We can obtain a more quantitative answer by examining the values of the following three forms of energy.

One form is the classical (Newtonian) potential energy $U_N(r)$ of the system of the two spheres given by:

$$U_N(r) = G \frac{M_{e1} M_{e2}}{r}$$

The second is to use (arbitrarily) the computed by PG masses at various distances and apply the same formula of potential energy (as we did in comparing the force equations):

$$U_{PG}(r) = G \frac{(M_{e1} - M_{e1r-loss})(M_{e2} - M_{e2r-loss})}{r}$$

where the loss of mass is the same for each sphere, namely, $M_{e1r-loss} = M_{e2r-loss} \equiv M_{er-loss}$

The third form of energy to compare with is taken from the energy-mass equation multiplied by 2:

$$E_{r-loss} = 2M_{er-loss}c_{ph}^2$$

where c_{ph} is the speed of photons. In prior versions of this report (v22), we “borrowed” the above equation from external theory in discussing various possibilities in the total energy balance. However, we have independently produced our own (PG) derivation of the same form involving the effective mass (see Section 29). As a result, we are confident in re-stating the interrelationships between the various forms of energy (and mass) in a system of bodies at various spatial configurations. CASE_4 computations presents a simple example to discuss below.

To the given pairs of (k, R) parameters, the corresponding effective masses are $M_{e1} = 2.30953136731102 \times 10^4$ kg and $M_{e2} = 5.97237 \times 10^{24}$ kg. We file the calculated values for $U_N(r)$, $U_{PG}(r)$ and E_{r-loss} in Table 19. In addition, we file the difference $U_N(r) - U_{PG}(r)$ providing a measure of the order of magnitude of deviation relative to the expected absolute values of potential energy. The latter provides a measure of the deviation from the expected Newtonian behavior, or “how much Newtonian” is this, or any other case. Now that we have adopted also the derivation of the equivalent energy from the mass loss at shorter distance, we can see that its magnitude is much higher than the corresponding classical, or PG potential energy loss. We have to interpret this as a transfer of energy not only between two spheres but mainly between the system of spheres and the external graviton medium flux. The two spheres comprise an open system exchanging energy predominantly with the surrounding medium having a flux intensity given by J_0 corresponding to a given value of maximum acceleration g_0 . The numerical values in this table were computed with $g_0 = 1000 \text{ ms}^{-2}$, which was originally set arbitrarily for the purposes of investigation while pending further work. We have found in later versions of this report that it should be $g_0 > 10^7 \text{ m/s}^2$. Hence, CASE_4 along with other cases should be computed again for much greater values of g_0 with the expectation that the two forms of potential energy should be much closer together with corresponding much lesser values in E_{r-loss} .

In conclusion, we have found that classical mechanics must be inadequate in the description of gravitational fields and the corresponding forces and energy equations.

17 Momentum or push gravity as the universal and unifying cause of all types of acceleration (force)

If gravity is finally proven to be caused by gravions under the working of PG, then it could be a logical conclusion that all forces may be attributable to a similar cause, albeit by different kind of push particles. What would then be needed is that each kind of particles have a mean free path much longer than the dimensions of the masses (particles) acted upon. This requirement is already fulfilled for planets and stars by gravions, to which we may also refer as the first type-I push particles. The force is then generated by the law of conservation of momentum and energy. This momentum force is well established in physics as it is also a tangible phenomenon, i.e. understood by common experience. We may then extend the proposal to apply to all kinds of force fields regardless of the size of the field generating body. This may be a sensible proposition, because size should not be an obstacle at least for all experimentally known particles. Given that the size of an atom is of the order of $\approx 10^{-9}$ m, we still have 16 orders of magnitude to reach the Planck particle, the length ℓ_P of which is defined as:

$r, \text{ m}$	$U_N(r), \text{ J}$	$U_{PG}(r), \text{ J}$	$U_N(r) - U_{PG}(r), \text{ J}$	$E_{r-loss}, \text{ J}$
6371002	1.4450E+12	1.4396E+12	5.3244E+09	1.5297E+19
6377371	1.4435E+12	1.4382E+12	5.2786E+09	1.5181E+19
6434710	1.4306E+12	1.4257E+12	4.9931E+09	1.4489E+19
7008100	1.3136E+12	1.3102E+12	3.4326E+09	1.0848E+19
7645200	1.2041E+12	1.2016E+12	2.4855E+09	8.5690E+18
8919400	1.0321E+12	1.0306E+12	1.4661E+09	5.8971E+18
9556500	9.6330E+11	9.6213E+11	1.1687E+09	5.0364E+18
12742000	7.2248E+11	7.2201E+11	4.6840E+08	2.6914E+18
25484000	3.6124E+11	3.6118E+11	5.6142E+07	6.4519E+17
50968000	1.8062E+11	1.8061E+11	6.9504E+06	1.5975E+17
101936000	9.0310E+10	9.0309E+10	8.6676E+05	3.9844E+16
203872000	4.5155E+10	4.5155E+10	1.0828E+05	9.9550E+15
407744000	2.2577E+10	2.2577E+10	1.3533E+04	2.4884E+15
815488000	1.1289E+10	1.1289E+10	1.6916E+03	6.2208E+14

Table 19: *Variation of various forms of energy of the system of spheres of CASE_4*

$$\ell_P = \sqrt{\frac{\hbar G}{c^3}} \quad (222)$$

where \hbar is the reduced Planck constant. The Planck length is about 10^{-20} times the diameter of a proton.

Thus, nucleons may be maintained by their own surrounding push (momentum) particles, the nucleus may be maintained by yet another kind of push particles, and so on for atoms, each group maintained by their own associated type of momentum particles. The universal situation may be that the space is filled by particles with a wide range of sizes (energies/wavelengths) corresponding to an equally wide range of mean free paths, acting as push particles to their matching (corresponding) relatively much bigger particles (bodies). The entire universe may then be thought as an agglomeration of varying concentrations of matter automatically sorting out themselves by the surrounding push particles. This proposition may then constitute a likely basis for a unification of all force fields in the cosmos from the smallest to the largest phenomena. Le Sage made a similar attempt to account for forces of different chemical strengths, by the existence of different species of “ultramundane” corpuscles of different sizes, whilst all this should be reconsidered and re-appraised in the light of modern particle physics, quantum mechanics, relativity and astrophysics.

Ultimately and inexorably, however, the above model only shifts the problem to what keeps the “ultimate” mysterious particle as a unity (re gravion), if not for an attractive force, according to Kant’s philosophical reasoning. However, the lack of understanding of the nature of an ultimate particle is not yet reason good enough to reject a possible unifying model that allows us to concentrate our attention more to a smaller “area” of the cosmos that underlies as a common denominator to all other processes.

From the above broad model, we may narrow down the cosmological questions to assuming the existence of types of particles corresponding at least to the known force fields. Thus, gravions are type-I push particles that mediate the gravitational force, type-II push particles are those mediating the electrical field forces, type-III those mediating the nuclear forces, etc. Already, in quantum theory the electric field is thought to be due to a continuous stream of exchange of photons (say, here type-II particles). Dibrov (2011) believes that the core of electrons and positrons remains stable by pressure of the bombardment of “fations”. The electron, in his proposed model, “*as against the static Abraham-Lorentz electron, is the dynamic object transforming the gravitational field energy into the energy of the electric field, and periodically exploding up.*” However, he probably means something very different to our proposed model in this report, because he talks about charge already being present in the electron, and he only tries to justify the re-emission of the “fation” energy in the form of electric field sub-particles. Considering various parameters quantitatively and his main conclusions, it is clear that his theory is not consistent with our findings. For example, “the active mass is not equal to the passive mass”, he discovers a “violation of equivalence principle for the electron” and that the “gravitation

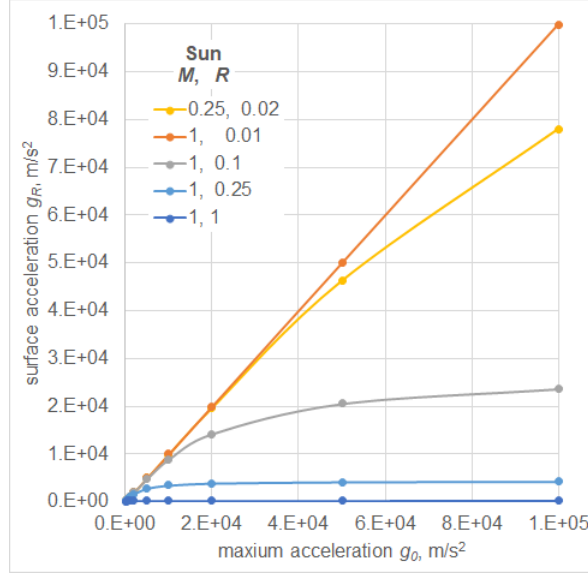


Figure 31: *Surface g_R against maximum g_0 for stars with mass and radius (M, R) in units of Sun mass and Sun radius.*

constant G is not equal to the actual one”, to mention a few aspects of his push gravity theory that are in clear variance to the ideas proposed herewith. Nevertheless, an "exploding electron" seems consistent with re-emission of absorbed graviton energy.

We may go on to elaborate on our general proposal (model). For example, the type-II particles, in particular, may be subdivided either in two sub-classes responsible for the positive and negative electrical force (such as opposite spin or an as yet unknown attribute), or may emanate from two complementary types of matter organization at the electron and positron level. The emanated energy (type-II) carriers exit as a result of the absorbed type-I push particles by protons and electrons, and so on and so forth.

In summary, for a field unification theory, it is logical and consistent to envisage and assume that all force fields are created by particles including gravity. This general idea of the underlying particles for all fields is then greatly facilitated by a push/momentum mechanism in a PG framework advanced in this report. A general push particle field principle may then be seen as one kind of self-similarity as used in fractal theory. Could self-similarity be used to recreate a new standard model in physics?

18 White dwarfs, neutron stars and black holes

Note: This Section has not been edited and is retained per original version_1 of this report, in order to track the developmental ideas through to current attempts towards a unification of a quantum push field theory; this can be found in chronologically later Section herewith.

It is reported that the gravitational field on a white dwarf is of the order of 10^6 m/s^2 , whilst that on a neutron star is of the order of 10^{12} m/s^2 , and much greater on black holes. If these extreme accelerations are caused by gravions (in that case being the universal cause of all gravitational fields), then it might be unlikely that we can practically detect them directly by the methods proposed here, because of the need for extremely sensitive gravimeters. However, if it were found that the maximum g_0 is, say, around 30000 m/s^2 by some careful measurement, then we would be faced to explain the super high values of acceleration on white dwarfs, neutron stars and black holes. Then, one possible explanation would be to assume that those extreme accelerations may be caused by different, more energetic types of push particles. Before we further speculate on these other hypothetical types of push particle, let us apply a little further the already found PG relationships below.

We continue our investigation from where we left off in Section 9.1. By increasing the maximum prevailing acceleration g_0 in the neighboring universe, we inversely decrease the corresponding k (see Eq. 65) by

$$k = \frac{\pi G \rho}{g_0} = \frac{3GM}{4g_0 R^3} \quad (223)$$

so that by keeping the mass and radius of a star constant, the PG equation is reduced to the value provided by Newton, namely, to $\frac{4}{3}\pi G \rho R = GM/R^2$, which is the saturation (asymptotic) value(s) observed

in Fig. 10, when k becomes sufficiently small.

Let us now see the values of surface acceleration g_R against the prevailing maximum acceleration g_0 possible in a particular space of the universe for stars having various combinations of masses M with radii R . This is shown in Fig. 31, where both mass and radius are expressed in units of Sun (\odot) mass and radius. The masses used are those of the apparent Sun mass but taken to be the real mass of a hypothetical star as a first approximation to get a feel of the situation. Then as expected, the pair $(M, R)=(1, 1)$ reproduces the curve in Fig. 10 very close to the abscissa (visibly touching it) with an asymptotic value approaching the Newtonian value of surface acceleration of our Sun. The additional curves now show the outcomes of different values of the pair (M, R) , which can be understood by the above Eq. 223: For any fixed, g_0 and M , the value of k increases very fast with a decrease of radius, which forces the surface acceleration to be well below the saturation values is reached, as noted by the curves on the figure. When R reduces below a sufficiently low value, k becomes so large that the factor A_R in PG becomes unity and $g = g_0$, which is the straight line at unity slope in the figure.

In the event that we can safely measure g_0 and find that this is not as high as on the surface of a dwarf, however, it may be sufficient to trigger gravitational collapse in the presence of a critical mass. After the collapse, a white dwarf is formed that may be sustained also by push particles of a different kind (type-II). Likewise, upon formation of a neutron star, the forces holding it together may further be provided by push particles of a third kind (type-III) as they evolve upon the onset of a further collapse. This proposal forms initially a qualitative model, which is depicted with some hypothetical quantitative dimensions in logarithmic scales (powers of 10) in Fig. 32. The validity of such a hypothesis should by all means be cross-examined against existing data and theories in astrophysics to be further refined or even rejected, if not appropriate.

For the general reader and to better describe the proposed model here, it is helpful to summarize the current understanding of these dense bodies by conveniently referring to a brief description provided in relevant articles by Wikipedia contributors (2019g). The summary descriptions below are needed to precede a new idea here attempting to connect the neutron star field with the atomic nuclear field, both unified under the proposed PG field model.

A white dwarf is a very dense stellar core remnant composed mainly of electron-degenerate matter. It has a mass like the Sun with a volume like the Earth. Because it no longer undergoes fusion reactions, it has no source of energy, so that it cannot support itself by fusion heat against gravitational collapse. It is supported by electron degeneracy pressure and is extremely dense. Accretion takes place by accumulating particles into a massive object, typically gaseous matter. Galaxies, stars, and planets, are formed by accretion processes. Neutrinos are radiated by white dwarfs through the Urca process (Wikipedia contributors, 2019f), which is a neutrino-emitting process playing a central role in the cooling of neutron stars.... White dwarfs have masses from about 0.07 to 10 M_\odot .

An astronomical body can collapse by its own gravity drawing matter inward toward its center. Gravitational collapse is a fundamental mechanism for structure formation in the universe. It can all start from relatively smooth distribution of matter gradually collapsing to form pockets of higher density, stars and planets, stellar groups and clusters of galaxies.

A giant star with a total of between 10 and 29 solar masses collapses to a neutron star (Wikipedia contributors, 2019c). Other than black holes, neutron stars are the smallest and densest stars with a radius on the order of 10 km and a mass less than 2.16 solar masses. They are produced from the supernova explosion of a massive star, and together with gravitational collapse achieve the density of atomic nuclei.

Binary systems of neutron stars can undergo accretion making the system bright in X-rays and a source of short-duration gamma-ray bursts, as well as produce gravitational disturbance. At soaring temperatures, electrons and protons combine to form neutrons via electron capture, releasing a flood of neutrinos. It is important for our model proposed here to quote verbatim from Wikipedia the following: *“When densities reach nuclear density of $4 \times 10^{17} \text{ kg/m}^3$, neutron degeneracy pressure halts the contraction. The in-falling outer envelope of the star is halted and flung outwards by a flux of neutrinos produced in the creation of the neutrons, becoming a supernova. The remnant left is a neutron star. If the remnant has a mass greater than about 3 M_\odot , it collapses further to become a black hole”*.

The temperature inside a newly formed neutron star is from around 10^{11} to 10^{12} Kelvin. However, the huge number of neutrinos it emits carry away so much energy that the temperature of an isolated neutron star falls within a few years to around 10^6 kelvin. At this lower temperature, most of the light generated by a neutron star is in X-rays.

A neutron star has some of the properties of an atomic nucleus, including density (within an order of magnitude) and being composed of nucleons. In popular scientific writing, neutron stars are therefore sometimes described as ‘giant nuclei’. However, in other respects, neutron stars and atomic nuclei are quite different. A nucleus is held together by the strong interaction, whereas a neutron star is held together by gravity. The density of a nucleus is uniform, while neutron stars are predicted to consist of multiple layers

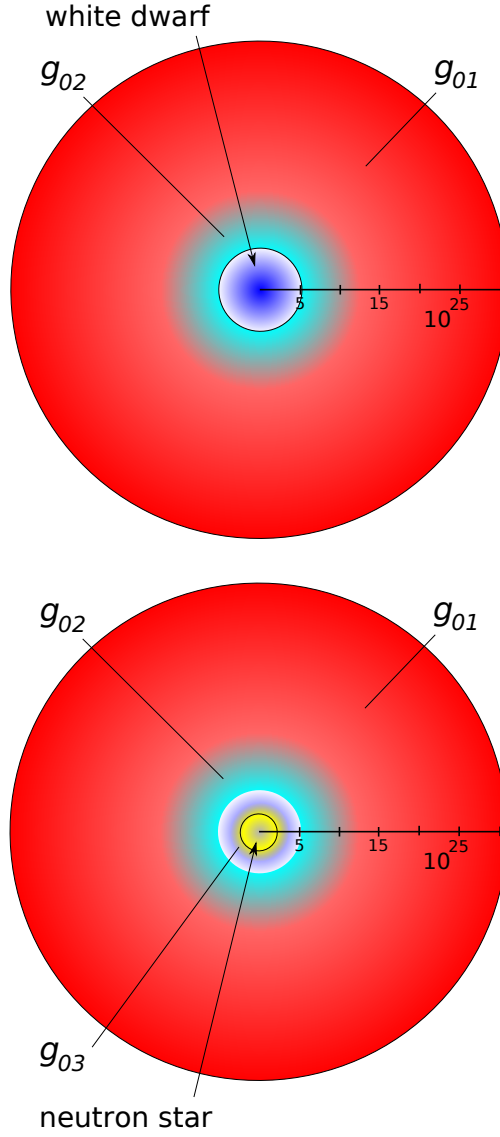


Figure 32: Diagrammatic perception of a white dwarf (above) with its surrounding PG type-II (g_{02}) field inside the universal type-I (g_{01}) field, and a neutron star (below) with its surrounding PG type-III field (g_{03}) inside a dwarf type-II (g_{02}) field inside the universal type-I (g_{01}) field; the scales in m are logarithmic and approximate.

with varying compositions and densities.”

It is the above last statement that we can seize upon to support the PG model here, namely, we say here **that a nucleus and a neutron star are both held by the same force: That force is the pressure exerted by the presumed type-III push particles.** We propose that the strong nuclear interaction is no different from the neutron star gravity, namely, both being created by push particles of the same type. In consequence of this model, the space around any atomic nucleus inside the electron orbitals is occupied by push particles holding the nucleus together. The current understanding is that this space seems relatively more "empty" than the interplanetary space, so there is nothing weird about our hypothesis that push particles small enough occupy this space fulfilling the requirements of PG with regard to mean free path and absorption coefficient of the nucleus. There is plenty of "room" for such superfine particles on the scale all way down to the Plank length. It may turn out that these push particles are x-rays and gamma-rays of sufficiently short wavelength, which would be consistent with the strong x-ray emission by neutron stars. That may also provide the existence/mechanism of x-ray emission by the orbital electrons in atoms adjusting to different energy levels, as well as somehow explain the original mystery of stable electron orbitals of accelerating orbital charges. Thus, the atom is a micro-neutron star created from (after) breaking down a neutron star. We might want to call the corresponding type-III push particles *neutrions* (neutron + $\iota\omicron\nu$) in analogy to gravions. However, in proposing this model, it may not be clear how to differentiate between a nucleus and a neutron particle, so that we may have to refine the various distinctions of push particles mediating strong and weak interactions and all other sub-nuclear forces. The proposed model is only a general approach towards a unification of fields, which requires the cooperation of particle physics and astrophysics.

The above proposed scheme for neutron stars and atoms may not be acting alone, as it requires the simultaneous cooperation of a type-II push particles holding electrons and nuclei together in the atom. In a similar fashion, white dwarfs are the plasma state by free electrons and nuclei having released their mediating binding (type-II) particles around the white dwarf. These mediating particles responsible for the appearance of electric field might be called *electrions* (from electricity + $\iota\omicron\nu$). "Neutrions" and "electrions" are finally redistributed after explosion to form atoms.

At any rate, the above general model could be described in more specific terms of particle physics such as: Gluons participate in the strong interaction in addition to mediating it. This is unlike the photons, which mediate the electromagnetic interaction but lacks an electric charge. Gluons also share this property of being confined within hadrons. One consequence is that gluons are not directly involved in the nuclear forces between hadrons. The force mediators for these are other hadrons called mesons. Although in the normal phase of QCD single gluons may not travel freely, it is predicted that there exist hadrons that are formed entirely of gluons — called glueballs. There are also conjectures about other exotic hadrons, in which real gluons (as opposed to virtual ones found in ordinary hadrons) would be primary constituents.

The above intermittent extracts from established theories and observations from astrophysics and particle physics serve only to stimulate further discussion, one way or another, that could involve the push theory principle consistent with the findings of this report.

In continuation to the proposed "aether of gravions" in Section 14.1 and generalized push particles in Section 17, it is envisaged that other types of push particles finally "leak out" into space together with gravions achieving some steady state concentration in various regions of space. Whilst their concentration is highest around their associated specific fields, which they mediate, like around white dwarfs, neutron stars and black holes, and various atomic and nuclear fields, the "aether" is a "soup" of various types of extremely fine particles. The "electrions" after mediating the electric field in matter, they leak out of bodies and fill the space. Thus, they might mediate also the propagation of photons in space, which is not an absolute vacuum, whilst they are also entrained by bodies. Electrions are also "energetic" particles, like gravions activating (or mediating) corresponding physical processes in electricity; they permeate not only space but also matter. Electrions seem to be responsible for charge and electricity, in a similar fashion to gravions being responsible for creating effective (active) mass, i.e. the conventional mass we are familiar with. Nikola Tesla, forgotten genius of electricity and the man who invented the twentieth century (Lomas, 1999), may have already envisaged the medium for the electric field and the propagation of lightning, when he was suggesting that we swim inside an inexhaustible source of energy.

18.1 More on mass, energy and black holes

We now continue from where we left off in Section 14.6 canvassing the possibility that black holes consist mainly of passive mass per Eq. 137.

From the preceding discussion on massive bodies in general, we have proposed the possibility that these bodies are surrounded by different layers of different fields generated by the corresponding different types of push particles. For the dynamics of such bodies (kinematics and kinetics) in push gravity, it is important

to consider the distance between any two given bodies. For long enough distance, they will be governed by our familiar long range gravity field due to gravions, but at closer range other types of field will take over or prevail, like the fields around white dwarfs, neutron stars and black holes. It is not yet known to the present author whether the proposed hypothesis agrees with data from astronomy and astrophysics. It is not known how the “gravitational” fields and masses have been calculated, whether these data are amenable to review, and overall if PG and the data can be inter-interpreted, re-interpreted, and/or mutually adapted, or the PG theory must be modified or be aborted. These questions need to be addressed by many more workers with appropriate expertise. Nevertheless, some tentative ideas are put forward next by way of trialing conjectures.

In a recent report, an active galactic nucleus (AGN) believed to be the explosion from a supermassive black hole has been announced (Giacintucci *et al.*, 2020). It looks like an outburst in slow motion that *“would take at least 240 Myr to rise to the current radius moving with the sound speed, which is an upper limit on the velocity, so the actual age would be greater than that”*. In our proposed model of a black hole, a small disturbance could create an instability to the spherical geometry exposing some internal mass near the surface to the action of push particles, in turn, setting off a chain reaction to a full blown explosion. The explosion would be necessary because, otherwise, the stable sphere can only hold a maximum limit of effective mass. As more passive mass is accessed by push particles, more effective mass is created by a process continuing for a long time. The internal passive mass of a black hole may resemble black powder waiting to explode. The end result is the creation of active mass (effective mass) in a huge cloud that will later start yet another cycle of galaxy and star formation according to prevailing theories.

The internal stuff, from which black holes are made of, is completely shielded from the action of push particles of various types, like gravions, electrions, neutrinos and black-hole-field push particles. All these types of particles can actually exist in all of our everyday materials according to the preceding model. Even black hole stuff may be present in the smallest possible quantities corresponding to what we initially have called “real mass”. By way of self-similarity, the universe is deconstructed and reconstructed recursively.

We may have a tangible illustration of particle-matter transformation to energy in the $E = mc^2$ equation and conversely.

The above may not be implausible, as there is some similarity with current theories about the Higgs boson (field) giving mass to subatomic particles. Without the Higgs field, we wouldn’t exist, i.e. mass would “evaporate”. Similarly, we may say that push particles maintain the integrity of material bodies at all levels of organization, whilst in the absence of said push particles (fields), the effective mass would cease to exist too. We may now have a reason, why the Higgs field exists. Matter cannot exist in absolute vacuum, and so PG theory is on the same page with some prevailing theories. There remains to work out an understanding on the relationship between gravions and black hole passive matter, as well as the interaction between gravions and all matter manifested in the universal constant Λ , i.e. the number of scattering events per unit mass thickness (area density).

Mathematics provide relationships about things, but not what the things are, whilst theorists often are not concerned as to what it means. Thus, we hope that PG can fulfill such a gap haunting several areas in physics. The physics/maths ratio needs a substantial overhaul, where physics lags behind mathematical formulations; mathematics is supposed to serve physics, whereas physics has become subservient to mathematics. For example, the mathematicians(?) invented the Higgs field, but they don’t tell us what it is, not to mention a long standing difficulty in conceptualizing relativity outside a narrow circle of high expertise scientists.

18.2 Total absorption layers and black holes

In continuation to the conceptualization of possible gravitational fields around massive bodies per Fig. 32, below we attempt to provide also a conceptualization of the interior of massive (very dense) bodies by some simple qualitative considerations.

In Sections 14.6 and 14.7, we found that the effective mass becomes concentrated towards the outer layers of a material body, be it a sphere, or a line segment, or any other shape, when we sufficiently increase the product $k \cdot \text{length}$. At a very high value of the latter product with a characteristic low value of contraction factor per Fig. 5, the effective mass is concentrated in a relatively thin outer layer resembling the event horizon (Schwarzschild surface). Associated with this is the limiting gravion parameter of maximum acceleration g_0 together with the governing Eqs. 149 and 150. From the preceding proposals about white dwarfs, neutron stars and black holes, they may also be characterized by their own corresponding limiting (maximum) acceleration parameters, so that we can suggest similar outer layer concentrations of effective masses due to absorption of the corresponding type of push particles. To clarify and avoid confusion about this emerging novel situation, we need to introduce an appropriate terminology of the more general case of the look-alike “event horizon” or “Schwarzschild” parameters with reference to gravions and other push particles, i.e. over and above the existing terminology. The established terms for event horizon and

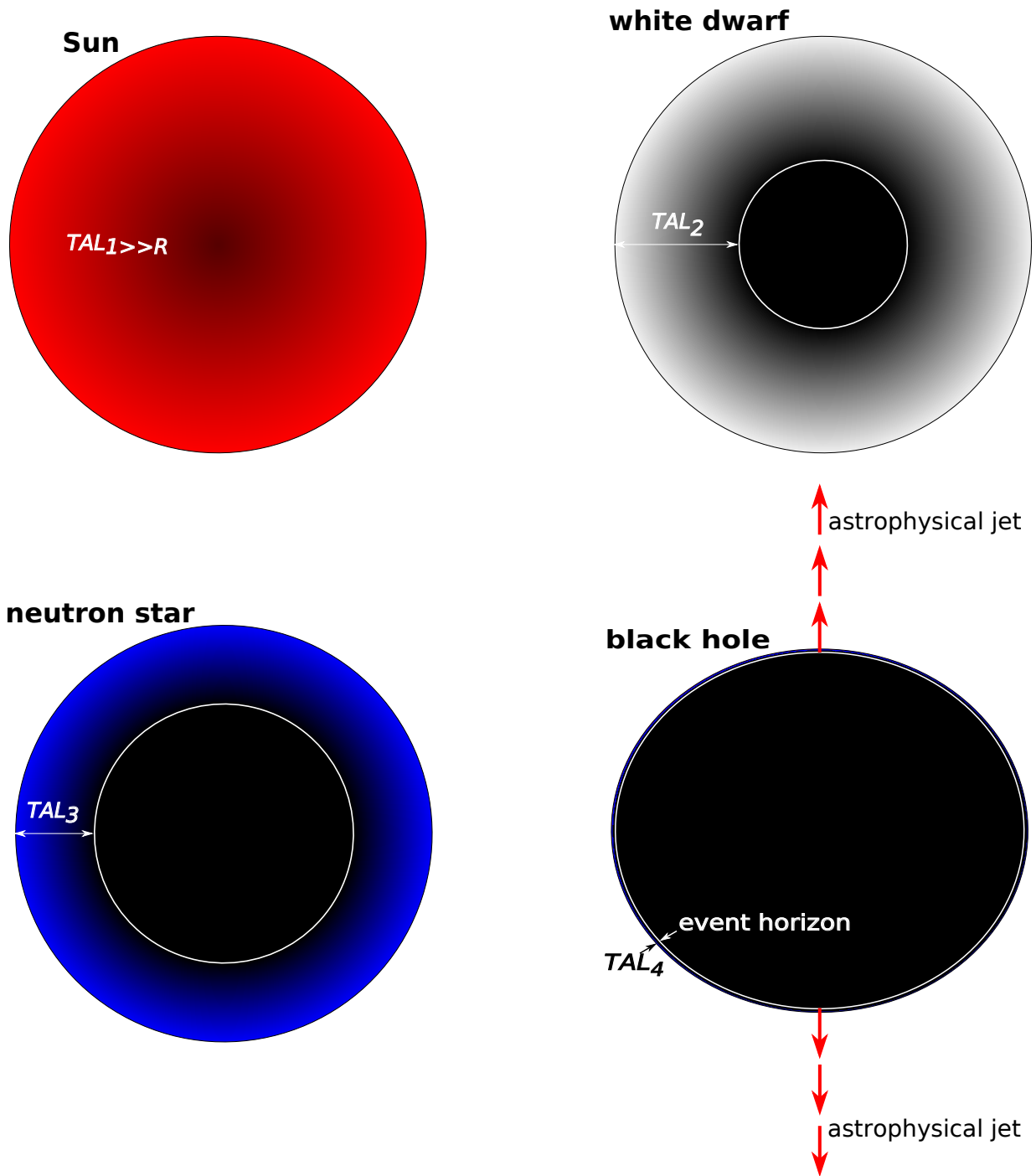


Figure 33: Diagrammatic perception of the Sun (upper-left), white dwarf (upper-right), neutron star (lower-left) and black hole (lower-right) with their corresponding total absorption layer

Schwarzschild radius are expressed differently from the corresponding ones arising from gravions. The well known Schwarzschild radius R_S is given by

$$R_S = \frac{2GM}{c^2} \quad (224)$$

whereas our PG limiting radius R_0 (at $A_R = 1$) due to gravions is given by

$$R_0 = \sqrt{\frac{GM_e}{g_0}} \quad (225)$$

A possible correlation (and numerical comparison) between the two quantities and the correspondence between the said event horizons should be done in conjunction with possible values of g_0 with different types of push particles. We can return to this issue after we outline the various regimes below. ~~In fact, a possible agreement of the above two equations seems to be born out during the development of push electricity reported in Section 21.~~ Later work reported in Section 18.4 has now revealed that there is a clear differentiation between the Schwarzschild radius of general relativity and the characteristic radius R_0 of push gravity.

From the Beer-Lambert law, we generally define an attenuation or absorption length as the distance inside a material, whereby the incident intensity drops to $1/e$ of the initial value; that is, the transmitted intensity decreases to about 37% with 63% being absorbed. We generally define the transmission fraction or transmittance T , and transmission depth τ by:

$$T = \frac{J}{J_0} = \exp(-\tau) = \exp(-k\chi) \quad (226)$$

where we use our parameters of k and χ with $\tau = k\chi$. We can also define a particular transmission depth resulting in an arbitrary amount of absorption of practically “all” gravions, say, 99% absorption allowing only 1% transmission. We designate such a depth with $\chi_{0.01}$, when $\tau_{0.01} = -\ln 0.01 = 4.60517 = k\chi_{0.01}$, so that $\chi_{0.01} = 4.60517/k$. For a line segment ℓ or radius R and, depending on the value of k , we can have $\chi_{0.01} \geq \ell$ or R . By convention and for practical purposes, we may define the 99% absorption layer, or any other convenient absorption fraction, as the “*total absorption layer (TAL)*”. Theoretically, there is no “total” absorption layer on account of the exponential form of the absorption, but in reality, we can assume there must be one by introducing a quantum mechanism of absorption in a quantum push gravity theory (QPG) later. ~~A rigorous quantitative presentation of the distribution of various PG parameters (hence of absorption layers) has been presented in Section 24.1,~~

With reference to Fig. 32, we can continue with the terms of push particles being “type-I”, “type-II”, type-III, “type-IV” and so on. Now, each of these bodies should have their own TAL for the corresponding type of push particle. We have also reserved more explicit terms for each of those types, like gravions, electrions, neutrions and possibly others to be used later as the need arises. We may use the Roman or Arabic numerals in ascending order of field strength or ascending order of generating process, something to be finally determined again later. The use/attachment of expressive (explicit) words have been used provisionally in this report, whilst their order may evolve and change as we more firmly establish the associated processes that generate those fields in PG. Thus, we can envisage a (nearly) total absorption layer relative to gravions and abbreviate it with a subscripted acronym TAL_1 or TAL_I (“*type-I total absorption layer*”). Similarly, we may apply the same scheme for subsequent denser bodies: We can envisage a “*type-II total absorption layer*” TAL_{II} or TAL_2 for white dwarfs, a “*type-III total absorption layer*” TAL_{III} or TAL_3 for neutron stars, also a “*type-IV total absorption layer*” TAL_{IV} or TAL_4 for black holes, and so on for other possible intermediate fields/bodies/particles. We initially (tentatively) think that these thicknesses may rank as $TAL_1 > TAL_2 > TAL_3 > TAL_4$.

By applying the workings of internal spherical field for the Sun, the internal contraction factor is only a little less than for Earth and both a little less than unity. By way of visual illustration (not to scale), we show the Sun’s distribution of effective mass in Fig. 33 (upper-left). Thus, we deem that $TAL_1 \gg R_{Sun}$. For a white dwarf, we may initially assume that $TAL_1 < R_{dwarf}$, for which a visual representation is provided in Fig. 33 (upper-right). Likewise, we have conceptualized a neutron star (lower-left) and a black hole (lower-right) in the same figure. We don’t know at this stage how the various types of push particles and total absorption layers may superpose or interact with each other and how we may rank them. We have not considered the possibilities of other, or intermediate situations, like the existence of quark stars.

At a later stage, we should compute the effective mass envelop of a black hole also in the shape of a rotating spheroid. We then find the dependence of the thickness of this envelop on the curvature of the spheroid. If the thickness is significantly less at the poles than at the equator, then an astrophysical jet could be formed at the poles on account of internal hydraulic pressure exerted by the envelop membrane

everywhere inside the body. This weakening at the poles may be further enhanced by forces due to rotation. Also, the size of the black hole can be significant for such a process, but all this remains to be answered by formulating the entire dynamics of such a system. As soon as the black matter is squeezed out and exposed to push particles of all kinds, it becomes effective (active) mass and literally “lights up”. This is consistent with observed jets of plasma material coming out from the center of galaxies presumably occupied by black holes. It is plausible that black hole matter is jettisoned by squeezing out initially non-inertial (passive and inert) mass to form astrophysical jets.

A rough analog, in some respects, to conceptualize black holes may be the formation of liquid droplets or soap bubbles in the atmosphere in the absence of gravity (e.g. inside the international space station). The surface tension plays a decisive role for the spherical shape of the smallest of droplets, whilst its role changes as more mass is accreted. When the droplets becomes very large, any small perturbation causes the droplet to wobble and deviate from the spherical shape. The eccentricity of a rotating bubble can be also a contributing condition. Some resemblance may take place with black holes but with properties unparalleled by our familiar bubbles: There is no surface “tension” per se, whilst the interior is an incompressible and non-inertial (conventionally) mass being literally inert and inactive. The interior does not generate any force but can be acted upon by the membrane forces. Black holes can in principle grow to arbitrary large sizes, but as they do so, they become more unstable by nearby disturbances and/or by rotation. A breach at the poles will squirt out inert mass at extreme acceleration and velocity while the exterior surface of the forming jet becomes activated. This situation is governed by new mechanics to be worked out.

Earlier, we referred to the difference between real and effective mass as “passive” mass $m_{passive}$ (per Eq. 137). We could also call it “black matter” or “black mass” and designate it with $m_b \equiv m_{black}$, which should not be confused with the term “dark” matter already in use by existing physics terminology but with a different meaning. Thus, we can write for the real mass (and matter) in PG:

$$m = m_e + m_b \quad (227)$$

Based on the above equation, we can say that there is some fraction of black matter even in ordinary objects. That fraction can be exceedingly small, moderate or excessive depending on the size and density of the object. There must be more of this stuff in the Sun than in the Earth. The amount of gray color-level showing in the diagrams in Fig. 33 gives some idea about it (not to scale). We may visualize more black matter towards the center of celestial bodies. In doing all this, it is important that we have only considered some average density throughout each of the above bodies, whereas in reality the density is variable. We have seen in Section 10 that actual density distribution can alter all other parameters involved. The same applies for the planets and stars, so that the picture conveyed by Fig. 33 for the Sun could be misleading. Those who have all the relevant data about the Sun may like to see how we can build the correct PG picture of the Sun. The same applies for all other bodies in Fig. 33 and not only. We have selected those four typical types of bodies, but all other intermediate bodies with all available data could be re-worked to fit, or to see if they can fit under PG.

The above is an initial conceptualization of what might happen around and inside stars and other massive bodies, but is subject to later modification as we develop and better understand PG theory. Even the proposed classification of various fields and various types of push particles may be entirely or partially incorrect needing proper adjustments along with corresponding fractions of effective and black mass, for example, if existing information on surface gravity of those bodies is revised.

In the above general scheme, we imply that the maximum value of a starting g_0 is sufficient to trigger the first transition of a star to a white dwarf. Depending on the literature source, the pressure at the center of the Sun may range between 3×10^{13} - 3.5×10^{16} Pa. This is expected to be well below the maximum pressure by gravions predicted by Eq. 36

$$p_{0g} = \frac{J_0}{c} = \frac{g_0^2}{\pi^2 G} \quad (228)$$

which will be known when J_0 or g_0 is finally measured. For a tentative $g_0 = 4 \times 10^4$ m/s², we have $p_{0g} = (4 \times 10^4)^2 / (\pi^2 G) = 2.43 \times 10^{18}$ Pa. Therefore, this pressure is consistent with existing requirements for a star on the main sequence to collapse to a white dwarf. The pressure at the core of Sirius B (white dwarf) is estimated to be $\times 10^6$ that of the sun, which means that we need a $g_{02} > 10^3 g_0$.

If the conceptualization of various bodies in Fig. 33 is generally correct, it would question the validity of existing methods for finding their mass, radius and distance. There shouldn't be a serious problem for the main sequence stars, if their contraction factor q is not far from unity. From the observed (intrinsic) brightness, color (temperature) and distance, the established measurements of mass and radius might involve only a small correction, but for stars outside the main sequence, in particular for white dwarfs etc, we may have significant discrepancies between existing values and reality. To address this problem, we would probably

also need to develop a concurrent quantum theory of push gravity. We need to re-appraise conceptions and requirements of established theories of nuclear particles and force fields. We now see that PG opens new possibilities for modeling our physical observations. For example, the Chandrasekhar curve may need re-adjustment, if we note some discrepancy with PG, rather than object to PG. We will return to the question of white dwarfs later after we attempt an inquiry at the small particles level. Like the flying shuttle weaves the fabric out of yarn, so may push particles weave the fabric of effective mass out of real mass (matter, or stuff). The material form of objects as we experience them is created from an amorphous substrate/matter through the action of gravions and other push particles by as yet unknown staged processes. We would need to bring together all particle physics data to date and attempt to explain them by PG.

One important corollary here is to indicate that the current scales of the cosmos may require adjustment. This should not be overlooked even if specific mechanisms above might turn out to be fallacious simplifications. Therefore, prospective criticisms against PG may themselves be based on false grounds. In turn, agreement or not by various theories (including GR) involving existing measurements of dwarfs, neutron stars and black holes may have to be revised. As a result, the findings of PG, like in Section 16 of the novel relationship between mass and force should not be dismissed (based on some other theory) until an integrated resolution of all emerging issues is obtained.

Note: The transmission depth τ defined above is based on an assumed exponential variation of J with depth. In a later development on mass-matter relationship in Section 24, we have derived the exact variation of several parameters as a function of radius in spherical geometry bodies. They are not pure exponential functions, but we can still define an equivalent or effective transmission depth to convey the same main ideas above.

18.3 Is the Big Bang an artifact?

Based on the preceding Section and further considerations below, the Big Bang theory is under question. The reasons of our query are presented in three groups:

(1) Because the methods for finding the mass, radius and distance of various celestial bodies require adjustments and corrections based on PG, a reappraisal of the Big Bang becomes necessary. The expansion of the universe is deduced from plotting the recessional velocity against distance, whereby the velocity is deduced from the redshift of distant bodies (Hubble's law). To the extent that redshift is based on photometric methods, which have already proved to be only an estimate by existing methods, PG adds additional reasons to further question the outcomes for the recession velocity of astronomical objects.

(2) The "tired light" theory has, by and large, been abandoned (it is said) as reason to reject the cosmological redshift. It has been questioned whether distortions of photons are created at the source or during their travel in space. However, until we can better determine the nature of photons with respect to their emission, transmission and absorption, tired light theory remains as a candidate for questioning the expansion of the universe. In this connection, PG is currently developing a new understanding of the nature of photons in Section 31.

(3) However, there is an additional reason for questioning the Big Bang: After considering all possible causes of the redshift, the remaining gravitational redshift may play the main reason for abandoning the expansion theory. It may be that the most massive bodies at very long distance overwhelm all other determinations of redshift from visible data. It is only those massive bodies that can be (are) visible and detected, while all smaller bodies at the same distance are not detectable due to light loss in the intervening distance. If that is what happens, then the redshift (spectroscopic and/or photometric) does not represent the entire contents inside the given visible distance. These largest bodies can be moving in equal numbers away or closer, but their gravitational redshift overwhelms the Doppler shift (red or blue). Therefore, the redshift on average can be biased in favor of the dominating massive bodies providing a misleading impression about the average motion of all visible bodies. In that case, the redshift predominantly represents "size" towards the outer regions of the universe (if it is mainly due to gravitational shift). The farther the distance, the more gravitational redshift (than recessional redshift) is represented in our measurements. It is said that gravitational redshift can take on a large range of values. Then size becomes very important, to an extent that overtakes the recessional redshift. In that case, we cannot claim that redshift (overall) of very distance objects represents velocity, but more so it represents size. By "size" we mean a combination of effective mass and real mass (per PG) together with radius, all of which relate to luminosity and distance. If the methods of measurement of mass, radius and distance require revision for all the reasons presented in the previous section and if light absorption during travel further complicates our measurements, then the redshift relationship to size and distance need to be reworked also. In that case, we would need to plot the size against distance, whereby the shape of the graph may not be linear any more (a shape to be found). In that case, the long established tenet of velocity versus distance relationship (Hubble's law) should be revoked.

In any case, we propose that the universe is uniform in all directions with regards to average velocities and sizes of all celestial bodies, however, not all of which are visible within the maximum visible universe. There are (maybe) equal numbers of bodies with redshift and blueshift in all directions. We mean at sufficiently (very) long distances, because PG allows variations of physical constants (like G) from region to region sufficiently apart. However, the most distant ones that are visible happen to be also the bigger, so that we inadvertently filter out the smaller ones during our observations. Our observations would then be biased and introduce an artifact by the outer visible galaxies in our thinking that they are moving faster than the closer ones. In that case, the Big Bang can be simply an artifact. It can be an artifact merely of the visible universe and not of the actual universe altogether, namely, observable and not observable (as defined by special relativity). Note: The “average” and “sufficient” words here have relative significance to be established by the actual data available in each referenced case.

The above requires considerable amount of work on both existing and new astrophysical/astronomical data, before we can accept it as a denial of the long established “big bang” belief. All this could be clarified, when cosmologists reappraise and review their methods of measurement now to be based on the new framework of PG. It is said that measuring photometric redshift is easier to use than direct distance measurements, but this is not only a crude method, it can also be wrong on account that it is not known how luminous objects are in reality. The use of such means to measure the masses of objects independent of the mass-to-light ratio may contribute to artifacts. These problems are convoluted by the new possibilities of reality revealed by PG as outlined in preceding and later sections of this report.

If PG does indeed provide a new real framework for new physics, and if astrophysical and astronomical measurements do indeed require a re-calibration, then not only the Big Bang should be reconsidered as unreal, but also all other competing alternative theories may stand on shaky ground (re cosmic microwave background (CMB), steady state model, etc.)

It is said that “*CMB radiation is landmark evidence of the Big Bang theory for the origin of the universe.*” However, even this should also be reappraised. In particular, it is said that “*With a standard optical telescope, the background space between stars and galaxies is almost completely dark. However, a sufficiently sensitive radio telescope detects a faint background glow that is almost uniform and is not associated with any star, galaxy, or other object*” (Wikipedia contributors, 2024b). The spectroscopic measurements in the space between visible galaxies may not be an empty space filled with “background” radiation after all that is independent of the ever present cosmic bodies. The allegation (or assumption) that the CMB is the remnant of the Big Bang may prove to be entirely arbitrary and the ensuing support for the Big Bang unwarranted. In that intervening gap, there is actually a practically infinite number of galaxies, of which only the most massive ones get their light through to us to see and measure. As we increase the angular resolution our spectroscopic/photometric measurements in that “space”, we may simply resolve clusters of those most massive bodies, which at the same time appear “redder and redder shifted”, on the micro-wavelength scale. In that case, the CMB may not be another confirmation of the Big Bang theory. Furthermore, the paradoxical discrepancy of the rate of expansion of the universe based on spectroscopic redshift and on CMB redshift (Hubble tension) might or might not be resolved, but this by itself does not solve the problem. It is beyond the means available to this author to carry out such work, which is left to ambitious cosmologists to work it out. This author only projects his philosophical tenets in physics on this matter by use of the available resources to him. The space can easily be filled with a cosmic fluid (e.g. gravions), and the space can be overall homogeneous and isotropic over sufficiently large scales.

If Big Bang becomes redundant, a lot of complicated theories will be unnecessary and our understanding could be greatly simplified. The universe could be much simpler than we have thought so far. If we start with a wrong premise (like universe expansion), we are constrained to formulate needlessly complex mathematical relationships only to comply with the wrong starting point of our theories. For example, take “*proper and comoving coordinates*” introducing only redundant hard-and-complex work for cosmologists. We may have misconceived the nature of the universe due to systematic biases and errors. The universe can easily be static and always comoving. Philosophically, the universe in its eternity must not change to something else overall, but it always flows within itself. The Big Bang is philosophically untenable. The vacillations between contracting or expanding universe must have been in vain. We advocate the “static” and “flat” universe, to the requirements of which we should comply from now on.

There is no need for the present author to delve deep into the long literature of the Big Bang and the expansion of the universe, since especially following the launch and use of the James Webb Space Telescope (JWST) a momentous debate has skyrocketed worldwide.

The “Hubble Tension” is a point of current controversy, and not only that. New contradictions expose a fundamental gap in the understanding of cosmos, so that “new physics” becomes necessary. We mentioned several reasons for that. A flaw also in the Lambda Cold Dark Matter model and Dark Energy driving

the expansion of the universe are under question too (Riess *et al.*, 2024). Even if the Hubble Tension is somehow resolved, it is still signaling New Physics (Freedman, 2024), while the Big Bang theory can still be an artifact.

We are bombarded with expressions like “*The Universe Has Stopped Expanding! James Webb Space Telescope Shocks the Entire Space Industry!*” We hear that “*Galaxies appear small, smooth and surprisingly old in the JWST, but according to the big bang theory, as space expands, they should appear larger as they move away due to the stretching of light: However, the galaxies become smaller as the distance increases*”... “*Even galaxies with greater mass and brightness bigger than our galaxy appear in the JWST images 2-3 times smaller than the previous images obtained by the Hubble telescope*”... Also “*the redshift is 2-3 times greater challenging the assumptions of an expanding universe. They must be exceptionally tiny to explain the optical illusion (mighty mouse galaxies)*” (Labbe *et al.*, 2023)... “*The age of the universe appears to be older than previously thought, if to explain the new findings with galaxies as big as our own, even after a few million years after the big bang*”... “*The number of redshifted galaxies above 10 is 100000 times greater than predicted*”... and “*if verified with spectroscopy, the stellar mass density in massive galaxies would be much higher than anticipated from previous studies on the basis of rest-frame ultraviolet-selected samples*” (Labbe *et al.*, 2023)... All of these and much more are not expected by “established” theories and the expansion of the universe is now seriously questioned. We hope that our PG theory provides the ultimate framework to arrive at a much better understanding of the cosmos. The absence of any mention of our theory (PG) in what appears to be a long and comprehensive list of “*Alternatives to general relativity*” (Wikipedia contributors, 2024a) leaves much to be desired about the status of physics today.

A concise article has also been written on this question separately by Danilatos (2024). It contains some fundamentals from PG theory together with an early explanation of a possibly expanding universe taken from Section 33.1.

18.4 Cosmological Redshift-Distance Relation without Universal Expansion

As of December 2025, further developments arising from later sections of this report, as well as from more recent work by the author, have led to results that extend and, in some instances, refine earlier parts of the present manuscript. A complete reconciliation and consolidation of the preceding and subsequent sections will be undertaken in a final integrated revision of the work. In the interim, the principal new findings—reported separately in Danilatos (2025)—are incorporated here in condensed form, with relevant extracts reproduced and adapted below

18.4.1 Cosmological Redshift:

Cosmological redshift is understood as the stretching of photon wavelength induced by the expansion of the universe. In the Friedmann–Lemaître–Robertson–Walker framework, the redshift parameter z relates to the scale factor $a(t)$ via

$$1 + z = \frac{a(t_{\text{obs}})}{a(t_{\text{emit}})}. \quad (229)$$

Empirically, for nearby galaxies, this leads to the Hubble–Lemaître law

$$v = H_0 D, \quad (230)$$

where v is interpreted as recessional velocity, D is the comoving distance, and H_0 is the present Hubble constant. The tension between early- and late-universe determinations of H_0 (Riess *et al.*, 2024), and the unexpected abundance of massive, evolved galaxies at high redshift revealed by JWST (Labbe *et al.*, 2023) (Naidu *et al.*, 2022; Kokorev *et al.*, 2023; Gottumukkala *et al.*, 2024; Giulietti *et al.*, 2024) suggest that the interpretation of z purely as expansion may require revision.

18.4.2 Gravitational Redshift in General Relativity

In GR, photons lose energy as they climb out of a gravitational potential well. For a static, spherically symmetric Schwarzschild field, the exact gravitational redshift of a photon emitted at radius r is

$$z_{g\text{GR}} = \frac{1}{\sqrt{1 - \frac{2GM}{rc^2}}} - 1. \quad (231)$$

Define the compactness parameter

$$x \equiv \frac{2GM}{rc^2} = \frac{R_S}{r}, \quad (232)$$

where R_S is the Schwarzschild radius. Then Eq. (231) takes the form

$$1 + z_{\text{gGR}} = (1 - x)^{-1/2}. \quad (233)$$

As $x \rightarrow 1$, the redshift diverges, which corresponds to the approach toward the event horizon.

However, all observed astrophysical objects have $x \ll 1$, even neutron stars where typically $x \sim 0.4$. Thus the gravitational redshifts actually observed in nature are very small, with measured values typically ranging from $z \sim 10^{-6}$ (solar surface) to $z \sim 0.3$ (extreme neutron star conditions). This is vastly smaller than cosmological redshifts ($z = 1\text{--}15$).

Figure 34 illustrates this behavior in the GR curve (red line). The additional curves in this figure result from and are explained by the continued work next.

Consequently, within the observable universe so far, large redshifts cannot be attributed to gravitational fields under GR.

The general-relativistic expression for gravitational redshift used here follows standard derivations in modern expositions (Carroll, 2004).

18.4.3 Newtonian Gravitational Redshift

Before comparing with PG theory, it is useful to revisit the Newtonian derivation of gravitational redshift using the effective-mass concept for photons. This derivation extends beyond the classical escape-velocity argument of Michell (1784) and produces a closed-form, exact Newtonian expression for gravitational redshift. Because this derivation forms the basis for a subsequent extension, and for good measure, we present all the detailed steps for reference when needed:

Let a photon of initial wavelength λ_r be emitted at radius r from a spherical body of mass M . Its local energy is

$$E_r = \frac{hc}{\lambda_r}. \quad (234)$$

Assuming the photon carries an effective mass

$$m_{\text{eff}} = \frac{E}{c^2} = \frac{h}{\lambda c}, \quad (235)$$

the infinitesimal work done against gravity when the photon climbs by dr is

$$dE = -\frac{GMm_{\text{eff}}}{r^2} dr = -\frac{GM}{c^2} \frac{E}{r^2} dr. \quad (236)$$

Thus

$$\frac{dE}{E} = -\frac{GM}{c^2} \frac{dr}{r^2}. \quad (237)$$

Integrate from r to ∞ :

$$\ln\left(\frac{E_\infty}{E_r}\right) = -\frac{GM}{rc^2}. \quad (238)$$

Exponentiate:

$$E_\infty = E_r \exp\left(-\frac{GM}{rc^2}\right). \quad (239)$$

Convert to wavelengths:

$$\frac{\lambda_\infty}{\lambda_r} = \exp\left(\frac{GM}{rc^2}\right). \quad (240)$$

Therefore, the Newtonian gravitational redshift is

$$z_{\text{gN}} = \exp\left(\frac{GM}{rc^2}\right) - 1. \quad (241)$$

To compare with GR, retain the compactness definition

$$x \equiv \frac{2GM}{rc^2}, \quad (242)$$

so that $\frac{GM}{rc^2} = \frac{x}{2}$. Then Eq. (241) becomes

$$z_{\text{gN}} = \exp\left(\frac{x}{2}\right) - 1. \quad (243)$$

As shown in Fig. 34 (orange curve for Newton), even at the limiting case $x = 1$ the Newtonian redshift saturates at

$$z_{gN}(x = 1) = e^{1/2} - 1 \approx 0.6487, \quad (244)$$

which is far smaller than typical cosmological redshifts.

Therefore Newtonian gravity, like GR, cannot account for large observed cosmological redshifts under conventional interpretations. So far, both GR and Newtonian predictions do not support our claim stated at the outset. The GR curve diverges as $x \rightarrow 1$, while the Newtonian curve approaches a finite value. In both cases, for realistic astrophysical objects, x stays well below unity, yielding redshifts far smaller than those observed in cosmology.

The above derivation follows treatments that interpret photon frequency loss via energy conservation in a Newtonian potential (Catto, 2014; Okun, 2006). More importantly, it is based on the *critical* understanding that converting the classical potential energy to a mass equivalent via $E = mc^2$ applies only when $A_R = 1$. This means that the exact Newtonian derivation of the gravitational redshift in Section 18.4.3 necessitates that the photon be treated (considered) as a highly compact body itself. Otherwise, we must introduce appropriate adjustments.

18.4.4 Gravitational Redshift in Push Gravity Theory

Push Gravity (PG) revises the understanding of mass and its distribution within a gravitationally active body. The key PG insight is the distinction between:

- *effective mass* M_e — the gravitationally active component generally for all bodies variously distributed, but particularly concentrated in an extremely thin Total Absorption Layer (TAL) for very compact bodies, and
- *black mass* — the gravitationally inert component generally for all bodies variously distributed in the interior that does not participate directly in gravitational absorption.

Both are components of *real mass*, or *hyle*. In PG, the standard gravitational parameter $\mu = GM$ is replaced by

$$\mu_{PG} = GM_e = A_R g_0 R^2, \quad (245)$$

where

- A_R is the absorptivity (dimensionless),
- g_0 is the universal maximum gravitational acceleration,
- R is the physical radius of the compact body.

This relation arises from the absorption dynamics in the TAL and replaces the conventional GM term throughout Newtonian-style gravitational interactions. Crucially, M_e is not concentrated at a point, nor does it correspond to the total rest mass. Instead, it describes the effective action of the absorption layer.

To compute the gravitational redshift in PG, one repeats exactly the same steps used in the Newtonian derivation—but replaces GM by the PG gravitational parameter from Eq. (245). This yields the exact PG redshift:

$$z_{gPG} = \exp\left(\frac{A_R g_0 R^2}{rc^2}\right) - 1. \quad (246)$$

Maximum Compactness in PG In PG, a maximally compact object is defined not by a singularity or coordinate pathology but by the saturation of absorptivity and surface acceleration:

$$A_R = 1, \quad g(R) = g_0. \quad (247)$$

Such bodies possess a limiting radius R_0 for a given effective mass M_e , determined through Eq. (245). The TAL becomes extremely thin, fully absorbing incident gravions mediating gravity. The interior mass becomes gravitationally opaque (no inertia, inert, gravitationally inactive) but not singular.

Substituting $A_R = 1$ and $R = R_0$ into Eq. (246) yields

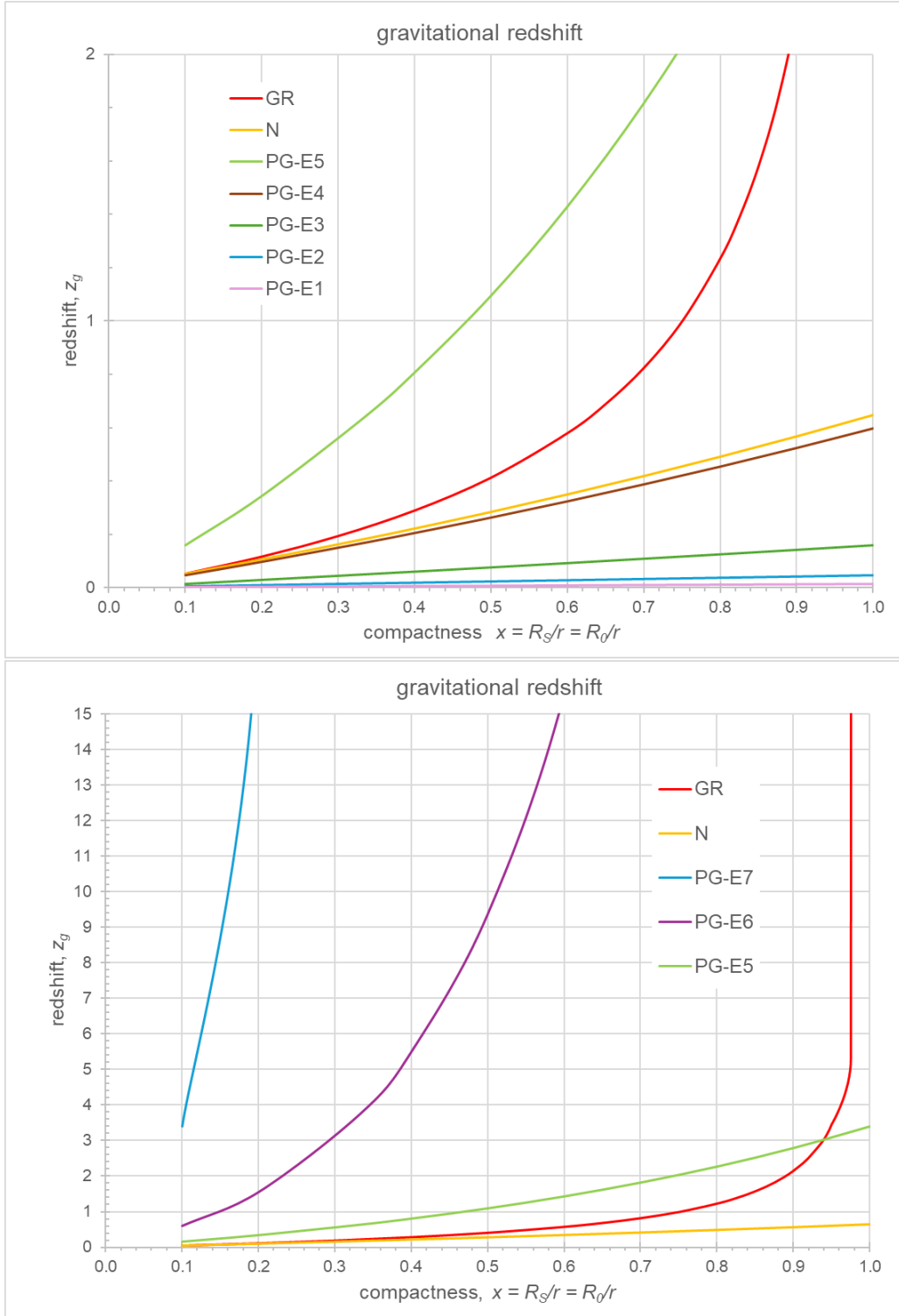


Figure 34: Comparison of gravitational redshift predicted by GR (red curve), the exact Newtonian effective-mass model (orange curve), and PG plotted against compactness values x . The PG model produces a family of curves corresponding to different effective masses, here shown as labeled powers E_n , $n = 1 \rightarrow 7$, representing compact objects with total mass $n M_\odot$. PG allows large gravitational redshifts even at moderate compactness, owing to its dependence on the physical radius R_0 of the compact body rather than on the theoretical Schwarzschild radius alone.

$$z_{\text{gPG}} = \exp\left(\frac{g_0 R_0^2}{rc^2}\right) - 1. \quad (248)$$

Define

$$p = \frac{g_0}{c^2}, \quad (249)$$

so that

$$z_{\text{gPG}} = \exp\left(p R_0 \frac{R_0}{r}\right) - 1. \quad (250)$$

This reveals that PG redshift depends sensitively on both the radius R_0 and the emission radius r . In contrast with GR and Newtonian gravity, PG allows substantial gravitational redshifts even far from $r = R_0$, provided R_0 is large enough.

For a direct comparison, we can now define the compactness factor by

$$x = \frac{R_0}{r} \quad (251)$$

and re-write the PG gravitational redshift as

$$z_{\text{gPG}} = \exp(p R_0 x) - 1. \quad (252)$$

Numerical Estimates Using a preliminary PG finding (see Section 31.5)

$$g_0 = 1.331942797 \times 10^9 \text{ m s}^{-2}, \quad (253)$$

we obtain

$$p = \frac{g_0}{c^2} \approx 1.4819862273 \times 10^{-8} \text{ m}^{-1}. \quad (254)$$

Compact bodies of increasing mass yield increasing values of R_0 in PG.

We can now complement Fig. 34 by illustrating the PG redshift in comparison to GR and Newtonian models. The PG redshift of Eq. (248) is shown against R_0/r for a sequence of values of R_0 corresponding to effective masses ranging from $1M_\odot$ to $7M_\odot$. The resulting PG redshifts can exceed unity by large factors, reaching and surpassing the observed redshifts of JWST high- z galaxies.

In this framework, extremely large redshift values arise not from cosmic expansion but from intense gravitational fields associated with very massive objects whose radii have been underestimated in standard and prevailing analysis.

These results challenge the interpretation that large observed redshifts necessarily imply cosmic expansion.

18.4.5 A Re-appraisal of Luminosity and Distance by PG Theory

Given the distribution of effective mass in PG, especially for compact objects whose gravitationally active mass resides within a thin TAL, the conventional relation between luminosity, mass, and radius requires a fundamental revision. In standard astronomy, the intrinsic luminosity of an object is treated independently of its gravitational structure. In PG, however, the geometry and mass distribution of the TAL directly influence both the emergent luminosity and the inferred distance.

18.4.6 Conventional Relation Between Luminosity and Distance

The observed flux f , intrinsic luminosity L , and physical distance D of an astronomical object are related by the inverse-square law:

$$f = \frac{L}{4\pi D^2}. \quad (255)$$

Here,

$$f = \text{apparent brightness (flux)}, \quad L = \text{intrinsic luminosity}, \quad D = \text{distance}.$$

18.4.7 Luminosity of Compact Bodies in PG

For general absorptivity values $A_R < 1$, the connection between A_R , effective mass M_e , and luminosity remains an open theoretical task. However, for maximally compact bodies satisfying $A_R = 1$, PG provides a clear simplification: the entire effective mass is concentrated in a thin TAL at radius R_0 . In such cases there is no need to model radiative transfer from an interior volume; the luminosity is set by surface processes at the TAL.

It is therefore plausible—and consistent with PG structure—to assume that the intrinsic luminosity scales with the surface area of the absorption layer:

$$L \propto M_e \propto R_0^2. \quad (256)$$

This contrasts sharply with GR-based compact objects, where luminosity is either severely suppressed or originates from accretion physics rather than a well-defined physical surface.

Distance as a Function of Flux and PG Radius Substituting the proportionality $L \sim R_0^2$ into Eq. (255), we obtain

$$D^2 \sim \frac{R_0^2}{4\pi f}, \quad \Rightarrow \quad D \sim \frac{R_0}{2\sqrt{\pi f}}. \quad (257)$$

Thus, knowledge of R_0 implies knowledge of distance.

Determining the Radius R_0 from PG Redshift The PG gravitational redshift for a compact body with $A_R = 1$ is provided by Eq. 250 being rearranged as

$$1 + z_{g\text{PG}} = \exp\left(p R_0 \frac{R_0}{r}\right), \quad (258)$$

Taking natural logarithms:

$$\ln(1 + z_{g\text{PG}}) = p R_0 \frac{R_0}{r}. \quad (259)$$

For emission from the physical surface of a maximally compact body in PG, $r = R_0$, hence

$$\ln(1 + z_{g\text{PG}}) = p R_0. \quad (260)$$

Solving for R_0 ,

$$R_0 = \frac{1}{p} \ln(1 + z_{g\text{PG}}). \quad (261)$$

Distance in Terms of Redshift and Flux Substituting Eq. (261) into the luminosity–distance relation gives

$$D \sim \frac{\ln(1 + z_{g\text{PG}})}{2p\sqrt{\pi f}}. \quad (262)$$

Thus, in PG, the distance to a remote compact object can be determined directly from its gravitational redshift and apparent flux without appealing to standard candles or cosmological distance ladders. The absolute luminosity scales with the radius of the TAL, which is itself fixed by the PG redshift.

This relation has major cosmological ramifications.

18.4.8 Minimum Mass for a True Black Hole in PG

In prevailing gravitational theories, particularly General Relativity, a black hole is defined as a compact object whose gravitational field prevents the escape of any electromagnetic radiation. This condition is formalized by the existence of an event horizon, beyond which all light paths are causally disconnected from distant observers. The defining physical assumption is therefore absolute light trapping, independent of wavelength or photon energy.

In the Push Gravity (PG) framework, the same operational criterion is adopted: a black hole is understood as an object from which no electromagnetic radiation can escape. However, because PG predicts a finite and continuous gravitational redshift rather than a divergent horizon, this definition raises a critical question

that is usually implicit rather than explicit in standard treatments: given that electromagnetic radiation spans a finite range of wavelengths, does a finite upper limit to gravitational redshift exist, beyond which no observable radiation of any wavelength can reach a distant observer?

In PG, gravitational redshift increases monotonically with compactness but remains finite for any finite mass. Consequently, a *true* black hole, defined as an object from which no light of any wavelength escapes, can exist only if the gravitational redshift exceeds a maximum physically meaningful value.

A natural upper bound on wavelength is obtained by considering the minimum conceivable photon frequency. Following the PG framework, we adopt a conservative lower bound of $\nu_{\min} \sim 1$ Hz, corresponding to a maximum wavelength

$$\lambda_{\max} = \frac{c}{\nu_{\min}} \approx 3 \times 10^8 \text{ m}. \quad (263)$$

Gravitational redshifts in astronomy are inferred from spectral lines, which typically lie in the optical band. A representative emitted wavelength may therefore be taken as

$$\lambda_{\text{emit}} \approx 5 \times 10^{-7} \text{ m}. \quad (264)$$

The maximum gravitational redshift consistent with these bounds is then defined by the wavelength ratio

$$1 + z_{g \max} = \frac{\lambda_{\max}}{\lambda_{\text{emit}}} \approx 6 \times 10^{14}. \quad (265)$$

For maximally compact objects with total absorptivity $A_R = 1$, the PG mass–radius relation yields the effective mass required to produce a given gravitational redshift. Solving Eqs. 245 and 261 for the limiting case with $z_{g \max}$ gives

$$M_{\min} = \frac{c^4}{Gg_0} [\ln(1 + z_{g \max})]^2. \quad (266)$$

Substituting the numerical values yields

$$M_{\min} \approx 1.05 \times 10^{38} \text{ kg} \approx 5.29 \times 10^7 M_{\odot}. \quad (267)$$

This result implies the existence of a finite minimum mass for a true black hole in PG. Objects below this threshold, regardless of compactness, must necessarily emit radiation at sufficiently long wavelengths and therefore cannot be completely dark. Because the mass scale depends only logarithmically on the choice of emitted wavelength, the existence of this threshold is robust against reasonable variations in spectral assumptions.

The PG framework therefore predicts that stellar-mass and intermediate-mass black-hole candidates are not strictly light-trapping objects, but instead extremely compact bodies with large yet finite gravitational redshifts. Only objects exceeding the above mass threshold qualify as true black holes in the strict physical sense. Horizon-scale imaging of Sagittarius A* and M87* by the Event Horizon Telescope (Akiyama, 2019, 2022) therefore probes the compactness of these objects, but does not by itself establish the existence of an event horizon in the general-relativistic sense. Within PG, such observations are compatible with extremely compact, high-redshift objects below or near the true black-hole mass threshold. This prediction differs fundamentally from the general-relativistic notion of black holes and provides a clear observational and conceptual distinction between the two frameworks.

The adopted upper bound on wavelength is not arbitrary, but corresponds to an objective physical limit. This wavelength is associated with the minimum physical quantum, termed the “planckion,” which acts as the push particle mediating the fifth force field identified as the Planck field (See Section 31). Such radiation is expected to be presently undetectable and lies well beyond the infrared and microwave ranges associated with the cosmic microwave background (CMB).

A key implication of this result is that the CMB need not be directly associated with true black holes, nor uniquely with an early hot Big Bang phase. Instead, within the PG framework and under the caveat of Section 18.4.9, the CMB may arise predominantly from cumulative gravitational and other redshift processes operating throughout an eternal universe, as discussed further at the conclusion of this article.

Note: For finding the above M_{\min} outcome, the value $g_0 = 1.331942797 \times 10^9 \text{ m s}^{-2}$ applied is the latest theoretically derived estimate within the PG framework. Existing terrestrial gravity measurements do not contradict this lower bound, in that no evidence has been found for a smaller effective value. Should future developments of PG establish a larger value of g_0 , the corresponding gravitational redshifts would

increase accordingly, thereby reinforcing—rather than weakening—the principal conclusion of this work: that gravitational redshift can attain very high values within the PG framework. At the same time, an increase in g_0 would reduce the minimum mass required for the formation of a true black hole, relative to the value derived above. This dependence has direct implications for the population, distribution, and observational interpretation of compact objects throughout the universe.

18.4.9 Caveat

In deriving Eq. 262 for determining distance from the redshift of massive bodies with absorptivity $A_R = 1$, it is tacitly assumed that the radiation reaching the observer has not undergone additional processes contributing significantly to the observed redshift. As discussed elsewhere in this paper, we do not exclude the presence of other redshift mechanisms (e.g. tired-light-type processes, scattering, or intragalactic absorption effects). Consequently, the present derivation of PG gravitational redshift applies strictly to those objects and distances for which such additional contributions are subdominant. In more general situations, supplementary terms or correction factors must be incorporated to account for all mechanisms contributing to the total measured redshift.

It must further be emphasized that astronomical redshifts are usually measured from the integrated light of entire galaxies, whereas the present analysis concerns the gravitational redshift associated with individual massive compact bodies that may be embedded within those galaxies. The total observed redshift should therefore be regarded as a composite quantity, arising from multiple contributions operating both within galaxies and along the line of sight through intergalactic space. The PG contribution becomes dominant when the gravitational redshift associated with compact absorption-layer structures exceeds the cumulative effects of Doppler, environmental, and propagation-related redshift mechanisms.

In practical terms, the PG gravitational redshift component dominates the observed redshift when

$$z_{gPG} \gg z_{\text{Doppler}} + z_{\text{ISM}} + z_{\text{IGM}} + z_{\text{other}}, \quad (268)$$

where z_{Doppler} represents kinematic contributions, z_{ISM} and z_{IGM} account for intragalactic and intergalactic propagation effects, and z_{other} denotes any additional redshift mechanisms (including tired-light-type processes, if present). In this regime, the total measured redshift is controlled primarily by the compactness and physical radius R_0 of the emitting TAL structure, as described by the PG framework.

This caveat also addresses the natural question of why such massive compact bodies are not commonly observed at relatively nearby distances, but instead appear predominantly at the largest observable distances. In the PG framework, this behavior arises from the combined effect of large intervening distances, various selection effects and intragalactic processes occurring in massive galaxies that host compact bodies capable of producing substantial gravitational redshifts. The central claim advanced here is that gravitational redshift, arising from PG compact absorption-layer structures, must play a significant—and potentially dominant—role in producing the largest observed redshifts, contrary to prevailing theory that regards gravitational redshift as entirely negligible in cosmological contexts. Nevertheless, the term z_{other} must account to the extent of why the most massive compact bodies are not commonly observed at relatively “nearby” distances.

Before attempting a detailed decomposition of the various contributions to the total observed redshift, a necessary first step is to reappraise existing astronomical and astrophysical data across the entire observable universe within the PG framework. Such a remapping is essential for isolating the PG gravitational redshift component, assessing its relative importance, and establishing quantitative criteria for its dominance.

18.4.10 Critical conclusion

The recognition of a minimum required mass for the formation of a true black hole has emerged from a more mature analysis of photon behavior within the Push Gravity (PG) framework. This result was reached only after the foundational elements of PG had been substantially developed, including the physical origin of gravity, the extension of the push principle to other interactions, the unification of fields, and the emerging structural understanding of the electron, positron, proton, and nucleus. Within this hierarchy, the photon may be regarded as a comparatively large-scale body relative to the fundamental push entities (planckions), and its role had not previously been examined in sufficient quantitative detail.

Under these later considerations, the photon becomes central to the operational definition of a black hole: namely, an object from which no electromagnetic radiation of any physically meaningful wavelength can escape. On this basis, a critical minimum mass follows naturally, below which complete light suppression is not possible, regardless of body absorptivity.

This result necessitates a revision of earlier terminology used throughout this work. Compact bodies characterized by maximal absorptivity $A_R = 1$ were previously referred to indiscriminately as “black holes”

across all mass scales, from subatomic structures to astrophysical objects. The present quantitative analysis shows that not all maximally absorptive and compact bodies qualify as true black holes in the strict physical sense defined above. Objects satisfying $A_R = 1$ but failing to meet the minimum mass criterion given in Eqs. 266 and 267 must therefore be regarded as distinct ultra-compact absorptive bodies rather than true black holes.

Until a systematic terminological revision of the present working book is completed, earlier usage of the term “black hole” for such lower-mass objects should be understood as provisional. Importantly, this correction does not invalidate the physical reasoning or conclusions developed elsewhere, but rather sharpens their interpretation in light of a more complete understanding of extreme compactness within PG.

19 Towards a quantum push gravity (QPG) theory

The explanation of gravity as arising from push particles (the gravions) already indicates the quantum nature of the generated field. However, so far we have described and discussed the absorption of gravions by material bodies in general without much regard about the nature of the absorbing body. We have introduced an absorption coefficient k only to denote the number of absorption events per unit length inside the body. So far, the body may be a continuum, inside which the absorption process takes place; the process obeys Lambert’s law on the propagation of general radiation or beam transmission inside matter. It is the interaction of push particles with another material entity that completes the phenomenon of gravity. We attempt to complement our study by investigating the other side (member) of this process, i.e. the absorbing body including material particles like protons and electrons. In doing so, we must be reminded about the provisos of Part Two, namely, that these attempts may be revised by the author and the readers freely without harm to the outcomes of Part One.

The attempted development of a quantum push gravity (QPG) theory here follows an independent path from existing quantum gravity and quantum field theories. This happens either because the theory is self-sufficient without the need to introduce extraneous concepts, or because of limitations already outlined in the introduction of this report, which make a thorough literature survey impractical. The connection with existing theories may be effected as it becomes apparent to this author now or in later writing, but the onus is mainly on the expert reader to take over from all the loose ends created by, or left off from this report. The present sections may extend beyond the original scope of providing an early mathematical background of a push gravity theory for the purpose of designing experimental verification of its principles. Pending such verification, we are only left with a continuation of the theoretical development and a compilation of thought experiments.

It is generally accepted that force fields are responsible for the force exerted between two particles, or the force is the result of the exchange of virtual-force-carrier-particles between the said two particles. The force field generated by each particle acts on the other particle. Furthermore, it is said that particles are interpreted as the quantum excitations of each field. Thus, photons are the excitations of the electromagnetic field, gluons are excitations of the strong gauge field, Higgs bosons are excitations of one component of the Higgs field and gravitons are presumed to be excitations of gravitational field or waves.

PG starts with a presumed existence of gravion particles, a consequence of which is the gravitational field. In that sense, gravions create (underlie) the gravitational field. If a disturbance of the steady-state gravitational field is thought of as a wave, and if the graviton (per literature) is that wave, then gravions and gravitons are two separate and different entities. The gravions precede the gravitons, and we were justified at the outset to introduce a new term for the push particle of gravity, namely, the gravion or type-I push particle. In subsequent extension of PG, we introduced the electrion (type-II) push particle underlying the electric field. As such and following a parallel reasoning as with gravity, we may say that a photon is a perturbation of electrions from their steady-state equilibrium. In other words, if the underlying quantum fields are more fundamental than particles, then we take it one step deeper by understanding that fields themselves are made up by more fundamental particles, the nature of which is yet to be comprehended. We may repeat the same reasoning for any other type of push particles responsible for other force fields. We realize that the term “particle” used here may differ from its meaning in the literature, so that we try to use the qualifier word “push” often.

In the following sections, we continue with possible forms of quantization of absorbing bodies, some absorption parameters and a description of the proton, electron and positron under the laws of PG.

19.1 Minimum absorption center (MAC)

A particle beam or any radiation, in general, traversing a material body may be scattered or absorbed by the body, partially or totally. That is, we may have partial or total reflection, partial absorption and scattering

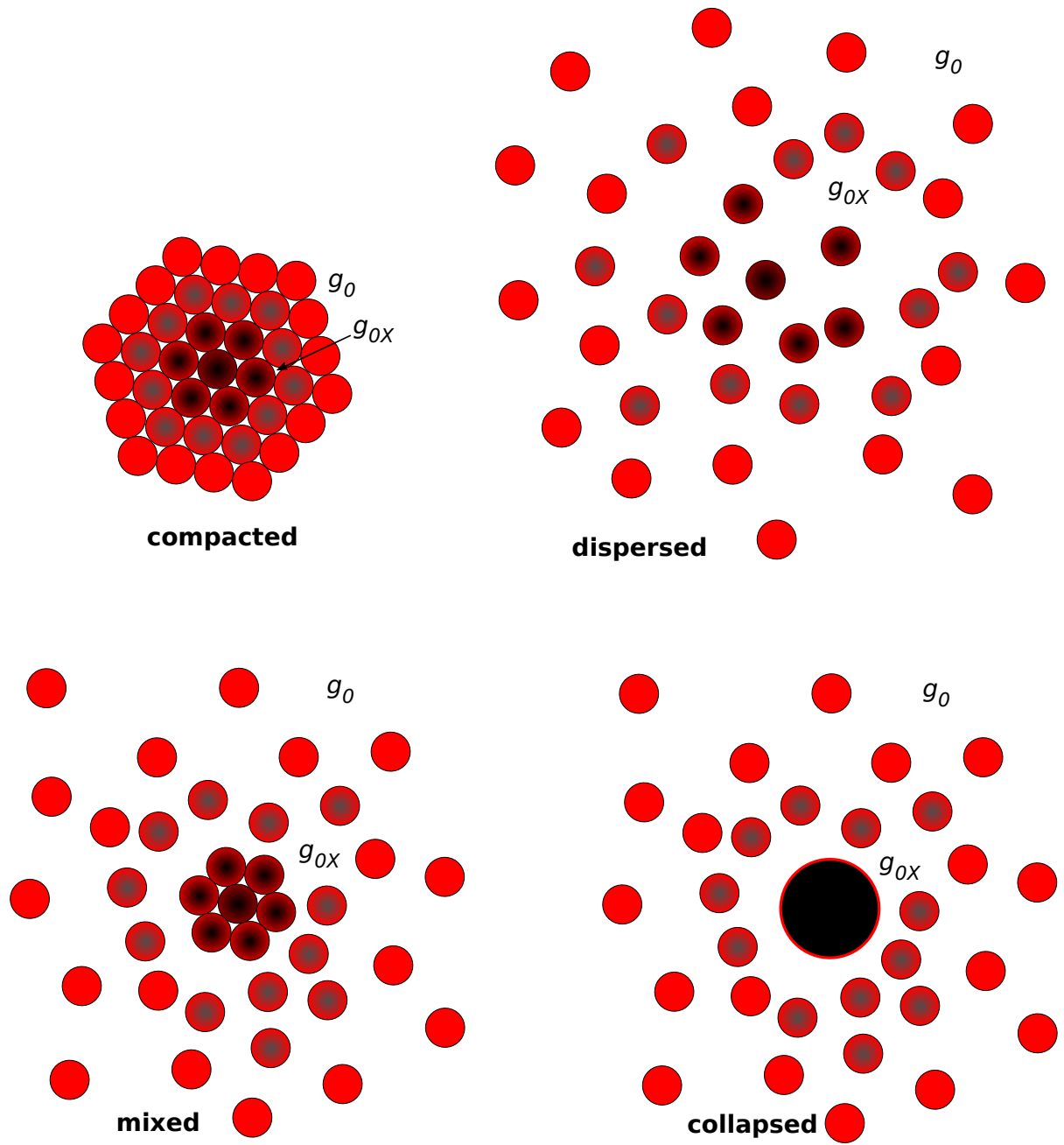


Figure 35: *Conceptualization and configurations of minimum graviton absorption centers*

or total absorption with concomitant changes in the reacting body. For push gravity, we have considered only total absorption of gravions as a necessary condition to develop the theory, whilst we defer consideration about some other type of scattering also taking place; we should stress that our going assumption applies only to gravity, i.e. other types of force field may behave differently.

Around the absorption "point" of a gravion, there must be a minimal amount of a material entity or mechanism performing the absorption process. This process must also allow additional gravions to accumulate up to a critical limit, whereupon the accreted gravions are lumped and emitted in another form of radiation by the reasoning proposed in Section 15.8. That is, the absorption "point" constitutes a minimum thermodynamic subsystem evolving by fluctuations in time to a state that can emit the accumulated gravion matter (and energy) as permitted by the fluctuation theorem. We may refer to this quantum subsystem or minimal material entity as gravion absorption center, or quantum gravion absorption center, or simply as minimum absorption center (MAC). The distribution of MACs depends on the nature and state of any given material body, be it a gas, liquid or solid, plasma, electron, nucleon, etc. Some conceivable distribution patterns are depicted in Fig. 35 to help in the ensuing analysis, but they are not the only ones, whilst other appropriate patterns can be devised as we evolve our understanding. A given MAC is drawn in full red color to indicate that it is fully active and free of any shadowing effect by other "neighboring" matter. A MAC can only be active or inactive, so that it should be drawn either red or black correspondingly. At and near the surface of a body, there is a maximum time exposure to push particles, whilst, as the depth inside the bulk of a material increases and due to the shadowing (shielding) effect by the overlaying layers, the time exposure decreases exponentially. In any situation, a MAC can be active or inactive, ON or OFF, one of two states, i.e. a process thought to be governed by a Poisson distribution probability. The variation of gray level in its mixture with red color in the diagrams describes just the time averages of them being between the active and inactive state, i.e. between effective or black mass (or matter).

The four spacial distributions shown in Fig. 35 are entirely arbitrary at this point of our understanding: They may be distributed at the highest packing order (compacted) as in a cuboctahedron, or at the most dispersed, or a mixed type of distribution. These distributions are determined by the fixed or averaged spacial distribution of matter determined by other forces, like the chemical bonds pertaining to the electric field. That means that another type of force field (say, the electric field) is also present and takes precedence prior to the gravion force field (gravity). If the hypothesis is correct that the other fields are also due to push particles, then those other push particles must be permeating in the interstices of matter at the appropriate scales to maintain the material body in its macroscopic form. We will consider the electric field in an upcoming version of the report, but we may remain with the gravitational (gravion) field for a while. The "collapsed" depiction of MACs in the provided diagram is an anticipated collapse of ordinary matter to the next or further finer-ingredient state, whereby the gravions can only penetrate a relatively small depth leaving the core as inactive mass with reference to gravions. However, this collapsed central region is a matter of concern whether we understand it correctly at this point, i.e. whether it is composed of plasma particles, neutrons, or quarks (not shown/resolved as finer spheres), or whether it is the ultimate black mass of a black hole. We have to return back to this section at a later stage of theory development.

It should be appreciated that the depictions in Fig. 35 are exaggerated in scale, because we already saw how little absorption takes place over the scale of planet sizes. The effects shown may become more evident above the scales of stars, etc. envisaged in the preceding Fig. 33.

19.2 Absorption coefficient vs. absorption cross-section

We can generally liaise microscopic with macroscopic processes, like those of microscopic particles with a (macroscopic) planet. We can apply the standard/general formulation of a directional particle beam scattering and absorption by a material body. Any macroscopic body may be composed of individual particles (including MACs) responsible for absorption events. Whether MACs may be thought of as particles themselves is a different question, because such "particles" may be impossible to isolate, or they may have an extremely short life to ever become observable. Nevertheless, we can say that the total number of absorbing particles, in whatever form, composing a planet would be the ratio M/m of the respective real masses of the planet and particles, of which the number density n is

$$n = \frac{M}{m} / \left(\frac{4}{3} \pi R^3 \right) = \frac{\rho}{m} \quad (269)$$

where R is the radius of the planet. A single particle has a characteristic radius R_0 , which defines a total absorption cross-section σ :

$$\sigma = \pi R_0^2 \quad (270)$$

The number of absorption events of a beam of gravions traversing our typical length ℓ is $k\ell$ with the generally known relationship for k :

$$k = n\sigma = \frac{\rho}{m}\pi R_0^2 \quad (271)$$

We also have from Eq. 118

$$k = \frac{\pi G \rho}{g_0} = \frac{\pi G \rho_e}{g_0 q} = \frac{k_e}{q} \quad (272)$$

where we similarly introduce a corresponding effective absorption coefficient k_e by:

$$k_e = \frac{\pi G \rho_e}{g_0} \quad (273)$$

and supplement yet another equation (formula) for the contraction factor:

$$q = \frac{k_e}{k} \quad (274)$$

The practical application of this effective absorption coefficient is that we can use the known effective mass of the used particle and the known effective mass of the planet, from the outset, to obtain a corresponding effective number density of the scattering particles:

$$n_e = \frac{\rho_e}{m_e} \quad (275)$$

The latter allows us to derive, or connect either of the absorption coefficients with the total absorption cross-section of the particle as:

$$k_e = n_e \sigma = \frac{\rho_e}{m_e} \pi R_0^2 = qk \quad (276)$$

The above method relates the microscopic absorption cross-sections with the macroscopic parameters of a planet, but the absorption cross-section can be taken to correspond to particles (including MACs) of any size with a given (absorption) effective mass. The particle can be an electron, proton, positron or any other body including the entire planet itself. In the latter case, from Eq. 225, the planet's minimum radius at $A_R = 1$ is

$$R_{0-planet} = \sqrt{\frac{GM_e}{g_0}} \quad (277)$$

Then we can write the following useful relationships:

$$k_e = n_e \sigma = \frac{\rho_e}{M_e} \pi R_{0-planet}^2 = \frac{3R_{0-planet}^2}{4R^3} = \frac{3GM_e}{4g_0 R^3} = \frac{\pi G \rho_e}{g_0} = qk \quad (278)$$

From the above equations, we can obtain the minimum absorption radius of the Earth (i.e. its absorption cross-section) as a function of the prevailing g_0 . For example, we get $R_{0-Earth} = 8.928614 \times 10^4$ m, a total absorption cross-section $\sigma_{Earth} = 2.504482386487 \times 10^{10}$ m² and $k = 2.31236 \times 10^{-11}$ m⁻¹ for $g_0 = 50000$ ms⁻², as can also be cross-examined against Table 2 with use of data from Table 3. Again, these values are produced based on an average density distribution of Earth and should be re-evaluated by proper accounting of the actual prevailing density situation in the future.

Note. The above numerical values can be updated given the later theoretical value of $g_0 = 1.331942797 \times 10^9$ ms⁻². That is, we get $R_{0-Earth} = 5.47 \times 10^2$ m, a total absorption cross-section $\sigma_{Earth} = 9.40 \times 10^5$ m² and $k = 8.68 \times 10^{-16}$ m⁻¹, also $A_R = 7.37 \times 10^{-9}$ and $q = 0.99999999585$,

19.3 Proton and electron parameters

Before we theorize a description of the electric field under push particle principles, we consider the gravion field (gravity) effect at the microscopic scales of proton and electron according to PG for a series of assumed cases with regard to their absorptivity and the amount of black mass possibly contained in them. We know that these particles have a gravitational mass, i.e. they have weight under gravity regardless of their very small size. We can use the available radius for proton, but no such radius is readily accepted for electron, for which it is said to be zero, or some very small value not yet found, or the so called "classical electron

radius”. We can return to these and other questions after we attempt to solve a series of cases in the form of exercises below. We take this approach initially, because of unknown parameters for these particles, with an intent to return for a another pass of computations later. None of the presented cases are claimed to represent actual cases, but they serve to alert us about some important issues.

19.3.1 Exercise: Proton parameters

Like for planets, we find the corresponding parameters for proton from Eqs. 145 and 147 given its (charge) radius and effective mass; the “charge” radius is used to be also the mass radius at this stage. The contraction q_p , absorption coefficient k_p and absorptivity A_{R-p} are given in Table 20 in the typical range for g_0 (we use p in the subscript for proton). We use the prevailing radius $R_p = 8.414000 \times 10^{-16}$ m and mass $m_{e-p} = 1.672622E \times 10^{-27}$ kg as its effective mass. We find that the contraction factor is very close to unity, which means that the real mass is very close to the measured effective mass.

From the above known parameters of proton, we find its total real mass m_p and its black mass component m_{b-p} from the contraction factor:

$$m_{b-p} = m_p - m_{e-p} = \frac{m_{e-p}}{q_p} - m_{e-p} = \left(\frac{1}{q_p} - 1 \right) m_{e-p} \quad (279)$$

We note that only an extremely small fraction of mass is inactive (black), whilst correspondingly the absorptivity is also very low. However, all these parameters may need revision as soon as the radius of the proton is further revised; in fact, we feel that such a revision is overdue, whilst PG will assist in doing so.

19.3.2 Exercise: Electron parameters in case of equal electron-proton real mass

The electron is considered an elementary or fundamental particle that cannot be decomposed to other particles, yet it presents some sort of a connection with proton by its constant (effective) mass ratio $\mu = m_{e-p}/m_{e-e}$, its equal but opposite charge and by both particles being stable in time (i.e. extremely long - if not infinite- lifetimes). The β^+ decay or “inverse beta decay” inside a nucleus is written by:

$$p^+ \rightarrow n^0 + e^+ + \nu_e \quad (280)$$

$$\bar{\nu}_e + p^+ \rightarrow e^+ + n^0 \quad (281)$$

where e^+ is a positron, ν_e is an electron neutrino and $\bar{\nu}_e$ an electron antineutrino. Likewise, the beta decay for the neutron (β^- decay) is written by:

$$n^0 \rightarrow p^+ + e^- + \bar{\nu}_e \quad (282)$$

It is said that all particles can be made from leptons. Without specifying the kinds of particles, the idea of building particles from other particles is consistent with the general concepts of PG and its framework. They could be described under PG too in balancing the energy and total mass yielding a tiny rest mass for

g_0	q_p	k_p	A_{R-p}	m_{b-p}
300	0.99999999704344	4.68513035281366E+05	5.25609157025589E-10	4.945210E-37
500	0.99999999822606	2.81107821135575E+05	3.15365494215353E-10	2.967133E-37
1000	0.99999999911303	1.40553910555320E+05	1.57682747107676E-10	1.483566E-37
2000	0.99999999955651	7.02769552745438E+04	7.88413735538384E-11	7.417906E-38
5000	0.99999999982260	2.81107821090695E+04	3.15365494215353E-11	2.967237E-38
10000	0.99999999991130	1.40553910544101E+04	1.57682747107676E-11	1.483618E-38
20000	0.99999999995565	7.02769552717388E+03	7.88413735538384E-12	7.418277E-39
30000	0.99999999997043	4.68513035144233E+03	5.25609157025589E-12	4.945890E-39
50000	0.99999999998226	2.81107821086207E+03	3.15365494215353E-12	2.967459E-39

Table 20: PG parameters for proton

the electron neutrino/antineutrino. We cannot enter into a detailed correlation or explanation of particle physics data under PG yet.

There seems to be a fundamental relationship between proton and electron, which can now be revisited under various possibilities presented by PG. These possibilities arise from the existence of and distinction between real, effective and black mass, which could presumably be used to establish that relationship. The possibility of combining gravion absorption with black mass in various proportions to produce effective mass for any given particle might assist existing theories in nuclear reactions and particle physics in general, as we might be able to better understand and explain the above reactions. For this purpose, we present some results in the form of a series of “exercises”, which might point to a direction, or provide the means to address the problem in due course.

For convenience, we repeat our previous equations: The radius of a particle is given by

$$R = \sqrt{\frac{Gm_e}{g_0 A_R}} \quad (283)$$

where in the limiting case of $A_R = 1$, we obtain the characteristic minimum radius R_0

$$R_0 = \sqrt{\frac{Gm_e}{g_0}} \quad (284)$$

It is said that electrons have zero radius, being point masses, or on account of its mass ratio with proton it may be less than 10^{-18} m, but the radius is as yet unspecified. There is also the classical electron radius of $R = 2.8179403227(19) \times 10^{-15}$ m, which, being greater than the proton radius, it is said to have only a theoretical value. Now, we could initially obtain a radius from the above formula, except that we don't know A_R . The value of $A_R = 1$ means an absolutely total absorption layer forming an effective mass with “zero” thickness. This would also imply an infinite, or extremely large real mass, which would be very difficult to explain. However, this idealized situation is simply a mathematical artifact that can be dealt with in a quantum PG. We can only accept a finite value for the real mass accompanied by a finite absorption layer thickness (TAL) for the existing (established) effective mass of the electron. We have no indication what the real mass of the electron may, or should be. That could perhaps be derived during a concerted effort to fit various existing data of the “standard model” or other data under the framework of PG. The present author is in no position to achieve this goal for lack of readily available knowledge of the existing vast pool of information. However, we can demonstrate by simple algebra how to go about with some tentative considerations in a possible relationship between proton and electron (or positron). In short, we can say that the electron is an opaque particle at $A_R \approx 1$ without the need to speculate on the structural details about how this takes place. However, all this leaves the case of the value $A_R < 1$ open for further investigation, with the understanding that the greater the departure from unity the more transparent the electron becomes.

We have generally considered the effect of shrinking a given constant spherical mass in Section 9.1. We apply this situation to the case of a proton and see what happens. Because its contraction factor is very close to unity and its absorptivity very small getting smaller at higher g_0 , it can be envisaged as being very “fluffy” or “compressible”. This is consistent with its structure of three quarks. In plain terms, the proton seems to be very “transparent” to gravions.

Initially, we consider what would happen, if we could compress the proton to a much smaller radius keeping its real mass constant. We re-write Eq. 145 both for a proton and an electron together with their contraction factors, whereby we also use the same real mass m for both:

$$m_{e-p} = q_p m = \frac{g_0}{G} A_{R-p} R_p^2 \quad (285)$$

$$m_{e-e} = q_e m = \frac{g_0}{G} A_{R-e} R_e^2 \quad (286)$$

[Note: the subscript $_e$ stands for “effective”, the subscript $_{-e}$ stands for “electron”, whilst the subscript $_p$ or $_{-p}$ stands for “proton”]. In other words, we consider that we compress the proton to such a radius that its effective mass reduces to become equal to the published (effective) mass of an electron, namely, $m_{e-e} = 9.1093837015 \times 10^{-31}$ kg. We expect that the effective mass of a sphere decreases, if we keep the real mass constant: Because A_R can never exceed unity, by arbitrarily reducing the radius in the above equations, the only compensation can be a reduction of the contraction factor and hence by a corresponding decrease of the effective mass.

The proton-to-electron mass ratio μ is well known to be:

$$\mu = \frac{m_{e-p}}{m_{e-e}} = \frac{q_p}{q_{-e}} = 1836.15267343 \quad (287)$$

where we have canceled the common m and also relate the above by:

$$\mu = \frac{A_{R-p} R_p^2}{A_{R-e} R_{-e}^2} \quad (288)$$

from which we find the electron radius as:

$$R_{-e} = \sqrt{\frac{A_{R-p}}{\mu A_{R-e}}} R_p \quad (289)$$

We can find the unknown A_{R-e} as follows: The contraction factor for the electron is given by:

$$q_{-e} = \frac{q_p}{\mu} = \frac{3A_{R-e}}{4kR_{-e}} \quad (290)$$

which yields the equation

$$\frac{3A_{R-e}}{4kR_{-e}} - \frac{q_p}{\mu} = 0 \quad (291)$$

The above can be solved first for the unknown product kR_{-e} (for electron), which appears also inside A_{R-e} (see Eq. 49), and from which we obtain A_{R-e} and then the electron radius from Eq. 289. We have done this numerically and list the final results in Table 21. Like for proton, we find the black (inactive) mass m_{b-e} for the electron (positron) under this particular condition of maintaining a constant real mass $m_p = m_{-e} = m$ by

$$m_{b-e} = m_{-e} - m_{e-e} = \frac{m_{e-e}}{q_e} - m_{e-e} = \left(\frac{1}{q_e} - 1 \right) m_{e-e} \quad (292)$$

Notable is the comparatively large black mass in the electron (positron). We also find and list the theoretical limiting radius R_{0-e} , which is the same and repeated in all tables for easy reference; the difference between the two radii $R_{-e} - R_{0-e} \equiv \Delta R_{-e}$ is discussed below.

Since the positron is the counterpart of the electron having the same effective mass, we could imagine the positron as being a compressed proton by the above means, or conversely, the proton as a “blown-up” positron. We are aware of the theory that the proton consists of quarks and muons, but the imagined contraction or expansion of real mass does not necessarily negate an internal structure of the proton as a function of that of a positron.

The above analysis presents only a methodology on how to deal with real and effective mass and with their associated parameters without claiming to have found the actual electron radius yet. The latter may have any value subject to the electron absorptivity factor A_{R-e} as it deviates from unity. The greater the deviation, the greater the electron radius. To be able to finally solve this question, we need to apply the above methodology in a way that produces outcomes consistent with other existing data and general information not only relating to electrons but also spanning the entire physical world at various scales.

The example analyzed above is just one possibility among many. There is a variety of combinations of effective mass with black mass, g_0 value and radius. We demonstrate some of those other possibilities below, which may later help us derive not only the electron radius but also the proton-to-electron mass ratio μ and other particle relationships.

[Note: Could PG theory help in the mysterious discrepancy of proton diameter measurements and other anomalies with muon technologies? From Wikipedia article on hadrons, we quote a relevant statement: “*In other phases of matter the hadrons may disappear. For example, at very high temperature and high pressure, unless there are sufficiently many flavors of quarks, the theory of quantum chromodynamics (QCD) predicts that quarks and gluons will no longer be confined within hadrons, "because the strength of the strong interaction diminishes with energy". This property, which is known as asymptotic freedom, has been experimentally confirmed in the energy range between 1 GeV and 1 TeV*”]

19.3.3 Exercises: Electron parameters in case of x:y gravion accretion

We can repeat the previous exercise by setting various other conditions between the different types of mass. We generalize the previous derivations for the following hypothetical particle relationship like:

$$p^+ \leftrightarrow e^+ + \nu \quad (293)$$

where ν is a hypothetical emitted or absorbed particle (in lieu of a known neutrino) with all particles being at rest with no kinetic energy, so that we write for their masses the inequality/equation:

g_0	q_{-e}	kR_{-e}	$A_{R_{-e}}$	$m_{b_{-e}}$
300	5.44617021326613E-04	1.37711414240144E+03	0.9999997363485721592	1.67171098512473E-27
500	5.44617021391021E-04	1.37711414223858E+03	0.9999997363485720969	1.67171098492693E-27
1000	5.44617021439326E-04	1.37711414211643E+03	0.9999997363485720501	1.67171098477857E-27
2000	5.44617021463479E-04	1.37711414205536E+03	0.9999997363485720267	1.67171098470439E-27
5000	5.44617021477971E-04	1.37711414201872E+03	0.9999997363485720127	1.67171098465989E-27
10000	5.44617021482801E-04	1.37711414200650E+03	0.9999997363485720080	1.67171098464505E-27
20000	5.44617021485217E-04	1.37711414200040E+03	0.9999997363485720057	1.67171098463763E-27
30000	5.44617021486022E-04	1.37711414199836E+03	0.9999997363485720049	1.67171098463516E-27
50000	5.44617021486666E-04	1.37711414199673E+03	0.9999997363485720043	1.67171098463318E-27
g_0	R_{-e}	R_{0-e}	ΔR_{-e}	k_{-e}
300	4.50173194740697E-22	4.50173135396290E-22	5.93444066960637E-29	3.05907628106260E+24
500	3.48702657227941E-22	3.48702611259961E-22	4.59679797757554E-29	3.94925049664415E+24
1000	2.46570013543645E-22	2.46569981039375E-22	3.25042702226488E-29	5.58508361306745E+24
2000	1.74351328613970E-22	1.74351305629980E-22	2.29839898939935E-29	7.89850099223745E+24
5000	1.10269462299327E-22	1.10269447762975E-22	1.45363515574359E-29	1.24886266179528E+25
10000	7.79722845496485E-23	7.79722742708958E-23	1.02787527601569E-29	1.76615851383658E+25
20000	5.51347311496635E-23	5.51347238814878E-23	7.26817577891135E-30	2.49772532355734E+25
30000	4.50173194740697E-23	4.50173135396290E-23	5.93444067308037E-30	3.05907628016721E+25
50000	3.48702657227941E-23	3.48702611259961E-23	4.59679797919012E-30	3.94925049595058E+25

Table 21: *Derived PG parameters for electron (positron) in the case of constant (equal) real mass between electron-proton.*

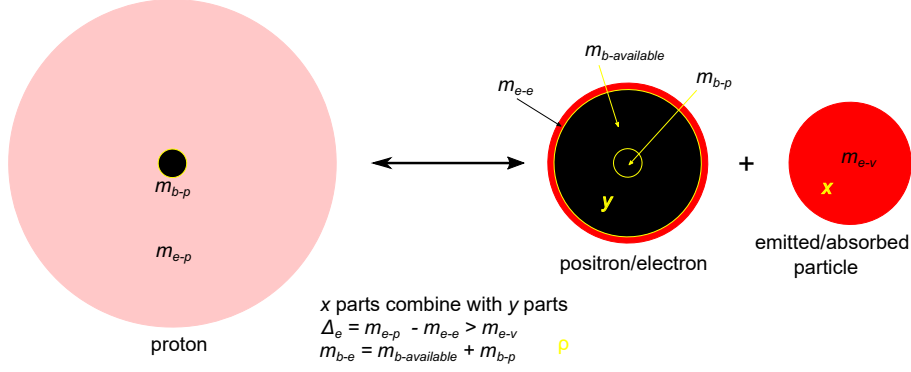


Figure 36: A hypothetical particle reaction between proton, positron(electron) and emitted/absorbed particle

$$m_{e-p} \geq m_{e-e} + m_{e-\nu} \quad (294)$$

where the masses of the positron and electron are the same ($m_{e-positron} = m_{e-e}$) and $m_{e-\nu}$ is the effective mass of the hypothetical emitted/absorbed particle in lieu the a known emitted neutrino. This hypothesis allows us to add mass to the positron(electron) from an external source, which can be via an accretion of gravions. This is a thought exercise extending the preceding special case. Fig. 36 is a schematic diagram to assist in the formulation of the equations for the general case below. It refers only to the masses without regard to “charge” of the particles, while the masses of positron and electron are used interchangeably; a mechanism to explain the charge sign is initially modeled in Fig. 76. Also, the distribution of masses is not properly depicted, like the black mass of the proton is not concentrated at the center but can be organically integrated with the structure of the proton.

Now, instead of keeping the same real mass for the electron and proton, we can try to vary the real mass from m_p to m_{-e} , or from m_{-e} to m_p and re-write their equations as

$$m_{e-p} = q_p m_p = \frac{g_0}{G} A_{R-p} R_p^2 \quad (295)$$

$$m_{e-e} = q_e m_{-e} = \frac{g_0}{G} A_{R-e} R_{-e}^2 \quad (296)$$

with corresponding contraction factors q_p and q_e . The absorptivities and radii of the proton and electron are still related via Eq. 288 (by dividing the above equations), but the contraction factors relate differently. It is easier to start by adding effective mass to the electron via gravion absorption, the total accretion of which is represented by the effective mass $m_{e-\nu}$ and depicted by the red colored absorbed particle in the figure. The proton’s effective mass can be written as a sum by

$$m_{e-p} = m_{e-e} + \Delta_e = \frac{m_{e-p}}{\mu} + \Delta_e \quad (297)$$

where we factor in their observed (effective) mass relationship μ between proton/electron(positron) and Δ_e is the fixed (known) effective mass difference between proton and electron:

$$\Delta_e = m_{e-p} - \frac{m_{e-p}}{\mu}$$

The above equation is only a starting approach to help build the required term Δ_e in various ways of combining added gravion mass with existing black mass in the electron to produce the effective mass of the proton; in this process, mass and energy are interchangeable in the summed terms by lumping them together. To build a proton from an electron(positron) in this way, we need an available amount of black mass $m_{b-available}$ in the electron over and above the final remnant black mass m_{b-p} in the proton, i.e. we must have for total real mass of the electron :

$$m_{-e} = \frac{m_{e-p}}{\mu} + m_{b-available} + m_{b-p} \quad (298)$$

with a total electron black mass being $m_{b-e} = m_{b-available} + m_{b-p}$.

Now, we can build the needed term Δ_e from a given amount of the “available” black mass ($m_{b-available}$) via the absorption of gravions in various ways. Let’s designate the mass (energy) of a single gravion by ω ,

which when absorbed adds a quantum of ω mass (energy) by itself to the absorbing center. We can generalize so that x accreted gravions (or mass parts) combine with y parts of black mass in the electron (positron), i.e. we make the rule $x : y$ with the meaning that an amount of $y\omega$ of the available black mass combines with an amount of $x\omega$ gravion mass to yield an amount of $x\omega + y\omega$ effective mass towards Δ_e for building the proton. In this connection, we envisage that the black mass is “granulated” with grains of ω mass each as we use gravion particles, but this granulation is not a necessary condition if just the right proportion of masses is used, whilst granulation is for convenience in envisaging our mathematical formulation. Thus, what we actually need is the fraction $x\omega/(x\omega + y\omega) = x/(x + y)$, from which we find the available (or needed) black mass fraction $y/(x + y)$ in the electron to be present by:

$$m_{b-available} = \frac{y}{x + y} \Delta_e = \frac{y}{x + y} \left(m_{e-p} - \frac{m_{e-p}}{\mu} \right) \quad (299)$$

We note that

$$\frac{x}{x + y} \Delta_e + \frac{y}{x + y} \Delta_e = \Delta_e$$

Then the total real mass of the electron (positron) should be:

$$m_{-e} = \frac{m_{e-p}}{\mu} + \frac{y}{x + y} \left(m_{e-p} - \frac{m_{e-p}}{\mu} \right) + m_{b-p} = m_{e-p} \left[\frac{x}{(x + y)\mu} + \frac{1}{q_p} - \left(\frac{x}{x + y} \right) \right] \quad (300)$$

where we used Eq. 279 for the proton black mass. From this, we derive the overall general equation for the electron contraction:

$$q_{-e} = \frac{m_{e-e}}{m_{-e}} = \left(\frac{x}{x + y} (1 - \mu) + \frac{\mu}{q_p} \right)^{-1} \quad (301)$$

that is used in the below equation (like in 291) to find all the electron parameters in the usual way:

$$\frac{3A_{R-e}}{4kR_{-e}} - \left(\frac{x}{x + y} (1 - \mu) + \frac{\mu}{q_p} \right)^{-1} = 0 \quad (302)$$

We solve the above equation with a Python script allowing sufficient precision, which finds, in turn, first the proton contraction factor q_p , then finds (solves for) the product kR_{-e} (being present also inside A_{R-e}), then the absorptivity A_{R-e} and finally the electron radius R_{-e} together with other parameters presented in the figures and tables herewith.

We can vary the fraction x/y in the range $0 \rightarrow \infty$. When $x = 0$, we recover Eqs. 290 and 291, i.e. the case for constant real mass without external contribution. When $x = \infty$, i.e. there is no need to have any available $m_{b-available}$ mass, so that the above equations reduce to:

$$q_{-e} = \left(1 - \mu + \frac{\mu}{q_p} \right)^{-1} \quad (303)$$

$$\frac{3A_{R-e}}{4kR_{-e}} - \left(1 - \mu + \frac{\mu}{q_p} \right)^{-1} = 0 \quad (304)$$

from which we found the results of Table 25; in this case, the added effective mass originates exclusively from external contribution. We present some examples for the electron parameters as before in Tables 22 through to 25 for a selection of ratios $x : y$. Furthermore, we have extended the computations to include more results (points) for this ratio in the range $0 \rightarrow \infty$ in Table 26 for two values of g_0 . The results are also presented for many more points in graph form with logarithmic scales in Fig. 37. These outcomes are discussed in more detail next.

19.3.4 Discussion

From the provided tables and graphs, we note some salient outcomes:

- The electron radius R_{-e} lies in the range $3.487 \times 10^{-23} \rightarrow 4.58 \times 10^{-19}$ m for the highest value of g_0 used and in a sub-range of the same for lower values of g_0 . The lowest value of radius is only slightly above the characteristic limiting electron radius $R_{0-e} = 3.4870261 \times 10^{-23}$ for the high g_0 (see Table 21).

g_0	q_{-e}	kR_{-e}	$A_{R_{-e}}$	$m_{b_{-e}}$
300	1.08864114983105E-03	6.88931527181105E+02	0.9999989465403999087	8.35855492809629E-28
500	1.08864115008840E-03	6.88931527018244E+02	0.9999989465403994106	8.35855492611821E-28
1000	1.08864115028141E-03	6.88931526896099E+02	0.9999989465403990371	8.35855492463466E-28
2000	1.08864115037791E-03	6.88931526835026E+02	0.9999989465403988503	8.35855492389288E-28
5000	1.08864115043582E-03	6.88931526798382E+02	0.9999989465403987382	8.35855492344781E-28
10000	1.08864115045512E-03	6.88931526786168E+02	0.9999989465403987009	8.35855492329945E-28
20000	1.08864115046477E-03	6.88931526780061E+02	0.9999989465403986822	8.35855492322528E-28
30000	1.08864115046799E-03	6.88931526778025E+02	0.9999989465403986760	8.35855492320055E-28
50000	1.08864115047056E-03	6.88931526776396E+02	0.9999989465403986710	8.35855492318077E-28
g_0	R_{-e}	$R_{0_{-e}}$	ΔR_{-e}	k_{-e}
300	4.50173372516083E-22	4.50173135396290E-22	2.37119792940316E-28	1.53036934044004E+24
500	3.48702794932163E-22	3.48702611259961E-22	1.83672201909637E-28	1.97569832255652E+24
1000	2.46570110915235E-22	2.46569981039375E-22	1.29875859531822E-28	2.79405936242182E+24
2000	1.74351397466081E-22	1.74351305629980E-22	9.18361010036657E-29	3.95139664406219E+24
5000	1.10269505845225E-22	1.10269447762975E-22	5.80822501263505E-29	6.24770666665878E+24
10000	7.79723153412487E-23	7.79722742708958E-23	4.10703529323719E-29	8.83559150156096E+24
20000	5.51347529226128E-23	5.51347238814878E-23	2.90411250647199E-29	1.24954133329852E+25
30000	4.50173372516083E-23	4.50173135396290E-23	2.37119793217784E-29	1.53036933954465E+25
50000	3.48702794932163E-23	3.48702611259961E-23	1.83672202038593E-29	1.97569832186295E+25

Table 22: *Derived PG parameters for electron (positron) in the case of variable mass rule 1:1*

g_0	q_{-e}	kR_{-e}	$A_{R_{-e}}$	m_{b-e}
300	7.03405088619216E-03	1.06619503325234E+02	9.99956015800314E-01	1.28593153158382E-28
500	7.03405089693614E-03	1.06619503162367E+02	9.99956015800180E-01	1.28593152960574E-28
1000	7.03405090499413E-03	1.06619503040216E+02	9.99956015800079E-01	1.28593152812218E-28
2000	7.03405090902312E-03	1.06619502979141E+02	9.99956015800029E-01	1.28593152738040E-28
5000	7.03405091144052E-03	1.06619502942495E+02	9.99956015799998E-01	1.28593152693534E-28
10000	7.03405091224632E-03	1.06619502930280E+02	9.99956015799988E-01	1.28593152678698E-28
20000	7.03405091264922E-03	1.06619502924173E+02	9.99956015799983E-01	1.28593152671280E-28
30000	7.03405091278352E-03	1.06619502922137E+02	9.99956015799982E-01	1.28593152668808E-28
50000	7.03405091289096E-03	1.06619502920508E+02	9.99956015799980E-01	1.28593152666830E-28
g_0	R_{-e}	R_{0-e}	ΔR_{-e}	k_{-e}
300	4.50183035975433E-22	4.50173135396290E-22	9.90057914308844E-27	2.36835897412741E+23
500	3.48710280215613E-22	3.48702611259961E-22	7.66895565122834E-27	3.05753828354135E+23
1000	2.46575403809933E-22	2.46569981039375E-22	5.42277055802827E-27	4.32401210310503E+23
2000	1.74355140107819E-22	1.74351305629980E-22	3.83447783879373E-27	6.11507655657349E+23
5000	1.10271872899698E-22	1.10269447762975E-22	2.42513672327273E-27	9.66878498921251E+23
10000	7.79739891015185E-23	7.79722742708958E-23	1.71483062272360E-27	1.36737268618470E+24
20000	5.51359364498498E-23	5.51347238814878E-23	1.21256836205313E-27	1.93375699751017E+24
30000	4.50183035975508E-23	4.50173135396290E-23	9.90057921795331E-28	2.36835896517295E+24
50000	3.48710280215647E-23	3.48702611259961E-23	7.66895568602239E-28	3.05753827660524E+24

Table 23: *Derived PG parameters for electron (positron) in the case of variable mass rule 12:1*

g_0	q_{-e}	kR_{-e}	$A_{R_{-e}}$	m_{b-e}
300	9.63934186896923E-01	4.93609383070407E-02	6.34409279086220E-02	3.40829627576949E-32
500	9.63934388663436E-01	4.93606548086926E-02	6.34405768227254E-02	3.40827649499800E-32
1000	9.63934539988376E-01	4.93604421849095E-02	6.34403135081781E-02	3.40826165941939E-32
2000	9.63934615650864E-01	4.93603358730108E-02	6.34401818508643E-02	3.40825424163008E-32
5000	9.63934661048362E-01	4.93602720858693E-02	6.34401028564632E-02	3.40824979095650E-32
10000	9.63934676180862E-01	4.93602508234885E-02	6.34400765249941E-02	3.40824830739864E-32
20000	9.63934683747113E-01	4.93602401922980E-02	6.34400633592591E-02	3.40824756561971E-32
30000	9.63934686269196E-01	4.93602366485678E-02	6.34400589706807E-02	3.40824731836007E-32
40000	9.63934687530238E-01	4.93602348767027E-02	6.34400567763915E-02	3.40824719473024E-32
50000	9.63934688286863E-01	4.93602338135836E-02	6.34400554598180E-02	3.40824712055235E-32
g_0	R_{-e}	R_{0-e}	ΔR_{-e}	k_{-e}
300	1.78728911805991E-21	4.50173135396290E-22	1.33711598266362E-21	2.76177691724670E+19
500	1.38443202859096E-21	3.48702611259961E-22	1.03572941733100E-21	3.56540832553048E+19
1000	9.78943307096927E-22	2.46569981039375E-22	7.32373326057552E-22	5.04221662552541E+19
2000	6.92218169123965E-22	1.74351305629980E-22	5.17866863493985E-22	7.13074837886423E+19
5000	4.37797483004940E-22	1.10269447762975E-22	3.27528035241965E-22	1.12746815598555E+20
10000	3.09569633264237E-22	7.79722742708958E-23	2.31597358993341E-22	1.59447973959889E+20
20000	2.18898809644638E-22	5.51347238814878E-23	1.63764085763150E-22	2.25493415301937E+20
30000	1.78730135825983E-22	4.50173135396290E-23	1.33712822286354E-22	2.76171874544013E+20
40000	1.54784840724023E-22	3.89861371354479E-23	1.15798703588575E-22	3.18895795258856E+20
50000	1.38443771734721E-22	3.48702611259961E-23	1.03573510608725E-22	3.56536326590157E+20

Table 24: Derived PG parameters for electron (positron) in the case of variable mass rule 49048:1.

g_0	q_{-e}	kR_{-e}	$A_{R_{-e}}$	m_{b-e}
300	9.99999457132400E-01	7.23823744995925E-07	9.65097802740621E-07	4.94519194260210E-37
500	9.99999674279410E-01	4.34294219814202E-07	5.79058771140844E-07	2.96711479371232E-37
1000	9.99999837139729E-01	2.17147052147437E-07	2.89529355710413E-07	1.48355693244071E-37
2000	9.99999918569909E-01	1.08573460670328E-07	1.44764602438909E-07	7.41778001932116E-38
5000	9.99999967428023E-01	4.34293033380708E-08	5.79057358979900E-08	2.96710643667659E-38
10000	9.99999983714062E-01	2.17145838196526E-08	2.89527779546803E-08	1.48354857586291E-38
20000	9.99999991857082E-01	1.08572239840062E-08	1.44762985274623E-08	7.41769645468789E-39
30000	9.99999994571422E-01	7.23810402746675E-09	9.65080531756552E-09	4.94510002005967E-39
50000	9.99999996742893E-01	4.34280805815849E-09	5.79041072535134E-09	2.96702287236387E-39
g_0	R_{-e}	R_{0-e}	ΔR_{-e}	k_{-e}
300	4.58240965125915E-19	4.50173135396290E-22	4.57790791990518E-19	1.57957013903598E+12
500	4.58240929714180E-19	3.48702611259961E-22	4.57892227102920E-19	9.47742097339680E+11
1000	4.58240953344043E-19	2.46569981039375E-22	4.57994383363003E-19	4.73870898187498E+11
2000	4.58241072706203E-19	1.74351305629980E-22	4.58066721400573E-19	2.36935244650012E+11
5000	4.58241488475362E-19	1.10269447762975E-22	4.58131219027599E-19	9.47738352600211E+10
10000	4.58242200653944E-19	7.79722742708958E-23	4.58164228379673E-19	4.73866959190235E+10
20000	4.58243632231437E-19	5.51347238814878E-23	4.58188497507556E-19	2.36931257094321E+10
30000	4.58245065424667E-19	4.50173135396290E-23	4.58200048111127E-19	1.57952688934228E+10
50000	4.58247932812879E-19	3.48702611259961E-23	4.58213062551753E-19	9.47698341267113E+09

Table 25: *Derived PG parameters for electron (positron) in the case of variable mass rule $\infty : 0$*

x/y	g_0	q_{-e}	kR_{-e}	$A_{R_{-e}}$	m_{b-e}	R_{-e}	ΔR_{-e}
0/1	1000	0.0005446170	1377.11414212	0.99999974	1.67171098E-27	2.46570014E-22	3.25E-29
	50000	0.0005446170	1377.11414200	0.99999974	1.67171098E-27	3.48702657E-23	4.60E-30
1/12	1000	0.0005899750	1271.23991918	0.99999969	1.54311783E-27	2.46570019E-22	3.81E-29
	50000	0.0005899750	1271.23991906	0.99999969	1.54311783E-27	3.48702665E-23	5.39E-30
3/10	1000	0.0007078865	1059.49145518	0.99999955	1.28593153E-27	2.46570036E-22	5.49E-29
	50000	0.0007078865	1059.49145506	0.99999955	1.28593153E-27	3.48702689E-23	7.77E-30
1/1	1000	0.0010886412	688.93152690	0.99999895	8.35855492E-28	2.46570111E-22	1.30E-28
	50000	0.0010886412	688.93152678	0.99999895	8.35855492E-28	3.48702795E-23	1.84E-29
10/3	1000	0.0023557305	318.37100771	0.99999507	3.85779458E-28	2.46570589E-22	6.08E-28
	50000	0.0023557305	318.37100759	0.99999507	3.85779458E-28	3.48703471E-23	8.60E-29
12/1	1000	0.0070340509	106.61950304	0.99995602	1.28593153E-28	2.46575404E-22	5.42E-27
	50000	0.0070340509	106.61950292	0.99995602	1.28593153E-28	3.48710280E-23	7.67E-28
54/1	1000	0.0290981784	25.75538124	0.99924624	3.03947453E-29	2.46662961E-22	9.30E-26
	50000	0.0290981786	25.75538112	0.99924624	3.03947452E-29	3.48834105E-23	1.31E-26
146/1	1000	0.0741617940	10.06309090	0.99506250	1.13721837E-29	2.47180964E-22	6.11E-25
	50000	0.0741617949	10.06309078	0.99506250	1.13721836E-29	3.49566672E-23	8.64E-26
49048/1	1000	0.9639345400	0.04936044	0.06344031	3.40826166E-32	9.78943307E-22	7.32E-22
	50000	0.9639346883	0.04936023	0.06344006	3.40824712E-32	1.38443772E-22	1.04E-22
$\infty/0$	1000	0.9999998371	2.1714705E-07	2.8952E-07	1.48355693E-37	4.58240953E-19	4.58E-19
	50000	9.999999E-01	4.3428080E-09	5.7904E-09	2.96702287E-39	4.58247932E-19	4.58E-19

Table 26: *Electron (positron) parameter variation with admixtures of effective/black_ mass (m_e/m_b) at two values of g_0*

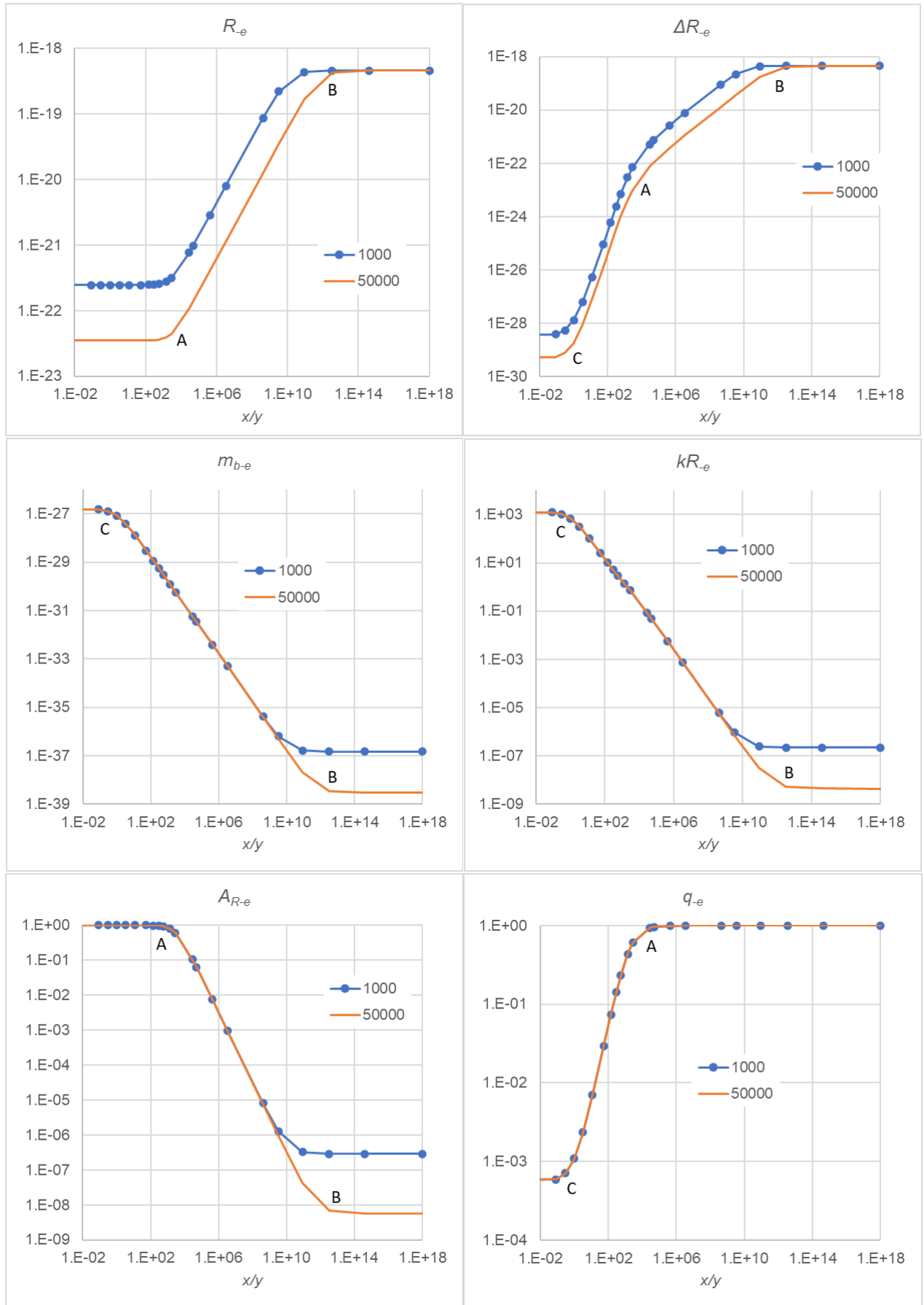


Figure 37: Plotting the electron parameters per Table 26 versus the ratio x/y for two fixed values 1000 and 50000 of g_0

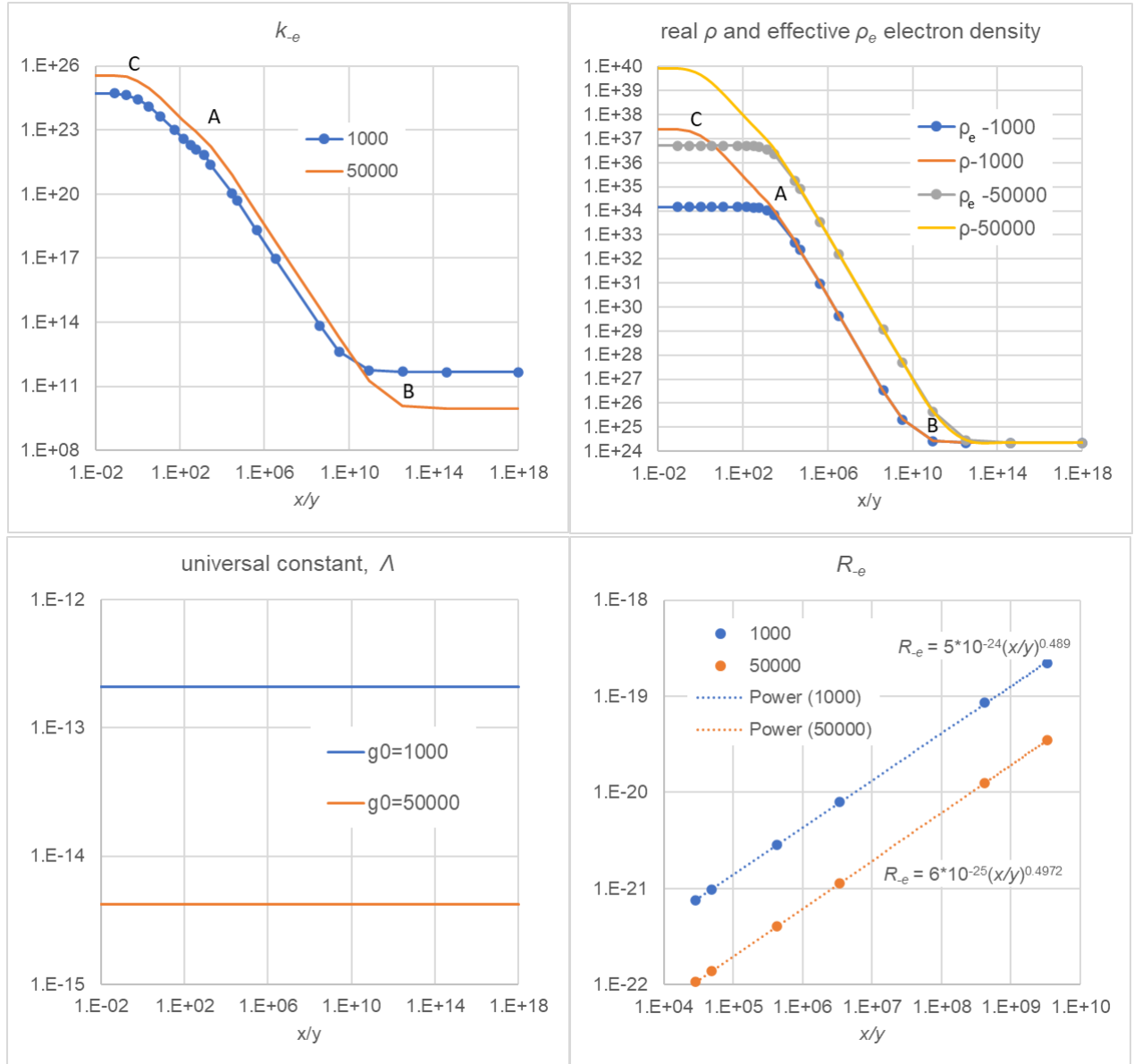


Figure 38: Absorption coefficient k_e , real ρ and effective ρ_e densities, universal constant Λ and repeat of the electron radius in the transition range versus ratio x/y for two values of $g_0 = 1000$ and 50000 ms^{-2} [Note: densities graphs corrected from previous version inadvertently inputting the wrong data columns]

- The slope (on log-log scales) of the radius variation is initially close to zero followed with a nearly fixed slope up to the maximum radius. The middle range of variation is re-plotted in Fig. 38, where the straight line is fitted with a power function for the two values of g_0 . There are two characteristic inflection points A and B at specific values of the ratio x/y .
- The radii difference ΔR_{-e} simply follows the variation of R_{-e} where R_{-e} is much greater than R_{0-e} , otherwise it shows some additional information: There is a new inflection point C very early before point A is shifted upwards. Point C occurs around $x/y=3/10$, point A around $x/y=560/1$ and point B around $x/y=3338337000/1$.
- Either only two combinations or all three of points A, B and C appear with each of the electron parameters at the same x/y .
- From the previous parameters, we have further extracted the absorption coefficient k_{-e} , the effective ρ_e and real ρ densities as well as the universal constant Λ as shown in Fig. 38. The latter constant depends only on the chosen g_0 and the values shown confirm those already provided in Table 2 for large bodies, as it should.
- All electron parameters present the usual “sigmoid” shape like in Fig. 3, except we have now used logarithmic scales for both axes, which allows us to distinguish differences at the very small scale of the ordinate axis: Thus all parameters are affected by a change in g_0 , except the contraction coefficient (albeit to a very small extent). It is interesting to observe how the effect of g_0 takes place in the ranges between points A, B and C. Furthermore, it should be noted that even where the curves appear indistinguishable, there is still some very small difference for all parameters per numerical values in tables (less than the fifth decimal place).

The above summary of results may be important in attempting to explain the properties of the electron and positron in this report but also by other workers in particle physics and cosmology in general. The electron radius seems to assume a finite value in a definite range as noted above.

The parameter ΔR_{-e} is many orders of magnitude smaller than the electron radius up to point A, whereupon it reaches about the value of the electron radius. This indicates that the absorption layer initially distributes itself around the characteristic (minimum) electron radius with $TAL_{-e} < R_{-e}$, until it becomes $TAL_{-e} \approx R_{-e}$ around point A. Afterwards, the radius “swells” up to point B and then it appears to have reached a saturation (maximum) value.

In this connection, it is important to quote from Dehmelt’s (Nobel prize) lecture on “experiments with an isolated subatomic particle at rest” (Dehmelt, 1989), where he suggests that “*the electron may have size and structure!*”. He calculates a radius $R \approx 10^{-22}$ m with an upper limit $R \approx 10^{-19}$ m. This is entirely consistent with our preceding values. Another “unofficial” report is found giving a more precise electron radius $R = 1.61 \times 10^{-22}$ m, but this and other formulae were “*published without detailed explanations of how they were derived*” (Sukhorukov, 2017-2020). This value can be found also in some of our tables in the preceding exercises, whilst Table 24 was specifically compiled to contain a case close to this value in the suspected range between 30000-40000 m/s² for g_0 ; this range was “suspected” from the Allais effect calculations in Section 12.4 of prior version v16 (or before) of this report.

If we have not provided a definitive answer yet, we have at least demonstrated the plausibility of PG schemes. The Standard Model does not allow a finite radius for the electron. However, if this is to be remodeled, then PG offers a candidate platform: The electron and positron having a finite mass can also have a finite radius, which depends on the relative amounts of the two types of real mass present. Since gravitation is not described by the Standard Model and a quantum theory of gravity is not yet established, the final observation of the top quark with a mass much larger than had previously expected, almost as large as a gold atom, it might make us think again with an understanding of the meaning of mass under PG.

Neutrinos with great range of energy and mass, from supernova neutrinos and solar neutrinos to cosmic neutrino background radiation with minimal energy may provide some hint on their possible role in PG. It is said that the three known neutrino flavors are the only established elementary particle candidates for dark matter, but they may also relate to black matter. To accommodate the large amount of all neutrinos in the universe, the summed masses of the three neutrinos must be less than 0.26 eV (1 eV = 1.782662×10^{-36} kg). We may be able to do away with the Standard Model’s neutrinos as fundamental point-like particles (no volume), whilst they involve mass differences between neutrino mass eigenstates. Loureiro *et al.* (2019) report a species of neutrino with a mass no greater than 0.086 eV, i.e. about $\times 10^7$ (times) smaller mass than an single electron. This implies the existence of physics beyond the Standard Model.

Neutrinos have been detected with a large variety of mass/energy in nuclear reactors and in South Pole IceCube Neutrino Observatory (Stein *et al.*, 2021), all of which may be attributed to fragments of black mass

from black holes and other massive bodies all the way down to atomic nuclei. For discussion purposes, we may consider the following two contradicting scenarios: (1) The black mass fragments become activated, as they are hurled away from the source, whilst they have subsequently high penetration range through material bodies. (2) The black mass fragments are difficult to detect, if they remain inactivated (inert) during their transit from the source to a detector event. These ghost particles then may have even superluminal speed of immense magnitude, if they are actually inert and without classical inertia meaning that they can be hurled from their source across the universe at unimaginable speed. However, the second scenario cannot justify the principle of imparting a push (momentum) required by PG. So, gravions themselves may be the smallest possible neutrinos (or neutrino like) from initially black mass traversing the universe and manifesting themselves as gravitation after they are absorbed by particles, planets, stars, etc. The universal constant $\Lambda = k/\rho$ is exactly the characteristic measure of this absorption. The nature of gravions is as yet unknown, so that confirmation of their existence and measurement of g_0 is an imperative step forward. This will greatly facilitate the further development of the theory.

The big range of neutrino energy chasing the tinniest particles is consistent with taking into consideration the novel possibilities now opened with PG on the finest structure of matter. We can now return to our hypothetical proton decay expression 293 and appreciate its purpose: Whilst no nuclear reaction like that has been observed, the end products of proton, electron (positron) and neutrinos are obtained via reactions 280, 281 and 282 with mediation of neutron and energy balancing terms in the equation. It seems that our black mass m_{b-e} calculated and plotted in Fig. 37 provides the ranges required for balancing the said reactions with observed neutrinos and energy. We note that the black mass may lie anywhere between $2.96 \times 10^{-39} \rightarrow 1.67 \times 10^{-27}$ kg. If the smallest species of neutrino is about $\times 10^7$ times smaller than the electron, i.e. about $m_{e-e} = 9.1093837015 \times 10^{-38}$ kg, then PG predictions (expected range of m_{b-e}) are consistent with experiment. The task is to determine the ultimate values of the electron parameters. This can only be done with further correlation of existing or new data, a task to be undertaken by relevant physics departments.

In all above connections, we would like to further quote from Dehmelt's lecture: "*The electron is a much more complex particle than the cosmon. It is composed of 3^C-3 cosmon-like d_c 's, but only two particles of this type formed the cosmonium world-atom from which sprang the universe. In closing, I should like to cite a line from William Blake. 'to see a world in a grain of sand...' and allude to a possible parallel - to see worlds in an electron -*". Our elementary investigation of the electrons and positrons in this section already reveals some exciting possibilities and prospects: If the electron has the smallest predicted radius, it would also have the highest density and the highest absorptivity close to $A_{R-e} \approx 1$. That means it has the characteristics of a black hole! Should this be shown to be the case, it would be a really extraordinary finding. Then it would be easier to think about electric charge and other properties of these fundamental particles. At the other end, should the electron have the highest possible radius predicted here, then there would be very little black mass with the lowest $A_{R-e} \approx 0$, i.e. it would be a "fluffy" object, with an effective mass equal to its real mass. Between the two extremes, it is also possible that the radius corresponds to the situation of point A on the presented graphs. It may be governed by statistics favoring an optimum state around this point. The governing statistics may be different from conventional quantum mechanics. Furthermore, we may have not exhausted all possible interpretations of the Heisenberg Principle to date. Also, as already said, the second law of thermodynamics should be considered in conjunction with the fluctuation theorem. All-in-all, we feel that there are some exciting possibilities under PG making its verification all the more urgent.

We can summarize our findings that may be used in particle physics thus: The preceding exercises demonstrate the new possibilities presented by various relationships between active (effective) and passive (black) types of mass in PG. The relative amounts of effective and black mass in a particle could accommodate the needs of particle physics. In the transformations between and among various particles, we should also consider the possible role of black mass that accompanies those transformations. Various neutrinos appear for balancing the equations of mass and energy involved. The instability and extremely short lifetimes of various particles may be attributed to their inability of containing less-or-equal to the critical mass that allows a push particle field to stabilize them as an independent entity. The large types of particles produced in nuclear reactors and elsewhere are generally fragments out of stable and unstable entities. Those fragments may not necessarily exist as independent entities inside the original particle, they may even not appear to exist at all in there. Theories contrived to reconcile their co-existence inside, for example, the nucleus or nucleons, may need reappraisal.

In the meantime, we may attempt to theorize about various possibilities in understanding the electron and positron. Neutronium and Neutron stars are said to have extremely high pressures and temperatures, nucleons and electrons are believed to collapse into bulk neutronic matter, called neutronium. This is presumed to happen in neutron stars. The extreme pressure inside a neutron star may deform the neutrons into some high packing order of neutrons like a cubic symmetry (Llanes-Estrada & Navardo, 2012). We

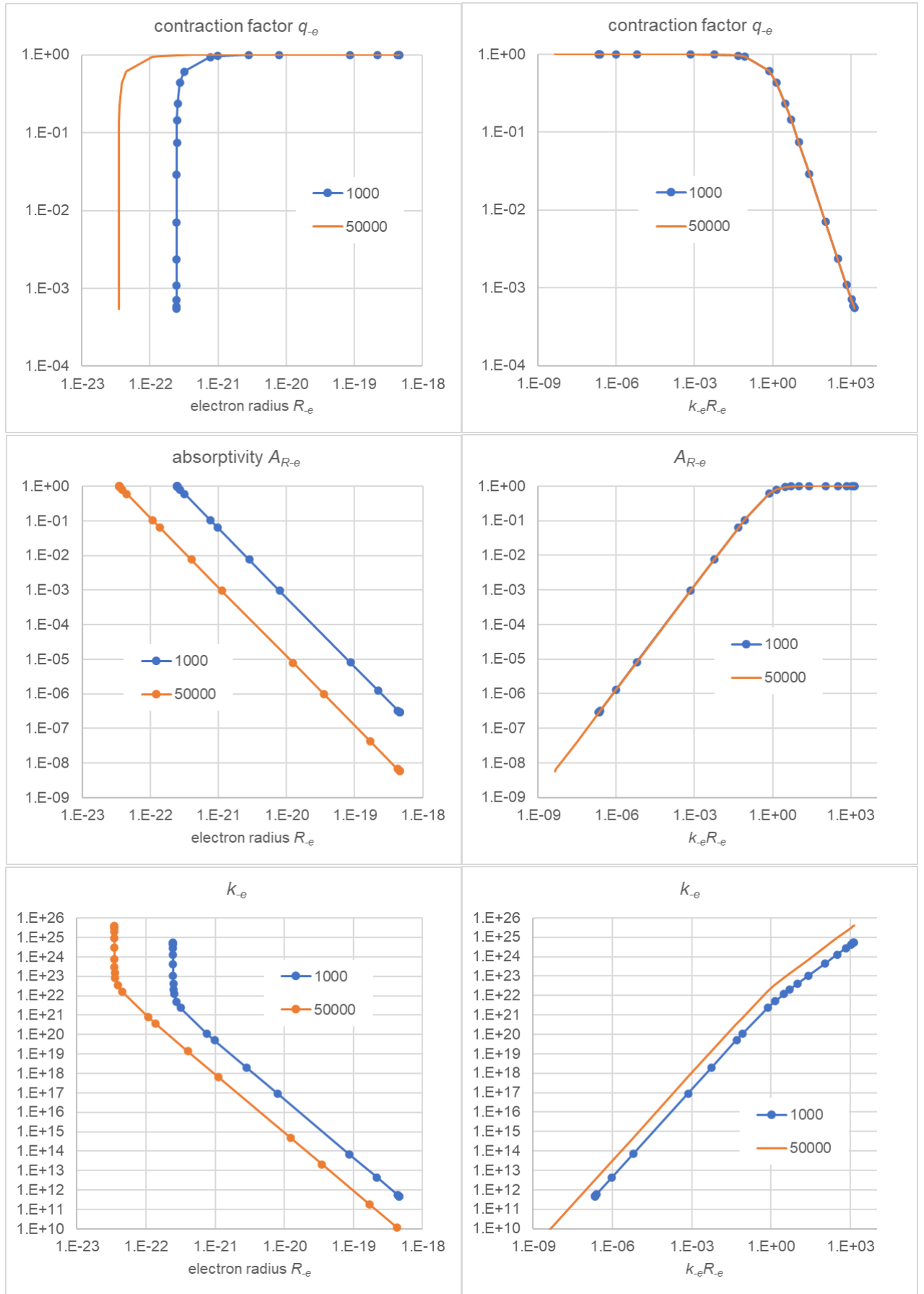


Figure 39: Plotting and comparing the electron parameters versus electron radius (left) and versus product $k_e R_e$ (right) deduced from previous plots for two fixed values 1000 and 50000 of g_0

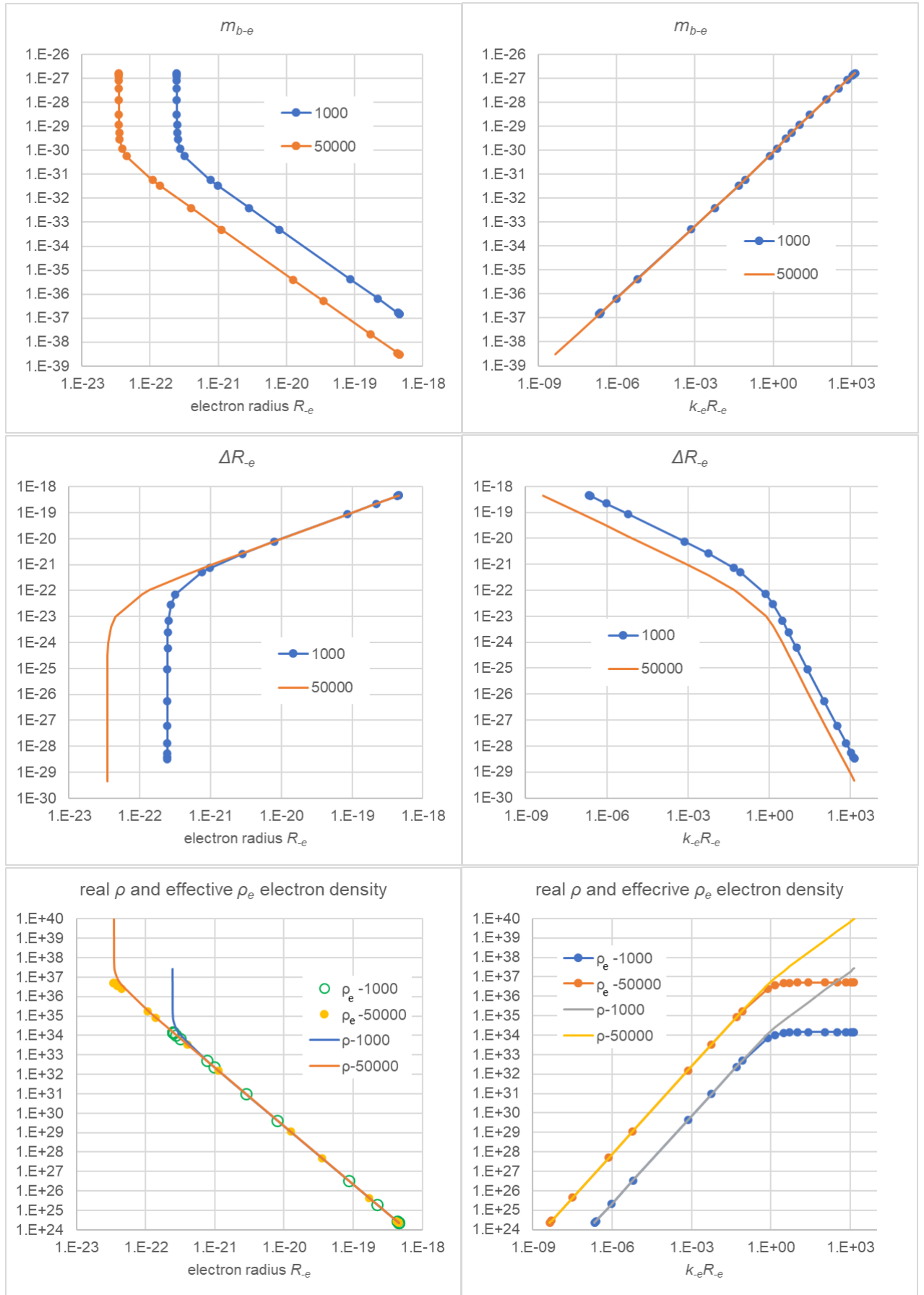


Figure 40: Plotting and comparing of more electron parameters versus electron radius (left) and versus product $k_e R_e$ (right) deduced from previous plots for two fixed values 1000 and 50000 of g_0

may then think that the interior of black holes could have still the highest packing order possible, like a cuboctahedron (see also “compact” shape in Fig. 35). With the small electron radii possible, the densities become extremely high per Fig. 38. It is for this reason that we selected most of the mass ratios x/y in the exercises herewith. We would like to examine if there is some characteristic correlation of the behavior of the electron parameters with the chosen ratios. For cuboctahedron, the count of successive layers of closely packed spheres is called frequency F , from which we find the number of the outermost layer spheres in a densely packed “ball” by:

$$\#outer_spheres = 10F^2 + 2 \quad (305)$$

and the total number of spheres by:

$$\#total_spheres = \frac{10}{3}F^3 + 5F^2 + \frac{11}{3}F + 1 \quad (306)$$

We note that point A occurs around $x/y = 308/1$, or $x/y = 560/1$, which correspond to $F = 4$ and $F = 5$. A visual observation may indicate that the outer three, or four layers could be sufficient to shield the central one sphere at the core of the “ball”; this would agree with such ratio of added effective mass to one unit of black mass. The ultimate aim is to hopefully find an explanation of the “mysterious” but firm number of $\mu = 1836.15$. We can return to this question later, while some other workers may like to take up this task.

The specific presentation of electron parameter variation with respect to the ratio x/y is aimed at the possibility of revealing some structural relationship, but the same data relate all parameters between themselves taken in arbitrary pairs. In preparation for the formulation of a push electricity (PE) theory in a following section, it is helpful to familiarize with all push gravity parameters, because the same appear also in other force fields. The equations we used to derive and describe these properties for electrons are relatively simple and straightforward, but the peculiar form of Eq. 144 and its dependence on the product kR may often lead us to some non-intuitive outcomes, or to an understanding that is not immediately obvious. Since graphic presentation is a good way to acquaint ourselves with these new parameters of PG, we have re-plotted the same numerical data in different pair combinations in Figs. 39 and 40. We juxtapose any given parameter against radius (left), and the same parameter against the characteristic product kR . There are many other combinations the reader may wish to display, but we prefer to standardize the plotting against the common dimensionless variable kR , which will also make the comparison during development of the electric field easier to comprehend.

19.4 Neutrino production

Based on later investigations, it seems that the tentative upper limit of g_0 used in the preceding plots could be an underestimate. Another upper limit may be $g_0 = 10^8 \text{ ms}^{-2}$ on account of Section 12, but also much higher values up to $g_0 = 5.56 \times 10^{51} \text{ ms}^{-2}$ according to Table 43 might be used. However, according to the understanding of Section 31, we should not exceed the value of $2.35 \times 10^{20} \text{ ms}^{-2}$, if the theoretical connection found between gravity and electricity is correct. Thus, we have considered the value of $1.0 \times 10^{20} \text{ ms}^{-2}$, but also $g_0 = 10^{42} \text{ ms}^{-2}$ for comparison. We have repeated all of the preceding computations for these three values of g_0 as well, from which we present a summary of results in Figs. 41 and 42.

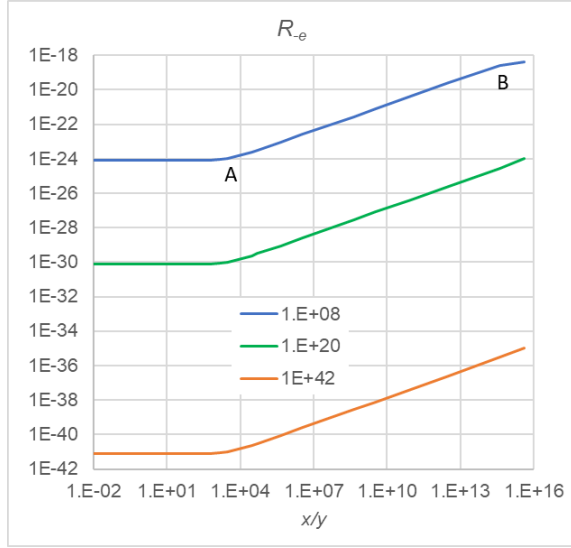
We note that the case for $g_0 = 10^{42} \text{ ms}^{-2}$ yields a minimum electron radius $R_{-e} = 7.8 \times 10^{-42} \text{ m}$, which is much smaller than the Planck length and should not be accepted. However, for $g_0 = 10^{20} \text{ ms}^{-2}$, the minimum radius $R_{-e} = 7.8 \times 10^{-31} \text{ m}$ is well suited by four orders of magnitude greater than the Planck length. This difference from the Planck length may be used to organize the anticipated structure of the electron. The case for $g_0 = 10^8 \text{ ms}^{-2}$ yields a minimum electron radius $R_{-e} = 7.8 \times 10^{-25} \text{ m}$. Without plotting, we also report that the value of $g_0 = 10^{26} \text{ ms}^{-2}$ yields a minimum electron radius $R_{-e} = 7.8 \times 10^{-34} \text{ m}$, while the value of $g_0 = 10^{28} \text{ ms}^{-2}$ yields a minimum electron radius $R_{-e} = 7.8 \times 10^{-35} \text{ m}$, both of which border closely with the Planck length.

Furthermore, the ΔR_{-e} variation in Fig. 41(b) for the middle case shows values less than the Planck length, which may indicate another adjustment for possible values of the electron radius and g_0 . We leave this to be worked out at a later stage.

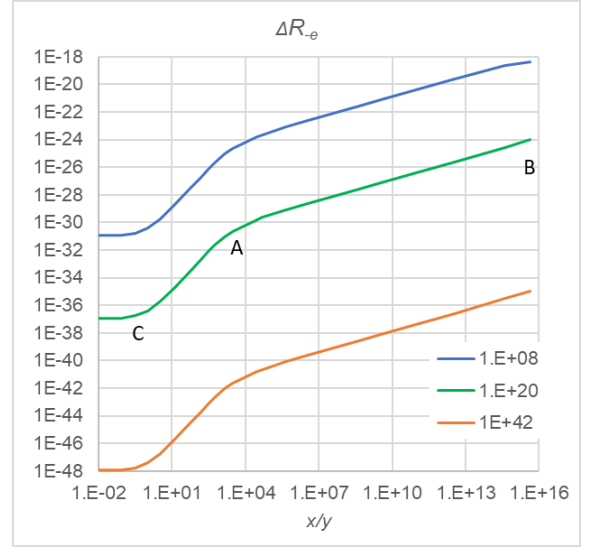
We add a new graph in 42(f) for the variation of:

$$m_{e-\nu} = \frac{x}{x+y} \Delta_e$$

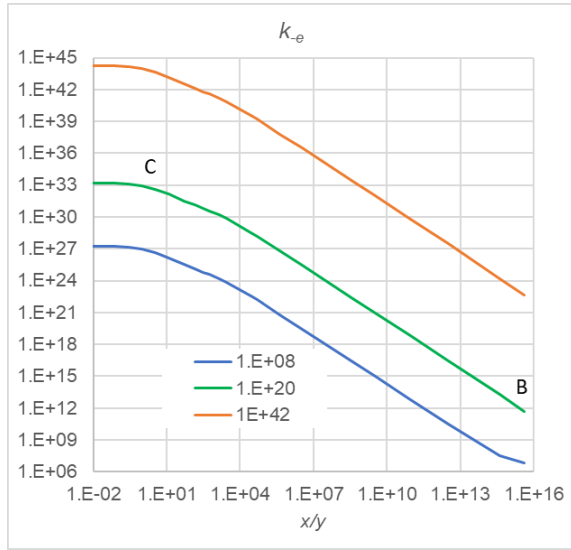
against x/y . It is plausible to think that the effective mass of the actual neutrino emitted in the beta decay is practically equal to its real mass and should be a point on this graph. The reported neutrino mass of



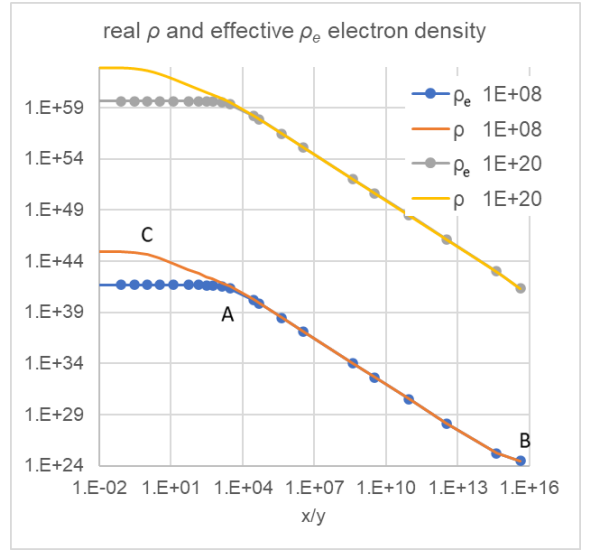
a



b

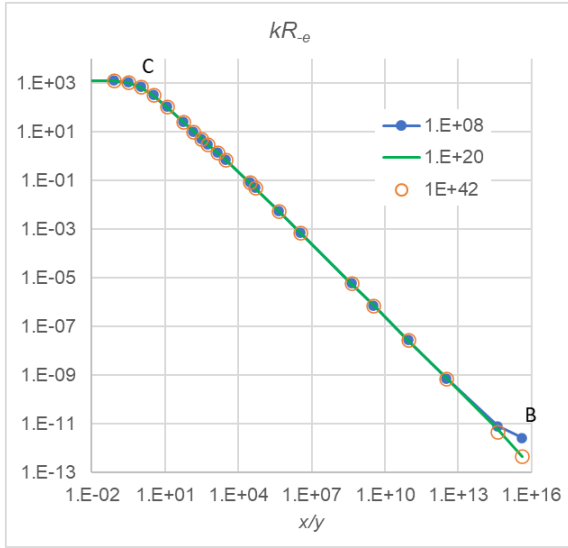


c

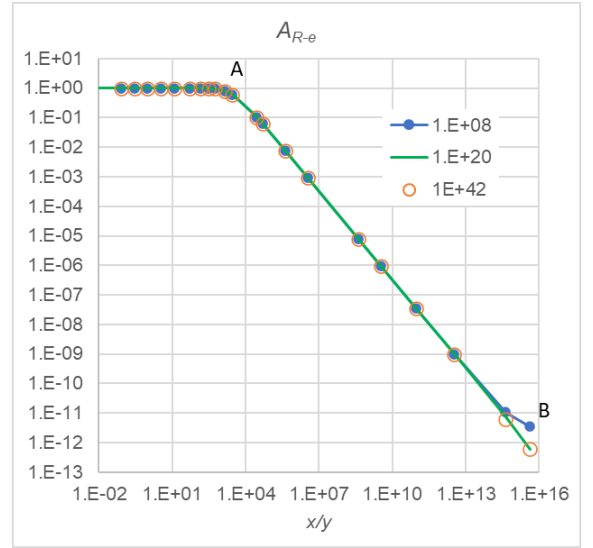


d

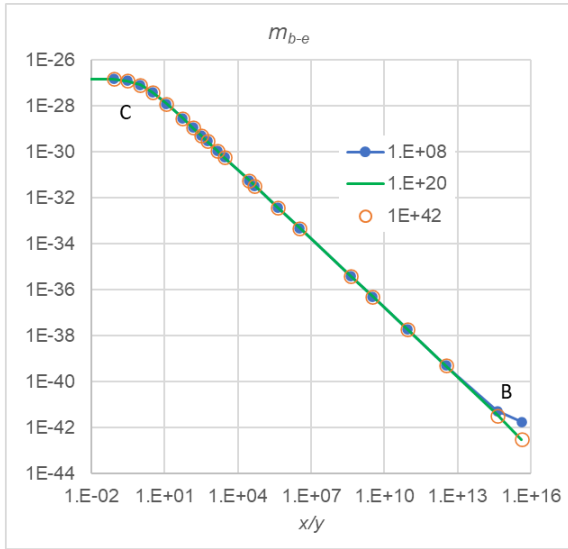
Figure 41: Plotting some electron parameters versus ratio x/y for two fixed values 10^8 ms^{-2} and 10^{20} ms^{-2} of g_0



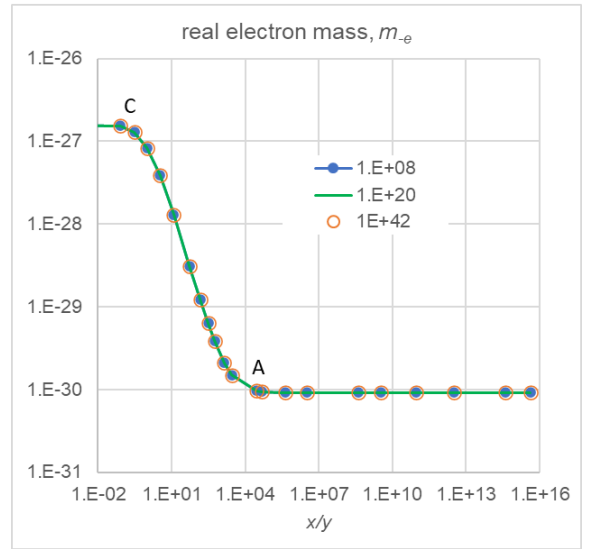
a



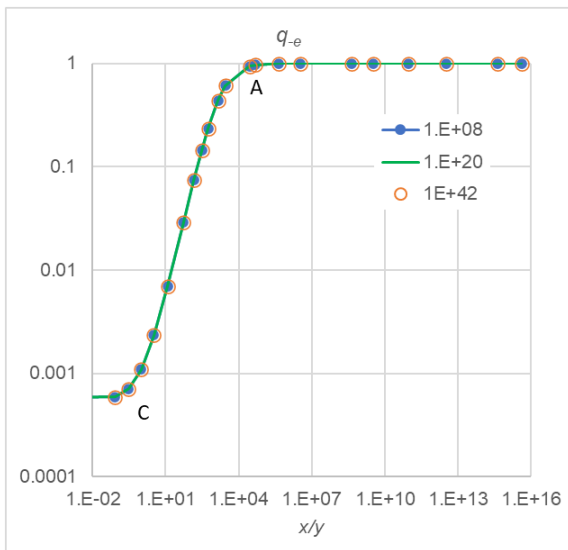
b



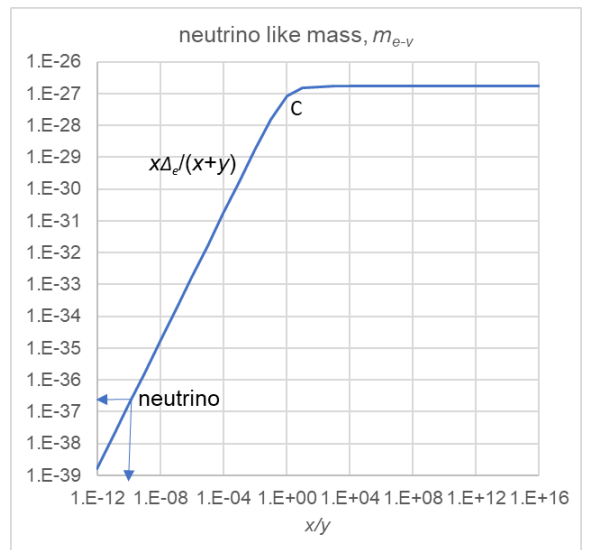
c



d



e



f

Figure 42: (a \rightarrow e) : Plotting some electron parameters versus ratio x/y for two fixed values 10^8 ms^{-2} and 10^{20} ms^{-2} of g_0 , (f): emitted/absorbed particle effective mass with actual neutrino point.

$m_{e-\nu} \approx 2 \times 10^{-37}$ kg corresponds on the graph to a value of $x/y \approx 1E-10$. That means only an extremely small amount of mass is emitted during beta decay. As we have previously found, there exists a critical mass that can be contained within a given radius of a body, so that if the proton mass is compressed just below the critical radius, then an excess amount of hyle is possible to exist. This small amount of hyle is ejected in the form of a neutrino and, when detected, appears as an effective mass equal to the measured neutrino mass.

Further, we note that this neutrino point is located in a region with lowest x/y values for all parameters. In particular, the electron radius in Fig. 41(a) remains practically constant in the low range of x/y . The latter finding, if correct, is useful to simplify further investigations, i.e. if we can narrow down among various values for the radius.

The electron radius is a function of the prevailing g_0 mainly, with negligible (if any) contribution of the trialed x/y interacting fraction. Then, for the two new possibilities of g_0 presenting above, we narrow down to the flat portions of the provided graphs yielding an electron radius between $7.8 \times 10^{-25} < R_{-e} \approx R_0 < 7.8 \times 10^{-31}$ m (in rounded figures). This can be seen directly from Eq. 289 (or graphs) with absorptivity almost unity. These very low value of radius might appear comforting for the anticipated “zero” value by the Standard Model while resolving the outstanding singularity problem.

The above finding may prove a useful practical outcome from the preceding “exercises”, which also serve to help in the understanding of the interplay among various parameters. We recognize that the above is based on several assumptions, which may appear arbitrary. We acknowledge the incompleteness of the proposition at this stage, but we can take away the method possibly useful in particle physics as an alternative research approach.

19.5 ADDENDUM_1 (May, 2025)

In consequence of latest findings in PG theory, we have now found a possible value of $g_0 = 1.33 \times 10^{-9}$. This permits us to re-work the preceding investigation based on an unknown range of possible values for g_0 . To facilitate the reader, we have done this revision along with other important outcomes in Section 31.5.

In fact, the hypothetical description of the proton, electron, positron and neutrino seems to be substantiated as a concept, while the preceding “exercises” acquire a good practical meaning in preparation for what is to come in particle physics.

This substantiates the reasons, for which we have not yet revised the entire work: It would be unwise and counterproductive to undergo the pains of doing so every time we achieve a new development and a new understanding. We purposefully retain the original writings of this report as a useful way to help the future reader understand the thinking process behind the entire work. It could also serve as a teaching method of this novel approach to physics.

20 Uncertainty Principle

We are well overdue for making a statement about the Uncertainty Principle (UP) in attempting to apply push particle theory at very small scales and entities. In fact, we are already working with entities assumed to be well below quantum mechanics levels. In attempting to find the radius of the electron at such small scales, the conjugate variable of momentum would be greatly uncertain. This is a concern compounded also by the as yet unspecified description of what this momentum (conjugate to radius) involves. Does it involve an oscillating mass of the electron? Which mass of the electron, the effective, the black or both masses? The radius itself would also be accompanied with an uncertainty, but how would that relate to the well defined characteristic minimum radius, or is the latter already ill-conceived? We have plotted a black mass of the order $\times 10^{-38}$ and a density of the order $\times 10^{40}$, which raise the question of how these variables and their conjugate variables enter in the uncertainty principle, or what the physical implication of the UP on these variables might be? In the next section, we will find even greater ranges of these and other variables, so can we proceed without prior application or some consideration of the UP?

The above questions and concerns are at the core of PG, especially when the latter is based on the transfer of momentum (impulse) by push particles, the nature of which is not yet specified or satisfactorily understood. A great uncertainty in momentum may be in direct conflict with the requirement of PG that gravions impart a definite impulse at the smallest of MAC targets.

UP could make the continuation of development of PG futile unless we can integrate UP and PG together. We readily acknowledge all of the above considerations. However, how do we know that UP is or must be a universal principle applicable even to push particles and their interactions? Furthermore, there are different interpretations or “schools” for UP with significant deviations and with no need to go through them all now. After all, UP is a “principle” creating again another dilemma if we should continue with the development of

PG or think more about the UP itself. We faced the same dilemma with the equivalence principle, which it seems that we can or we have overcome. Now, we have the option to continue without the uncertainty principle, at least tentatively, in order to see what outcomes we can obtain and then return to it with a judgment. After all, it may be more plausible to assume a deterministic sub-quantum-mechanics level than proclaim a universal applicability of UP everywhere. We opt to continue without a full investigation of the consequences of UP on PG, only as a way that would allow us to get at least an idea what the outcomes are if we follow this path. We might even have a better understanding of quantum mechanics, if we were willing to investigate first, as we have already been doing from the outset in this work. If we are in search of a “game changer”, we must be prepared to work outside principles that may be responsible for the constraints and impasses of the theories based on them. This is the purpose of science. After all, EP and UP are just “principles” that science has adopted to build all hitherto mainstream current theories. We reserve the right to pursue an investigation tentatively without these constraints, i.e. on the “what if” approach for anyone willing to see the outcomes first and then decide.

In other words, a statement of awareness on the above issues is a provisional license that may allow us to proceed even if we appear to trespass the uncertainty principle. We intend and hope to remedy this shortcoming after we gather sufficient information by means of an expanded PG theory.

By no means do we dispute the validity of the uncertainty principle and quantum mechanics (QM). We only want to move beyond this if and where possible. We only make brief statements in this section to let us move forward elsewhere. The presented report is only an optional investigation not a claim, but may become one if and when it is verified.

Actually, we have suggested that QM might be explained on the basis of PG. The big picture of modern physics should include a deeper and possibly hidden layer of subatomic world, which may lie beyond the uncertainty principle. The introduction of “virtual particles” and the mysterious electric field accompanying the electric charge may be replaced by real processes of real “particles”. If a conventional particle generates(?) an output field (e.g. electron \rightarrow electric field), it must also have an input of something. We cannot exclude that the processes at sub-QM levels are perfectly deterministic. A “particle” is an excitation according to QFT, but our introduced “push-particle” is not a particle in the sense of QFT. Perhaps, we should coin another name, but “push particles” lie well below the scale of QFT “particles”. Whereas QM describes and is valid at the scale of QFT particles, it would be arbitrary to want to forcefully apply it also at the scale of push particles. Therefore, without abandoning the achievements of QM, we might be able to explain it in a tangible way instead of attributing mythical properties beyond human comprehension. That is, UP may be reformulated to include an underlying determinism, which will also put an end to the persistence of different interpretations and schools vying for the truth. We are optimistic that the following work will put to rest any concerns.

A critical analysis of the origins of Heisenberg’s Uncertainty Principle has been presented by Michaud (2024). It is shown that this principle to be a hindrance to further fundamental research about elementary particles at the subatomic level. We quote from his concluding remarks that: “... *This confusion has lasted for a full century in the case of phase-wave velocity, contributing to the establishment of the Uncertainty Principle as an ontological axiomatic principle, thus enormously limiting the scope of research projects in fundamental physics, at least for the subatomic level of magnitude, and for much longer in the case of the relationship between the Coulomb force and the gravitational force, unduly delaying any coherent research into gravitation*”.

21 Push Electricity (PE)

We have proposed that the push particle principle be extended to explain all other known force fields. We attempt to do this for the electric field next. The outcomes seem to have far reaching effects in physics.

Because mass is a key “ingredient” across all force fields, we summarize the greater notion of matter already developed throughout previous sections even if we appear to be repetitive:

(a) The conventional mass appears either as inertial or gravitational mass in different situations, but they are axiomatically assumed to be the same according to the equivalence principle (EP). Both forms start with a common rest mass thought to be also an intrinsic property.

(b) In PG, we have come up with the notion of real mass, which is the same as matter, i.e. all the material (stuff) from which any object is composed of. The real mass is then subdivided into effective mass and black mass. The effective mass is understood to be the active or activated component liaised with a force. The black mass is a purely inert, passive, or inactive component without the conventional “inertia”. The effective mass is created by the absorptive action of push particles, e.g. of gravions in gravity and electrions in electricity as we will say. Effective mass is a relative and measurable quantity, whilst real mass is an absolute quantity. They are both measured in the same units of mass and their difference is the amount

of black mass. The amount of effective mass is relative to whether a body (real mass) is close or very far away from other bodies (real masses). For a lone body, its effective mass is determined by the intensity of flux of particular type of push particles in the surrounding space. It is the rate of push particle and energy absorption that determines the effective mass, which is different for a lone body or for a body with other neighboring bodies. We have found a relationship between force and effective mass between two spherical bodies in Section 16. The effective mass of a lone body can be said to coincide with the conventional intrinsic mass. From this common point of agreement, we have a departure of the meaning and measure of the effective mass from the conventional inertial and gravitational mass. This departure is imperceptible for “ordinary” bodies of Newtonian mechanics, but becomes increasingly significant for neighboring dense bodies. In particular, the effective mass generally decreases by proximity with another body in contrast with conventional gravitational mass. We have briefly cautioned what may happen to the effective mass of a body orbiting around another body or accelerated in space by a rocket. In the latter case, we think that it increases in similar but not necessarily exactly the same mathematical fashion as the conventional inertial mass, and not only mathematically but also in a material sense. While we await a proper assessment of the latter case, we can still proceed to investigate the static electric field next.

We should note that the term “matter” in this report includes also “antimatter” that is well known and used in physics. This is only because we lack a commonly agreed word to include both “matter-antimatter” in elsewhere terminology. For this reason we have often used the less elegant word “stuff” to denote everything that material bodies or objects are made of including the force fields themselves. Then we can state that “stuff is conserved”, which leads us to unite the fields. We do not subscribe to a mere mathematical conception/description of force fields in the belief that only some common underlying stuff can unite them. Otherwise, physics could be reduced to a mathematical idealism, and cosmos could be the product of human existence, not the reverse. By all this, of course, we enter the realm of philosophy.

For the time being, we juxtapose only gravions and electrions and, if our findings prove successful or promising, we may continue on with other fields of force. The examination of these two fields may present us with an opportunity of their unification prior to a general push field theory (PFT).

21.1 General relationships

Little is known about the mysterious and intriguing electron: We don’t know what holds it together, what fixes its mass and its possible radius, or the nature of its electric charge. By the same token, we can say the same about the positron. We know, or consider, that the electron is a persistent and reliable “atomon” (=uncuttable), i.e. indivisible particle so far, whilst the positron has a very short life. We want to describe and quantify the electric field in a similar fashion as the gravitational field. Initially we ignore the repelling effect of same sign charges and bypass the concept of charge. The electric field between an electron and a positron (in lieu of a proton) is the simplest way resembling an “attracting” gravitational field, for which we may afford to use similar derivations. We don’t use the similar proton-electron system to avoid possible complications on account of the different proton mass and structure. The apparent similarity between Coulomb’s law and gravitational law prompts us for this approach. Upfront we can expect that the only difference should be a difference in magnitudes, since we know that the electric field is by far much stronger than the gravitational field.

Under the provisos set in the preceding sections, our intention is to consider the options below as a first pass of the theory and then return and weed out any discrepancies that may appear. So far, we rely on the type (nature) of push particles and regard their mean-free-path as a critical parameter in delineating various fields. We delay the use of the wavelength concept until we see the need for it.

Since the real mass is the stuff that is conserved, it should be invariant under the simultaneous presence of both gravitational and electric fields. Then we think that the radius corresponding to the real mass is also invariant between the fields. The latter radius might be disputed presumably by a theoretical arrangement of a collision experiment in electromagnetic field that would produce only a “charge” radius. Instead, we have produced a theoretical electron radius from a gravitational field by PG considerations in preceding Section 19.3. Sharing Dehmelt’s vision, we also assume that the electron has an absolute finite (real) radius determined by its real mass, i.e. independently and prior of any applied measuring methods or an assumed nature’s indeterminism. At any rate, should any objections be raised, we can always return after we proceed as repeatedly suggested.

For the electric field and its associated electrion, i.e. push particle type-II, we can apply the same equations as for the gravitational field simply by introducing the subscript 2 (2) following the same terminology used in previous sections. Thus, we write G_2 for universal “electrical” (big G_2) constant, m_{2e-e} for effective mass, A_{2R-e} for absorptivity, q_{2-e} for contraction factor, k_{2-e} for absorption coefficient, g_{02} for maximum acceleration, J_{02} for flux 2 density (intensity), Λ_2 for new universal 2 constant, m_{2b-e} for black mass, ρ_{2-e} for real density, R_{02} for characteristic minimum radius, $\Delta_2 R_{-e}$ for radius difference, and product $k_{2-e} R_{-e}$

for the characteristic dimensionless variable. We may use no subscript or occasionally the subscript 1 (₁) for the gravitational field, like $g_{01} \equiv g_0$.

Since the real mass m_{-e} of the electron (positron) is the same under both fields (i.e. $m_{2-e} = m_{1-e} \equiv m_{-e}$), we immediately have that:

$$m_{-e} = \frac{m_{e-e}}{q_{-e}} = \frac{m_{2e-e}}{q_{2-e}} \quad (307)$$

or

$$m_{2e-e} = \frac{q_{2-e}}{q_{-e}} m_{e-e} \quad (308)$$

If the radius R_{-e} for the electron (positron) is the same (i.e. $R_{2-e} = R_{1-e} \equiv R_{-e}$), then:

$$R_{-e}^2 = \frac{G m_{e-e}}{A_{R-e} g_0} = \frac{G_2 m_{2e-e}}{A_{2R-e} g_{02}} \quad (309)$$

or

$$g_{02} = \frac{m_{2e-e} G_2 A_{R-e}}{m_{e-e} G A_{2R-e}} g_0 = \frac{q_{2-e} G_2 A_{R-e}}{q_{-e} G A_{2R-e}} g_0 = \frac{G_2}{G} \frac{k_{-e}}{k_{2-e}} g_0 \quad (310)$$

where we used also the general equation $q = 3A_R/(4kR)$. [Note: Throughout this report we often expand an equation to include various forms and parameters, because they can be easily referenced, verified and better understood as we experience new variables over conventional physics].

We also have a corresponding characteristic limiting radius R_{20-e} for each value of g_{02} :

$$R_{20-e} = \sqrt{\frac{G_2 m_{2e-e}}{g_{02}}} = R_{-e} \sqrt{A_{2R-e}} \quad (311)$$

so that we can again define the two radii difference ΔR_{-e} by:

$$\Delta R_{2-e} = R_{-e} - R_{20-e} = R_{-e} \left(1 - \sqrt{A_{2R-e}}\right) \quad (312)$$

Further, from the known (given) m_{e-e} , m_{2e-e} and q_{2-e} and the equation of contraction factor below:

$$q_{2-e} = \frac{3A_{2R-e}}{4k_{2-e}R_{-e}} = \frac{m_{2e-e}}{m_{e-e}} q_{-e} \quad (313)$$

we solve first for the unknown product $k_{2-e}R_{-e}$ (also contained in A_{2R-e}) and then we deduce k_{2-e} and A_{2R-e} from the given electron radius.

The new universal constant Λ_2 and other parameters of the electric field are given below from the corresponding parameters of the gravitational field without further comment:

$$\Lambda_2 = \frac{k_{2-e}}{\rho} \quad (314)$$

$$\Lambda_2 = \frac{\pi R_{-e}^2 A_{2R-e}}{m_{2e-e}} = \frac{\pi R_{-e}^2 A_{R-e}}{m_{e-e}} \frac{k_{2-e}}{k_{-e}} = \Lambda_1 \frac{k_{2-e}}{k_{-e}} \quad (315)$$

$$J_{02} = \frac{c g_{02}}{\pi \Lambda_2} = \frac{k_{-e}^2 G_2}{k_{2-e}^2 G} \frac{c}{\pi \Lambda_1} g_0 = \frac{k_{-e}^2 G_2}{k_{2-e}^2 G} J_0 = \frac{k_{-e}^2 G_2}{k_{2-e}^2 G^2} \frac{c}{\pi^2} g_0^2 = \frac{c G_2}{\pi^2} \frac{k_{-e}^2}{k_{2-e}^2} \left(\frac{m_{e-e}}{A_{R-e} R_{-e}^2} \right)^2 \quad (316)$$

$$J_{02} = \frac{c}{\pi^2 G_2} g_{02}^2 = \frac{c}{\pi^2 G^2} \left(\frac{k_{-e}}{k_{2-e}} g_0 \right)^2 \quad (317)$$

$$\frac{k_{-e}}{k_{2-e}} \frac{g_0}{g_{02}} \frac{G_2}{G} = 1 \quad (318)$$

$$\frac{J_{02}}{J_0} = \frac{g_{02}^2}{g_0^2} \frac{G}{G_2} = \frac{k_{-e}^2 G_2}{k_{2-e}^2 G} = \frac{g_{02}}{g_0} \frac{k_{-e}}{k_{2-e}} \quad (319)$$

The above considerations require generally two alternative effective masses, which may be in question because the electron “mass” is generally considered to be well established. If the effective mass created by (or corresponding to) electrons were generally different from that created by gravions, it would presumably be contrary to our experience with mass measurements of the electron and established theories. Masses with an

electric charge are generally measured inside electric (and/or magnetic) fields, but they are also measured in macroscopic charge-neutral-form inside the gravitational field and found to be the same in the sum-total of all particles comprising a given material body. No distinction is generally made for the masses inside electric and gravitational fields in compliance with the Equivalence Principle. Nevertheless, we wish to go through the exercise of the available options below.

The above general relationship by Eq. 308, states that the ratio of the two effective masses is equal to the ratio of the two corresponding contraction factors for the two fields. We have now two options to consider, namely, that the two masses are equal $m_{2e-e} = m_{e-e}$ for the sake of preserving the equivalence principle, or distinctly different $m_{2e-e} \neq m_{e-e}$. The unequal masses case clearly violates the EP, but we have already concluded in Section 16 that EP should not be a constraint that we always have to adhere to.

Addendum:

As a separate supplementary relationship often encountered in conventional physics is the product Gm_e called “standard gravitational parameter” μ_{sp} , which we can also express in our parameters as:

$$\mu_{sp} = Gm_e = A_{R-e}R^2g_0 \quad (320)$$

This is often quoted to be the “best known or measured quantity”. We can also introduce a corresponding “standard electric parameter” μ_{2sp} for the electric field by

$$\mu_{2sp} \equiv A_2g_{02} = A_{2R-e}R_{-e}^2g_{02} = G_2m_{2e-e} \quad (321)$$

Noted that the sub-scripted symbol $\mu_{subscript}$ here denotes a different parameter from the plain μ previously used for the proton-to-electron mass ratio.

We can also transfer other corresponding equations from the summary Section 6.5 and elsewhere in Part One of this report for use in the electric field.

21.1.1 Case with equal masses $m_{2e-e} = m_{e-e}$

Let’s assume that the gravitational mass of the electron m_{e-e} is equal to its electrical mass m_{2e-e} . Then $q_{2-e} = q_{-e}$ and $k_{2-e}R_{-e} = k_{-e}R_{-e}$ from Eq. 50 of contraction; then $k_{2-e} = k_{-e}$ and $A_{2R-e} = A_{R-e}$. As a result, the above Eq. 310 between fields reduces to a simple formula of proportionality:

$$g_{02} = \frac{G_2}{G}g_0 \quad (322)$$

In electricity, the Coulomb force F_2 at distance r between an electron and a positron charge e is

$$F_2 = \frac{1}{4\pi\epsilon_0} \frac{e^2}{r^2} \equiv b \frac{e^2}{r^2} \quad (323)$$

where for simplicity in expressions we use Coulomb’s factor $b = 8.987552E+09 \text{ m} \cdot \text{N}^2/\text{C}^2$ instead of the electric permittivity constant ϵ_0 . We may now theorize that the same force is generated by a corresponding effective electron mass m_{2e-e} at the same distance:

$$F_2 = G_2 \frac{m_{2e-e}^2}{r^2} \quad (324)$$

where G_2 is the (electrical) universal constant for this field. By equating the two expressions of the same (equal) force, we derive

$$G_2 = b \frac{e^2}{m_{2e-e}^2} = 2.7803909099 \times 10^{32} \text{ m}^3 \text{ kg}^{-1} \text{ s}^{-2} \quad (325)$$

where we used for the charge $e = 1.6021766340 \times 10^{-19} \text{ Cb}$ and the established effective electron mass $m_{2e-e} = 9.1093837015 \times 10^{-31} \text{ kg}$. From this, we derive the remaining corresponding PG parameters for the electric field as summarized without further comment below:

$$\Lambda_2 = \frac{\pi R_{-e}^2 A_{2R-e}}{m_{2e-e}} = \Lambda_1 \quad (326)$$

$$J_{02} = \frac{cg_{02}}{\pi\Lambda_2} = \frac{cg_0}{\pi\Lambda_1} \frac{G_2}{G} = \frac{G_2}{G} J_0 = \frac{cG_2}{\pi^2 G^2} g_0^2 = \frac{cG_2}{\pi^2} \left(\frac{m_{e-e}}{A_{R-e}R_{-e}^2} \right)^2 \quad (327)$$

$$J_{02} = \frac{c}{\pi^2 G_2} g_{02}^2 = \frac{c G_2}{\pi^2 G^2} g_0^2 \quad (328)$$

$$g_{02} = \frac{G_2 m_{2e-e}}{A_{2R-e} R_{-e}^2} = \frac{G_2 m_{e-e}}{A_{R-e} R_{-e}^2} \quad (329)$$

$$F_2 = G_2 \frac{m_{2e-e}^2}{r^2} = \frac{g_{02}}{g_0} G \frac{m_{e-e}^2}{r^2} = \frac{g_{02}}{g_0} F_1 \quad (330)$$

where F_1 is the gravitational force and how it relates to the electric force F_2 .

Now, we try to understand the physical meanings for this case of equal masses in the two fields. We need to introduce the number density n_ω for gravions with a quantum energy ω and the number n_ε density for electrions with a quantum energy ε and relate them via the corresponding energy flux densities with J_0 and J_{02} by:

$$J_0 = n_\omega \omega c \quad (331)$$

$$J_{02} = n_\varepsilon \varepsilon c \quad (332)$$

$$\frac{J_{02}}{J_0} = \frac{n_\varepsilon \varepsilon}{n_\omega \omega} = \frac{G_2}{G} = 4.1659538241 \times 10^{42} \quad (333)$$

The equation $k_{-e} = k_{2-e}$ found says that the number of absorption events per unit length is the same for the gravion and the electrion. Then we must have $n_\omega = n_\varepsilon$, otherwise the accrued absorption events would be different for gravions and electrions resulting in different effective masses that would contradict the case of equal masses here. Thus the above equation is simplified to:

$$\frac{J_{02}}{J_0} = \frac{\varepsilon}{\omega} = \frac{G_2}{G} = 4.1659538241 \times 10^{42} \quad (334)$$

Then we face a dilemma to reconsider the interpretation of the meaning of effective mass: The impulse transmitted to the common effective mass by each electrion is G_2/G times the impulse transmitted by each gravion. This means that the effective mass is proportional to the number rate of push particles not to the energy rate (power) and each electrion is not reduced to an equivalent number of gravions after absorption, otherwise the effective mass should be by many orders of magnitude greater. The reasoning of the electrion “dissolving” to equivalent gravions after absorption forces a contradiction of terms, unless the electrion is a type of matter that retains its identity after absorption. In other words, the electrion must have some unique attribute like, say, the conventional charge which is conserved. In other words, the electrion is not lumped together with the absorbing matter, it is not integrated with stuff of the electron but its entity is preserved inside the electron. Then, we may as well identify it with our well known charge. By this then, we conclude that the charge of an electron originates by absorption of peculiar electrions being small push particles with a density flux J_{02} in the surrounding space. Then, gravions and electrions perform different functions upon absorption in their own right and their own separate identity. We are forced to conclude that whilst the electrion imparts much greater impulse and energy into the absorbed center, the effective mass is not increased in proportion but remains the same. Such a conclusion and re-interpretation of “effective” mass may be difficult to incorporate into a unifying theory of fields and matter, if not met with an outright rejection. Nevertheless, we must keep note of this case, if keeping true to our scientific endeavor.

21.1.2 Case with unequal masses $m_{2e-e} \neq m_{e-e}$

Let us now investigate the challenging case of unequal effective masses between the two fields. Given the identical form of Coulomb’s law with the gravitational law, we are tempted to replace Coulomb’s charge with effective mass, as if the electric field were to be considered like a gravitational field. In other words, we set the numerical value of the electrical effective mass equal to the numerical value of the electron charge as a likely case of unequal gravitational and electrical masses. We cannot immediately envisage any reason for another choice of a numerical value of electrical mass without upsetting the well established physics of electricity. Thus, we set:

$$m_{2e-e} \equiv 1.6021766340 \times 10^{-19} \text{ kg} \quad (335)$$

and so the universal electrical constant should be numerically equal to b :

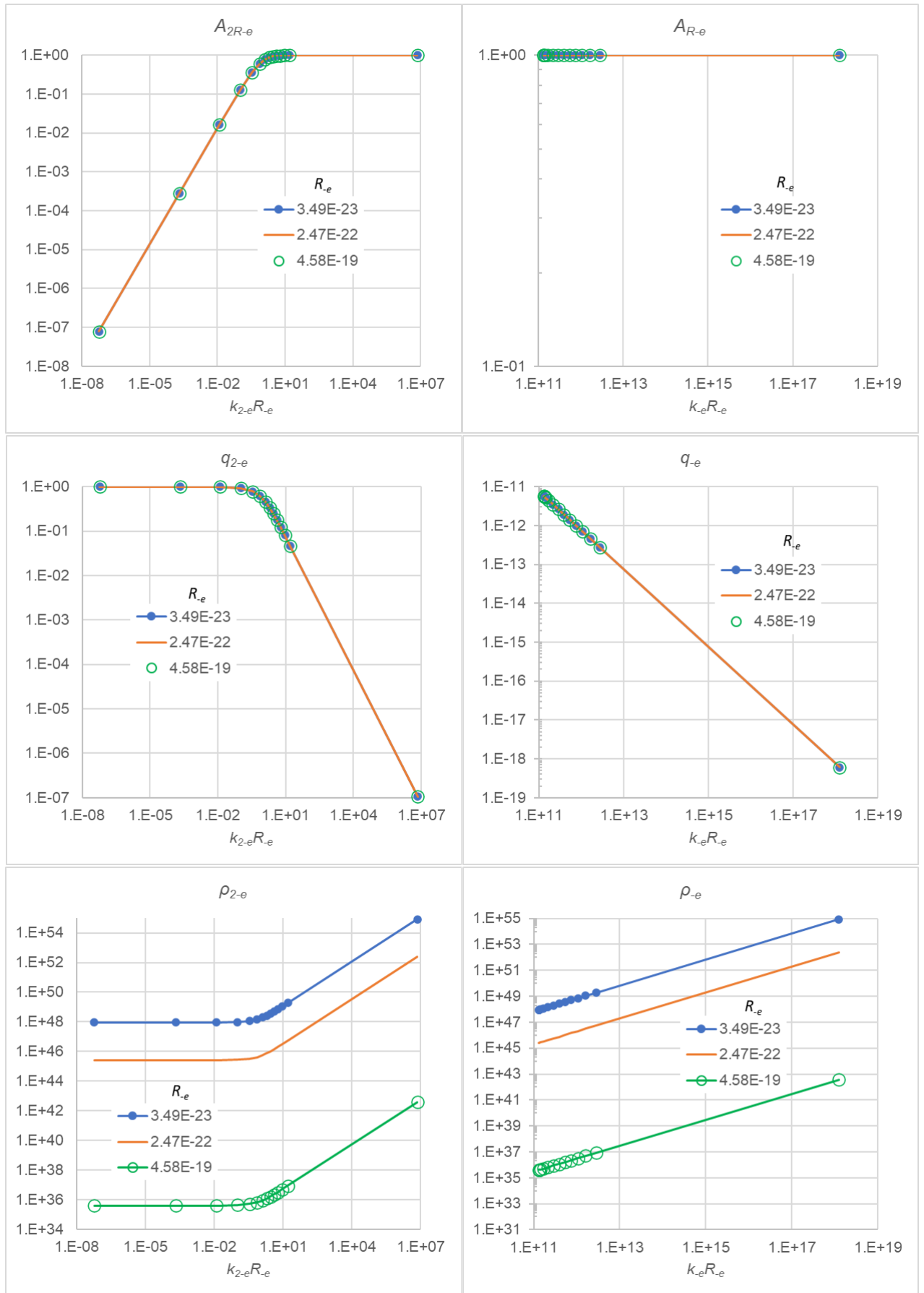


Figure 43: Electron parameters against the electrical product $k_{2-e}R_e$ (left) and same juxtaposed against the gravitational product k_eR_e (right) for three extreme cases of fixed electron radii.

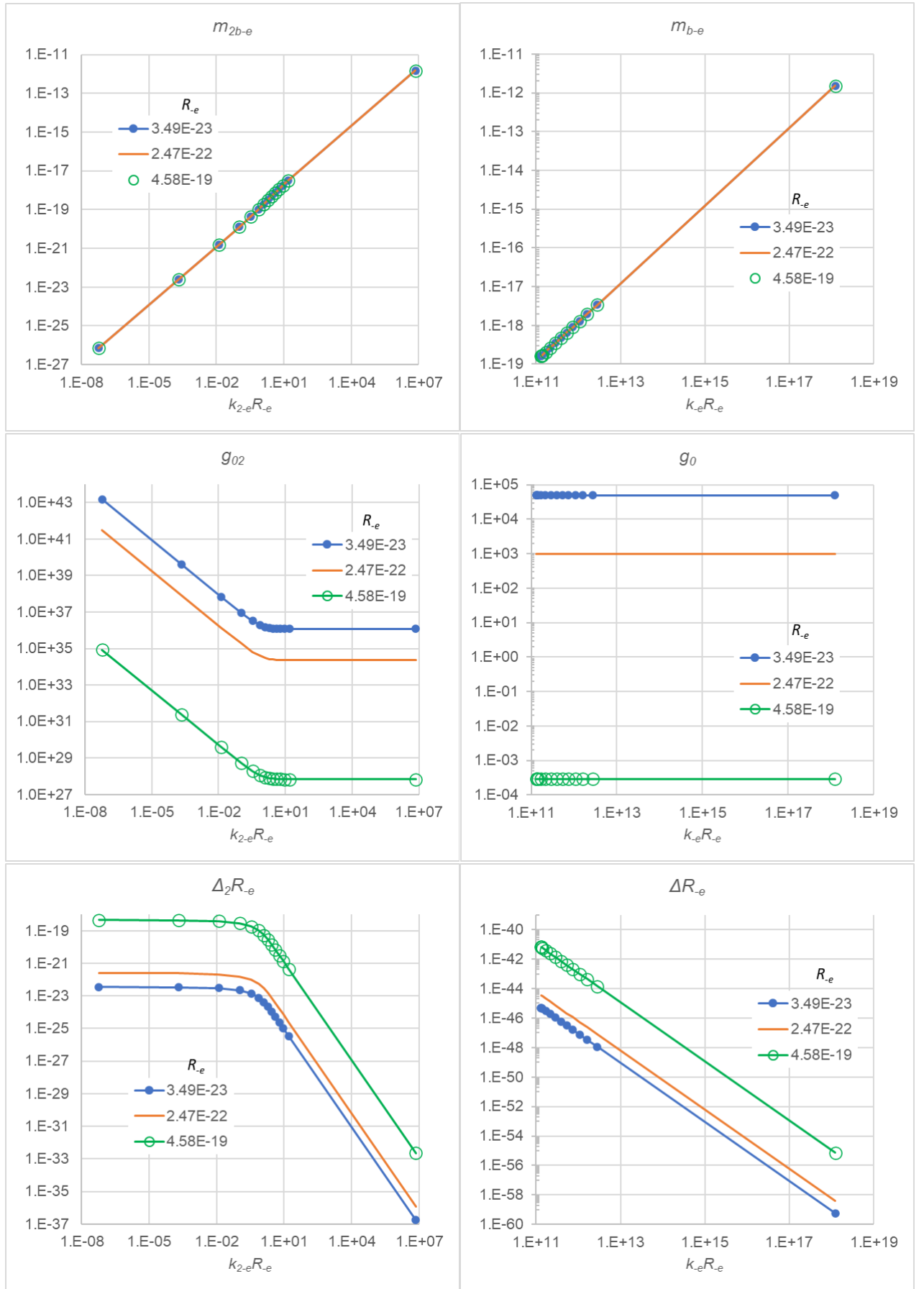


Figure 44: Electron parameters against the electrical product $k_{2-e}R_{-e}$ (left) and same juxtaposed against the gravitational product $k_{-e}R_{-e}$ (right) for three extreme cases of fixed electron radii.

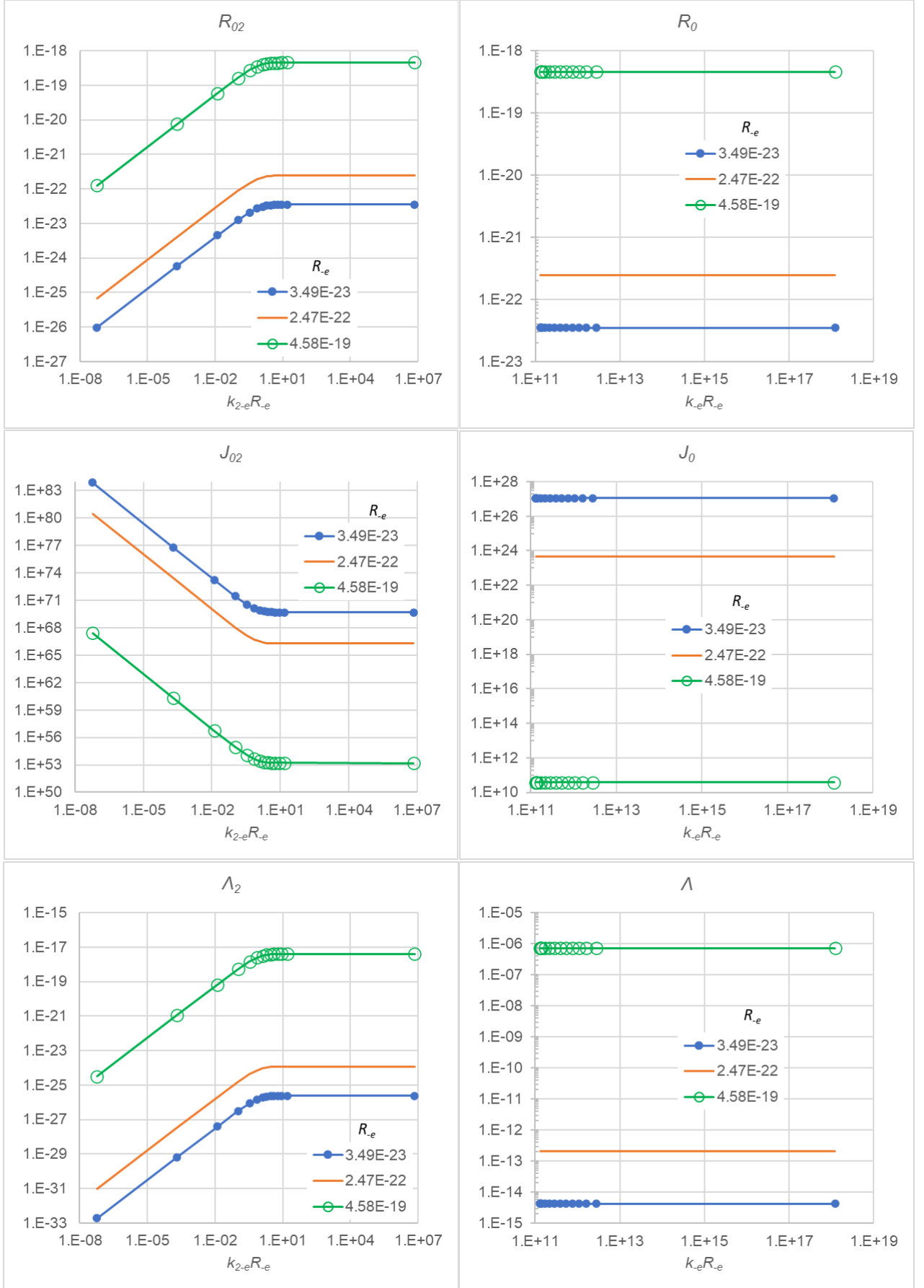


Figure 45: Electron parameters against the electrical product $k_{2-e}R_e$ (left) and same juxtaposed against the gravitational product k_eR_e (right) for three extreme cases of fixed electron radii.

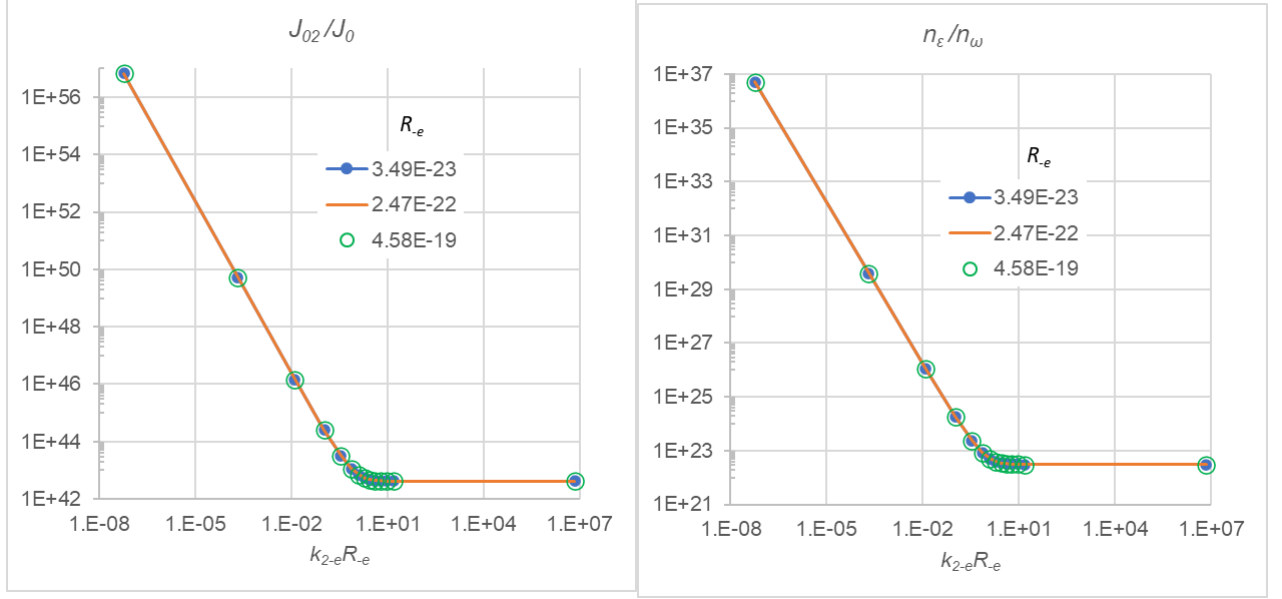


Figure 46: Ratios of density flux (left) and number density (right) of corresponding push particles of electrical over gravitational fields against electrical product $k_{2-e}R_e$ for three extreme cases of fixed electron radii.

$$G_2 \equiv b = 8.987552 \times 10^9 m^3 kg^{-1} s^{-2} \quad (336)$$

i.e. a greatly different value from Eq. 325 for this parameter. Coulomb's law is then replaced with a gravitational-like law, as previously by:

$$F_2 = G_2 \frac{m_{2e-e}^2}{r^2} \quad (337)$$

Substituting the electrical mass in terms of PG parameters as we did for the gravitational mass via Eq. 308, we obtain:

$$F_2 = G_2 \left(\frac{q_{2-e}}{q_{-e}} m_{e-e} \right)^2 \frac{1}{r^2} = \frac{k_{2-e} g_{02}}{k_{-e} g_0} \frac{q_{2-e}^2}{q_{-e}^2} G \frac{m_{e-e}^2}{r^2} = \frac{k_{2-e} q_{2-e}^2 g_{02}}{k_{-e} q_{-e}^2 g_0} F_1 \quad (338)$$

where F_1 is the gravitational force and how it relates to the electric force F_2 .

We find some numerical values and see the consequences of the above derivations. For the known (given) ratio of the two effective masses, we find the magnitude of contraction ratio:

$$Q = \frac{q_{2-e}}{q_{-e}} = \frac{m_{2e-e}}{m_{e-e}} = 1.75882001076(53) \times 10^{11} \quad (339)$$

i.e. the electrical effective mass is 11 orders of magnitude greater than the gravitational mass and so are the contraction factors. This is the known electron charge-to-mass quotient, which is not a tautology or a mere change of the word charge with the word mass, as we will shortly realize by introducing and understanding the physical meaning and consequences below.

The above "quotient" expresses an enormous difference between the two masses that cannot be reconciled if we start with (accept) the gravitational parameters already calculated for the electron in Section 19.3, because the contraction factor and the absorptivity cannot be greater than unity in either the gravitational or electric field. The only way to apply the above relationships between the two fields is to start with a range of values for the electrical field and work backwards (in reverse) to find the corresponding parameters for the gravitational field. Since we have no idea about choosing a range for g_{02} (as we did for g_0), we can choose a range for the contraction or the absorptivity both known to vary in the range between zero and one. We opted to do so by choosing the absorptivity as the independent (starting) variable with a selection of representative values in the range $0 < A_{2R-e} < 1$. Then we find all other electrical parameters corresponding to these values of A_{2R-e} and all corresponding gravitational parameters from the above relationships between the two fields. The only proviso in doing all these computations is that we have to specify (choose) an arbitrary electron radius at least among the range of radii already found from the gravitational field. For every choice of radius value, we obtain a different family of relationships between

all other parameters. We present results for three electron radii at the extreme cases previously found in Section 19.3. Two radii are taken from the lowest values at $g_0 = 1000 \text{ ms}^{-2}$ and $g_0 = 50000 \text{ ms}^{-2}$, namely, $R_{-e} = 2.46570013543645 \times 10^{-22} \text{ m}$ and $R_{-e} = 3.48702657227941 \times 10^{-23} \text{ m}$ from Table 21, and one maximum radius $R_{-e} = 4.58247932812879 \times 10^{-19} \text{ m}$ from Table 25 with $g_0 = 50000 \text{ ms}^{-2}$. Having calculated the corresponding values of all parameters, we can plot any arbitrary pair of them and observe their variation. We have done this by plotting parameters against the generalized products $k_{2-e}R_{-e}$ and $k_{-e}R_{-e}$ for the electric and gravitational field juxtaposed in the left and right columns in Figs. 43, 44 and 45.

There are many conclusions to draw from those graphs, some of which are given below.

We note that for the electric field there is generally a straight line portion of the graphs corresponding to a Newtonian mass, another straight line portion corresponding to a prevailing black mass and an inflection region corresponding to a transition between the two masses. This is because we have purposefully chosen a wide range of values of the variable $k_{2-e}R_{-e}$ to cover all regimes of electron absorption. In contrast, the juxtaposed parameters for the gravitational field are all straight lines well beyond the Newtonian masses and into the total absorption of black masses as judged by the very near unity value of the absorptivity, or the very near zero values of the contraction factors, all with extremely low values of variation invisible by the drawn lines. The graphs were produced with an excel worksheet not permitting precision with more than 15 decimal places, so the absorptivity appears a parallel line very close to unity, but there is no need to zoom in such small details here.

Another salient feature is that the black mass of the electron should be many orders of magnitude greater than that worked out by the exercises on possible electron-proton relationship in previous Section 19.3. The large amount of possible black mass in the electron (positron) may allow even more flexibility to find not only the ultimate relationship between proton and electron but also to explain many other relationships in nuclear and particle reactions, where these three particles are present. Importantly, we have not found a unique single value of possible black mass yet, as we only have a large range of possible electron densities J_{02} . However, we learn that black mass can be used as a “wild” card for fitting and understanding many or all particles already found for the Standard Model and beyond. This is a next task that can only be undertaken by the relevant experts. We only reveal the new possibilities now opened by PG.

Another salient feature found by examining the graphs for g_0 is that it requires an extremely low value of $g_0 = 0.0002895 \text{ ms}^{-2}$ with the maximum radius used, which is unacceptable. It must be understood that for any fixed radius R_{-e} the variation of g_0 appears constant on the graphs, but there is an invisible but extremely small variation. For example, in the case with $R_{-e} = 4.58 \times 10^{-19} \text{ m}$ the variation is beyond the 25th decimal place, with $R_{-e} = 2.47 \times 10^{-22} \text{ m}$ beyond the 19th decimal place and with $R_{-e} = 3.49 \times 10^{-23} \text{ m}$ beyond the 16th decimal place. In practice, this means that if we could measure experimentally the gravitational g_0 , then we can determine the electron beam radius. To these fixed values of g_0 and R_{-e} there corresponds a range of values for the electron g_{02} . The actual value for g_{02} will then have to be determined by other means such as from existing data in particle physics and possibly from similar relationships between subsequent field strengths, until we close the “loop” of necessary relationships.

In Table 27, we present possible magnitudes of the maximum (limiting) electrical acceleration g_{02} and density flux J_{02} against the gravitational g_0 for the cases of equal and unequal masses using Eqs. 322 and 310 correspondingly. We see (as expected) that there is a one-to-one correspondence between electrical and gravitational fields for the case of equal masses. However, for every given value of g_0 at a fixed radius, we have a corresponding range of values for g_{02} and J_{02} in the case of unequal masses, where we equated the electrical mass to the charge of the electron. [Note: The above range of values are by far much greater than the minimum requirement of $g_{02} > 10^3 g_0$ to achieve expected core pressures in white dwarfs.]

Now, we can describe further the meaning of the case with unequal masses in the two fields with energy flux densities J_0 and J_{02} . We use Eqs. 331 and 332 again, but with $n_\omega \neq n_\epsilon$ we obtain the corresponding ratio of flux densities from Eq. 316 as:

$$\frac{J_{02}}{J_0} = \frac{n_\epsilon \epsilon}{n_\omega \omega} = \frac{G_2 k_{-e}^2}{G k_{2-e}^2} = \frac{G}{G_2} \frac{g_{02}^2}{g_0^2} = \frac{g_{02}}{g_0} \frac{k}{k_{2-e}} \quad (340)$$

Then we can relate the ratios $\frac{\epsilon}{\omega}$ and $\frac{n_\omega}{n_\epsilon}$ as:

$$\frac{n_\epsilon}{n_\omega} = \frac{\omega}{\epsilon} \frac{J_{02}}{J_0} = \frac{\omega}{\epsilon} \frac{G_2 k_{-e}^2}{G k_{2-e}^2} = 1.347 \times 10^{20} \frac{k_{-e}^2}{k_{2-e}^2} \frac{\omega}{\epsilon} \quad (341)$$

or the same by

$$\frac{n_\epsilon}{n_\omega} = \frac{\omega}{\epsilon} \frac{J_{02}}{J_0} = \frac{\omega}{\epsilon} \frac{G}{G_2} \frac{g_{02}^2}{g_0^2} = 7.426 \times 10^{-21} \frac{g_{02}^2}{g_0^2} \frac{\omega}{\epsilon} \quad (342)$$

	$m_{2e-e} = m_{e-e}$		$m_{2e-e} = 1.6E - 19$	
g_0	g_{02}	$\frac{J_{02}}{J_0}$	g_{02}	$\frac{J_{02}}{J_0}$
300	1.24979E45	4.16595E42		
500	2.08298E45	4.16595E42		
1000	4.16595E45	4.16595E42	2.4E34 \rightarrow 3.0E41 ($R_{-e}=2.47E-22$)	4.16575E42 \rightarrow6.83450E56
2000	8.33191E45	4.16595E42		
5000	2.08298E46	4.16595E42		
10000	4.16595E46	4.16595E42		
20000	8.33191E46	4.16595E42		
30000	1.24979E47	4.16595E42		
50000	2.08298E47	4.16595E42	1.2E36 \rightarrow 1.5E43 ($R_{-e}=3.49E-23$)	4.16575E42 \rightarrow6.83450E56

Table 27: Relationship between g_{02} of electric field and g_0 of gravitational field for equal masses case (left columns) and $m_{2e-e} = 1.6E - 19$ kg case (right columns) with two electron radii at $g_0 = 1000$ and 50000 ms^{-2} .

If we set

$$\frac{\omega}{\varepsilon} = \frac{G}{G_2} \quad (343)$$

then

$$\frac{n_\varepsilon}{n_\omega} = \frac{k_{-e}^2}{k_{2-e}^2} = \frac{G^2 g_{02}^2}{G_2^2 g_0^2} \quad (344)$$

In other words, the impulse transmitted to the different effective masses by each electron is a lot greater than the impulse transmitted by each graviton but a lot smaller than the impulse of the electron in the case of equal masses. The ratio of these impulses will be determined if and when we know the number density ratio n_ω/n_ε . These numbers may be easier to physically justify in a subsequent modeling for the two fields using the unequal masses case. The ratios of flux densities and number densities for the two fields are plotted in Fig. 46.

We will use the above findings further in building an electricity model and draw more conclusions and insights in the course of more detailed development of the theory.

21.1.3 Extended range of electron parameters

Based on the extended range of electron parameters in the preceding Section 19.4, it is pertinent to also extend the inter-relationships between gravitational and electric fields. To be able to make some headway forward, we adopt the case of unequal masses between the fields given by section 21.1.2. That is, we use the radii between $R_{-e} = 7.8 \times 10^{-25}$ m and $R_{-e} = 7.8 \times 10^{-31}$ m corresponding to $g_0 = 1 \times 10^8$ ms^{-2} and $g_0 = 1 \times 10^{20}$ ms^{-2} , from which we present a selection of results in Figs. 47 and 48. We juxtapose corresponding quantities for the two fields and we provide the ratio of four corresponding constants between electricity and gravity as well; we need the ratios for further development in Section 31.1. Now, the graphs in Fig. 48 appear to be independent of the electron radius; however, this needs to be checked for each constant: The contraction factors q_1 and q_2 seem to differ beyond the 41st decimal place between radii cases, while the absorptivities differ beyond the 60th decimal place, when increasing the precision in the Python script used. This precision is lost, when we further process the Python outputs with an excel spreadsheet giving only 14 decimal places (good enough **only** for plotting the results). It is important to note that the two values of g_0 at which we establish the two electron radii are reproduced on the graphs of $g_0(k_{-e}R_{-e})$ as they should, but they are not exactly constant; there is a second order variation invisible on the graphs in the way we previously reported. We should always bear in mind the special characteristics of the absorptivity curve

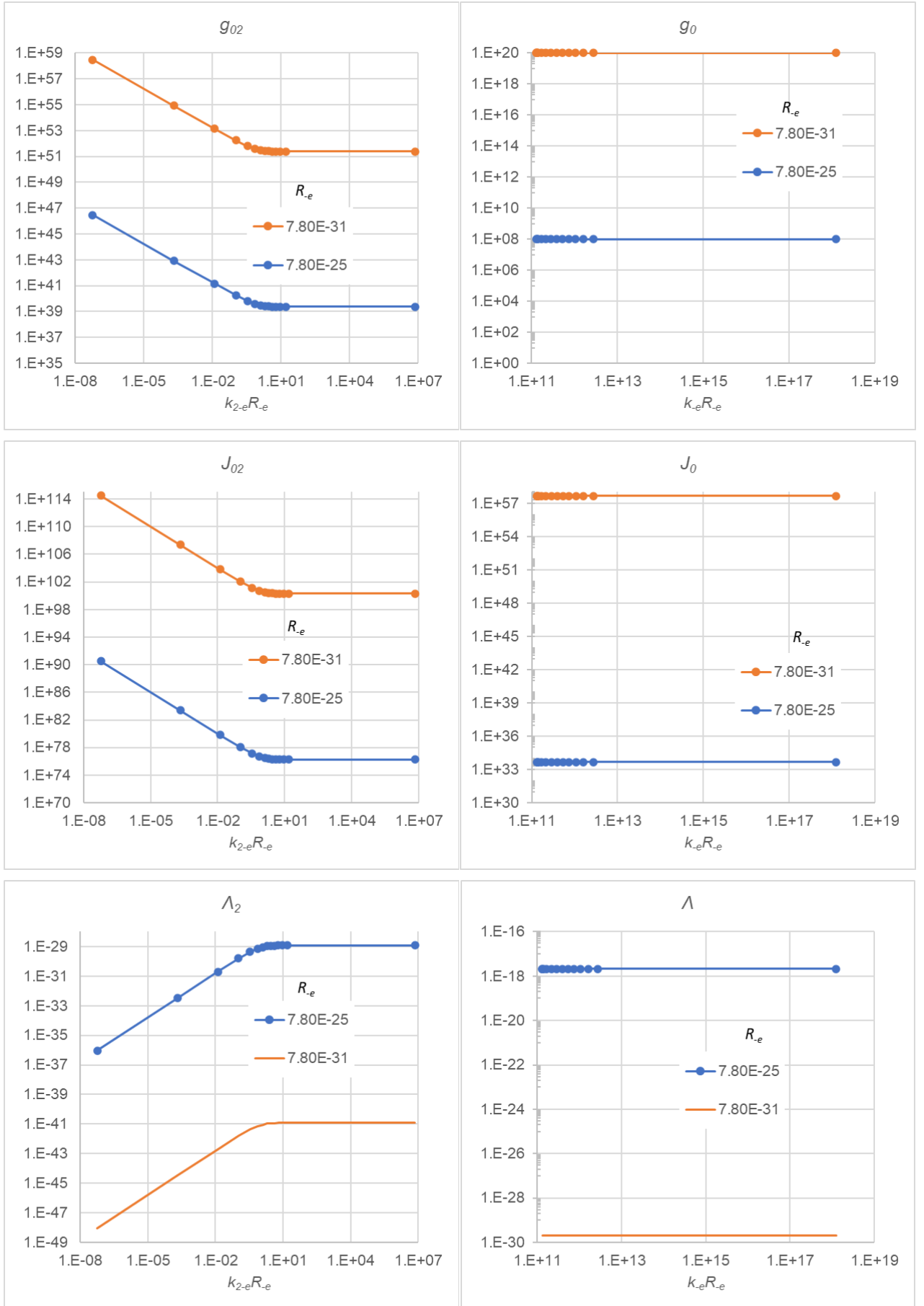


Figure 47: Electron parameters against the electrical product $k_{2-e}R_e$ (left) and same juxtaposed against the gravitational product k_eR_e (right) for two cases of fixed electron radii.

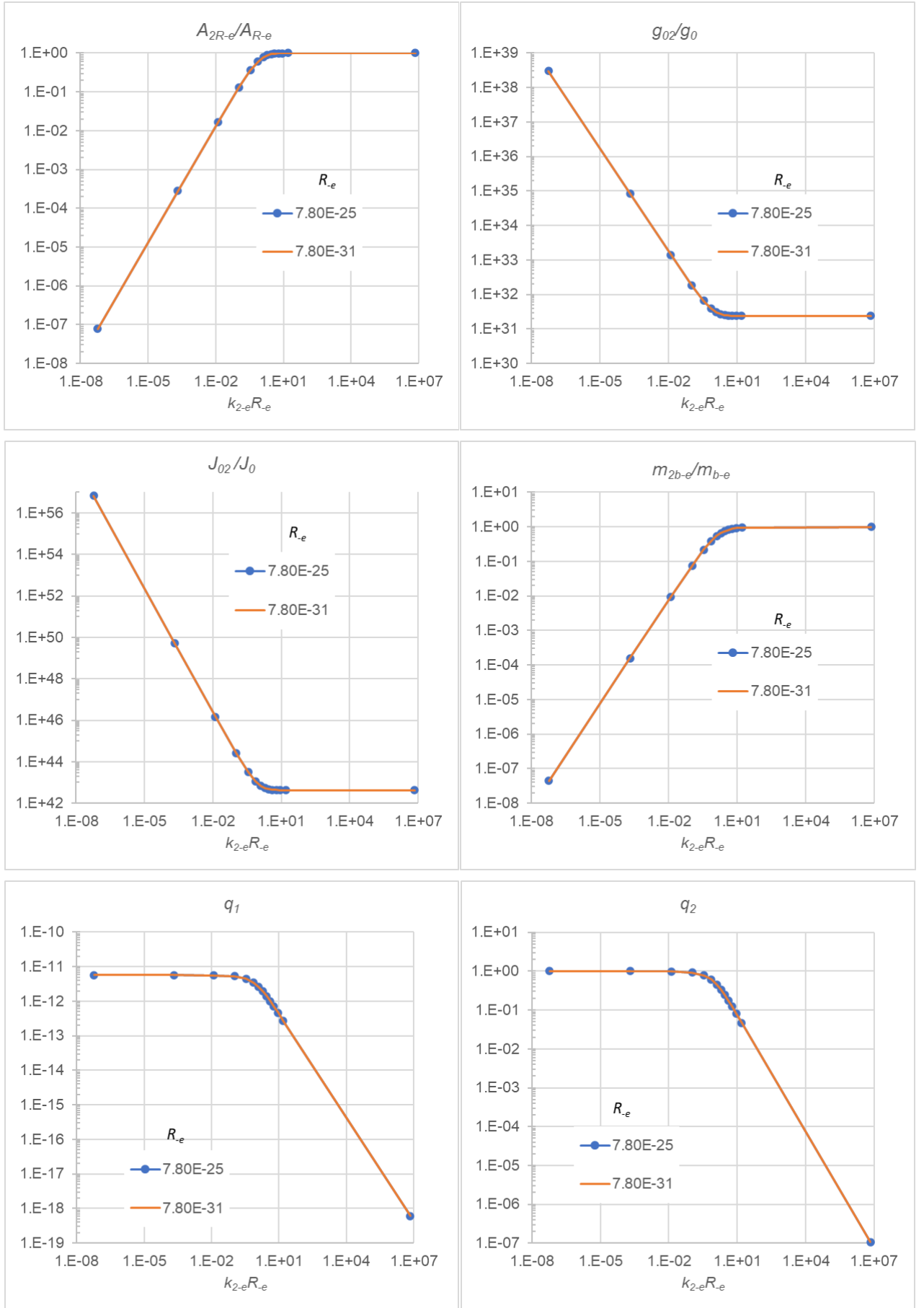


Figure 48: Ratio of corresponding constants of the electron in electricity over gravity, and contraction factors against the electrical product $k_{2-e}R_e$ for two fixed electron radii R_e .

in the early graph of Fig. 3, whereby this function varies extremely slowly at very low and at very high values of the product kR . The closer the absorptivity approaches unity the more undetectable the variation becomes. This is a fundamental property that has gone undetected in physics experiments. Thus, part of the graph $g_{02}(k_{2-e}R_{-e})$ representing the electrical mass also varies extremely slowly. We contend that this imperceptible and undetected variation of electrical mass has tricked physicists to believe that the electrical mass is an independent constant entity for which they coined the term “charge” and studied it in a separate chapter for electricity. We investigate the case of near unity absorptivities in subsequent sections in an effort to unify gravity with electricity.

21.1.4 ADDENDUM _2 (May, 2025)

In consequence of latest findings in PG theory, we have now found a possible value of $g_0 = 1.33 \times 10^{-9}$. This permits us to re-work the preceding investigation based on an unknown range of possible values for g_0 . To facilitate the reader, we have done this revision along with other important outcomes in Section 31.5.

In the preceding theory, we have arbitrarily equated the numerical value of “charge” to the electrical mass for the reasons provided. This may have raised serious objections, i.e. if we are allowed to do so between systems using different units. Even so, the preceding investigation has provided novel insights, which by-and-large make good sense for connecting gravity with electricity. It seems that we have now found a genuine equivalence conversion of units between Coulomb (for charge) and kg (for electrical mass).

This substantiates the reasons for which we have not yet revised the entire work: It would be unwise to undergo the pains of doing so every time we achieve a new development and a new understanding. We purposefully retain the original writings of this report as a useful way to help the future readers understand the thinking process behind the entire work, and possibly as a teaching method of this novel approach to physics.

21.2 Minimum emission centers (MEC)

According to the third postulate of PG theory, “gravions (or energy) absorbed are also re-emitted in a different form of particles (energy) with much shorter mean free path so as not to pertain (mediate) further to gravitational force, but likely to pertain to other types of forces or reactions”. That is, the rates of absorption and emission (decay) are equal in the steady state with a characteristic time constant, as we have also discussed in Section 15.7.1. The number-rate of absorbed gravions and the number-rate of emitted particles differ in inverse proportion to the energy of each type of push particle. They differ by many orders of magnitude as we have found for both cases of equal or unequal electron masses in the two fields. Having previously introduced the minimum absorption center (MAC), we can now introduce equivalently a minimum emission center (MEC) for and around points distributed inside any material body. That is, we can say that every “point” of a body appears “dark” with respect to gravions and “bright” with respect to emitted push particles, which we have tentatively called electrions, but may be called with any other name according to their function. At this point of development we don’t know if the nature of a MAC or the type of push particle absorbed or both determine the nature of emitted push particles. For an electron and positron, in particular, we may guess that they are type-II push particles (electrions) subject to possible revision later.

Let us concentrate on the electron and positron here. The acceleration (force) around them may be generated as follows: The sphere of Fig. 2 used for founding gravity is now considered an electron. Now, there is an excess amount of emitted electrions inside the differential solid angle subtended by O, not a depletion as applied for gravions. This will produce a repulsive force in the opposite direction. The emitted electrions ε^- will be produced along lines of sight from O with an emission coefficient k_{2-e} inside the sphere, corresponding to the gravion absorption coefficient $k \equiv k_1$. Therefore, we expect a net emission factor, or acceleration and force expressed by the same formulas as in the gravitation field. Thus the repulsive force should have the same form as the corresponding attractive force expressed by Eqs. 330 or 338 for equal or unequal electrical masses between the fields.

With the above understanding, we can adopt a similar reasoning for the positron as being the source of MECs radiating electrions ε^+ with a positive attribute. We can combine these ideas to build an electrical push model next.

By virtue of the above description, there are various possibilities about the proposed MACs and MECs. They may be equal in number and distribution, or vary to explain differences between gravity and electricity. They perform certain functions, two of which are the absorption of gravions ω and the emission of electrions ε^- or ε^+ . In building a model, we are entitled to allocate attributes in similar fashion as practiced by other theories like “flavors”, “colors”, “exclusive” principle, etc. We hope to be able to explain any introduced attributes as PG theory evolves, otherwise we simply augment the list of incomprehensible properties. The

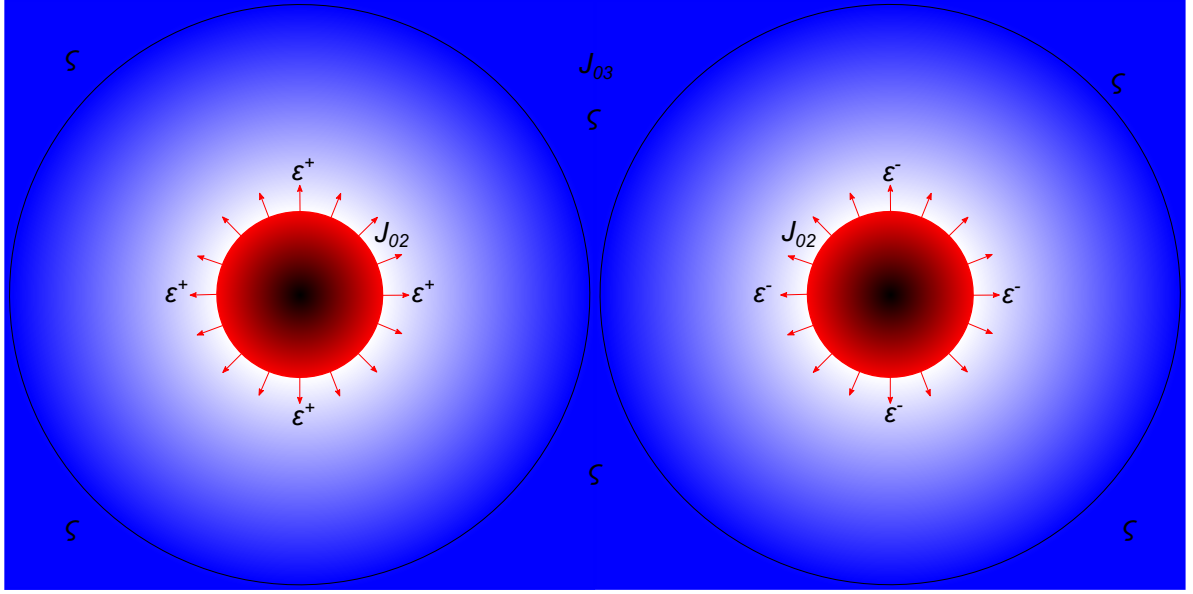


Figure 49: *Primary somion field ς (blue background) with flux density J_{03} generating secondary emitted electron field ε^+ or ε^- with flux density J_{02} at the electron and positron surface correspondingly.*

task of physics should be to make the cosmos understood by humans and not appeal to human weakness to evade the task.

21.3 Unifying gravitational and electric fields

From the numerical examples worked out for the force and other parameters for the electron, it is immediately clear that the gravion density is too weak to produce enough electrions to generate the electric force, i.e. if gravions are re-emitted as electrions. Therefore, there must be another source of push particles type-III that we call “*somions*” (ς) [see below note (*) for terminology], which after being absorbed by an electron generate the required flux density J_{02} of emitted electrions ε^- . We require that this other source has a density flux $J_{03} \geq J_{02}$ producing a maximum secondary acceleration g_{02} at the exit surface of electrons and positrons and all the other parameters that we worked with for the electric field. This rightly evokes the question about the origin and extent of the source of somions ς , i.e. if they are “locally” stagnating in the “vacuum” inside material bodies or they pervade the outer universe (“vacuum”) as well. Are they recycled locally or are they supplied continuously from outside?

Since electrons and positrons contain MECs, they are emitters of electrions and appear as “bright-gray” bodies generally, not as “dark-gray” bodies like in the case of gravity. The depth distribution of bright MECs is an open end question to determine together with nuclear force fields later as needed.

We now need to disengage the functions of the primary supply density J_{03} of somions from the secondary supply density J_{02} of electrions. To assist in this, we describe an outline of a model as follows:

Fig. 49 shows an electron and a positron surrounded by a dense medium of somion particles ς . These particles have a uniform density and move homogeneously in all directions presumably at the constant speed of light. They are characterized by a uniform flux density J_{03} . We posit that the mean free path of these particles is much smaller than atomic sizes, so that no attractive force is generated by them between electron-proton in an atom (or electron-positron in the figure) by way of absorption from J_{03} , as it happens with gravity (note that the diameters and distance in the figure are disproportionate). We further posit that push particles ε^- and ε^+ emitted from the electron and positron correspondingly have a mean free path much longer than the atomic dimensions (also the dimensions in the figure). We show this emission by red arrows emanating from the surface of the particles, where the maximum intensity J_{02} takes place. This maximum decreases with the inverse square distance law as expected by Coulomb’s law for the electric field. The latter field is not fully shown by the diagram, but we can extrapolate the red arrows emanating from the surface of each particle. The signs $+$ and $-$ designate two attributes of the emitted electrions the nature of which remains to be explained. These attributes are introduced to explain the repulsive force between two electrons or between two positrons, and an attractive force between an electron and a positron (as in proton). For convenience, we may refer to them as “positive” and “negative” electrions but without the meaning of “charge” conventionally known for the electron and positron (or proton). In consequence of

the relatively much longer mean free paths, these secondary electrions ε^+ and ε^- are thought to be much lighter (less mass/energy per particle) than the primary neutral somions ς . A positive electron striking a positron is probably reflected, and so a negative electron is probably reflected from an electron. Instead of reflection, there may be absorption and re-emission via a processing mechanism if a final model requires it. In either case, the electrions create repulsive forces between electrons or between positrons.

We proceed step-by-step in building a model. For now, we further posit that a negative electron is readily absorbed by a positron, like a positive electron is absorbed by an electron. At the point of this absorption (MAC), the previous mechanism of electron generation and emission (MEC) is neutralized and momentum is transferred from the impinging ε^+ or ε^- to the receiving electron or positron. In this way, we may also say that MECs are “annihilated” or lost, i.e. the mechanism is lost but not the incoming electrions that may re-emerge as something else in another “grouping” that is not pertaining to the process of generating the electrical force. We need to stress that the “annihilation” here is about the mechanism (or MEC) without annihilation of matter from the absorbing body or the absorbed electron. As a result of this annihilation, there will be a shortage of electrions between and across an electron and a positron.

What eventually happens to the emitted electrions, if they do not meet with an electron or positron, does not concern us here yet; it is another open end to be dealt with as needed later, but we must assume that they dissipate or drain out to a steady-state density orders of magnitude below the density of emitted electrions at close range to the nucleus. Orbital electrons are already relatively far from the nucleus and may experience a density somewhere between the maximum J_{02} and the background electron aether. We do not attempt to address several questions until we have a more complete theory about other known force fields and until we can fit the general approach of PG with specific experimental information from particle physics and other related data. Then we should be able to learn how the background density dissipates or drains out and what happens to the absorbed electrions with annihilated MECs. This is only an initial qualitative attempt towards connecting electricity with gravity pending a quantitative analysis of the model. By conjecture, we anticipate similar outcomes as from the gravitational computations in the Appendices with a difference arising from the background electron flux superimposed on the emitted electron flux. We are compelled to have or produce an explanation for the outcomes and choices of electrical parameters used in this section.

If electrions are practically reflected without prior deep absorption, then electrons and positrons should appear like white-holes in an opposite sense to black-holes. In that case, the values for J_{02} and g_{02} should be in a range corresponding to $k_{2-e}R_e > \sim \times 10$ according to Figs. 44 and 45. That is $J_{02} \sim \times 10^{68}$ and $g_{02} \sim \times 10^{35}$, for which there is practically no variation. Thus, electrons and positrons may be like black holes with respect to gravions and bright holes with respect to electrions. In that case, we may be much closer to understanding what happens physically when an electron comes sufficiently close to a positron: The adjacent surfaces coalesce, the masses merge and re-emerge as two gamma rays, and other particles. That is because a particle with an effective mass twice that of the electron (positron) cannot be sustained under PG rules. An explanation of the coalescence of electron-positron like this may help dissolve the long standing mysteries of “matter-antimatter”.

In consequence of the above description of the model, we can account of the repulsive and attractive forces as mediated by the exchange of electrions with same or opposite sign attribute. This may be a counterpart of the concept of “virtual” particles exchanged and transmitting force found in existing literature. Our model then explains known behavior of charges. However, the next key here is to explain the nature of positive and negative attribute of the emitted electrions by the electrons and positrons towards completing a unification theory. This outstanding attribute might relate to spin or revolution or another physical property, and we might be able to draw from the experimental data that have led to the Standard Model, if now the same data can be re-appraised under PG.

In drawing a parallel between Fig. 2 for establishing other force fields, we do not know at present about the depth distribution of MACs and MECs in relation to somions and electrions. They might penetrate deep enough or they may be restricted to an event-horizon-like layer. We bear this in mind when we attempt to reconcile experimental data and adapt this model accordingly.

In a macroscopic material body we expect a huge number of electrions around emitted from local sources like in Fig. 49 effectively producing a background of equal number density of ε^+ and ε^- in the “vacuum” away from the sources. As a result, we must superimpose the effect of this homogeneous background to the local picture of 49. Pending a detailed computation, we anticipate that the effect of this background on the total local force to be practically negligible. Also, whilst the ε^+ neutralize a number of MECs on an electron, an equal number is recreated continuously by somions. The same applies for a positron. An electron must be so organized internally as to always have a net amount of MECs specializing in ε^- emission and the positron in ε^+ emission. It is generally the short range interactions emanating from the immediate and near neighbors which determine the electrical force in atoms and between atoms. Now, the mean free path and

range of ε^+ and ε^- depends on the surrounding medium (nature and state of material, like permittivity), but it must be consistent with observed macroscopic electric properties. A macroscopic electric field arises from an excess of ε^+ and ε^- on/from the corresponding “charged” bodies. We cannot complete the model until we can take into account an integrated flow and inter-conversions of push particles from all available sources of various force fields around.

We need to calculate the details of distribution of ε^+ and ε^- at both the microscopic and macroscopic level to gain a new insight of the ultimate mechanisms of electricity. For example, push electricity may provide a direct explanation also of the Casimir effect on account of the inhomogeneous distribution of ε^+ and ε^- around surfaces at close range. Also push electricity should explain long range observations like discharging and atmospheric lightning.

Most importantly, we have not accounted yet why the electrical mass should be constant by equating it numerically with the charge. Like with gravitation, we should be having a variable electrical mass with distance, say, from the nucleus of the atom. We can offer the following initial explanation: The electron has an intrinsic electrical mass m_{2e-e} acquired in a region where it is free from surrounding spherical nuclei. That region is characterized by a fixed density flux of electrions, from which the intrinsic electrical mass emerges. Whilst this mass is variable with distance from another spherical mass, it is not variable with distance from a “charged” flat plane. It is known that the electric force on a charge is independent of distance from an infinite plane conductor at fixed potential. Even simpler, we know that the force in a homogeneous electric field between two parallel plane conductors is independent of location. By increasing the potential of the conductors, we increase the electrical mass of the electron, generally speaking. For determining the charge of the electron, the experimental fields applied by Millikan and Fletcher create a net excess of effective mass due to extra electron flux created by the external field only and not by changing position in the field. That is, we only vary the total flux of J_{02} . However, the magnitude of the extra applied flux is much-much smaller than the naturally prevailing electron flux by many orders of magnitude. The naturally prevailing electron flux is that around a bound or “free” electron, the magnitude of which remains to be found. Thus the variation of electrical mass is practically vanishing and undetectable during experiment. This is the reason why we have invariably found the electron charge to be constant, whereas in reality it is not, if our push electricity theory can be verified. In other words, we do expect theoretically a significant net excess of effective mass to accrue on an electron with decreasing distance from another electron with spherical geometry, but we do not expect any net excess mass to accrue on an electron with variable location in a uniform electric field. In practice (experiment), if the position of an orbital electron from the nucleus in an atom changes slightly, the surrounding electron flux variation may not be measurable either, whereby motion must be considered too. The added effect of the external field itself is practically insignificant and presumably undetectable to date. The naturally prevailing density of electrions trumps the applied fields during our charge measurements. The variation of electrical mass due to proximity with another electrical mass like the in-situ electrical mass of the electron in the atom remains an issue to investigate. This is another loose end to pick up on the way towards completing a push particle theory for all known forces.

We note reported values of the electron charge up to the 9th decimal place, which seems to be out of the expected range of charge variation vs. experimental applied electric field. Theoretically, if we could conduct measurements better than that to detect variation of the electron charge as a function of the applied field, then that would be a direct way to verify push electricity.

We should be able to independently confirm a similar theorem for the constancy of gravitational or electrical effective mass of a spherical body from an infinite plane sheet of matter (neutral or charged) using the fluxes of gravions and electrions as we did in Appendix C and E.

21.3.1 Precursor of nuclear field

The short mean free path relative to atomic sizes described above for neutral somions ς may be very long relative to nuclear sizes. In the latter case, nuclear particles would be pushed against each other, i.e. they would appear attracted to each other like with a strong force holding the nucleus together. In other words, we have a situation like with gravions but with an immensely greater flux density. Also, the weak nuclear force might not need a separate reservoir of push particles. The nature of the absorbing particles may determine the interaction with various types of push particles. Furthermore, the nuclear force arising from somions can be strong enough to overcome the repelling forces between the positive charges “residing” somewhere inside the protons. This is all a matter of the reservoir of somions having enough density to accommodate both electrical and nuclear forces by way of properly apportioning the absorptivity and emissivity of each constituent of an atom. This apportioning must be properly balanced out to preserve the real mass and energy of atoms being coupled with surrounding push particles (so far gravions, somions and electrions). The system of atoms and push particles must complete a “loop” of a continuous flow of real mass. This model will be finally complete when we can relate these push particles in closing the said loop.

Alternative to the the above suggestion (but unlikely), there is also the (theoretical) possibility that J_0 (and g_0) is far (immensely) stronger than we expect to ever be able to measure, in fact so strong as to be the primary source from which all other secondary push particles draw from, like secondaries in required in J_{02} and/or other flux densities J_{0x} with x as required. However, this possibility might extinguish our desire for a direct verification of PG, which makes it (again) imperative to organize some independent testing measurements for the gravion flux J_0 (or g_0).

Yet a simpler explanation for the presence of somions may be non other than they are gravions with the same mean free path and intensity (density) as the hypothesized somions. This idea is in accord with gravions being characterized by an appropriate distribution of density over mean free paths. In other words, the gravion density varies by orders of magnitude that corresponds to the magnitudes of force of various fields, like nuclear and electric fields. Correspondingly, the mean free paths also vary by many orders of magnitude commensurate with the range of forces of the said fields. This is further discussed in Section 33.4

[Note (*). We have determined the term “somion” like this: Since we think that the pool of push particles may be a common source for the electric and nuclear forces and since these forces create or hold the atom together and since atoms make up the everyday bodies that we experience, we want the new term to relate to embodiment. We mean something pertaining to the creation of bodies, or to the fleshing out of objects. Thus “bodions” might have been one, which could probably raise some eyebrows. Another term might be “union” since it unifies and unites particles, but it seems a too common and likely confusing word. So we decided for a more exotic name from Greek word “σώμα” for “body” and adding our suffix “-ίον” (ion), as we did for gravion and electrion. That is, “soma” + “ion” = “somion”. The symbol for somion could be sigma σ , but this has had many other uses and so we coined the variant-sigma ς . “Somation” (from known somatic) is a bit longer for economy, also “formion” in body-forming might be a bit less descriptive. Thus, somion is not more unsuitable than gluon, which would be a good choice too, if it were not already in use (unless we made it “gluion:” for consistency with “ion”). Somion implies the function of gluon but for a larger group of composite particles and atoms. If the nucleus is found to be held together by its own special push particles, we have used the term “nuclions”, but all these are in a state of revision subject to how exactly the theory evolves. A review could be due any time.]

21.4 Discussion

The oil drop experiment by Millikan and Fletcher for measuring the elementary electric charge is now perfectly understood in physical terms without the use of an exotic “charge”. The oil drop becomes stationary by the equally opposing flows of gravions and electrions imparting a total of equal impulses. The same particle, namely, the electron has two distinct masses each acted upon by different types of push particles with different strength. In a stationary steady-state situation, both gravitational and electrical masses appear to be constant, whilst possible variations have been beyond detection to date. The “constant” electron charge may not be absolutely constant after all, as now revealed by PE, but we can have a simple explanation for its constancy too. If our theory is correct, the consequences are enormous even for the structure of the atom in view of the possibility that the in-situ electrical mass is different from the constant “charge” used to date. This could influence novel theoretical modeling of the atom and quantum mechanics. However, the picture is incomplete until we formulate the magnitudes of both electrical and gravitational effective masses in motion that actually (finally) yields the known constant effective mass or “charge”. Here, we repeat the thought process on the variation of gravitational mass in a stationary or moving state per Section 16.2, as it is also further developed in following sections.

Another issue may appear to be during finding the mass-to-charge ratio (m/Q) in electrodynamics experiments, which can be performed away from a planet, i.e. believed to be independent of the influence of gravity. There, it appears that we need the use of an inertial mass of the electron resisting the action of the electric force. However, even far enough from a planet, we have the ever present gravion flux creating an effective mass, which appears to resist (presenting classical inertia) an applied force. We have said that this apparent resistance is due the gravions acting via the activated part of the real matter. Thus, we have again the action by gravitational and electric fields on the same particle with different masses emerging from the energy rate of absorption from the respective fields. Again, there would no mystery of a separate and needless entity of “charge”, had we properly understood the meaning of mass used conventionally. In other words, we could have understood the above experiments in a straightforward and natural manner without the intervention of an “equivalence principle”. If our understanding could be verified, then we would be justified by proclaiming at the outset in version 1 of our reports that this principle is redundant. In fact, it would be worse than redundant, because it may have created a lot of needless mathematical physics around it. In fact, we still need a lot of basic mathematics to further develop PG and PE in the manner we have used in Section 16. With a similar approach, we should quantify the creation and variation of electrical mass. We listed the cases that we have not addressed yet in Section 16.2 and mentioned the need to incorporate

a PE theory, an outline of which we have only started to describe qualitatively. The case of accelerating a body inside a gravitational and/or an electrical field remains incomplete. Even so, we have achieved a good understanding of the nature of both fields as we also understand that Newton’s gravitational law and Coulomb’s law are the same differing only in the type of effective mass used without the need of a distinct and cloudy entity like charge. The case of a falling “mass” in gravity corresponds to a falling “charge” in an electric field. When one of the two is driving the movement, the other is receiving the effects appearing as inter-conversion between mechanical and electrical energy. We have dealt only with a stationary steady-state situation for both fields, whilst Section 14 remains only a “stub” open for further work. In this respect, one worker alone cannot accomplish the entire task, should some readers feel that we leave many loose ends or obfuscate the problems. The groundwork of the theory should by now be sufficient to warrant participation of readers keen to solve all the ensuing issues.

Corollary: It is said that the mass-to-charge ratio (m/Q) in high energy particle accelerators remains constant and, because the charge is invariant, the mass must also be invariant and equal to the rest mass; it is then concluded that the relativistic mass increase is not an actual mass increase but only a theoretical consideration. However, we now lay bare the possibility that charge actually being also a mass may be subject to a simultaneous increase by the same factor that cancels out in the quotient. There is plenty of black mass converting to effective mass at the elementary particle level without creating new atoms. This possibility should raise an alarm about what really happens.

The reduction of all fields to push particles together with real mass in bodies provides a more tangible basis to understand and analyze in lieu of a mathematical abstraction by merely allotting a “force” to every point of a field by quantum field theory. For example, the electromagnetic potential field may have a real physical substrate rather than being mathematical concept(s) not readily comprehensible by humans. All push particles may be thought of as being a form of matter, so that we are left with finding how they relate or transform to each other through the mediation of other material bodies (e.g. electrons, positrons, neutrons protons, etc) containing also black matter in the right amount to fit experiments. The substrate of fields in PG and PE is a form of real mass (stuff) that is conserved during transformations. One such transformation is to the effective mass. Black mass is another form of real mass with probably a true “zero-ground-state” that can be excited to effective mass at different states.

Another corollary of the above description is that we may be able to explain the underlying mechanism of the classical conservation of energy (potential and kinetic) as being one of conservation of gravions together with their momentum, if for example electrions upon absorption are equivalent to the absorption of a lump of gravions.

If the advent of electrical mass in lieu of “charge” creates a sensible basis for the unification of gravity with electricity, but at the cost of the equivalence principle, then why not do it? After all, Kajari *et al.* (2010) have already forecast such a possibility by their study on “inertial and gravitational mass in quantum mechanics”.

In view of the quantitative analysis and results, we can also return to the proton and review its black mass to fit with our upgraded finding for the electron on account of the electrion field. We can envisage that the “charge” in the proton is still connected to a fractional mass corresponding to that of a positron because of the composite nature of proton. The quark model of the proton may provide one form of connection with the evolving theory here by modeling the quarks with appropriate combinations of effective and black mass. However, we must also consider alternative possibilities about the structure of the proton. In this regard, we note some recent reports by Vayenas *et al.* (2020); Vayenas & Grigoriou (2020) claiming a fundamental departure from the Standard Model. They propose a “rotating lepton model” with a three-neutrino ring around a positron. Whilst this may be at odds with other theories, it may be consistent with our findings about mass so that the idea of revolving sub-particles may be validated with appropriate modifications. For example, their model for the neutron involving three revolving neutrinos around a stationary neutrino at the center may not explain the observed neutron magnetic moment, but we might use a different combination of revolving, rotating and spinning particles to explain the neutron properties: It might involve a central binary system of a positron (or electron) with a heavy neutrino both acted upon by gravitational force at very close range, around which revolve correspondingly an electron (or positron) together with one or more light neutrinos all acted upon by gravions while the electron and positron are acted upon also by electrions. Such a system would display a neutral charge but have a magnetic moment by the orbiting charge. There may be better combinations of particles among the plethora of experimentally existing particles to improve or replace the alternative proposed combinations of particles just mentioned. Revolving and rotating/spinning systems of smaller particles at the ultra-small scales inside all known/unknown particles seems a plausible way to proceed, if we wish to move beyond the Standard Model. If it can be shown that gravions, somions and electrions are sufficient to explain all known forces, the model can be simplified greatly. Then it may be that all composite particles are made of much fewer elementary particles in one way or another, such as

Vayenas et al. propose or variant(s) of it; their model might warrant a closer examination and attention by authoritative experts. Of course, even if all this could explain the known forces, we would still be left with Kant's query of how the elementary particles themselves are held together, but we do not aspire to reach the "ultimate" end by the present theory other than having made a bold stride forward.

By the same token, another "unofficial" theory on "*a sensible model for the confinement and asymptotic freedom of quarks*" (Watkins, 2020b) and on "*estimates of the mass densities of up and down quarks and estimates of the outer radii of the small, medium and large up and down quarks*" (Watkins, 2020a) may also be considered in relation to another possible "charge" distribution inside a proton under our interpretation of charge by PG. Again, the present author is in no position to support or reject any of those claims, other than to state the need for some new understanding of hadrons. We should not reject an alternative theory only on grounds of disagreement with existing theories and principles, or by the prejudicial demand that any new theory must only constitute an extension (continuation) of and subject to existing theories. We more probably need a radical breakout before we can determine some common grounds and return with an all encompassing theory. At the moment, we can speculate various possibilities, or at best we can sideline the problem until we can think of compatible models for hadrons and other particles. We hope that a better particle model will be found under the platform of a general PG, but that work is left for the relevant scientific community to accomplish.

Furthermore, the structure of the electron and positron could be entirely remodeled based on evolving theories of toroidal vortex structures (Rankine, 1855; Kelvin, 1867; Parson, 1915; Bulgac *et al.*, 2014; Falconer, 2019) as are proposed in following sections.

It is said that hadrons feel the strong nuclear force, but leptons do not, whilst all particles feel the weak nuclear force. Now, we may think that both forces may arise from the pool of somions, if their flux density is sufficient to satisfy the production of both electric force and nuclear forces. To this end, the presence of black matter in various particles may be such as to satisfy all experimental nuclear reactions.

Our above model per Fig. 49 may be enriched or modified by incorporating any compatible aspects of other existing field theories. For example, the zero-point energy (ZPE), or zero-point radiation and ground state energy may correspond to the somion concentration, a kind of an aether. The term ZPF is in reference to quantum electrodynamics (QED) vacuum dealing with electromagnetic interactions between photons, electrons and the "vacuum", or to the quantum chromodynamics (QCD) vacuum dealing with color charge interactions between quarks, etc. A "vacuum" is viewed as the summation of all zero-point fields, the "vacuum state" in quantum field theory (QFT) with an energy density relating to the cosmological constant coefficient in the temporarily added term of the field equation of the general relativity. In this connection, we have correspondingly introduced and used the gravion flux density J_{01} and now the electrion flux density J_{02} and/or somion J_{03} . From the flux densities and Eq. 16, we may obtain a total energy density C , equivalent to the cosmological constant, as:

$$C = \frac{2J_{01}}{c} + \frac{2J_{02}}{c} + \dots + \frac{2J_{0x}}{c} = \frac{J_{0-total}}{c} \quad (345)$$

where x is the x^{th} known type of push particles. We note that our previous symbol Λ is also used in the literature to denote the "vacuum" cosmological constant, so care should be taken to avoid any confusion arising from the use of this symbol. Our Λ denotes a new "cosmic" constant (in lieu of G) being different from the above energy constant C , but both bearing a direct relationship with each other. The above ideas might assist in removing the "infinite zero-point energy and the need for re-normalization". In the event that the somion flux density provides a common source for all fields other than gravity, then the above equation would be simplified to:

$$C = \frac{2J_{01}}{c} + \frac{2J_{03}}{c} \quad (346)$$

Initially, we have no guide about the range of the somion or electrion flux density. Perhaps, we may have such a guide by previous Eqs. 224 and 225 on Schwarzschild radius and PG limiting radius. We had hoped to find an agreement once we find the maximum acceleration of other force fields. We can now try our preceding findings for the electric field. By equating the radii obtained for the Schwarzschild and PG derivation, we obtain for the required maximum acceleration g_{0max} :

$$g_{0max} = \frac{c^4}{4G_{max}M_{maxe}} \quad (347)$$

where the subscript *max* denotes the strongest force field producing an effective mass M_{maxe} and constant G_{max} , if all other fields are orders of magnitude weaker than this. Using the values for the electrion field in the case of unequal masses in the above equation, we find $g_{0max} = 1.4 \times 10^{42} \text{ ms}^{-2}$. This is the value of

J_{02} around and between the graphs for the two smaller electron radii of $\sim 10^{-22}$ and $\sim 10^{-23}$ m at around $k_2 R_{-e} \approx 10^{-7} \rightarrow 10^{-8}$ in Fig. 44. We do not expect an exact agreement between PG and GR, especially if one theory is better than the other. However, an astonishing compatibility is obtained by these values bearing in mind that we converge from totally independent derivations. In addition, we see convergence with Dehmelt (1989) and Sukhorukov (2017-2020) for the radius of the electron.

In contrast, using the case of equal masses, we get $g_{0max} = 7.97 \times 10^{30} \text{ ms}^{-2}$, which conflicts the corresponding range in Table 27. That is, we would need an unacceptably (unnatural) low value for g_0 for this value of g_{02} leading to an impossible situation. This seems to be a strong argument against the case of the gravitational mass being equal to the electrical mass.

We can obtain an interim energy cosmological constant by using the above value of $g_{02} = 1.4 \times 10^{42} \text{ ms}^{-2}$: The corresponding flux density is $J_{02} \approx \times 10^{82} \text{ Jm}^{-2}\text{s}^{-1}$, so that the cosmological energy constant may be around $C = 2J_{02}/c \approx 2 \times 10^{74} \text{ Jm}^{-3}$ ignoring the relatively much smaller contribution from the gravitational flux density of $2J_0 \approx 2 \times 10^{26} \text{ Jm}^{-2}\text{s}^{-1}$. The actual J_{02} may be finally found to be several orders of magnitude less, which means that the difference from the energy cosmological constant is used for nuclear forces, like we proposed for the somion density, i.e. $J_{03} = J_{0max}$. However, we may ask if the energy density of vacuum is the same inside and outside a material body, which may be one reason for the big discrepancies found in the literature. It may be that there is a stagnation density of energy accompanying celestial bodies that is different from the rest of the universe, or different in various regions. We have already assumed the latter variability to be the case throughout this report.

The above cross-correlation example, if proven correct, indicates that there are probably many other examples of cross-examination between PG and existing data. Then this should serve as an invitation for the broad scientific community to start transferring their information on the PG platform in the hope that they will help PG to develop but, conversely, also their information to be better explained.

Note: The above is an early account of a subject further investigated in Section 31, but compares well with new findings.

22 Action and reaction

We can now illustrate a conceptualization of the effects of gravitational and electrical fields between two macroscopic material spheres as shown in Fig. 50. The gravitational (effective) mass of the spheres is depicted with red color (top pair) and the electrical (effective) mass in blue color (middle pair). To avoid possible confusion, it should be noted that the color coding for each field here is different from that used in previous or other figures; also the density variation is not computed but it is only an indicative schematic (graphic) illustration. We have learned in Section 16 that the force arises from the loss of effective mass during the interaction of two spheres, which (loss) is depicted by yellow color (top pair). Correspondingly, we expect that an electrical force arises from the excess of effective electrical mass during interaction via same attribute electrions. While corresponding forces arise from the loss and excess of corresponding effective masses, these forces are distributed and exerted throughout the entire effective masses. We have not yet described the detailed distribution of electrical mass at the atomic level, but we may skip ahead and say that a shortening (albeit extremely small) of the distance between electrons prevails where there is compression, which means that a net excess amount of electrions is stored between atomic charges (masses) within each atom at a steady-state. This excess amount gives rise to an excess amount of electrical mass which becomes equal to the loss of gravitational mass, at equilibrium, as it is shown also in yellow color in the middle pair of spheres. The depth distribution of the electrical loss must be the same for both fields. The end result is a null force schematically depicted by the spherical distribution of red color for a restored effective mass in the bottom pair of spheres. The red color depiction is again approximate and without computation, to indicate the distribution of effective mass towards the outer surface with mass loss towards the center of the spheres shown again in yellow; the net effect is to restore the “lone” sphere distribution of effective mass.

It must be clear again that the schematic depiction above is about macroscopic bodies and not the interaction between elementary electrons. Until we find the correct quantitative relationships, the latter particles behave like a black-hole with respect to gravions and either (a) like a white hole or (b) like a bright hole with respect to electrions. The distribution of those masses would look like a very thin or thick meniscus accordingly (see gravitoids in Fig. 113) as each particle is facing the other. The magnitude of the absolute values will differ by many orders of magnitude between the two types of masses, which is not possible to depict graphically and simultaneously in the figures provided. The distribution of effective masses and their loss or excess for elementary particles can be computed accordingly but left for future work as needed.

In effect, we have explained the underlying processes during action and reaction between stationary macroscopic bodies. This involves a redistribution of the rate of absorbed push particles that is also an

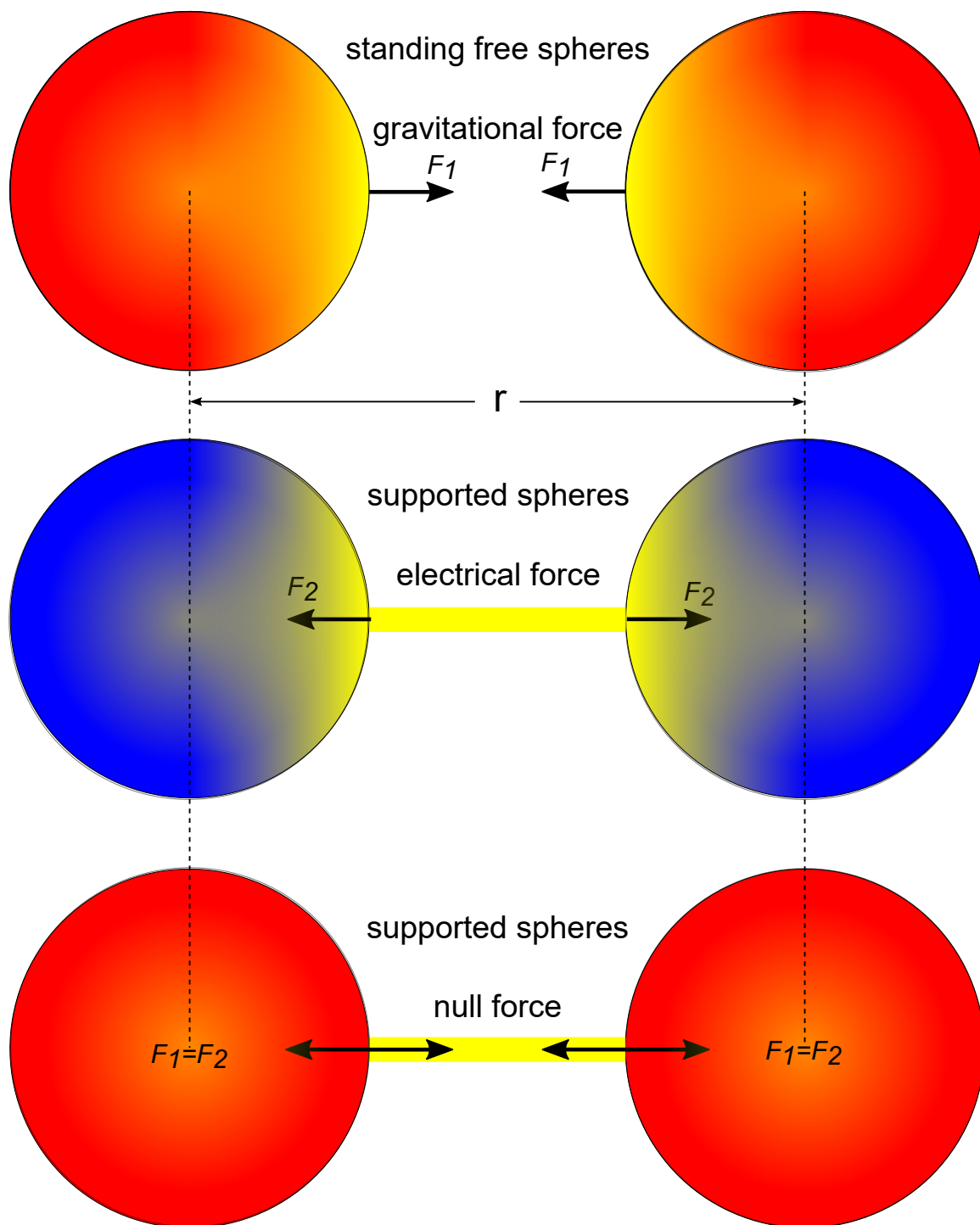


Figure 50: *Unification of gravitational and electric fields: Red represents gravitational effective mass, blue electrical effective mass and yellow the loss of effective mass being the same in both fields. The resulting gravitational F_1 and electric F_2 forces arising from the equal mass loss are also equal*

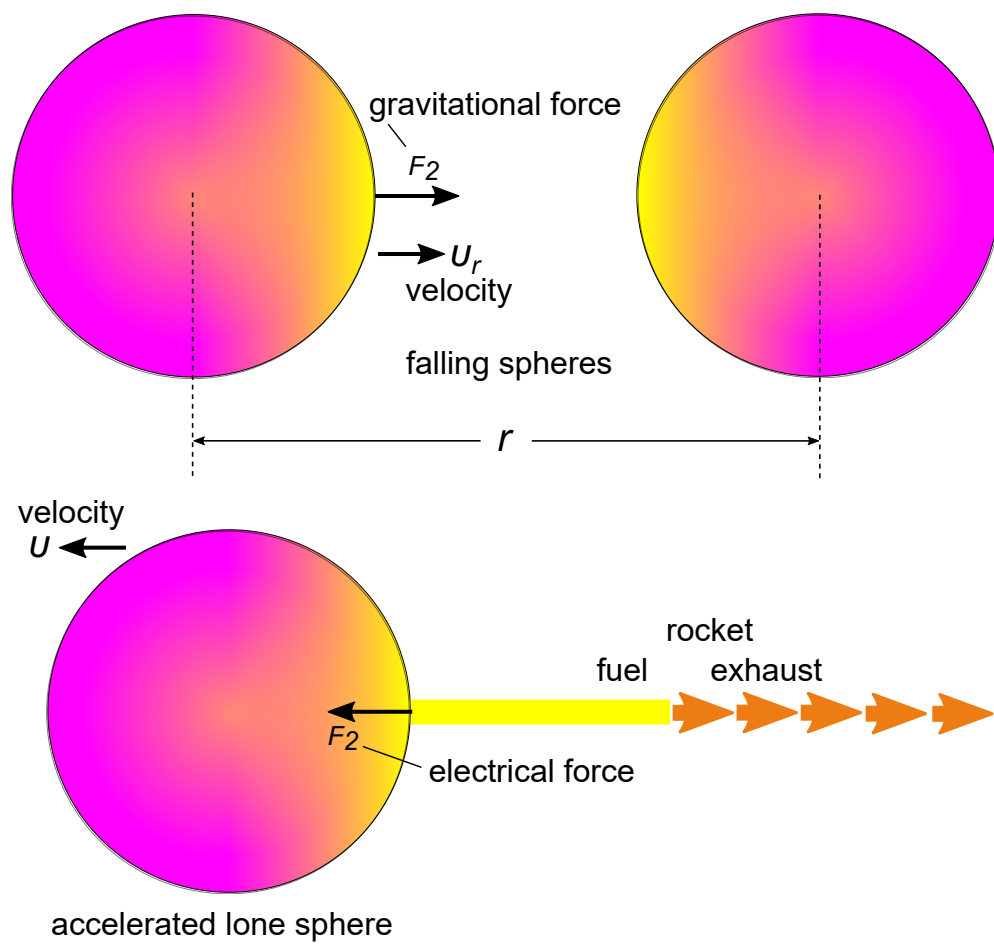


Figure 51: *Falling spheres (top) and rocket acting on sphere (bottom)*

exchange and variation of effective mass. At first, it may look like electrions are squeezed out from the rod and transferred to the sphere, but actually they are squeezed out of the sphere itself locally (at the atomic/molecular level) originating from the local pool of electrions and transferred back into the sphere to replenish the loss of gravitational effective mass due to the shadowing by the other sphere. This is reminiscing of the piezoelectric effect converting mechanical compression to electric voltage and vice-versa. In combination, the ultimate balance of masses is supplied from the pool of gravions and electrions pervading the “vacuum” within and outside material objects. This may complete, for now qualitatively, the incomplete picture anticipated in Section 16.

The above description may also serve first for a qualitative description and introduction to a proper development of a dynamic push particle theory for Section 14. This can be done by upsetting the static equilibrium of the picture in Fig. 50 in any of the following two ways:

(i) Remove one sphere leaving the rod acting on the other sphere like a rocket per Fig. 51(bottom). Then the sphere has no mass loss on account of the presence (shadowing) of the other sphere, but retains the net excess electrion rate as long as the rod acts on the sphere imparting acceleration. While the acceleration persists, the net excess of electrions accrues real mass in the form of effective and black mass. It is important that this accrual takes place inside elementary particles of the atoms not by creating new atoms; in other words, the chemistry is preserved. This continues for the duration of acceleration. When the rod (rocket) ceases to act, which is the practical situation, acceleration ceases, the body moves at constant velocity but retains an excess mass establishing a new steady-state energy exchange rate with the surrounding gravion flux. It remains to work out how exactly the new equilibrium flux is distributed around the moving sphere. There must be an equal rate of absorption of gravions at least from the back and front in the direction of velocity to avoid drag. The rate of absorption and emission around the perpendicular direction may differ, but this plane of symmetry does not affect the constant velocity. During acceleration, it is the electric field (electrions) driving the body whilst the gravion field acts as buffer in a passive manner for the balancing of energy flow consisting of push particles. Energy flows from the electrion medium to the gravion medium. We attempt to write equations for the mass accrued at constant speed below.

(ii) Remove the supporting rod between the two spheres per Fig. 51(top). Then the internal compression in each sphere will be undone and the emanating excess electrions will vanish over a very short transition time, during which masses of different types vary and redistribute themselves. The force present from the net rate of loss of gravions (= effective mass loss) will accelerate the spheres closer to each other increasing the said loss on account of proximity. We attempt to quantify the situation of falling spheres also below.

23 Mass versus speed

This is in continuation of Sections 14.7 and 16 dealing with variation of mass against distance or speed, under the understanding on developments on electricity and electron structure in preceding sections. We test and investigate a conjectural relationship between velocity and parameter kR of a moving material sphere for two distinct situations: (a) acceleration by a rocket away from (outside) other gravitational fields and (b) acceleration of a falling sphere on another under their gravitational field.

It is still undecided how to correctly handle special relativity under PG in order to start working out the dynamics of push gravity. In the interim, we have attempted a trial connection between the Lorentz contraction factor and the PG contraction factors in Section 14.7. With some further analysis and in view of the findings on mass composition of the electron (positron), we can obtain a new insight of this attempt. We use again the conjectures for connecting speed v to absorptivity A_R . A close agreement was obtained with one hypothesis by setting:

$$\frac{v^2}{c^2} = A_R = 1 - \frac{1}{2k^2 R^2} + \frac{\exp(-2kR) \cdot (2kR + 1)}{2k^2 R^2} \quad (348)$$

The above conjecture is arbitrary and can be replaced by another form as suggested previously. The simplest variation is to apply a power form of the above equation, like:

$$\left(\frac{v}{c}\right)^n = A_R \quad (349)$$

where n may be chosen in a way to yield outcomes consistent with experiment. We will discuss this possibility afterwards.

In the following, we first use the above Eq. 348 to help us draw some important conclusions, which may not differ if we use or find other relationships later, including some not yet proposed; it is worthwhile to ponder on the outcomes of the following investigation. The work of these sections here is undertaken under the provisos set at the outset of Part 2, that is, they have an exploratory purpose and by no means bound the groundwork of Part 1.

23.1 Rocket acceleration

First, we compare the ratio of *relativistic mass* m_{rel} over the *rest mass* m_0 used by $\gamma = m_{rel}/m_0$ simultaneously with the PG ratio of *real mass* over *effective mass* given by $1/q = m/m_e$. We actually repeat the findings of Fig. 21 by now explicitly plotting the ratio of masses from the two theories, because we will continue to use various types of masses in continuation to these plots. The results are given in Fig. 52(a) in the same range of kR as before for the three cases, namely, of a “sphere”, “line” and “Lorentz” (left ordinate axis), where we also plot the corresponding speed fraction v/c on the secondary axis (right ordinate axis). The same three cases are re-plotted against the more familiar variable of speed fraction v/c in (b). As expected, we repeat the close agreement between $1/q$ and γ factor for the “sphere”. If our relational conjecture is correct, then this is an important outcome beyond just a good or fortuitous agreement, as found below.

We note in Fig. 52(b) that the speed ratio v/c starts from a non-zero value, because we arbitrarily started with a non-zero value of kR . This is a consequence of the applied Eq. 348 stating that only at the limit of zero kR would we have a non-moving body. This means that the absorption coefficient k (or absorptivity A_R) is practically zero at zero velocity. The latter condition may have only theoretical meaning or importance, because we must actually start with some finite value of absorptivity, i.e., A_R is non-zero before the sphere starts moving. In this case, Eq. 348 yields a speed-like quantity for a stationary body, which we may call *intrinsic speed* v_0

$$v_0 = c\sqrt{A_R} \quad (350)$$

This appears to be a misnomer for a non-moving body in the absolute reference frame of the gravion medium, but we introduce it for uniformity of terms in the ensuing formulation. At any rate, this speed corresponds to an initial (starting) value $(kR)_0$, or k_0R for a fixed sphere radius R , as given by:

$$\frac{v_0^2}{c^2} = A_R = 1 - \frac{1}{2k_0^2 R^2} + \frac{\exp(-2k_0 R) \cdot (2k_0 R + 1)}{2k_0^2 R^2} \quad (351)$$

Noted that we want to retain the notation A_R instead of a would be more appropriate A_{R0} for what should now be called the *intrinsic absorptivity*, because we prefer to avoid changing the notation in all of the preceding work; it is exactly what we have used and meant under the static regime of our theory. As we move in a range $kR > k_0R$, absorptivity increases monotonically to values which we designate by $A_{Rc} > A_R$, where the subscript c ($_c$) refers to “*composite*”, as in composite absorptivity pertaining to combined (integrated) intrinsic and kinetic (moving) components of absorptivity. The term “composite” means the same as the term “current” (like *current effective mass*) in previous discussion of Section 16.1, but “composite” now ensures the presence of actual speed. From the absorptivity, we aim to derive the corresponding types of mass like real, effective, black and now kinetic and composite masses being simply proportional to types of absorptivity by the ubiquitous equation:

$$M_e = \frac{g_0 R^2}{G} A_R \quad (352)$$

Because the masses are additive quantities, so are the absorptivities. Therefore, the *composite absorptivity* A_{Rc} in the range $k_c R > k_0 R$ is the sum of the intrinsic absorptivity plus a component of absorptivity arising from the actual speed v of the moving body. Let us call the latter component as the *kinetic absorptivity* $A_{R\kappa}$, so that we have :

$$A_{Rc} = A_R + A_{R\kappa} \quad (353)$$

Then we obtain the *composite speed* v_c from the relationship:

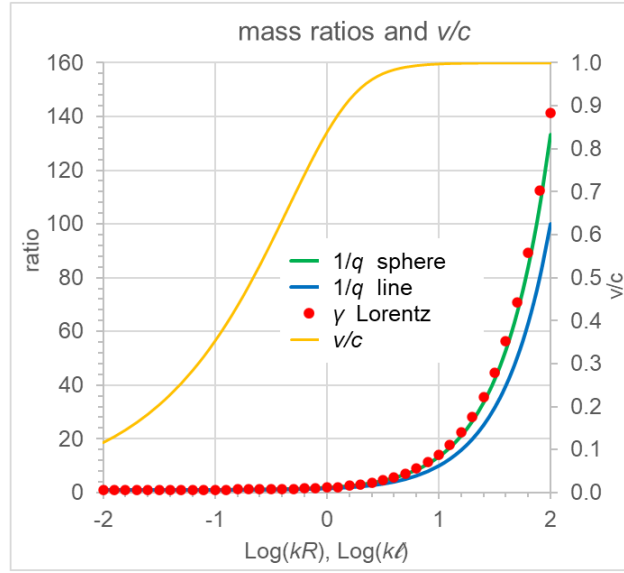
$$\frac{v_c^2}{c^2} = \frac{v_0^2}{c^2} + \frac{v^2}{c^2} \quad \text{or} \quad v_c^2 = v_0^2 + v^2 \quad (354)$$

where we reserve the notation v without subscript for the actual speed to be consistent with convention. The corresponding absorptivities then are given explicitly by:

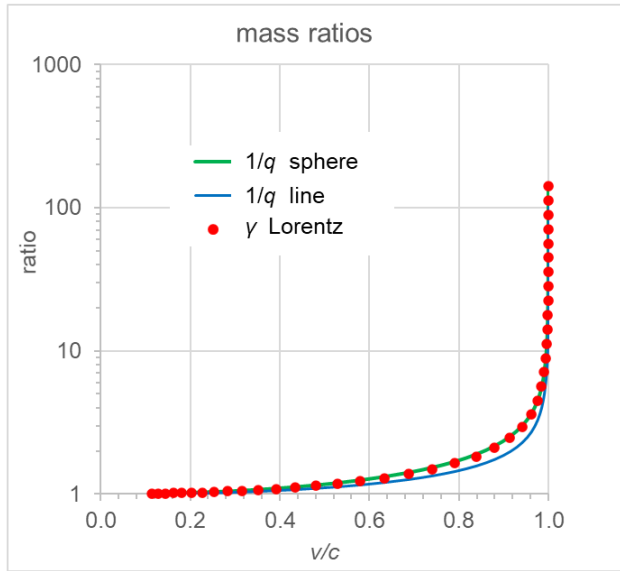
$$\frac{v_c^2}{c^2} = A_{Rc} = 1 - \frac{1}{2k_c^2 R^2} + \frac{\exp(-2k_c R) \cdot (2k_c R + 1)}{2k_c^2 R^2} \quad (355)$$

$$\frac{v^2}{c^2} = A_{R\kappa} = 1 - \frac{1}{2k_\kappa^2 R^2} + \frac{\exp(-2k_\kappa R) \cdot (2k_\kappa R + 1)}{2k_\kappa^2 R^2} \quad (356)$$

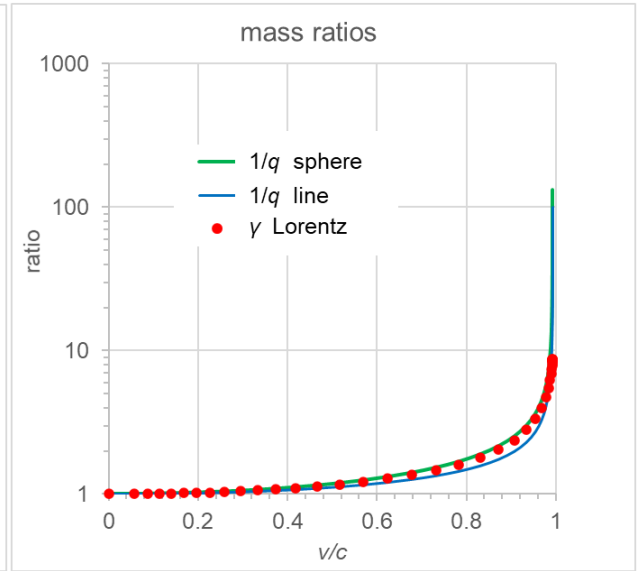
Among the three types of speed introduced above, only v is the real one, while the other two (v_0 and v_c) have theoretical significance (initially) in the formulation derived. However, the composite absorptivity A_{Rc}



a



b



c

Figure 52: (a) Mass ratios and speed against kR , (b and c) mass ratios against speed.

may be viewed as the absorptivity in the reference frame of the moving body, like the intrinsic absorptivity is with reference to the stationary frame of the gravion medium.

As a result, we adjust the graphs on contraction factors against actual speed using:

$$A_{R\kappa} = A_{Rc} - A_R \quad (357)$$

We substitute velocities for absorptivities per above to obtain:

$$\frac{v^2}{c^2} = 1 - \frac{1}{2k_c^2 R^2} + \frac{\exp(-2k_c R) \cdot (2k_c R + 1)}{2k_c^2 R^2} - A_R \quad (358)$$

As demonstration, we use again the starting (arbitrary) value $k_0 R = 0.01$ to establish an intrinsic A_R at $v/c = 0$ and plot the same mass ratios against speed (v/c) for $kR \equiv k_c R > k_0 R$ in Fig. 52(c). It should be noted that the deviation between GR and PG, (γ and $1/q$) now becomes greater towards high speeds. This deviation decreases if we start at smaller starting values of $k_0 R$ instead of the arbitrarily chosen 0.01. Smaller $k_0 R$ implies operation closer to Newtonian regime. Higher $k_0 R$ means starting to move a denser body, which has a higher intrinsic velocity v_0 . As a result, GR using the lesser actual speed v yields a lesser value for γ than PG using a corresponding higher composite speed v_c yields a higher value for $1/q$. Now, if one of the two theories is correct, the other should be wrong. We think that GR has not been verified at very high speed with v/c very close to unity for macroscopic bodies, while with small particles the existence of real and black mass has not been taken into account. Therefore, we may not dismiss PG being the correct one. In the latter case, we anticipate much higher real mass than a corresponding relativistic mass (theoretical or real), the significance of which can be thrown into question.

We can readily find the corresponding contraction factors, effective masses and real masses from previous known equations. We only need to qualify these new quantities as being *intrinsic*, *kinetic* or *composite* accordingly. Thus we use the notations m , m_κ and m_c for the real masses, m_e , $m_{e\kappa}$ and m_{ec} for the effective masses, m_b , $m_{b\kappa}$ and m_{bc} for the black masses and q , q_κ , q_c for the contraction factors and so on for other variables.

To avoid possible ambiguity, we summarize the old and new notations and symbols of the variation of mass of a moving sphere in Fig. 53: This is for a sphere with radius $R = 1$ m, for which we set (arbitrarily) $k_0 R = 0.01$ and $g_0 = 1000 \text{ ms}^{-2}$. The latter values determine the intrinsic (lone and stationary) effective mass m_e at the start of the abscissa. We note that it is already a very massive body at this value of kR (left point). From Eq. 352, we find and plot the new effective mass in motion m_{ec} that we termed “composite effective mass” and is the sum of masses corresponding to Eq. 353:

$$m_{ec} = m_e + m_{e\kappa} \quad (359)$$

where $m_{e\kappa}$ is the kinetic mass. The real mass in motion m_c (composite real mass) is found from the effective mass divided by the contraction factor to be:

$$m_c = \frac{4g_0 R^2}{3G} k_c R \quad (360)$$

which is the straight line graph in 53(a). It must be noted that $m > m_e$ at the starting point of $k_0 R$, but the difference is not visible on the graphs. The difference $m_{bc} = m_c - m_{ec}$ is the *composite black mass*. For good measure, we plot the same masses against the corresponding real velocity in the same figure on the right (b), where we also add the relativistic mass. We note the significant disagreement of the latter with the real and effective masses, where the m_{rel} lies consistently below the PG masses. The disagreement is due to the choice of this unusually dense sphere, which has a large intrinsic “velocity”. If we chose an ordinary density sphere, the disagreement would be exceedingly small as the reader can easily verify (e.g. use a steel sphere with $\rho_e = 7500 \text{ kgm}^{-3}$ and $R = 1$ m characterized by $k_0 = 1.57 \times 10^{-9} \text{ m}^{-1}$ at $g_0 = 1000 \text{ ms}^{-2}$, or $k_0 R = 3.15 \times 10^{-11}$ with a more likely $g_0 = 50000 \text{ ms}^{-2}$). It is this difference (small or big), which we find that GR may have missed. Hopefully, we have correctly accounted for this miss now. [Note: The apparent much better agreement in Fig. 52 is because we use the mass ratios, not the absolute values of masses].

We have examined the situation of a continuous application of force (acceleration), but we need also to consider what happens at cessation of acceleration. There must be initially an “instantaneous”, actually extremely short duration, transition of some internal re-adjustment of masses followed by a new steady state situation of the body moving at constant speed. This transition is needed to restore the effects of “deformation” of the internal electric field that took place at the outset of application of force, but the cumulative effects accruing in the entire acceleration period must remain intact after this transition under a new steady-state rate of gravion absorption and emission. These matters are pending examination in conjunction with and after investigation of a falling body and then of possible internal structure of matter at the fundamental level in following work.

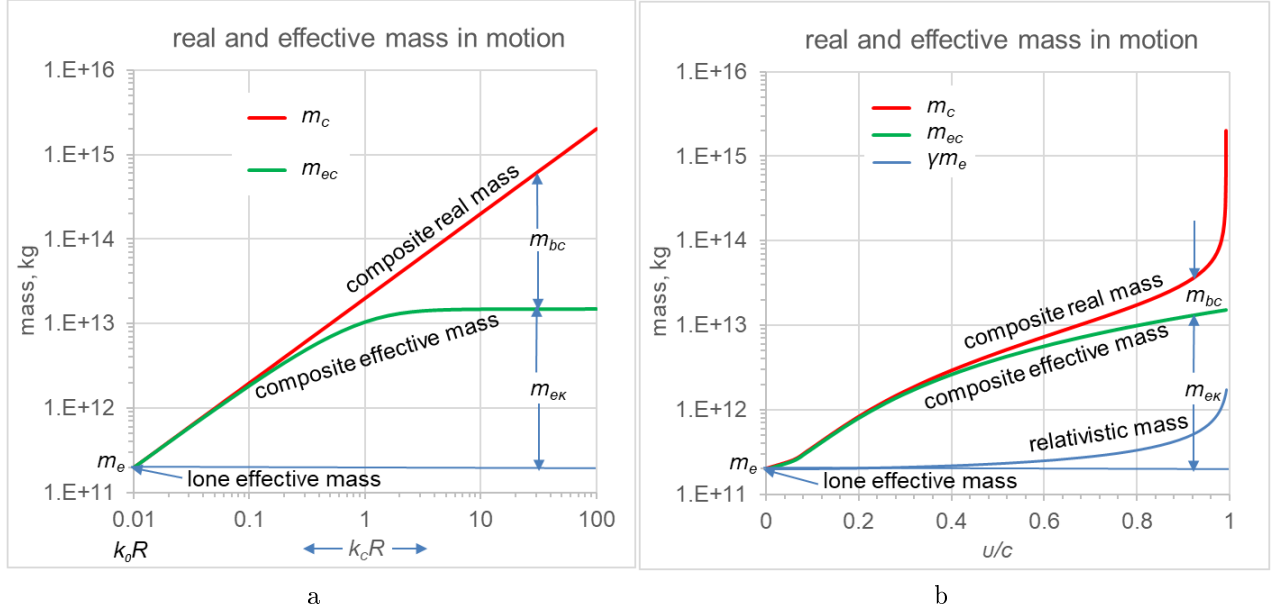


Figure 53: Composite real mass m_c and composite effective mass m_{ec} of a moving material sphere starting with an intrinsic effective mass m_e at $v/c=0$ are plotted against kR in (a) and against v/c in (b), based on Eq. 348; the relativistic mass is added for comparison.

Note: Compare Eq. 354 with relativity equation $E^2 = (m_0^2 c^2 + p^2) c^2$ or

$$\left(\frac{E}{c^2}\right)^2 = m_0 + \frac{p^2}{c^2} \quad (361)$$

which corresponds to Eq. 359 relating composite_effective, effective and kinetic masses. The difference between the two theories lies in the understanding that the effective mass per PG corresponds to the “rest” mass per SR, but they are not the same. Our effective mass varies with speed, which added to the kinetic mass yields the total (composite) effective mass. It is said that “relativistic mass corresponds to the total energy” which we could relate to the composite mass here.

Further, we can briefly see what the effect is on the mass-speed relationship, if we use Eq. 349 in the case of $n = 1$, or $n = 4$ (we already investigated the case with $n = 2$) below. That is, we if we use the alternative conjecture of:

$$\frac{v}{c} = A_R \quad (362)$$

or

$$\left(\frac{v}{c}\right)^4 = A_R \quad (363)$$

We plot the alternative mass-speed relationships in Fig. 54a for $n = 1$. We can see by comparison with the previous Fig. 53b that the accrued kinetic mass is now greater for any given speed. The opposite effect is if we use $n = 4$, the quantitative relationship for which is plotted in Fig. 54b. Hence, it is possible to adjust the accrued mass as needed in later theoretical formulations. In the latter case, it looks like the effective mass is much closer to the relativistic mass up to considerable speed of $v/c \approx 0.2$; could that mean that this is sufficient agreement, if relativistic mass has not been experimentally verified with sufficient accuracy above this speed? Otherwise, could we adjust the conjecture to achieve the experimentally required accuracy? Interestingly, both effective and real mass move closer together up to around $v/c \approx 0.8$, meaning that the black mass accrued is not great, but becomes so as we approach very close to the speed of gravions.

Introducing again a distinction between intrinsic, kinetic and composite absorptivities, we sum them by Eq. 353 in the form of speeds by the above alternative conjectures to obtain correspondingly:

$$\frac{v_c}{c} = \frac{v_0}{c} + \frac{v}{c} \quad (364)$$

or

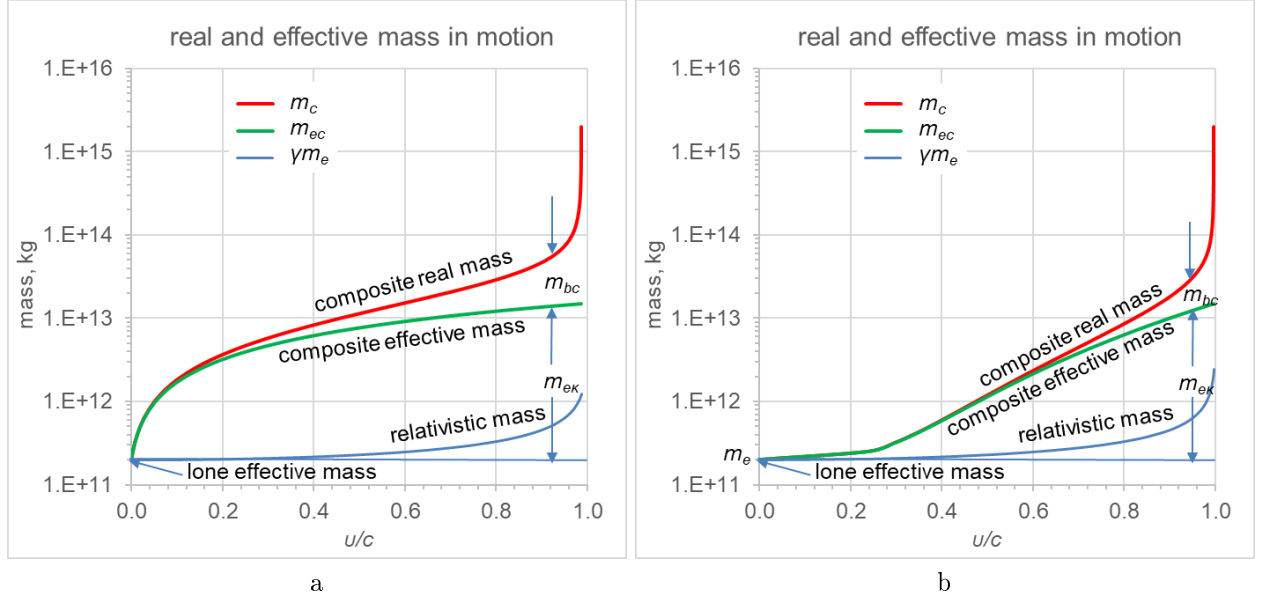


Figure 54: *Composite real mass m_c and composite effective mass m_{ec} of a moving material sphere starting with an intrinsic effective mass m_e at $v/c=0$ are plotted against v/c , for alternative conjectures (a) with power of $n = 1$ and (b) with power of $n = 4$; the relativistic mass is added for comparison.*

$$\left(\frac{v_c}{c}\right)^4 = \left(\frac{v_0}{c}\right)^4 + \left(\frac{v}{c}\right)^4 \quad (365)$$

The issue of speed-mass relationship is taken up again in Section 23.2.2.

Alternatively, we might want to force an equation between our contraction factor q and Lorentz factor L $q = L$ as proposed by Eq. 184, to but not carried through yet. From that equation, we derive the relationship between speed and absorptivity (connected to mass) for sphere and line, as we did in Section 14.7:

$$\frac{v^2}{c^2} = 1 - q^2 \quad (366)$$

Sphere

$$\frac{v^2}{c^2} = 1 - \left(\frac{3A_{R\kappa}}{4k_\kappa R}\right)^2 \quad (367)$$

$$\frac{v_0^2}{c^2} = 1 - \left(\frac{3A_R}{4kR}\right)^2 \quad (368)$$

$$\frac{v_c^2}{c^2} = 1 - \left(\frac{3A_{Rc}}{4k_c R}\right)^2 \quad (369)$$

We have done the calculations and plotted the results for this case too. However, the graphs are very close to those presented in Fig. 53; we can only a small numerical shift on the corresponding speed axis for the relativistic mass. This outcome is expected on account of the very close graphs for the two factors seen in Fig. 21. The reader may like to repeat our computation steps as follows:

We set an initial value of $k_0 R = 0.009999999999 \approx 0.01$ and find A_R . Then for any subsequent $k_c R$ we have the A_{Rc} yielding the kinetic absorptivity from:

$$A_{R\kappa} = A_{Rc} - A_R \quad (370)$$

which we solve for $k_\kappa R$, namely, the equation:

$$1 - \frac{1}{2k_\kappa^2 R^2} + \frac{\exp(-2k_\kappa R) \cdot (2k_\kappa R + 1)}{2k_\kappa^2 R^2} - (A_{Rc} - A_R) = 0$$

Finally, the speed ratio is given by:

$$\frac{v}{c} = \sqrt{1 - \left[\frac{3(A_{Rc} - A_R)}{4(k_\kappa R)} \right]^2}$$

The initial value of $k_0 R$ was chosen very close (not equal) to 0.01 to avoid a singularity in solving the above equation at this point $k_0 R$ and then increased the step by the factor of $10^{0.1}$ up to $k_\kappa R = 100$ spanning the typical 4 orders of magnitude variation.

If we wish to apply the “line” contraction factor, we may proceed like:

Line

$$\frac{v^2}{c^2} = 1 - \left(\frac{A_\ell}{k\ell} \right)^2 = 1 - \left(\frac{1 - \exp(-k\ell)}{k\ell} \right)^2 \quad (371)$$

where the contraction of material line q_ℓ is given by Eq. 51 and the line-absorptivity $A_\ell = 1 - \exp(-k\ell)$ was defined in Eq. 182.

We can retrace our steps in the entire Section 23 for both rocket acceleration and falling acceleration using the above speed-absorptivity equations.

23.2 Falling body acceleration

We further apply the above formulations in the special case of two spheres falling to each other. However, we already found that this is a different situation, so that we must adapt the previous derivations properly. One difference is that with a rocket acceleration we have the action of an electric field from the “outside”, whereas in the case of a falling body we have action of the gravitational field within itself. There is no outside accretion of mass (by an “external” agent like a rocket), only a variation of the existing falling mass(es) by gravity. We have seen this in Section 16, where the distance between gravitating spheres is an additional parameter to be incorporated in our derivations of motion. Those simple findings are enough to see that “falling body acceleration” is different from the “rocket acceleration”. We simply cannot assume any equivalence, as will also become more evident below. Now, we need to introduce the additional parameter of distance r and incorporate it as an additional subscript ($_r$) accordingly.

It is instructive to continue on from the three cases worked out in Section 16 for static pairs of material spheres. We start with CASE_1 involving the Earth and Moon. We calculate the components of effective mass for the Moon falling to Earth. We previously found the effective mass of a stationary and unsupported Moon at various distances. However, the effective mass of a falling Moon is increased by the kinetic mass component over and above the static one. Therefore, we must distinguish the effective masses in previous Tables 12 and 13 by denoting them as m_{er} for *static effective mass at distance r* . As explained previously, “static” means that the sphere is stationary at distance r but without any supporting means. If the sphere is moving at r in consequence of prior falling, then we use m_{erc} for the *composite (current) effective mass at distance r* . For the lone (very far away) effective masses of the Moon and Earth we maintain the same subscripts in m_e and M_e correspondingly for the masses but now with lower and upper case letters in lieu of numerals (1 and 2); we use one plain upper case R for the radius of the “smaller” sphere falling towards the “larger” sphere in the three cases (we do not examine the falling of the “larger” sphere to the “smaller” one at present). Now, the static effective mass plays the role of an intrinsic mass at each distance, if we apply the same preceding formulation for the composite effective mass used in rocket acceleration; the rocket force is replaced by the force of the impulse of the graviton difference rate of absorption along the line of fall.

We found that Newton’s gravitational law is applicable provided we use the intrinsic (lone) masses in calculating the force vs. distance. Then, regarding the potential energy, we can use:

$$E_{potential} = \int_{\infty}^r F dr = \int_{\infty}^r G \frac{M_e m_e}{r^2} dr = G \frac{M_e m_e}{r} \quad (372)$$

which is equally shared by the two bodies. However, the speed obtained from the corresponding equivalent kinetic energy (by the action of the same force) depends on the behavior of mass during fall. If we arbitrarily use a constant mass m_e as in the classical derivation of the kinetic energy of the system:

$$E_{kinetic} = \int_{\infty}^r F dr = 2 \int_{\infty}^r \frac{dp}{dt} dr = 2 \int_{\infty}^r \frac{d(m_e v_r)}{dt} dr = 2m_e \int_{\infty}^r \frac{dv_r}{dt} v_r dt = m_e v_r^2 \quad (373)$$

r , m	m_{er} , kg	m_{erloss} , kg	m_{rc} , kg	$m_{er\kappa}$, kg	m_{br} , kg	m_r , kg
12742000	7.342882E+22	4.7876E+19	7.34960070E+22	1.57E+16	6.7167536E+19	7.34959912E+22
25484000	7.346527E+22	1.1431E+19	7.35325113E+22	7.87E+15	6.7234253E+19	7.35325034E+22
50968000	7.347387E+22	2.8281E+18	7.35411257E+22	3.93E+15	6.7250002E+19	7.35411217E+22
101936000	7.347599E+22	7.0524E+17	7.35432505E+22	1.97E+15	6.7253887E+19	7.35432486E+22
203872000	7.347652E+22	1.7620E+17	7.35437796E+22	9.83E+14	6.7254854E+19	7.35437786E+22
407744000	7.347666E+22	4.4043E+16	7.35439115E+22	4.92E+14	6.7255095E+19	7.35439110E+22
815488000	7.347669E+22	1.1010E+16	7.35439444E+22	2.46E+14	6.7255155E+19	7.35439441E+22
∞	7.347670E+22	0	7.35439552E+22	0	6.7255175E+19	7.35439552E+22

Table 28: *Dependence of various types of mass on distance of the Moon from Earth per prior CASE_1.*

the resulting speed refers only to this constant mass. which is not consistent with a variable mass m_{er} vs. distance found previously in PG. Use of the above Newtonian speed to generate the kinetic mass ($m_{e\kappa}$) by a presumed conjecture in Eq. 348 would be incorrect at least in principle. Nevertheless, we can establish procedures and relationships below, which do not affect the analysis, discussion and conclusions, other than some second order of magnitude numerical differences. After all, if PG speed is different from Newton, the difference has not been possible to measure to date. Contingent upon this clarification, we may use Newtonian mechanics to derive the corresponding speed at distance r for the Moon (to start with) by:

$$v_r^2 = G \frac{M_e}{r} \quad (374)$$

From the above, we obtain the absorptivity $A_{Rr\kappa}$ at this distance by

$$A_{Rr\kappa} = \frac{v_r^2}{c^2} = G \frac{M_e}{c^2 r} \quad (375)$$

Then the kinetic mass component of the composite effective mass at the same distance is

$$m_{er\kappa} = \frac{g_0 R^2}{G} A_{Rr\kappa} = \frac{g_0 R^2}{G} \frac{v_r^2}{c^2} = \frac{g_0 R^2}{c^2 r} M_e \quad (376)$$

The total or composite effective mass at distance r is

$$m_{erc} = m_{er} + m_{er\kappa} \quad (377)$$

The corresponding absorptivities are

$$A_{Rrc} = A_{Rr} + A_{Rr\kappa} \quad (378)$$

By substitution, the above equation becomes:

$$1 - \frac{1}{2k_{rc}^2 R^2} + \frac{\exp(-2k_{rc}R) \cdot (2k_{rc}R + 1)}{2k_{rc}^2 R^2} = G \frac{m_{er}}{g_0 R^2} + G \frac{M_e}{c^2 r} \quad (379)$$

which we solve for $k_{rc}R$ and then obtain the composite contraction factor q_{rc} at this distance. From the composite effective mass we also obtain the real mass m_r at each distance. The results are provided in Table 28, where we have transferred the masses m_{er} and m_{erloss} along with the same distances from Table 13. Subject to the above clarification on mass variation, we repeat the same procedure for CASE_2 and CASE_3 in compiling Tables 29 and 30. We include these tables to show any small numerical differences and variations where they occur, which are not visible in subsequent graphical form.

It is necessary to point out that the “kinetic” type of PG mass introduced above is not the same with another “kinetic mass” that we could theoretically derive from the Newtonian kinetic or potential energy of two mutually falling spherical bodies given by

$$E_{potential} = G \frac{m_e M_e}{r} = m_e v_r^2 = E_{kinetic} \quad (380)$$

We understand that orthodox (conventional) physics may not accept us to think that the above energy is convertible to mass, i.e. something outside the conventional or Newtonian intrinsic (rest) mass. However,

r , m	m_{er} , kg	m_{erloss} , kg	m_{rc} , kg	$m_{er\kappa}$, kg	m_{br} , kg	m_r , kg
6371002.0	7.9414E+14	6.8921E+14	1.193639E+15	1.05E+10	3.99492E+14	1.193614E+15
6371063.7	7.9448E+14	6.8887E+14	1.194452E+15	1.05E+10	3.99964E+14	1.194427E+15
6371637.1	7.9657E+14	6.8678E+14	1.199452E+15	1.05E+10	4.02869E+14	1.199427E+15
6377371.0	8.0869E+14	6.7466E+14	1.228731E+15	1.05E+10	4.20028E+14	1.228705E+15
6434710.0	8.6487E+14	6.1848E+14	1.372847E+15	1.04E+10	5.07967E+14	1.372819E+15
7008100.0	1.0576E+15	4.2575E+14	2.015524E+15	9.56E+09	9.57913E+14	2.015484E+15
7645200.0	1.1562E+15	3.2718E+14	2.494737E+15	8.76E+09	1.33856E+15	2.494687E+15
8919400.0	1.2634E+15	2.1995E+14	3.264946E+15	7.51E+09	2.00153E+15	3.264877E+15
9556500.0	1.2967E+15	1.8668E+14	3.601683E+15	7.01E+09	2.30500E+15	3.601604E+15
12742000.0	1.3851E+15	9.8300E+13	5.036353E+15	5.26E+09	3.65130E+15	5.036225E+15
25484000.0	1.4600E+15	2.3312E+13	8.830150E+15	2.63E+09	7.37011E+15	8.829845E+15
50968000.0	1.4776E+15	5.7588E+12	1.200624E+16	1.31E+09	1.05286E+16	1.200586E+16
101936000.0	1.4819E+15	1.4355E+12	1.349491E+16	6.57E+08	1.20130E+16	1.349464E+16
203872000.0	1.4830E+15	3.5861E+11	1.396041E+16	3.29E+08	1.24774E+16	1.396026E+16
407744000.0	1.4833E+15	8.9637E+10	1.408436E+16	1.64E+08	1.26011E+16	1.408428E+16
815488000.0	1.4833E+15	2.2408E+10	1.411584E+16	8.21E+07	1.26325E+16	1.411580E+16
∞	1.4834E+15	0	1.412635E+16	0	1.26430E+16	1.412635E+16

Table 29: *Dependence of various types of mass on distance of the small dense sphere from the large dense sphere per prior CASE_2.*

r , m	m_{er} , kg	m_{erloss} , kg	m_{rc} , kg	m_{erk} , kg	m_{br} , kg	m_r , kg
12742000	1.384834E+27	9.8516E+25	5.03111536E+27	5.26E+21	3.64628E+27	5.03098791E+27
25484000	1.460029E+27	2.3322E+25	8.82903258E+27	2.63E+21	7.36900E+27	8.82872789E+27
50968000	1.477591E+27	5.7593E+24	1.20060756E+28	1.31E+21	1.05285E+28	1.20056950E+28
101936000	1.481915E+27	1.4355E+24	1.34948947E+28	6.57E+20	1.20130E+28	1.34946246E+28
203872000	1.482992E+27	3.5861E+23	1.39604103E+28	3.29E+20	1.24774E+28	1.39602608E+28
407744000	1.483261E+27	8.9637E+22	1.40843570E+28	1.64E+20	1.26011E+28	1.40842803E+28
815488000	1.483328E+27	2.2408E+22	1.41158362E+28	8.21E+19	1.26325E+28	1.41157976E+28
∞	1.483351E+27	0	1.41263499E+28	0	1.26430E+28	1.41263499E+28

Table 30: *Dependence of various types of mass on distance of the smaller dense from larger dense sphere per prior CASE_3.*

since we have already moved away from this restriction, it would be arbitrary to avoid juxtaposing and cross-examining this quantity (actual or not) vis-à-vis with all other types of mass already introduced in our theory. This quantity can be tested together with the ubiquitous equation $E = mc^2$ used for our conversion, i.e. by dividing the above potential (or kinetic) energy by c^2 as:

$$m_{potential-at-r} \equiv m_{pr} = \frac{m_e v_r^2}{c^2} = G \frac{m_e M_e}{rc^2} \quad (381)$$

where we prefer the subscript “p” ($_p$) to avoid confusion with the subscript “ κ ” ($_{\kappa}$) already allotted to the PG kinetic mass. Then the ratio of these two masses is:

$$\frac{m_{erk}}{m_{pr}} = \frac{g_0 R^2}{G m_e} \quad (382)$$

From the above, we could obtain the highly sought limiting acceleration:

$$g_0 = \frac{m_{erk}}{m_{pr}} \frac{G m_e}{R^2} \quad (383)$$

if we actually knew the value of m_{erk} , but we do not, because the tabled values for it are based on the assumed values of g_0 arbitrarily chosen to be $g_0 = 10^3 \text{ ms}^{-2}$ for CASE_1 and $g_0 = 10^5 \text{ ms}^{-2}$ for CASE_2 and CASE_3. Then, if the conversion of potential energy to mass by division with c^2 were to be correct, i.e. if we wanted to have $m_{erk} = m_{pr}$, we would obtain:

$$g_0 = \frac{G m_e}{R^2} \quad (384)$$

The above finding is important, because we also have the universal Eq. 352 for g_0 , so that the only way to have them equated by:

$$\frac{G m_e}{R^2} = \frac{G m_e}{A_R R^2} \quad (385)$$

is on the condition that $A_R = 1$, or, in practice, close enough to unity! This indicates that if we knew the diameter and the mass of a particle opaque to gravions, then we could deduce the g_0 sought. We could have come to this understanding earlier by the known

$$g_0 A_R = \frac{G m_e}{R^2} \quad (386)$$

but we have now found this result by connecting kinetic mass to potential mass via $E = mc^2$. Conversely, the latter equation is experimentally applicable with very dense bodies. It would be nice if could measure the electron radius. However regarding measurement of g_0 , it may still be more practical to resort to some of the direct methods proposed in Part 1.

Next, we can see how the above theoretical considerations fare in comparison with the tabled results for the three computed cases. To facilitate reading of the various combinations and types of mass, for convenience and clarity in the ensuing reporting, we include a summary Table 31 with explanations of the

Symbol	Definition
m	real mass of static lone body
m_e	effective or intrinsic mass of static lone body
m_b	black mass of static lone body
m_c	composite real mass of lone body at speed v
$m_\kappa = m_c - m$	kinetic real mass of lone body at speed v
m_{ec}	composite effective mass of lone body at speed v
$m_{e\kappa} = m_{ec} - m_e$	kinetic effective mass of lone body at speed v
m_{bc}	composite black mass of lone body at speed v
$m_{b\kappa} = m_{bc} - m_b$	kinetic black mass of lone body at speed v
m_r	real mass static at distance r
m_{rc}	composite real mass moving at distance r
m_{er}	effective or intrinsic mass static at distance r
m_{erc}	composite effective mass moving at distance r
m_{br}	black mass static at distance r
m_{brc}	composite black mass moving at distance r
$m_{r\kappa} = m_{rc} - m_r$	kinetic real mass moving at distance r
$m_{er\kappa} = m_{erc} - m_{er}$	kinetic effective mass moving at distance r
$m_{br\kappa} = m_{brc} - m_{br}$	kinetic black mass moving at distance r
$m_{rloss} = m - m_r$	loss of real mass static at distance r
$m_{erloss} = m_e - m_{er}$	loss of effective mass static at distance r
$m_{brloss} = m_b - m_{br}$	loss of black mass static at distance r
$m_{rcloss} = m - m_{rc}$	loss of real mass moving at distance r
$m_{ercloss} = m_e - m_{erc}$	loss of effective mass moving at distance r
$m_{brclloss} = m_b - m_{brc}$	loss of black mass moving at distance r
m_{pr}	potential mass static at distance r
v	real (actual) speed of lone body (moving outside gravity)
v_0	intrinsic (notional) speed of lone body by m_e
v_c	composite (notional) speed of lone body (moving outside gravity)
v_r	real (actual) speed of falling body (inside gravity)
v_{r0}	notional speed of falling body (inside gravity) by static m_{er}
v_{rN}	Newtonian falling speed from infinity to r
v_{rPGs}	real (actual) PG falling speed from infinity to r by static m_{er}
v_{rPGc}	real (actual) PG falling speed from infinity to r by composite m_{erc}
v_{r1rPGc}	real (actual) PG falling speed from r_1 to r by composite m_{erc}

Table 31: *Summary of terminology on masses and speeds tabled, plotted and analyzed.*

various mass symbols used. The numerous types and combinations of mass is not a trivial or pedantic exercise, because their theoretical existence may indicate corresponding existence of material structures at the fundamental level of particles.

With regard to density of mass in the three cases examined, mention of a “dense” or “very dense” sphere simply implies operating away from Newtonian mass on the sigmoid curve of A_R against kR . Unfortunately, we do not have the actual value of g_0 yet, which has compelled us to use a hypothetical range for it, or some arbitrary values as in the example cases here. This creates some unavoidable complexity in reporting and understanding the real world situation. Thus, the choice of g_0 for the Moon corresponds to $k_0R = 0.00122$ placing it closer to Newtonian situation, while for CASE_2&3 we have $k_0R = 7.071$ placing them close to saturation on the absorption curve. We expect a much higher than $g_0 = 1000 \text{ ms}^{-2}$, which would correspond to a much lower k and kR , i.e. even closer to Newtonian situation for the Earth-Moon system, but these clarifications should help understand the results provided. It is imperative to conduct some of the proposed experiments to determine the actual g_0 and then repeat the computations to establish the actual k for real systems of bodies.

In Fig. 55(a,b,c), , we plot the m_{pr} , m_{erk} , m_{erloss} and m_{rcloss} for each of the three cases. In Newtonian CASE_1, the effective mass loss is practically (not exactly) the same as the real mass loss, whereas the kinetic mass is far above the potential mass and both far below the effective mass. In contrast, the kinetic mass is practically (not exactly) the same as the potential mass in CASE_2&3, while the effective mass loss and real mass loss have separated out both lying above the potential and kinetic masses by orders of magnitude. These are important outcomes: They confirm Eq. 385 in that potential mass is (nearly) the same as kinetic mass for very dense but not for Newtonian bodies. This might seem at first that energy does not balance out in all cases. However, according to our understanding, mass is a continuous steady state rate of energy transfer between gravions (absorption) and (possibly) electrions (emission), or between different fields. The classical (conventional) potential energy represents only the agent for achieving conversion of one form of mass to another during fall (variation of distance). When we lift an object, we spend work to achieve the process of the said mass conversion to which we partner with the surrounding fields. In any energy balance we have to include not only our energy (work) but also the partnered energy. It is like the mechanism of a heat pump in an air-conditioning system, namely, we spend a small amount of energy for the pump (electrical motor) to transfer a much larger amount of energy between two different temperature reservoirs. Correspondingly, in Newtonian mechanics, we spend a small amount of potential energy (i.e. mass) to generate a much larger amount of PG kinetic mass. However, if we use extremely dense bodies, then our potential energy expended transforms almost entirely to kinetic mass. Understood that the processes described are reversible. This understanding is compatible with particle physics confirming the conversion of mass to energy, because we may assume that the particles involved are extremely dense, as we have already found for the electron and positron. Hence, the equivalence Eq. 385 blends harmoniously with $E = mc^2$ that was used to derive it. It would be profitable to trace back the original work (founding steps) in the derivation of the latter equation.

Furthermore, we also find that the total (real) mass decreases with distance between the two falling spheres in all cases. We present comparative graphs in the same Fig. 55(d). This indeed contravenes conventional theories. The conventional “rest mass” is sacrosanct. However, all types of PG mass vary with distance, including the real mass. This might at first be disturbing, but we may quickly dismiss any concerns: If the mass of a falling body decreases, it does not mean that it loses atoms or chunks of matter, but rather that it radiates push particles without changing the known structure of matter (within a certain range of conditions). This is what happens to an electron falling towards a nucleus. We are accustomed to x-rays emitted by electrons. We can claim that a similar situation exists also with a falling body in a gravitational field, except that we have not been able to detect such radiation yet, neither for a falling Moon on Earth, nor by variation of the distance of planets in elliptical orbits. Such radiation would be of extremely low frequency and extremely low intensity for us to detect. However, we do detect radiations from heavy bodies in astrophysics, so that our PG theory of mass may apply and help us understand better the astronomical/astrophysical observations available now or in the future.

In corroboration of the above, we may also note in (d) of the same figure that CASE_2 may approximately represent also an electron-proton analog system by comparing the radii used: The ratio of “large_dense” to “small_dense” radii is of the order 10^6 , while the proton/electron ratio can be in the order between 10^6 and 10^7 per Section 21.1.2. Since we found that the density of the electron is very high with a much lower proton density (making a good analog system with our spheres), then we may conclude that the variation (loss) of mass displayed in the figure is plausible. It would be very useful to repeat another test case with two “small_dense” spheres of equal diameter to simulate an analog for the fall between an electron and a positron. All this requires a lot of work which may take time to do unless readers decide to contribute to this and many other open topics.

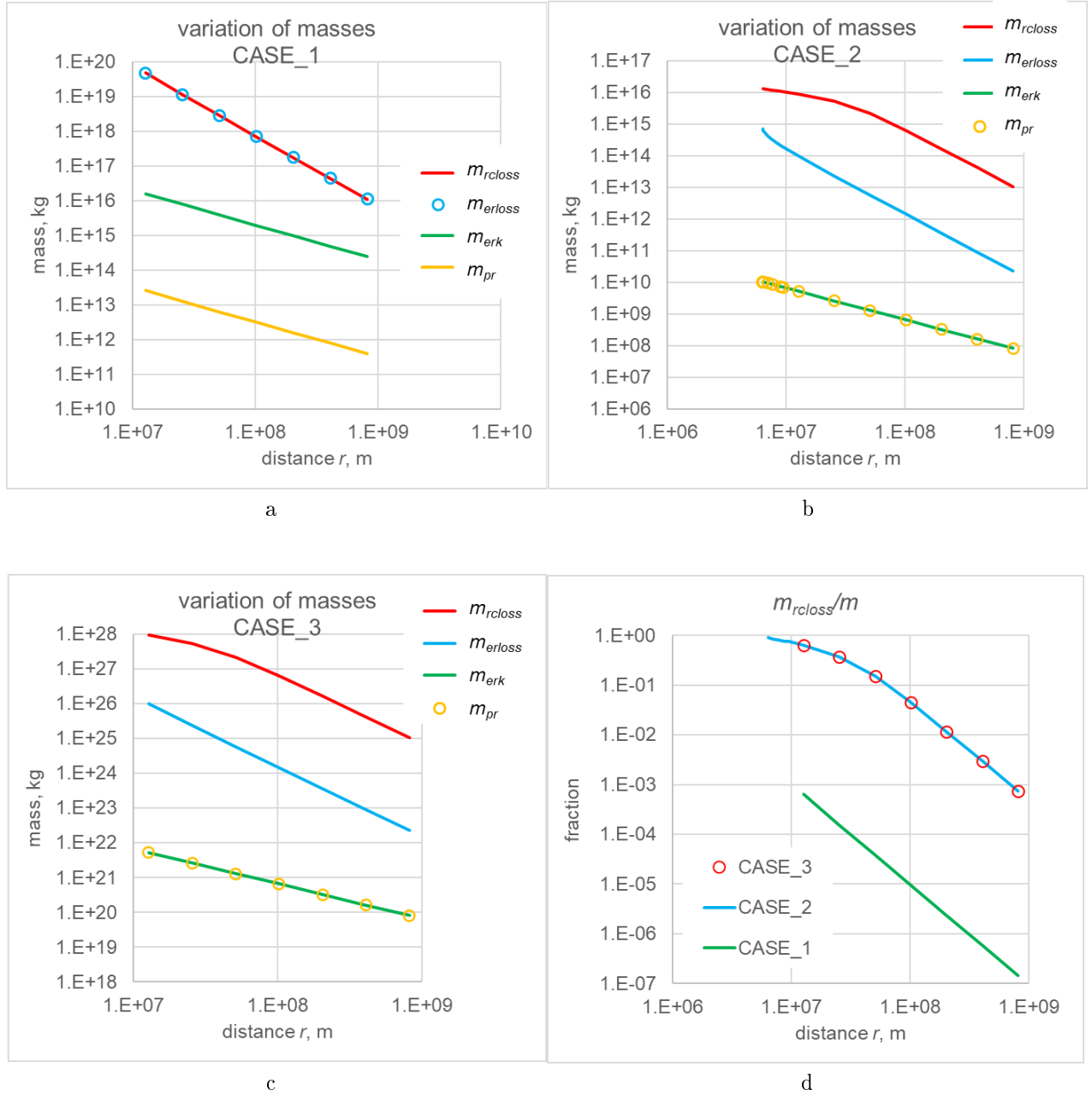


Figure 55: (a, b and c) Variation of different type of masses against distance in continuation of CASE_1, CASE_2 and CASE_3 per Section 16 in absolute values; (d) real mass loss in fractional (normalized) values.

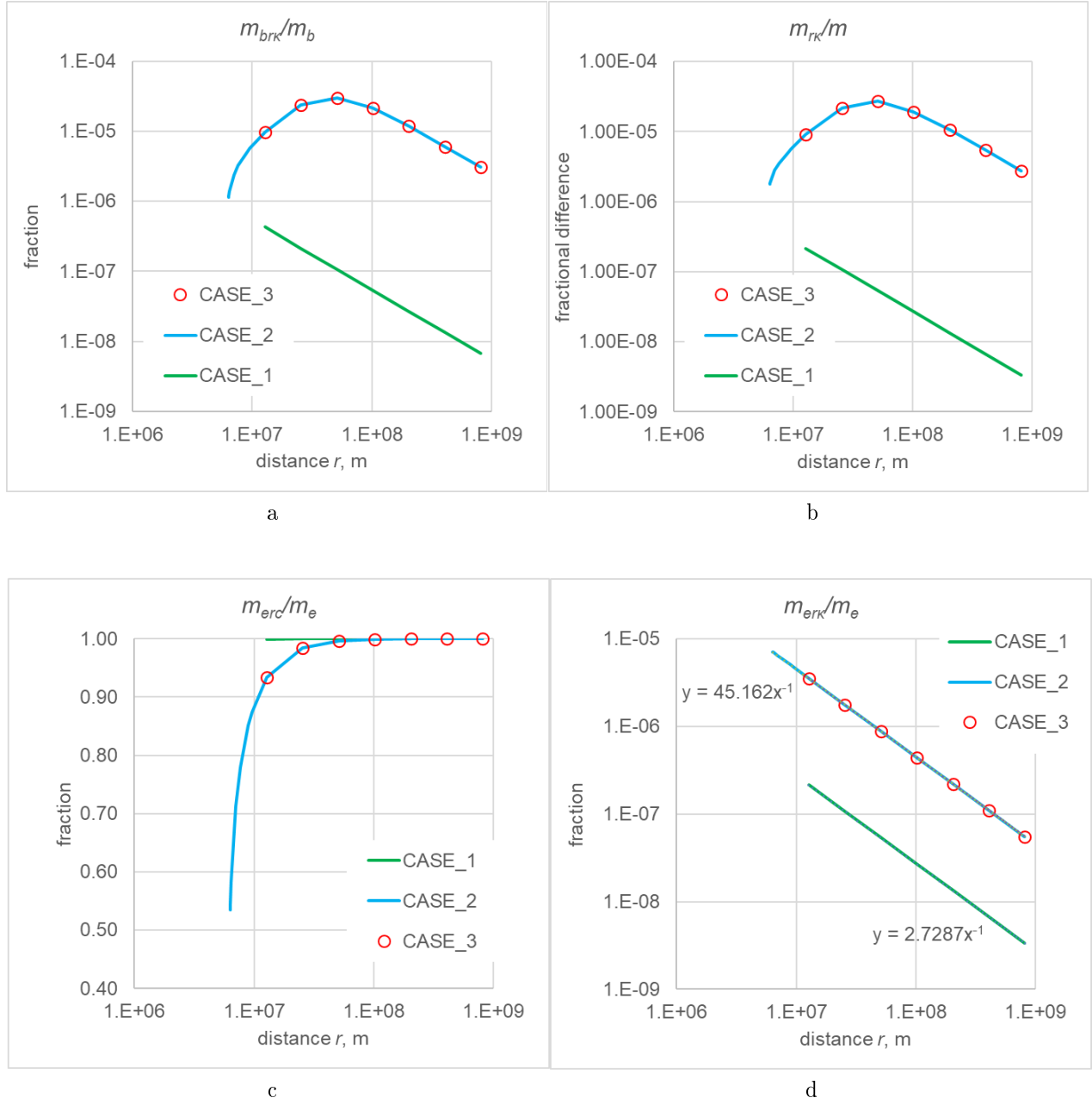


Figure 56: Fractional (normalized) variation of various types of mass against distance.

The above findings may also provide evidence about a long standing question, or paradox, about the orbiting electron not emitting radiation. Our PG theory provides the answer: At fixed orbiting radius and numerically fixed speed there is no change of the real mass, hence there is no radiation emitted. If this might seem difficult to accept, we can suggest a physical explanation too: The centripetal force (acceleration) should accrue kinetic mass per Fig. 53 but the “fall” should also emit an amount of mass simultaneously resulting in a null effect. The rate of mass accrual (due to falling acceleration) must offset the rate of mass loss (due to distance decrease); we should be able to confirm this by carrying out analytical and/or computational work later, like in Appendix E. Readers may be encouraged to take up this work too, like many other works where we leave off unfinished tasks. However, the processes taking place during motion in PG dynamics will be better understood when we can correctly learn about the structure of fundamental particles once and for all.

Now, the exact distribution and other aspects of radiation emission may be speculated. The emission should be generally uniform around the falling sphere, otherwise it would affect the force along the direction of fall. However, this uniformity may be distorted at short range and/or with dense bodies resulting. Electrodynamics may be re-appraised on a PG platform.

The results presented in the tables and equations are only part of the big potential ushered. As a further example, we have also plotted the variation of other fractional masses or combinations thereof against distance in Fig. 56. While black mass may not contribute to inertia and force, it is part and parcel of the entire body structure accompanying the static and kinetic effective masses. There are corresponding fractions of black mass like *static black mass at r* m_{br} , *kinetic black mass at r* $m_{br\kappa}$ and *composite black mass at r* $m_{brc} = m_{br} + m_{br\kappa}$. We normalize and plot the fraction $m_{br\kappa}/m_b$ in order to compare the outcomes for all three cases on the same Fig. 56(a). Likewise, we plot the *kinetic real mass at r* $m_{r\kappa} = m_{rc} - m_r$ normalized by $m_{r\kappa}/m$, i.e. over the intrinsic real mass to compare the results again for all three cases in Fig. 56(b). The latter mass is the radiation (mass loss) emitted initially if we release the body fixed at r with a support rod as shown in Fig. 50; on the hypothesis that the stationary-and-supported sphere has the original intrinsic (lone) mass, upon release it must rearrange the internal mass types so that it acquires the computed static effective and black masses at this distance of an unsupported-and-not-moving sphere. Actually, this re-arrangement must be very fast determined by the magnitude of gravion and electrion exchange rate. That is what must be happening when we release a body from some altitude to start a free fall. This action-reaction process represents a transition period of time during which the body starts falling without having achieved any appreciable speed. In future studies we can examine the mathematical details of this transition. For now, we are satisfied about the general state of a stop-fall regime. That is, the dynamics of the falling sphere depends also on the point of start of the fall (the distance r). We can use the same mathematical derivations accordingly.

We are further interested in the shape of the two curves (a) and (b) of Fig. 56. For the cases of highly dense bodies, there is a maximum presumably representing some internal process in the structure of real mass. Suffice it here to note this finding until we attempt to understand better what the internal structure might be.

We add two additional sets of plots in the same Fig. 56, namely, for the *normalized composite effective mass* m_{erc}/m_e in (c) and the *normalized kinetic mass* $m_{er\kappa}$ in (d). The curves in (c) appear numerically identical with the ratio of forces in Fig. 26, but actually they are different derivations with unequal values:

$$\frac{m_{erc}}{m_e} > \frac{m_{er}M_{er}}{m_eM_e} \quad (387)$$

The seeming equality on the graphs is due to the chosen numerical values of the variables involved as can be easily verified. With variables differing by many orders of magnitude, it requires high precision computations if to avoid misleading impressions. Nevertheless, we note this similarity that might lead us to new relationships and understanding further down the track.

The curves in (d) confirm a relationship found between masses and distance if we use the previous equations by:

$$\frac{m_{er\kappa}}{m_e} = \frac{g_0 R^2 M_e}{c^2 m_e} \frac{1}{r} \quad (388)$$

The straight lines fitted on the log-log plots yield the equations $y = 2.7287x^{-1}$ for CASE_1 and $y = 45.162x^{-1}$ for CASE_2&3, i.e. an inverse to the distance relationship as predicted above or the same originally given by Eq. 376. The kinetic mass and potential energy behave the same, but they are generally unequal unless the absorptivity is close to unity.

We supplement the above presentation with the additional CASE_7 and CASE_4 now provided in Section 16.3 with corresponding results here in Figs. 57 and 58.

Type of mass	kg
m_e, r_∞	2.30953136731102E+04
m, r_∞	2.30953136931349E+04
m_b, r_∞	2.00246358872391E-05
m_{er}, r_{min}	2.30102108923897E+04
m_{erloss}, r_{min}	8.51027807205368E+01
m_{erc}, r_{min}	3.34405290986513E+04
m_{rc}, r_{min}	3.34405291406330E+04
m_{brk}, r_{min}	4.19817015868788E-05
m_{rcgain}, r_{min}	1.03452154474984E+04
m_{erk}, r_{min}	1.04303182062616E+04
m_{pr}, r_{min}	1.60772894666244E-05

Table 32: *Representative masses of the small sphere of CASE_4*

We comment first on CASE_7, which follows the same trend with previous cases: The variation of kinetic $m_{er\kappa}$ and potential m_{pr} masses are practically the same but not exactly equal, like we found previously for the dense bodies; the loss of real composite m_{rcloss} and effective m_{erloss} masses increases monotonically as the spheres approach each other. That is, there is a monotonic shedding of real mass with decreasing distance, most of which takes place within a few radii of distance, considering the logarithmic scale of mass loss. The fractional kinetic black mass $m_{br\kappa}/m_b$ and the fractional kinetic real mass $m_{r\kappa}/m$ at distance r follow practically the same trend and values without being equal. The fractional composite effective mass m_{erc}/m_e and the fractional kinetic effective mass $m_{er\kappa}/m_e$ at distance r are again similar at different scales for all these cases.

CASE_4 is in clear departure from the other cases: The real mass loss defined by $m_{rcloss} = m - m_{rc}$ yields a negative value. To show this on logarithmic scale along with the other masses, we changed the sign and renamed it by $m_{rcgain} = m_{rc} - m$, because we now have a net gain of mass. The small test sphere with earthly density and only 1 m radius is characterized by a very small absorptivity and black mass, so that the effective and real masses are very close to each other. The corresponding variation of effective mass with position (m_{er}) is also extremely small to the extent that the accrual of kinetic mass during fall overwhelms all positional variation of mass loss. The real mass gain is practically equal to the kinetic mass with both being only a little under the effective lone mass of the falling sphere. Indicatively, we list some representative values of the various types of mass for the small sphere of this case in Table 32.

The above outcomes may come as surprise and for possible rejection based on existing expectation and experience. In fact, they may be contrary to data and astronomical observations and measurements of meteors and comets. However, this is no reason to discard the attempted approach. First of all, these masses are the result of the arbitrary use of Eq. 348 while they can be drastically reduced via, say, Eq. 363 up to great speeds (see also Fig. 54).

As stated previously, the use of Newtonian speed to connect with mass variation for a falling body is arbitrary but has been applied on the assumption that it would provide first order magnitudes, upon which we have already derived important lessons. We proceed to substantiate our assumption in the next two subsections, but the answers provided are themselves subject to other simplifications, which should not invalidate our hitherto conclusions. The simplifications used have other important ramifications emanating from the cumulative effects of speed computations.

We first consider the case where the falling spherical mass has a variable effective mass $m_{er}(r)$ with distance alone but not with speed yet, followed by the case of having both variations. This is a novel situation completely outside conventional physics, for which we must make our position clear: We must recognize the distinction between the two different causes of mass variation, namely, one positional variation based on the firm PG outcomes of Section 16, and another based on a proposed/speculated mass accrual (variation) determined by the given speed at any point in space and moment in time (speed-variation of mass). The first variation is fundamental to the static PG theory of Part 1 of this report, but the second

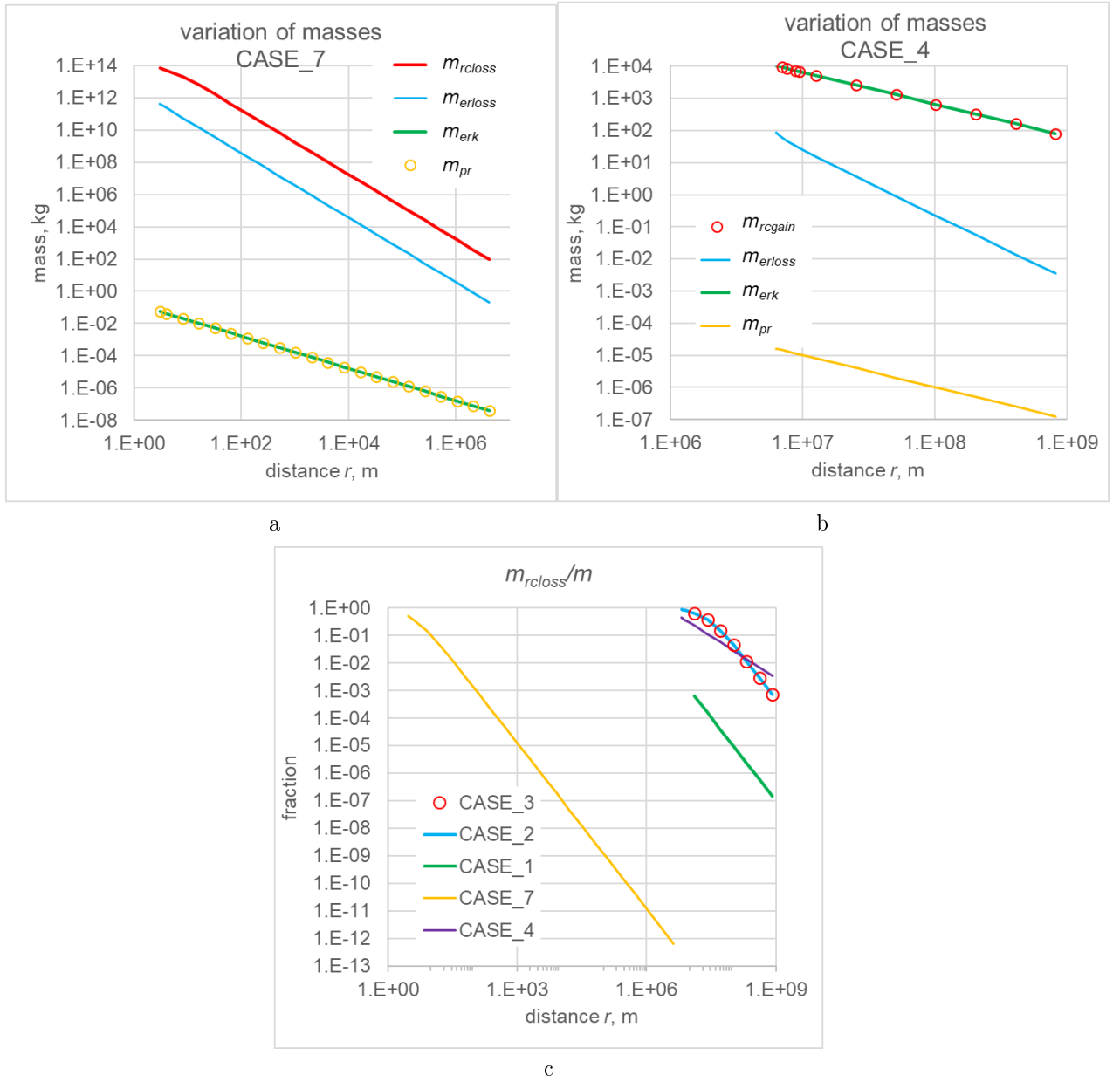
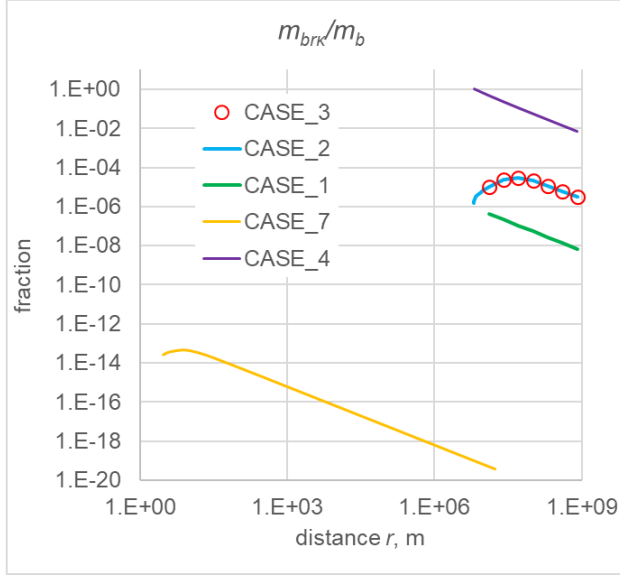


Figure 57: (a) Variation of different type of masses in absolute values against distance for CASE_7, (b) same for CASE_4 and (c) real mass loss in fractional (normalized) values for all cases together

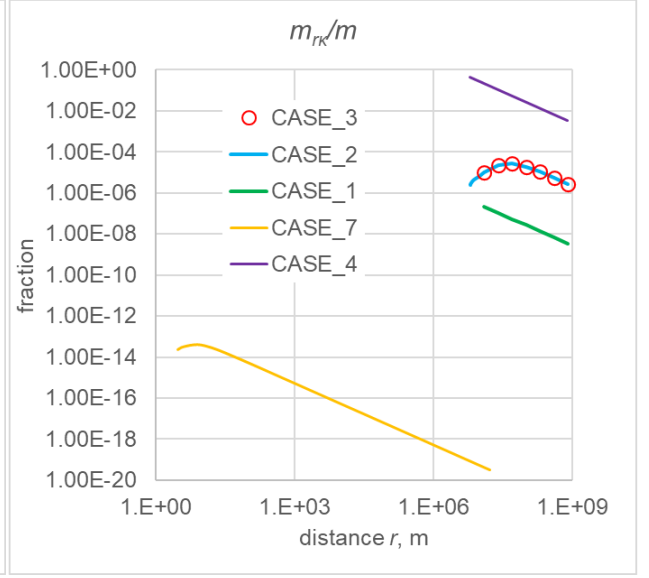
variation remains to be worked out and proved, albeit also fundamental in the development of a dynamic PG theory. We skirmish with the latter development in Part 2 of this report. We attempt to explore the possibility of arriving at a dynamic theory with as little as possible reliance on conventional principles. The delay in doing so is the idea that the dynamics of motion depends also on the structure of matter at the fundamental level, i.e. motion and structure being intimately connected. We provide a sample of these ideas later, so that it should be appreciated why we have created several incomplete openings with the aim to return to, or somebody else to take over from where we leave off.

23.2.1 Speed from static mass variation

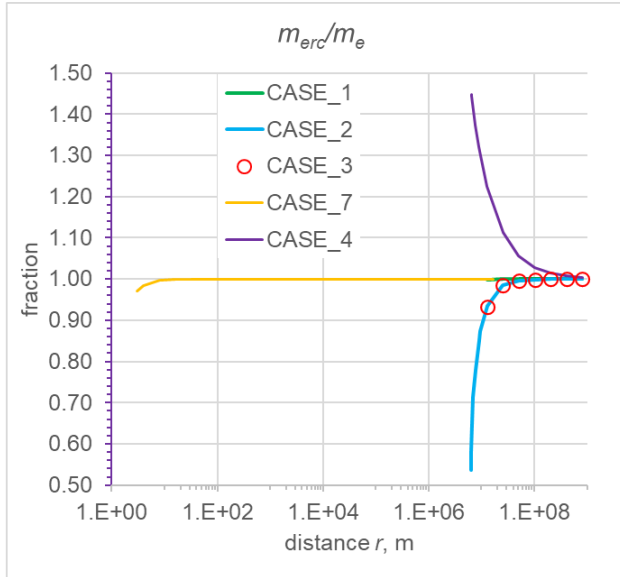
The difference between Newton and PG is that the same force acts on different masses, namely, on a constant (invariable) mass in Newton, but on a variable mass now in PG. The force is the same in both situations but the outcomes on speed and motion are different. The work done and the kinetic energy is the same in both cases, but the resulting speeds differ as they are used by different masses. The kinetic mass ($m_{e\kappa}$) created by a presumed conjecture in Eq. 348 is left out for now (to be applied in the next section), so that we can secure a novel outcome even if the said conjecture is abandoned or modified later.



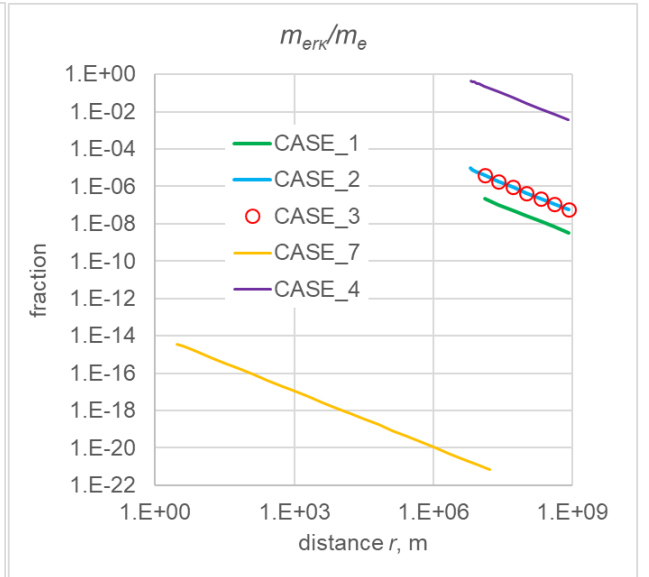
a



b



c



d

Figure 58: *Fractional (normalized) variation of various types of mass against distance adding CASE_7 and CASE_4 together with all previous ones.*

We follow the mathematical steps for the work done by the same force on the variable mass below:

$$\begin{aligned} E_{kinetic} &= \int_{\infty}^r F dr = 2 \int_{\infty}^r \frac{dp}{dt} dr = 2 \int_{\infty}^r \frac{d(m_{er} v_r)}{dt} v_r dt = 2 \int_{\infty}^r \left(v_r \frac{dm_{er}}{dt} + m_{er} \frac{dv_r}{dt} \right) v_r dt \\ &= 2 \int_{\infty}^r \left(v_r^2 \frac{dm_{er}}{dt} dt + \frac{1}{2} m_{er} \frac{dv_r^2}{dt} dt \right) = 2 \int_{\infty}^r \left(v_r^2 \frac{dm_{er}}{dr} + m_{er} \frac{dv_r^2}{dr} \right) dr \end{aligned}$$

There remains now to furnish the effective mass $m_{er} = m_{er}(r)$ so that we can find the speed $v_r = v_r(r)$ as a function of distance by solving the differential equation:

$$2 \int_{\infty}^r \left(v_r^2 \frac{dm_{er}}{dr} + m_{er} \frac{dv_r^2}{dr} \right) dr = G \frac{M_e m_e}{r} \quad (389)$$

We use again the notation of capital M for the “gravitating” mass and lower case m for the “falling” mass. Strictly speaking, both spheres are gravitating and falling relative to each other as we use the variable distance r in the equations. For the function of $m_{er}(r)$, we can use the variation of effective mass computed in Section 16. The corresponding tables provide the variation of mass in numerical form. The graphs show the mass loss, which deducted from the “lone” mass m_e can also provide the required mass here. We draw attention again to the behavior of mass loss and the associated asymptotic line. The correct approach should be to apply the numerical outcomes on mass calculation using the computational methods in the Appendix for solving the above differential equation. We are not equipped to do that at present, but we can apply the asymptotic analytical function in an attempt to estimate at least the order of magnitude of the ensuing falling speed. Thus, from the general Eq. 204 for mass and Eq. 213 for the asymptotic line, we write again here:

$$\begin{aligned} m_{erloss} &= \frac{g_0}{4\pi^2 G} S_{F0} \\ S_{F0} &\equiv \frac{\pi A_1 \pi A_2}{r^2} = \frac{\pi^2 A_{R1} A_{R2} R_1^2 R_2^2}{r^2} \\ m_{erloss} &= \frac{g_0}{4\pi^2 G} \frac{\pi^2 A_{R1} A_{R2} R_1^2 R_2^2}{r^2} = \frac{g_0}{4G} \frac{A_{R1} A_{R2} R_1^2 R_2^2}{r^2} \equiv \frac{d}{r^2} \end{aligned} \quad (390)$$

where

$$d = \frac{g_0}{4G} A_R A_{R2} R^2 R_2^2 = \frac{\Lambda G M_e m_e}{4\pi G} = \frac{G M_e m_e}{4g_0}$$

We reintroduce the notation R_2 for the “gravitating” sphere radius but retain the plain notation R for the “falling” sphere radius. The required effective mass of the falling sphere is the difference of the loss mass from the effective lone mass:

$$m_{er} = m_e - m_{erloss} \quad (391)$$

from which the derivative with respect to distance is

$$\frac{dm_{er}}{dr} = \frac{2d}{r^3}$$

We use the above to re-write the differential equation in a form ready for integration and find the unknown speed squared as $y \equiv v_r^2 = v_r^2(r)$. We proceed in obvious steps with comments as needed:

$$\begin{aligned} \int_{\infty}^r \left(4v_r^2 \frac{d}{r^3} + \left(m_e - \frac{d}{r^2} \right) \frac{dv_r^2}{dr} \right) dr &= G \frac{M_e m_e}{r} \\ \int_{\infty}^r \left(4y \frac{d}{r^3} + \left(m_e - \frac{d}{r^2} \right) \frac{dy}{dr} \right) dr &= \frac{G M_e m_e}{r} \end{aligned}$$

We divide both members of the equation by d :

$$\int_{\infty}^r \left(\left(\frac{m_e}{d} - \frac{1}{r^2} \right) \frac{dy}{dr} + 4 \frac{y}{r^3} \right) dr = \frac{4g_0}{r} \quad (392)$$

whereby it is important to note that the falling mass m_e is entirely eliminated from the equation:

$$\int_{\infty}^r \left(\left(b - \frac{1}{r^2} \right) \frac{dy}{dr} + 4 \frac{y}{r^3} \right) dr = \frac{a}{r}$$

where

$$b = \frac{4g_0}{GM_e} \quad a = 4g_0$$

By differentiating, we need to solve the equation of the form:

$$\left(b - \frac{1}{r^2} \right) y' + 4 \frac{y}{r^3} = -\frac{a}{r^2} \quad (393)$$

The solution for y is readily found to be:

$$y = \frac{\int -\frac{ae^{\int \frac{4}{r(b r^2 - 1)} dr}}{b r^2 - 1} dr}{e^{\int \frac{4}{r(b r^2 - 1)} dr}} \quad (394)$$

$$\int_{\infty}^r \frac{4}{r(b r^2 - 1)} dr = 2 \ln \frac{b r^2 - 1}{b r^2} \quad (395)$$

$$\begin{aligned} y &= \frac{\int \frac{-a \exp \left(2 \ln \frac{b r^2 - 1}{b r^2} \right)}{b r^2 - 1} dr}{\exp \left(2 \ln \frac{b r^2 - 1}{b r^2} \right)} = \frac{\int -a \frac{b r^2 - 1}{b^2 r^4} dr}{\left(\frac{b r^2 - 1}{b r^2} \right)^2} = \frac{\frac{a(3 b r^2 - 1)}{3 b^2 r^3}}{\left(\frac{b r^2 - 1}{b r^2} \right)^2} = \frac{a(3 b r^2 - 1)}{3 b^2 r^3} \frac{b^2 r^4}{(b r^2 - 1)^2} \\ y &= \frac{a(3 b r^2 - 1)r}{3 (b r^2 - 1)^2} \end{aligned} \quad (396)$$

Reverting to the original parameters and denoting the obtained PG speed from static mass at r by v_{rPGs} with $y = v_r^2 \equiv v_{rPGs}^2$, we finally obtain:

$$v_{rPGs}^2 = \frac{4g_0 \left(\frac{12g_0}{GM_e} r^2 - 1 \right) r}{3 \left(\frac{4g_0}{GM_e} r^2 - 1 \right)^2} = \frac{4g_0 \left(\frac{12}{A_{R_2}} \frac{r^2}{R_2^2} - 1 \right) r}{3 \left(\frac{4}{A_{R_2}} \frac{r^2}{R_2^2} - 1 \right)^2} \quad (397)$$

We can immediately see that the above formula reduces to the familiar Newtonian $v_{rN}^2 \rightarrow GM_e/r$ when $r^2 \gg \frac{GM_e}{4g_0}$, or $\frac{r}{R_2} \gg \frac{\sqrt{A_{R_2}}}{2}$, or when $A_{R_2} \rightarrow 0$, in other words when we approach closely to the Newtonian regime. Beyond Newton, we arrive at a different speed, which, however, is the same for all falling bodies. The latter appears to be consistent with prevailing experience and conventional physics, namely, that all bodies fall with the same speed. However, according to the findings in Section 16.3, the falling body parameters should not be eliminated from our differential equation above, because they are ever present albeit imperceptibly in the first place. It is only because we used the linear asymptotic equation of mass loss when the falling mass was eliminated in step of Eq. 392. After all, by way of symmetry, we should have the absorptivity of both spheres involved, not only one as provided by the above equation. Then, the speed should be a function of the properties of the falling body, which presumably has escaped our experiments to date, because of its extremely small effect within the framework of our experiments. However, this can become important in long space travel between planets whereby even the smallest deviation from Newtonian mechanics would appear as an anomaly, such as those anomalies already on record.

For the present purposes, we can use the above derived equation of speed to see at least the magnitude of deviation from Newton. We do so later in tables and figures together with the outcomes of the next section including the kinetic mass.

23.2.2 Speed from composite mass variation

Here, we investigate the possibility of the falling spherical mass being dependent on both distance and speed. That is, we follow the corresponding steps as previously by using the composite mass function $m_{erc}(r, v_r)$ by including the kinetic mass component generated by the speed at each distance r , namely:

$$m_{erc} = m_{erc}(r, v_r) = m_{er}(r) + m_{er\kappa}(v_r) = m_e - m_{eloss} + \frac{g_0 R^2}{G} \frac{v_r^2}{c^2} \quad (398)$$

where we initially use Eq. 348 between speed-mass. We now arrive at a new differential equation to solve by proceeding in the same way as before. To make it more general, we can replace the starting falling point from infinity to a finite initial distance r_1 and follow the same steps without or little further comment below:

$$\begin{aligned} E_{kinetic} &= \int_{r_1}^r F dr = 2 \int_{r_1}^r \frac{dp}{dt} dr = 2 \int_{r_1}^r \frac{d(m_{erc} v_r)}{dt} v_r dt = 2 \int_{r_1}^r v_r d(m_{erc} v_r) dr \\ &= 2 \int_{r_1}^r \left(v_r \frac{dm_{erc}}{dt} + m_{erc} \frac{dv_r}{dt} \right) v_r dt = \int_{r_1}^r \left(2v_r^2 \left(\frac{\partial m_{erc}}{\partial r} + \frac{\partial m_{erc}}{\partial v_r} \right) + m_{erc} \frac{dv_r^2}{dr} \right) dr \end{aligned} \quad (399)$$

$$\begin{aligned} E_{kinetic} &= \int_{r_1}^r \left(2v^2 \left(\frac{d}{r^3} + \frac{g_0 R^2}{c^2 G} \frac{dv_r^2}{dr} \right) + \left(m_e - \frac{d}{r^2} + \frac{g_0 R^2}{G c^2} v_r^2 \right) \frac{dv_r^2}{dr} \right) dr \\ &\equiv \int_{r_1}^r \left(2y \left(\frac{d}{r^3} + \frac{g_0 R^2}{c^2 G} y' \right) + \left(m_e - \frac{d}{r^2} + \frac{g_0 R^2}{G c^2} y \right) y' \right) dr \\ &= \int_{r_1}^r \left(2y \frac{d}{r^3} + 2y \frac{g_0 R^2}{c^2 G} y' + \left(m_e - \frac{d}{r^2} + \frac{g_0 R^2}{G c^2} y \right) y' \right) dr \\ &= \int_{r_1}^r \left(\left(m_e - \frac{d}{r^2} + \frac{g_0 R^2}{G c^2} y + 2y \frac{g_0 R^2}{c^2 G} \right) y' + 2y \frac{d}{r^3} \right) dr \\ &= \int_{r_1}^r \left(\left(m_e - \frac{d}{r^2} + 3 \frac{g_0 R^2}{G c^2} y \right) y' + 2y \frac{d}{r^3} \right) dr \\ &= \int_{r_1}^r \left(\left(m_e - \frac{d}{r^2} + 3 \frac{g_0 R^2}{G c^2} y \right) y' + 2y \frac{d}{r^3} \right) dr = G M_e m_e \left(\frac{1}{r} - \frac{1}{r_1} \right) \\ &\int_{r_1}^r \left(\left(\frac{m_e}{d} - \frac{1}{r^2} + 3 \frac{g_0 R^2}{d G c^2} y \right) y' + 2y \frac{1}{r^3} \right) dr = \frac{G M_e m_e}{d} \left(\frac{1}{r} - \frac{1}{r_1} \right) = 4g_0 \left(\frac{1}{r} - \frac{1}{r_1} \right) \end{aligned} \quad (400)$$

$$\int_{r_1}^r \left(\left(\frac{4g_0}{G M_e} - \frac{1}{r^2} + 3 \frac{g_0 R^2}{d G c^2} y \right) y' + 2y \frac{1}{r^3} \right) dr = 4g_0 \left(\frac{1}{r} - \frac{1}{r_1} \right)$$

where we have use the replacements

$$a = 4g_0, \quad b = \frac{4g_0}{G M_e} = \frac{4}{A_{R_2} R_2^2}, \quad d = \frac{G M_e m_e}{4g_0} = \frac{M_e A_R R^2}{4}, \quad h = \frac{4g_0^2 R^2}{G^2 M_e m_e c^2}$$

and simplify the form of the equation as:

$$\int_{r_1}^r \left(\left(b - \frac{1}{r^2} + 3hy \right) y' + y \frac{2}{r^3} \right) dr = a \left(\frac{1}{r} - \frac{1}{r_1} \right) \quad (401)$$

By differentiating, we arrive at the differential equation:

$$\left(b - \frac{1}{r^2} + 3hy \right) y' + y \frac{2}{r^3} = -\frac{a}{r^2} \quad (402)$$

The solution of this equation is again readily available and given by:

$$y = \frac{-b + \frac{\sqrt{c_1 h r^4 + 6 a h r^3 + b^2 r^4 - 2 b r^2 + 1} + 1}{x^2}}{3h}$$

where the integration constant c_1 is determined by the speed at r_1 . To simplify the present investigation, let us start with zero speed at r_1 getting the equation:

$$y = \frac{-b + \frac{\sqrt{c_1 h r_1^4 + 6 a h r_1^3 + b^2 r_1^4 - 2 b r_1^2 + 1} + 1}{r_1^2}}{3h} = 0$$

from where we obtain the constant:

$$c_1 = -\frac{6a}{r_1}$$

By substituting and restoring our parameters from the interim substitutions, we finally obtain for the falling PG speed v_{rPGc} from composite mass at r over the gravion speed c squared, the formula:

$$\frac{v_{rPGc}^2}{c^2} = -\frac{A_R}{3} + \sqrt{\frac{A_R^2}{9} + \frac{2g_0 A_R A_{R_2} R_2^2}{3c^2} \left(\frac{1}{r} - \frac{1}{r_1}\right) - \frac{A_{R_2} A_R^2 R_2^2}{18} \frac{R_2^2}{r^2} + \left(\frac{A_{R_2} A_R R_2^2}{12} \frac{R_2^2}{r^2}\right)^2} + \frac{A_{R_2} A_R R_2^2}{12} \frac{R_2^2}{r^2} \quad (403)$$

where A_{R_2} and A_R are the absorptivities for the gravitating and falling spheres accordingly given by the familiar general equation:

$$A_R = \frac{Gm_e}{g_0 R^2} \quad (404)$$

For speed notations see also a summary in Table 31. We discuss the above results next. It should also be noted that we use the words “speed” and “velocity” interchangeably in this work, while in other languages these words have only one translation (e.g. $\tau\alpha\chi\acute{o}\tau\eta\varsigma$ = tachytes or tachytis in Greek, re tachyon, etc.)

This work remains incomplete: The exact solutions to the differential equations involved require resources beyond those available to this author at present, but other workers are encouraged to make a contribution in this direction, if to move forward faster. We only attempt to introduce some dynamics in PG, i.e. new physics, which constitutes an opportunity for mathematicians to make a new contribution. We have grouped various situations by way of several “CASES” with regard only to two interacting spherical bodies, but the problem is greatly complicated in a multi-body problem like the solar system. We need devoted mathematics and software engineering to properly address a new and evolving chapter of physics, a task clearly beyond the means available to this author.

23.2.3 Speed investigation

The speed formula 397 based only on positional variation of effective mass but not on the speed itself would not be consistent with accrual of mass proposed during rocket acceleration, with an upper speed limit; that is, any kinetic mass, if present, would be inertia-less. The second speed formula 403 is consistent with a composite effective mass and would be closer to a true representation of reality, if the conjectural Eq. 351 between speed and absorptivity (or mass) were to be true; that is, the kinetic mass may be treated like effective mass acted upon by a force.

On the above basis, we can now see the effects of revised falling speeds for all CASES_1_2&_3. It is instructive to find the deviation from Newtonian mechanics, the falling speed for which we denote by v_{rN} . We do this by plotting the ratio of speeds squared v_{rPGs}^2/v_{rN}^2 and v_{rPGc}^2/v_{rN}^2 in Fig. 59. The effect is to obtain a higher PG speed than Newton, which quickly diminishes as the distance increases. The departure from Newton follows the same trend as in previous comparisons with other parameters (e.g. for the force per Fig. 26). We can better understand these results by examining also the numerical values of kinetic and composite masses for all three cases next.

Tables 33, 34 and 35 provide a comparison of kinetic masses corresponding to (or generated by) Newtonian, static and composite speeds; the Newtonian kinetic mass is copied from previous tables for convenience of comparison. We note that all kinetic masses have same order of magnitude or very close values, with the greatest deviation for CASE_2. The difference does not affect the main points of discussion based on

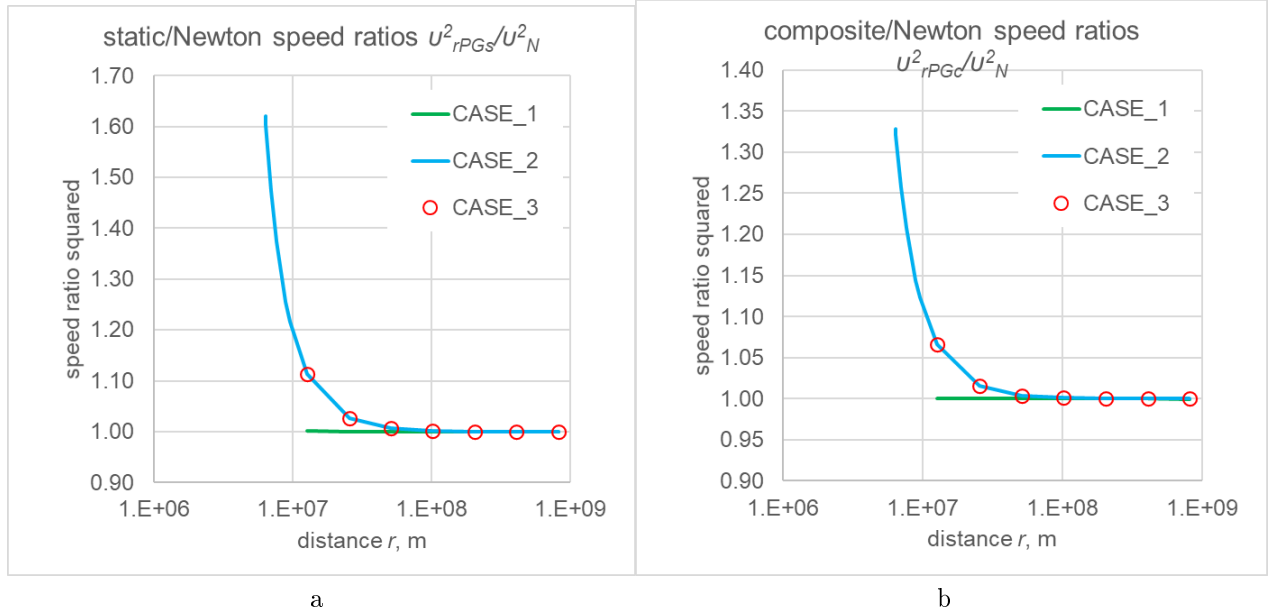


Figure 59: *Ratio of speeds_squared against distance in (a) using static mass and (b) using composite mass for CASES_1, 2&3.*

Newtonian speed. The corresponding speed ratios squared are also given in the last two columns noting a monotonic decrease close to unity at long enough distance; the distance in meters is given in multiples of Earth radii doubling with each point.

Similarly, the corresponding composite masses are provided in Tables 36, 37 and 38. We can verify again the similar values with the greatest effect resulting in CASE_2, all of which also do not affect the preceding discussion.

We have the same conclusion for the added CASE_7, namely, there is no visible difference for the kinetic and composite real mass loss between applying Newtonian or PG composite speed according to Fig. 60a. However, this does not apply for CASE_4 according to Fig. 60b, which is further investigated with more specific examples below.

Therefore, there is no need to redraw the graphs obtained for the cases in the previous section using Newtonian speed, or revise the ensuing findings and considerations. One remaining correction would arise from replacing the asymptotic function of Eq. 390 used above with the actual falling static effective mass m_{er} resulting by the computational means applied in Section 16 or by an analytical function, if it exists; additionally, a correction may be required by a modified relationship between absorptivity and mass (analytical, if it exists, or otherwise) in lieu of the conjectured equation. Still, we expect only second order difference on top of the previous one for the given cases. Therefore, the opening presentation of this Section 23.2 need not be altered only because it was based on Newtonian speeds. However, there would be a practical difference of the preceding analysis by way of a cumulative effect on the speed over a long trajectory between planets or between a planet and spacecraft. This is an important difference that is examined in the following Section.

Now, CASE_4 represents a family of objects from our immediate experience, as opposed to very massive, large or dense bodies lying beyond the ordinary range of perception. We have already seen the different behavior of the associated masses in Table 32 and Figs. 57 and 58 drawn according to Section 16.3. We can use cases like this to further investigate the equations of falling speed and see if they are consistent with surrounding experience. Actually, current experience dictates that our predictions should be untenable, because “*all bodies fall with equal speed*”, unless our predictions fall within the experimental errors prevailing to date.

Both equations involve the distance r and the unknown limiting acceleration g_0 . We do a preliminary examination of the behavior of the second Eq. 403, whereby we do have a variation of speed due to the absorptivity A_R of the falling body. The numerical results in Table 39 indicate that the effect of parameter g_0 seems to be minor: We note a very small variation of the ratio v_{rPGc}/v_{rN} in a wide range of absorptivity over many orders of magnitude and over a wide range of the limiting acceleration (g_0) at a fixed final distance from Earth, namely, at $r = 2R_2 = 12742000$ m. However, the absorptivity A_R of the falling body is decisive in the determination of the final speed. In a range of $A_R > 1.0E - 08$, the PG speed is very close to Newtonian speed with a ratio either a little below or a little above unity. This behavior is consistent with the outcomes from various cases: The kinetic mass adds very little in all those cases except CASE_4, where

r , m	$m_{er\kappa}$ kg, with v_{rN}	$m_{er\kappa}$, kg with v_{rPGs}	$m_{er\kappa}$, kg with v_{rPGc}	v_{rPGs}^2/v_{rN}^2	v_{rPGc}^2/v_{rN}^2
12742000	1.5735021E+16	1.5751131E+16	1.5744680E+16	1.001024	1.000614
25484000	7.8675107E+15	7.8695231E+15	7.8687168E+15	1.000256	1.000153
50968000	3.9337553E+15	3.9340068E+15	3.9339059E+15	1.000064	1.000038
101936000	1.9668777E+15	1.9669091E+15	1.9668964E+15	1.000016	1.000010
203872000	9.8343883E+14	9.8344276E+14	9.8344117E+14	1.000004	1.000002
407744000	4.9171942E+14	4.9171991E+14	4.9171971E+14	1.000001	1.000001
815488000	2.4585971E+14	2.4585977E+14	2.4585974E+14	1.000000	1.000000
∞	0	0	0	1	1

Table 33: *Dependence of kinetic mass and speed ratio_squared on distance per prior CASE_1 and comparison using Newtonian speed v_{rN} , static speed v_{rPGs} and composite speed v_{rPGc}*

r , m	$m_{er\kappa}$ kg, with v_{rN}	$m_{er\kappa}$, kg with v_{rPGs}	$m_{er\kappa}$, kg with v_{rPGc}	v_{rPGs}^2/v_{rN}^2	v_{rPGc}^2/v_{rN}^2
6371002.0	1.0515014E+10	1.7037378E+10	1.3973175E+10	1.620291E+00	1.328878
6371063.7	1.0514912E+10	1.7037026E+10	1.3972951E+10	1.620273E+00	1.328870
6371637.1	1.0513966E+10	1.7033751E+10	1.3970866E+10	1.620107E+00	1.328791
6377371.0	1.0504513E+10	1.7001085E+10	1.3950061E+10	1.618455E+00	1.328006
6434710.0	1.0410908E+10	1.6681671E+10	1.3745758E+10	1.602326E+00	1.320323
7008100.0	9.5591065E+09	1.4077247E+10	1.2016979E+10	1.472653E+00	1.257124
7645200.0	8.7625143E+09	1.2045208E+10	1.0581013E+10	1.374629E+00	1.207532
8919400.0	7.5107265E+09	9.4244672E+09	8.5961329E+09	1.254801E+00	1.144514
9556500.0	7.0100114E+09	8.5254105E+09	7.8763469E+09	1.216176E+00	1.123585
12742000.0	5.2575086E+09	5.8506967E+09	5.6042391E+09	1.112827E+00	1.065950
25484000.0	2.6287543E+09	2.6980243E+09	2.6700494E+09	1.026351E+00	1.015709
50968000.0	1.3143771E+09	1.3228948E+09	1.3194781E+09	1.006480E+00	1.003881
101936000.0	6.5718857E+08	6.5824895E+08	6.5782412E+08	1.001614E+00	1.000967
203872000.0	3.2859429E+08	3.2872670E+08	3.2867362E+08	1.000403E+00	1.000241
407744000.0	1.6429714E+08	1.6431369E+08	1.6430704E+08	1.000101E+00	1.000060
815488000.0	8.2148572E+07	8.2150640E+07	8.2149806E+07	1.000025E+00	1.000015
∞	0	0	0	1	1

Table 34: *Dependence of kinetic mass and speed ratio_squared on distance per prior CASE_2 and comparison using Newtonian speed v_{rN} , static speed v_{rPGs} and composite speed v_{rPGc}*

$r, \text{ m}$	$m_{er\kappa} \text{ kg, with } v_{rN}$	$m_{er\kappa}, \text{ kg with } v_{rPGs}$	$m_{er\kappa}, \text{ kg with } v_{rPGc}$	v_{rPGs}^2/v_{rN}^2	v_{rPGc}^2/v_{rN}^2
12742000	5.2575086E+21	5.8506967E+21	5.6042391E+21	1.112827	1.065950
25484000	2.6287543E+21	2.6980243E+21	2.6700494E+21	1.026351	1.015709
50968000	1.3143771E+21	1.3228948E+21	1.3194781E+21	1.006480	1.003881
101936000	6.5718857E+20	6.5824895E+20	6.5782412E+20	1.001614	1.000967
203872000	3.2859429E+20	3.2872670E+20	3.2867362E+20	1.000403	1.000241
407744000	1.6429714E+20	1.6431369E+20	1.6430704E+20	1.000101	1.000060
815488000	8.2148572E+19	8.2150640E+19	8.2149806E+19	1.000025	1.000015
∞	0	0	0	1	1

Table 35: Dependence of kinetic mass and speed ratio_squared on distance per prior CASE_3 and comparison using Newtonian speed v_{rN} , static speed v_{rPGs} and composite speed v_{rPGc}

$r, \text{ m}$	$m_{erc} \text{ kg, with } v_{rN}$	$m_{erc}, \text{ kg with } v_{rPGs}$	$m_{erc}, \text{ kg with } v_{rPGc}$
12742000	7.34288394267474E+22	7.34288394428572E+22	7.34288394364059E+22
25484000	7.34652770181904E+22	7.34652770202028E+22	7.34652770193965E+22
50968000	7.34738756500709E+22	7.34738756503224E+22	7.34738756502215E+22
101936000	7.34759966340501E+22	7.34759966340816E+22	7.34759966340689E+22
203872000	7.34765247337708E+22	7.34765247337747E+22	7.34765247337731E+22
407744000	7.34766564250449E+22	7.34766564250454E+22	7.34766564250452E+22
815488000	7.34766892244818E+22	7.34766892244818E+22	7.34766892244818E+22
∞	7.34767000000000E+22	7.34767000000000E+22	7.34767000000000E+22

Table 36: Dependence of composite mass on distance per prior CASE_1 and comparison using constant Newtonian speed v_{rN} , static speed v_{rPGs} and composite speed v_{rPGc}

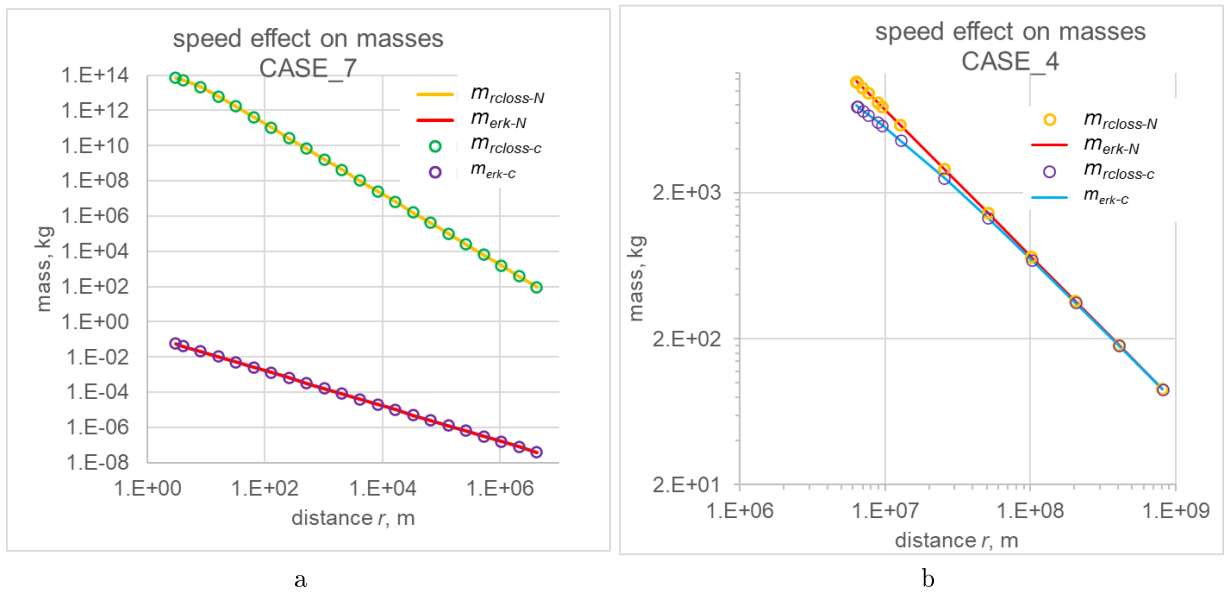


Figure 60: Speed effect on real mass loss and kinetic mass by applying Newtonian and composite speeds in (a) for CASE_7 and in (b) for CASE_4

r , m	m_{erc} kg, with v_{rN}	m_{erc} , kg with v_{rPGs}	m_{erc} , kg with v_{rPGc}
6371002.0	7.94147138242287E+14	7.94153660606427E+14	7.94150596403506E+14
6371063.7	7.94488228598695E+14	7.94494750712234E+14	7.94491686637396E+14
6371637.1	7.96583043838863E+14	7.96589563624548E+14	7.96586500739456E+14
6377371.0	8.08703233104536E+14	8.08709729676536E+14	8.08706678652915E+14
6434710.0	8.64879251436736E+14	8.64885522199615E+14	8.64882586286389E+14
7008100.0	1.05761101120192E+15	1.05761552934288E+15	1.05761346907430E+15
7645200.0	1.15618076737692E+15	1.15618405007037E+15	1.15618258587526E+15
8919400.0	1.26341138212519E+15	1.26341329586583E+15	1.26341246753153E+15
9556500.0	1.29668049750239E+15	1.29668201290149E+15	1.29668136383782E+15
12742000.0	1.38505541527468E+15	1.38505600846280E+15	1.38505576200522E+15
25484000.0	1.46004099803422E+15	1.46004106730425E+15	1.46004103932934E+15
50968000.0	1.47759306210703E+15	1.47759307062470E+15	1.47759306720794E+15
101936000.0	1.48191568110883E+15	1.48191568216921E+15	1.48191568174437E+15
203872000.0	1.48299223039647E+15	1.48299223052888E+15	1.48299223047580E+15
407744000.0	1.48326104136967E+15	1.48326104138622E+15	1.48326104137957E+15
815488000.0	1.48332818800946E+15	1.48332818801152E+15	1.48332818801069E+15
∞	1.48335051422818E+15	1.48335051422818E+15	1.48335051422818E+15

Table 37: *Dependence of composite mass on distance per prior CASE_2 and comparison using constant Newtonian speed v_{rN} , static speed v_{rPGs} and composite speed v_{rPGc}*

r , m	m_{erc} kg, with v_{rN}	m_{erc} , kg with v_{rPGs}	m_{erc} , kg with v_{rPGc}
12742000	1.38483965472048E+27	1.38484024790860E+27	1.38484000145102E+27
25484000	1.46003136003934E+27	1.46003142930937E+27	1.46003140133446E+27
50968000	1.47759250212494E+27	1.47759251064261E+27	1.47759250722585E+27
101936000	1.48191564673190E+27	1.48191564779228E+27	1.48191564736744E+27
203872000	1.48299222827079E+27	1.48299222840320E+27	1.48299222835012E+27
407744000	1.48326104123612E+27	1.48326104125267E+27	1.48326104124602E+27
815488000	1.48332818800111E+27	1.48332818800317E+27	1.48332818800234E+27
∞	1.48335051422818E+27	1.48335051422818E+27	1.48335051422818E+27

Table 38: *Dependence of composite mass on distance per prior CASE_3 and comparison using constant Newtonian speed v_{rN} , static speed v_{rPGs} and composite speed v_{rPGc}*

$r = 12742000 \text{ m}$				
$g_0 =$	1000	10000	50000	100000
A_R	v_{rPGc}/v_{rN}	v_{rPGc}/v_{rN}	v_{rPGc}/v_N	v_{rPGc}/v_{rN}
1.0E-13	0.117236	0.117236	0.117236	0.117236
1.0E-12	0.206925	0.206924	0.206924	0.206924
1.0E-11	0.359383	0.359376	0.359375	0.359375
1.0E-10	0.593533	0.593498	0.593495	0.593495
1.0E-09	0.851810	0.851676	0.851664	0.851662
1.0E-08	0.976295	0.976050	0.976028	0.976026
1.0E-07	0.997716	0.997443	0.997419	0.997416
1.0E-06	1.000046	0.999770	0.999745	0.999742
1.0E-05	1.000281	1.000005	0.999980	0.999977
1.0E-04	1.000304	1.000028	1.000004	1.000000
1.0E-03	1.000307	1.000030	1.000006	1.000003
1.0E-02	1.000307	1.000031	1.000006	1.000003
1.0E-01	1.000307	1.000031	1.000006	1.000003

Table 39: *Speed ratios against absorptivity at selected values of g_0 using Earth as the gravitating body with a falling sphere from “infinite” distance to a perigee of $r = 12742000 \text{ m}$*

the kinetic mass overtakes the positional net loss of mass; this happens when A_R is very small.

Equivalently, we next plot the same speed ratios v_{rPGc}/v_{rN} against absorptivity for a set of final distances starting from infinity in Fig. 61(a). We note that all curves shift closer to Newton speed at long final distance. This is again important indicating that Newtonian mechanics can be applied at long enough distance from planets in interplanetary travel, but a modification becomes due as we approach a planet. The same effect is re-plotted in (b) of the same figure showing the variation of speed ratio against distance at selected absorptivities. While all graphs start from greater than unity ratios at long enough distance, they invariably undershoot unity at shorter distance. The deviation is quite large raising concern about the veracity of such outcomes.

The above are generalizations of situations similar to CASE_4. We get a better feel also by choosing for comparison two different materials of beryllium (Be) and lead (Pb) with diameters even smaller than 1 m. A similar deviation can be seen if we plot the same speed ratio against the radius of the falling sphere per Fig. 62a, since radius and absorptivity are interdependent. Corresponding to this, we further plot the absolute speed of these spheres in a smaller (more practical) range of radii in 62b.

We don’t have data of falling bodies from “infinity” to compare with the numerical values between “experiment” and our findings and see if these outcomes are correct or even reasonable. However, we have applied Eq. 403 for sets of falling spheres from a height of 10 m on the surface of Earth at a guessed $g_0 = 40000 \text{ ms}^{-2}$. We used the example of Be and Pb materials with sphere diameters 0.001 m, 0.01 m and 0.1 m. The time difference $\Delta t = t_{Be} - t_{Pb}$ is found to be 0.017394 s, 0.001782 s and 0.000179 s correspondingly. These values clearly fall within the detectable time range and cannot be accepted. However, while these values are no good, they are not “catastrophic” either, in the sense that their discrepancy can be manageable. The numerical values plotted are no reason to reject or abandon the preceding theory, because they can be explained by the assumptions from which the equations were deduced. The equation of speed based on positional variation of mass (static speed) always yields ratio values above unity. The transition to below unity values by the equation for the composite speed is due to the accrual of mass in excess of the positional loss. We used the conventional equation between kinetic and potential energy, so that for any fixed potential energy between two points, an increase of mass would result in a reduction of the end speed. The increase of mass by use of 403 is determined by the applied conjecture of Eq. 348, but the increase of mass would be a lot less if we had used Eq. 349 with $n = 4$ as seen by Fig. 54. In the latter case, the composite speed would be considerably higher and closer but always below the static speed. There is an interplay between the two

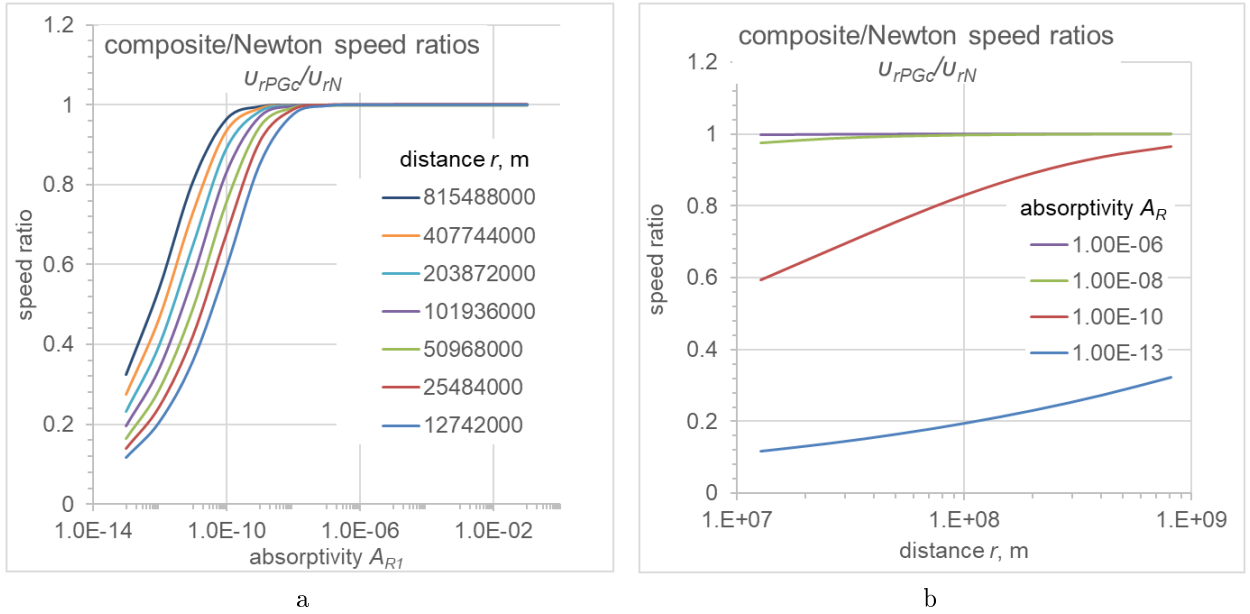


Figure 61: Ratio of speeds (a) against absorptivity at fixed final distances and (b) against distance at fixed absorptivities of the falling body

speeds, which we hope it to be such that to bring the theory in agreement with reality. The problem would still be that the effects would remain undetectable for falling bodies from a height of 10 (or similar) meters, but they might become detectable from an interplanetary “height” fall.

There are additional parameters requiring adjustment and determination, such as the true value of g_0 that is to be used in our work. We can see this by plotting the final falling velocity from 10 m height v_{10c-Pb} of the lead sphere, the same v_{10c-Be} of the beryllium sphere and their difference $\Delta v = v_{10c-Pb} - v_{10c-Be}$ against a wide range of g_0 values in Fig. 62c. This is done for the middle radius $R_1 = 0.01m$, but similar (almost inversely proportional) is the situation for the other radii too. Therefore, there is ample room for adjustment of the theoretical parameters to meet reality. This is an important conclusion confirming an early corollary of Section 14.3 that “All bodies fall at equal rates... if and only if they have the same contraction factor q ”, which relates to the same absorptivity. The problem is that the classical experiments of measuring velocity involve bodies all having practically equal absorptivities and thus not measurable by our equipment. If we had a body with an unusually high density for comparison, then we would have detected the difference.

It might also be said that meteors and comets provide data that do not (presumably) support any deviation of speed from that worked out by applying Newtonian mechanics. However, the question here is about their mass, not just speed and trajectory. How do we measure their mass? Is it measured by reliable independent means or is it deduced by applying/relying on the Newtonian laws of motion? How do we know if their effective mass thus deduced is not a composite type of mass as introduced herewith? The question of mass is a key question in modern physics and applies to all moving bodies in astronomy and elsewhere. We have introduced a new conception of mass that can be put to the test by numerous proposals throughout this report. The different kinds of mass in Table 31 might be explained by and correspond to different material structures. We continue with modeling of the electron and positron in a following Section 25 with some interesting possibilities. The role of kinetic mass might be connected with to propulsion of a body to motion with some degree of contribution to the ideas of inertia, action-reaction, etc; i.e., it might have a dual function. It might play a role in offsetting the graviton “drag”. So far, the theory is incomplete pending further development but mainly pending experimental research like the newly proposed next.

23.2.4 Interplanetary testing of falling speeds: Effect of shape, direction and contraction factor

The preceding findings lend themselves for another possible verification of PG theory involving tests during interplanetary spacecraft trajectories. A recent “space test of the equivalence principle” (STEP) with orbiting satellite measurements failed to establish any deviation from the Equivalence Principle (Touboul *et al.*, 2019). However, this negative outcome is consistent with our PG theory: We found that the real and effective mass of an orbiting object remains constant for all spherical objects and densities, whereby the associated speed and acceleration should be invariable for all objects. However, we should expect a continuous net variation of

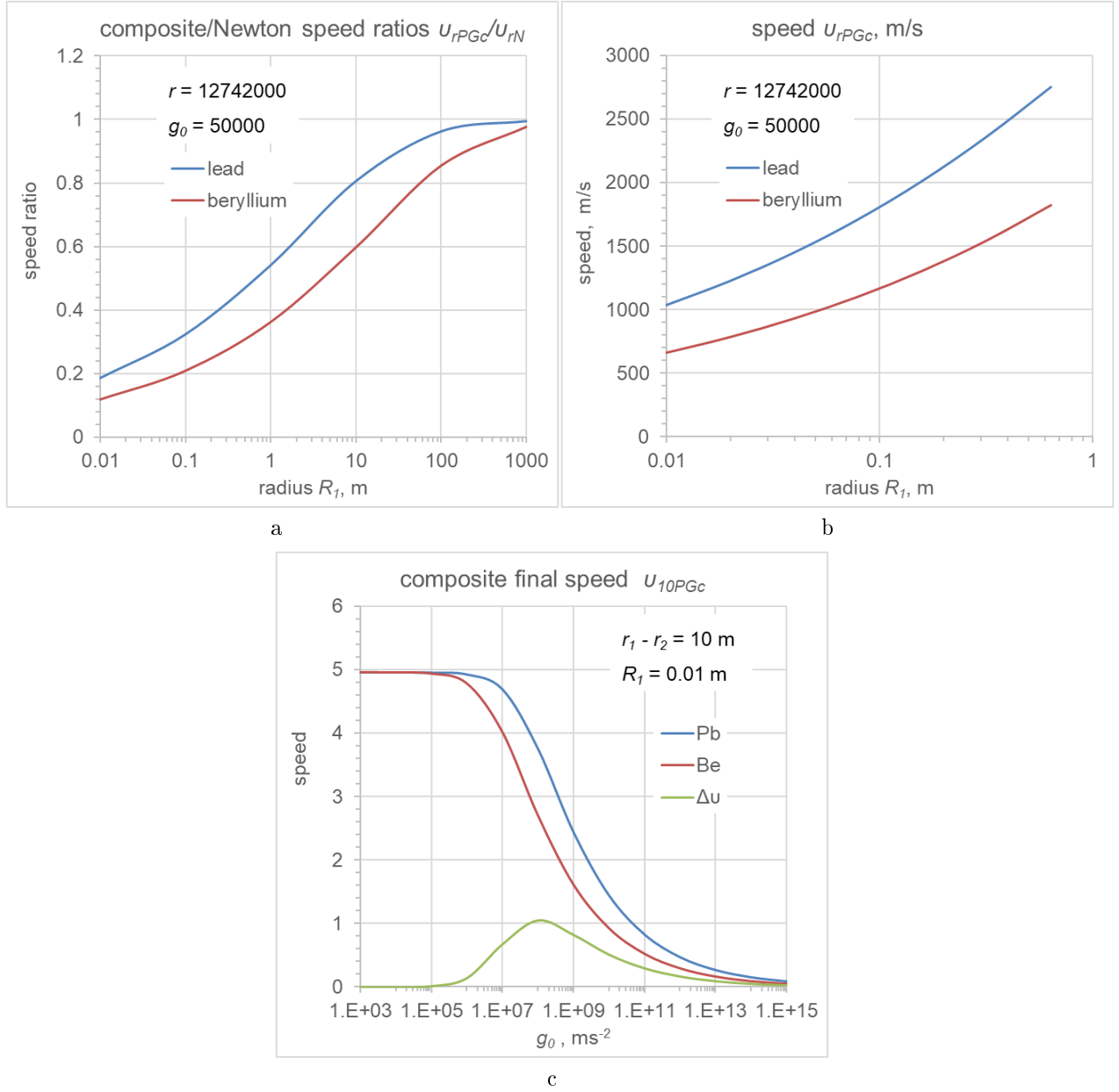


Figure 62: Comparison of final speeds for beryllium (Be) and lead (Pb) spheres falling from infinity to $r = 12742000$ m against falling sphere radius in the form of (a) Speed-ratio v_{rPGc}/v_{rN} and (b) absolute composite speed v_{rPGc} . (c) Final falling speed from 10 m height of beryllium and lead spheres with $R_1 = 0.01$ m together with their difference Δv plotted against universal acceleration g_0 .

mass during fall in an interplanetary trajectory with an associated variation of speed, which can be subjected to the test by an experiment. Even the incomplete solution of Eq. 403 predicts different falling speeds. Also, even if there is no connection between speed and mass, the first Eq. 397 completed with the absorptivity of both bodies in a future correction predicts different speeds with a measurable effect over a long falling trajectory.

In fact, we have found that not only different density bodies fall with different speeds, but different size objects of the same material would also fall at different speeds, because they present different absorptivities (per Fig. 62a&b). We note that the effect of radius may be even greater than the effect of material nature, per (a).

Based on the above finding, we could perform a variety of experiments involving different combinations of body shapes, sizes and materials. Indicatively, we have illustrated some examples in Fig. 63. We show a pair of two equal radius spheres (#3 and #4) of lead and beryllium per preceding analysis, but also added two identical flattened bodies (#1 and #2) with one oriented parallel and the other perpendicular to the direction of fall. The experiment is supposed to take place between two rocket firings for correcting the trajectory, so that the fall is always free of disturbance by rocket force. We should choose this trajectory, if possible, to be the last leg of fall in an inbound trajectory with the longest possible pause of rocket engine activity.

The pair of flat bodies shown could have the shape of disk or any other convenient shape. However, this is a different case than the spherical geometry we have worked with so far. We would need to repeat the same PG computations by replacing the sphere with another desirable shape. One candidate shape is that of an oblate spheroid as depicted in Fig. 63 by #1 and #2. It is not immediately obvious if those two bodies would deviate or not during fall. We might initially think that the first (#1) with its major axis parallel to the direction of acceleration would fall faster, if it is associated with higher absorptivity. However, the subtended angle is smaller than the second body (#2), so that the combination of solid angle and absorptivity might cancel each other out. Both of these identical bodies (#1) and (#2) have equal lone absorptivities very far away from a planet, so that it is not obvious if they would retain equal absorptivities in different direction inside the gravitational field. The variation of static effective mass at different proximity locations from a planet need to be worked out using the methods presented in the Appendices by replacing the spherical geometry with spheroidal one. The non-obviousness of the effect of falling orientation can be appreciated by considering the overall picture of macroscopic and microscopic structure of any given geometry body: Fig. 64 conveys an idea for the case of a “rod” in continuation of the configurations of prior Fig. 35. The shielding (depicted by shading) of the absorption centers is greatly exaggerated for demonstration only of the envisaged effects on absorptivity in the three situations involving the same amount of particles; the dark (gray) shading illustrates the amount of black matter created when the rod moves from infinite distance to a given approach inside the gravitational field of a planet. The effect is shown approximately and grossly exaggerated to demonstrate the change of black mass (and absorptivity) with a change in configuration or rod direction relative to the direction of the surrounding gravitational field. Actually, a single-stranded rod of MACs would have an infinitesimally different absorptivity at different orientation (the solid angle being infinitesimally small), but as we add strands to build a macroscopic rod, the difference may become measurable. At any rate, the study of relative orientation could be included in the experiment to confirm or disprove in advance theoretical computations.

Judging from the “STEP” experiment, the complexity of practical details involved is appreciated. These details might be the same, simpler or even more complex in the proposed test here. For example, spinning the disks might be an option for maintaining orientation, but it might complicate an as yet unknown effect on the mass-energy relationship during fall. This and other parameters require prior, during, or a post experiment assessment.

The influence of orientation during free fall, if real, would have important theoretical ramifications but may also have important practical applications. We suggested in Section 14.3 that changing the orientation between the inbound and outbound leg of the trajectory during a flyby mission could result in a difference of speed at corresponding points of the two legs. That was based on the assumption that the spacecraft is made to exhibit a greater effective mass in one part of the orbit than in the other, but this remains both theoretically and in practice unproven. Another possibility was to vary the mass configuration by way of an opening or folding fan-like system.

Yet another conceivable mechanism for performing such a test is shown by the collapsible sphere of a toy shown in Fig. 65. The effective mass is greater in the expanded form (a) than in the collapsed form (b). The transformation between the two forms (collapsed and expanded) involves the supply (or release) of some energy commensurable with the associated gravitational field of the toy sphere itself. The amount of this energy must be extremely minute in comparison with the energy involved during fall of the same toy sphere towards a planet. The preceding findings that the falling speed is a function of absorptivity (or

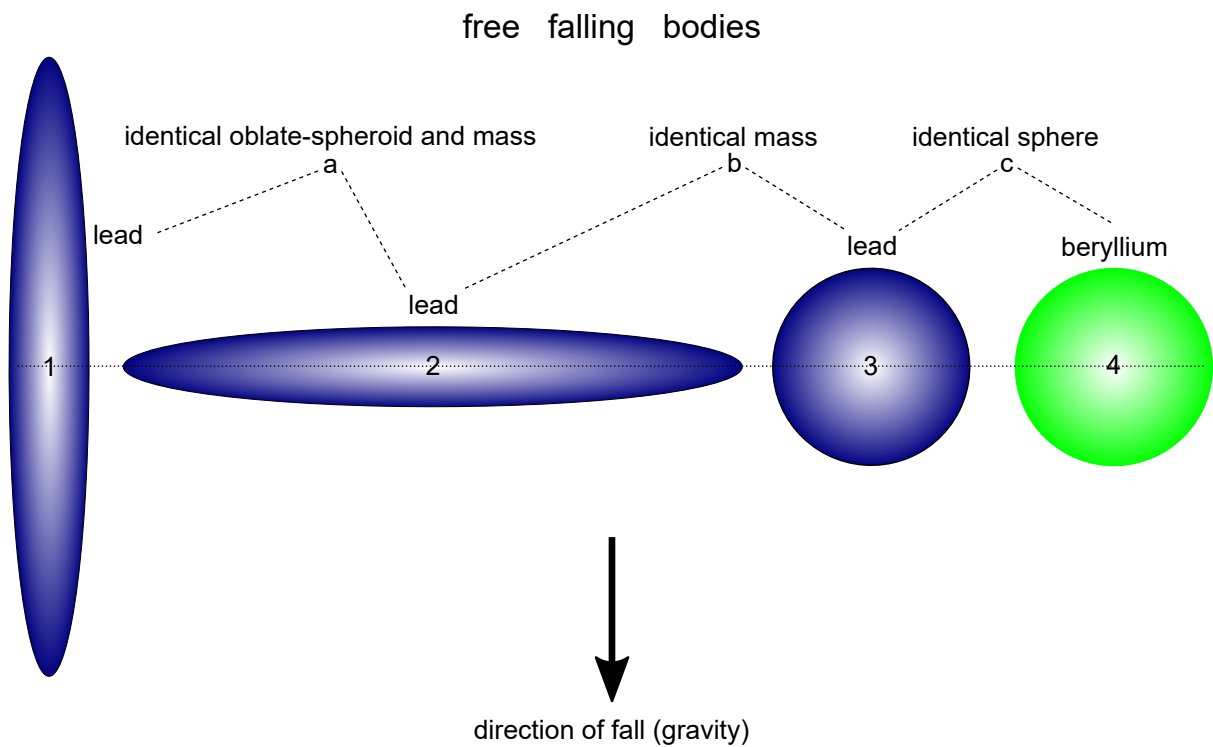


Figure 63: *Inter-planetary spacecraft experiment with four (1, 2, 3, 4) free falling bodies in pairs of (a) identical oblate spheroid masses with different orientation, (b) equal masses with different shapes and (c) equal sphere size but different materials.*

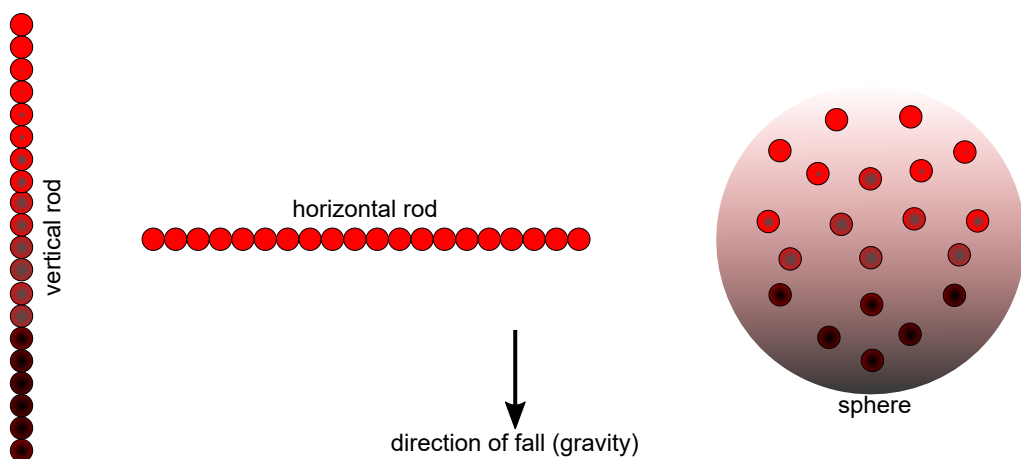


Figure 64: *Absorption centers (MACs or particles) fixed in a rod configuration directed along the gravity direction (i.e. vertical), or perpendicular to it (i.e. horizontal); same particles re-distributed in a spherical configuration*

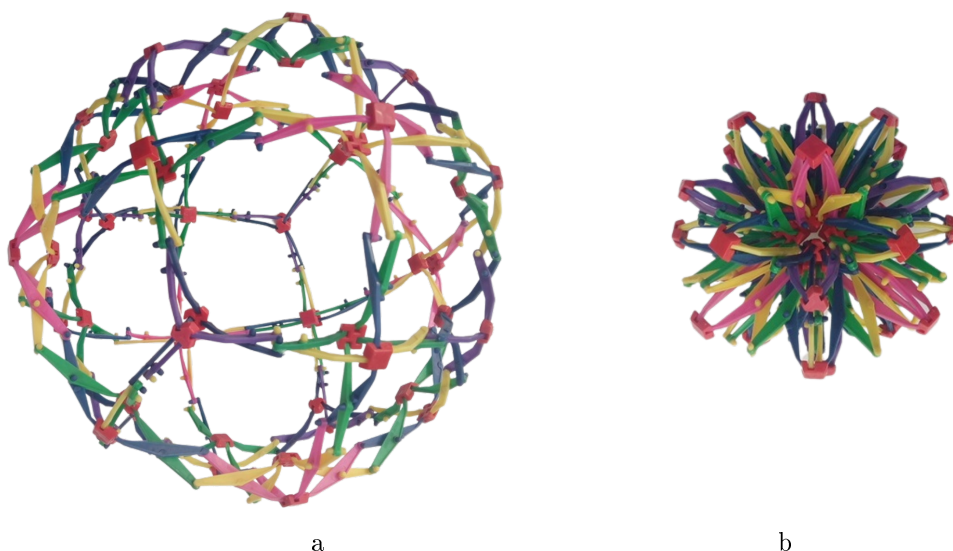


Figure 65: *Toy sphere in (a) expanded form and (b) collapsed form*

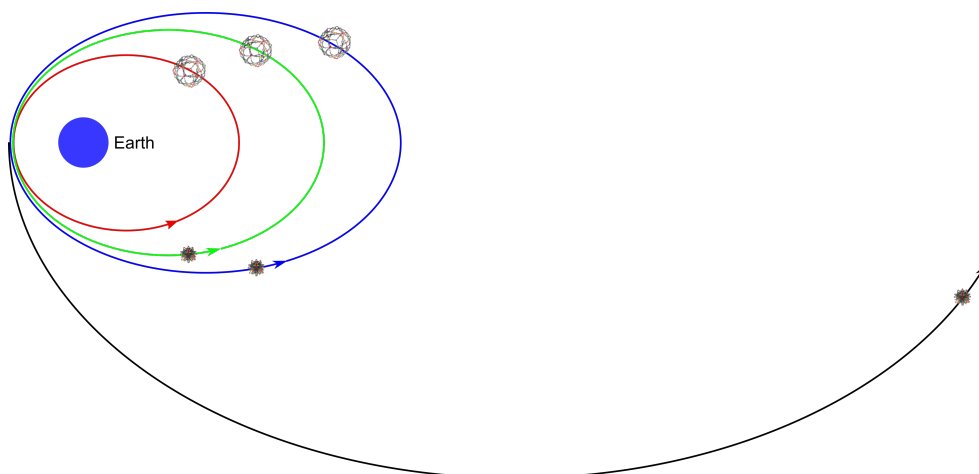


Figure 66: *Schematic of principle: Cascade flyby acceleration and escape velocity obtained with the “toy sphere” falling towards the perigee in the expanded configuration while ascending towards the apogee in the contracted configuration (simplified and exaggerated trajectories)*

contraction factor) implies that if we can somehow vary the absorptivity during flight, then we should also vary the speed, if we are to preserve the energy of the body. That means that we can brake or accelerate the body accordingly. The effect may be very small if we can vary the absorptivity only by a very small amount, but over a long flight, the cumulative effect should be measurable. Furthermore, *“This would result in incremental accretion of energy until it can reach escape velocity and then repeat the same process around a bigger planet (e.g. Jupiter), or the Sun”*, per early statement of Section 14.3. We understand that if two spheres like that, one expanded and the other collapsed, start together at the apogee, they should both return at the apogee simultaneously, but they would pass around the perigee at different times: The contracted one would pass before the expanded one, but then the faster one would decelerate faster during the outbound leg so that the expanded one will catch up and arrive at the same time at the apogee. Now, if we consider one only sphere to start in the expanded configuration at the apogee all the way to the perigee, whereupon it contracts, it should reach and surpass the apogee where it started from. This is because it would have a lesser potential energy than it started with, so that it can continue the “ascend” to a new apogee before it starts a new descend. However, around the new apogee, it could expand again to increase its effective mass. This will be done at the cost of only a practically negligible energy. Doing so is like “inhaling” mass via graviton absorption, which results in an increased potential energy at the new apogee at negligible cost.

We can build on the preceding description as with reference to Fig. 66. We initially spend energy

to establish an elliptical orbit, say around Earth, by a spacecraft equipped with a mechanism to vary its absorptivity in a manner analogous to the toy sphere. The initial (innermost) elliptical orbit (in red) is established in the expanded configuration at the cost of given rocket energy. Then we can initiate and repeat a series of the previously described sequence of maneuvers: At the perigee, it collapses and travels all the way to a new greater apogee, whereupon it expands again to travel to the perigee, whereupon it collapses, and so on. This is repeated a number of times, resulting in a cascade gain of apogee distance. We have likened the actions at the apogee and perigee to “inhaling” and “exhaling” mass, in and out. We have suggested it to be an equivalent process taking place like with a heat pump, whereby an electrical motor pumps heat (energy) “out of thin air” at a small cost. Our analog is pumping mass out of the gravion gas. There are more details around the orbit to contend with, but they all cancel out in the overall scheme. For example, we can ignore the gain or loss of kinetic energy from the tangential component of velocity at the apogee, because it is generally less from the corresponding tangential kinetic energy at the perigee. Now, the trajectories drawn in the figure are simplified to demonstrate the principle and the intended effect, but the flight engineer can later draw the correct ones. We have not accounted for possible precession and distortion from symmetrical shapes due to the variation of velocity at the corresponding points.

The presence or not of a concurrent variation of kinetic mass would not change the overall outcomes of the above proposed scheme.

To avoid disappointment for a forthcoming (anticipated) “free” space travel, we must warn that the above described effect may be so small that it might take 100 years to achieve some moderate increase of apogee with current technology for shape transformation. However, if we could find means to effectively vary the density (to contract and expand) of an orbiting spacecraft, then the promise could become rewarding. In the meantime, the practical benefit of PG speed variation might be in controlling trajectories over a long haul accordingly by accelerating or braking a spacecraft with minimal (negligible) energy expenditure, provided the total effect is significant. The latter is to be quantified in later PG theory and engineering. Also it could furnish direct explanation for the flyby anomaly and perhaps for the Pioneer anomaly as well. We should investigate if it can also explain, at least in part, the Mercurian precession. Above all, the immediate benefit would be to validate our PG theory, which would place us in an advantageous position to progress in many other areas of scientific and technical endeavor.

23.3 Speed addition

If our theory is verified, then we have effectively arrived at a novel way to compose speeds according to Eq. 354. This supplies an alternative solution to the speed transformation in special relativity.

The actual speed of a body depends on and is limited by the composite absorptivity possible. The upper limit of absorptivity is unity, which imposes an upper limit to the effective mass and the associated speed, since the two are one-to-one connected. With given intrinsic absorptivity A_R , the kinetic absorptivity $A_{R\kappa}$ can only be in the range:

$$0 \leq A_{R\kappa} < 1 - A_R \quad (405)$$

which provides also a limited range for the real speed:

$$0 \leq \frac{v^2}{c^2} < 1 - \frac{v_0^2}{c^2} \quad \text{or} \quad 0 \leq v^2 < c^2 - v_0^2 \quad (406)$$

In other words, the intrinsic speed v_0 takes on a real meaning in the sense that it sets a handicap for the real speed of any given body: A heavy (dense) body cannot go as fast as a light body. In all this, it is implied that zero real speed is with reference to the gravion medium. A passenger in a train with real speed v_1 has already committed a composite value of speed over and above the intrinsic one before boarding the train. The passenger moving forward (or shooting a bullet) with additional speed Δv will find it more difficult to acquire that additional speed than prior to boarding the train (provided any subtle differences could be measured no matter how small they would be). The additional speed will result in a real speed $v_2 = v_1 + \Delta v$ to be computed with reference to the stationary gravion system, giving:

$$\frac{v_1^2}{c^2} = A_{R\kappa 1} = A_{Rc1} - A_{R1} \quad (407)$$

$$\frac{v_2^2}{c^2} = A_{R\kappa 2} = A_{Rc2} - A_{R2} \quad (408)$$

$$\Delta v = v_2 - v_1 = c\sqrt{A_{R\kappa 2}} - c\sqrt{A_{R\kappa 1}} = c\sqrt{A_{Rc2} - A_{R2}} - c\sqrt{A_{Rc1} - A_{R1}} \quad (409)$$

which is the speed seen by the moving train reference. This gives the “transformation” (better the real speed) of v_2 relative to the stationary (absolute) system and Δv relative to the moving (train) system. The addition of speeds is straightforward with the provision that they cannot acquire arbitrary values other than those constrained by the absolute stationary medium.

When we establish another suitable equation to relate speed with absorptivity (and effective mass) in lieu of the conjectured Eq. 348, then we can adjust and expand the above equations accordingly.

23.4 Review and discussion

The present Section 23 is effectively a first attempt to usher some dynamics in PG theory initially developed only for stationary bodies. It is sort of an introductory rehearsal for the deferred Section 14 towards a dynamic push gravity theory. It is only a trial attempt based on a conjectured relationship between speed and mass, which we hope to approach from more fundamental principles in later development. In any case, the attempt remains to be completed with further work using more detailed mathematical analysis and accompanying computations. The preceding presentation contains some simplifying assumptions and relationships that we discuss below by way of alerting to remaining issues.

The absorptivity formula used in Eq. 349 was derived for a stationary lone sphere under omnidirectional graviton flux with spherical symmetry. Gravitons are being absorbed with radial depth of penetration converting “neutral” (inactive) real mass to effective mass. By the introduction of speed of a sphere, we may not assume that the spherical symmetry of the distribution of effective mass is maintained. Intuitively, we may expect a distribution of the total effective mass towards axial symmetry around the direction of velocity, but this is not clear (for now) how it takes place. It is not clear whether the intrinsic effective mass of the lone sphere is redistributed lumped together with the kinetic mass accrued at any given speed, or the kinetic mass accrued is superimposed to the lone mass. We accept that the kinetic mass must be reversible (added or subtracted) as a function of speed, which is the reason why we introduced the term “kinetic” mass to separate it out from the “intrinsic” mass. The kinetic mass must also be such that it counteracts (neutralizes or bypasses) the drag expected to appear from classical considerations. Possibilities for this to happen are canvassed in Section 25. It is difficult to envisage such mechanisms operating on amorphous matter. This prompts us to hypothesize the existence of some suitable structures around (or by) the minimal absorption-and-emission centers (MACs-MECs). One candidate structure is the vortex, which we also attempt to introduce for modeling the electron and positron in the following section. Vortices are built around axial symmetry, which we need during the introduction of kinetic mass.

In considering the free fall acceleration vis-à-vis the rocket acceleration, we have an overlap of common issues, but we also have unique issues with each of these situations. In rocket acceleration, we can understand the accrual during acceleration and radiation (release) of mass during deceleration. The addition and subtraction of mass takes place via an electrical field by the rocket. However, in free fall acceleration, the graphs show a net radiation (release) of mass, which is surprising. We can understand that the effective mass decreases with position and concurrently increases with falling speed, but any variation of total mass begs further questions and investigation. In fact, this is another opportunity to see the difference between rocket acceleration and falling acceleration, contrary to the Equivalence Principle.

To address the above concerns, it has been necessary to further study the mass-matter relationship by expanding our PG in the following Section 24. Before that, we need to spell out the details of how various parameters have been calculated and graphed for the falling body in the current section. We do so even if all the equations have been known and often applied in preceding work.

From given k and R for each sphere, we obtain the intrinsic (lone) values at infinite separation distance $r = \infty$ for A_{R_1} and A_{R_2} from the general equation:

$$A_R = 1 - \frac{1}{2k^2 R^2} + \frac{\exp(-2kR) \cdot (2kR + 1)}{2k^2 R^2}$$

The corresponding contraction factors q_1 and q_2 from the general equation:

$$q = \frac{3A_R}{4kR}$$

The corresponding effective masses $m_e \equiv m_{e1}$ and $M_e \equiv m_{e2}$ similarly from:

$$m_e = \frac{g_0 A_R R^2}{G}$$

The corresponding real masses $m = m_1$ and $M = m_2$ from:

$$m = \frac{m_e}{q}$$

After that, we need to decide what speed to use during fall, like Newtonian speed v_{rN} , PG static speed v_{rPGs} , or PG composite speed v_{rPGc} , so that we can calculate the kinetic absorptivity $A_{Rr\kappa}$ at distance r from:

$$A_{Rr\kappa} = \left(\frac{v_r}{c}\right)^2$$

where we adopt Eq. 349 with $n = 2$.

The corresponding kinetic (effective) mass $m_{er\kappa}$ from:

$$m_{er\kappa} = \frac{g_0 A_{Rr\kappa} R^2}{G} \quad (410)$$

The total (composite) effective mass from:

$$m_{erc} = m_{er} + m_{er\kappa}$$

where m_{er} is the static effective mass at r computed per Appendix E. From the latter, we find a static absorptivity A_{Rr} :

$$A_{Rr} = \frac{G m_{er}}{g_0 R^2} \quad (411)$$

and a composite A_{Rrc} at r from:

$$A_{Rrc} = A_{Rr} + A_{Rr\kappa} \quad (412)$$

Then we can find the product $k_c R$ for the composite absorptivity by solving the equation:

$$A_{Rrc} = 1 - \frac{1}{2k_c^2 R^2} + \frac{\exp(-2k_c R) \cdot (2k_c R + 1)}{2k_c^2 R^2}$$

from which we find the contraction factor for the composite mass:

$$q_{rc} = \frac{3A_{Rrc}}{4k_c R}$$

The latter is used to find the real mass at r m_{rc} from:

$$m_{rc} = \frac{m_{erc}}{q_{rc}}$$

Then the total black mass in motion at this distance r m_{brc} is:

$$m_{brc} = m_{rc} - m_{erc}$$

and the loss of real mass m_{rcloss} from:

$$m_{rcloss} = m - m_{rc}$$

For the static parameters, we correspondingly find first the static product $k_r R$ by solving the equation:

$$A_{Rr} = 1 - \frac{1}{2k_r^2 R^2} + \frac{\exp(-2k_r R) \cdot (2k_r R + 1)}{2k_r^2 R^2}$$

and then we get the static contraction factor q_r at that distance:

$$q_r = \frac{3A_{Rr}}{4k_r R}$$

The static real mass m_r :

$$m_r = \frac{m_{er}}{q_r}$$

The static black mass m_{br} :

$$m_{br} = m_r - m_{er}$$

Finally, the loss of static real mass m_{rloss} is obtained from:

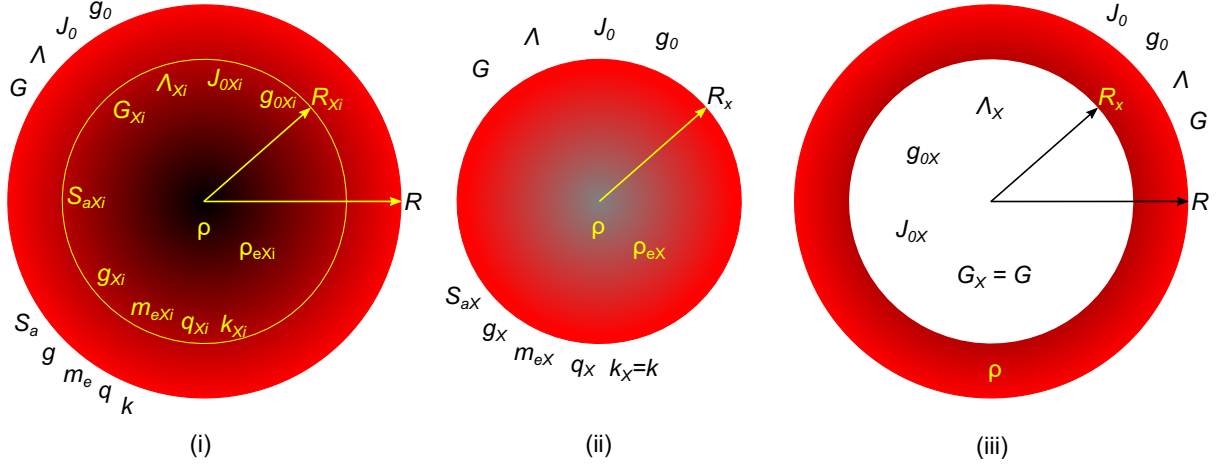


Figure 67: *Internal vs. external spherical parameters and gravitational fields.*

$$m_{rloss} = m - m_r$$

The provision of exactly all the equations used in producing the graphs in this section may now help the reader to better stay in tune with what they mean. Our main concern above regards both Eqs. 411 and 412, whereby we insert the equation of absorptivity as it applies for lone bodies with effective masses distributed around a spherical symmetry. This is not the case for a falling sphere, where m_{er} must be axially distributed around the axis of fall, and $m_{er\kappa}$ is a new unknown type of mass with probably also a distribution around the same axis of fall. Therefore, the derivation of a composite absorptivity A_{Rrc} based on the equation for a lone body is only simplifying but arbitrary. Therefore, some of the graphs in this section (e.g. the total real mass) should be treated with caution until we can find an alternative approach for a dynamic PG. It is ascertained that m_{er} is correctly computed as a total mass following an integration, but we could also establish its distribution during the integration in future work. These concerns prompt us to undertake further work in the following section and return to them afterwards.

24 Mass-matter relationship

This theory has continually evolved from simple absorption relationships producing parameters with new understanding and without a priori knowledge. For example, the concept and parameter of “real mass” was necessitated as a substrate to facilitate the absorption of gravions. This led us to distinguish it from the “effective mass”, which is the activated component bearing the classical inertia as opposed to the remainder component that must be inertia-less and thus termed as “black mass”. This then has necessitated the understanding of black mass and its association with the assumed substrate; by the same token, we need to understand the association of all forms of mass with a presumed common substrate. In order to achieve this, we need to further develop the meaning and relationships of these and other parameters inside a material sphere including their connection to corresponding equations outside the sphere “in vacuum”; then we can attempt to find the desired association with the said (presumed) substrate (or matter).

We have already produced the variation of internal acceleration of a sphere in Section 8. We did the same in Section 14.6 with emphasis on the outermost layer of a very dense spherical body, after which we introduced (arrived at) the concept of black mass. It is now pertinent to review, refresh and generalize those relationships including others inside a material sphere. Since the intensity of radiant flux of gravions remains unknown, we have to theoretically continue on varying this parameter and find how all else vary with this. Equivalently, we can vary any other interdependent parameter that may be more suitable to understand or experiment with and deduce all others therefrom. In this Section, we opt to maintain a constant (fixed) real density ρ inside a fixed radius R of sphere as a more “tangible” approach in deriving the other parameters. For example, Eq. 118:

$$k = \frac{\pi G \rho}{g_0} \quad (413)$$

yields an inverse relationship between k and g_0 so that by choosing a series of values for k , we can find or imply a corresponding series of values for g_0 in a region of the universe with constant G and given ρ .

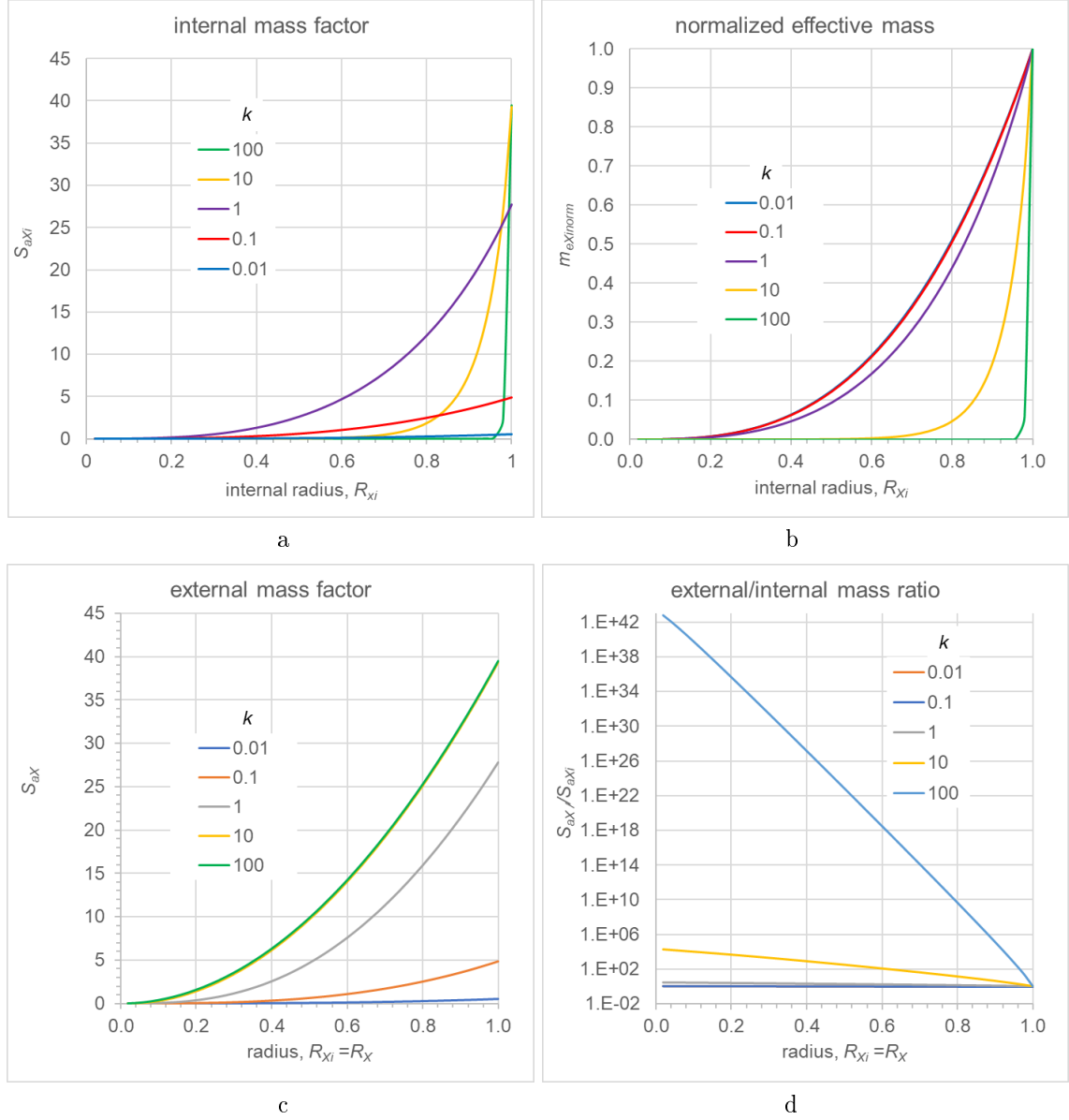


Figure 68: *Internal and external mass factors, internal effective mass and ratio of external/internal mass.*

Alternatively, for a given g_0 , we can choose a set of fixed values of k to which correspond a set of fixed values of ρ . We establish fundamental equations and theorems as an introduction to later analysis of more complex systems. The main purpose is to consolidate our understanding of the physical meaning of novel parameters that will reappear in future developments; it will be appreciated below that the physical meaning becomes convoluted and sometimes confusing as we move from external (vacuum) to internal condition with a given material density.

We reproduce the schematic representation of a massive star from Fig. 33 now in Fig. 67 with the aim of quantifying the schematic color shading of the internal properties. This figure illustrates three situations:

- (i) The variation of various parameters (properties) at any internal point X_i inside the sphere such as radius R_{Xi} , effective mass m_{eXi} , Λ_{Xi} , etc. in contrast to the external ones R , m_e , Λ , etc.; we introduce the subscript (i) for the internal parameters.
- (ii) The creation of a new “external” partial sphere from the internal partial sphere with the same radius, namely, with $R_X = R_{Xi}$, in order to find the relationship of the parameters between these two spheres; we compare various internal parameters with corresponding ones for spheres of the same radius and real density but without the outer shell, i.e. for spheres exposed to the influence of the “vacuum” g_0 as opposed to the internal spheres exposed to an internal g_{0Xi} .

- (iii) The removal of the material of the internal sphere leaving a hollow space (“vacuum”) with corresponding parameters characterizing a new internal “universe” surrounded by a material shell absorbing (shielding) in part the external graviton flux.

The subscript (i) helps avoid ambiguity and is used even if it may be redundant (obvious that something is internal), the absence of which refers to a sphere exposed to external “vacuum”. Thus, R_{Xi} replaces the R_X in Fig. 7, and the fractional radius becomes R_{Xi}/R , where we always have $R_{Xi} \leq R$; R_X is herewith reserved for a free to vacuum sphere like in (ii) but with $R_X = R_{Xi}$.

We should note that the “internal” realm regards not only solid or liquid bodies but also gaseous bodies including the heliosphere, all of which are considered non-vacuum, whilst some allow the motion of other material bodies like planets. For the present purposes, we do not include the interior of subatomic particles (electrons, protons, neutrons, etc); we consider all bodies with a given distribution of matter that is fixed either by their chemistry or by fixed statistical processes like in gases and the heliosphere.

24.1 Internal vs. external parameters (constant real density)

For the internal spherical field in (i) of the above figure, we derived the variation of a few parameters against fractional internal radius (R_X/R) per Fig. 8, which we now complement by deriving also the distribution of other parameters for a general case, starting with the effective mass and density.

Mass We examine the distribution of effective mass with radius. The computed characteristic absorption area S_a for any sphere continues to mean S_{aR} for the external total sphere (with R) to be distinguished from S_{aR_X} for the external partial sphere (with R_X) and $S_{aR_{Xi}}$ for the internal partial sphere (with R_{Xi}). In Appendix D.2.2, point O always refers to an internal point defining an internal radius over which we integrate; that is, R_O now strictly refers to an integration variable in the range $0 \leq R_O \leq R$, or $0 \leq R_O \leq R_{Xi}$, or $0 \leq R_O \leq R_X$.

Eq. 702 used for the total (external) sphere is now re-written for the external partial sphere as :

$$S_{aX} = \int_0^{R_X} M_{aO} \cdot 4\pi k R_O^2 dR_O \quad (414)$$

and for the corresponding internal partial sphere as:

$$S_{aXi} = \int_0^{R_{Xi}} M_{aO} \cdot 4\pi k R_O^2 dR_O \quad (415)$$

which multiplied by $\frac{1}{4\pi\Lambda}$ yields the internal effective mass m_{eXi} at radius R_{Xi} .

It must be noted that this (m_{eXi}) partial mass is different from the (total) effective mass m_e uniformly apportioned to the same internal radius, and stated by the expression:

$$m_{eXi-apportioned} = m_e \frac{R_{Xi}^3}{R^3} \neq m_{eXi} \quad (416)$$

whereby m_{eXi} is an actual effective mass by an actual internal absorption process, whereas $m_{eXi-apportioned}$ is a deemed effective mass from the outer (total) effective mass mathematically allocated; this distinction is needed during later derivations. The above notation is temporary and may later be replaced by a more consistent and more meaningful one after we take stock of the needs of this continually evolving theory.

For this and other parameters it will help our theoretical development to normalize them over their characteristic value at the outer surface. Thus, the normalized internal effective mass is:

$$m_{eXi norm} = \frac{m_{eXi}}{m_e} = \frac{S_{aXi}}{S_{aR}} \quad (417)$$

We apply the above definitions and derivations to obtain the effective mass inside a sphere for a set of fixed absorption coefficients k (and real density ρ): Thus, Fig. 68(a) shows the variation of factor S_{aXi} (being proportional to effective mass) and (b) the variation of the normalized factor over its maximum value at $R_{Xi} = R$ (being equal to the normalized effective mass). For this and all other parameters, we choose five indicative values for $k = 0.01, 0.1, 1, 10, 100 \text{ m}^{-1}$. By setting the outer radius equal to unity ($R = 1 \text{ m}$), the internal radius R_{Xi} at any point X is normalized over the outer sphere radius. At the lowest of values of k the variation is very small becoming negligible as we approach the Newtonian condition, whereas at the

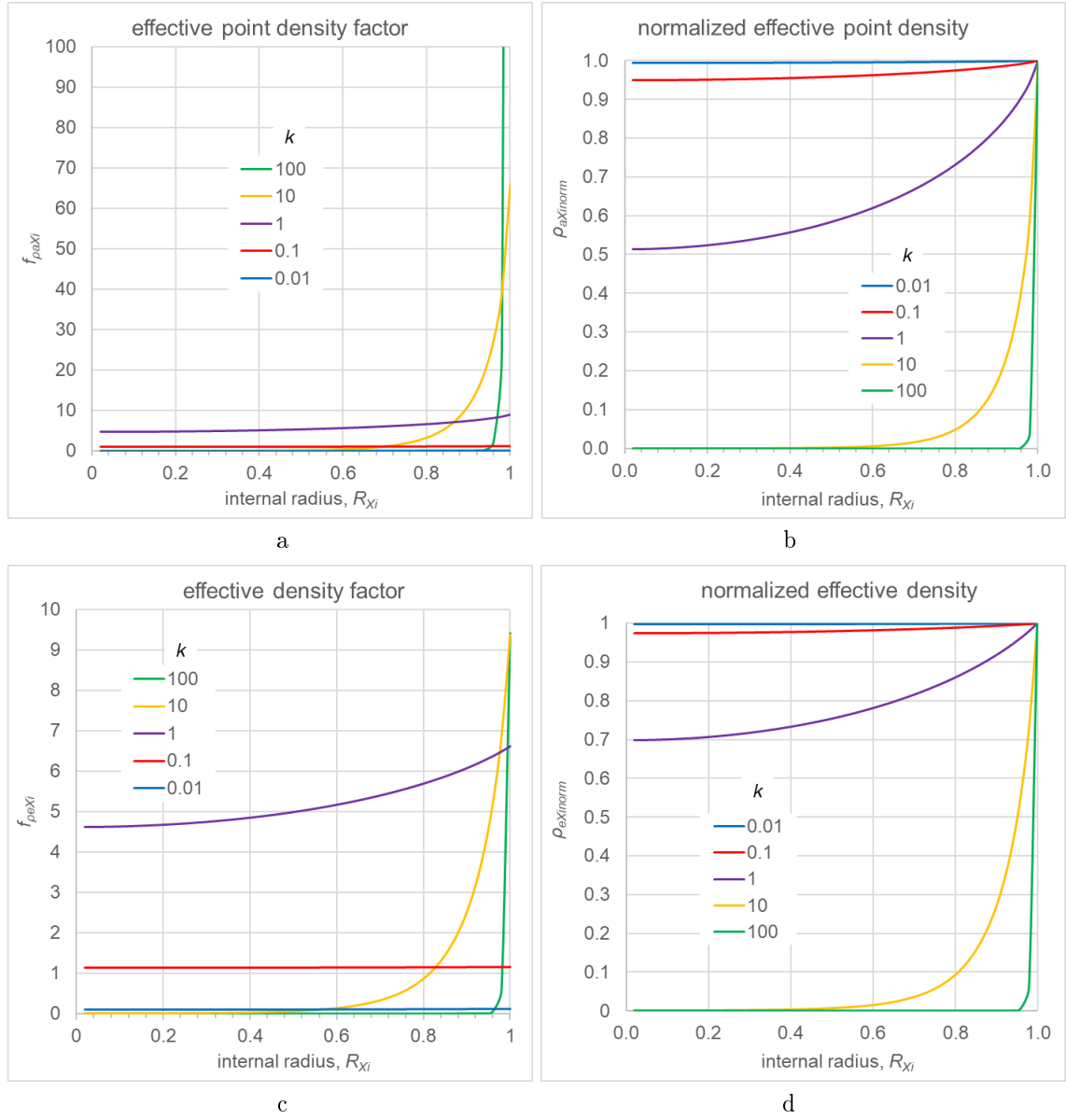


Figure 69: (a) *Effective point density factor*, (b) *normalized effective point density*, (c) *effective density factor* and (d) *normalized effective density*.

highest values the internal effective mass is concentrated very close to the outer radius with close to zero value elsewhere.

Unlike m_{eXi} , the real mass m_{Xi} at any internal radius is governed simply by a geometrical factor that uniformly apportions the total real mass:

$$m_{Xi} = m_{Xi-apportioned} = \frac{R_{Xi}^3}{R^3}m$$

and the normalized internal real mass is:

$$m_{Xi norm} = \frac{m_{Xi}}{m} = \frac{R_{Xi}^3}{R^3} \quad (418)$$

Now, with reference to Fig. 67 again, the extracted sphere (ii) has a different effective mass in the vacuum medium according to Eq. 414 as shown in Fig. 68c. The difference is more obvious by plotting the ratio S_{aX}/S_{aXi} in (d) of this figure. The acquisition of mass is negligible in the Newtonian regime, but it becomes increasingly significant to at high values for the higher and highest density spheres.

The real density ρ (and associated absorption factor k) used in the derivations herewith is (are) unknown in the first place. We obtain this from the well known equation:

$$g_0 A_R - g_R = 0$$

with the known (best if measured) acceleration g_R at the surface establishing the equation:

$$g_0 \left(1 - \frac{1}{2k^2 R^2} + \frac{\exp(-2kR) \cdot (2kR + 1)}{2k^2 R^2} \right) - \frac{4\pi G R \rho_e}{3} = 0$$

that is solved for the unknown k provided that we have establish the actual value of g_0 . In conventional physics, we assume that the measured density ρ_e is invariant with radius. However, we have shown that the effective density measured should vary with radius while it is the real density that is invariant. A variable measured density with radius may be thought to be contrary with experience, but we allege that this is due only to our inability to measure extremely small density variations with sufficient accuracy for Newtonian bodies. If we could know the true effective density of a given spherical material with different radii, then the above equation would yield a constant absorption factor k and a constant real density for the given material. In all this, we also assume that there is no phase transformation (transition) and that the given material nature is invariant with radius. The latter assumption would be true over a certain radius range. In other words, we need only one good (sufficient) measurement of the density at a given radius with which we find the real density (and k) of a material, after which we can calculate the effective density with any other radius at constant k according to Fig. 69. All this necessitates that we have previously established the actual prevailing value for g_0 by some independent means once and for all. We should use a special notation for the actual g_0 to distinguish it from all its hypothetical values in a certain range that we often used throughout this report only because it is as yet unknown. The latter practice could easily lead to some confusion between assumed (variable) g_0 and an actual g_0 when it enters in our equations. Here, we use a bold faced g_0 for the actual one as typed in the last equation above (as often stated, we need to rationalize a new set of terminology and notations for PG theory as soon as we obtain sufficient data for its requirements). For experiments with ordinary falling bodies (like in Figs. 62 and 63), the possible effect of variable density with radius is by far much smaller than the other issues first needed to be addressed in Section 23.2.3. In any case, the fact there remains that the falling speed depends on the absorptivity per Eq. 403 so that care must be ultimately taken to include all possible effects with correct formulations.

Density A corresponding derivation is provided in Appendix D.2.2, where the effective density at an internal point X is found from Eq. 703 to be:

$$\rho_{e-point} = k M_{aO} \cdot \frac{1}{4\pi \Lambda} \quad (419)$$

It must be noted again that $\rho_e \neq \rho_{e-point}$, since the effective density ρ_e was introduced as an average density of an effective mass m_e , in lieu of the Newtonian mass, uniformly distributed inside a spherical body. We should have denoted it by the usual average symbolism $\bar{\rho}_e$ and should have reserved ρ_e for the effective point density; this can be done during a later re-write of this report, but for practical (convenience) interim purposes, we now introduce the temporary symbol $\rho_a \equiv \rho_{e-point}$; it should be appreciated that this work is an exploratory project yielding new physics with variables not anticipated from the outset. The subscript (a) here denotes an activated density at a point resulting from the absorption of gravions at that point,

whilst ρ continues to denote the "real density" at the same point and ρ_e the effective density throughout the entire sphere with radius R .

Then for internal point X_i we rewrite the above as:

$$\rho_{aXi} = kM_{aO} \cdot \frac{1}{4\pi\Lambda} \equiv f_{\rho aXi} \cdot \frac{1}{4\pi\Lambda} = \frac{M_{aO}}{4\pi} \rho \quad (420)$$

The point density at the surface is given by setting $R_O = R$ (or $R_{Xi} = R$) in Eq. 703 to yield the value of the surface M_a factor as

$$M_a = \int_0^{\pi/2} \exp\left(-kR\sqrt{1 - (\sin\varphi)^2}\right) [\exp(+kR\cos\varphi) + \exp(-kR\cos\varphi)] \cdot 2\pi \sin\varphi d\varphi \quad (421)$$

by which we obtain the normalized point density $\rho_{aXi\text{norm}}$ as:

$$\rho_{aXi\text{norm}} = \frac{\rho_{aXi}}{\rho_a} = \frac{M_{aO}}{M_a} \quad (422)$$

We can see the variation of the effective point density in Fig. 69(a) by plotting the proportional factor kM_{aO} ($f_{\rho aXi}$) and the normalized effective point density in (b) for the same set of fixed values of k . The trend is similar to the variation of effective mass, but we can now display a quantitative representation for each parameter. We thus reproduce the general picture of what we already found for a specific numerical example in Section 14.6.1 with Fig. 19 and schematically shown with Fig. 33. This was our conception and description of what happens in very dense bodies, like white dwarfs, neutron stars and black holes, for which we established an effect resembling to the conventionally described as an "event horizon".

We can further distinguish the corresponding derivations for the effective density: From effective mass, we obtain the effective density ρ_{eXi} and normalized effective density $\rho_{eXi\text{norm}}$ by:

$$\rho_{eXi} = \frac{S_{aXi}}{V_{Xi}} \cdot \frac{1}{4\pi\Lambda} = \frac{3S_{aXi}}{4\pi R_{Xi}^3} \cdot \frac{1}{4\pi\Lambda} \equiv f_{\rho eXi} \cdot \frac{1}{4\pi\Lambda} \quad (423)$$

$$\rho_{eXi\text{norm}} = \frac{\rho_{eXi}}{\rho_e} = \frac{S_{aXi}R^3}{S_{aR}R_{Xi}^3} \quad (424)$$

We plot the effective density factor $f_{\rho eXi}$ and the normalized effective density $\rho_{eXi\text{norm}}$ in Fig. 69c&d. The difference between point effective density and effective density is readily seen.

The above outcomes are inline with what we have already found previously, namely, that the effective mass is concentrated towards the outer surface, a negligible effect for Newtonian masses but becoming increasingly significant and important for heavy (dense) bodies.

Acceleration and contraction factor By our new notation, the internal PG acceleration g_{Xi} given by Eq. 96 is now written as:

$$g_{XiPG} \equiv g_{Xi} = \frac{g_0}{\pi} f_{gXi} \quad (425)$$

while the acceleration at the surface is:

$$g_R = g_0 A_R \quad (426)$$

whereby we can normalize the internal acceleration by:

$$g_{Xi\text{norm}} = \frac{g_{Xi}}{g_R} = \frac{f_{gXi}}{\pi A_R} \quad (427)$$

This is plotted in Fig. 70a. Close to Newtonian regime, we have a linear relationship against radius, as expected, but greatly diverging for denser bodies.

The contraction factor q was first introduced as the ratio of PG-acceleration over Newton-acceleration, whereby the first (PG) yields the actual force by an effective mass and the second the force that would be exerted by the real mass acting under Newton's gravitational law (as if effective). It was then found that the same factor is produced by the ratio of effective over real mass like also for a series of other variables. We want here to investigate how the contraction factor behaves as an internal parameter. We may start with the internal contraction factor as the ratio of the internal masses by:

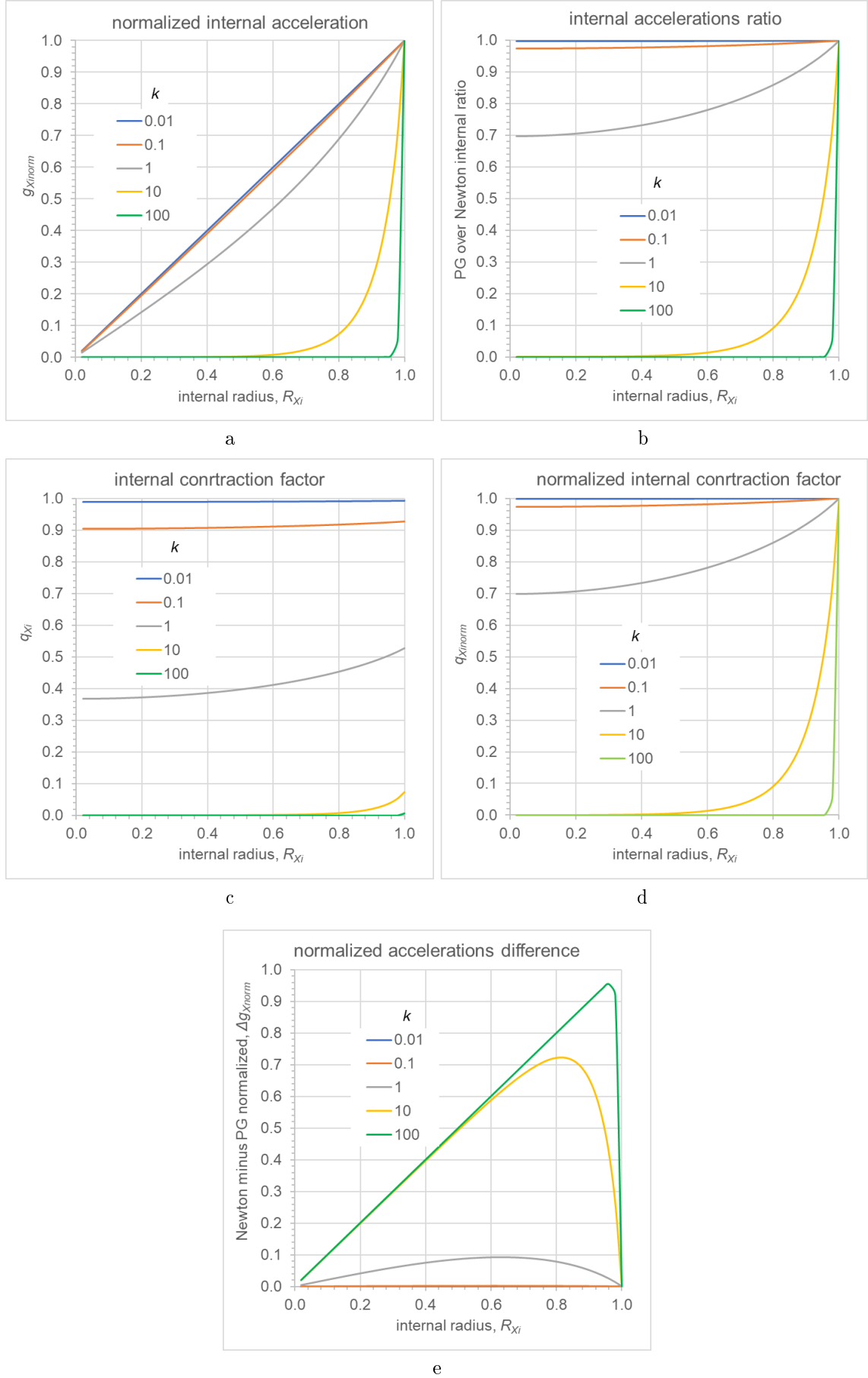


Figure 70: Internal acceleration and contraction parameters.

$$q_{Xi} = \frac{m_{eXi}}{m_{Xi}} = \frac{S_{aXi}}{4\pi\Lambda} \frac{3\Lambda}{4\pi R_{Xi}^3 k} = \frac{3S_{aXi}}{16\pi^2 R_{Xi}^3 k} \quad (428)$$

We can normalize the internal contraction factor over its value q at the outer surface (i.e. at $R_{Xi} = R$):

$$q_{Xinorm} = \frac{q_{R_{Xi}}}{q} = \frac{\frac{m_{eXi}}{m_{Xi}}}{\frac{m_e}{m}} = \frac{\frac{m_{eXi}}{m_{Xi}}}{\frac{m_e}{m}} = \frac{m_{eXinorm}}{m_{Xinorm}} = \frac{S_{aXi}}{S_{aR}} \frac{R^3}{R_{Xi}^3} \quad (429)$$

Let us now return to the original formulation of contraction factor from accelerations:

$$q_{Xi} = \frac{g_{XiPG}}{g_{XiN}} = \frac{\frac{g_0}{\pi} f_{gXi}}{\frac{Gm_{Xi}}{R_{Xi}^2}} = \frac{\frac{g_0}{\pi} f_{gXi}}{G \frac{4}{3} \pi \rho R_{Xi}} \quad (430)$$

where we treated the real mass acting under Newton to yield an acceleration g_{XiN} .

However, in Section 8 we used Eqs. 96 and 98 in the ratio, namely:

$$\frac{PG-g_{Xi}}{Newton-g_{Xi}} = \frac{\frac{g_0}{\pi} f_{gXi}}{\frac{Gm_{eXi-apportioned}}{R_{Xi}^2}} = \frac{\frac{g_0}{\pi} f_{gXi}}{\frac{4}{3} \pi G \rho_e R_X} \quad (431)$$

where for good reason we used the apportioned effective mass $m_{eXi-apportioned}$ per Eq. 416. The purpose was then to find the difference between expected Newton-acceleration and PG-acceleration at various depths for prospective measurements on Earth. As a result, we have corresponding Eqs. 430 and 431 differing only in the densities ρ and ρ_e . As we now attempt to formalize the relationships for the internal and external regimes, we need to see the needed adjustment in the terminology used in preceding Section 8. The significance of this adjustment is found by taking the ratio of the two derivations in Eqs. 430 and 431 above:

$$\frac{\frac{q_{Xi}}{PG-g_{Xi}}}{\frac{PG-g_{Xi}}{Newton-g_{Xi}}} = \frac{\frac{m_{eXi-apportioned}}{m_{Xi}}}{\frac{m_{eXi-apportioned}}{m_{Xi}}} = \frac{m_{eXi-apportioned}}{m_{Xi-apportioned}} = \frac{m_e}{m} = q \quad (432)$$

Therefore,

$$\frac{PG-g_{Xi}}{Newton-g_{Xi}} = \frac{q_{Xi}}{q} = q_{Xinorm} \quad (433)$$

In other words, the ratio of accelerations provided in Section 8 with Fig. 8 must be understood to be the normalized contraction factor according to the generalized definitions in the present Section; the contraction factor continues to comply with its original formulation. The same observation applies also to Fig. 19 using the same ratio of Eq. 431, where we have now changed prior q_X to q_{Xinorm} ; that was plotted specifically close to the outer surface of a very dense sphere (as example) to demonstrate the extreme concentration of effective mass very close to the surface. We have now elucidated the exact meaning of internal versus external properties for these cases. The variation of internal contraction factor and the normalized one are plotted in Fig. 70c&d. The internal accelerations ratio per Eq. 431 is also plotted in Fig. 70b yielding identical graphs with (d) as expected above.

The numerical difference of accelerations with depth presented in Table 1 remains correct, while we further investigate again the same difference for the current set of k coefficients here. The internal Newtonian acceleration as given above is proportional to the internal radius, whilst at the surface is given by $g_0 A_R$; this is linearly distributed with radius expressed also as:

$$Newton-g_{Xi} = g_0 A_R \frac{R_{Xi}}{R}$$

from which we subtract the $PG-g_{Xi}$ to obtain the difference as a function of radius (and depth):

$$\Delta g_{Xi} = Newton-g_{Xi} - PG-g_{Xi} = g_0 A_R \frac{R_{Xi}}{R} - \frac{g_0}{\pi} f_{gXi} \quad (434)$$

We used the above equation to plot the said difference in Fig. 8 and Table 1 for Earth with $g_0 = 1000 \text{ ms}^{-2}$. It is useful to generalize this function by dividing by g_0 , as a special (only here) normalization for this particular quantity, namely, by:

$$\Delta g_{Xi\text{norm}} = \frac{\Delta g_{Xi}}{g_0} = A_R \frac{R_{Xi}}{R} - \frac{f_{gXi}}{\pi} \quad (435)$$

which we plot in Fig. 70e. From this, we can readily reproduce the graph in Fig. 8 for the values of k , R and g_0 applied in the example there.

Finally, we can complement the formulas of effective density at Xi by:

$$\rho_{eXi} = q_{Xi}\rho$$

and the normalized effective density:

$$\rho_{eXi\text{norm}} = \frac{\rho_{eXi}}{\rho_e} = \frac{q_{Xi}\rho}{q\rho} = q_{Xi\text{norm}}$$

which is also confirmed by the provided graphs for these parameters.

Absorptivity and absorption coefficient For a given g_0 , the absorptivity A_R of the outer sphere (i) in Fig. 67 is known in connection with absorption coefficient k and radius R and by:

$$A_R = 1 - \frac{1}{2k^2 R^2} + \frac{\exp(-2kR) \cdot (2kR + 1)}{2k^2 R^2}$$

so that for the sphere (ii) it is

$$A_{R_X} = 1 - \frac{1}{2k^2 R_X^2} + \frac{\exp(-2kR_X) \cdot (2kR_X + 1)}{2k^2 R_X^2}$$

because k is the same for the same real density ρ . For consistency, the internal sphere in (i) having radius R_{Xi} must be characterized by an internal absorptivity $A_{R_{Xi}}$ in connection with an internal g_{0Xi} and internal absorption coefficient k_{Xi} by:

$$A_{R_{Xi}} = 1 - \frac{1}{2k_{Xi}^2 R_{Xi}^2} + \frac{\exp(-2k_{Xi}R_{Xi}) \cdot (2k_{Xi}R_{Xi} + 1)}{2k_{Xi}^2 R_{Xi}^2}$$

The outer material shell depicted by (iii) in the above figure reduces the outermost flux intensity from J_o to J_{oXi} and the maximum acceleration from g_0 to g_{0Xi} . We can derive $A_{R_{Xi}}$ and k_{Xi} by solving the equation

$$q_{Xi} = \frac{3A_{R_{Xi}}}{4k_{Xi}R_{Xi}} \quad (436)$$

first for the product $k_{Xi}R_{Xi}$ and then deduce $A_{R_{Xi}}$ and k_{Xi} from the given radius R_{Xi} .

Again, we can normalize these internal quantities over their values at the surface by:

$$A_{R_{Xi}\text{norm}} = \frac{A_{R_{Xi}}}{A_R} \quad (437)$$

$$k_{Xi\text{norm}} = \frac{k_{Xi}}{k} \quad (438)$$

with which the contraction factor relates by

$$q_{Xi\text{norm}} = \frac{A_{R_{Xi}\text{norm}}}{k_{Xi\text{norm}}R_{Xi\text{norm}}} \quad (439)$$

as can also be readily confirmed from Eq. 436. We show the above internal absorption coefficients and absorptivities in graphical form in Fig. 71a,b,c&d. For comparison, in Fig. 71e&f we also show the absorptivity of external partial sphere (ii) of Fig. 67 as well as the ratio of absorptivities of internal-over-external partial spheres. Interestingly, we note that the normalized absorptivity in (d) is greater than unity within a limited range of values; also the ratio in (f) is also within a particular range. We should later examine what the significance of those limiting values might be.

There are subtle differences in some expressions that we need to spell out if to avoid errors easily taking place. The internal acceleration factor can be written by alternative equations as:

$$f_{gXi} = g_{Xi\text{norm}}\pi A_R = g_{0Xi\text{norm}}\pi A_{R_{Xi}} \quad (440)$$

based on Eqs. 96 and 427.

It is worth noting that if the absorptivity of the external partial sphere shown in Fig. 71e is re-plotted against the product kR_X (reduced radius), we obtain the familiar sigmoid shape for external absorptivity as seen in Fig. 72a, but not the same for the internal absorptivity as seen in (b) of the same figure.

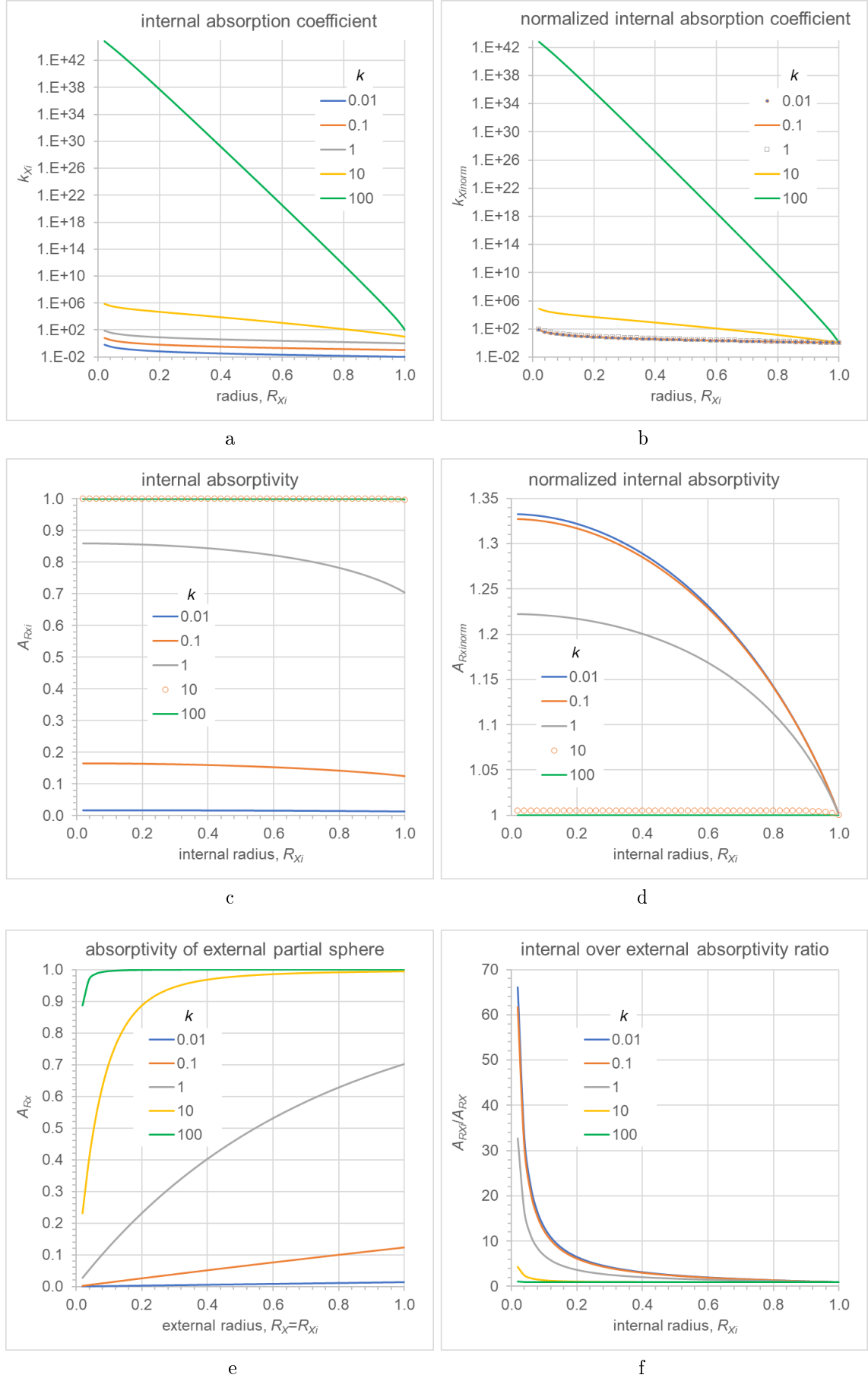


Figure 71: *Absorptivity and absorption coefficients.*

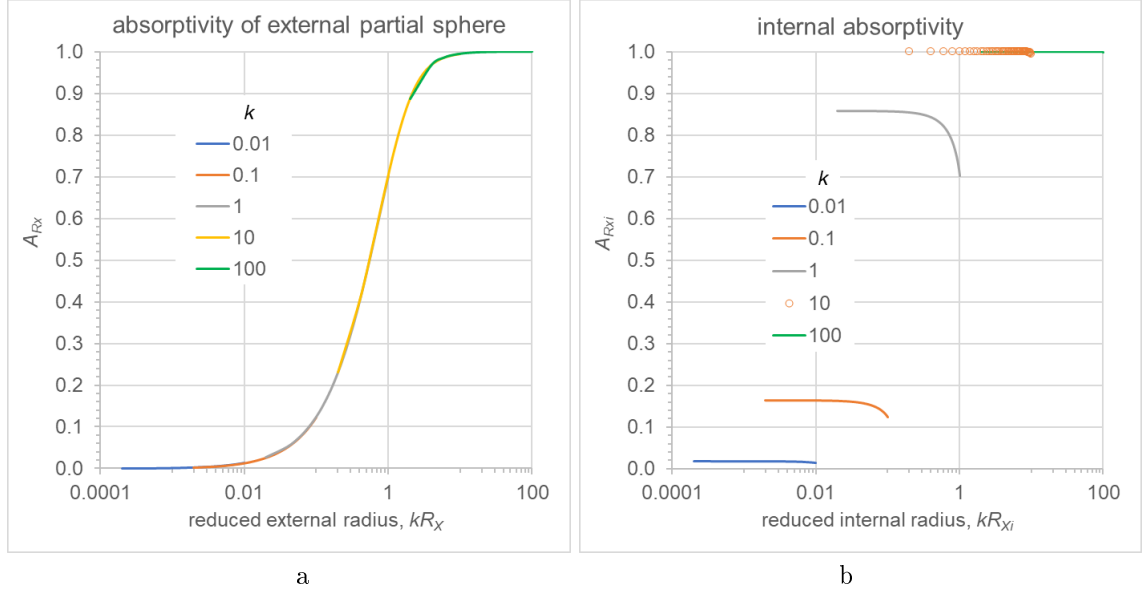


Figure 72: *Absorptivities against reduced radius.*

g_0 , Λ_{Xi} , J_0 and G We have already established the connection between external g_0 and internal g_{0Xi} (see Eqs. 96 and 97), so that the normalized $g_{0Xinorm}$ is:

$$g_{0Xinorm} = \frac{g_{0Xi}}{g_0} = \frac{g_{Xi}}{g_0 A_{R_{Xi}}} = \frac{f_{gXi}}{\pi A_{R_{Xi}}} \quad (441)$$

[Note: The $g_{0Xi} = g_{0Xinorm} g_0$ has now been corrected in the preceding Fig. 8 for $g_0 = 1000 \text{ ms}^2$, whereby we inadvertently used the ratio given by Eq. 427 in previous versions of this report, i.e. we used A_R instead of $A_{R_{Xi}}$]. We can now see the variation of this generalized parameter in Fig. 73a.

For consistency in the formulation for the internal acceleration g_{Xi} , we replace the external universal constant G by G_{Xi} in

$$g_{Xi} = \frac{G_{Xi} m_{eXi}}{R_{Xi}^2} \quad (442)$$

The external Λ constant becomes internally Λ_{Xi} , so that from the corresponding Eqs. 78 like:

$$\Lambda = \frac{\pi G}{g_0} \text{ and } \Lambda_{Xi} = \frac{\pi G_{Xi}}{g_{0Xi}}$$

we deduce the normalized constant Λ_{Xinorm} :

$$\Lambda_{Xinorm} = \frac{\Lambda_{Xi}}{\Lambda} = \frac{\frac{\pi G_{Xi}}{g_{0Xi}}}{\frac{\pi G}{g_0}} = \frac{G_{Xinorm}}{g_{0Xinorm}} \quad (443)$$

where we have also introduced the normalized universal constant G_{Xinorm} by:

$$G_{Xinorm} = \frac{G_{Xi}}{G} \quad (444)$$

We can further process this per Eq. 442 as:

$$G_{Xinorm} = \frac{g_{0Xi} A_{R_{Xi}} R_{Xi}^2 m_e}{g_0 A_R R^2 m_{eXi}} = \frac{g_{0Xi} \Lambda_{Xi}}{g_0 \Lambda} = \frac{g_{0Xi} k_{Xi}}{g_0 k} = g_{0Xinorm} \Lambda_{Xinorm} = g_{0Xinorm} k_{Xinorm} \quad (445)$$

We connect the internal flux intensity J_{0Xi} via the known Eqs. 38 below:

$$G = \frac{J_0}{c} \Lambda^2 \text{ and } G_{Xi} = \frac{J_{0Xi}}{c} \Lambda_{Xi}^2$$

$$J_0 = \frac{cg_0^2}{\pi^2 G}$$

$$J_{0Xi} = \frac{cg_{0Xi}^2}{\pi^2 G_{Xi}}$$

The normalized internal flux intensity then is:

$$J_{0norm} = \frac{g_{0Xi}^2 G}{g_0^2 G_{Xi}} = g_{0Xinorm}^2 G_{Xinorm}$$

From Eq. 445 we deduce:

$$k_{Xinorm} = \Lambda_{Xinorm} \quad (446)$$

Also:

$$\begin{aligned} g_{Xi} &= \frac{g_0 f_{gXi}}{\pi} = \frac{G_{Xi} m_{eXi}}{R_{Xi}^2} = \frac{G_{Xi} S_{aXi}}{4\pi \Lambda R_{Xi}^2} = \frac{G_{Xi} g_0 S_{aXi}}{4\pi^2 G R_{Xi}^2} \\ f_{gXi} &= \frac{S_{aXi}}{4\pi R_{Xi}^2} \frac{G_{Xi}}{G} \end{aligned} \quad (447)$$

which relates the integrals in the factors f_{gXi} and S_{aXi} .

For convenience in further processing the above formulas, we transfer some useful equations below:

$$\Lambda = \frac{\pi A}{m_e} = \frac{\pi R^2 A_R}{m_e} = \frac{\pi G}{g_0} = \frac{k}{\rho} = \frac{cg_0}{\pi J_0} \quad (448)$$

and together with Eqs. 413 and 441 we transform the normalized universal constant as:

$$G_{Xinorm} = \frac{g_{0Xi}}{g_0} \frac{k_{Xi}}{k} = \frac{g_{Xi}}{g_0 A_{R_{Xi}}} \frac{k_{Xi}}{k} = \frac{g_{Xi}}{\pi G A_{R_{Xi}}} \frac{k_{Xi}}{\rho} = \frac{g_{Xi}}{\pi G A_{R_{Xi}}} \Lambda_{Xi} = \frac{g_{Xi} \pi R_{Xi}}{\pi G m_{eXi}} = \frac{g_{Xi}}{G \frac{m_{eXi}}{R_{Xi}^2}} = \frac{g_{Xi}}{g_{Xi}} = 1 \quad (449)$$

which we highlight below:

$$G_{Xinorm} = 1 \quad \text{or} \quad G_{Xi} = G \quad (450)$$

As a result we can also simplify other parameters as:

$$\Lambda_{Xinorm} = \frac{1}{g_{0Xinorm}} \quad (451)$$

$$J_{0norm} = g_{0Xinorm}^2 \quad (452)$$

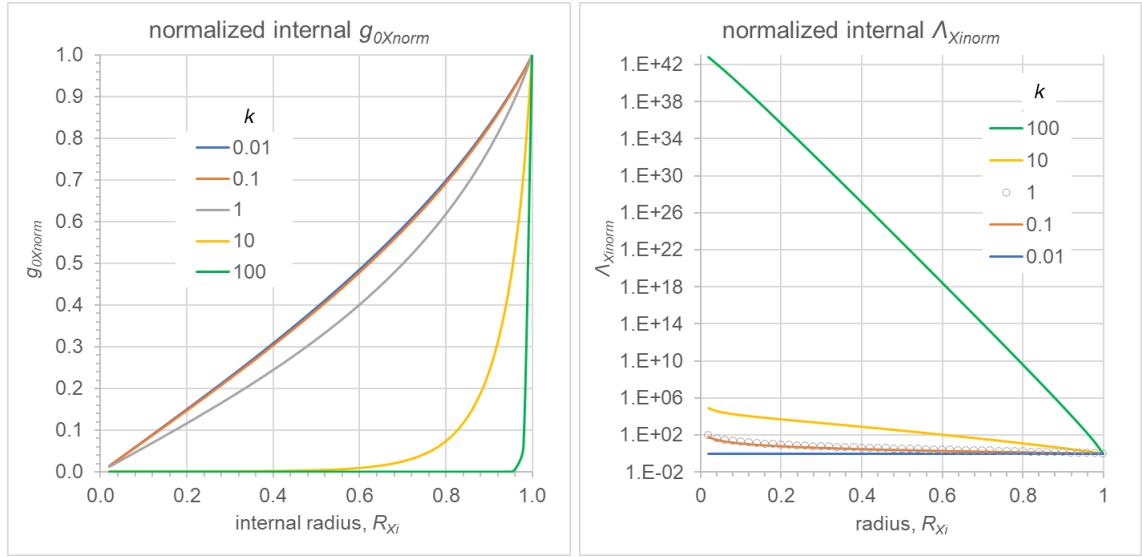
$$f_{gXi} = \frac{S_{aXi}}{4\pi R_{Xi}^2} \quad (453)$$

We can see the variation of the generalized internal parameters Λ_{Xinorm} and J_{Xinorm} in Fig. 73b&c.

The constancy of the internal universal gravitational constant per Eq. 450 has also been verified computationally via Eq 445 to always give:

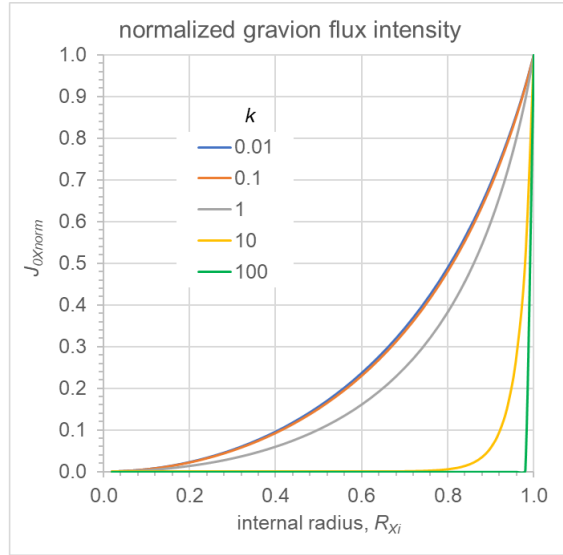
$$g_{0Xinorm} \Lambda_{Xinorm} = 1 \quad (454)$$

which we show by the graph in Fig. 73d. There is an oscillation for $k = 100 \text{ m}^{-1}$ of extremely small magnitude around unity. This arises from “round off” errors produced by the integration routine in the python program used. We can set an arbitrary precision for all other computations except for the integration routine that is governed by its own precision limits: As soon as we exceed some set level of precision, an error warning is issued. We purposefully present this limitation to warn potential users that high precision algorithms are often required to avoid misleading results. It may be that a devoted integrator must be developed to take on special requirements of PG theory.

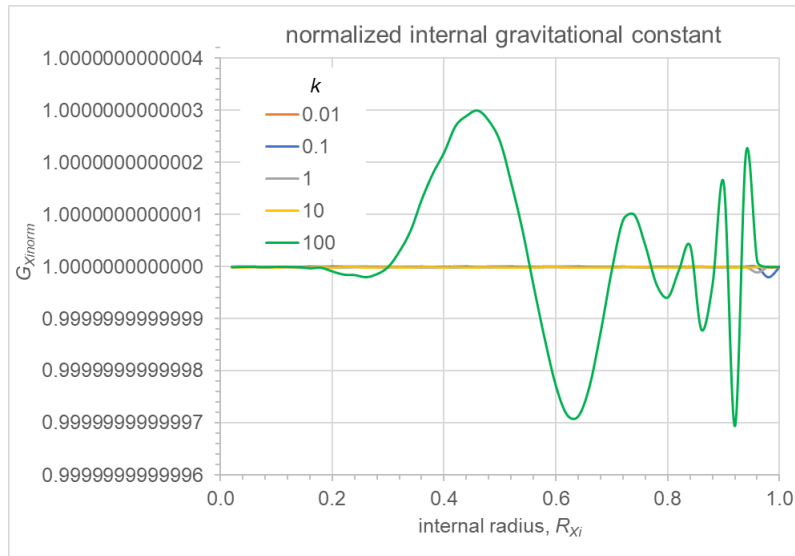


a

b



c



d

Figure 73: Internal parameters of g_{0Xi} , Λ_{Xi} , J_{0Xi} , G_{Xi} .

Miscellaneous discussion. The penultimate step of:

$$g_{Xi} = G \frac{m_{eXi}}{R_{Xi}^2}$$

in Eq. 449 is justified by the fact that m_{eXi} is the actual effective mass inside the sphere with radius R_{Xi} and not the apportioned Newtonian effective mass per Eq. 416; this m_{eXi} must produce the same acceleration whether it is derived from the action of the external g_0 (or J_0) as above or the action of the internal g_{0Xi} (or J_{0Xi}) as below:

$$g_{Xi} = G_{Xi} \frac{m_{eXi}}{R_{Xi}^2}$$

which can only happen if and only if $G_{Xi} = G$.

This outcome was not directly obvious at the outset of our formulations, while we had to introduce the general possibility of an unknown G_{Xi} in the equation above. In fact, having regard to the dependence of G via Eq. 39, we have already contemplated that the universal gravitational is a different “constant” at various remote locations in the cosmos. That understanding still remains valid whilst the new finding of $G_{Xi} = G$ concerns, so far, only the internal gravitational field inside a material body. We only need to adjust our speculated variation of G inside the heliosphere in Section 13 or elsewhere as regards internal situations. However, we still have a deviation from Newton’s gravitational law inside matter now not on account of a variable G but rather on account of variable m_{eXi} over and above the variation of mass on account of the two sphere interaction, in vacuum), established in Section 16. The two-sphere mass variation is ultimately consistent with Newton’s law, but we now have an extra variation of mass due to the internal field in the heliosphere presumed to consist of a very dilute matter that allows the motion of planets. Presumably, the density of heliosphere increases significantly as we approach the Sun, so that planet Mercury experiences the most of a variable mass arising from the variation of internal properties. Similarly, among various solutions for the Pioneer anomaly (a slowing slightly more than expected) offered so far, we can also propose that it is due to a slight continuous increase of effective mass as it approaches the outer reaches of the heliosphere; this should result in a deceleration of the spacecraft. The nature and physics of the presumed very dilute matter in the heliosphere is a separate issue to focus on later.

The above finding is most important for a deeper understanding of the universe. We have now learned that the big_ G must remain constant throughout an extended region comprising the heliosphere and beyond. How far beyond is a matter of conjecture and speculation. Since $G = \frac{J_0}{c} \Lambda^2$ and considering that Λ remains constant as an external (vacuum) parameter at constant J_0 (or Φ_0), then G will change only when J_0 changes. If gravions behave like a gas, then it is their mean free path (mfp) that could determine the size of the region beyond which the intensity of J_0 may change. It may remain constant for a much wider region well far greater than the mean free path of gravions, i.e. for a far too expansive region, until and unless there are events that can generate the said intensity variation. The suggestion of a mfp for gravions may appear incompatible with our understanding of the behavior of photons, but we have proposed that gravions and photons are different entities. This idea is further elaborated in Section 25.

We initially restricted Fig. 67 to “ordinary” bodies, not necessarily Newtonian, but we could include very dense systems, in which case we should involve the corresponding parameters of other fields, like the electric field in Section 21; this would involve a change of G to $G_{2-electric}$. We can extend a similar analysis for the electric field in later developments aiming to unify the two fields.

The process of normalization of various internal quantities (parameters) over their value at the surface has simplified their equations like 451 and 452. The finding that the normalized universal constant G_{Xinorm} is unity raises the question whether this constant might be redundant after all and that the use of big G in conventional equations is the result of the way that the problem of gravitation was formulated. It is a constant of proportionality in an equation obtained by experiment and observation. Actually, big G is already absent in our Eq. 91. Furthermore, there are no masses involved but only absorptivities, Λ and g_0 . We replace Newton’s gravitational law by another equation (law) that involves no mass and no big G . Any godly attributes to these parameters may not be well deserved after all, while our reverence can now be directed to gravion flux and hyle (see next Section). It is now PG parameters that we need to consider and understand. We may have more to say on this in later development of PG.

Furthermore, the internal properties seem to be dependent on their value at the surface. The surface appears to be a reference boundary. Depending on the density of mass, variation of internal properties may be very small in the Newtonian regime, but variation increases with depth (distance from the surface) faster with increasing density (see “*total absorption layer (TAL)*” in Section 18.2). The sharpest variation occurs in neutron stars and finally in black holes whereby the “surface” has a finite thickness with spatially fastest transition from an external to internal regime having lost total communication from the outside. We may

generalize this description by saying that the surface of any material sphere is a boundary through which “information” is transferred from the outside to the inside, or that the inside properties start with those from the outside at the surface and then are modified in conjunction with the density of the material sphere. We might like to call this surface an “event horizon” under a new generalized meaning as opposed to the conventional meaning of the event horizon of black holes. Our difference then is a matter of quantity, i.e. our event-horizon may be very extended (in thickness) well beyond the size of the material sphere itself, or shorter than the radius of the sphere. Black holes create the shortest possible transition of the event horizon, which is real and tangible, in distinction from a mysterious mathematical surface, beyond which numerous claims and hypotheses have been made on what actually happens.

The above qualitative description has by now been quantitatively expressed via equations among various parameters. In particular, the acceleration factor f_g by Eq. 43 for an external point O at distance r from the center of a sphere is $f_g = \pi A/r^2$ all the way to the surface where it becomes a characteristic $f_{gR} = \pi A_R$, after which it becomes $f_{gXi} = g_{0Xi} \pi A_{R_{Xi}}$ per Eq. 441; the latter contains (expresses) a transition from external (vacuum) g_0 regime to an internal g_{0Xi} regime of matter.

Throughout the above derivations we attempted to introduce notations in a way that would prevent confusion. When this is not fully achieved, we should make appropriate amends. Specifically, we need to do so for the factors S_{aXi} and f_{gXi} as already applied, We note that they are both “internal” parameters, however, both involving the external k in the integrals; they are internal factors “seen” or created from the outside. For good measure, we re-state them below:

$$S_{aXi} = \int_0^{R_{Xi}} M_{aO} \cdot 4\pi k R_O^2 dR_O$$

which in the limiting case at the outer surface of the sphere yields:

$$S_{aR} = \int_0^R M_{aO} \cdot 4\pi k R_O^2 dR_O = 4\pi^2 R^2 A_R$$

Looking from the inside, we might feel inclined to use the internal absorption coefficient k_{Xi} in an analogous formulation by:

$$S_{aXi-internal} = \int_0^{R_{Xi}} M_{aO} \cdot 4\pi k_{Xi} R_O^2 dR_O = 4\pi^2 R_{Xi}^2 A_{R_{Xi}}$$

which is numerically different from the prior S_{aXi} on account of $k \neq k_{Xi}$, i.e. these two absorption area factor are:

$$S_{aXi} \neq S_{aXi-internal} \quad (455)$$

In any case both of the above parameters should yield an identical internal effective mass m_{eXi} when multiplied by the corresponding factors like:

$$S_{aXi} \cdot \frac{1}{4\pi A} = m_{eXi}$$

$$S_{aXi-internal} \cdot \frac{1}{4\pi A_{Xi}} = \frac{4\pi^2 R_{Xi}^2 A_{R_{Xi}}}{4\pi A_{Xi}} = \frac{\pi R_{Xi}^2 A_{R_{Xi}}}{A_{Xi}} = m_{eXi}$$

with the last member of the second equation obtained by use Eq. 448 internally. The two factors relate via the equations:

$$\frac{S_{aXi}}{A} = \frac{S_{aXi-internal}}{A_{Xi}}$$

$$S_{aXi} = \frac{S_{aXi-internal}}{A_{Xi} \text{norm}} = g_{0Xi} S_{aXi-internal} \quad (456)$$

Similarly, the internal acceleration factor f_{gXi} is computed based on the external k , but if we feel inclined to use the internal k_{Xi} , then we would obtain a numerically different factor:

$$f_{gXi-internal} = \pi A_{R_{Xi}}$$

which is not the same as that obtained by Eq. 95, namely:

$$f_{gXi} \neq f_{gXi-internal}$$

In any case both of the above parameters should yield an identical internal acceleration g_{Xi} when multiplied by the corresponding factors like:

$$f_{gXi} \cdot \frac{g_0}{\pi} = g_{Xi}$$

$$f_{gXi-internal} \cdot \frac{g_{0Xi}}{\pi} = \pi A_{R_{Xi}} \frac{g_{0Xi}}{\pi} = g_{Xi}$$

where the product $g_{0Xi}A_{R_{Xi}}$ (internally) corresponds to the product g_0A_R (externally). The two factors relate via the equations:

$$f_{gXi}g_0 = f_{gXi-internal}g_{0Xi}$$

$$f_{gXi} = g_{0Xi}norm f_{gXi-internal} = g_{0Xi}norm \pi A_{R_{Xi}} \quad (457)$$

The above subtle details, if unnoticed, can result in significant errors. This helps us also understand the different effect between k and k_{Xi} . In setting up computation equations, we use a constant k for all and through all bodies having the same real density, but it can vary when the density varies according to the constant ratio $\Lambda = k/\rho$. We do all this from an external point of view. Nonetheless, we can obtain equivalent outcomes also from an internal point of view according to the experience of graviton flux at an inside point of a material; the latter depends on the internal distribution of density, which attenuates the external graviton flux. In that case we can use the k_{Xi} at that point. The latter is variable with variable radial position in a spherical body. Therefore, this clarification should dispel possible misconceptions about the constancy or not of the absorption coefficient. Our computations have been set up correctly so far.

In this Section we have initiated an understanding of internal versus external parameters (properties) that can be appended to Part 1 of this report later. More investigation and formulations may continue in future work, its current form of which remains incomplete for the time being. Many important topics remain open. Furthermore, many details need to be worked out as, for example, the limiting values on the graphs in Fig 71d may (or may not) be important. Also, we have often established mathematical derivations based on the physics (physical considerations) but the same derivations should result from pure mathematical manipulations as well. PG has ushered a bonanza for mathematicians to make important contributions and help further expand the new physics. Archimedes is reported to be the first to have used physics to prove mathematical theorems in his codex Netz (2007).

24.2 Mass and hyle

We have demonstrated once more that mass is not a sacrosanct entity by being invariant and conserved. It is rather a property of a substrate along with other properties (parameters) entering inter-relationships that describe a mode of existence of the substrate. This substrate has been also described as “stuff” or matter that is generally something vague or unknown. It may be that the word mass has been subliminally implied to mean matter (stuff) with an attached force or acceleration that we can experience and measure. In fact, mass in English means a body of matter, which must have been the initial intention of the meaning of this word in early physics too. However, the word means a constant of proportionality between force and acceleration in established physics. The ordinary meaning of the word mass is divorced from its meaning in physics. It remains a question if and what relationship exists between the ordinary meaning of mass (as matter) and its meaning in physics. If they are separate entities, we must say so or introduce another word for mass. Even the word “matter” is divorced from “ant-matter”, so that we have no word for the possibility of describing the “stuff” that may underlie both matter and anti-matter. We are prejudiced to accept that the cosmos exists in the form of matter or anti-matter. If we want to break away from this prejudice, then we need to clearly define mass, matter, anti-matter and the possible underlying substrate (or stuff) of everything. The easiest or practical way is to introduce a new term for this (so far hypothetical) substrate and continue investigating the true physical meaning of the existing terms of mass, matter and anti-matter.

We propose that an underlying entity exists universally and it is measurable. For this, we need an unambiguous word (term). The words mass and matter seem too worn out and confusing. Short of adopting the word stuff for this purpose as being too colloquial in the English language, we might want to resurrect the ancient Greek term of “*hyle*” per Wikipedia contributors (2022). Historically, the term *hyle* ($\nu\lambda\eta$) fits in perfectly well with our purposes. Let its symbol then be the letter upsilon \mathcal{Y} .

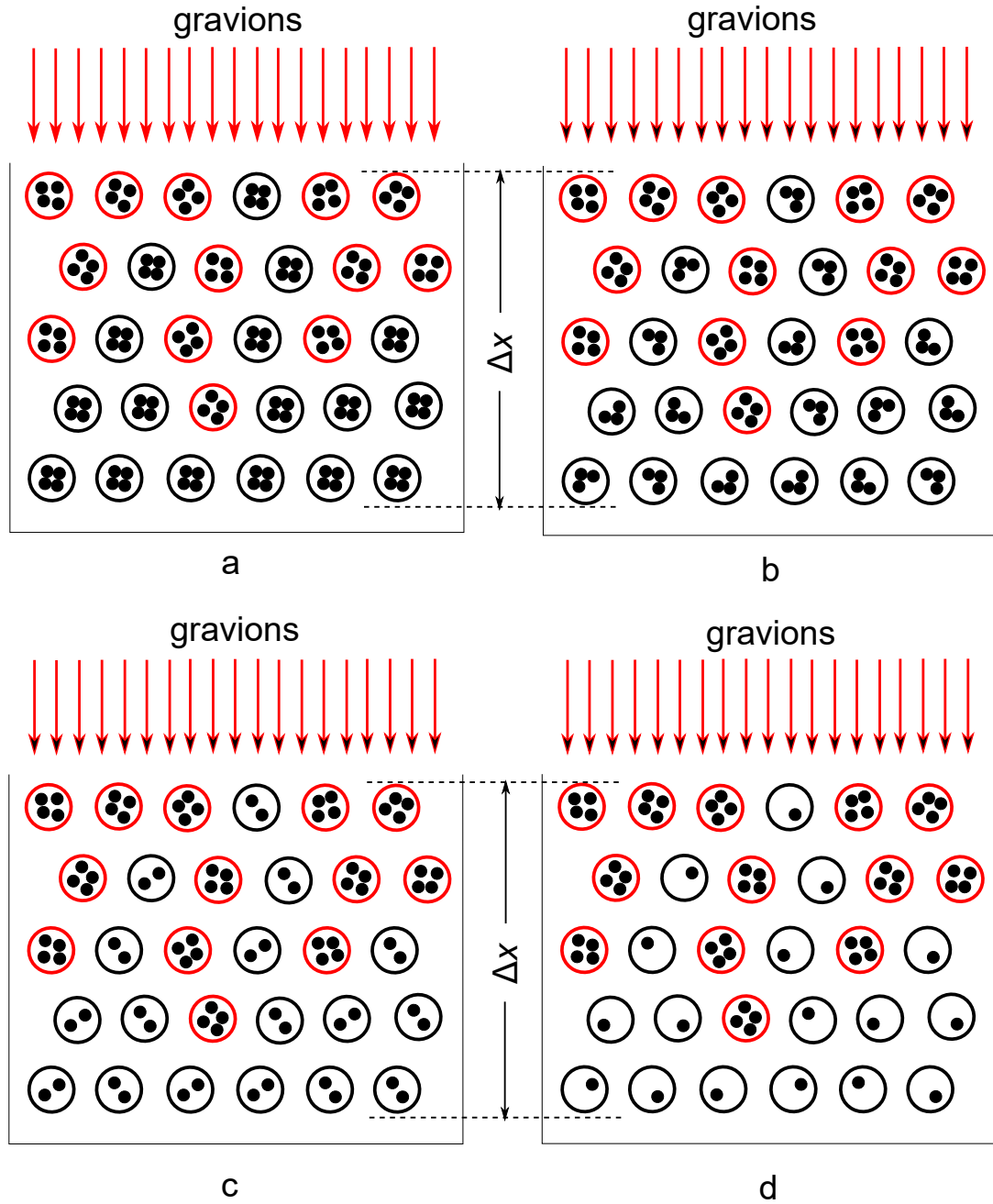


Figure 74: *Macroscopic body: Effective mass as red circles, black mass as black circles and hyle (or matter) as black grains; arriving gravions combine their hyle with black hyle to create effective mass in various proportions per (b), (c) and (d) but have no hyle in (a).*

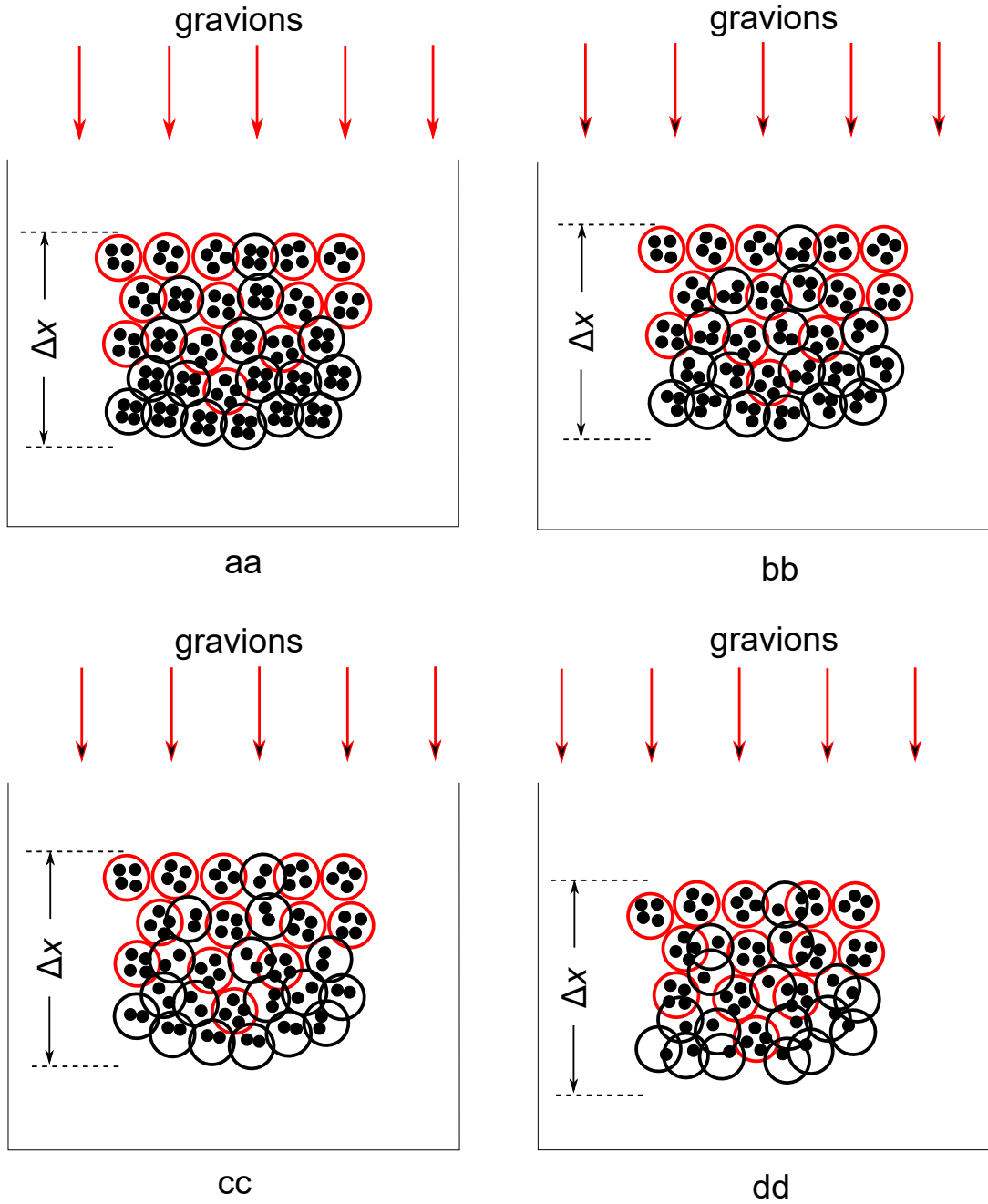


Figure 75: *Fundamental body: Effective mass as red circles, black mass as black circles and hyle (or matter) as black grains; arriving gravions combine their hyle with black hyle to create effective mass in various proportions per (b), (c) and (d) but have no hyle in (a).*

Whether we can identify the entity of hyle with one of the known quantities like energy, or the radiant flux of gravions Φ_0 , or some other remains to be seen. We don't aim to solve this fundamental question here, other than make an attempt to conceptualize a connection or relationship with mass as used in physics and in PG theory in particular. This is needed especially because we have often stated that *real-mass* is the substrate upon which gravions act (or being absorbed and released). It might be questionable that we allowed the word “mass” to be included in our terminology in the first place. This took place at the outset of our inquiry whereby we needed an absorbing substrate that lay dormant until it was activated by gravions to produce an effective-mass. It was clear that we referred to or implied a dormant mass waiting to be activated, so that it had to be a “mass-in-waiting” and we coined the term “real-mass”. Afterwards, we saw that it was the effective mass that had inertia, not the real-mass by itself. With that background and followup developments, we are in a better position now to make appropriate adjustments, which can maintain consistency with all our preceding PG findings.

To ease possible objections to our approach, we can say that the concept of hyle is not inconsistent with current theories. For example, one can continue stating that photons do not have a rest mass but at the same time we can also state that photons contain or are made of hyle. Photons is a mode of existence of hyle, like electrons are and so on and so forth. Energy is also a form of (or mode of existence) of hyle but we do not predispose ourselves on how to understand the connection between form and hyle yet. We have found that mass is proportional to the rate of absorption of energy or better, for a spherical body, according to Eqs. 194, 202 and 204

$$M_e = \frac{W}{4cg_0} = \frac{S_a}{4\pi\Lambda} \quad (458)$$

it is the rate of energy absorption/desorption per unit gravion-speed per unit of maximum-acceleration. This remotely resembles the original intention of the meaning of mass as matter, it is only a process riding on the back of hyle. We feel more certain to consider hyle as the underlying medium of that process and all other processes. This then may be the only way to strive towards a theory of everything. Hylism (= materialism) is set apart from dualism and idealism. If a theory of everything strives also to unify the cosmos, this can be conceivably achieved on the basis of monism as provided by a dynamic materialism. We consider this to be a sound basis of physics science.

We attempt to conceptualize and quantify the above approach via a series of diagrams. We assume that hyle can be quantified and quantized. In Fig. 74, we depict hyle with small black spheres (grains) each representing a single quantum or fixed multiples of quanta of hyle. The circles surrounding them depict the corresponding property of mass, which is either effective mass drawn in red color or black mass drawn in black color. Mass and hyle are thus separate entities but are interconnected via some process. This process for black mass is a deemed one, it does not exist yet, it is a potential or latent process in waiting until gravions are absorbed. The hyle with its red circle may be the minimum absorption (emission) center (MAC or MEC). For ordinary macroscopic bodies, these centers are distributed throughout and kept apart via the chemical structure of the body; hence they are shown at fixed separations uniformly. The MACs/MECs exist at subatomic level withing “elementary” particles. By “elementary”, we do not mean structure-less particles, in fact, we have proposed that conventional elementary particles are more likely to have structure (e.g. see our further electron modeling). We only wish to ensure that in this figure MACs do not migrate around the macroscopic body but kept apart via a given phase of hyle. They may migrate and redistribute themselves within each elementary particle. The effective mass is more concentrated toward the surface of the macroscopic body in the direction of incoming gravions; the representation is grossly exaggerated where black mass appears to be the only population after a certain depth. This is not the case with ordinary matter before some phase transition is triggered, say, to plasma phase. In ordinary matter the relative concentration of effective and black mass is not great enough as to induce a phase transition. This is a question to be taken up for what happens in stars and their cores, in white dwarfs and so on. We consider that the depiction of hyle in Fig. 74 is consistent with experience of ordinary matter up to the size of planets. At subatomic level, the situation is different as we will discuss in the next Fig. 75, with which we need to intermittently alternate to be able to convey our thinking.

Gravions travel in all directions but we have singled out only a net amount of them in a particular direction over an elementary depth Δx ; this fraction of gravions is responsible for the force exerted on the layer of hyle. If we wanted to calculate the total gravion absorption over the same layer, then we should have shown all gravions absorbed by the layer (energy is in the sum but force is in the net difference of gravions).

Referring specifically to the first diagram of Fig. 74a, we associate the same proportional amount of hyle to both effective and black mass, e.g four (arbitrarily) quanta (or multiples thereof) per MEC (in effective mass) or latent MEC (in black mass). The real-mass density is uniform throughout the body and corresponds also to a uniform hyle density. The real-mass is composed of the two fractions of effective and

black mass, each having their own specific distributions across Δx , for example, as they were determined in the preceding analysis for a sphere. For this case, the gravions absorbed do not alter the content of hyle but they somehow manage to activate the hyle hidden in black mass to hyle presenting as effective mass. In this case, the constancy (invariance) of hyle necessitates that the absorbed gravions have no hyle themselves. One might rush to suggest that they are “only energy without mass”, but such a statement is inconsistent with our initiated approach above. With our approach, we should state that gravions, in this case, must be of an entirely different entity of an entirely different nature without hyle; it is inconceivable (to us) that such an entirely different entity can interact with hyle, unless gravions and hyle have a common denominator via which they can interact. The situation of Fig. 74a is tantamount to dualism, which we have rejected. Further debate on this is left for general philosophy, or to other physicists who may like to take it up too.

As a result, the following three diagrams in Fig. 74b,c&d are the accepted classes of possibilities for our purposes. They all show accrual of hyle by the incoming gravions in different proportions, like 1:3, 2:2 and 3:1, i.e. all fractions greater than zero. The relative numbers of effective and black masses are all exactly the same as in (a) under the same uniform real-mass density. Each gravion conveys one quantum of hyle, which may combine with a certain number of body-hyle quanta, or one body-hyle quantum may combine with a certain number of gravion-hyle quanta to produce an activated center of mass; note that the arrowheads contain black color to indicate the conveyance of hyle, unlike the arrowheads in full red for case (a). It is unknown in what proportions of gravion-hyle to body-hyle the interaction forms activated mass. It is the task of particle physics to reconcile these proportions with existing data. We only propound the basis on which to proceed with PG when considering gravion absorption.

By the above scheme, we have the possibility (a mechanism) of maintaining the real-density ρ of a macroscopic body constant along with variable effective mass as that when we vary the distance between two material spheres per Section 16. The computations there were conducted under a constant k (hence ρ) and radius R for macroscopic spheres. We did not have re-arrangement of the fixed atoms, but we had a decrease of effective mass with a decrease of distance by way of radiation (or absorption) of hyle from within subatomic structures; by “radiation” we mean desorption of hyle and not necessarily radiation of electromagnetic waves. This variation of hyle might be experienced as radiation of mass or energy if our instruments were made to detect such signals and if they were sensitive enough. In any case, during this process, the real-mass remains constant but not the total hyle contained in the moving bodies. This understanding provides a great relief on possible physical processes involving the notion of constancy or variability of mass and hyle; real-mass enters as a parameter in our measurements during processes riding on hyle.

The situation is different at the subatomic (“fundamental” or elementary) particle level, as we try to depict in Fig. 75. MACs/MECs are created and redistributed inside a given particle with concomitant variation of the radius of the particle. We have used the same proportions of gravion-hyle combining with body-hyle in four cases corresponding to the four cases in the diagram for the macroscopic body. Case (aa) does not accrue hyle from gravions, it represents dualism and is not considered further. The remaining three cases (bb), (cc) and (dd) are possibilities to be taken into account. However, now both hyle-density and mass-densities are variable as they are free to re-arrange and re-distribute themselves within a variable radius particle while they are squashed close together as much as possible. This was the case when we attempted to build a proton from an electron in a series of exercises in Section 19.3.

We need to clarify that black mass (and its hyle) is not a “dead” entity. Only because it is shielded from gravions we call it “black” or inert relative to gravions. For example, see proposed modeling of electron in preceding and following sections. Black mass exists in its own world, it is just another mode of existence of hyle. The latter is necessary for the above modeling of mass and hyle. Black mass must be structured in self contained units and not in an amorphous agglomeration of hyle grains. In an amorphous black mass, gravions could be added or subtracted arbitrarily without any sensible outcome. To illustrate this point, black mass may consist of self contained vortices initially randomly oriented in a sphere. While they happen to absorb gravions, they could be oriented in the direction of incoming gravions, which makes them activated. As all the activated vortices are directed towards the center of a sphere, they exert a pressure keeping the sphere as a unified (integral) body. A vortex reverts back to the inactive state (black mass) as soon as it emits the extra absorbed gravions. That is why we have included “one” black mass circle at the surface in Fig. 74 to indicate the statistical nature of MACs and MECs and the dynamics of effective vs black mass throughout the entire body. We discuss in more detail the possible presence of vortices in the following section, but we need to move back-and-forth in our presentation to be able to convey our thinking. The hypothesis of vortex structures is not binding or limiting the PG theory, as other, more suitable, structures may be proposed later. However, the presence of some structure at the fundamental level seems inevitable for a consistent theory of PG. The conjecture of speed-mass relationship is thought of on the basis of a connection between speed and structure. It would be best if we could derive this relationship from first principles, from a synthesis

of acceptable relationships; the failure or success of our conjecture is only an initial tentative attempt and should not bear on the overall theory of PG (see also clarification at the outset of Part 2).

A distinction between macroscopic and microscopic (fundamental) level of hyle is critical in the development of PG. Failing to do this has led prior attempts on PG to failure or criticism and rejection. An initial step in connecting the two levels was made in Section 19.2 followed by various ensuing developments. Certain changes at the fundamental level leave the macroscopic body apparently “intact”, in the sense, for example, that its chemistry is conserved. It is analogous (not the same) with isotopes. The very high “thermal” energy absorption in PG that is feared to “melt” the planet instantly takes place within particles that are decoupled from the macroscopic observable properties. They do not melt. As explained in Section 15.8, the second thermodynamics law need not be violated either. The absorption takes place at the MAC level passing through “all” states over a very short time during which there is a favorable state capable of emitting the absorbed energy via another non-gravitational particle. This is allowed (or expected) by the fluctuation theorem. The second thermodynamics law is complemented by the fluctuation theorem law. This consideration is not more untenable than similar prevailing theories of “vacuum fluctuations”, etc. These are steady-state processes at the microscopic level of a stable macroscopic body. The above description explains the main possible process, which may not be the only (100%) one. There may be a statistical smaller amount of emissions that couples with the macroscopic body and result to a certain degree of heating, which may be exactly the internal heating of planets (in part also of stars, etc.). An analogy may be seen with electromagnetic radiation of a given wavelength being reflected by a body at a different wavelength with some remnant amount of heating. With gravions, the analogy differs by way of quantity (intensity) and quality (type), i.e. by way of one field converting to another as described in preceding sections.

The distinction between macroscopic and microscopic levels applies not only to ordinary bodies (planets, etc.) but also to stars, white dwarfs, neutron stars, etc. Only at the stage (phase) of black holes macroscopic and microscopic levels may coalesce, but can only vaguely be described at present. We need firmly develop a sound and consistent PG theory for most of the other phases before we venture into the ultimate structure of fundamental particles and black holes (likely to be similar). We cannot do this here.

The above convey only a minor part of the big picture, because the electrical mass (charge) is not sacrosanct either. We should draw similar diagrams for the electric field and electrions. Therefore, based on the materialist approach, we should associate hyle to the electrical mass too. This should be many orders of magnitude more than the amount of hyle associated with gravitational mass. We say the same for other types of mass (if any) corresponding to other force fields. On this basis, we now better understand that the decrease of effective mass towards the center of a macroscopic sphere is accompanied (or complemented) with an adjustment of electrical mass in the fashion envisaged by prior Fig. 50. The variations due to gravion flux may be negligible in comparison with the levels of electrion flux. In other words, the variation of gravitational mass is negligible relative to the absolute levels of electrical mass on which the said particle or body is structured. That is, we should not be misled by the exaggeration depicted by the provided qualitative diagrams. We need to combine both gravitational and electrical masses to convey the full picture of hyle, which is impractical to perform by gross diagrams. We need a rigorous mathematical description of both electric and gravitational fields individually and in combination as the best way to unify them. Clearly, this can be done in future work, while we only attempt here to lay the basis for further developments.

In unity, all types of mass ride on the substrate of the entire (total) hyle. In working out various relationships for the gravitational field, we may have, at some point, to consider concurrently also the presence of electric field while we introduce and quantify the total hyle involved. It is often said that “only about 5% of objects is stuff while the rest is energy”. However, the issue of stuff is sidelined, or muted, nothing is said about it, it is left to subliminal conceptions of the reader. This may be because the theory is based on mathematical deductions with no substance ever coming into play. Physics has been reduced to subjective mathematical idealism. It is well overdue to restore physics to its objective basis. PG provides this opportunity. In any closed system, the total hyle is conserved. Hyle must be the first and foremost entity that is conserved in the universe. Hyle exists in motion. The conservation of momentum and energy are different expressions in the form of measurable parameters (quantities) of the conservation of hyle. Hyle is the common quantifiable thread unifying our mathematical descriptions of the universe. This is how we envisage the possibility of arriving at a theory of everything.

We may establish a relationship between real mass and hyle following an analogous approach to the exercises for building a proton from an electron in Section 19.3.3. We always have the equation $m = m_e + m_b$. With the help of the diagrams in Figs. 74 and 75, we note that the number of the total circles (red and black) represent the total (real) mass. The total of the contents of these circles represents the total amount of hyle \mathcal{T} , which depends on the mixing parts of gravion-hyle x and parts of black-mass-hyle y producing $x + y$ parts of effective-mass-hyle. The ratio $(x + y)/y$ is the factor by which the effective mass apportions hyle over and above the hyle apportioned by the black mass. If we denote by $C_{\mathcal{T}}$ the amount of hyle per

unit of black-mass, then the black-hyle $\Upsilon_b = C_\Upsilon m_b$, the effective-hyle $\Upsilon_e = C_\Upsilon m_e(x+y)/y$ and the total hyle Υ is:

$$\Upsilon = \Upsilon_e + \Upsilon_b = C_\Upsilon \frac{x+y}{y} m_e + C_\Upsilon m_b \quad (459)$$

Referring to Figs. 74 and 75, cases (a) and (aa) have $x = 0, y = 4$; cases (b) and (bb) have $x = 1, y = 3$; cases (c) and (cc) have $2, y = 2$; and cases (d) and (dd) have $x = 3, y = 1$. For cases (a) and (aa), the above equation reduces to:

$$\Upsilon = C_\Upsilon (m_e + m_b) = C_\Upsilon m \quad (460)$$

stating that hyle is simply proportional to the real mass. At the outset we suggested that real mass may be the substrate or matter by which gravions are absorbed to create the effective mass portion of the total real mass. It was implied (intuitively) that $C_\Upsilon = 1$. All our hitherto equations involving the various types of mass are valid. We now extend the meaning of mass as corresponding to a certain proportion of hyle being the actual substrate upon which the gravions act. That is, we now shift the substrate to be a separate entity, of which mass is one property. That is, if we want to accept and adopt the materialist basis of cosmos, then we need to introduce hyle and liaise it to real mass in accordance with the Eq. 459, where the fraction $(x+y)/y$ remains to be found; it must comply with experimental data from various fields of physics.

The meaning of mass has been deciphered by the "Novel quantitative push gravity/electricity theory poised for verification". The gravitational constant G is redundant. Thus, "stuff" and mass are not the same thing, nor are they proportional to each other. This theory seems consistent with Higgs's ideas in some respects. We can establish some correspondence between the two: Stuff (now termed "hyle") by itself has no inertia or mass until it is activated by gravions, the underlying (creator of) field stuff (hyle); compare this idea with the contemporary idea that "the field gives mass" (we now say that the gravions give mass to hyle). We now have a tangible understanding of mass, field, and hyle.

In the light of these developments, it would be necessary, when we will re-write the PG theory, to take care to maintain consistency of terminology both within the theory and as much as possible with established terms in physics. For example, to avoid a re-write of the term "mass" in established literature, we can identify it with "effective mass" in PG, and so on, namely,

mass \equiv *effective mass*
real mass \equiv *hyle*
hyle minus mass \equiv *inert mass* \equiv *black mass*.

Note to be added to our response to criticisms in Section 15: The above ideas and analysis are all consistent with current theories on the coupling of energy to all forms of matter. In other words, our PG theory is not refuted by current theories as is claimed by Wikipedia contributors (2018), namely, that: *"Based on observational evidence, it is now known that gravity interacts with all forms of energy, and not just with mass. The electrostatic binding energy of the nucleus, the energy of weak interactions in the nucleus, and the kinetic energy of electrons in atoms, all contribute to the gravitational mass of an atom, as has been confirmed to high precision in Eötvös type experiments.[50] This means, for example, that when the atoms of a quantity of gas are moving more rapidly, the gravitation of that gas increases. Moreover, Lunar Laser Ranging experiments have shown that even gravitational binding energy itself also gravitates, with a strength consistent with the equivalence principle to high precision – which furthermore demonstrates that any successful theory of gravitation must be nonlinear and self-coupling.[51] [52] Le Sage's theory does not predict any of these aforementioned effects, nor do any of the known variants of Le Sage's theory."* Our variant of PG theory is not refuted by the above quotation. It seems that the objection should now be withdrawn. However, Wikipedia editors resist to provide even a mere reference to (without adopting) the present variant of PG by invalid reasons for breach of Wikipedia rules. In fact, Lunar Laser Ranging (LLR) should be used during solar eclipses to investigate the predicted PG effect formulated in Section 12.4 and not for the falling rates of Moon and Earth in general, which are not expected to differ according to our PG theory too (see Section 23). Our stance on the equivalence principle has been discussed and explained on many occasions throughout this report, but LLR is still awaiting application for a possible gravitational anomaly.

24.3 Continuation from Section 23.4

Equipped with the lessons above, we can now supplement the discussion in Section 23.4. In the case of acceleration during free fall (i.e. not involving an electric field as in rocket acceleration), we have computed the variation of effective mass m_{er} with distance r between two spheres. As one sphere is shielded by the

other, it is like being an internal sphere but only in part; there is only a partial directional shielding of the gravion flux, not a complete shielding around a full 4π solid angle as in Fig. 67a&c. The computation of static m_{er} was correctly performed under a fixed external k for a fixed real density ρ . Static m_{er} decreases according to the finding for a two sphere system with concomitant increase of black mass so that their sum $m_r = m_{er} + m_{br} = m$ remains constant in the static situation. However, the corresponding (static) total hyle varies in accordance with Eq. 459. As the falling sphere acquires a speed, kinetic effective mass is added according to a conjectured relationship per Eq. 349, by which we have to make further assumptions about how this happens. If the kinetic effective mass is created by absorption of extra gravions from the direction of fall activating black mass, then the total (composite) real mass must remain also constant:

$$m_{rc} = m_{erc} + m_{brc} = m \quad (461)$$

It remains to be found about how hyle varies during fall. In contrast, during rocket acceleration, the accrued kinetic effective mass could originate from absorption of electrions, which themselves may be agglomerations of organized gravions, such as vortices (see next section); then we may have a net accrual of real mass via the electron absorption and an absolute accrual of hyle during rocket acceleration.

Returning to the case of falling acceleration per above equation, an adjustment of the variation of masses is required in related figures, e.g. Fig. 55 and others. Still, a difficulty (or question) arises from the use of a kinetic mass formula per Eq. 410 pertaining to spherical symmetry of absorption, which seems not to be the case for a falling sphere. It may be that our conjectured mass-speed relationship should be based on the absorptivity of a material-line per Eq. 182 or a thin-rod aligned in the direction of velocity. This would require a repetition of computations to establish all related parameters for a thin-rod in lieu of a sphere in future work. Until then, we draw attention to certain deficiencies of some of the preceding results. The variation of real mass was intriguing for some time leading to the current valuable investigation of internal parameters and the introduction of hyle. The variation of m_{er} as plotted is correct and a variation of m_{erc} is subject to a re-appraisal of the mass-speed relationship. From these variations there exists an emission of hyle instead of real mass, which yields an equivalent outcome to what we subliminally perceived via a loss of mass. The distinction between mass and hyle is a key issue. Pending proper rectification, we leave those graphs unchanged as they may also help a discussion and a deeper understanding of all the issues involving mass and now hyle.

24.4 Internal vs. external parameters (variable real density)

Work to formulate the problem of external acceleration from two concentric spheres with different densities was presented in Section 10. We should examine the variation of internal properties for that case too, as well as for the general case of a sphere with spherically variable density (i.e. as a function of radius). We need to establish a set of theorems governing all parameters involved. This investigation is left for later work due to other work constraints by this author. Other workers are welcome to make a contribution in this or related area too.

The heliosphere would be a practical application of that study. We have speculated on the influence on elliptical orbits of planets and Mercury above based on the finding for a uniform density of the sphere. With some reservation (until rigorously proven), we might qualitatively accept the same consideration for a variable density heliosphere. We might consider that the hyle above the aphelion and below the perihelion would have some equivalent effect of some equivalent uniform distribution, so that only the variation in the layer between aphelion-perihelion would make a quantitative difference; the latter is thought to be very small, but it could become conclusive when this is computed rigorously.

25 Further electron/positron modeling

In view of the preceding sections and analysis, we can discuss various possibilities and draw some important corollaries below. The accrual or diminution of real mass during acceleration and deceleration may not be properly explained without a concomitant understanding of the structure of material particles. The latter can be achieved by progressive modeling in continuation from the general proposal in Fig. 49.

First, we outline the general background on which all such modeling may be constructed. If accrued real mass (effective plus black mass) is a function of speed and vice-versa, then we can have a tangible interpretation of the kinetic mass concept. We have learned that effective mass is proportional to the energy rate of absorption that is proportional to the rate of gravion absorption. Furthermore, if gravions are thought of as particles of a gas (or aether), then we have two distinct possibilities regarding the distribution of gravion speeds:

(a) They all have the same constant speed as opposed to a Maxwell–Boltzmann distribution of molecular speeds in a ideal (classical) gas. That is, we consider gravions belonging to a “monochromatic” gas, for which we may derive corresponding relationships between the gravion speed and the propagation of a disturbance (or excitation) speed (like sound speed or light speed). In that case, we expect the (individual) gravion speed to be greater than the propagation speed (presumably c) by some factor to be worked out later. For example, this factor is $5/3$ for monatomic gases using classical mechanics but relativistic effects, if applicable, may also be taken into account. The important idea here is that each gravion has a dual nature of “body” and “speed”. The body-and-speed are integrated in a single entity to what makes a gravion. That is body-and-speed are objectively inseparable.

(b) They have some characteristic distribution of speeds (not necessarily Maxwell–Boltzmann). Such a possibility means that gravions are entities capable of exchanging and/or transferring speeds during interaction between them. If the “body” is invariable, then the speed must be variable. The variable speed might be continuous or discontinuous (quantized). The speed is some sort of a separate entity that can be exchanged and/or transferred from gravion to gravion. Hence, we have to accept a dual nature of matter but with separable entities of speed and body, each having its own “nature”.

The combination of having a variable body with invariable speed refers back to the first possibility by “sticking” the two gravions together (somehow) or getting them to move parallel and very close to each other. Otherwise, we would have fractional gravion bodies sticking together, a combination that we will not be dealing with here. The combination of having both a variable body and a variable speed refers back to the second possibility, because if the two gravions stick together to vary the mass but have a different speed, it means that the speed is a separable entity. We think that we could adopt either (a) or (b) of the above possibilities among other combinations that might also be proposed.

Those two possibilities lead to the dilemma about the deeper meaning of “body” and “speed”. We prefer to adopt initially the first case (a) and investigate the consequences. If not satisfied, we can always return to case (b) accordingly. The reason for opting to examine the (a) case first is because it offers a common denominator of the smallest quantum of matter, namely, the moving-gravion with an overall (integrated) invariable identity. A moving gravion then represents a quantum of momentum (impulse). In other words, momentum is quantized and the minimum amount is that of the moving gravion. The duality of its nature is inherent in the gravion from the outset of the theory. Then, we are left with the task of modeling the gravions in building other push particles, conventional particles and material bodies (forms of matter) in general and ultimately the cosmos. This is the subject/task of subsequent developments in PG. We only initiate some preliminary ideas.

Based on the above choice, we can arrive at a better understanding of the nature of effective and black mass. We have said that effective mass is the activated part of real mass and black mass is the inactive (inertia-less) part with “true” zero classical inertia and zero energy. This might seem to demand that we choose the second possibility (b) rather than the first (a) per above, because only then could we achieve gravions with zero speed (at rest), presumably packed with maximum density inside a black hole. In contrast, (a) demands that we would have highly packed gravions incessantly moving/colliding with each other at an extremely high density. The latter density could never reach the theoretically limiting density of gravions at rest. Essentially, we would have a medium of moving gravions with an extremely high density flux J_{0black} of black matter. In the case of a black hole, this would be enveloped by an effective mass layer (the event horizon) separating it from the surrounding field created by push particles of type-x, with a density flux J_{0x} . To maintain the black mass core stable, it would require that $J_{0x} > J_{0black}$, which is overall inconsistent with black mass having the highest possible density. However, the latter inconsistency can be resolved as follows:

Two gravions may be considered at rest relative to each other if they happen to move in parallel with the same velocity, the presumed fixed gravion velocity. Similarly, we may consider a swarm of gravions moving parallel with each other in a stream inside the surrounding chaotically moving gravions of a generally static, on average, gas. In this situation, we can invoke the classical gas dynamics laws. A static gas is characterized by a static pressure, whereas a gaseous stream is characterized generally by both a static and a dynamic pressure. For example, a gas flowing through an aperture from a region of high pressure to region of low pressure generates a jet (stream) whereby the chaotic molecular movement is converted to orderly stream movement. The static pressure converts to dynamic pressure during expansion. If the low pressure region is a vacuum, the gaseous stream passes from subsonic to supersonic velocity and finally to hypersonic and beyond velocity when all static pressure is converted to dynamic pressure. This is how a molecular beam is formed. Linear streams of gravions inside a surrounding static gas of gravions must be enveloped by a layered transition zone of gravions flowing with increasing order (uniformity of velocity) towards the axis of the stream.

Linear particle beams having a finite length would be rare and cannot contribute to building stable

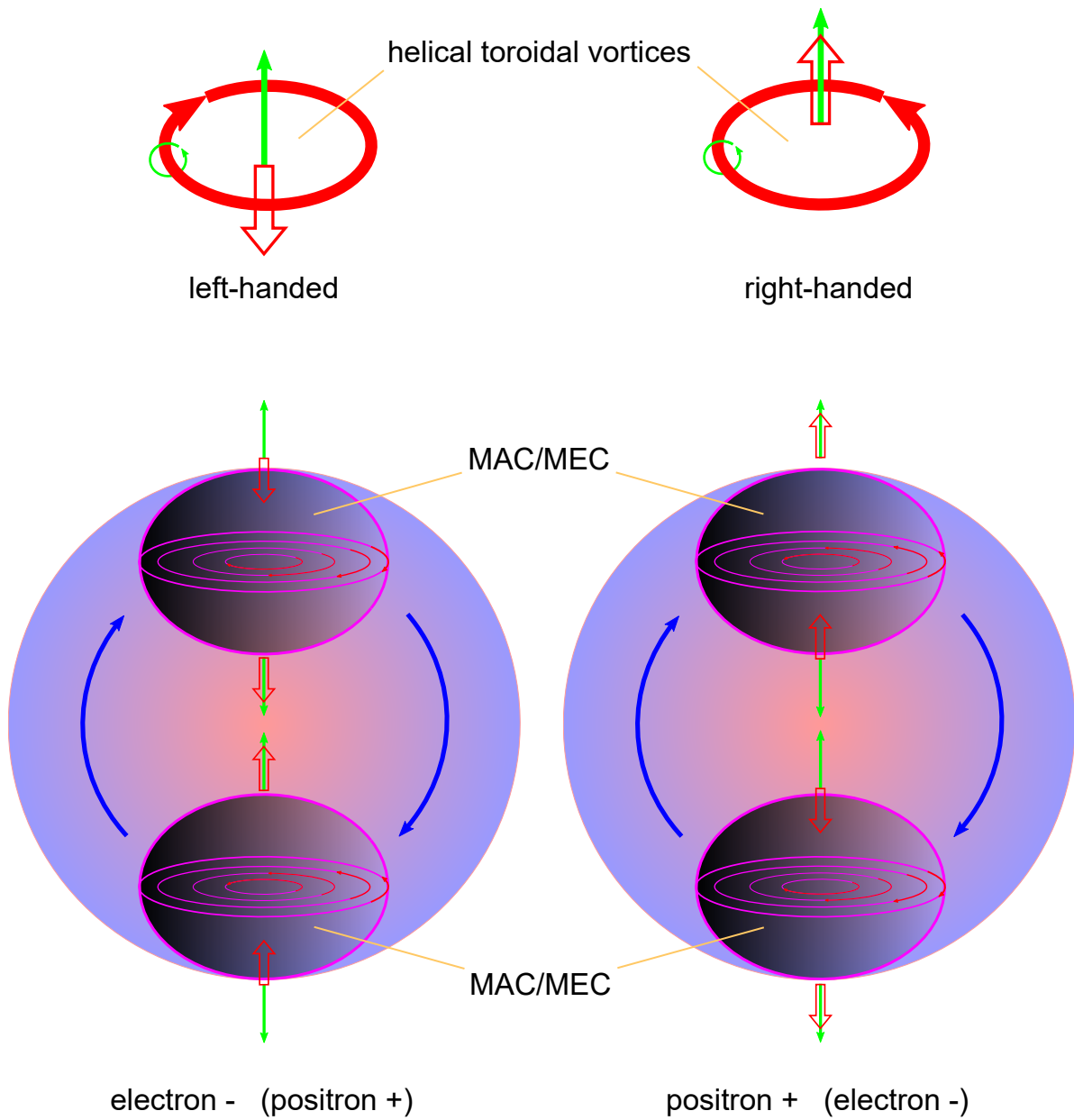


Figure 76: Pairs of MEC (MAC) at fixed distance and spinning in opposite directions emit outwardly either left-handed or right-handed helical toroidal vortices as negative or positive electrons; minimal structure for the electron and positron.

structures. However, with certain conditions present, it is possible to form circular streams of particles in the form of a vortex. Thereby, gravions in such a vortex are drawn from the periphery towards the axis and flow out along the axis in two opposite directions, like a double cyclone, back-to-back, in space. This provides a good scheme of a structure acting both as absorber and emitter, with which to simulate our MAC and MEC concepts. By such means, we can also describe the behavior of a rotating black hole in the shape of a disk, ellipsoid, sphere or shaft. In principle, we can have gravions at uniform (constant) velocity with increasing angular velocity inversely proportional to the radius from the axis of rotation. That would be the state of black mass, namely, a fluid with nearly all (or mostly) dynamic pressure and only a vanishing static pressure towards the axis. This is then the black mass that is enveloped with a layer characterized by a fast transition between dynamic and static pressure. This layer constitutes the event horizon that should be amenable to quantitative analysis to fit the best observations available by astrophysics. In such a model, the interior of black holes may then look like laminar flow but with vanishing low friction towards the axis. Because it is completely isolated from the outside push particles of various types, it presents no inertia to the outside world but maintains a huge amount of dynamic (latent) energy stored until it can be released during a black hole disintegration (explosion). In other words, black mass is still thought to be classically inertia-less but with “zero-point-energy” being the zero static energy (pressure) coexisting with latent dynamic energy due to the dynamic pressure of the rotating gravions. The latter description may bring PG close to current understanding of super-fluidity based on QED theory. Questions about the shape of a black hole, like spherical, ellipsoid or disk, should also fit available data. This in principle description of a black hole may also explain the accrual of real mass from equatorial periphery and emission via the polar regions in the form of hydrodynamic jets.

By similar means we may be able to describe also the structure of some elementary particles like electrons and positrons. They do not necessarily have to be exactly like the above hypothetical structure of a black hole. What we need is the application of Bernoulli law in analogous situations of gas and liquid flows of ordinary matter. In fact, there is a variety of forms of flows, from which we may use those that yield structures and properties consistent with particle physics data. Lord Kelvin (1867) already attempted to describe the structure of atoms with toroidal vortices. In fact, this trend continued for decades culminating to a description of chemistry (atoms and molecules) based on vortices until 1915 (Parson, 1915) before modern ideas prevailed to date. We do not propose to revert back to Parson’s chemistry, but we can attempt to follow a similar path for the modeling of elementary particles, which are considered to be structure-less by prevailing theory. Such an approach is particularly promising under our platform of PG theory. Key to those old theories was a conceived stability of toroidal vortices to the extent that they could form permanent structures of matter, like atoms and molecules. On these principles, Papathanasiou & Papathanasiou (2020) have proposed a theory of everything based exclusively on “*stable ring-shaped cyclones within the pressure field of a universal ideal gas*”.

For our purposes, we need not restrict ourselves to the use only of Kelvin’s vortices, but also consider a great many variations of similar structures based on dynamic flows. For example, Consa (2018) has proposed a new semi-classical model of the electron charge with helical solenoid geometry. In lieu of such a charge distribution, we may assume real matter distributions of the same or similar form. Thus, in PG we may consider the “ring electron model” and the “helical solenoid model” combining toroidal and poloidal currents of gravions or other push particles in fractal layers. The number of fractal layers will be determined by the needs of a PG model replacing the Standard Model but consistent with existing data.

Our general proposal here is a combination of (a) uniform forms of flow of particles with (b) chaotic push particle flow inducing gravity and/or electricity. That is, specialized flows of push particles constitute the fundamental structures of matter and material fields, all immersed inside superstructures of matter propelled by pushing fields of various types.

We attempt to use these ideas in further modeling the positron and electron shown in Fig. 49. If Kelvin’s vortex atoms did not prevail in the understanding of structure of atoms and molecules, or for being the panacea for “everything”, similar structures seem plausible and appealing for substructures of elementary particles on the platform of PG. In particular, they could be the key for subatomic structures and more so for the structure of the electron and positron, in particular. That is what we propose now in more detail by Fig. 76. This is an early attempt to take advantage of a helical-toroidal-vortex flow, which could embody the presumed positive and negative attributes of electrions. We are not aware of extensive research on such flows, but it seems that they can form stable entities behaving like particles. Plain toroidal vortices may bounce off each other or merge, and various observations have been made with smoke ring guns. The helical toroidal vortices are rotating vortex rings around the axis of the ring. All vortices propagate along the ring axis in the direction of the central flow of the torus. A helical toroidal vortex can be formed by a rotating “smoke ring gun”. In our case, we could postulate a spinning body (like a neutron star, black hole or electron) pumping out material in the form of rotating toroidal vortices from its poles. Discrete vortices would be

emitted by a pulsating spinning body. Now, the material coming out of an electron could be rotating vortices of gravions. Such hypothetical entities would fit the requirements of electrions. They can be right-handed (or positive +) when the vector of velocity points in the same direction as the vector of rotation, and left-handed (negative -) when these vectors point in opposite directions with each other. Also, we may posit the existence of at least two MACs acting also as MECs. Somions are absorbed by each spinning MAC while concurrently acting as MEC emits positive electrions from one pole and negative electrions from the opposite pole. The pair of MECs (MAC) shown in the figure are disposed in opposition along their axes, so that they always emit the same type of electrion outwards from the electron or positron. Now, what happens to the same type of electrions emitted in-between the oppositely spinning pair of MECs is a matter of conjecture for now: We suppose that they repel each other if they happen to collide or are reflected if they happen to strike the other MEC across. We have said that the mean free path of electrions should be very long relative to atomic scale, but if the pair of opposing MECs are practically aligned along their common axis, then the question is reduced to the statistics of this alignment. We can safely assume that there is a wobble between these axis so that the probability of collisions between electrions in this confined region between MECs may allow a degree (rate) of collisions. Leaving quantification of this question aside for now, we may qualitatively say that there can be a net repulsion between the pair of MECs due to net statistical bouncing of electrions imparting a net momentum in an outward sense. However, this outward force is counter acted by the surrounding somions imparting a gravity-like force in the opposite direction. We have said that somions may act like the nuclear force in atoms, so that they may also act in a similar manner in keeping the two MECs together inside an electron or positron. This situation then poses the question of stability. Do they move like in a binary system or do they require a stabilizing third body or more bodies to be present? We cannot address this question, until we earnestly attempt to quantify all these and other processes that may be present. For example, we may not exclude the presence of other particles contributing to the overall structure and stability of the electron (positron). We may be able to compose a minimum structure of particles acted upon by somions and gravions, and rotating in conformity according to classical laws or other laws as needed. By such methodology, we may be able to explain also the proton, which could be composed like a positron but with additional matter (real mass) of other stabilizing particles. Likewise we could build the neutron.

25.1 Discussion

The possibility of existence of the above structures for electrons and positrons may be questioned, since we have not considered detailed mathematical or experimental evidence to support such claims yet. However, the main purpose now is to initiate thinking in this direction for possible working structures. We have already discussed some questions above, but others may be equally or more important. ~~For example, it is important to explain why the electron is stable but not the positron on account of their equivalent structures. The stability of proton might give us a clue.~~ For now, gas and fluid dynamics with emphasis on the above special flows seem to constitute important tools for the development of a complete PG theory. Recent work has applied these tools to quantized superfluid vortex rings in a Fermi gas (Bulgac *et al.*, 2011), and to planetary atmospheres and vortex movements in the vicinity of active galactic nuclei (Bannikova *et al.*, 2016). Also, a recent overview has been provided by Falconer (2019). Furthermore, computational simulations of gas flows like that by Bird (1995) could become indispensable tools in the study of force fields.

The possibility of making material structures and particles by way of various forms of circular motion from the chaotic random motion of particles opens a new way to study and understand cosmology. Early glimpses of this can be gathered by some direct quotations from Bulgac *et al.* (2011): *...“A notable property of superfluids is their ability to sustain quantized vortex lines (3, 4), which, unlike classical hydro-dynamical vortices, have a quantized velocity circulation.... Abrikosov predicted that many quantized vortices self-organize into a triangular lattice (6)... In excited superfluids, vortices have a complicated time evolution; they cross and reconnect, a process extensively studied in Bose superfluids, which leads to quantum turbulence (9) and which, unlike turbulence in classical hydrodynamics, is realized basically in the absence of dissipation.”... A spherical projectile flying along the symmetry axis leaves in its wake two vortex rings.... Moreover, the system organizes itself in an almost perfect vortex lattice after the stirring is turned off. Even more surprising is that the system remains a superfluid, even when stirred at supercritical speeds“...*

It seems that we can have a better understanding, or more options in the behavior of an electron. This particle can easily appear in different modes of existence when free and when it is bound in a atom or molecule. Consa's deterministic description of the orbital electron is helpful to conceive an upgraded structure: Whereas he describes the electron as helical toroidal vortex comprising toroidal and poloidal currents of charge distributed around the nucleus of an atom, we think that this may be the locus of trajectories of a single electron moving around the nucleus. This would resolve the huge discrepancy in the size of an electron between the two models, namely, Consa's electron having the size of an atom (i.e. its

orbital), while we may have a much smaller size between $10^{-22} - 10^{-23}$ m (per preceding findings) moving along Consa's trajectories. Alternatively, we can go along with the quantum mechanical description of the electron orbital but again as being the probability of locating our PG electron inside such an orbital. In both cases, we maintain that the electron is a very small particle in motion around the nucleus in one way or other, but neither a QM continuum (wave cloud) nor a helical solenoid continuum of electrical current. We do not need to invoke the electrical charge as a distinct entity. Fractalization may also be taken into account to devise structures at various levels, like "*heavy solitons*" shown to be vortex rings Bulgac *et al.* (2014).

The notion of quarks may be compatible particles per above: Quarks may be combinations of MECs (MACs) in such a way that we may bridge experimental data with our theory. For this purpose, the electron model proposed may be a model for each quark existing in stable triplets. or having three pairs of MECs in some alternative stable configuration. Furthermore, the display of *zitterbewegung* at the Compton scale may also be exhibited by modeling around the proposed scheme in Fig. 76, which may also be consistent with certain QED aspects.

The proposed electron/positron model may help understand also the connection of accrued mass with the speed of a moving body. It is challenging to attempt to understand the mass-speed relationships proposed and to attempt to conceptualize the situations depicted in Figs. 50, 51 and 76. A moving body with constant speed relative to the gravion frame of reference is acted upon by a null total force, which can take place only if the rate of gravion flux from the advancing is the same as from the receding direction of motion in order to avoid drag. The effective mass of the moving body is greater than the effective mass at rest, whereby the extra effective mass is accrued during acceleration by the action of the rocket in Fig. 51. This is obtained by the excess rate of electrions absorbed from the receding direction via a process yielding an increment of both effective and black mass in the accelerated body. As soon as the rocket action ceases, there is a new steady state equilibrium of gravion absorption with the surrounding flux density J_0 . An observer inside the famous "accelerated elevator" would report a real mass injection apportioned between the effective and black fractions, if the observer could detect push particles and monitor the building grains of matter. The elevator is integrated with the rocket body-with-fuel (elevator system) while the ejected propellant causes the excess electrions to accelerate the elevator system. A stationary observer (outside the elevator) with similar capabilities of detection would observe both the accrual of mass and the displacement of the elevator system. During deceleration via a rocket system again, the ejected propellant travels in the advancing direction with additional mass imparted from the stored excess mass in the rocket system. The accreted mass is preserved at constant speed without affecting its chemical constitution but the atoms become more massive in the form of extra effective and black mass.

The above description might spare us from the "twin paradox" and other effects now not necessary to address. However, there may come a point at sufficiently high speed when matter has to transform to another phase: Atoms may become plasma, then neutrons, then black matter and whatever transpires in all possible transitions. Our traveler inside the gedanken elevator would see those transformations provided consciousness survives beyond matter transformation. Such may be the fate of a falling body into a black hole.

Prior to any presumed phase transition of matter, the moving body must acquire some fundamental variation of structure at sub-elementary level that distinguishes it from its stationary state structure. If the chemistry is preserved, then some attribute may vary at the subatomic level over and above a plain quantitative accumulation of matter, and in a way that is reversible during deceleration. This may involve, for example, an alignment of the spin of MACs and MECs, in a fashion similar to nuclear magnetic resonance (NMR). The pushing particles in a particular direction of motion might provide the mechanism of alignment for a fraction of the total composite mass. The so "aligned" fraction of mass may coincide with the kinetic mass. By such or similar means, a moving body would be distinguishable from a stationary one by all observers, i.e. stationary or traveling with the body. Kinetic mass may be the distinguishing feature of a moving body. Therefore, further examination of the definitions in Table 31 may contribute in the modeling of matter at the fundamental level.

The circular movement of matter at the smallest and higher fractal scales is compatible with black mass, effective mass and push particles of gas-like media, such as gravions, electrions and somions. These is a continuous interchange of matter between its various forms. It seems that the classical "flux" of fields is an actual physical event of push particle flow: The magnetic flux in a solenoid, the electric flux from positive and negative charges and the gravitational flux are all representing a flow of material particles, all of which we think can be finally reduced to gravions.

The equation $E = mc^2$ holds quite well in transforming potential energy to mass, or (better) potential mass to kinematic mass when applied to very high density mass. Furthermore, PG reveals a wider range of mass types, the conversion of which via that equation yields outcomes that we may not experience directly

in conventional physics, like the heat-pump effect (principle) applied between force fields, like electrical and gravitational fields. We can now close the energy-mass balance sheet properly. The “invisible” black mass is part of the total real mass equation that is absent in prior theories and practice.

The connection of motion to structure may be a way to make progress in understanding space-time, the dynamics of PG and the connection between speed and mass. The vortex structure may be at the basis of this hypothesis. A minimal effective mass may be that of a MAC/MEC. By way of illustration, we might simulate a moving vortex to a jet engine. In a stationary sphere, the effective mass is spherically distributed with the statistical average of the vortex vectors all pointing towards the center of the sphere with zero net sum. When the sphere moves, we may have a partial alignment of the vortices along the direction of velocity. A one-to-one correspondence exists between velocity and kinetic mass, which is composed of aligned vortices. This is one example of connecting speed to structure. We might find alternative and better structures for this purpose. This approach opens new vistas for experimentation and/or theoretical work. For a deeper appreciation of this proposal, we may quote from Feyerabend (2010) again: “*The consistency condition which demands that new hypotheses agree with accepted theories is unreasonable because it preserves the older theory, and not the better theory. Hypotheses contradicting well-confirmed theories give us evidence that cannot be obtained in any other way. Proliferation of theories is beneficial for science, while uniformity impairs its critical power. Uniformity also endangers the free development of the individual.*”

25.1.1 Lord Kelvin’s vortex atom

While the proposed model for electrons and positrons is admittedly speculative, its adoption entails a similar description for related particles like protons, neutrons and photons. This might trigger further ideas with regard to important unsolved issues in physics. The vortex modeling of electrions composing electrons, if also used for other particles, may usher a novel perspective for understanding and explaining phenomena like the slit experiment and quantum entanglement.

Vortex in lieu of “wave packet” is our proposal herewith. It is the constituent building block of “particles” such as electrons, protons and photons. The particles (excitations) of quantum field theory are now thought to be composed of other real entities. The vortex exists in 3D space and can yield the wave-forms we experience upon its interaction with (or incidence upon) surfaces. This may also seen as “collapse” of the vortex upon a “surface”. The latter may correspond to the “collapse” of the wave function of quantum mechanics upon measurement (detection) of the particle. Lord Kelvin described the atom by way of a vortex as shown in Table 40. This is a copy-paste from his original paper, where we have added an arrow to indicate the direction of propagation. It is a traveling entity at high speed c , not a stationary atom envisaged by Kelvin; this is similar to the rings of air shot out of vortex cannons. Atoms and molecules have been described very well by modern quantum theory, which is by no means challenged and its successes are not disputed. We only shift the Kelvin model to describe entities many orders of magnitude smaller than the level of quantum mechanics.

We have (tentatively) identified the electrion to be a single traveling Kelvin vortex. We have further used a combination of vortices to describe the electron and positron. Appropriate combinations may be devised to describe the structure of protons, neutrons and photons, some more complex, some rather simpler. We are only taking one step towards attributing some structure, about which Dehmelt (1989) felt compelled to surmise.

Kelvin’s schematic complements our visualization of a possible reality. The “particle” of an electron or a photon is not one homogeneous individual “particle” in the customary sense of the word. It is the sum-total of the synergy of sub-processes involving a huge number of other much smaller entities, like electrions, which are further made up by even smaller entities (perhaps, the gravions). Vortices form over a relatively extended space (albeit extremely minute to us). This possibility can readily explain the phenomenon of duality, i.e. of “particle” and “wave” exhibited by the same “particle”. By such means, we may better envisage the possibility of an electron or photon going through a double slit “simultaneously”. That is, it is not a single “particle paradoxically” passing through both slits, but parts of what appears to us to be a single particle. It remains to explain how these parts of the particle simultaneously “excite” or trigger the slit surfaces to reproduce the “particle” on the other side of the slits. The waves, in general, that we experience are inherent in or part of vortices. The wave interference of light that we record on a screen behind the slits are the outcome of the incidence of more complex entities, such as vortices. We now need to encompass these phenomena in a wider vortex theory. Vortices are not everyday customary (obvious) experiences, while they possess some extraordinary properties. Workers in this field are called upon to consider research along the lines envisaged herewith for push gravity.

Quantum entanglement (the ability of separated objects to share a condition or state), may then be given another perspective in terms of the vortex theory. Vortices provide the spatial expanse of particles (otherwise apparent points) and hence it may also explain the connection (entanglement) of opposite spin vortices, i.e.

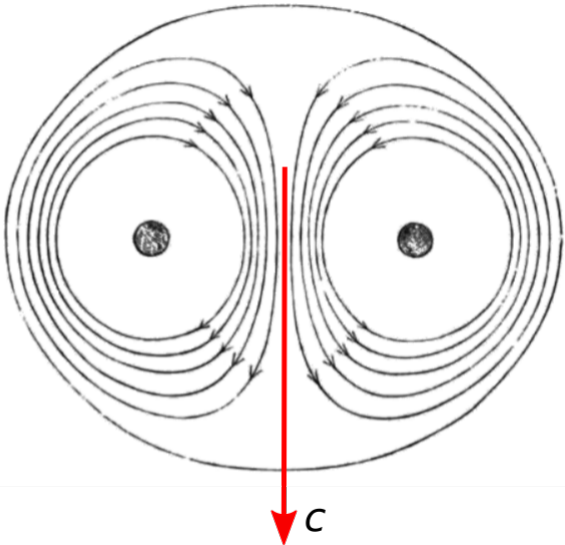
Multi-level universe		
	entities	forces
	galaxies	cosmic weather, gravitational, electromagnetic, nuclear fields
	white dwarfs, neutron stars, black holes	gravitational, electromagnetic, nuclear fields
	planets, stars	gravitational fields
	atoms, molecules	electromagnetic fields
Kelvin vortex 	particles, electrons, protons, photons	electromagnetic, nuclear fields
	electrons, somions	electromagnetic, nuclear fields
	gravions	gravitational fields

Table 40: *Schematic of the vortex atom published by Lord Kelvin (1867) now proposed as building unit (element) for particles like electrons, protons and photons, with corresponding forces (fields)*

particles at a distance (spooky action at a distance). What is unclear now is whether the said vortices are traveling objects like in vortex cannons or moving formations like water waves without moving (transferring) of water at a distance. In addition, we have to ascribe a minimum set of attributes to the gravion enabling us to construct the vortex. Such attributes, for example, could be a quantum (minimum) vector of space-time-momentum with a collision (interaction) rule between gravions. This could be the starting entity by which the universe is made and all our theories must comply with.

In 40, we have included the schematic of the Kelvin vortex to indicate its relative position in a multilevel universe. It is placed at scales much smaller than the atom, i.e. much smaller than the range of validity of quantum mechanics. Quantum electron dynamics may then have to undertake the appropriate adjustments in describing superstructures above gravion and vortex levels. The current field theories encompass a number of levels, below and above which forces can be explained by alternative means. At galactic and super-galactic levels, we have proposed that cosmic weather determines what appear to be problematic phenomena for prevailing gravitational theories. The concept of mean free paths and the distribution of hyle over these paths becomes a key concept in our theory. The universe is self assembling at various levels separated by many orders of magnitude under an auto-sorting process of particles and bodies over a range of mean free paths. A universal medium (hyle) is distributed in a way that may explain our observations over a wide range of orders of magnitude (see more in Section 33.4).

By no means do we claim veracity of the above proposals and ideas. We only wish to indicate that we may need to start with a radical new approach to explain our accumulated large amount of data. This includes certain principles like the speed of light being the ultimate speed of the universe. If our hypothesis that photons are themselves a superstructure of other much finer processes, then speed of light is only the speed observed for this superstructure making it arbitrary to assume the same speed for its components. The above ideas of “mean free paths” and “collisions” (or interactions) at the levels of gravions and electrions may provide us with novel means to formulate a novel concept of the universe.

In fact, it seems that we are arriving at some important conclusions that are consistent with contemporary findings elsewhere in physics, albeit not everywhere. For example, we have learned that gravions create or “give” mass to hyle. This is consistent with the notion “that Higgs field gives mass to fundamental particles”. By the same token, we have further learned here that electrions create, or “give” charge to electrons (charged particles, another form of hyle). Is this a coincidence, or have we arrived at some fundamental truths about cosmology via another simpler and perhaps more precise way? This may be answered by those best learned experts of quantum field theory and the Higgs field. It may be about time to put aside certain “principles” that have locked physics in an impasse. It maybe about time to adopt the principle of similitude and fractals as the basis for understanding the multi-leveled cosmos. It may be that the gravion defines the quantum of space-time-momentum, whilst the rest of the universe is being built by gravions at different configurations and concentrations. The concept of atom proposed by Democritus has gone through a round about trip via our established chemistry/atomic/nuclear/quantum theories, all of which will finally come to rest on the ultimate “atom” being none other than the gravion.

26 Particle physics

26.1 Moving particles

In view of the new definitions and findings about speeding material bodies, we need to review the meaning of various masses previously derived for the proton, electron and positron in Sections 19.3 and 21, and similarly for other particles to be considered later.

The notion of intrinsic speed for a macroscopic body is connected with the intrinsic mass of a lone-and-stationary body with respect to the gravion gas (medium). However, this body consists of internally moving atoms and molecules (moving particles). These particles then have a composite mass each, the sum-total of which constitutes the intrinsic mass(es) of the macroscopic body. If we could bring all the particles to rest at the absolute zero temperature, then each particle would be left with an intrinsic mass of its own, the sum-total of which would constitute a new intrinsic mass for the macroscopic body. The intrinsic mass of the “frozen” body would clearly be less than the intrinsic mass of the body at “room” (elevated) temperature.

We can apply the same logic to sub-atomic particles even though we may not have the technical means to “freeze” them. All our measurements and experimental data on those sub-atomic particles refer to moving particles. We previously used the known masses for the proton, electron and positron under a static PG theory. However, those masses were actually the composite masses for each of those particles according to our latest understanding. Thus, the effective mass of an electron previously designated as $m_{e-electron} \equiv m_{e-e}$ actually represents the composite effective mass of a moving electron and should be reassigned as $m_{ec-electron} \equiv m_{ec-e}$. Similarly, the proton should be shown as $m_{ec-proton} \equiv m_{ec-p}$. Having said that

these moving particles have a “composite” mass, leaves an open question if they also have an intrinsic mass of their own too. We need not answer this question here, other than point out this possibility. The latter depends on their possible internal structure, which we attempted to conceptualize in the previous section. For consistency, it is reasonable to assume that they do have an intrinsic mass, at least a theoretical one that would be had if the particle could be captured stationary inside the gravion medium.

The above considerations are important in view of Eqs. 406 and 409 on speed range and speed addition. The electron was found to be a very dense particle meaning that its absorptivity is very close to unity. If that absorptivity corresponded to its intrinsic mass, then its intrinsic speed would already be very high leaving minimal room for additional speed. In other words, we would have great difficulty to speed up the electron from its rest position, which is contrary to experience. We understand now that this contradiction does not occur because the masses we used are composite masses at already great speeds. To achieve the latter situation (already fast moving particle), should they have an intrinsic mass, it must be very small that allows all the known possible range of speed for the electron.

The above understanding is the counterpart of similar understanding of current theories, whereby material bodies are said to be composed of about 95% “energy” and 5% “mass”. We may arrive at similar descriptions but in terms of various forms (types) of mass, all of which are part of real mass. It seems that PG may “encompass” existing theories, which have missed out on black mass and internal structure of “fundamental” or “elementary” particles. Therefore, we need to return to these issues after, or better in conjunction with modeling of the structure of moving particles.

The above are only opening remarks for what may become a chapter of particle physics in later developments.

26.2 WIMP, WISP and dark matter

It is said that about 85% of the universe consists of dark matter. If this must be the case because of prevailing theories, then it can be consistent also under the PG platform. The only qualification is to say that the dark matter must also correspond to effective mass under PG, which, in turn, is further accompanied by an appropriate amount of black mass. In short, dark matter and black mass are different notions, not mutually exclusive and can coexist. The quantitative relationship between effective and black mass depends on the size of dark matter particles.

It is said that the weakly interacting massive particles (WIMPs) are hypothetical particles among various candidates for dark matter. They are broadly thought to be new “elementary” particles interacting via gravity and other force(s) as weak or weaker than the weak nuclear force; they are beyond the Standard Model. Since they do not interact with electromagnetic force, they may have a simpler structure than the one outlined for electrons/positrons in our preceding model. They may be more “elementary” having a kind of “amorphous” structure, but still have some structure in the arrangement between effective and black mass. Being more massive than neutrinos, they move slower under our PG relationships between absorptivity and mass outlined above. They are relatively large spheres (still particles) interacting via push gravity via gravion absorption. Experts on dark matter research may continue to study various candidates of particles like neutralino (WIMP) and axion (WISP) under the PG platform. The fundamental issue, however, remains if the search for dark matter is justified by being based on existing theories, should those theories need revision. Dark matter is necessitated to explain why rotating galaxies don’t tear themselves apart. However, this is not necessary to be the case under PG, but PG does not exclude dark matter for whatever other purpose. We have already accounted for black mass expelled in the form of jets from black holes and other dense bodies. This mass may be “sprayed” in the form of particles being activated by gravions to form WIMPS, which consist of a black mass core enveloped by activated effective mass. They are minute black holes as particles, like electrons/positrons might be, but without the internal organization of the latter; i.e. they lack emission of vortex structures and they are “electrically” neutral. If WIMPs exist, their properties may be unlike those originally predicted. In the latter case, we have to re-appraise the entire background of our research efforts.

In the above context, a successful detection of dark matter does not solve the outstanding problems in physics. Detection of some rare WIMPs in the laboratory does not prove that we found the 85% missing matter “needed to prevent the galaxies from falling apart”. It does not disprove PG theory either, which can explain the integrity of galaxies even without dark matter. However, PG can easily accommodate dark matter, which is likely to exist simply as another component of the cosmos not yet detected.

27 Literature survey

As stated at the outset of this report, the special circumstances of the author have not allowed extensive referencing to all and various diverse fields of science having a direct connection with this development. This work is mostly self-reliant, but it is natural and welcome that our findings overlap and agree in most respects with prior literature. After all, we should all converge in agreement with experimental data. We seek an understanding for many omissions in literature references. We intend to study prior literature that comes to our attention, as also we prefer to make proper and meaningful attributions instead of a mere reference listing. Historically, works on push gravity are rare and practically non-existent in the “mainstream” scientific literature. Worse than that, PG has been considered a “finished” or “discredited” theory by several authors including well known celebrities in physics. Under these circumstances, it requires a lot of courage by someone to come forward in an attempt to revive, develop and promote this theory. At any rate, we feel that a substantial body of work has been presented by now warranting due attention; the majority of the theory, especially its methodology and many important conclusions, is unique.

For a while, we will continue to provide our findings as long as this is possible and work on the literature will be mentioned intermittently under this new section, which for the moment is only a “stub”. We welcome suggestions to improve on all kinds of omissions.

Long after Fatio and Le Sage proposed their principle, a relatively early comprehensive analytical work on the pushing force between two bodies has been presented by Darwin (1905). Interestingly, it is the year that physics took a completely different course for the following century and more.

Just briefly, it is important to mention that some recent works by Meis (2020), Meis (2022) and Meis 2025 has come to our attention: It appears that quantum electron dynamics (QED) theory may independently predict the existence of push gravity, or push electric field. It may make it worthy to investigate the radiation pressure of the electromagnetic quantum vacuum field felt by bodies.

{To be read and included where relevant: (Fedosin, 2018), (Fedosin, 2015b), (Fedosin, 2012), (Fedosin, 2017), (Fedosin, 2015a)} Likewise, Fedosin (2021) reporting “*on the structure of the force field in electro gravitational vacuum*” has clearly adopted the principle of push gravity. Furthermore, Simaciu (2006) has made a contribution to the development of the theory with absorption of gravitational interaction. We should examine if and to what extent those theories can interbreed with our approach to PG.

It seems that another perspective of the atomic structure outlined by Hunt (2019) may be compatible with our fledgling model for nuclear force in Section 21.3.1. Our *somion* medium may correspond to the description that “*nucleus of every atom is held together by energy in the form of a standing wave originating from the nucleus and surrounding it*” (Hunt, 2019). PG pressure and standing waves are compatible.

It seems also that the ideas of “a superfluid theory of everything” reported by Fedi (2016) are compatible with our further modeling of the electron and the cosmos in Section 25. This work may deserve special attention for possible inclusion in the development of our PG theory.

The inclusion of certain works herewith does not imply endorsement or overall agreement with our theory.

28 Elastically back-scattered gravions

Lahres (2023b) recently presented a lecture entitled “*What if the basic force "gravity" is basically repulsive?*” and now followed by “*Effects of different interaction mechanisms between hypothetical gravions and matter on Push Gravity theories*” (Lahres, 2023a).

He used the Ansys Speos software to simulate the effects of absorption and scattering using a presumed analogy between optical radiation and gravitational repulsive radiation. The results confirm that an apparently attractive force is generated between two bodies from the pushing forces (impulses) by a background radiation of particles. in the following two cases:

- (a) When the particles are absorbed and
- (b) When the particles undergo anisotropic elastic scattering in the backward direction (elastic back-scattering) similar to Rayleigh-scattering.

When the particles undergo isotropic elastic scattering, no net force can be generated between the two bodies. Case (a) is consistent with our #3 principle at the outset Section 3. However, case (b) is a new theoretical proposal not yet considered in the present work. Our response to it is outlined below.

We can allow this theoretical case by considering Fig. 2 as follows: In lieu of absorption, we may assume that a gravion undergoes an elastic back-scattering event at 180 degrees angle. This will impart an impulse twice as strong as the impulse generated by an absorbed gravion. Therefore, we can follow and reproduce the same equations to finally arrive at Newton’s gravitational law by Eq. 38. We only need to replace the absorption coefficient k with an elastic-back-scattered-gravion (ebsg) coefficient k_{ebsg} . In that case, the often used absorptivity would be replaced by a reflectivity factor. The latter is thought to be a different function,

perhaps more complex, if it can be an explicit integration formula at all. Meis (2020) and Meis (2022) has proposed a total (elastic) reflection of kenons to produce a gravitational field probably like elastic gravions would do. In any case, this requires considerable work and then to find out what modifications would be required to the followup reported work here.

The advantage of this theoretical possibility is that there is no energy absorbed, which is one way to overcome the main objection to PG theory requiring very high energies and presumably resulting in destruction of planets and bodies. Furthermore, we may allow some energy to be absorbed by near elastic back-scattering to a degree that would be consistent with the heating of the core of planets, the high heating of stars, etc.

One disadvantage of this is that, for now, it is initially restricted to weak gravion-planet interaction leading to Newton's law per given equation, but it is not obvious what would happen for very dense or large bodies. When the elastic back-scattering is repeated from much greater depths of dense bodies, the equations derived for the general gravitational law (in PG) by Section 5.2 need to be modified accordingly. Elastic multiple back-scattering will tend to produce an isotropic end scattering out of a sphere, which does not generate gravity. Lahres has found (by simulation) that *“as multiple scattering becomes more relevant, it makes the scattering on large scale isotropic again”*. However, this needs to be further investigated either by analytical means or some direct simulation Monte Carlo (DSMC) method (Bird, 1995).

Another disadvantage might be that, in a total elastic scattering regime with no energy transfer at all, we may not hope for a unification of different fields (e.g. gravitational-electric), because these fields would be compartmentalized with no possible “communication” or coupling between them.

The possibility of elastic gravion scattering does not refute or invalidate our theoretical considerations and derivations based on a gravion absorption regime together with re-emission of energy in another form of particles. However, all this needs to be born in mind along with further advances of PG theory.

Part Three (3)

In this new Part, we attempt to synthesize and extend some of the findings, ideas and theses in the preceding Part 1 and 2. The main reason for separating this part out of the preceding ones is to allow even more freedom in putting on record a series of proposals and theories that, in the event of invalidity, should not diminish the importance or validity of what has preceded this. Thus, Part 1 is thought to be at least a valid mathematical derivation of gravity, whilst Part 2 is an extension based on theoretical proposals in direct connection with Part 1. Part 3 presents also assumptions intimately connected with the previous parts, but with an increased risk of invalidity. Nevertheless and while speculative to a great extent, it is not necessarily less likely to be correct; it can, in effect, provide a least a road-map for other more significant developments ahead.

We apply again the approach of “what if” without being bound by conventional constraints in certain situations, but always ready to recant. We start with some further considerations of the energy-mass relationship. We plan to follow with some attempts in understanding possible details of the gravion properties in conjunction with hyle organization and with a further elaboration of the electron/positron model proposed in Section 25. We feel that there is a boundless potential for reappraising physics and intend to record out thoughts in the ensuing versions of this work.

29 The energy-mass equation in PG

We attempt to establish a relationship between energy and mass in PG analogous or the same with the conventional $E = mc^2$. Actually, this Section may contain fundamental material in the development of PG theory and may qualify to extend Parts 1 and 2 with it during a later re-write of the report. We work by steps in the following subsections.

29.1 Gravion momentum vs maximum acceleration g_0

We endeavor to find first a relationship between gravion momentum vs. maximum acceleration g_0 to be used in following derivations. Based on early derivations in Part 1, we find that the factor f_g in Eq. 43 given by:

$$f_g = \frac{\pi A}{r^2} = \frac{\pi R^2 A_R}{r^2} \quad (462)$$

provides a coefficient for the component of gravion momenta (impulses) contributing to the generation of acceleration g_r towards the center of a sphere illustrated in Fig. 2. The proportionality for the acceleration

is provided by Eq. 46, namely, by the product $\frac{J_0}{c}\Lambda$. This means that, if there is some effective mass M_{er} acted upon by a force F_r at point O set at distance r , the acceleration g_r is

$$g_r = \frac{F_r}{M_{er}} = \frac{J_0}{c}\Lambda f_g$$

Now, we move the point O on the surface ($r = R$) and make the sphere to have a totally absorbing material with unity absorptivity ($A_R = 1$). This situation is schematically depicted in Fig. 77(b) with a black sphere having a red surface representing the entire effective mass. We choose an infinitesimal surface area dS on the sphere with effective mass dM_e around point O, and the acceleration now symbolized by g_R is

$$g_R = \frac{dF_R}{dM_{eR}} = g_0$$

where dF_R is the force normal to the differential surface area exerted on dM_{eR} by the incident gravions. Because the absorptivity is unity, the field acceleration at the surface is the maximum possible g_0 .

We can assume that the surface element may be small enough so that only one gravion is incident during the entire gravion interaction time t_g . The elementary effective mass becomes the mass M_{eg} created at the body by the single gravion, i.e. $dM_{eR} = M_{eg}$. Each gravion is absorbed over interaction time t_g with (an average) deceleration c/t_g transmitting its momentum to M_{eg} with a force F_g at a random direction. This may appear to be a gross assumption, but we may use a mechanical analogue, for example, of a rope (string) impinging longitudinally on a body in free space, at constant speed c ; there is a continuous accrual of momentum for the duration of this interaction. In reality, the "rope" can be replaced by a very thin line of distributed momentum by some medium or entity. We can describe the transfer of momentum via some specified function of time, like a vibration, which, however may prove to be redundant even incorrect; an arbitrary transfer of the waveform of photon transmission might be counterproductive to the understanding of gravions. In any case, we wish to find the outcomes of this assumption first, while we are always free to revoke it later and return to this point with a refined type of interaction.

The difficulty is that we do not know the details about the nature and attributes of the gravion yet, beyond the initial principles, and specifically that it carries a momentum p_g imparting an impulse on the body. However, momentum by conventional mechanics requires velocity and mass. If the gravion is giving mass to other bodies, what might give mass to itself? We would have to accept that there is another level of finer push particles to give mass to it, and so on. To end this impasse, we adopt the classical mechanics of momentum transfer to apply to the single gravion for the present purposes. That is, we initially assume that a gravion does have an effective mass of its own, which is intrinsic to it and is one of its attributes; the quantum mass of the gravion, designated by M_{ig} , is invariant and indivisible. We have dropped the subscript e and replaced it by i , because we adopt an "intrinsic" property of mass with conventional inertia in a conventional meaning of momentum. Then, its momentum $p_g = M_{ig}c$ produces a force $F_g = M_{ig}c/t_g$ during deceleration, while it is pushing the corresponding body mass M_{eg} with equal force at some random direction at point O. To obtain the normal force F_{gR} on mass M_{eg} , we must multiply by the factor f_{gR} given above:

$$F_{gR} = \pi \frac{M_{ig}c}{t_g}$$

where we have used $f_g = \pi$ on the surface (from Eq. 462 and $A_R = 1$) by averaging over a large number of gravions. The above force is equal to the force by the gravitational field $g_0 = g_R$:

$$g_0 M_{eg} = \pi \frac{M_{ig}c}{t_g} \quad (463)$$

which finally yields the desired maximum acceleration to be:

$$g_0 = \pi \frac{M_{ig}}{M_{eg}} \frac{c}{t_g} \quad (464)$$

The above equation is a general finding, which may be used as a guide to various possible outcomes. We know nothing about any of the factors in the right hand side of the equation, except, perhaps, for M_{eg} by knowing the total effective mass M_e of a spherical body and hypothesizing a total number N of individual quantum absorbing centers yielding $M_{eg} = M_e/N$.

A given g_0 can be produced in various ways according to the above equation. One way might be by inversely proportional pairs of M_{ig} and c . However, it is not appealing to assume superluminal or subluminal

speeds, but more appealing to set the gravion speed equal to the speed of photons $c = c_p$. Another way is to assume [proportionality](#) between M_{ig} and t_g in a constant ratio M_{ig}/t_g in the above formula. This means that the gravion mass can be extremely small with a corresponding extremely short interaction time. The latter is a fundamental question similar to that arising from established theories that a photon has zero rest mass but non-zero energy and momentum. In our simple (even simplistic) formula, we cannot have zero gravion mass, because it would require an instantaneous (zero) interaction time. However, we can think that neither the gravion mass nor the interaction time are zero, but their ratio is fixed albeit with some very small values of each. This can provide some insight by the ensuing analysis about what may be happening.

There is also the theoretical possibility that the product $M_{eg}t_g$ is fixed, so that for shorter interaction time, the generated effective mass is bigger. Hence, the interaction time remains to be determined.

Last but not least, we also have the possibility of both the gravion mass and induced quantum effective mass in the absorbing body to be exceedingly small. By “exceedingly small” we mean relative to hitherto known “particles” or minimal known entities (structures) in nature. In the latter case, we could set both masses to be equal without much concern. This is not a trivial excuse for the assumptions made about an intrinsic (as opposed to relativistic) mass of a gravion moving presumably with the speed of light. It would be in violation of special relativity (SR) and the initially assumed relativistic nature of the gravion per principle #5 at the outset. However, only by going around a prevailing theory (per “what if” method), can we achieve some new insights in the current section that can retrospectively justify the hypothesis (*).

To move forward, we can get some valuable insights even with setting some arbitrary values in the above equation. We can trial first the conjecture that the intrinsic gravion mass is equal with the emerging effective mass in the body, namely, $M_{ig} = M_{eg}$ getting the simpler form:

$$g_0 = \pi \frac{c}{t_g} \quad (465)$$

We will use the above equation together with PG equations already derived between energy and mass. However, care must be taken not to introduce the factor $f_g = \pi$ twice in deriving various expressions, in which we already choose the component of acceleration or flux density in the axial direction for spherical bodies (normal to the surface). If the flux component along the axial direction has already been taken into account, then we should drop π and use only the equation $g_0 = \frac{c}{t_g}$, as we may do sometimes without warning.

(*) The introduction of an intrinsic mass for the gravion is done for the specific purposes of this section, while only effective mass is used elsewhere and throughout this report. The retention or not of intrinsic mass for the gravion is deferred until later developments of PG theory.

It is important to note that gravion and photon are different entities (at this stage). Light (photon) theory and SR may not be applicable to gravions. We have already proposed that electrions (mediators of the electric field) are superstructures of gravions, whilst photons may also be some superstructure of gravions. At this stage, we see at least a correspondence (similar attributes) between gravions and photons with a relationship remaining to be established. The relationship may be the same or similar to that proposed by Meis (2020) between kenons and photons. However, we think that this similarity exists as a fractal similarity and that kenons and gravions may differ by many orders of magnitudes. Kenons operate at quantum-mechanical level, while the gravions presumably operate at sub-quantum-mechanical level. For example, they may differ by the numerical quotient (see Eq. 339), so that it is plausible that kenons may be identified with electrions. For these reasons, we have taken the liberty to assign an “intrinsic” mass to gravions with no implications to photons. We are not making a judgment about the zero rest mass of photons per quantum field theory. Nevertheless, we could accept the same for gravions too as follows: With a gravion momentum p_g , the force exerted on the receiving body is dp_g/dt and Eq. 463 can be re-written as:

$$g_0 M_{eg} = \pi \frac{dp_g}{dt} = \pi \frac{p_g}{t_g}$$

assuming uniform interaction over time and resulting in the following equation:

$$g_0 = \pi \frac{p_g}{M_{eg} t_g} \quad (466)$$

for g_0 to have as general equation in lieu of Eq. 464. We can stop at the above and move no further, but we are entitled also to apply the conjecture that $p_g/M_{eg} = c$. This conjecture attributes no rest mass to the gravion itself, but it uses an effective mass created by the incident gravion on the resting body. In the latter case, we return to Eq. 465, which we intent to use in the subsequent analysis. All this is done on the stated basis of this part, in order to see what the outcomes are.

29.2 Macroscopic sphere

We wish to reproduce and carefully trace the steps used in the derivation of what can constitute fundamental issues in physics, but have probably escaped due attention in a multifaceted and multilevel exposition of novel developments throughout this report. We start with derivations using a macroscopic sphere below.

29.2.1 Absorptivity $A_R < 1$

We continue further with the investigation of the relationship between energy and mass originally developed in Sections 15.7 and 16 and specifically by Eq. 191. The latter equation relates the effective mass “given” (emerging, or appearing) to a spherical body by the incoming radiation of gravions in the form of power (energy per unit time) absorbed by the body. It was worked out for a spherical geometry body and involves the totality of gravions crossing the sphere from all possible directions along all chords and diameters of the sphere for any absorptivity of a given material. The general case with $A_R < 1$ is depicted in Fig. 77(a).

We retrace the steps back to a starting point now with Eq. 188

$$J_{aR} = \pi J_0 A_R \quad (467)$$

which provides the absorbed density flux per unit surface area of the sphere from all directions inside a hemispherical solid angle, i.e by integrating from 0 to $\pi/2$. We should note that this is (was) generally absorbed gravions in the bulk of the sphere passing through an elementary surface area dS of the sphere. The fraction of gravions absorbed inside the sphere depends on the absorptivity A_R value; for ordinary bodies this is a very small fraction of unity. Then, we multiply by the total surface area of the sphere ($4\pi R^2$) to obtain the total absorbed density flux, i.e. the total energy per unit time, or power W as:

$$W = \frac{dE}{dt} = 4\pi^2 J_0 A_R R^2 \quad (468)$$

By replacing J_0 from Eqs. 73 and 78, we finally obtain:

$$\frac{dE}{dt} = 4cg_0 M_e \quad (469)$$

For later consideration, we need to note that the effective mass appeared from the referenced PG equations and not from the starting equation (point) above. The concept of effective mass was first introduced by PG in Section 6.2. It is the necessary mass to account for the measured acceleration of a spherical body. This was an important development in PG needing another “bigger” more “inclusive” mass, namely, the existence of a “real mass” for any body, over which gravion absorption takes place.

We can understand the above derivation better by comparing it with another form to be derived later, if we convert it again back to the per unit surface area form like:

$$\frac{\partial^2 E}{\partial t \partial S} = \frac{4cg_0 M_e}{4\pi R^2} = 4cg_0 \frac{dM_e}{dS}$$

providing the absorbed power per surface unit area as a function of the effective mass in the bulk of the sphere per corresponding surface unit area through which the power passes. We keep the energy and mass differentials differential below:

$$\frac{d^2 E}{dt} = 4cg_0 dM_e$$

By choosing dS small enough to allow (presumably) the creation of only the minimum possible effective mass M_{eg} at a time, we can set $dM_e = M_{eg}$. Furthermore, we can designate the corresponding (required) energy absorbed by E_g with $dE = E_g$ and re-write the above as

$$\frac{dE_g}{dt} = 4cg_0 M_{eg}$$

We substitute g_0 from Eq. 465 without π , as we already applied $f_g = \pi$ for the axial component of the density flux in Eq. 467, and obtain

$$\frac{dE_g}{dt} = 4c \frac{c}{t_g} M_{eg}$$

where t_g is the interaction time, over which we integrate to get

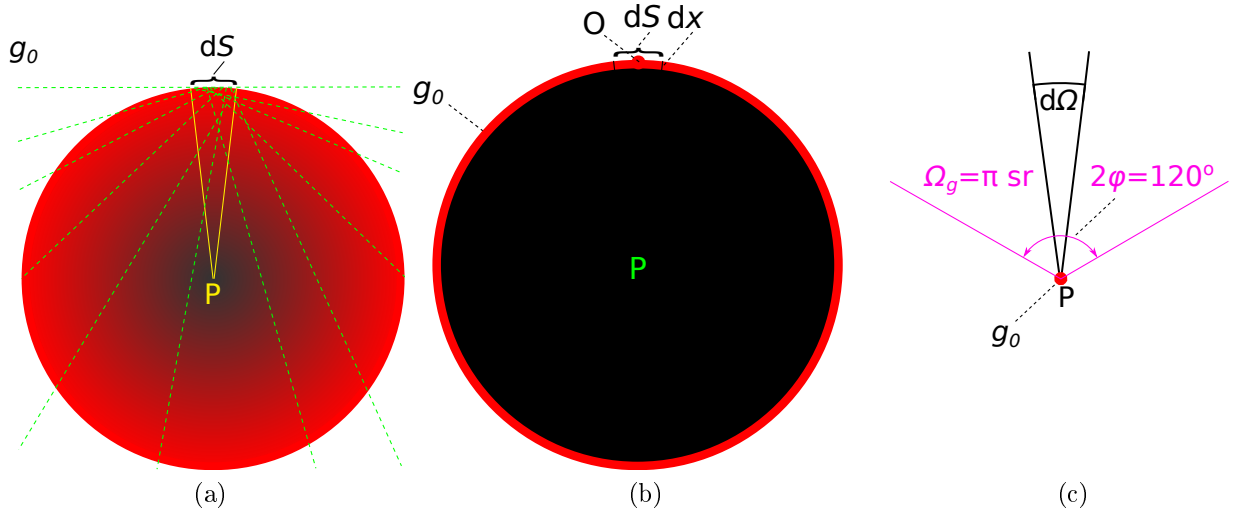


Figure 77: *Energy-mass relationship in PG for: (a) macroscopic ordinary sphere, (b) macroscopic sphere with unity absorptivity and effective mass (in red) over the surface, (c) minimal (microscopic) sphere at P with unity absorptivity, and elementary solid angle $d\Omega$ integrated up to Ω_g for a single gravion,*

$$\int dE_g = \int 4 \frac{c^2}{t_g} M_{eg} dt$$

$$E_g = 4c^2 M_{eg} \quad (470)$$

Lumping together all concurrent incident gravitons (from all directions for the entire spherical surface), we can obtain an almost (formally) identical energy-mass relationship with the familiar conventional one:

$$E = 4M_e c^2 \quad (471)$$

except for the factor 4 and the unknown gravion speed. If this is equivalent (identical) with the conventional equation, then must have $4c^2 = c_p^2$ giving a gravion speed half of the photon speed c_p . Such an outcome has been of some concern, but we may be able to resolve the seeming discrepancy by the subsequent analysis.

29.2.2 Absorptivity $A_r = 1$

The preceding case is general and is applicable for all values of A_R . The single quantum mass of M_{eg} is located somewhere in the bulk of the sphere. However, in deriving the substitution for g_0 by Eq. 465, we used $A_R = 1$ with having “pure” effective mass at the surface of a sphere in Fig. 77(b). It is worthwhile for this exploratory work to repeat the derivation procedure again specifically for this case too. Dealing with a surface mass alone capturing all incident gravitons may be easier to understand.

$A_R = 1$ means that all gravitons are absorbed at the surface and none in the bulk any more (mathematically, it means that the limiting case of A_R actually approaches extremely close to unity). Then we have from Eq. 467:

$$J_{aR} = \pi J_0$$

from which we arrive again at the:

$$\frac{\partial^2 E}{\partial S \partial t} = 4cg_0 \frac{dM_e}{dS} \quad (472)$$

except now dM_e is at the surface element dS . We reduce the latter until a single gravion impinges in order to set again $dM_e = M_{eg}$, with $dE = E_g$. Following the same steps, we reproduce the same outcomes:

$$E_g = \int 4cg_0 M_{eg} dt = 4cg_0 M_{eg} t_g$$

Replacing g_0 from Eq. 465, we finally obtain again:

$$E_g = 4c^2 M_{eg} \quad (473)$$

Lumping together all concurrent incident gravions:

$$E = 4c^2 M_e \quad (474)$$

29.3 Minimal sphere

We supplement and further confirm the same outcome by a new approach (case), which, in addition, can reveal the potential mechanism responsible for the said factor of 4. We reduce the size of the general case sphere to an extremely small radius having the effect that only a few gravions cross it. The sphere practically becomes point-like located at the center P of the previous sphere in Fig. 2. Also, the previous point O coincides now with the center P as is shown in Fig. 77(c). This point maybe thought of as the minimum absorption center (MAC) being activated (designated by red color), when a minimum number of gravions are absorbed, or being turned off converted to black matter. We juxtapose the quantitative transition from macroscopic to microscopic case and stress that the transition becomes also qualitative: Whereas in (a) gravions crossing along random chords and diameters are absorbed anywhere in the bulk of the macroscopic sphere, now, in minimal sphere (c) all these off-center traces are eliminated practically leaving only those gravions arriving in the vicinity of P. The exact trajectory inside the point-like minimal sphere is irrelevant. Now, the minimal sphere is located at the apex of a cone with a given solid angle $d\Omega$. This sphere randomly and relatively rarely receives gravions from all possible directions inside the full 4π solid angle. By this arrangement, we can choose a sufficiently small angle $d\Omega$ so that only one gravion strikes during the entire interaction time t_g . All incident gravions inside this cone are absorbed by the minimal sphere, for which the absorptivity is unity ($A_R = 1$) and the acceleration of the gravitational field at this point is equal to the maximum possible acceleration g_0 . Eq. 191 can now be used to describe the per unit solid angle gravions if we divide by 4π giving:

$$\frac{\partial^2 E_g}{\partial \Omega \partial t} = \frac{1}{\pi} c g_0 M_{eg} \quad (475)$$

where E_g is the energy rate carried by presumably a single gravion and M_{eg} is the corresponding effective mass given to the minimal sphere traveling inside the elementary solid angle $\partial\Omega$. The energy rate per steradian is proportional to mass via the product $c g_0$. We substitute g_0 from Eq. 465 again without π (already included in deriving the whole sphere):

$$\frac{\partial^2 E_g}{\partial \Omega \partial t} = \frac{1}{\pi} c_g \frac{c}{t_g} M_{eg} = \frac{c^2}{\pi t_g} M_{eg} \quad (476)$$

$$E_g = \int \int \frac{c^2}{\pi t_g} M_{eg} \partial \Omega \partial t = \frac{c^2}{\pi t_g} M_{eg} \Omega_g t_g = c^2 M_{eg} \frac{\Omega_g}{\pi} \quad (477)$$

where we have integrated over time in the interval $0 \rightarrow t_g$ and over solid angle in the interval $0 \rightarrow \Omega_g$, where Ω_g remains sufficiently small to ensure that no other gravion is concurrently incident during the entire gravion interaction time t_g . Lumping together all minimal spheres in a macroscopic body, we arrive at an energy-mass relationship similar with the conventional one, except for the factor Ω_g/π and gravion speed:

$$E = \frac{\Omega_g}{\pi} M_e c^2 \quad (478)$$

If we set $\Omega_g = \pi$ steradian and $c = c_p$, we arrive exactly at the conventional energy-mass equation:

$$E = c_p^2 M_e \quad (479)$$

However, if we had integrated up to 4π in the minimal sphere in Eq. 477, we revert back to the same result as we did for macroscopic spheres:

$$E = 4c^2 M_e \quad (480)$$

The persistence of the factor 4 seems to be unavoidable and correct. This requires an explanation, which may come about by the minimal sphere derivation as analyzed and discussed in the following section.

NOTE: In fact, the starting equations of PG, namely, of radiance Eq. 1 and flux density Eq. 2 are at the core of the above results. These equations describe mathematically a flowing energy either as a continuous medium or as a discrete particle medium. In the continuum case, the minimal sphere can be arbitrarily small and still (always) receive some radiance, but in the discrete particle case, we can have a prolonged vacuum state, i.e. without any gravions (see also NOTE 29.4.6); actually, this has a philosophical

connotation, undertone or feeling about empty or not space to be invoked later. In both cases, we need to consider a spherical space, inside which we can still find radiance. This allows us to calculate the amount of flux density that traverses the sphere. In the Appendix, we have used two approaches to compute the total flux density in a sphere, namely, the “bulk” method integrating all events inside the sphere, or the “surface” method computing exactly the same outcome (both methods are equivalent). The surface method is more direct and equally obvious. We have applied the surface method in this Section. We conclude that the factor of 4 is a consequence of the mathematical processing of the starting equations leading to the power-mass relationship, for which we seek a physical explanation next.

29.4 Corollaries and discussion

29.4.1 The 3+1 mass scheme

If we choose to match PG with conventional physics regarding the energy-mass equation, then $\Omega_g = \pi$ and $c = c_p$, otherwise we need an explanation for the discrepancy appearing by the factors $\frac{\Omega_g}{\pi}$ and 4 in Eqs. 471 and 478. Hopefully, the discrepancy is legitimate caused by some physical process under PG, while we accept the veracity of the conventional equation.

The derivation based on macroscopic spheres involves the entire body “activated” from all directions simultaneously, i.e. from the full 4π solid angle. This is exactly 4 times the possible solid angle Ω_g proposed (used) for a single graviton interacting alone and unimpeded by any other graviton in the minimal sphere. This leaves “room” of $3\Omega_g$ solid angle for interaction by another 3 gravitons concurrently. Because Eqs. 471 and 474 refer to the total absorbed energy, the appearing factor 4 includes all the absorbed gravitons. Therefore, the attribution of a corresponding energy E_g to a single graviton instead of four gravitons was not warranted. We should have written (denoted) it by a better symbol like $E_{4g} = 4E_g$, in which case the macroscopic sphere derivations need to be amended by

$$4E_g = 4c^2 M_{eg}$$

producing

$$E_g = c^2 M_{eg} \quad (481)$$

from which, lumping together all concurrent incident gravitons in the sphere, we obtain an energy-mass relationship identical with the conventional one but with a graviton speed, instead:

$$E = c^2 M_e \quad (482)$$

In other words, reduction of a macroscopic sphere to the hypothetical minimal sphere can be made by allowing not only a single but four independent gravitons to interact with it. This is consistent with omnidirectional absorption of macroscopic spheres involving the factor 4 in their equation. However, the 4 concurrent gravitons interacting with the minimal sphere explain only the fourfold amount of absorbed energy. However, this is still inconsistent with the production (emergence) of only 1 M_{eg} that is required for a given (measured) gravitational field with intensity g . A fourfold amount of absorbed energy should be associated with a fourfold amount of effective mass and a fourfold intensity of the associated gravitational field. A contradiction emerges.

The above contradiction can be resolved by understanding the way, by which we defined and introduced the “effective” mass at the outset. The term “effective” for mass and other parameters was first necessitated and introduced in Section 6.2, to which the reader must refer. It is only the effective mass that is associated with a given gravitational field. The effective mass is required to be present by a certain amount to generate the measured acceleration (and force) by a spherical body. It is correct to state that 1 M_{eg} is required to generate a maximum acceleration of g_0 at the minimal sphere in Fig. 77(c), only if the other three gravitons combined together do not generate a net force (acceleration). In that case, we can have the energy of 4 gravitons being absorbed but only one creating the associated gravitational field. The possibility of this happening is explained in Fig. 78, reference to which is made below.

It is possible to construct an equilateral triangular prism, such that each triangular face subtends exactly $\pi/2$ sr (steradian) at the center of the prism, while each of the three rectangular lateral faces subtends exactly π sr. We can only have one graviton falling inside the $\pi/2$ solid angle with nothing falling from the opposite direction in the opposite $\pi/2$ solid angle as a necessary and sufficient condition for a graviton to impart an impulse. The said two halves make up the required $\Omega_g = \frac{\pi}{2} + \frac{\pi}{2} = \pi$ during integration of Eq. 477. It is only this graviton that is responsible for the 1 M_{eg} associated with g_0 . The remaining three separate Ω_g valued at π

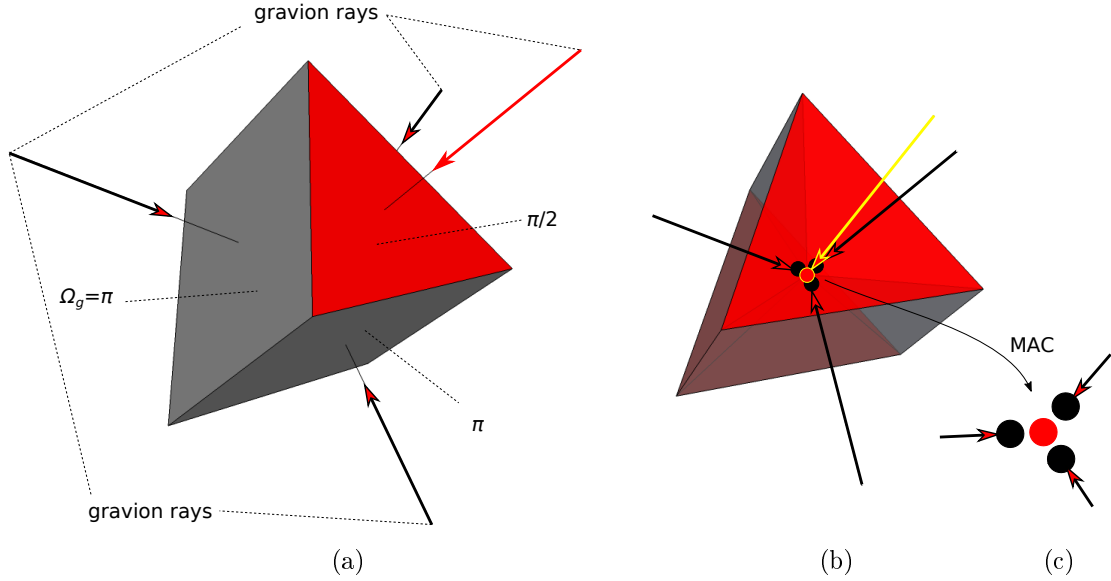


Figure 78: 3+1 mass scheme: Equilateral triangular prism with 3 lateral rectangular faces subtending π steradian each and 2 triangular faces subtending $\pi/2$ steradian each. (a) opaque faces, (b) transparent faces (c) minimal absorption center (MAC) with effective mass in red and black masses in black.

sr each accept only one graviton each and generate three co-planar impulses adding to zero resultant impulse. The zero force produces no gravitational field around, while gravitons and energy are absorbed. Thus, in this and previous derivations, when we reduced the total effective mass M_e to that of a single graviton, we implied that the incident graviton had a corresponding energy E_g , but the starting formula does not guarantee this. The formula correctly provides a quadruple amount of energy, but we did not suspect that 3/4 of it was consumed by a physical process without producing gravitational field. Now, the 3+1 gravitons explanation theoretically resolves the issue. Only 1/4 of gravitons generate effective mass and acceleration, while 3/4 “lateral” gravitons do not contribute to a net force (or gravity), but they are responsible for the additional energy density flux and an associated non-effective mass. We have previously called this non-effective mass “black mass”. Black mass has already been introduced in consequence of graviton shadowing, in general, in spherical bodies as already described throughout this work. See, for example Fig. 33. Thus the 3+1 scheme now accounts for 3/4 of black mass at the “elementary” level, but does not account for all the black mass in a given sphere. There is another amount of black mass arising from the value of the absorptivity A_R . Hence, we can expect much more black mass in the universe from all the sources put together. Black mass is our answer to “dark matter” albeit being very different with different origin and notions.

The above 3+1 mass scheme may appear extraordinary in the sense that it is possible to happen especially with randomly traveling “corpuscles” like gravitons. However, there can be an organic connection between bodies and graviton radiation as we shall see below. Also, the solid angles are only schematically drawn in Fig. 78 to demonstrate only the possibility (principle), while in reality the shape of the same size solid angles may be adjusted to the particular structure of the absorbing unit of hyle.

In all above, it is implied that the entire mass scheme proposed involves statistical averages of large numbers of gravitons over time. Furthermore, we need structural stability of the absorbing entity independent of the gravitational field. These and other issues will be dealt with separately later.

Therefore, Eqs. 478 and 471 differ by the factors $\frac{\Omega_g}{\pi}$ and 4, only because we integrate partially up to π in one case and up to 4π in the other case. We now have a better way to express the actual relationship of an actual process relating power to effective mass and to mass in general. The proportionality between total power absorbed and effective mass is always given by the universal product $4cg_0$. Conventional physics seems to miss out on the full energy-mass process, as we further analyze the classical (effective) mass and its equivalent energy in the continued discussion. This “missing” part is not an error, while it may be explained subsequently.

While the PG power-mass Eq. 191 has been derived since the early stages of this report, it was only after “pedantic” examination of the same result by various approaches as in Fig. 77 (and others) that we seem to have understood the intriguing factor of 4. In particular, it was the minimal sphere in (c) that set us on a productive course to realize that the full spheres in (a) and (b) can yield an error free equation if they are hiding a fundamental physical process.

29.4.2 Intrinsic versus effective mass

The introduction of an “intrinsic” mass for gravions was necessitated above in attempting to derive the conventional energy-mass equation. Otherwise, we have derived the more general Eq. 469 providing a power-mass equation with the two quantities connected via the product of cg_0 . The effective mass is a derivative quantity entering after the initial Eq. 468 of power absorption leading to the final power-mass Eq. 469 without any prior assumptions about an intrinsic mass of the gravion. Now, having attributed an intrinsic mass to the gravion in Eq. 464, we can repeat the same procedure from Eq. 468 without the intermediate step introducing the effective mass, i.e. without PG. In other words, the gravion flux density J_0 already possessing classical mass literally gives mass to absorbing bodies. For this, we still assume that bodies behave like sink holes with an absorption time constant (or time interaction delay t_g) to incoming massive gravions from the outside around collecting them under a steady-state at equilibrium. With these provisos, we proceed as follows:

We consider again a spherical body with total absorption for simplicity, although an A_R factor could be written along. Let us denote by N_0 the number flux density of gravions (number of gravions per unit time per unit area) in any particular direction. For a differential surface area ∂S on the sphere, the integrated total incident number flux (from all directions in 2π) is given again by

$$N_{aR} = \pi N_0 = \frac{\partial^2 N}{\partial S \partial t}$$

with corresponding intrinsic mass M_i flux

$$M_{iaR} = \pi M_{i0} = \frac{\partial^2 M_i}{\partial S \partial t} = \frac{\partial^2 N}{\partial S \partial t} M_{ig}$$

By denoting again the single gravion energy by E_g , the flux density is $J_0 = N_0 E_g$. For a differential surface area ∂S on the sphere, the integrated total incident flux is given again by

$$J_{aR} = \pi J_0 = \pi E_g N_0 = \frac{\partial^2 E}{\partial S \partial t}$$

The density flux is also given by the product $J_0 = Pc$ where P is the pressure on a surface element normal to the direction of J_0 (this pressure has been denoted by p_g elsewhere, but p_g is used for gravion momentum in this section). The component normal to a spherical surface element ∂S is

$$J_{aR} = \pi Pc$$

The pressure being force per unit area, or time rate of momentum per unit area (in any direction) can be obtained by

$$P = \frac{\partial^2 N}{\pi \partial S \partial t} M_{ig} c = \frac{\partial^2 M_i}{\pi \partial S \partial t} c$$

from which we obtain

$$J_{aR} = \frac{\partial^2 E}{\partial S \partial t} = \pi Pc = \frac{\partial^2 M_i}{\partial S \partial t} c^2$$

We integrate the above first with respect of time to obtain a per surface element energy-mass relationship:

$$\frac{\partial E}{\partial S} = \frac{\partial M_i}{\partial S} c^2$$

and then integrate over the entire sphere surface getting

$$E = \int \frac{\partial M_i}{\partial S} c^2 \partial S = \frac{\partial M_i}{\partial S} c^2 \cdot 4\pi R^2 = M_i c^2$$

having set $M_i = \frac{\partial M_i}{\partial S} \cdot 4\pi R^2$. Thus, we have obtained the famous equation without further ado.

To compare the above outcome with our PG corresponding power-mass derivations, we revert back to:

$$\frac{\partial^2 E}{\partial S \partial t} = \frac{\partial^2 M_i}{\partial S \partial t} c^2 = \frac{\partial^2 M_i}{\partial S \partial t} c g_0 t_g = \frac{\partial M_i}{\partial S} c g_0$$

where we have used Eq. 465 without π (already applied) and taken $\partial t = t_g$. We then integrate with respect to surface and obtain the total power for the spherical body as:

$$\frac{\partial E}{\partial t} = \int \frac{\partial M_i}{\partial S} c g_0 dS = \frac{\partial M_i}{\partial S} c g_0 \cdot 4\pi R^2 = c g_0 M_i$$

This intrinsic mass M_i is the aggregate mass simply accrued from the gravion intrinsic masses and has not been imposed (or necessitated) by any requirement arising from the associated (measured) accelerating field. We have used Eq. 465 generating push acceleration but this acceleration is not yet connected to (or emanating from) any body mass (effective or not) and is not connected with prior PG equations. However, the power absorbed is the same both in prior PG derivation and intrinsic mass derivation setting an equality by identity:

$$\frac{dE}{dt} = 4c g_0 M_e = c g_0 M_i$$

yielding a relation between the two kinds of mass as:

$$M_e = \frac{M_i}{4}$$

The difference is important. The effective mass was previously introduced in the corresponding PG Eq. 469 as a necessary mass (imposed) to reproduce the measured (existing) gravitational field around a given material sphere. Here, the intrinsic mass is simply accrued from surrounding gravion carriers of mass. The difference is subtle, but fundamental, because the factor 4 in PG derivation quadruples the absorbed energy (not the effective mass). The difference between the two theories (methods, or approaches) is that for the same energy absorbed, PG produces only 1/4 equivalent to classical (intrinsic) mass. Conversely, classical mass would produce a fourfold stronger gravitational field, which is invalid, because the existing field is explained only by $1M_e$.

Thus, $M_e = \frac{M_i}{4}$ stating that only 1/4 of the intrinsic mass of the sphere is used while 3/4 of it is somehow unseen. Notwithstanding this, the conventional equation still yields a correct amount of energy but it misses an energy that would be produced from a hidden mass should that hidden mass be also converted to a detectable form of radiation (say during an atomic bomb explosion). Later, we suggest that this “missing” energy may escape in some other form that could be detected if we were properly looking for it.

For good measure, we can finally verify explicitly the above derivations by a backwards substitution of equations and draw a final conclusion. Let us see if it is correct that the effective mass is indeed 1/4 of the intrinsic mass. If it is, then the following equation must be an identity:

$$M_e \equiv \frac{1}{4} \frac{\partial M_i}{\partial S} \cdot 4\pi R^2$$

We substitute the left hand effective mass from PG equations, while maintaining the intrinsic mass in the right hand member of the equation during the following steps:

$$\begin{aligned} \frac{\pi R^2}{\Lambda} &= \frac{\partial M_i}{\partial S} \cdot \pi R^2 \\ \frac{1}{\Lambda} &= \frac{\partial M_i}{\partial S} \\ \Lambda &= \frac{1}{\frac{\partial M_i dx}{\partial S dx}} = \frac{1}{dM_i/dV} \frac{1}{dx} = \frac{k}{\rho_i} \end{aligned} \tag{483}$$

Above, we have multiplied numerator and denominator by an infinitesimal thickness dx over which a gravion is absorbed. For total absorption, the coefficient k must be $k = 1 \text{ \#events over the depth } dx$, so that $1/dx = k$. We further recognize that the intrinsic density is $\rho_i = dM_i/dV$ finally yielding the ratio k/ρ_i corresponding to the original definition of the universal constant $\Lambda = k/\rho$ in terms of real density in PG. If we now set the real density to be identical with the intrinsic density, then we have shown the veracity of the equations used. This means that the effective mass is indeed 1/4 of the intrinsic mass. There remains to interpret the meaning of identifying the intrinsic mass with real mass.

The above derivations follow the conjecture of setting $M_{ig} = M_{eg}$ at the outset of 464. Thus, we could temporarily challenge the above analysis as follows: Alternatively, we could eliminate the 4 factor in PG equations by setting $4M_{ig} = M_{eg}$ at the outset conjecture. Then, the theoretical landscape would be different. Then, four concurrent gravions would be creating $1 M_{eg}$, but they should all impinge simultaneously normal to the surface, otherwise they would result in a deficient gravitational field. In other words, they should all four act as one fourfold-massive gravion without any other concurrent gravions falling from any other

direction. In that case, the special hyle configuration in Fig. 78 would be redundant. By following the same steps, the relationship between real-mass and intrinsic-mass would replace Eq. 483 with the following final one:

$$\Lambda = \frac{k}{4\rho_i} \quad (484)$$

which would imply that the real density is fourfold the intrinsic density:

$$\rho = 4\rho_i$$

The above outcome is difficult to comprehend or to model. It dictates that all gravions create effective mass but only in groups of 4 from the same direction concurrently and with no other gravion from any other direction. This is most unlikely to happen statistically. It seems rather an impossibility when creation of effective mass should be a most frequent and continuous event to occur all the time.

Therefore, the 3+1 mass scheme devised by Fig. 78 seems much more likely to occur as it also appears to reflect a physical structure at the fundamental level of gravitational mass. We may have to take it into account towards building the natural world from a gravion basis; we give it an initial preference in the following discussion, without prejudicing other possibilities if they exist. In the meantime, it remains to find if intrinsic mass is needed after all. In any case, we have made a further contribution towards understanding the meaning of mass in general.

29.4.3 Electrical mass-energy equation

The above findings and analysis further enforce our confidence in PG theory and compel us to expand the energy-mass relationship by Eq. 478 to apply universally to any effective mass and not only to gravitational effective mass. We now propose to apply it to other types of effective mass, like the electrical mass introduced for charged particles, e.g. for the electron and positron in Section 21 ushering the push electricity theory. By our symbol convention introduced there, the effective electrical mass m_{2e-e} for an electron should now be equivalent to an energy correspondingly given by:

$$E_{2e-e} = c_e^2 m_{2e-e} \frac{\Omega_e}{\pi} \quad (485)$$

where E_{2e-e} is the equivalent electron energy stored in the electrical mass of the electron and c_e is the electron speed (electron being the push particle for the electric field). If this is true, then we have introduced the concept that an electron (or positron) encapsulates far more energy than its ordinary effective (classical, gravitational) mass. The extra energy can be calculated by the numerical quotient given by Eq. 339, i.e. by about 11 orders of magnitude more than ordinary (gravitational) mass. The idea of “splitting the atom” in atomic physics, may have its counterpart in PG theory of electricity by the idea of splitting the electron! This might sound extraordinary, but one never knows, until PG theory is put to the test. “Splitting the electron” might be seen in (and better explain) the enormous amount of energy observed in astrophysical explosions, in particular, during the end phase of neutron stars forming black holes. We may assume that “charge” (electron and positron) collapses in a black hole. Using the terminology of the electrical mass and electric field of an electron, we can correspondingly write the power-mass equation as:

$$\frac{dE}{dt} = 4c_e g_{02} m_{2e-e} \quad (486)$$

If $c_e = c_p$, then we should have for an electron with electrical mass m_{2e-e} an equivalence equation like:

$$E_{2e-e} = 4c_p^2 m_{2e-e}$$

The main thrust of the ideas herewith suggest that conventional “energy” and “mass” have been introduced by a historical evolution of physics without adequately being explained (or understood). Thus, mass was introduced either as a proportionality constant between an applied force and acceleration of a body, or as proportionality constants for two bodies attracting each other (after Newton). This was followed by the equivalence principle for the said constant(s) of mass, and “mass” has been consequently involved in our physics equations ever since as a fundamental (intrinsic/invariant) constant. Had we followed the Fatio idea about gravity being “pushing” and not “pulling” in nature, physics might or could have followed a different path without a misconceived parameter of mass. Mass is not sacrosanct and is not conserved. It is only the property of momentous-hyle that is conserved. The equations of motion can be re-written by novel equations containing yet alternative quantities, such as gravion radiation intensity, universal constant Λ , absorptivity, maximum acceleration and force. If electrical charge is also mass, and if other types of force are connected

to other types of mass, then we are on a correct path to unifying all types of force; they are all generated by push particles via momentum transfer, the difference among them being only a matter of degree.

Important for now is the question: Could the 3+1 mass scheme devised by Fig. 78 provide a hint for the structure of the electron? If this scheme is also applicable to the electron, it appears to reflect a physical structure at the fundamental level of electrical mass also, i.e. of conventional charge. It seems to correspond to the three-quark-electron-concept, except that our structural units could be distributed inside an electron (positron) in sufficient numbers (quantities). They maybe distributed to form a superstructure according to the electron model presented by Fig. 76 in Section 25. Consistent with current theories (presumably), the quark having $e/3$ charge is not a single independent sub-particle (substructure) of the electron, but 1/3 of components of distributed entities within another structure of the electron. In that case, it would be impossible to separate the “quarks” without ruining the “charge” structure, a fact consistent with current theories and experiments, but it provides some explanation. Certainly, these new ideas are speculative, but they can at least trigger the interest of particle physicists to consider PG as a basis towards building the natural world.

29.4.4 Gravion ray length and interaction time

Beyond the above outcomes, we can independently derive some further corollaries also from the other important (or critical) Eq. 464. Again, we assume that it is a valid equation, even in a gross approach, because there may be fine details of interaction, but we have them evened out for now. This can provide by itself some preliminary and useful outcomes below, even in gross terms. Among the various possibilities of varying the factors involved (already outlined), we start by considering the conjecture of Eq. 465. That is, we equate an assumed “intrinsic” gravion mass with the elementary body effective mass without prejudicing other remaining possibilities, to which we may return later, if needed. Assuming also that gravion speed is equal to the speed of photons ($c = c_p$), we can get a feel of the order of magnitude among the interdependent quantities g_0 and t_g . Having initially simplified the interaction process to be continuous, homogeneous and steady, like a “rope”, or momentum string impinging longitudinally on a free body, the gravion must be associated with a “length” given by $s_g = ct_g$. As a consequence, we can consider the following situations.

For the speculated (in Part 1) approximate value of $g_0 \approx 4 \cdot 10^4 \text{m/s}^2$, we derive $t_g = c_p/g_0 \approx 7.5 \cdot 10^3 \text{s}$. This means that the gravion has a length of $s_g = c_p t_g \approx 2.25 \cdot 10^{12} \text{m}$, which maybe like the length of a wave packet, if it has photon-like properties and if the photon can be correctly described by a “wave packet”. This gravion length would be of the order of 15 astronomical units. These values of interaction time and length are an extraordinary outcome, for which we need to seriously ponder over. In any case, it seems to be both an interesting and important finding.

If g_0 is greater than the above value, as it is likely to be, then the gravion length would be proportionally shorter. Therefore, we may have found an approximate upper limit for the longest gravion length, say, around 15 a.u. Even a few orders of magnitude less than that still represent an important finding to consider seriously. In fact, such an outcome is consistent with Meis theory (Meis, 2020). He has independently forecast the existence of push radiation at extremely low photon frequency, as it is clearly stated (on page 8) that: “... *it is worthy investigating whether gravitation originates from the radiation pressure of the electromagnetic quantum vacuum field (Push Gravity) felt by the bodies in their own frame depending on their charge densities [16]. ... Therein, it is important to mention that a well-elaborated model of Push Gravity has been developed recently [23] and the similarity of “gravions” to the electromagnetic vacuum fluctuations would be of great interest to be investigated in detail.*” See also Meis (2022) page 963. Therefore, our finding (very long gravion lengths) on its own adds a good incentive to consider it properly and to undertake relevant experimental work to test its validity.

The prospect of gravions having a length measured in astronomical units and engaging over a relatively long time interval is consistent with the idea expressed at the outset of our theory that bodies are “bound” to gravity like via some kind of a “lattice”. For convenience, we quote from Section 14.5 that “*Yet, by further iterative thinking, we can make the inventive step that, instead of the gravion-lattice **activating** the effective mass to resist, it is the lattice itself that resists the movement of the body (matter) by engaging via the effective (active) part of the mass. The effective mass is passive by itself, except that it is somehow tied to the activating gravions. In consequence then, we can safely state that the entire mass is actually passive and hence it has no inertia; what appears as inertia of the mass (or part thereof), it is actually the resistance of the gravions opposing the mass to change its kinetic state.*”

The above interpretation of our equations is still valid even with much shorter interaction times of t_g , in which case g_0 may assume extremely high values practically putting them well outside the detection limits of our contemporary instruments.

Thus, to complete our investigation, we need to consider cases of much higher values for g_0 , like $g_0 \approx 10^{12} \text{m/s}^2$ for black holes. While we have proposed that such very high values maybe explained by different

types of push particles, we have not yet excluded the possibility of the black hole gravitational field being due to only type-I (gravions) push particles or, equivalently, that all other proposed types of push particles have degenerated to gravions in a compressed cloud initially at maximum density, but later expanding with a density decay over relatively long astronomical time. Regardless of the actual situation, we can use the above equation to obtain the corresponding values $t_g \approx 3 \cdot 10^{-44}$ s and $s_g \approx 9 \cdot 10^4$ m for $g_0 \approx 10^{12}$ m/s². Even in this case, the interaction time and gravion length seem to be relatively long in comparison with life times usually encountered in particle physics.

We can go also to the extreme case by assuming that the gravion length is of the order of Planck length, namely, $s_g \approx 10^{-35}$ m. In this case, we obtain $t_g \approx 3 \cdot 10^{-44}$ s and $g_0 \approx 10^{52}$ m/s². In the case where g_0 is so high, we will have to abandon any hope for terrestrial experiments to verify PG; we will only be left to investigate, understand and interpret astrophysical observations based on PG, as indirect means for its verification.

As can be seen, our theory can initially accommodate a wide range of values for its variables including interaction times, lengths and masses. It is a matter of matching the available data from particle physics and astrophysics with PG general findings. It would be better to match PG with observations and experiments rather than with existing invalid theories.

The life time t_g (interaction time) and length s_g of gravion rays may have far greater significance than mere common place “lives” have in particle physics. They provide an excellent clue about the meaning of mass, which has remained a key issue in physics. According to our understanding, effective mass is a rate process of energy absorption. To maintain mass as a stable entity entering our equations in physics, a “practical” life time of gravions is necessary to have. If the life time is exceedingly short, we would need an exceedingly large amount of flux density. If we were to take the numerical example of $s_g \approx 9 \cdot 10^4$ m with $g_0 \approx 10^{12}$ m/s² in black holes as an extreme limit, we would still have a gravion length of 90 km, which appears to be relatively still very long. If lengths of astronomical units are also possible with lower values of g_0 , then we can understand how the (humanly apparent) stability of effective mass is maintained. Bodies are “tied up” with “zillions” of concurrent gravion rays from all directions extending far out in space. When a gravion is interacting with a MAC, it commits the MAC to this interaction for a considerable time in human experience and would resist a change in status. A MAC must be structured with “receptor” sites to allow absorption of gravions. For example, we have proposed a 3+1 mass scheme for such receptor sites. We can then envisage a legitimate resistance to any “external” force to change the connection (binding) between bodies and gravions, which could explain classical “inertia” (=resistance). Philosophically, why should bodies present any resistance to their state of motion for no reason whatsoever? That has been a mystery and accepted only as an axiom. However, we have now proposed a reason: Matter (hyle) is initially inert and presents no resistance unless and until it is activated by gravions to acquire effective mass thereby becoming bound. From the outset, we arrived at the idea of “real mass” having no classical inertia, while only a part of it, the effective mass, has classical inertia. We pointed out also that “inertia” is a misnomer if the word originates from the word “inert”. In any case, it seems now that gravity and “matter” are interconnected in an unexpected way via pushing gravion rays interconnecting the wider “space” with structural units of bodies at the most elementary level possible. Gravity is exogenous to bodies but in union with them. The latter union then constitutes a sound basis for the long awaited unification of particle physics with macrocosm, it constitutes a basis of hyle for a unification theory of the cosmos.

We will return to the “gravion ray length” concept following a first attempt to connect the gravion with an actual physical property: See the following section, with more in Section 30.1.

29.4.5 Planck-constant versus gravion-constant and theoretical g_0

As noted before, there seems to be a similarity or correspondence in certain attributes between gravions and photons, but this should be treated with caution, until we can probably establish the relationship. Thus, we note the correspondence between gravion ray length s_g and light wavelength λ , gravion interaction time t_g and light wave period T along with photon frequency ν and gravion frequency $\nu_g = 1/t_g$. Concomitant with all this, we can further note a correspondence between Planck constant h and gravion energy E_g . Since we have $E = h\nu$ meaning that there is a characteristic energy numerically equal to h at 1 Hz, we can have, in summary, the following correspondence:

$$s_g \rightarrow \lambda$$

$$t_g \rightarrow T$$

$$\nu_g = \frac{1}{t_g} \rightarrow \nu$$

$$s_g \nu_g = c \rightarrow c_{ph}$$

$$E_g \rightarrow E_{ph} = h \cdot 1Hz$$

The above distinction is made to clarify that there should be no misinterpretation of various graviton relationships presented in this work with existing light (photon) equations and theories. There remains to be found what exactly the above correspondence is, without excluding also an identity between them. This issue is investigated in subsequent Section 30 with some preliminary considerations also given below.

The photon energy $E_{h\nu}$ is given by the well known energy equation $E_{h\nu} = h\nu$, with h being the Planck constant and ν the frequency of the photon. This energy is transmitted (emitted or absorbed) in a time interval $t_{h\nu}$, so that its power is

$$W = \frac{dE_{h\nu}}{dt} = \frac{h\nu}{t_{h\nu}}$$

Specifically, a photon with energy at $\nu = 1$ Hz contains a “unitary” photon energy $E_{uph} = h \cdot 1Hz$. We apply Eq. 469 with $c = c_{ph}$ and without the factor 4 subject to the interpretation of 3+1 mass scheme in Section 29.4, but we can do an adjustment for this factor if and where needed. To this photon, we have a unitary effective mass by:

$$\begin{aligned} E_{uph} &= m_{uph} c_{ph}^2 \\ m_{uph} &= \frac{h \cdot 1Hz}{c_{ph}^2} \end{aligned} \quad (487)$$

We substitute the values $c_{ph} = 299792458$ m/s and $h = 6.62607015 \times 10^{-34}$ J·Hz⁻¹ at $\nu = 1$ Hz and obtain a unitary Planck photon mass $m_{uph} = 7.37249732 \times 10^{-51}$ kg. This means that every “sine-wave” (over a period of oscillation T , between two consecutive peaks) in a continuous photon wave-train has a small but fixed (invariable) “mass”. This small mass multiplied by the frequency with wave-length equal to the Planck length yields the known “Planck mass”, which is different from the above m_{uph} . We will later set (or assume) the graviton energy to be:

$$E_g = E_{uph} = h \cdot 1Hz \quad (488)$$

The transmitted power by a photon with frequency $\nu = 1$ Hz, if applied to the PG power-mass equation, would “create” an effective mass M_{eg} by

$$\frac{dE}{dt} = \frac{h \cdot 1Hz}{t_g} = c_{ph} g_0 M_{eg} \quad (489)$$

We multiply the above Eqs. 487 and 489:

$$\frac{h \cdot 1Hz}{t_g} m_{uph} = c_{ph} g_0 M_{eg} \frac{h \cdot 1Hz}{c_{ph}^2}$$

to obtain a derivation for g_0

$$g_0 = \frac{m_{uph}}{M_{eg}} \frac{c_{ph}}{t_g} \quad (490)$$

which is the same as Eq. 464, With $m_{uph} = M_{eg}$ both being the same per their introduction, we also reproduce.

$$g_0 \approx \frac{c_{ph}}{t_g} \quad (491)$$

We intend to investigate further and utilize the above derivations in later work.

For good measure and understanding of the above derivation, let us use a similar derivation from rocket technology: The acceleration a of a rocket is given by textbook derivation as

$$a = \frac{v_e}{m} \frac{\Delta m}{\Delta t} - g$$

where v_e is the exhaust velocity, m the total mass of the rocket at time t with Δm the amount of exhaust mass in time interval Δt inside the Earth's deceleration g . The same acceleration would be achieved by a body with the same mass as the rocket, if the body is impinged by the same amount and rate of material by an external source. If this external source is exactly one gravion with mass m_{uph} impinging in time interval t_g on a massless body, which happens to acquire a mass M_{eg} during the interaction, then we produce Eq. 490 by setting also $v_e = c_{ph}$ and $g = 0$. This case provides a familiar experience to consider whether it can be transferred under the assumed gravion-hyle interaction. There may be some repercussions of this consideration towards understanding the nature of the gravion itself and the nature of its interaction during absorption by hyle in subsequent theoretical development. The concept of “mass” being delivered by a gravion and the concept of “mass” emerging inside the impacted body should be thoroughly thought out once and for all. In that case, if a gravion is somehow re-emitted following an elastic interaction (if any), then this process should be accompanied by a reverse loss/emission of an equivalent gravion mass. Is “mass” something that we have artificially introduced by early theories that needs to be discarded altogether, or is it something that has a physical significance to carry forward with our new theory? In any case, we currently understand that mass is accompanied by hyle and vice versa, but the two entities are not equivalent or the same. Hyle is permanent and invariant, but not the emerging mass in a macroscopic (composite) body (see Section 24.2).

We substitute the above value of g_0 (Eq. 491) in our general power-mass equation below:

$$\frac{dE}{dt} = c_{ph} \frac{c_{ph}}{t_g} M_e$$

from which we obtain a general expression for the effective mass M_e :

$$M_e = \frac{\frac{dE}{dt} t_g}{c_{ph}^2} \quad (492)$$

This equation states that the mass of any body depends on the energy absorption rate (power) $\frac{dE}{dt}$ multiplied by the gravion interaction time t_g . We can better understand the significance of this important equation, if we start thinking about a macroscopic body like a planet. The energy absorption rate depends on the absorption coefficient k , which is the number of absorption events per unit length in the body. It is all those events that take place in time t_g , which add up to produce the numerator of the fraction in the above equation. It is the synergy of concurrent absorption events adding up to produce an effective mass, the absorptivity and the associated acceleration g of the given planet. This understanding applies to any absorbing body, including a single photon, for which we initiate a new study in the following Section 30 and onward. The idea of synergy and concurrency applies all the way down to MAC/MEC size structures first described by the 3+1 mass scheme in Fig 78.

As a corollary of PG theory, we derive that the (classical) “energy” E in a given body is:

$$E = \frac{dE}{dt} t_g \quad (493)$$

which corresponding to its (classical) “mass” M now better explains the well known equation of mass-energy:

$$M = \frac{E}{c_{ph}^2}$$

except that we should better use PG notation for an effective mass M_e , but also for an effective energy E_e (not yet explicitly mentioned up to now), that is:

$$M_e = \frac{E_e}{c_{ph}^2} \quad (494)$$

This is important, because the well known energy-mass equation does not involve or say anything about a coexisting or collateral matter (hyle) in any given body. The hitherto conventional “mass” and “energy” have left out of consideration the bigger picture of the universe containing hyle (real mass) and not simply “mass”. “Mass” has been a key issue in physics for a very long time, actually since Newton. It is quite possible that the true meaning of mass has been uncovered for the first time by our novel PG theory. The importance of this analysis has been already reflected in cosmology, the expanding universe and the Big Bang explained in Sections 18.2 and 18.3. There, it is pointed out that the astronomical and astrophysical measurements correspond only to visible phenomena leaving out of consideration the real mass (matter, or hyle), real size

and real distance. The missing part of the universe as interpreted by PG could be a much better description than the missing “dark matter” and “dark energy” necessitated by established physics. PG provides a greater framework to describe the cosmos, whereas prevailing theories describe only a subset of it. PG could be the New Physics to describe the universe and overcome the ever emerging impasses by prevailing theories.

Therefore, it is critical to find the value for t_g . It might range starting from as short as the Planck time up to an upper limit remaining to be found. All this depends on whether the gravion acts singly, or cooperatively with multiple units of itself, like in a continuous ray of gravion units. We have already speculated gravion-rays in the preceding Section. We need to determine if we should use a gravion-ray interaction time t_{g-ray} in lieu of t_g in Eq. 491.

Note 1: The below text is deleted, because it was based on a probably premature idea about gravion-rays and photons that was intended to explore in a later development of the theory.

If the general energy-mass equation $E = mc^2$ is valid, which we also derived by PG means in Section 29, then we must have that $t_g = 1$ s in above Eq. 491, giving:

$$g_0 = \frac{c_{ph}}{1s} \quad (495)$$

The physical significance of this potential finding remains to be decided, because it depends on other PG parameters like the absorption factor k . This is further investigated in necessary subsequent work following Section 30. The experimental measurements of g_0 proposed in Section 12, or other equivalent parameters like k , J_0 , n_0 , A etc., would greatly facilitate the theoretical endeavors to establish a theoretical g_0 herewith. This depends on values of those other parameters in a way that makes it imperative to break out of a cyclical conundrum. We need to firmly establish one PG parameter either experimentally or theoretically to free us from many diverse theoretical combinations and speculations, and help us move forward fast.

Note 2: The above presentation raises several issues (like the relation between gravion t_g and photon period T , and much more, which will be addressed in a subsequent version of the report in Section 31 currently under development.

Actually, the power-mass equation contains the factor 4, which we should not omit if our 3+1 mass scheme at the fundamental level or an equivalent one can explain its presence, so that we should better write the equation in full as:

$$M_e = \frac{\frac{dE}{dt} t_g}{4c^2} \quad (496)$$

By virtue of Fig. 78, only $\frac{1}{4}$ of the total absorbed energy rate associates with the effective mass, i.e. we have an effective energy E_e provided by the integral (with a fixed steady-state power absorption):

$$E_e = \frac{1}{4} \left(\frac{dE}{dt} \right)_{fixed} \int_0^{t_g} dt = \frac{1}{4} \left(\frac{dE}{dt} \right)_{fixed} t_g \equiv \frac{1}{4} \frac{dE}{dt} t_g \quad (497)$$

leading to $E_e = m_e c^2$. The latter is more general than the conventional $E = mc^2$ in that it provides the effective mass, which is a subset of the real mass. We can better understand the significance of this important equation, if we start thinking about a macroscopic body like a planet. The energy absorption rate depends on the absorption coefficient k (the number of absorption events per unit length in the body). It is all those events that take place in time t_g , which add up to produce the numerator of the fraction in that equation. It is the synergy of concurrent absorption events adding up to produce an effective mass, the absorptivity and the associated acceleration g of the given planet. This understanding applies to any absorbing body, including a single photon. The idea of synergy and concurrency applies all the way down to some minimum size structures of absorption and emission centers (MAC/MEC) first described by the 3+1 mass scheme.

We can finally see that classical “inertia” appears every time we attempt to change the characteristic fixed $\left(\frac{dE}{dt} \right)_{fixed}$ power absorption exhibited by any given material body. This happens when we accelerate or decelerate the given body. “Inertia” is not some innate propensity for resistance by the body itself, but a resistance by the gravitational field to reconfigure itself with the body’s change of kinetic status. Inertia is not a property of the body or “mass”, but a resistance by the gravitational field to reconfigure its steady state power absorption in connection with a body. The body mediates this resistance of the gravitational field, as the body is the only tangible and visible medium to us.

In continuation to the above analysis, there arises the question about the importance of the interaction time t_g and its possible or not physical connection with the other constants like g_0 and J_0 , i.e. about why

should the interaction time constant be related to g_0 via Eq. 491. Conversely, why should g_0 be uniquely dependent on t_g , when we know that g_0 is also derived from J_0 , which can vary from region to region of the universe. We have already found the relationships between external and internal constants in Section 24.1. We may add also that the gravion density flux in close proximity to an astrophysical explosion may be much higher than an average value of “free space” of the universe. Therefore, the gravion interaction time does not by itself uniquely determine the other constants. Those other constants statistically determine the integration time of Eq. 497 in conjunction with the gravion interaction time. Whereas the interaction time is fundamentally necessary towards establishing an effective mass of an object, it is not sufficient. Therefore, we may conclude that the fundamental equation between power and mass requires an integration time to be worked out theoretically or experimentally. For the purposes of further developments in this report, we should use an integration time t_i in lieu of the interaction time t_g pending also the establishment of a mathematical connection between the two.

$$g_0 = \frac{c}{t_i} \quad (498)$$

29.4.6 Drag and miscellaneous issues

It is understood that the equation $E = mc^2$ has been verified by various experimental measurements quantitatively with negligible error. This raises the question again if the factor of 4 in our derivations is due to some subtle mistake in the procedures adopted. If not, could the experimental measurement be missing a form of energy not easily detected, like, for example, in the form of gravitational waves or particles slipping through our detectors? Perhaps, measurements during an atomic bomb explosion could provide maximum intensity of fugitive forms of energy to look for. This author is not aware if the entire energy released during an atomic explosion is accounted for, i.e. if it has been measured and found to agree with the mass-energy equivalence equation. Effective mass is responsible for the energy released and detected in an atom bomb, while black mass released presumably goes undetected; it might contribute to the addition of gravions that could increase gravity by a relatively small amount around the point of explosion and could be detected if we were looking for it (like a weak gravity burst, a gravity wave). Gravity waves are released from massive astrophysical explosions, which presumably free also our hidden black mass in the form of gravions and other components, i.e. the component in the 3+1 mass scheme plus the component associated with the absorptivity factor A_R . The type of hyle components released in astrophysical explosions in all forms is a matter for future research. Ghost particles already detected, neutrinos and other particles identified or not (known or not) are likely to be the remnants of such explosions along with gravion rays. The mass-hyle relationship outlined in Section 24.2 becomes more relevant here.

Like effective mass, classical energy is not sacrosanct either, if we have correctly deciphered its place in the universe: The classical energy is only that part of it flowing around that is absorbed by a given body to generate the corresponding classical mass (now effective) of the body surrounded by a gravitational field. The energy-mass equivalence has described only those two quantities that are in continuous interdependence under a steady state dynamic equilibrium with gravion flux. There is much more gravion energy radiating in the universe, as there is much more latent “mass” inside all bodies and much more in stars, white dwarfs, neutron stars and black holes. Energy and mass are not intrinsic to a body, they are not generated by the body itself alone, but they rather have an exogenous source in the universe.

In consequence of the above understanding, we propose to conduct new measurements during an atomic bomb explosion. We should attempt to measure subtle gravity variation with good gravimeters in an underground bunker at sufficient depth to separate all other types of radiation arriving from the bomb at sufficient distance. Gravity and other radiation generally precede the mechanical disturbances by seismic and heat waves. If possible, we might look for subtle differences in the speed between gravity rays and photon radiation. Similar measurement can be conducted from the distance of an international space station (instead of a bunker), if we are lucky to collect enough gravity waves to trigger a gravimeter. A more extreme experiment could be based on an atomic explosion in space. In any case, this proposal is added to our list of possible ways to verify PG theory. Clearly, this proposal would succeed if and only if there are independent (free) gravions released and if they are in sufficient numbers.

“Curvature” or “bending of space” may turn out to be only a corollary of mathematical idealism in lieu of the existence of force as fundamental and measurable property of nature. Force, distance, time and acceleration are our first call for understanding nature. Energy is $(force) \times (distance)$, so that when effective mass is converted to energy during an atomic bomb explosion, it is the destructive forces that we evidently experience. By PG theory, another type of mass, if converted to anything at the same time, remains to be tested.

We should note that the mathematical differentials for solid angle and time have been replaced by finite

quantities. We may wonder about the real physical significance of the quantities Ω_g and t_g , to which we also surmise a finite length $s_g = ct_g$. The length s_g may be the length of a continuous “ray” that is continuously interacting over a time interval t_g inside a solid angle $\Omega_g = \pi$ sr. Over and above the present considerations, the various possibilities for the distribution of Ω_g can later help us in modeling the minimum absorption center (MAC) defined in Section 19.1. This may mean that a MAC can interact with up to 4 gravions at a time. This may have to do with the structural order of the MAC permitting only one gravion interaction inside each quarter Ω_g sr. The co-existence of tiny MAC entities supposed constituents of known particles (like electrons), together with rays of possibly astronomical lengths could provide an entirely novel basis for understanding hyle (matter) in physics. It might help decipher the “spooky action at a distance” (entanglement) and much more. This and other properties may be used towards proposing models for the gravion and the MAC (concurrently being also a MEC = minimum-emission-center). The continuity of interaction in time is a necessary condition for the existence of effective mass. If the time interval t_g is shorter due to a higher value of g_0 , then we get an increased rate of gravion incidence on average resulting in the same given effective mass. It seems that a “durable” interaction (via t_g) is a necessary condition for the presence of effective mass and structure, for only during this time hyle can be engaged in organized patterns with gravions. Two gravions may not occupy the same site, hence the idea of Ω_g being a property of MAC. Conceptually, the gravions operate on material bodies like viruses operate on living cells. They occupy specific sites and are part and parcel of bodies and surrounding space together.

NOTE: When we integrate over the solid angle up to π limit presumably for a single gravion, mathematically, it is implied that “energy” flux is a continuous quantity over which we integrate (see also NOTE: 29.3). This may not seem consistent with the presence of a single gravion. However, the significance may be that the structure of a MAC is such that it allows only one event of interaction at a time. Once the gravion-MAC interaction ensues, there is an unbroken “bond” between them so that no other gravion inside the associated π solid angle can engage with the given MAC. Otherwise, we would have to have a “continuous energy” converging within that angle. We tend to accept more that the gravion is a “corpuscle” but with certain attributes (like length) to be found out, not a 3D filling continuum. These considerations may sound too detailed and too far fetched, probably wrong at this early development, but there is no harm to make a record of these thoughts for future reference. In the meantime, we may apply them towards modeling of various systems.

Before we learn about the quantitative interplay of these parameters, we should at least verify PG in principle in order to recruit many workers in this field. This is a key stage in science, so that we may re-assess and re-appraise all relevant data from all related branches of physics. Pending this, we can only proceed theoretically: The above advances provide good ground for thinking about the nature of gravions and attempting to provide some modeling next.

The present idea (proposal) of a triangular prism playing a role in the structure of MAC/MAC gives further support to an earlier suspicion (proposal) that electrons and protons may contain geometrical structures such as cuboctahedron (See 19.3.3). It is logical to think that at the extreme fundamental level of nature there is not much left by way of diversity, other than geometrical diversity with different shapes made out of gravions (gravion packing order).

We have envisaged that a MAC is ON or OFF every time and during interaction with a single gravion, or (now) quadruples of gravions. The accrual of gravions continues until it reaches a critical state when it emits another type of particles, like electrions. When we introduced the idea of MAC, we made no commitments about the number of gravions interacting concurrently. Furthermore, the distribution of the said characteristic solid angles may be favored towards the equator and away from the poles of an oblate MAC, while the same entity acting as MEC emits inside specified solid angles distributed more towards the poles. The MAC and MEC is one entity embodying a steady-state equilibrium of hyle flow.

An oblate MAC/MEC is more absorbent in the directions towards the equator and less towards the poles. This idea is consistent with a mechanism proposed in Section 25 to account for the critical “problem of drag” in moving bodies through gravions. For convenience, we copy the same as follows: *“The connection of motion to structure may be a way to make progress in understanding space-time, the dynamics of PG and the connection between speed and mass. The vortex structure may be at the basis of this hypothesis. A minimal effective mass may be that of a MAC/MEC. By way of illustration, we might simulate a moving vortex to a jet engine. In a stationary sphere, the effective mass is spherically distributed with the statistical average of the vortex vectors all pointing towards the center of the sphere with zero net sum. When the sphere moves, we may have a partial alignment of the vortices along the direction of velocity. A one-to-one correspondence exists between velocity and kinetic mass, which is composed of aligned vortices. This is one example of connecting speed to structure.”*

Furthermore, in complement or in lieu of the above explanation, we may also propose a scheme like the “Pauli exclusive principle” introduced to reconcile the then new requirements for electron orbitals. The interaction of gravions with bodies may be governed by an exclusive rule stating that an established “bond” between gravion and body-receptor cannot be broken by another incident gravion, unless an external force (acceleration/deceleration) is applied to change the kinetic status (and mass) of the body. Upon release of the said force, the body maintains its new acquired kinetic status with a new steady state of gravion-body-bonds, meaning that the body moves with constant velocity without experiencing the drag expected from classical mechanical corpuscles.

The above arguments clearly indicate that we have to free ourselves from established preconceptions and misconceptions about mass, energy and drag. While PG is by no means a proven theory yet, we have to resist objections like when PG is described as “an example of a failed theory... that *does not work*, because of the drag it predicts would be experienced by moving bodies, *so that is the end of that theory*” (Wikipedia contributors, 2019b)(*). Proclaiming the end of PG theory is rather an example of a failed prior PG implementation method, that is holding back further progress in science for too long.

(*) Quotation in full: *In 1965 Richard Feynman examined the Fatio/Lesage mechanism, primarily as an example of an attempt to explain a "complicated" physical law (in this case, Newton's inverse-square law of gravity) in terms of simpler primitive operations without the use of complex mathematics, and also as an example of a failed theory. He notes that the mechanism of "bouncing particles" reproduces the inverse-square force law and that "the strangeness of the mathematical relation will be very much reduced", but then remarks that the scheme "does not work", because of the drag it predicts would be experienced by moving bodies, "so that is the end of that theory"*

While Wikipedia is an invaluable source of information, unfortunately, it can be abused by cooperating editors with specific agendas. Sometimes, roaming groups misinterpret and misapply the Wikipedia rules as they see fit, but with detrimental outcomes. Nevertheless, it retains a great potential to be and become a free domain with uncensored facts for all.

30 Gravion as fundamental unit and its attributes

This section and subsections below are currently under development with various issues pending further work. The idea of a gravion ray length in Section 29.4.4 and the unitary photon wavelength in Section 29.4.5 may be underpinned by a common cause. That gravion may have both astronomical dimensions and yet interact with matter at sub-quantum mechanical level is an outcome (corollary) to be explained. We have already discussed the possibility that a gravion represents a unit of length, time, momentum and possibly an intrinsic mass (or better, unit of hyle). By a “unit”, we mean that this is an “ultimate” quantity, or an absolute quantum, i.e. an indivisible unit (entity) from which all else can be built. The latter possibility would be a major advance, if confirmed. For this, we need to know (or define) its behavior to everything external to it, leaving the description of the internal nature of this unit for future work. The next level up from this unit is an absorbing body (center) with a possible geometric structure. The latter may coincide with a known “particle” so far considered an indivisible quantum, except that we may now find, or say, that that this “quantum” is made up by other true indivisible quanta. To do this, we need a way to introduce (create) circular motion and spin emanating from the properties of the absolute quantum unit. We need to synthesize these and other possibilities and reconcile them with existing experimental data. We are presently attempting some initial modeling of the gravion and its interactions with other gravions, but also with some minimum absorption and emission centers themselves made up of gravion configurations. Prior to that, we attempt to formulate an approach departing from long established conceptions about photons without contradicting established experiments. As we first digest our new proposals, we will be in a better position to develop specific models of the gravion and its interactions subsequently.

We have developed our PG theory based on the understanding that gravions of sufficient mean free path (mfp) are responsible for the gravitational field without proposing any specific mechanism, via which the accruing gravions are re-emitted, but which is postulated at the outset of the theory. The emission should take the form of some other type of particles (composed by gravions) not pertaining to gravity. Working out an emission mechanism is deferred until we can propose models of material structures of hyle that conform with observed forms of nature. This approach for gravity was extended to explain and apply to all other force fields that are created by corresponding other types of “heavier” (composite) push particles, the accrual of which is balanced out by a corresponding emission of yet different types of particles. We proceed to propose the types of push particles that are consistent with the hitherto developed theory of PG along with emitted different types of particles in conjunction with appropriate modeling of structures for known and new particles and entities. We hope that this method of theoretical development will yield (or contribute

towards) the long awaited “theory of everything”. We start with a proposed connection between gravion and photon.

Here, we continue on from Section 29.4.5, in particular, by attempting to relate the gravion to the photon. There is a vast literature on theories of the photon, only part of which we have been able to access. To this extent, we are cognizant of the diversity of these theories to which we wish to add our own under the framework of PG. Readers who adhere to existing theories are bound to disagree with our presentation, so the decision to proceed with this report is not done lightheartedly. Our aim is to add an alternative position based on the extensive novel ideas already presented in this report. Readers can decide if there are at least some aspects worthy of integrating with their own conceptions about photons and quantum field theory. This would be especially useful if some workers can adopt the PG framework and wish to modify or add their own proposals to help the aims of PG. An attempt is made to correlate the quantum mechanical wave packet to push particles, but the diversity of published ideas is enough justification that entitles us to proceed with our own work. In the search for new physics and for solutions on the impasses of the Standard Model (Wikipedia contributors, 2023), we are well placed to proceed as in the following sections. [Note: For the diversity of opinion, one can find some literature in discussion fora here, here, here, here and here.]

30.1 Gravion as the Planck unit of photon

Note: The below presentation raises several issues, which will be addressed in subsequent versions of the report in Section 31 under development.

Again, emanating from the analysis in Sections 29.4.4 and 29.4.5, we are led to think that the “different types of push particles” referenced there may simply correspond to a different rate of incidence by gravion quanta traveling at the speed of light. We arrive at this conclusion as follows: In the “unitary” quantum at $f = 1$ Hertz, the unitary energy ($E_{uph} = h \cdot 1Hz$) and unitary momentum ($p_{uph} = m_{uph}c_{ph} = h \cdot 1Hz/c_{ph}$) properties were spread out (distributed) over a distance numerically equal to c_{ph} , but the same energy and momentum is also distributed over a distance inversely proportional to the frequency of any given photon. Should we then (or can we) redefine the Planck units with an alternative system of more natural units, whereby 1 (unity) describes a single wave period at any frequency and always contains the same amount of energy and momentum (and mass, better, hyle by PG)? Could a quantum with the unitary quantum energy of $E_{uph} = h \cdot 1Hz$ at the Planck length constitute the ultimate building block of the universe, and this block be (coincide with) the gravion? An affirmative answer would mean that a photon with frequency ν is composed by ν gravions, whereby they are separate entities but configured in a special formation making up what we know as photon. This was assumed to be the case in attempting to find the value of g_0 by Eq. 490.

In a reference system traveling along with this quantum, its internal properties appear invariable regardless of the observed (external) frequency. It is only for an external reference frame that time and space are “created” (observed) as we compare the different frequencies (and wavelengths) of photons. The “smallest” wavelength (e.g. the known Planck length and Planck time) can be used as a measure of all others, time-wise and space-wise. Corresponding to these, we have derived the smallest unitary mass $m_{uph} = 7.37249732 \times 10^{-51}$ kg, as opposed to the established (published) Planck mass 2.176434×10^{-8} kg bearing no relevance to our proposal here. Similarly, the other established (published) Planck units of mass, energy and momentum are set aside and replaced for our purposes with what we term “unitary” quanta of these properties as they characterize the gravion just defined.

We can now think of the possible connection among the proposed different types of push particles for different force fields, like plain gravions, electrions, somions, neutrions, etc., all of which were introduced independently of photons for each case in attempting to develop a general [push](#) quantum field theory. The derivation of g_0 by Eqs. 490 and 491 based on photons is similar with Eq. 464 and 465 based on gravions, lending to the idea of connecting the gravion to the photon, specifically via the Planck constant introduced to explain the black body radiation over a century ago. We move forward per above by adopting that photons are composed by initially independent entities with energy $E_{uph} = h \cdot 1Hz$, to which we may refer as “*universal-gravions*” serving for other fields in “packages” at corresponding different frequencies, or rates of emission, incidence and absorption. However, for simplicity of terminology and to avoid editing the hitherto presented theory, we can retain the term “gravion” without qualifying adjectives (or a new term). The originally introduced gravion for gravity can be configured in packages or groups to generate composite push particles that mediate all other force fields per prior proposals about different types of push particles. Thus consistency of terms is retained.

Per above, a photon with frequency ν is a group of ν gravions. If all of them are lined in a straight line, they would be apart from each other with a distance equal to the photon wavelength λ . To start with, we can set this distance to be the required mean free path (mfp) in PG, i.e. $mfp = \lambda$. A photon in this configuration would have a length equal to the velocity of light, i.e. $c = \lambda\nu$. We understand, that this is not

the case, as we will also see from the very short interaction times in the photoelectric effect. However, in lieu of a straight line gravion sequence, we can have (theoretically) much shorter gravion sequences in parallel to make up a total of ν gravions while preserving the observed wavelength and hence the required mean free path for PG. In consequence, we propose that photons of all possible "sizes" (i.e. frequencies) constitute a gas like medium. They may be likened to "molecules" composed of ν gravion "atoms". In that gas, we have mean free paths of all sizes according to the expected wavelengths of all photons. There are gravions with very long (enough) mfp (wavelengths) as required to produce gravitational fields. Likewise, there is a range of mfp (wavelengths) to produce the much stronger electric fields, and so on for various other force fields of much greater strength. All these coincide with the various types of push particles often mentioned in the preceding PG theory. Of course, the said types of push particles need not only be in the form of photons, but they can be in more (or less) composite forms as we will analyze further below. In short, photons are continuous sequences of gravions at a given mean free path, which appears as wavelength, and which are woven in spatial configurations (packets or groups) to be worked out later. In any case, photons are divisible down to their constituent gravions.

Thus, push particles need not be a continuous ray with a distributed energy and momentum as discussed in Section 29.4.4 in order to produce a gravitational field, but the mathematical analysis undertaken there remains valid. The only continuous "ray" that **must** exist is that of the unitary gravion defined above over its own Planck length, which we will consider in subsequent models of the gravion itself. The same applies for all other field "rays" now to be replaced with groups or sequences of gravions at certain inter-gravion distance (i.e. mfp, or wavelength). The main departure from prior theories we make here about the photon is that wave-length pertains to a regular (repeated) distribution of gravions in space, where gravions are defined by and relate to the said unitary photon above. The distribution of gravions inside a photon wavelengths may take on various configurations to be investigated later, with no specific commitment on the exact configuration (e.g. vortex, helix or other) made here.

We could readily derive the distribution of gravions over frequency and mean free path from Planck's distribution law, if that law contained (described) the entirety of hyle inside the black body cavity at a given temperature. It is already said that the law breaks down above a certain temperature, to which we add that it also breaks down at very low temperatures (maybe already accepted), and so on. Nevertheless, we use this law below only as an aid to convey our proposed theory on linking gravions with photons and all forms of hyle. We pretend it is valid, after which we can propose the need to be completed by later theoretical and experimental work. Planck's law for the energy density distribution is:

$$u_\nu(\nu, T) = \frac{8\pi h \nu^3}{c^3} \frac{1}{\exp\left(\frac{h\nu}{kT}\right) - 1} \quad (499)$$

By dividing the above by the Planck constant h , we obtain the number density distribution $n_\nu(\nu, T)$ of gravions along the frequency by:

$$n_\nu(\nu, T) = \frac{8\pi \nu^3}{c^3} \frac{1}{\exp\left(\frac{h\nu}{kT}\right) - 1} \quad (500)$$

This is plotted in Fig. 79(top) for the typical temperatures $T = 3000, 5000$ K. In addition, we plot for $T = 10000, 100000, 100000000$ K. The latter two temperatures are those presumably prevailing on white dwarfs and neutron stars respectively.

Although it is said that the above law is not valid above some very high temperature, it is interesting to note that the maximum occurs at $\nu_{peak} = 5.88 \times 10^{18}$ Hz for neutron stars and at $\nu_{peak} \approx 5.88 \times 10^{15}$ Hz for white dwarfs, as can be seen from the graphs, or more precisely calculated from Wien's displacement law using $b = 5.099 \times 10^{-3}$ mK when parameterized by frequency.

The corresponding gravion number density distribution $n_\lambda(\lambda, T)$ over "wavelength" λ now replaced with mean free path ($\lambda \equiv mfp$ sparing one symbol for the other in the formula) is given by:

$$n_\lambda(\lambda, T) = \frac{8\pi c}{\lambda^5} \frac{1}{\exp\left(\frac{hc}{\lambda kT}\right) - 1} \quad (501)$$

and plotted in Fig. 80(top). The maximum for neutron stars occurs at $mfp = \lambda_{peak} = 2.89 \times 10^{-11}$ m and for white dwarfs at $mfp = \lambda_{peak} = 2.89 \times 10^{-8}$ m, or more precisely calculated from Wien's displacement law using $b = 2.89 \times 10^{-3}$ mK when parameterized by wavelength.

The above finding is consistent with the requirements of push particles like somions, etc. For example, the value of $mfp \approx 2.56 \times 10^{-11}$ m is about four orders of magnitude greater than the size of hadrons, and

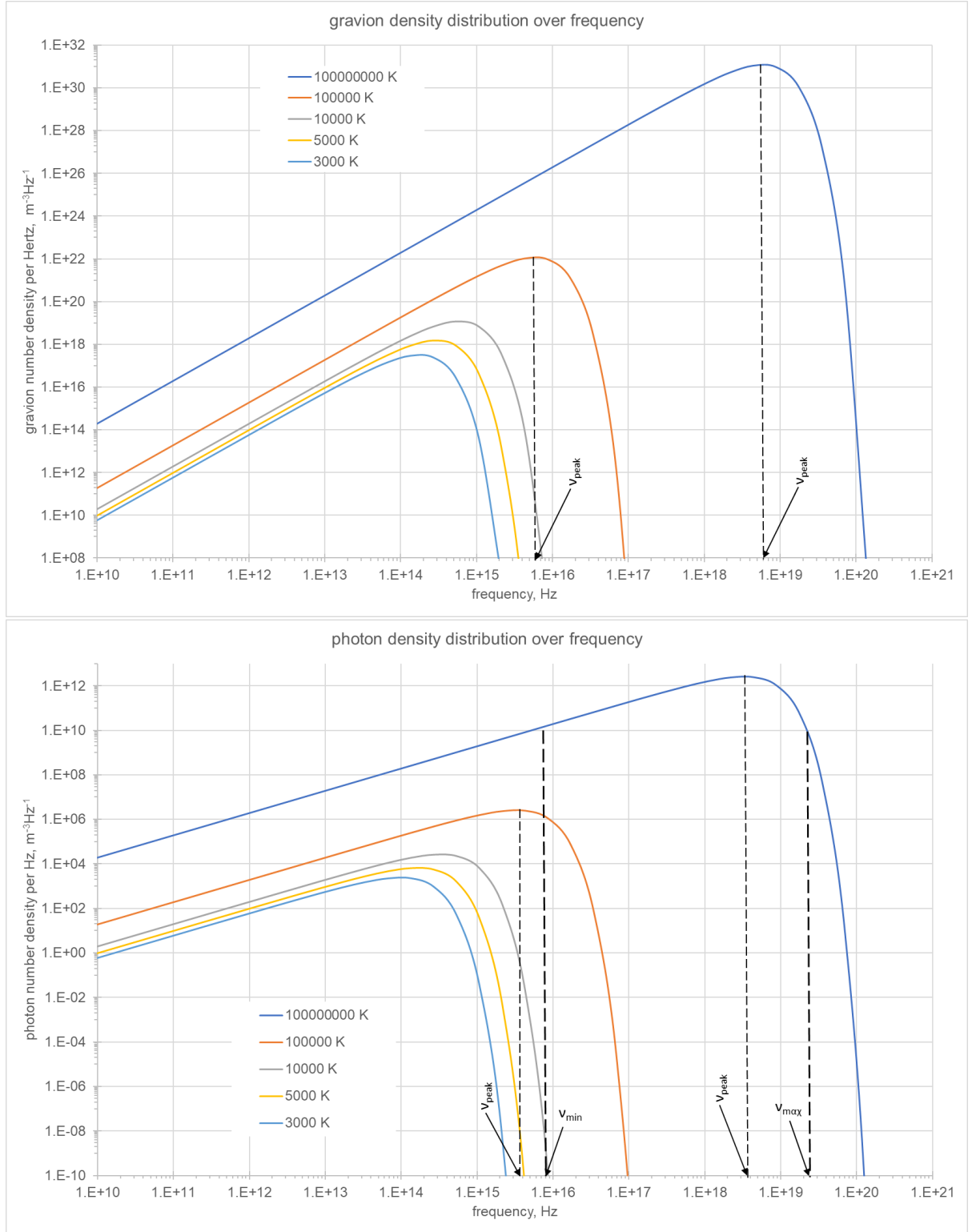


Figure 79: (top) Gravion number density distribution vs. frequency, (bottom) photon number density vs. frequency

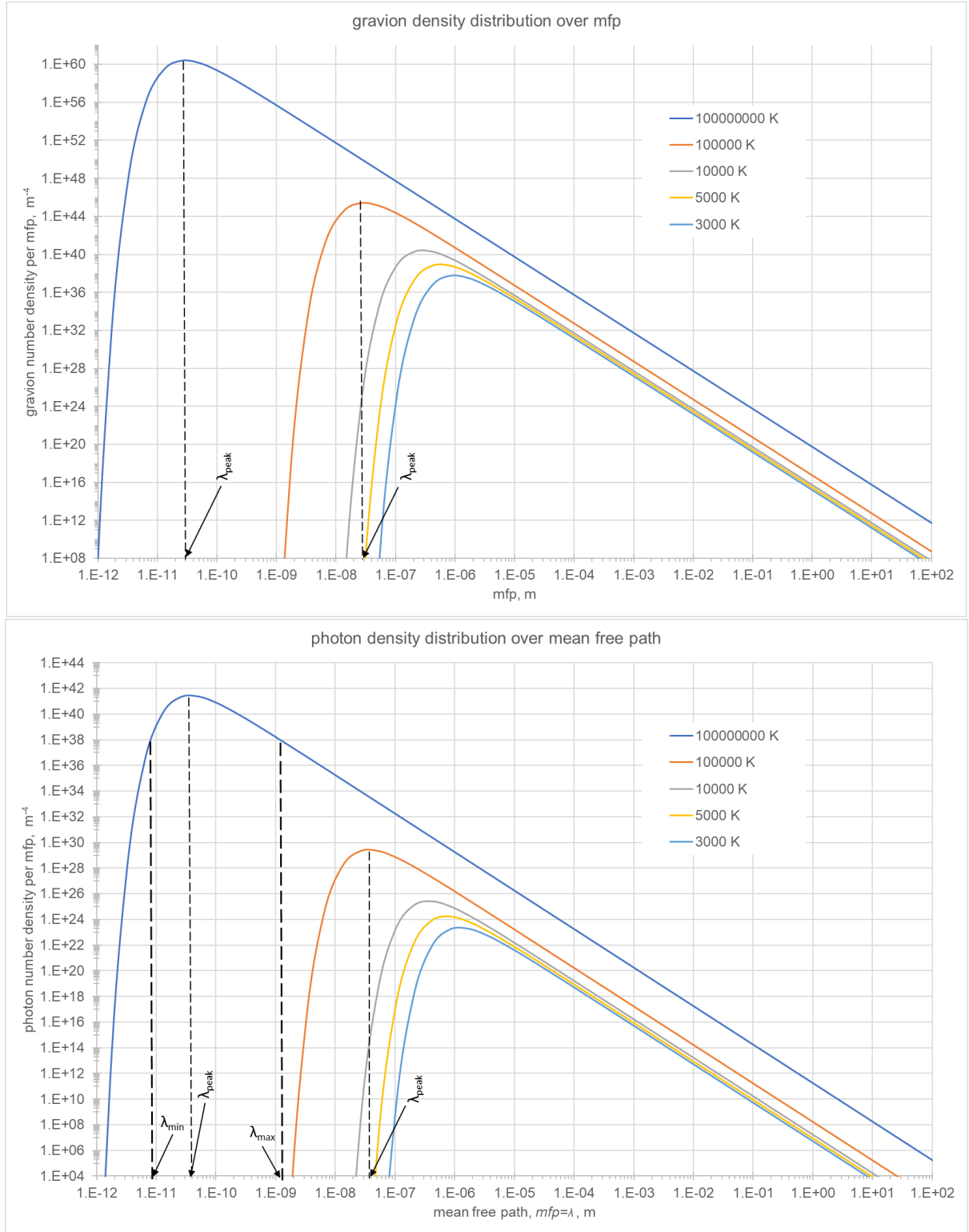


Figure 80: (top) Gravion number density distribution vs. mean free path (mfp), (bottom) photon number density vs. mfp

the value of $mfp \approx 2.62 \times 10^{-8}$ m is consistent with keeping the nucleons pushed (bound) together, as is required in the plasma phase of white dwarfs and in the nucleus inside the atoms of ordinary matter phase.

We will also need the distribution of photon number density against frequency ($n_{ph\nu}$) and against mean free path ($n_{ph\lambda}$), as they are juxtaposed in the corresponding Figs. 79(bottom) and 80(bottom). These are used towards the derivation of the equations that unify all force fields according to Section 30.5. The photon number densities are obtained by dividing the Planck law by each photon energy $h\nu$ yielding a modified law over frequency distribution as:

$$n_{ph\nu}(\nu, T) = \frac{8\pi\nu^2}{c^3} \frac{1}{\exp\left(\frac{h\nu}{kT}\right) - 1} \quad (502)$$

with $\nu_{peak} \approx 3.8 \times 10^{15}$ Hz for neutron stars and $\nu_{peak} \approx 3.8 \times 10^{18}$ Hz for white dwarfs, which are close to the peaks of gravion distributions.

The photon number density over mean free path becomes:

$$n_{ph\lambda}(\lambda, T) = \frac{8\pi c}{\lambda^4} \frac{1}{\exp\left(\frac{hc}{\lambda kT}\right) - 1} \quad (503)$$

with $mfp = \lambda_{peak} \approx 3.8 \times 10^{-11}$ m for neutron stars and $mfp = \lambda_{peak} \approx 3.8 \times 10^{-8}$ m for white dwarfs, which are close to the peaks of gravion distributions.

NOTE: With hindsight, we could and perhaps should have used the term “free path” instead of “mean free path”; the latter arises from and refers to inter-gravion mean-free-paths in given photons and not, strictly speaking, to the mean free path of the entire content of gravions in the universe. We aim to address this issue again later. We leave the description here as is to allow us to make headway by stages in this new and untied exposition of physics.

We need to work out a temperature for interplanetary space and plot the corresponding Planck distribution curve over mean free path. The integral of that curve above a certain mfp should yield the gravion density over the mfp range used, from which we can obtain the prevailing g_0 for the given space range. Unfortunately, this was tried and failed, when we used Planck’s law as is. For example, Pluto is a little less than 40 AU distance from the Sun. A photon wavelength that long (or more), i.e. $\lambda = mfp \approx 5.9 \times 10^{12}$ m, corresponds to a frequency of $\nu \approx 5 \times 10^{-5}$ Hz, or a period of $t_g = 2 \times 10^4$ s. When we attempted to integrate the Planck curves in the range of mfp greater than this low limit of integration using a Python program integrator, we could not get it to converge. This is logical, because photons with solar-system wavelengths are presumably unknown. If neutrinos pass through our planets undetectable, we shouldn’t expect to detect gravions (the finest of all particles), let alone gravions to be readily described by Planck’s law. At any rate, we mention all this as a guide for what to expect from a law used only as an aid to promote the hypothesis of a possible connection between photons and gravions.

Now, we know that photons have momentum and exercise pressure upon incidence. This pressure is very small for visible light and ordinary macroscopic bodies. However, the pressure can be significant at the right scale and the right concentration of photons with respect to the size of impacted bodies. For example, take atomic nuclei and their constituent nucleons. They can behave in a similar manner to the way macroscopic bodies behave when impacted by gravions. Matter is compacted to form (near) spherical planets. Nucleons and nuclei can be compacted, say, by x-rays and gamma rays, as they meet the requirements of mfp (being comparatively very long) and body size. Actually, all photons with greater mfp act cumulatively, including our gravions at the outset of the theory, all in addition to the main compacting push particles for the respective nucleon. We know that photons have “weight” and gravitational (or relativistic) mass. The same applies to particles, including electrons and positrons, as well other particles of verified existence, all of which are acted upon by gravity. Even photons have “weight”, as it is known that the trajectory of photons is bent by stars. That is, we can say that all photons with “wavelength” (mfp) less than a certain limit create a force field around them. That limit presumably assures enough material to behave like gravitational body. The strength of the associated field is relative to the particle size (by “mass”, or frequency) and the total impacting push particles. Under this scheme, we are left with the task of finding the quantitative relationships among all these variables, when we attempt to create a model of particle physics.

Gravions are responsible for maintaining the integrity of bodies, like planets, by exerting compression forces. We have used the hypothetical “somions” for this purpose on atomic scale particles, to which gravions are superimposed only by a relative flux density. Their corresponding fields are always “attractive”, which alone may not be sufficient to explain the long term stability of the ordinary universe.

Furthermore, we also need to explain repulsive forces as those by electrical charges but also by nucleons at very short range. There are secondary push particles like electrons composed of primary gravions (or

photons). They may be like the modeled electrions in Section 25 with the attributes of spin and rotation. They have the capability of creating both attractive and repulsive forces. They are emitted to balance out the absorption of the “attractive” particles (like somions and gravions). The repulsive action (fields) of the secondary push particles counteracts the attractive action of primary push particles resulting in the stability of nuclei (consisting of nucleons) and atoms (consisting of nuclei and electrons). The proposed electron and electrion models serve only to illustrate one possible way to explain repulsive fields like by same sign “charges” and similarly by hadrons at very short range; it is likely that more refined models (push particle configurations) will be devised to account for and unify all observed particle properties. The presented models are based on the possibility of vortex formations and in the ability of gravions to create circular motion and spin. PG has been based initially on linear motion, but less has been said about rotary motion, in general. We previously relied on rotary motion coming into existence only by chance, but we now propose that circular motion comes about by the intrinsic properties of the gravion (see following sections).

The above explanation of various fields, however, raises some important issues, especially with regard to energy balance, distribution and the **energy** cosmological constant. It is not possible to immediately address these issues, other than outline them with some initial thoughts. A high density of photons around nucleons and inside atoms would presumably result in a blowout of the atoms, if there is no equal pressure by other photons from the outside surrounding “vacuum”. The photon gas would have the same average concentration everywhere in the universe with a distribution of mean free paths corresponding to various fields. That would mean that we are surrounded by a photon gas at its highest temperature all the time, which is contrary to experience. However, we said that the Planck law is consistent with experiment, whereby the only contribution to the energy density arises from the detected photons (alone) accounted for in Figs. 79 and 80 at the given temperatures. Random “single” gravions permeate the universe creating gravity as the only trace for us to experience.

The above problem is circumvented in QFT by the definition or by properties attributed to the multiplicity of fields spread out everywhere, but there seems not to be a consensus as to what these fields are, or they are understood differently by different workers. It is said that everything is vibrations in a vast web of quantum fields. A field is a region where every point has a physical quantity associated with it. Some say that they are more than mere mathematical maps, as they are physical objects that fill otherwise empty space. Others say that nothing is made of fields, which are only mathematical probes of what may happen if a material object is put into it; or fields are typical potential energy but not energy. This is the cosmological problem arising generally. This problem may be obfuscated by theorizing that fields are mere mathematical properties and particles come into existence only upon excitation of the underlying fields. This seems like the universe arises out of mathematical ideas without the heat catastrophe problem we surmised for PG. It is said that things appear via fluctuations from “vacuum”. Can we also claim that a “pure” free gravion gas corresponds to “vacuum” out of which arise organized forms of gravions like photons, electrons and particles in general?

Our ultimate aim is to condense the rules of any theory and to make everything using just one rule.

When a wave is transmitted through a medium, it is an energy that is transmitted while the medium is “stationary” (i.e not propagating, or transferred, along a direction) . However, if energy consists of particles (quanta) and if energy is ultimately hyle (matter), then in a continuous propagation of a wave emanating from a source, it must be hyle (matter) that is transmitted in the wave-train. The source must be emitting matter (particles) that displace the medium particles in such a way that a net flow of matter from the source to the receiver takes place. If the particle is seen only as a disturbance of the medium (energy), then we introduce a duality whereby the disturbance is a state of the medium and the state itself is a distinct entity from the medium. The duality of wave-particle thus arises. However, we propose a different approach, namely, that medium and particles are of the same substance (hyle) at the ultimate fundamental level of nature, at the level of gravions.

The above issues (radiation catastrophe, duality, etc.) can be overcome by assuming that the distribution of photons varies from one region of the universe to the other and from within atoms and nuclei to the surrounding regions (or “vacuum”) accordingly as to create the observed fields in accordance with the distribution of mean free paths. The stability of atoms is owed to the stability of the structure of their constituents, which is the ultimate result of both rectilinear and curvilinear motion starting at the gravion level. The seeds of this proposal can be found also in Section 25 and elsewhere in this report. While it was argued there that circular motion could arise by way of chance, we can model to gravion in a way that promotes circular (rotational and spin) motion spontaneously during gravion-gravion interactions (collisions). By such means, we have inter-conversion and co-existence of the two kinds of motion from the ground level of the gravion to all higher levels upwards of hyle organization. These and other issues will be addressed as we develop the theory by stages. While the theory remains incomplete, there should be no reason to abandon it. Below, we proceed with supporting arguments to be used as basis in subsequent modeling of the gravion.

The Second Law of Thermodynamics (SLoT) is counter-acted by the Fluctuation Theorem (FT) as discussed in early Section 15.8. A closed system goes through a very large number of states, the majority of which is randomness, but every now and then it achieves some degree of order defining structures. It may take relatively very long time to alternate between disorder and order depending on the size of the system and the internal speed of the units composing the system. Molecular gases is an example. Atmospheric storms form out of the chaotic molecular movement every now and then. In a finite system composed of entities moving at the speed of light or close to it (like gravions), we may envisage the formation of structures appearing with high frequency in our time scale. These structures are fluctuations undoing the randomizing power of the SLoT. Thus, a given entity may be accruing gravions (or other particles), but every now and then it may also be emitting larger structures so that there is a steady state equilibrium that stabilizes the entity in existence. The “every now and then” can be extremely short times at atomic and fundamental particle levels relative to human level. With this background in mind, we can proceed in modeling structures without fear of violating some law of nature, provided that we can show a working organic synthesis of the modeled parts of the universe. We continue to apply the trial-and-error method as the only way to deal with a completely novel theory like PG.

The above flow of alternating states between order/disorder may be favored by certain attributes of the unit components of the system. For example, if the units have dipole-like characteristics of some kind (mechanical, or whatever) as opposed to spherical characteristics, then formation of vortices and vortex stripes can take place (*Klaus et al., 2022*). Suffice it to quote the opening paragraph from that work: “*Since the first experiments on gaseous Bose–Einstein condensates (BECs), the observation of quantized vortices has been considered the most fundamental and defining signature of the superfluid nature of such systems. Their very existence sets a unifying concept encompassing a variety of quantum fluids from liquid helium (Donnelly, 1991) to the core of neutron stars (Pines & Alpar, 1985) and from superconductors (Gallemí et al., 2020) to quantum fluids of light (Lagoudakis et al., 2008). Their classical counterparts have as well fascinated scientists from different epochs and fields as vortices are found in many scales of physical systems, from tornadoes in the atmosphere to ferrohydrodynamics*”. We contend that the SLoT should not be presented for an outright rejection of models in attempting to unify the flows of hyle among and between various levels of organization, starting from the smallest entities (sub-nuclear particles) to the largest (galaxies). We should be free to theorize and trial various models until the models can explain all the observed systems. This is a big task and should not be thwarted at the first difficulty, if the road-map set out by PG can be maintained for sufficient time by sufficient sections of the scientific community.

30.1.1 Divisibility of the photon and the double slit experiment

Below is a compilation of thought-notes to reinforce and illustrate the above ideas without harm if some overlap or repetition is allowed. They further outline the core ideas that could form a basis for subsequent modeling of various entities.

Miscellaneous: Photons are organized in a particular way by some emitting source, e.g. by electrons moving between orbitals in an atom. Similarly, they are emitted by nucleons and so on. By the same token, they are also capable of being absorbed by a receiver atom (or entity). We can continue to interpret the known light phenomena (black body radiation, photoelectric effect, etc.) under our proposals. The proposed divisibility of photons now introduced, allows more degrees of freedom that can interpret outstanding phenomena like the dual nature of photons, the double slit experiment, various experiments with interferometers and much more. Photons are creations by certain mechanisms in atoms, electrons and nuclear particles. These mechanisms may be seen as “zipping” gravions together to make photons. This is a pending task of modeling the known particles (as photon emitters) with structures that allow the emission and absorption of photons. The electron orbitals and particle energy levels in atoms and nuclei can be imposed by some kind of resonance between mfp (re “wavelength”) for any given size of particle. In short, we can say that waves are nothing more than regular (periodic) spatial patterns of gravions. Under the apparent duality of wave-particle, there is actually a manifestation of regularity in the density (wave) of gravions (particles) embodied by a photon.

In other words, photons with the longest wavelength are the hitherto perceived by PG single gravions with the longest mfp and statistically distributed in a long wave-like pattern; they can serve the postulates set at the outset of PG and, hence, they can be responsible for gravitational fields. Similarly, shorter and shortest wavelengths are responsible for much stronger force fields. All this means that what we referred to as “gravion ray length” and possible g_0 values in Section 29.4.4, should now be seen to correspond to the different values g_{01} ($\equiv g_0$), g_{02} , g_{03} of the different types of push particles theorized towards a general quantum push field theory in Section 19 and elsewhere in this report. The universe is self organized by entity-size in relation to corresponding mfp (re “wavelength”) in a photon gas.

Let us examine the consequences of the above ideas with regard to prevailing theory and established experiments. It is customary to consider the photon as a wave-packet constructed by interference of waves in a certain wave-number range $k - \Delta k < k < k + \Delta k$ (momentum space) corresponding to a frequency range $f - \Delta f < f < f + \Delta f$ along the propagation line in the range $x - \Delta x < x < x + \Delta x$ (position space) governed by the uncertainty principle of $\Delta p \Delta x \geq h/4\pi$. Let's replace the notion of the mathematical wave packet made by superposition of waves in a range of frequencies with an equivalent packet of coexistence of real particles (gravions) with corresponding apparent mfp (wavelengths). We replace the mathematical quantum wavepacket with a structured photon made out of real fundamental quanta, the gravions. In other words, the phrase that a wave-packet is a group of frequencies is consistent with a reality that a particle (like a photon) is a group of other particles (gravions) coexisting over a region of space-time. When the group strikes an object, it "collapses" producing all the experimental observations on record. We now think that photons are emitted "ready made" formations by an electron prior to the photon's emission and propagation. We need not think in terms of a mathematical interference of waves of an infinite length along the propagation line, but better to think as an organization of real entities (gravions) first organized and then exited as soon as the conditions are correct among the various statistical fluctuations inside the electron. The photons exhibit their presence only in a particular organization of gravions, otherwise the gravions would not be detected as light (if they existed free and randomly at the given mfp, or like neutrinos). For example, neutrinos are just another form of gravion groupings (photons) of various sizes that generally go undetected, either as particles or waves on account of their very long "wave" lengths. Neutrinos are thought to be light particles with sizes between single gravity-gravions and the longest wavelength detectable photons. These are not seen in black body radiation experiments. Could they be deduced theoretically by extending (applying) the Planck law at the appropriate temperatures? We proposed doing the same for gravitational gravions above.

Our description of photons may explain interference phenomena requiring the wave nature of photons. Given now that the photon is concurrently composed of individual real quanta (gravions), half (or part) of them can pass through each the double slits and recombine behind the slits on the receiving interference screen. They may not recombine exactly to form the same photon but they yield the same observed effect like the original photon becoming split and then regenerating at the screen, This may be achieved via mechanisms at the surface of the slit edges acting like a mechanical analog of the Huygen's principle in wave propagation (that every point on the current wavefront acts as a source of secondary spherical waves). The experimental observation now seems logical if the photon is no more an indivisible quantum, but an agglomeration of a huge number of other indivisible particles. There is no paradox any more, since the photon is naturally divisible consisting of, say, 10^{15} true quanta in a corresponding frequency photon. This large number of quanta lend themselves to be organized to what we call a photon and with such an organization capable of explaining all observations. We defer a determination of the exact structure of photons, but we may initially theorize it to be a multi-stranded helix, or some form of a vortex. "Wavepackets" composed of discrete sine-waves in a narrow range of frequencies need not "annihilate" themselves by interference everywhere along the propagation line except in the region of the packet itself, as is generally believed. All the required corresponding real components may spiral around each other in a particular way over the group length during propagation but "collapse" upon arrival at a particular material surface with the appearance of wave patterns. The "length" of the traveling packet needs to be small enough to explain the "instantaneous" emission of photo-electrons. Actually, "instantaneous" in reality is a finite time interval, say, $< 10^{-9}$ s corresponding to a distance of $s = 10^{-9} c_{ph} \approx 0.3$ m, over which its structure is "woven" from strands of gravions in a corresponding range of frequencies (= rates of transmission). If a photon at $\nu = 10^{15}$ Hz is made by a single strand (train) of gravions, it would need an interaction time of 1 second, so that if its interaction time is actually much shorter, like 10^{-9} s, we should have $10^{-9}/10^{-15} = 10^6$ parallel strands of gravions to explain the interaction time, or the strands woven in a helical configuration taking even shorter time to eject a photoelectron. In this scheme, we view the gravions a "sprays of bullets" shot out from a multiple-barrel machine gun (metaphorically speaking). They all hit the target electron cooperatively. A single strand capable of "lift-off" would take a long time to free the target photoelectron, while one million "sprays of gravions" acting in unison (parallel) would free the photoelectron correspondingly faster. Rocket science can provide the quantitative relationships needed between rates of parallel gravions for an electron to overcome potential energy between orbitals. In conclusion, we can replace the wave-packet notion of QM with an actual gravion-group in making up a photon.

The interaction time used above implies that the photon exhibits a length during its collision with a photoelectron. Xu (2021) has reported on the "*the size and shape*" of a single photon as being a property of a photon shown in its collision with a charged particle. This approach is consistent with our proposals, while the workings of that report may be a more general consideration without the specific notion of "splitting" the photon, as we do here. Furthermore, Aidelsburger *et al.* (2010) have reported on ultra-fast interaction times by single-electron emission. They studied ultra-fast diffraction of photons to generate electron pulses

shorter than 100 fs. This means that we should replace the 10^{-9} s factor with at least 10^{-13} s resulting in a much shorter photon length with a much greater number of “parallel” gravion sprays pointing towards rather a vortex type of formation than a long multi-stranded helix. Pertinent to all this is also the two-photon photoelectric effect reported by Richard (1962). Although the two-photon electron extraction is rare, it shows that if photons cooperate simultaneously, they can produce a photoelectron (PE), which then shows that it is not the frequency alone that is a necessary condition, but the combined cooperative total power and energy that is critical. If 3 or 4 photons could cooperate with a total energy not less than that required to extract the electron, we should have a PE liberated, except that such an event is statistically extremely rare to take place and be observed. We may consider the electron struck by several bullet sprays belonging to independent photons fired and received in parallel, but this does not happen in practice to produce a measurable effect. It is only the single photon that can supply parallel gravion sprays with the required energy and frequency that is capable of yielding a PE. By proper experimental measurements, we may be able to measure the exact interaction times and determine the number of “parallel” gravions as means towards deciphering the photon structure.

As said above, the divisibility of a photon can better (perhaps completely) explain light interference by the particle nature of photon with a wave appearance being only a distribution of its constituent gravions along the propagation line. An interferometer using the splitting of a laser beam via mirrors, and filters to reduce the intensity of the beam, produces results that need not be a paradox. A regular intensity laser demonstrates the usual electromagnetic intensity (amplitude) that can be reduced down to a single photon. Interference patterns are still observed with single photons, even if the difference of the travel length of the split beam is very high (say 1 m). This can be now explained by assuming that even a single photon is splittable to two components that can recombine and interfere to produce the observed experimental outcomes. If this is possible and true for a photon, then it should also be possible for an electron displaying wave characteristics. After all, an electron is a higher organization of gravions where a superposition of splitability applies. If this is possible for an electron, it should also be possible for a nucleon, as well as for a nucleus. By the same token, it should be possible for molecules too. This means that all these particles could be split and pass through a double slit by sequentially decomposing and re-emerging at the other side as waves of its components. It is not known to this author how exactly the latter experiments are performed and if atoms and molecules re-emerge whole on the other side, or only the individual particles-constituents form wave-like patterns. We present all this as a logical consequence of the push particle principles that we have embraced, even if this hypothesis might seem far fetched and extraordinary, away from the established conceptions about photons and particles. The jury should wait for judgment and allow the proposed method to conclude all necessary investigations.

The above proposed scheme (or guide) for structuring the photon in subsequent PG theory can be subjected to the test and refinement in explaining the hitherto experimental data by various scientific disciplines. For example, the “strands” of gravions that compose a photon can vary in frequency (gravion rate) within a particular range of frequencies as to explain the finite width of spectral lines. By numerous other observations, we hope to be able to apply “reverse engineering” to determine the structure of photons. Likewise, in fact concurrently, we should be able to determine the structure of electrons and all other known particles in physics.

The Standard Model having multiple elementary (fundamental) particles seems unlikely to be correct. Deconstructing this model and replacing it with another one based on a single invariant unit, like the gravion, seems more appealing. For example, it is plausible that we can replace gluons, pions and mesons of all kinds with push particles of the appropriate kind to obtain traction. We should be able to rebuild an alternative PG Model with a single gravion (fundamental) particle. Gravions can maintain the integrity of electrons, protons and neutrons and many of the other particles of the Standard model as their nature requires. There is a photon structure function in QFT, which may be re-considered in conjunction with above proposals leading to a synthesis of a better understanding of the photon. The QFT function is defined by the process $e + \gamma \rightarrow e + \text{hadrons}$, which may be integrated with above analysis and check if all these characteristics are borne out by experiment.

Not least, we should mention that in Table 31 we summarized the various types of mass and speeds in PG theory, while we have just initiated a PG particle theory in Section 26. For a photon, if we initially assume that its “composite” speed v_{phc} is equal to its actual speed $v_{phc} = c_{ph}$, then all its mass is kinetic m_{κ} with zero real and effective mass at rest; the latter would be consistent with relativity. However, we need not maintain such a consistency, if PG extends beyond the realm of relativity. It may be that the overwhelming mass of a photon is a composite mass m_c containing a composite effective mass m_{ec} plus a composite black mass m_b , starting with “tiny” rest real-mass containing “tiny” rest effective and black components of mass. The composite effective mass (of a moving photon) m_{ec} contains kinetic and starting effective components of mass. All in all, a photon (per PG) has a composite speed v_{phc} , an actual speed c_{ph} and a composite mass

m_c . It should be noted that black mass has no classical inertia (to an external of a given body force) and can travel/accelerate without resistance to/at any speed. Black mass is part of the real mass needed to act as substrate for the activated (effective) mass being created by absorbed gravions at the MAC/MEC level. In other words, a photon has structure with at least one or more MAC/MEC sub-units. Our PG mass (m_{ec}) need not be (or attached to) either a relativistic mass, or a rest mass. It can be thought of as a definition of a general effective mass that can be reduced to a “rest” and/or “relativistic” mass under certain assumptions. Should we do that, then the adherence to relativity is not breached by re-writing the relativistic equation as

$$E_{ph} = m_{ec}c_{ph}^2$$

In other words, relativity is a subset of (or contained by) PG, whilst assigning a mass to photons (m_{ec}) is an entitlement by PG theory.

The Ehrenfest theorem might help explain or bridge QM probability distributions with actual distributions of a deconstructed photon to gravions. It might turn out that QM is a macroscopic description of a much finer world governed by its own rules of gravion interactions. Often in modern physics, mathematics describe one type of macroscopic metaphor (particles) and also can describe another macroscopic metaphor (visible waves), but difficult to be properly imagined by humans so far. We hope that our scheme of a photon-gravion relationship can demystify those difficult to understand experiments. We have presented plausible arguments that point us to a particular direction. Experiments, old and new, may verify or not the proposed ideas. We need to go beyond existing theories with new general postulates to arrive at a new general theory.

The photon is a convoluted sequence of gravion quanta created and emitted by some particle (electron, nucleon). At this point, we propose that the gravions inside the photon may interact (or not) among themselves with a mean free path equal to the observed wavelength of the photon. If the inter-gravion distance is not statistically variable with an average value, then a fixed free path (distance) should be explained with appropriate modeling of the photon.

In conclusion, the photon is not a physically indivisible quantum particle. “Splitting the photon” is now a realistic option to use and apply, like “splitting the electron” was previously proposed. It is the Planck constant that belongs to a true quantum unit, namely, the gravion. Max Planck’s monumental work was not brought to its logical conclusion and has not been applied to its full potential by all hitherto theories.

We have re-appraised the nature of photons in a way that continues to explain various experimental effects like the Compton and photoelectric effects. We next attempt to model the gravion in a way that could help in the building of particles including photons.

Literature survey on photon divisibility: We did not resort to finding prior experiments or prior theoretical works in support of our proposed divisibility of the photon, because we could initially arrived at it independently. Nevertheless, this is now briefly undertaken below. While PG field theory is not contingent upon direct experimental (physical) photon division, the latter would provide *prima facie* support, if shown possible. It seems that we need to reappraise all possible factors contributing to the observed interference experiments. Thus, it seems that only (relatively) lately the question “*Do we count indivisible photons or discrete quantum events experienced by detectors?*” has been rightly asked by Roychoudhuri & Tirfessa (2006). We have also queried what exactly comes out and behind the double slits in the context of wave interference observed with electrons, atoms and molecules. Those authors state the inability of highly successful quantum formalism to provide “*the microscopic picture of the processes undergoing during QM interactions; that is left to human imaginations allowing for sustained controversies and misinterpretations*”, while they underscore “*the paradoxes that arise with the assumption that photons are indivisible elementary particles based on the obvious but generally ignored fact that EM fields do not operate on (interfere with) each other.*” They also “*suggest experiments to validate that the amplitude of a photon wave packet can be split and combined by classical optical components using the specific example of an N-slit grating*”. Thus, the divisibility proposed refers to classical (continuous) waves, which, however, supports our proposal, provided that the “wave” be exchanged with our mean free path notion of gravions. After all, it seems that “*Planck never accepted that the photons themselves, containing quantized energy at emission, were indivisible packets as they propagate out*”.

It is relevant to also consider a claim by Panarella (2005) that no single photons have been detected, while he has proposed a “photon clump” theory to explain his observation. It is inside this clump that “*the individual photons are arranged in a geometrical wave pattern, much like a wave distribution. In this sense, therefore, the photon clump is both a particle and a wave and the model thus reconciles two concepts which are normally a source of some debate, namely the Dirac’s notion that a photon interferes only with itself, and the pilot wave concept of de Broglie. In fact, as far as the interference of a single photon with itself is*

concerned, such statement can now be reinterpreted as meaning that a photon clump contains all the elements of interference in itself, namely maxima and minima, because in the clump there are maxima and minima of photon number density distribution. As far as the pilot wave of de Broglie is concerned, its reality and its real meaning are readily retrieved from this model. It is, in fact, the interaction among photons responsible for guiding them on a wave distribution within a clump. Rather than being separate entities, the particles and their wave geometrical distribution are coexisting and inseparable properties of what should now be said an element or an “atom” of light” (quotation from Panarella (1987)).

In effect, we have proposed an analogous description of the photon like Panarella does for the photon “clump” or “atom of light”. We are proposing that photons being divisible, are diffractively (by Huygens principle) spreading “classical” wave packets from the edges of the slits, immediately after which they come together and interfere in discrete directions; by blocking one of the two slits, we simply prevent the interference, and so there is no paradox any more.

The “atom” of light may correspond to the 3+1 scheme we proposed previously. The photons being push-particles in the electric field, may then require 3+1 photons to register an elementary electric force unit, like the corresponding single graviton in the gravitational field. In that case, Panarella’s light atom is an artificial one, while the single photon is by itself an “atom” of light, a push particle with an as yet structure to be specified. Our generalized field theory (See Section 30.5) seems to be consistent with a tweaked Panarella’s account for photons. Furthermore, Dirac’s notion that a photon interferes only with itself is contained in (consistent with) our proposal that a photon consists of gravitons that can interfere with themselves by being parts of the same photon.

Considerations reported by Grangier *et al.* (1986) should not affect our proposed photon divisibility, while we support a continued exploration along the lines by Prasad & Roychoudhuri (2009).

Liu (2010) and Liu (2011) have reported a direct experimental observation of the divisibility with a modified double slit experiment. However, it seems that little or no attention Liu’s work has received to date, even a negative or critical response on the validity or not of that work. It may be that it is not considered a properly reviewed paper and that the English text needed a better presentation. Nevertheless, it potentially contains important experimental findings for consideration. The interpretations of the experiment calling for direct challenge of existing theories might also contribute to apparent lack of due interest. However, a modified double slit experiment of light is presented with a spatial shape filter to manipulate the shape of cross section of the laser beam used. The laser light is directed to pass through only one or two slits, so the “which-way information” is predetermined before the photons pass through the slits.

The Principle of Complementarity is tested and the relationship of Englert–Greenberger duality verified (per Liu). It seems that the experiment shows that each photon passes both slits. In that case, the photon is divisible. Liu proposes that the photon has a “bright spot” and “extended part (EP)” around the spot. The bright spot is the observable part, while the EP part has been unknown before. “*The interaction of EP governs the motion of the bright spot in free space. Without the EP from the other slit, the interference pattern was changed to diffraction pattern magically*” according to Liu. We need more of this type of sustained experimental effort, if we desire genuine progress even in opposition to established theories of the photon.

The probability wave of QM is just an abstract way of looking at what is actually happening in reality underneath the apparent wave. The photons appear to determine in which direction (trajectory) to go immediately after they leave the double slits as soon as the interference condition is met for the first time. In other words, we should seek proof that photons exist before they interfere in the dark fringes of the spectrum on the screen, otherwise could these regions have been determined shortly behind the double slits? Again, how do we get canceling of waves in the dark fringes? The pilot wave theory (de Broglie – Bohm theory) may better apply in explaining Liu’s experiment. The “EP part” may correspond to the pilot wave that contains the “bright spot”.

30.2 Gravion modeling

Note: The below presentation raises several issues, which will be addressed in subsequent versions of the report in Section 31 under development.

We present some mechanical models of the graviton in a way to help us conceptualize an entity that initially transcends common experience. This necessitates the introduction of imaginary elements to construct what at first appears to be fictional, even in a naive manner. However, this is done with an aim to sequentially (iteratively) finally synthesize the entity of the graviton and its nature, and then its interaction with other gravitons. The endeavor is evolving.

We start our inquiry by using some imaginary materials together with conventional (classical mechanics) concepts about distance, time, velocity, mass and momentum and, initially, without regard to some findings in our preceding theory, to which we will return later. We create a mechanical model as depicted in Fig.

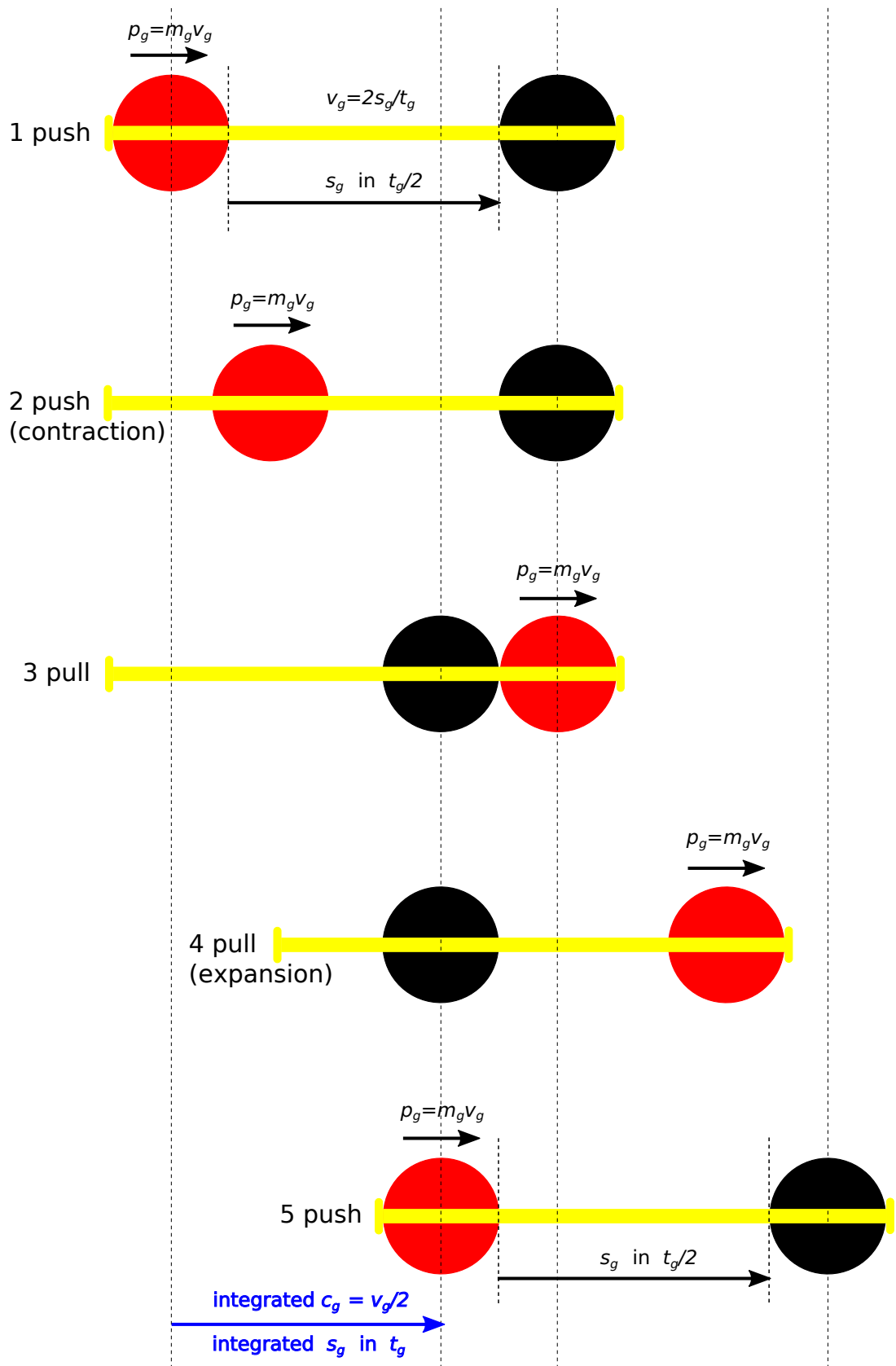


Figure 81: *Gravition model principle: Elastically colliding spheres, moving (red) with stationary (black) by sliding along a frictionless/inertia-less rod with end stoppers (yellow) in steps 1 to 5.*

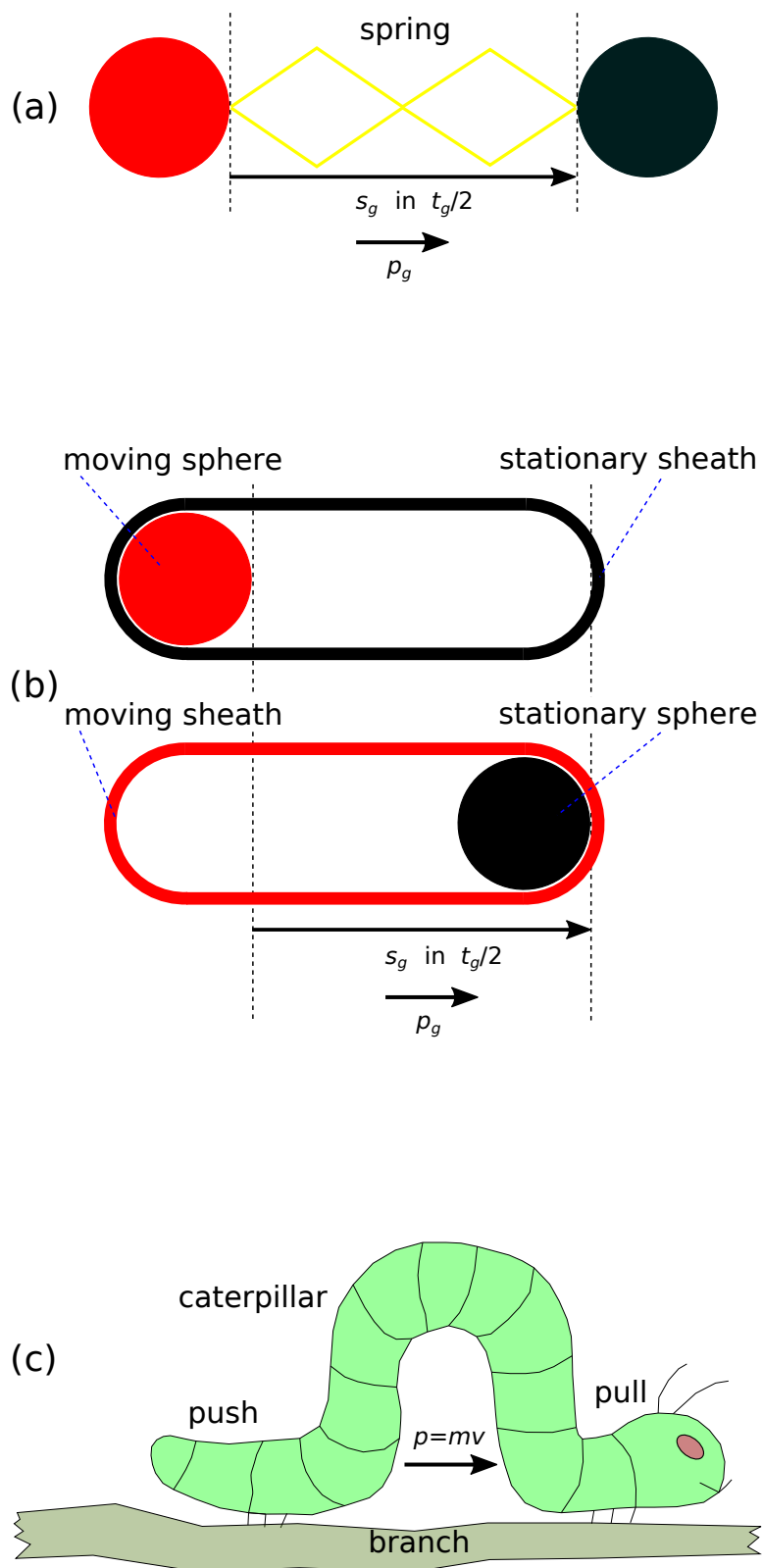


Figure 82: Gravion model - conceptualizations: Spheres with strings and caterpillar

81. It consists of two identical spheres with classical mass m_g each (i.e. without regards to the concepts of “effective”, “real” and “black” mass ushered by PG), one moving (in red) and one stationary (in black). They are made with totally elastic materials (arbitrary property), so that they exchange energy and momentum by classical considerations, when they collide. The spheres are constrained to slide along a frictionless rod (in yellow) piercing diametrically both spheres. The rod has stoppers at its ends to prevent the spheres from moving more than a distance s_g apart. Furthermore, the rod hypothetically exhibits no classical inertia, i.e. by being massless (also arbitrary property).

Having set the initial condition as above, we can follow what happens subsequently: The red sphere moves for a internal distance s_g in time $t_g/2$, i.e. with internal velocity $v_g = 2s_g/t_g$ during steps 1 and 2, after which it collides with and pushes the stationary sphere by exchanging momentum $p_g = m_g v_g$ (and velocities) as indicated by the exchange of red and black colors in step 3. After that, the now second moving sphere travels again for an equal distance s_g and time $t_g/2$ (in step 4), after which the constraining yellow rod pulls the lagging behind stationary sphere again exchanging velocities (step 5). The latter action completes a cycle of spheres movement restoring the system to its starting configuration, so that the cycle can repeat itself again indefinitely. This is a composite system with one of its halves moving while the other half being stationary. It is a push-pull system undergoing contraction between steps 1-3 and expansion between steps 3-5. The system advances with an overall (integrated) velocity $c_g = s_g/t_g$, but with a kind of a jerky stop-go motion observed from an outside reference system. Observed from inside in a reference system moving (a) with one or the other sphere at velocity v_g or 0, the observer sees the other sphere approaching, colliding and departing repeatedly with abrupt (discontinuous) reversal of direction of velocity of the other sphere and (b) with the average two-sphere system velocity $c_g = v_g/2$, the observer sees both spheres approaching each other, colliding and departing from each other simultaneously repeating the same pattern and position indefinitely. It would be unlike an ordinary (spring) oscillator with “smooth” displacement and reversal under some continuously variable force.

We have not defined the radius of the spheres, which clearly determine the magnitude of expansion/contraction via the length s_g . Should these magnitudes be needed to allow the model to yield certain outcomes compatible with experience, they are left open to work out accordingly.

Now, we recognize that ordinary experience presents no materials with exactly 100% elastic collisions and nowhere with a massless rod, so that the described model is admittedly imaginary. Moreover, the classical idea of mass has been found to be an emergent quantity described by Eq. 469. Effective mass is generated by the absorption of gravions, so that the two massive spheres inside our gravion model make so sense, if it is the gravion that creates mass. If we were to follow a similar (PG) generation of mass for those two spheres, we would require yet some other type of “push” particle at a smaller scale and repeat the same process for mass creation. However, the latter requirement would only shift the problem to yet a lower (deeper) level of the universe and so on ad infinitum. The same applies to the classical concept of energy. Therefore, our “trespass” on considering a “massless” rod and “totally elastic” material spheres by classical standards is already “forbidden” by our push gravity theory by way of inconsistency. These difficulties would have been compounded if we had used a conventional elastic spring in lieu of a stiff rod as is shown in Fig. 82(a), because that would imply a variable potential energy in the spring, for which we have no explanation either at this lowest level of the universe. A gravitational potential is generated by gravions around planets (and particles) because of absorption of gravions from a given density flux of gravions around the given body, i.e. “potential” is an after effect of PG and not a preexisting attribute of the push particle itself. If that potential is inherent in the gravion and in the spring, that would require again a lower level of push particles and so on. Then (there), fractions of energy smaller than the total energy of the gravion would be exchanged between the spring and the spheres. The latter requirement would be inconsistent with our hitherto PG theory, whereby energy is composed by the (discrete) absorption of gravions without resorting to a lesser entity within the gravion itself, unless we wish to shift the problem to deeper levels of the universe, again. In other words, the arbitrary mechanical model lays bare the cyclical problems inherent in our conventional concepts of mass and energy, potential and kinetic energy. No less, it exposes the problems we have with length and time, which we may take for granted (classically) but are presumably sorted out by the general theory of relativity (GR). We have now come to a critical point to say or do something about it with our PG theory too. As with the Standard Model (SM) and GR arriving to certain concepts with some of them being beyond ordinary experience, beyond “human” conceptions and capabilities, so with PG, we may demand the acceptance of the gravions behaving in a similar way to the way our imaginary model does. We demand that we disregard the presented internal details of it, but accept its overall external appearance and behavior, namely, as an entity existing and propagating with a momentum property continuously but discontinuously, or continuously discontinuously, as one (initial) attribute of the gravions. As another (second) attribute, we will consider what happens when two gravions interact. Before we undertake the latter step of interactions, let us reinforce the attempted description with some similar variants of the model.

Equivalent models can be constructed in different ways. For example, the rod and the second sphere can be replaced with a sheath having a mass equal to the mass of the first sphere, which is enclosed by the sheath as is shown in Fig. 82(b). The initial condition starts with a stationary sheath and the sphere moving again with internal velocity $v_g = 2s_g/t_g$, where s_g traveled before it collides with sheath in time $t_g/2$. Subsequently, the sheath travels the same distance in the same time until it pushes the stationed sphere, in order to start a new cycle of motion that continues indefinitely. This is a more realistic model that can be done provided we can eliminate friction between sphere and sheath. It could be realized and tested to a good extend in a space station. It will appear moving intermittently, like the previous push-pull system with a discontinuous-continuous motion along a straight line.

The above gravion models (in principle) could be even more crudely but lively be likened with the motion of a type of a caterpillar moving on a tree branch as shown in Fig. 82(c), or a jelly fish in water. However, these living examples require a medium, like a branch and water, to move along. The purpose of the caterpillar (or jelly-fish) is only to show that we require our gravion model to constitute one and indivisible unity as seen from an outside reference system. Like a caterpillar is an indivisible entity with a seemingly (roughly) discontinuous-continuous motion, we assign such an attribute to our principal gravion model but without an external medium as an initial attempt. Our aim is first to investigate what we may do with such an entity towards building higher levels of organization. Should that possibility be established with consistency for higher structures of hyle, we may return to investigate the inside nature of our model once more at a future stage. Since both the caterpillar and jelly-fish require an external medium to move along, we may require a QFT field for this purpose, the excitation of which is the caterpillar or jelly fish. However, we can bear this notion in mind and retract to it if only we have to resort to it later. Our representation is only to stress that a gravion is an organism behaving as it does for all external reference systems, without having to inquire about its internal workings at this stage.

30.2.1 Planck units in PG

The above is a general description of the gravion model without commitment to actual values of s_g , t_g and p_g along with accompanying components of m_g , E_g and v_g . Per preceding Section, we can start by setting $s_g = \ell_P$, $t_g = t_P$ (Planck units) and $p_g = p_{uph}$ along with accompanying components of $m_g = m_{uph}$, $E_g = E_{uph}$, $c_g = c_{ph}$ and $v_g = 2c_{ph}$.

We should note that the internal energy is equal to the external energy in the presented models. That is, if we may consider the model to be similar to a diatomic molecule with two degrees of freedom having an internal vibration and an external translation, then the equipartition of energy theorem already holds intrinsically for this system. There remains to see what happens to the rotational movement, if present, in a gas consisting of interacting gravions.

It will be useful to spell out the Planck units especially the ones to be used here: In the following analysis. it will be helpful to deal with Planck units, as they allow us to easily see and compare the relative magnitudes of the various parameters we examine. We do this by tweaking around various established designations (symbols) along with our already used symbols, in an effort to establish consistency and avoid confusion in subsequent derivations and analysis. If we alternate between various symbols, we can resort back to this summary for confirmation of what we mean. We designate the known Planck length to define the Planck unit of length as $1 P_\ell \equiv 1 \ell_P$. For example, we write for a length x that it is $x = 5 P_\ell$ to mean five Planck units of length, which converted to SI units is $x = 5 \times 1.616255 \times 10^{-35} = 8.081275 \times 10^{-35}$ m. Similarly, the unit of time is written as $1 P_t \equiv 1 t_P = 5.391247 \times 10^{-44}$ s. Hence the unit of velocity is $1 P_c = 1 \frac{P_\ell}{P_t} = c_P \equiv c = c_{ph}$ and of momentum is written as $1 P_p$, from which we obtain the derived units

of mass as $1 P_m = 1 \frac{P_p}{P_\ell/P_t} \equiv m_P = m_{uph}$. We think that momentum is a fundamental quantity, in which space, time and mass are incorporated and coexist, i.e. a gravion does not exist without exhibiting any one of these properties. Mass is only a mode of existence of the gravion and of hyle (matter). Space and time are components of spacetime in relativity, to which we add mass as to compose hyle.

Our Planck units are summarized in Table 41. The units in bold face are different from those provided (established) by Wikipedia contributors (2024f).

property	symbol	PG units symbol	SI equivalent units
Planck length	ℓ_P	1 P_ℓ	1.616255×10^{-35} m
Planck time	t_P	1 P_t	5.391247×10^{-44} s
Planck mass	$m_P = m_{uph}$	1 P_m	7.372497×10^{-51} kg
Planck velocity	$c_P = c = c_{ph}$	1 P_c	299792458 m/s
Planck momentum	$p_P = m_P c$	1 P_P	2.210219×10^{-42} kg m/s
Planck energy	$E_P = h \cdot 1\text{Hz}$	1 P_E	$6.62607015 \times 10^{-34}$ J
Planck force	$F_P = E_P / \ell_P$	1 P_F	40.996438 N
Planck acceleration	$a_P = c / t_P$	1 P_a	5.5607×10^{51} m/s ²
other		1 P	

Table 41: *Adopted Planck units for PG*

30.3 Gravion-gravion interaction

A single gravion described by Figs. 81 and 82 “moves in space” on a “straight line” as seen by an external “stationary” observer, and shown in Fig. 83(a) . We have placed words in quotes to indicate that we apply our preconceptions about the meaning of those words. One may rightly argue that all those words are arbitrary and meaningless in a universe composed by a single gravion. This is overcome by proceeding to enrich the universe with multitudes of such gravions while allowing them to interact with each other. The concept of interaction between separate entities is taken from every day experience, whereby we distinguish the pre-interaction and post-interaction state of a pair of gravions.

With reference to the given model, we are faced with various choices about the process of interaction and the “rules” that may govern this process. One case is that the moving sphere of one gravion “collides” with the stationary sphere of the other gravion. Another case is that the moving spheres from both gravions “collide”. In both cases and by strictly classical mechanics, momentum and energy transfer between individual spheres (components of gravion) would result in the modification of the momentum and energy of each gravion separately, while conserving the total energy and momentum in the system of the two interacting gravions. Furthermore, any of those collisions would generally result in a rotation of each gravion. They would generally result in a chaotic movement of tumbling and rotating and “oscillating” gravions similar to a diatomic gas in classical statistical mechanics. However, such an outcome would ruin our presumed invariability and stability of the modeled individual gravions. For this reason, we purposefully stipulate that the interaction obeys some rule that preserves the invariability of the modeled gravion. This means that the energy and linear momentum along with their internal structure are preserved. This leaves only the possibility of change of orientation of the two colliding mechanical dipoles relative to each other. The otherwise chaotic post-interaction movements will now be restricted only to circular paths for each gravion after collision. The simultaneous tumbling superimposed with push-pull gravion motion will be converted to a circular path of equal radii and opposite sense of rotation. They both move along the circumference of equal circles. An internal observer would not notice any difference before and after “collision”, while an external observer would notice only a movement along the circumference of circles with the gravion axes always tangential to the circumference. The pre-interaction linear paths as depicted in Fig. 83(a) are transformed to circular paths (c) after interaction (b). This rule generally holds for all subsequent interactions. except for “head-on” collisions resulting in linear post-collision paths. All linear paths are, of course, limiting curvilinear paths with very large radius (or very small curvature). This collision behavior is yet incomplete to be worked out by further details that will finally endow the gravion-gravion interaction “rule”.

We can describe the gravion interaction rule by surmising some quantitative relationship between the radius of the ensuing circular path and the collision angle φ as depicted in Fig. 84. For any given collision path angle, there is a component of momentum (πi) along the bisector of the angle and a component (πi) normal to it. The gravions exchange these components of momenta leading to a radius commensurate to (a function of) the longitudinal component with a curvature commensurate to (a function of) the lateral component. Thus, near-head-on and near-tail-on gravion collisions lead to high radius circular paths in opposite directions for each case. Collisions at (close to) right angles lead to the highest curvature and smallest radius. The smallest radius is taken to be $1/2 P_\ell$, whilst we have chosen an arbitrary maximum of radius in the range up to 50 orders of magnitude on a logarithmic scale. The gravion statistics determines

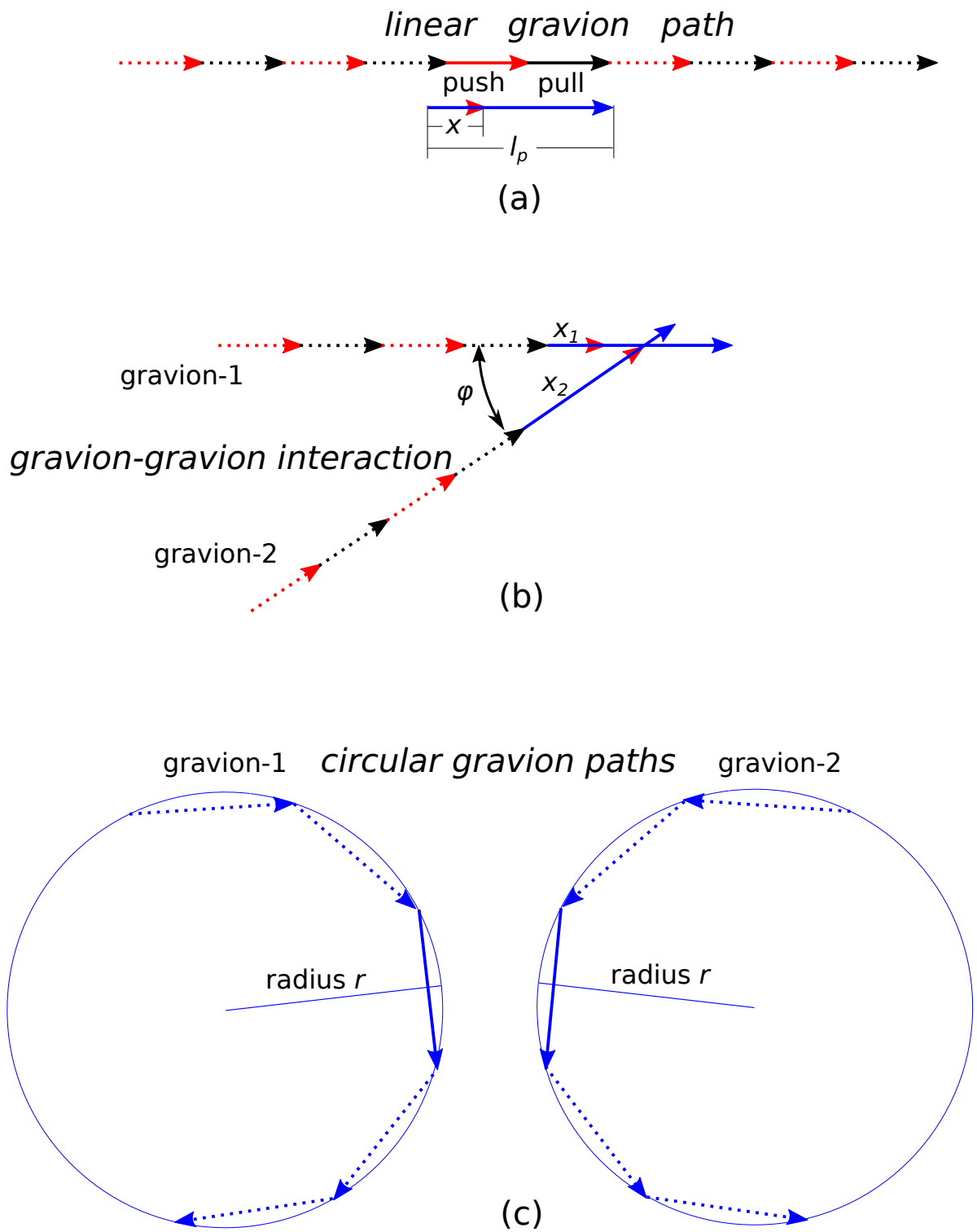


Figure 83: Gravion-gravon interaction: (a) linear path, (b) gravon collision with angle φ and (c) resulting circular paths in opposite directions.

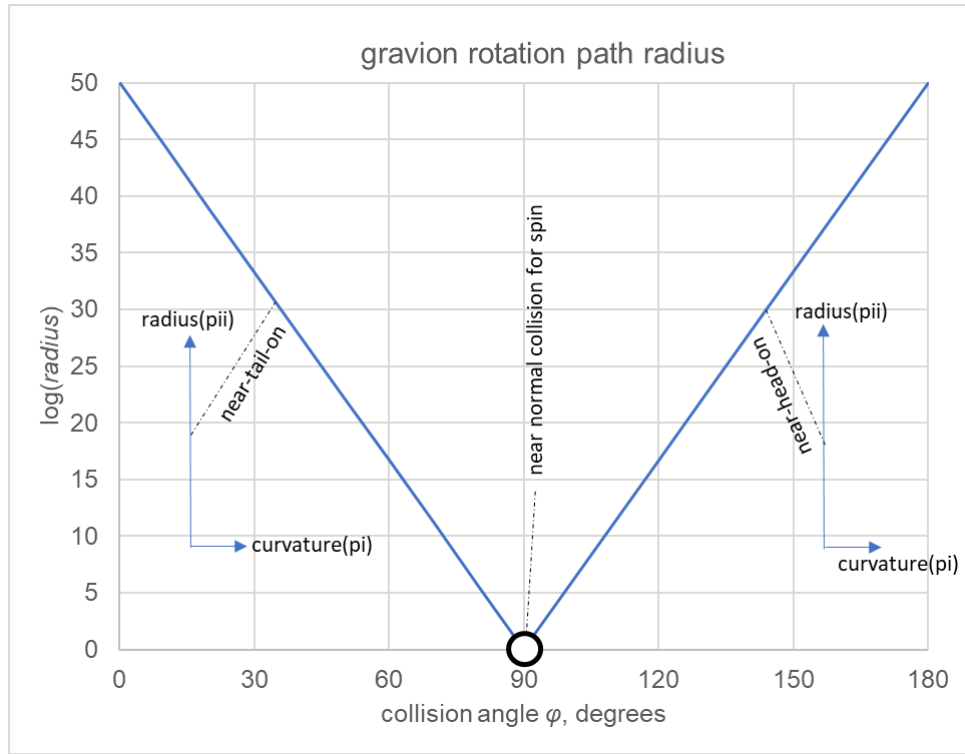


Figure 84: Gravion circular path radius r vs. collision angle φ

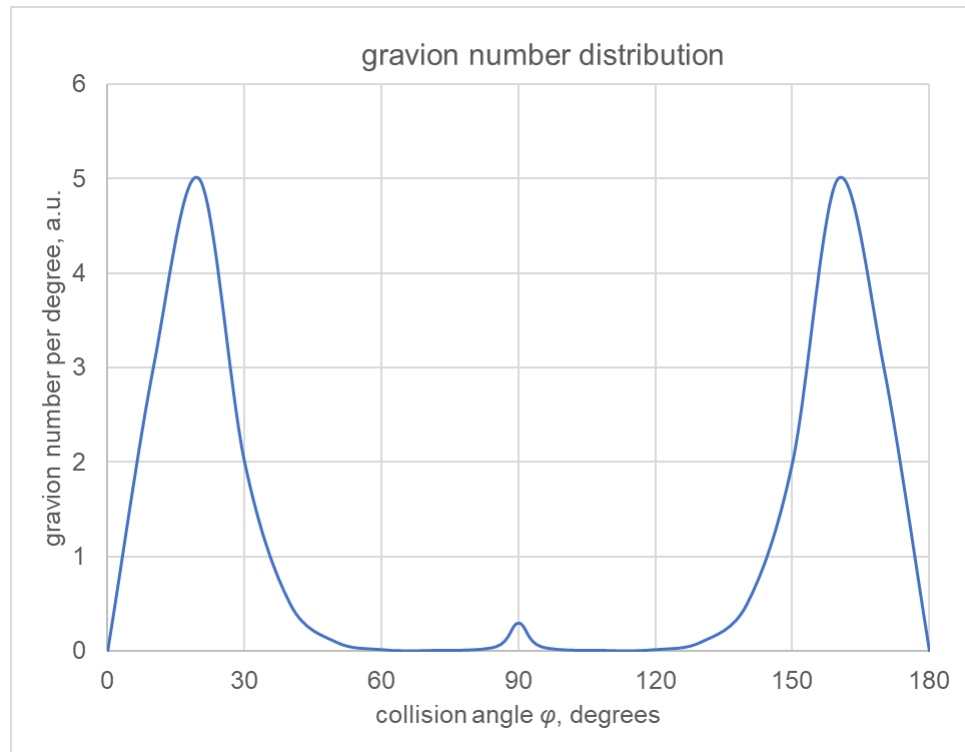


Figure 85: Gravion number/radius distribution in arbitrary units post collision over collision angle: An arbitrary gravion distribution for discussion purposes to be adjusted as needed.

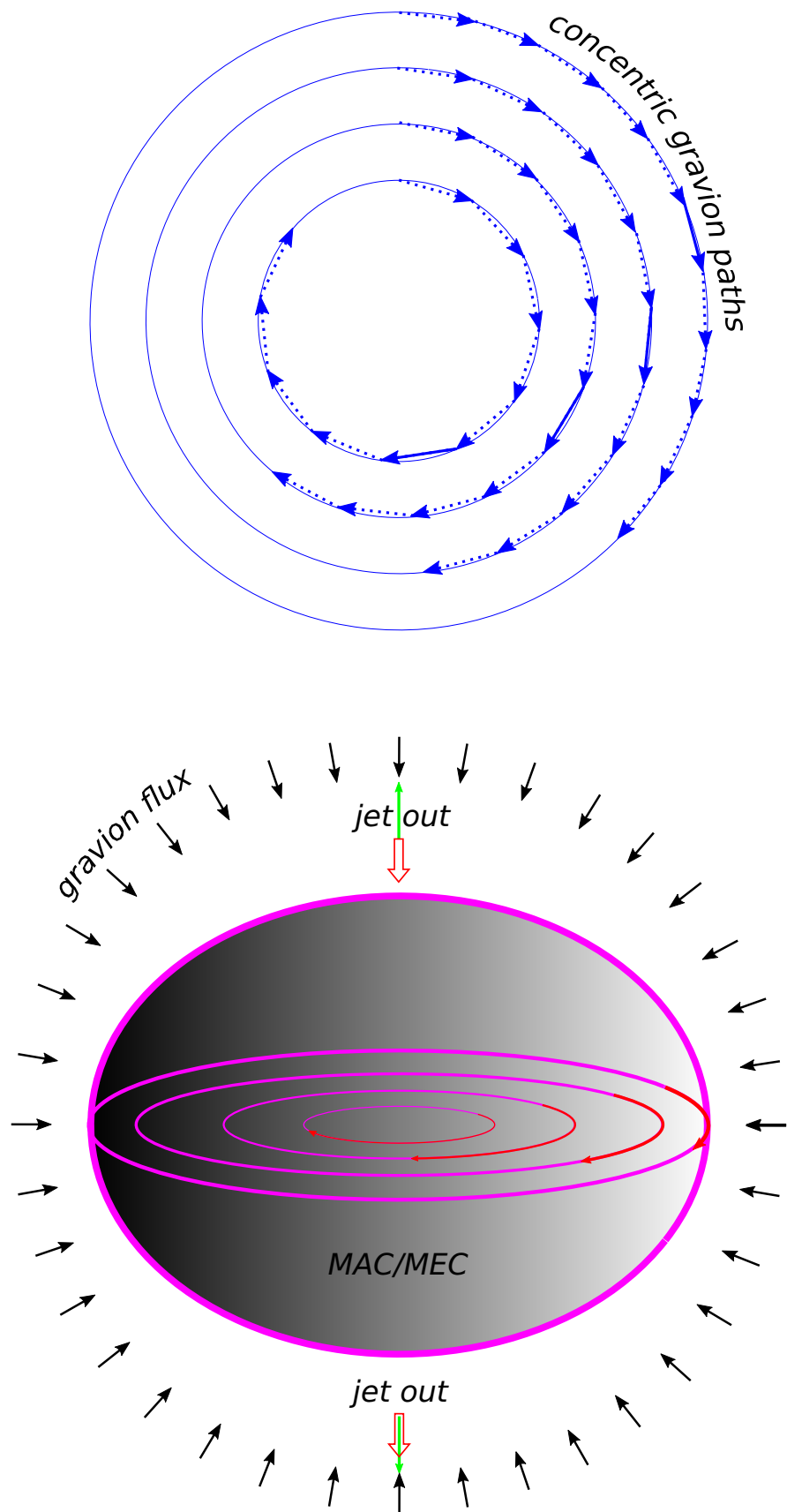


Figure 86: *MAC/MEC formation*

the distribution of mean free paths and radii (or curvatures) at corresponding densities of hyle throughout the universe.

We may paraphrase the above description of gravion interaction only to consolidate the concept of the proposed rule: The gravions behave internally always the same, namely, they continue moving along the line of their connecting rod simultaneously as the said rod rotates around along the circumference of a circle. The latter compels us to think that we do not need to (or should not yet) investigate the internal details “during” the gravion-gravion interaction, except to impose the said rule that preserves the integrity of each gravion after each interaction. Each gravion is invariant for an internal observer who is oblivious about its external trajectory. Trajectory is perceived only by an external observer who notices generally circular paths. In other words, each gravion follows the push-pull pattern except not on a straight line any more but on the circumference of a circle defining equal length chords on the said circumference. By prejudice and symmetry, we make the rule to say that the two gravions move on circles of equal radius and opposite direction of rotation, after the interaction. By such means, we do not violate classical conservation of momentum for the whole of each gravion (as an integral entity) in readiness to build higher level of organization and in consistency with human observations.

The above rule may be endowed with further attributes to obtain consistency with anticipated quantum mechanics. The gravion itself is a sub-quantum-mechanical entity defining a quantized path. We may then impose the condition that the length of the circumference of a circular path be an integral multiple of the gravion arc length subtended by the length of the gravion (as arc chord). If we take the length of the gravion to be ℓ_P , then the smallest circumference would be $\pi\ell_P$ with the gravion flipping back and forth along the diameter of the circle, or spinning by discrete π radians. The next “allowed” circular path contains 3 gravion chords with a quantized rotational angle of $2\pi/3$ radians, the next with an angle of $\pi/2$ radians and so on. In general, the rotational angle may be quantized. At the same time, with fixed linear speed, a gravion completes a rotation with faster time at smaller radius, reaching extraordinary angular velocities (oscillation like motion) at unitary diameter ($1 P_\ell$). The provision of such or other details to the interaction rule is discussed now provisionally subject to the needs of later building of higher hyle structures. Accordingly, we may endow additional “sub-rules” whereby the function (relation) of radius may depend not only on the collision angle φ but also on the relative position of the impact point along the length of each gravion, all this pending an investigation of the outcomes starting with the simplest of rules; the impact point is shown at x distance in Fig. 83(a) and being x_1 and x_2 during collision of gravion-1 and gravion-2, but we may not need to know this detail (actual or not) until and unless it is required for building known particles.

It would be interesting to set up a computer simulation of gravion interactions based on the above set of rules to find out the statistical outcomes in a gravion gas, like formation and dissolution of patterns of gravion concentrations. In particular, the scheme in Fig. 82(b) is amenable to computer simulation, as it might be also to an experimental investigation in a space station.

The main thrust of the gravion-gravion interaction is that circular paths are spontaneously created without the need of a centripetal force being present. There is no force field present at the gravion level. Motion and patterns of motion in a large population of gravions are determined by the inherent properties of the gravions themselves. If we can achieve circular motion this way, we have made a big leap towards building all higher forms of hyle, which is then the subsequent task of PG.

The formation of circular paths is accompanied by a rotation of the gravion around a midpoint of the dipole vector of the gravion. This represents a certain amount of energy, which must be provided from somewhere. If the energy of the gravion is invariant, then no energy can be converted to rotational energy, and circular motion would be impossible. This issue is addressed next.

First, we deal with the energy of the rotational motion of the gravion with a relatively large radius r in Planck units. Applying classical mechanics, the energy of rotation E_{rot} is

$$E_{rot} = m_g \omega^2 r^2 = m_g c^2 = E_g = 1 P_E \quad (504)$$

where ω is the angular velocity of the gravion moving on the circumference of circle with radius r . The angular velocity ω becomes equal to the spinning angular velocity of the gravion rotating (spinning) around its length mid-point with radius $\ell_P/2$ ($=1/2 P_\ell$) with a spinning energy E_{spin} given by

$$E_{spin} = m_g \omega^2 (\ell_P/2)^2$$

The ratio of the two energies is

$$\frac{E_{spin}}{E_{rot}} = \frac{\ell_P^2}{4r^2}$$

If the rotation radius r is of the order of known particle sizes, such as neutrons, a numerical outcome of the above ratio yields extraordinary values. We can see this with some numerical examples. Let's take

the neutron radius of 8×10^{-16} m to be the radius r of the rotation circle of the gravion. In Planck units, this is $r = 8 \times 10^{-16} / 1.616255 \times 10^{-35} = 4.9497 \times 10^{19} P_\ell$, which gives for the above energy ratio a value of 1.02×10^{-40} , which is an exceedingly small fraction of the unitary gravion energy.

According to a tentative electron radius value of $\times 10^{-23}$ m (see Section 21.1.2), it becomes $r = 10^{-23} / (1.616255 \times 10^{-35}) = 6.187142 \times 10^{11} P_\ell$ (Planck units). The above ratio of energies for this electron radius becomes 6.53×10^{-25} , which is still an extremely low value. There is a lot of range left to reduce the rotation radius for other particles (entities), say, down to $r \sim \times 10^2 P_\ell$ yielding an energy ratio of $\sim 0.25 \times 10^{-4}$. For example, structures like MAC/MEC can be that small and still have a negligible amount of spin energy for possible circulating gravions in these structures.

The question remains about how to account for the gravion spin energy, if the gravion cannot share its own energy (being invariant). For the greatest range of possible rotational radii, we might resign with the “fact” that the extremely low fraction of energy required can be allowed for the largest range of collision angles corresponding to sufficiently large radii. In other words, the gravion-gravion interaction results in a very slight nudging of the gravion vector starting to rotate at an extremely low rate thus forcing the gravion to continue its near “translational” motion around the circumference of a relatively large circle.

Nevertheless, the above leaves a remaining small range of the shortest radii not allowed for the proposed rotation at all. The alternative option for this is to allow conversion of all the translational energy to local spin energy, so that both gravions oscillate-and-spin only, without translation. This amounts to only two degrees of freedom between spin and rotation with equal energy each. Prior to collision we had also two degrees of freedom, namely, translation and “oscillation” with equal energy each. In other words, at near normal collisions, both gravions spin around the mid-point of their vector, actually flipping back-and-forth between 0 and 180 degrees in a simultaneous “oscillation” and spin. In the final analysis, the gravion gas intrinsically creates (or obeys) the equipartition theorem, but with only two degrees of freedom in two separate classes (groups) of gravions: One class is characterized with curvilinear motion containing “oscillation” + translation and the other class with rotational motion containing spin + oscillation superimposed; both classes are characterized by an invariant gravion energy being equal to $1 P_E$.

To reconcile the above requirements, we may combine them in a special distribution law of the number of gravions per degree of angle (or per rotation radius) at a given collision as qualitatively depicted by the distribution graph in Fig. 85. This graph should be read in conjunction with the previous one in Fig. 84 establishing the corresponding number of gravions with a given radius, so that the distribution of gravions over gravion radius is qualitatively represented by the same graph. For a relatively wide range from just below 90° and from just above 90° collision angle, there should be only scarce occurrences of resulting radii, if any, but with two maxima, namely, one far away from normal incidence angle and another close-and-around 90° . The relative intensities of the two maxima and the actual distribution graph is left for future investigation in order to obtain consistency with existing experimental data. It may be that the occurrence of spinning (flipping back-and-forth) gravions by far outweighs the population of gravions with large radii, i.e. contrary to the peaks shown in the graphical example. This is connected with the **energy** cosmological constant. We discussed the **energy** cosmological constant by Eqs. 345 and 346 in Section 21.4, but we need a more developed theory to proceed on this.

The total angular momentum before and after interaction is zero, meaning that the two gravions rotate and spin in opposite directions.

Should the interaction rule described (qualitatively) by Figs. 84 and 85 be valid, we would have obtained some fundamental ground for building all sorts of higher structures.

30.3.1 Synthesis

We summarize the status of the attempt to model the gravion. We have used our macroscopic experience in attributing various properties to the gravion. These properties are momentum, energy, distance, time, mass and velocity. We lump them in four properties, namely, time rate of energy (W), time rate of distance (c), acceleration (g_0) and mass (m) in our fundamental PG equation

$$W = 4cg_0m$$

This equation is more fundamental (general) than $E = mc^2$, as we have already presented. It applies in an external reference frame on an assembly of interacting gravions. We have elaborated how force and acceleration emerge from gravion absorption and gravion momentum transfer from the outset of PG. These properties lose meaning from inside a single gravion. Externally, we perceive a concept of energy, which we may identify with the number of gravions taking part in a particular external process. Likewise, velocity, acceleration and mass are external attributes, all of which are inter-dependent via a common denominator, namely, the gravion. Gravion is what it is. From what it is, we experience all its external behavior. This is

a philosophical issue to bear in mind, while we endeavor to use it successfully in building up the universe. Our approach should be dialectic, a back-and-forth process.

Therefore, the qualitative graphs in Figs. 84 and 85 need not have a justification based on the classical mechanics of our experience. They can be both qualitatively and quantitatively what they have to be in order to explain all higher level structures. In lieu of starting with a set of “fundamental” particles (Standard Model), we propose to start with a single fundamental “particle” (entity) endowed with a set of fundamental properties such that all other particles, bodies or entities are emergent but all having the common denominator of the single fundamental particle. Only then we can explain, for example, the proton-electron mass ratio, and so on.

Hence, all criticisms about our model are welcome on condition that better ideas can be offered to achieve the above goal in the framework of PG.

30.4 Gravion absorption/desorption and hyle organization

The gravion-gravion interaction resulting in circular and spin motion is a critical qualitative advance for the theory of PG. The circular trajectories and spin can be fundamental in the organization of the universe. In Section 25, we needed the existence of circular motion to construct a model of the electron/positron along with the minimum absorption and emission centers (MAC and MEC) long speculated from the outset and throughout this work. The possibility of circular gravion motion was attributed to a rare but possible chance event maintained by some continual tangential collision, whereas this is now based on a fundamental property of gravions in a most frequent occurrence. The latter provides a more plausible hypothesis on which to evolve our PG theory. Circular motion is now the rule when the said interaction occurs. This does not negate our #1 principle of PG requiring the existence of sufficiently long mean free paths in the gravion-gravion interactions. The existence of a fraction of gravions in the universe fulfilling this condition continues to apply. This is not inconsistent with the simultaneous presence of relatively dense structures composed of gravions organized by circular motion. In fact, this is needed for the long mean free path gravions to be absorbed by some dense and stable structures distributed over and composing ordinary bodies acted upon by gravitational forces, i.e by long mfp gravions.

Structures with circular motion are common throughout the universe. Apart from long scale circular motion of planetary systems and galaxies, corresponding micro-structures have been widely reported. As mentioned before, this is supported in the reports by *Klaus et al. (2022)*, *Donnelly (1991)*, *Pines & Alpar (1985)*, *Gallemí et al. (2020)* and *Lagoudakis et al. (2008)*. These reports are consistent with our assumption that gravions can also be organized to form the required structures in modeling the electron and positron. Those structures require circular motion. We require some minimum organization of gravions to form the basic (stable) MAC/MEC, which we have redrawn from Section 25 in Fig. 86. The absorbing-and-emitting centers are presumably rotating-and-spinning structures (spherical or ellipsoid). Gravions uniformly impinging from all directions on a MAC are absorbed by being re-ordered and entrained into the circular motions of the system and gradually transferred from the outer layers towards the inner layers. As they approach the axis of the rotating system, they may form helical toroidal vortices exiting the MEC from and near its poles. Internal gravion collisions in a MAC would tend to randomize, while gravitational pressure might tend to re-order the overall structure by pressing towards the axis. While the exact operating mechanism of internal organization of a MAC/MEC remains unknown and any description is for now speculative or even naive, we hope that similar mechanisms operating in the given reports provide a good basis for further thinking.

Consideration of stable vortex structures self-forming from “dipolar” (vector) gravions frees us from the requirement of the push principle to operate at the smallest scale of such structures, i.e. these structures to be formed only by push particle action. Otherwise, that requirement would occur ad infinitum leading to an impasse in PG theory. Our gravion model might be sufficient by way of generating the primary (fundamental) circular paths presumably necessary for building vortices and higher structures. Thus, we may assume that a MAC/MEC is a minimal self-sustained structure (let’s call it “particle”, too, for convenience) that occasionally absorbs gravions on account of its relative size to the surrounding gravion density. The absorbed gravion interacts with the structured internal gravions of the particle per assigned interaction rule, but it is overall overcome and entrained by the particle via a combined pressure force and vortex stability mechanism. The absorbed gravions reach a steady-state by simultaneously exiting in organized clusters from the polar regions of the particle.

Now, it is important to note that the absorption of gravions by a rotating/spinning MAC constitutes a purely elastic event as seen from within the MAC. It is only a gravion-gravion interaction within the MAC. It is a re-orientation of a linear (or near linear) external motion to a short range circular internal motion of a required curvature. An outside observer sees a pure absorption of gravions. The outside observer sees also an emission of different type of particles, much bulkier like the helical toroidal vortices emanating from the poles (or thereby) of the MEC. The MAC operates simultaneously as MEC. The differentiation between

MAC and MEC as described by the model satisfies the requirements for gravity generation, as they are truly absorbed from all directions transferring their momentum to the structure. The emission of other type of particles does not outdo the gravity effect, as they only create the basis of another higher level force field, namely, the envisaged (or other) electric field. Needles to say that there may be some continuous distribution of the exiting particles from the poles towards the equator, which could result in a oblate spheroid shape of the particle. These and other details and possibilities are left for future work, while they are mentioned only tentatively and are not binding on the theory of PG, in general.

We should point out that the terms elastic and inelastic are used with their conventional meaning. A particle is said to be elastically scattered by a body when the same particle emerges out of the body without any loss of energy, whereby “body” can be a star, planet, atom, nucleus or sub-nucleus entity. When this particle emerges out with some loss of energy, it has undergone an inelastic interaction (collision). When an inelastic scattering has taken place, the missing energy is taken up by the body at some level of its organization. If the energy is taken up at the atomic or molecular level, then it appears as heat in the body with a concomitant increase of temperature. We have claimed that the gravions are absorbed at sub-atomic levels of organization, whereby the energy is decoupled from the thermal energy level of the body. The deposited energy reaches a steady-state at sub-atomic level as it is eventually re-emitted in some other form of particles. Having now introduced the idea that the gravion is invariant, including the non-absorption of “energy” or hyle in any form, we have necessarily reached an absolutely elastic level of the universe. The theoretical possibility also exists that a gravion can create gravity by elastic scattering out of a given body on condition of anisotropic scattering per Lahres (2023a), or better by 180° back-scattering. In any case, classical energy would be fractioned and parted within any given gravion, if it ever underwent inelastic collisions, but this possibility has been excluded. By this realization, we can say that the universe as a whole is ultimately, or fundamentally, “elastic”. “Inelastic” processes concern only the above gravion organized structures, where “absorption” is possible and relative. The universe eventually “bottoms out” at the gravion level. It re-bounces without any loss of/for anything. Hence, we need to reappraise the concepts of energy and mass, elasticity and friction. The universe is overall (ultimately) frictionless. It is in perpetual motion and there is nothing strange about it. Strange appear now some misconceptions that we need to revise.

One such misconception, as already pointed out elsewhere, is that of mass. We learn very early in physics courses that “mass is conserved”, where mass is loosely understood and mostly thought to be “an amount of matter or substance” (“mass” being a misnomer). We have now come to learn that it is hyle with its momentum that is conserved (see Section 24.2 and Eq. 459), whereby hyle is not a mere word replacement for mass. Hyle and mass are entirely different entities with different equations and relationships. Energy goes along the same way. We may now understand that $E = m_{\text{classical}}c_{ph}^2$ should mean $E = m_e c_{ph}^2$, which, in turn, raises the question what might be meant by $E = m_{\text{real}}c_{ph}^2$, or perhaps $E = m_{\text{real}}c_g^2$. All this leads to thinking that the primary conservation in the universe is that of gravions, or better stated, of the moving (flowing) hyle.

It is generally accepted that mass and matter (hyle) are different things, but we often subconsciously identify mass with matter, so that when we find via PG that two objects lose mass as they approach each other, it is considered unacceptable (intrinsic mass being invariant). Our understanding of mass is that it is a measure of the rate of energy (i.e. power) absorption at a steady state, which varies with variation of distance between objects. In fact, not only mass varies but also matter (hyle) varies, which appears as emission or absorption by each body as they transit from one steady state to another steady state. The emission/absorption of photons by electrons changing orbitals is the same phenomenon. Electricity and gravity are both force fields differing only quantitatively by many orders of magnitude in strength and resulting in measurable radiation in electricity but not in gravity. The mass of a free electron has been measured to be 9.1×10^{-31} kg, which is many orders of magnitude greater than the mass of emitted/absorbed photons: A photon mass, at $\nu \approx 10^{15}$ Hz, is $m_{ph} = h\nu/c_{ph}^2 = 6.62607015 \times 10^{-34} \times 10^{15}/(3 \times 10^8)^2 = 7.36 \times 10^{-36}$ kg, i.e. 5 orders of magnitude less, so that a variation of mass in the electron is plausible to occur in its bound states, where its mass is not directly measurable (presumably); like in gravity, a “lone” (free) electron is not the same as the bound electron. The effective masses of two macroscopic bodies decreases with distance (albeit not measurable), but the effective electrical masses between a proton and an electron also decrease but by a measurable amount being the emitted photon. This is more pronounced and directly measurable at the nucleus level, which is known as the “mass effect”: The mass of a nucleus is less than the sum total of the individual masses of the protons and neutrons.

In applying the above ideas, let us consider some numerical examples. We note that the circumference length of neutron is $2\pi r = 3.11 \times 10^{20} P_\ell$. A sequence of gravions that long corresponds to the order of magnitude of frequencies of gamma rays emitted out of nucleus.

For the said electron $2\pi r = 3.887 \times 10^{12} P_\ell$, the corresponding gravion sequence length provides low

frequencies beyond the infrared limit. The mid-range visible light frequency is around 6×10^{14} Hz. If the latter is the length of a photon (gravion) sequence (in Planck units) enveloping the electron, then the radius to it should be $6 \times 10^{14} / 2\pi = 9.55 \times 10^{13} P_\ell$, which in SI units yields 1.543×10^{-21} m. The values of the electron radius were tentative, so that this one here is plausible, and the method used could provide reverse engineering for the determination of the size and structure of the electron.

The as yet unexplained fixed proton/electron mass ratio is indicative that they both should have a structure with multiple sub-units common to both. When we can construct the proton and the electron out of gravions, then we should also be able to derive this ratio.

All above numerical examples are indicative only to spur us forward for more detailed investigation of hyle structures. If our approach could explain the emission of photons by nucleons and electrons, we might use similar methods to build all the known particles and their properties. However, this task would require the greater contribution by the scientific community in particle physics and elsewhere.

30.5 Field unification - General

Based on the preceding analysis, we can now attempt to summarize all those ideas in a general form of interconnecting various force fields. If each photon $h\nu$ acts as a push particle in a corresponding field with maximum acceleration $g_{0\nu}$, the corresponding power-mass equation would be

$$W = \frac{dE}{dt} = c_{ph} g_{0\nu} M_{\nu e} \quad (505)$$

where now $c = c_{ph}$ and $M_{\nu e}$ is the corresponding field mass type (like electrical, etc.). For a single photon (push particle) the above becomes

$$\frac{dE}{dt} = \frac{h\nu}{t_{h\nu}} = c_{ph} g_{0\nu} M_{h\nu e} \quad (506)$$

where $t_{h\nu}$ is the time interval of the energy $E_{h\nu} = h\nu$ being transmitted (absorbed) and $M_{h\nu e}$ is the per photon effective mass generated in that field denoted by the subscript ν . The latter mass is a multiple $[\nu]$ of the gravion mass M_{eg} created by each gravion contained in the photon:

$$M_{h\nu e} = [\nu] M_{eg}$$

where $[\nu]$ is a pure (dimensionless) number defined by

$$[\nu] \equiv \frac{\nu}{1\text{Hz}}$$

For the photon energy, we can also write in terms of gravion energy:

$$h\nu = E_{h\nu} = [\nu] E_g$$

Having proposed in Section 30.1 that all photons can act as push particles at correspondingly stronger force fields, Eq. 506 essentially becomes the single photon power-mass equation, which is connected with the gravitational field via the gravion generated effective mass as:

$$\frac{h\nu}{t_{h\nu}} = c_{ph} g_{0\nu} M_{h\nu e} = c g_{0\nu} [\nu] M_{eg} \quad (507)$$

For a macroscopic body, the given field mass generated is denoted with $M_{\nu e}$ in Eq. 505 and is a multiple of $M_{eh\nu}$ in proportion to the power W .

As an example of a “stronger” field being the electric field, we can replace the above symbols for acceleration and effective electric mass with those used in Section 21.1. Thus, with the electron being the absorbing body, we would write for its effective electrical mass $M_{\nu e} \equiv m_{2e-e}$ for consistency of terms with Section 21.1. Of course, there we proposed the electrion as being the push particle for the electric field, in particular, and not a plain $h\nu$ photon. Still, the electrion is also composed by a special configuration of $[\nu]$ gravions, so that the PG power-mass equation can be applied as above. Therefore, this is the way forward, from where we left off the initiation of push electricity (PE) theory in Section 21.

Likewise, we can continue, from where we left off the attempt to unify gravitational with electric field in Section 21.3 together with the nuclear fields in Section 21.3.1. By such means, we can derive the long awaited grand field unification theory in a quantitative way.

In preceding versions of this report, we used the notation $g_{01} \equiv g_0$ for gravitational field, g_{02} for electric field, g_{03} for nuclear or other field and so on. Now, the subscript ν in $g_{0\nu}$ denotes the maximum acceleration created by a given density of $h\nu$ photons with $mfp = \lambda$. It should be appreciated that some inconsistency

of notation and symbols has been unavoidable due to novel developments that were not anticipated, when early notations were introduced. This will be sorted out in a final review of this report.

Here, ν is a relatively large number with many orders of magnitude. We have to determine the range of corresponding wavelengths (mfp) from a minimum value λ_{min} to a maximum value λ_{max} , all of which contribute to the generation of a given field. Correspondingly, there is a range of frequencies from a maximum value ν_{max} to a minimum value ν_{min} , all of which contribute to the generation of the same field. In principle, the integration of curves by Eqs. 503 and 502 in Figs. 79(bottom) and 80(bottom) and in the said ranges would provide the total number density $n_{0\nu}$ (or $n_{0\lambda}$) of ~~gravions~~ photons for the given field now indexed with subscript 0ν or 0λ . We formalize this as:

$$n_{0\nu} = \int_{\nu_{min}}^{\nu_{max}} n_{ph\nu}(\nu, T) d\nu = n_{0\lambda} = \int_{\lambda_{min}}^{\lambda_{max}} n_{ph\lambda}(\lambda, T) d\lambda$$

In practice, this may not be possible for all fields to derive from the existing Planck law curves, like the gravitational field as mentioned before. In fact, it may not be possible for any field, unless we can ascertain that Planck's law accounts for all push particles for a given field. In any case, we can continue with formalizing some immediate governing equations: The total number density $n_{0\nu}$ relates to the energy density by $u_{0\nu} = n_{0\nu} \langle E_{h\nu} \rangle$, where $\langle E_{h\nu} \rangle$ is the average photon energy $h\nu$ in the above range of integration. We derive the energy flux density (intensity) by

$$J_{0\nu} = \frac{c}{4\pi} u_{0\nu}$$

From the flux density and using Eq. 87, we derive the maximum acceleration first for a gravitational field by:

$$\begin{aligned} g_0 &= \frac{\pi J_0}{c} \Lambda = \frac{\pi^2 J_0}{c g_0} G \\ g_0^2 &= \frac{\pi^2 J_0}{c} G = \frac{\pi}{4} u_0 G \\ g_0 &= \frac{1}{2} \sqrt{\pi G u_0} = \frac{1}{2} \sqrt{\pi G n_0 E_g} \end{aligned} \quad (508)$$

Then, the corresponding generalized equation for a field indexed as $g_{0\nu}$ is:

$$g_{0\nu} = \frac{1}{2} \sqrt{\pi G_\nu n_{0\nu} \langle E_{h\nu} \rangle} = \frac{1}{2} \sqrt{\pi G_\nu n_{0\nu} [\nu] E_g} \quad (509)$$

to be used in the corresponding power-mass equation for the given field. An example of $G_\nu \equiv G_2$ has been trialed for the electric field in Section 21.1.2. Finally, we can re-write the power-mass equation using the notation with the integrated total number density/energy of push particles for a given field as:

$$W = \frac{dE}{dt} = c g_{0\nu} M_{\nu e} \quad (510)$$

We have tentatively used some numerical values in the above equation and arrived at some important results to be discussed during later reporting. The matters raised relate to the **energy** cosmological constant and cosmology in general. This is a major topic that cannot be sensibly touched upon here and now.

Following the above procedures, we can work out all higher fields above the gravitational one, all of which are based on the common denominator graviton. In the process, we might establish that there are more types of force field including a gradation of fields not yet envisaged by current theories of hyle structure. That is, the integration ranges yielding the $n_{0\nu}$ (or $n_{0\lambda}$) can be adjusted accordingly: In that case, we might have to reconsider and re-appraise even the atomic structure and much more. For example, the electrical mass of the electron (tentatively, equated numerically with "charge") may concern only the free electron, whereas the bound electron could have a variable electrical mass. Similarly with hadrons, which are presumably measured in a free state, while we know that they have a deficit of mass in the bound state. The new understanding is that the hadrons variant mass is intimately implicated with the hadrons structure, which we propose now to relate and unify across various particles with a common denominator being the graviton.

However, the above work requires the contribution by workers from all relevant fields holding all the relevant experimental data. All this data should be mapped out in the framework according to the push particle principles of the series of this report.

In short, it seems that we have in principle worked out the road map for a unification of all force fields. We have derived the most general fundamental quantitative relationships needed with further detailing by continuing work.

It is said that the gluons are carriers of the strong force binding quarks together to form composite particles like protons, neutrons and electrons. The bosons are carriers of the weak force. The photon is the force carrier of the electromagnetic field. According to PG, it may be that the gravion is the carrier of the force in gravity. Gluons, bosons and photons may be formations of gravions, each class acting as push particles in their corresponding fields.

Can a photon be split into two virtual components that can readily be recombined to a photon like the original one? This may occur in the double slit experiment and in half silvered mirrors. A photon could temporarily dissociate in two “virtual” components that recombine behind the slit without violating the rules for spin, and that applies for other particles like electrons, atoms and molecules, with transient splitting and superposition at the sub-photon level of their structures.

In the end, we may find that a photon is not an elementary particle (with no further division) and is not a particle of the fundamental force, because electromagnetic force is not fundamental; we have proposed that this force is a higher order gravitational like force (see Section 21).

The above presentation raises several issues, which are worked out and will be presented in subsequent versions of the report in Section 31 under development.

30.6 Interim remarks

We have made the point that investigating deeper into the gravion itself may only lead to shifting the original cosmological problem. Should the provided attributes of gravions be compatible with (i.e. produce) the higher known levels of organization of the universe observed by humans, it would be a great advance towards the long awaited unification theory of the cosmos. The inner workings of the gravion itself could be deferred for later work, while the bulk of the science would have entered on a new productive path. We may overcome the fictional parts of the gravion models if the overall gravion attributes may be sufficient to explain all the higher level structures. Our approach is teleological, namely, we assign such properties or attributes to gravions for a particular purpose, i.e. for producing known particle and bodies at higher levels in the universe.

By logical deduction, we have arrived at a fundamental unit of time and a unit of distance yielding the unit of velocity and momentum as attributes of the unit of hyle, which is the gravion. By allowing gravion-gravion interactions governed by a given set of rules, we arrive at 2D and 3D dimensional space structures that can be measured in the fundamental units of hyle. Gravions are organized in higher level stable units for whatever reasons to be established as we advance our PG theory.

From the very first version of this work in Section 18, we proposed that the maximum force field in white dwarfs, neutron stars and black holes was determined by corresponding different types of push particles leading to the highest order of magnitude for black holes. We have further allowed the possibility that g_0 is itself of the highest intensity required in the universe for black holes having the highest absorptivity; the relatively very low values of g measured for planets and stars may be only due to their very low density, with intermediate values of white dwarfs and neutron stars. Therefore, this is an open question for PG to make a determination on how to go about the distribution of hyle given now the possibility that MACS/MECS may constitute the densest units already distributed throughout the universe. The different types of push particles for electric and other fields can still apply, but their range and intensity interplay with the distribution of hyle in the cosmos. We had rather hoped that g_0 has the lowest value that would be accessible to our measuring instruments, but nature is not based on human wishes or preferences. This serves yet as another reminder for the urgency of conducting the appropriate tests, but now also of the tenacity required in pursuing this theory to its logical conclusions, even if the tests initially fail to show positive outcomes in gravity measurements.

Vortices make sense as auto-existing systems in the cosmos at its smallest scale; PG takes over above those minimal levels in the “intermediary” scales (say, inside galaxies), while cosmic weather predominates at the highest scales. Whereas Papathanasiou & Papathanasiou (2020) propose the “cyclone” model of the universe at all scales, we propose that rotational motion is prevalent at the smallest scale, whilst it is the push particle fields that take over at the higher scales, in fact, both processes coexisting at all scales but with an inverse kind quantitative relationship. There is nothing strange with self-organizing vortex type structures, as are already reported to exist at very low temperatures. Superfluidity/superconductance are now commonly accepted modes of existence of nature. MAC/MEC structures need not be much different and hence no more strange than some experimental realities. If we have difficulty in comprehending them because they surpass ordinary experience, they should not be less acceptable for PG purposes than a similar situation already arising for the Standard Model and GR theories.

Given the novel outlook of mass and energy provided by PG, the classical objection that “planets would melt down in a short time” by the required gravion absorption seems to become redundant and of no further

concern. The other “main” objection of the “drag problem on planets” that would allegedly be caused by the random movement of the gravion “corpuscles” was in a way incorporated in possible equations relating absorptivity with velocity in Section 23. A similar drag has been referred to in the literature as “radiation friction” in consequence of light pressure, which opposes the movement of matter. The forces of light pressure exerted on the two sides of a moving body would be unequal as more radiation will be reflected on the surface at the front of the motion than on the back surface. This problem for photons and presumably for gravions may be explained by the new considerations of circular gravion motion as follows:

The drag on planets, not slowing them down, may be explained by an assumed concomitant circular motion of gravions with enough intensity to compensate for the unwanted drag. Since we now readily anticipate that circular motion of gravions is commonplace in the universe, and since they can obtain all possible radii, circulating gravions around stars could be present. Circular gravion motion accompanying the orbit of planets may have been established since primordial times during formation of planets and stars. The orbital rotation of planets is still governed primarily by centripetal gravitational forces with only very slightly (imperceptibly) assisted by orbital gravions as well. The intensity of this assisting force in the forward direction may be orders of magnitude smaller than the centripetal gravitational force and only close to, if not equal, to the drag force anticipated (allegedly) by the randomly moving background gravions. While such a hypothesis might explain the drag away on orbiting planets, it would still have a drag on bodies moving on a straight or near straight line eventually bringing them to a halt. The latter is contrary to our expectation, or more precisely, to our assumed expectation. We have actually never followed (observed, or experimented with) any body traveling on a straight line ad infinitum! We have never witnesses such a body coming to an eventual stop (due to drag), which might actually happen if we could follow it. That is, the drag problem by gravions is as arbitrary as the lack of the required evidence to prove it, while it is only based on established theoretical preconceptions that can themselves be wrong. In conclusion, all hitherto presented objections to the primitive Fatio theory of push gravity should be removed and allow freedom for science to move forward.

In appreciation for Planck’s law re-drawn in Fig. 80, we seem to be staring at the secret code of the entire cosmos (if our preceding field theory is correct). In the “middle” range of the spectrum of light lies the code for all visible things to humans. In broad terms, to the “right” of this range lies the code of the invisible electrical and gravitational phenomena, which humans experience but have not fully come to grips with. To the “left” lies the code of radiation effects (x-rays, gamma rays, etc.) along with formation of “material” bodies from the smallest to the largest (particles, atoms, planets, stars and more). In all of its manifestations, the code consists of a common denominator, namely, the gravion, which unifies the entire cosmos as we experience it. All this is a hypothesis for further investigation.

However, to consolidate the above vision, it would be helpful, in the meantime, to see other workers making contributions in this direction. Therefore, the world scientific endeavor should diversify its search on new frontiers. We have added more reasons and possibilities now like: The speed-mass relationships, energy-mass equivalence derivation, spacecraft trajectory engineering, explanations for known anomalies, testing of the push-force principle, the gravion being a Planck unit, field unification theory grasped and much more for a fully fledged PG theory. This is poised for verification by a number of feasible experiments and potential data available within the reach of many laboratories and organizations around the world (e.g. see Section 12). Particle physics is a major source of already existing experimental data that may fit in and be readily explainable by PG. Only experiment will determine, which of the canvassed ideas in this report is the best suitable for a correct PG theory; some tentative proposals failing this test should be replaced with better ones. Theoretical expansion of the theory is also promising with a hope to attract commensurable interest.

In conclusion, PG must be incorporated in the body of official and mainstream science and must remain on the table as an active candidate for possible explanations of existing data and theories for sufficient time before it may ever be abandoned again.

31 Grand PG synthesis of gravions in gravion-rays and photons

There are several issues arising from preceding Sections of this Part of the Report, which are initially addressed below by a synthesis of prior proposals together with new ones being gradually presented next.

We have already proposed that all known force fields are mediated via push particles of different types, namely, gravions in gravity, electrions in electricity, etc. for other higher strength fields. The gravions, or type-I particles are associated with a maximum acceleration $g_0 \equiv g_{01}$. The electrions, or type type-II particles are associated a with maximum acceleration g_{02} , and so on for other fields. At present, we continue on an initial investigation in Section 21 ushering push electricity and its possible connection with push gravity. In view of our latest understanding, we revisit the attempt to evaluate the parameters of these two fields, their inter-connection and upgrade/update our conclusions.

Throughout this report and regarding the ultimate value of the maximum acceleration g_0 , we have canvassed two alternative hypotheses for understanding the type-I (gravity) and type-II (electricity) particles:

One hypothesis is that each type corresponds to a different concentration of the same push particles presumably resulting in the two values of g_0 and g_{02} . Essentially, we only have gravions alone but with a wide distribution of free paths, which presumably could accommodate and mediate all fields according to the required flux density with an appropriate mean free path (mfp) for each field. In other words, a fraction of the gravion “gas” with the greatest but suitable mfp mediates the gravitational field with g_{01} , another fraction of lesser but suitable mfp mediates the electrical field with g_{02} and so on for the remaining push fields of higher strength. We have in mind that different concentrations corresponding to different mfp are closely related to the different material structures from particle-size to galaxies, and to the concepts of absorption and emission of these structures. We apply this approach first to the gravitational and electrical fields. If successful, we may possibly extend it to higher order fields later. This has been an ad hoc idea that is tested below in the context of Kelvin’s teaching: *“I often say that when you can measure what you are speaking about, and express it in numbers, you know something about it; but when you cannot measure it, when you cannot express it in numbers, your knowledge is of a meagre and unsatisfactory kind.”*

The second hypothesis is that each type of push particles corresponds to a different combination of gravions. However, in view of the introduction and identification of the Planck unit with the gravion in Section 30.1, we now wish to expand this idea to gravions themselves as being a combination of the smaller Planck units. For example, such a combination can be a straight line sequence of Planck units acting in unison and thus constituting a single gravion. This idea is supported by the ensuing investigation. Thus, we are compelled to introduce yet another term of the sub-gravion unit being the Planck unit, namely, the *planckion* (from Planck+ion), which is consistent with our prior terminology and also facilitates the exposition of the evolving PG theory. The planckion characteristic constants, used also as natural measurement units, are as we have already provided in Table 41.

Thus, type-I may be just Planck units (planckions) acting as gravions, but we now extend it to include also a special array of planckions acting as a gravion, in either case mediating the gravitational field. Then, type-II push particles are also a special agglomeration of planckions in some other organized configuration acting as electrions that mediate the electric field.

Next, we proceed to test the two hypotheses in an interchanging way between gravity and electricity. All references to these two hypotheses also made or implied in all our chronologically prior reporting are superseded and reappraised by the present and subsequent theory.

31.1 Connection between gravity and electricity

The situation we examine is better understood by depictions in Fig. 87. In case (a), we depict a gas of planckions acting as gravions. Thus, we show gravions (planckions) traveling in random directions each with an accompanying free path until it interacts with another gravion. The free path may be very long (*fp1*), or much shorter (*fp2*). The question is whether we can have such a distribution of free paths as to be able to comprise a fraction of them sufficient for a gravitational field and another fraction sufficient for an electric field.

In (b) we depict planckion-rays acting as single gravions. They may be likened with a molecular gas. Planckion rays act cooperatively in a manner to be modeled later according to the presenting needs of the theory, but they count as single push particles for gravity. Initially, planckions don’t have to be bound together as long as they can be produced, emitted, transmitted and absorbed in that configuration by some source, or MAC/MEC units. They may be emitted like a bullet spray from a machine-gun and subsequently interact as a group unit with a body or with another gravion-ray. They act in lieu of our hitherto single gravions, when they impinge on a body. We do not negate the prior consideration that single gravions (now planckions) are indivisible, nor the proposed initial model for them in Section 30.2. In fact, we have already considered the theoretical situation where the gravions can constitute long rays of some kind of units in Section 29.4.4 and elsewhere.

The present investigation has been prompted from the possibilities opened by the theoretical Eq. 491 for a possibly known value of g_0 with a t_g value from Table 41 instead of an unknown range of g_0 values applied in all chronologically prior reporting. We have thought that we should better use the integration time t_i given by Eq. 498, but because this remains unknown, we can achieve a good insight, if we use the interaction times for now. The interaction time is a physical prerequisite for later superimposing a statistical model of the gravion gas with an actual integration time connecting mass with power absorption. We can derive some fundamental relationships and conclusions based on the interaction time alone. Also, we can constrain the investigation if we first assume the Planck values in Table 41.

We can further narrow down the investigation on push electricity of Section 21 by adopting the premise that the electron charge is numerically equal to the electrical mass (see Section 21.1.2). Then, we can use

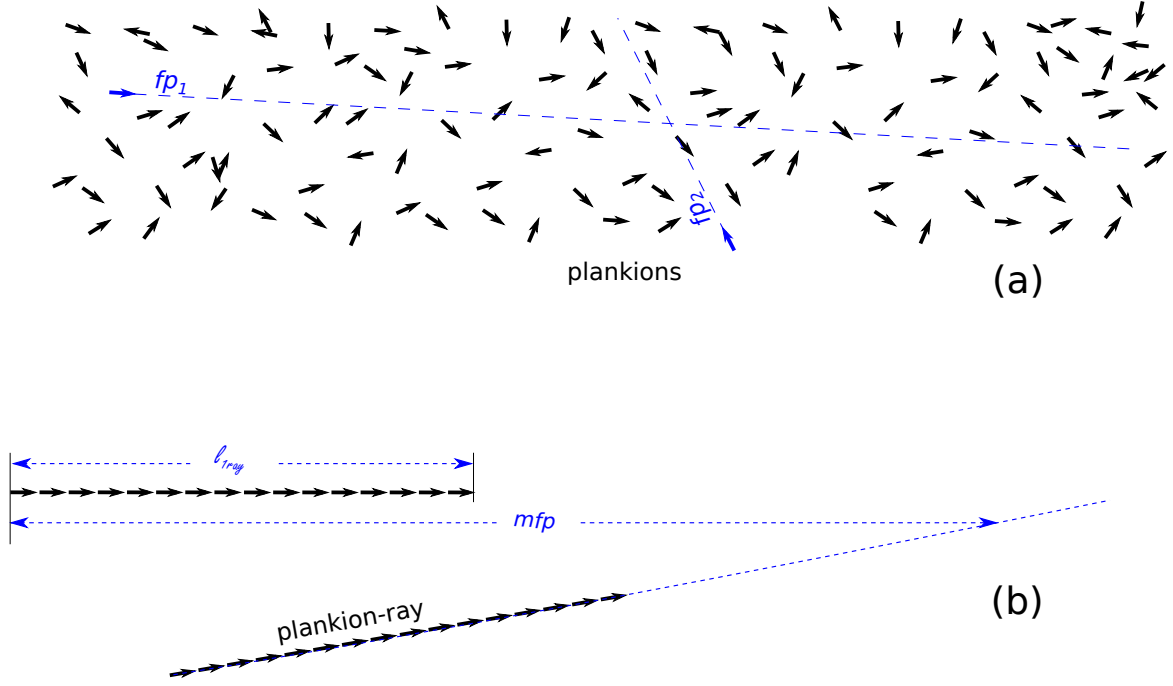


Figure 87: (a) Random single gravion (planckion) gas and (b) gravion-ray (planckion-ray) gas.

the electron as an important physical link between gravity and electricity and use the known charge-to-mass-quotient for the derivation of various constants for the respective fields.

For convenience, we summarize the relationships among alternative universal constants as they are applied again here. These are the gravion density flux J_0 , the maximum acceleration g_0 , the gravion energy density of free space u_0 , the gravion number density of free space n_0 and the constant Λ (deserving an overdue name). The only difference is that they are now theoretical values based on the starting equation:

$$g_{0theory} \equiv g_{0th} = \frac{c}{t_1}$$

where we introduce the subscript *theory* and (*th*) before we can finish up later with actual (or final theoretical) values of the same constants. We have compiled their expressions for evaluation in columns and rows of Table 42; they have the same form for both gravity and electricity in all cases with corresponding subscripts. In particular for Λ we could set $\Lambda_{1th} \equiv \Lambda_{01th}$ and $\Lambda_{2th} \equiv \Lambda_{02th}$, but we show the previously used symbol for consistency pending an overall revision of symbols at a later stage. For the gravion interaction times we use t_1 for gravity and t_2 for electricity, each to be equated with particular trial values as we move along.

We start with the Planck time t_P as the gravion interaction time $t_g = t_P$ per Table 41, which yields a maximum acceleration:

$$g_{0th} = \frac{c}{t_P} = a_P = \frac{c^2}{\ell_g}$$

where the gravions (planckions) have an ultimate small length ℓ_g . Then, we obtain a first evaluation of the gravity constants as shown in the column for single planckions under gravity in Table 43. We include the gravion length (initially, Planck length) and the gravion energy (initially Planck energy) in the expanded form of the same equations:

$$u_{0th} = \frac{2J_{0th}}{c} = \frac{2g_{0th}^2}{\pi^2 G c} = \frac{2c}{\pi^2 G t_g^2} = \frac{2c^3}{\pi^2 G \ell_g^2}$$

from which the gravion number density is derived by dividing the energy density with the gravion energy E_g :

$$n_{0th} = \frac{u_{0th}}{E_g} = \frac{2c}{\pi^2 G t_g^2 E_g} = \frac{2c^3}{\pi^2 G \ell_g^2 E_g}$$

The constant Λ_{1th} is obtained directly from:

gravity (gravions)			electricity (electrons)		
type_01	single planckions	gravion-rays	type_02	single planckions	electrons
x	1	x	y	1	y
$gravion_length$	$\ell_g = \ell_P$	$\ell_g = x\ell_P$	$electron_length$	$\ell_2 = ct_2$	$\ell_2 = ct_2$
t_1	$t_1 = t_P$	$t_1 = xt_P$	t_2	t_2	t_2
g_{0th}	$g_{0th} = \frac{c}{t_1}$	$g_{0th} = \frac{c}{t_1}$	g_{02th}	$g_{02th} = \frac{c}{t_2}$	$g_{02th} = \frac{c}{t_2}$
J_{0th}	$J_{0th} = \frac{cg_{0th}^2}{\pi^2 G}$	$J_{0th} = \frac{cg_{0th}^2}{\pi^2 G}$	J_{02th}	$J_{02th} = \frac{cg_{02th}^2}{\pi^2 G_2}$	$J_{02th} = \frac{cg_{02th}^2}{\pi^2 G_2}$
u_{0th}	$u_{0th} = \frac{2J_{0th}}{c}$	$u_{0th} = \frac{2J_{0th}}{c}$	u_{02th}	$u_{02th} = \frac{2J_{02th}}{c}$	$u_{02th} = \frac{2J_{02th}}{c}$
n_{0th}	$n_{0th} = \frac{2J_{th0}}{cE_g}$	$n_{0th} = \frac{2J_{0th}}{cE_{grav}}$	n_{02}	$n_{02th} = \frac{2J_{02th}}{cE_2}$	$n_{02} = \frac{2J_{02th}}{cE_2}$
Λ_{1th}	$\Lambda_{1th} = \frac{\pi G}{g_{0th}}$	$\Lambda_{1th} = \frac{\pi G}{g_{0th}}$	Λ_{2th}	$\Lambda_{2th} = \frac{\pi G_2}{g_{02th}}$	$\Lambda_{2th} = \frac{\pi G_2}{g_{02th}}$

Table 42: Comparative universal constants equations of gravitational and electric fields

$$\Lambda_{1th} = \frac{\pi G}{g_{0th}} = \frac{\pi G t_g}{c}$$

Next, we examine what the values of the corresponding constants should be in the electric field, provided that it exists the speculated fraction of single gravions with proper mean free paths mfp_2 shown in Fig. 87(a) and with sufficient flux density. We have no idea as yet about the values of those mean free paths, nor do we have a quantitative relationship of the distribution of properties of the entire gravion gas. However, the evaluation of the corresponding equations for the electric fields yields some immediate results.

As we constrain our current investigation around some fixed electron parameters, we set a symbol for the electron charge-to-mass ratio (quotient) by $Q \equiv e/m$; we need it in the equations connecting the fields. We apply and extend Section 21.1.2 by identifying the numerical value of the electron charge to be equal with our electrical mass of the electron. Thus, we have:

$$Q = \frac{m_{2e-e}}{m_{e-e}} = \frac{G}{G_2} \frac{g_{02th}}{g_{0th}} \frac{A_{2R-e}}{A_{R-e}} \quad (511)$$

Since the value of Q is known per Eq. 339, we solve the above for g_{02} in terms of g_0 (already done also by Eq. 310) as:

$$g_{02th} = Q \frac{G_2}{G} \frac{A_{R-e}}{A_{2R-e}} g_{0th} \quad (512)$$

The ratio of absorptivities is initially unknown, but a likely value is unity according to Sections 21.1 and 19.3 and later discussion in 21.1.3. Then, we can simplify like:

$$g_{02th} = Q \frac{G_2}{G} g_{0th} \quad (513)$$

The corresponding interaction times t_1 and t_2 between the fields relate via the equations:

$$t_2 = \frac{c}{g_{02th}} = \frac{cG}{QG_2g_{0th}} = \frac{G}{QG_2} t_1 \quad (514)$$

or conversely by:

gravity (gravions)			electricity (electrions)		
type_01	single planckions	gravion-rays	type_02	single planckions	electrions
x	1	2.37E+31	y	1	1.00E+10
$gravion_length$	1.62E-35	3.83E-04	$electron_length$	6.82E-67	1.62E-35
t_1	5.39E-44	1.28E-12	t_2	2.28E-75	5.39E-44
g_{0th}	5.56E+51	2.35E+20	g_{02th}	1.32E+83	5.56E+51
J_{0th}	1.41E+121	2.51E+58	J_{02th}	5.86E+163	1.05E+101
u_{0th}	9.39E+112	1.67E+50	u_{02th}	3.91E+155	6.97E+92
n_{0th}	1.42E+146	1.07E+52	n_{02}	5.90E+188	1.05E+116
Λ_{1th}	3.77E-62	8.93E-31	Λ_{2th}	2.14E-73	5.08E-42

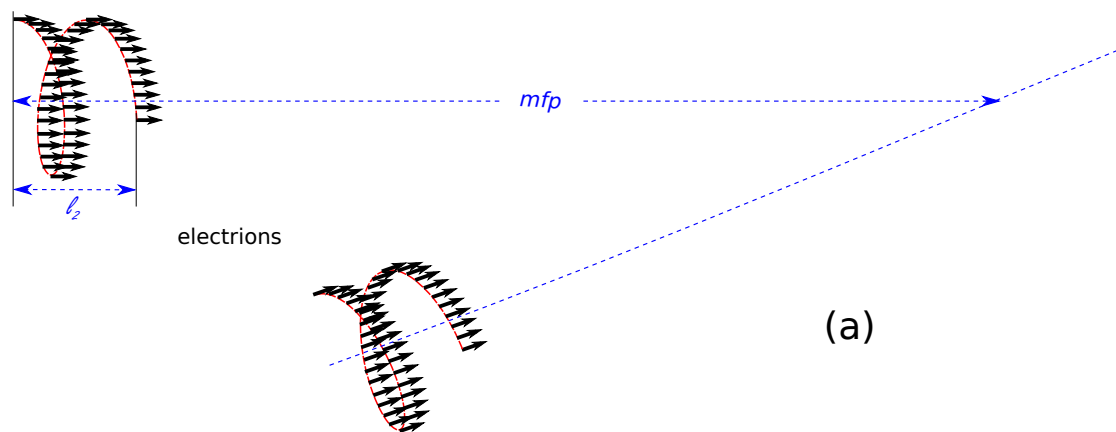
Table 43: Comparative values of the universal constants of gravitational and electric fields obtained by the equations of the corresponding cells of Table 42.

gravity (gravions)			electricity (electrions)		
type_01	single planckions	gravion-rays	type_02	single planckions	electrions
x		5.56E+43	y		1.00E+10
$gravion_length$		8.99E+08	$electron_length$		3.79E-23
t_1		3.00E+00	t_2		1.27E-31
g_{0th}		1.00E+08	g_{02th}		2.37E+39
J_{0th}		4.55E+33	J_{02th}		1.90E+76
u_{0th}		3.04E+25	u_{02th}		1.26E+68
n_{0th}		8.24E+14	n_{02}		1.91E+91
Λ_{1th}		2.10E-18	Λ_{2th}		1.19E-29

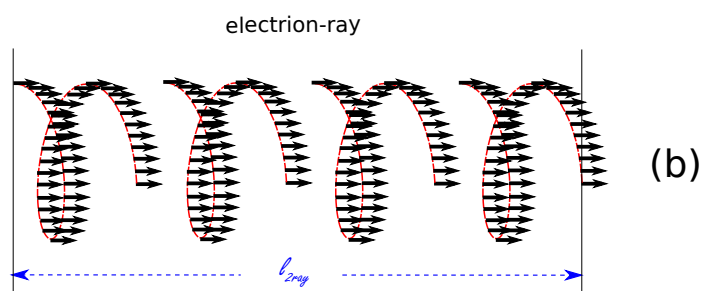
Table 44: Comparative values of the universal constants of gravitational and electric fields obtained by the equations of the corresponding cells of Table 42 starting with $g_0 = 10^8 \text{ ms}^{-2}$

gravity (gravions)			electricity (electrions)		
type_01	single planckions	gravion-rays	type_02	single planckions	electrions
x		2.37E+36	y		1.00E+05
$gravion_length$		3.83E+01	$electron_length$		1.62E-30
t_1		1.28E-07	t_2		5.39E-39
g_{0th}		2.35E+15	g_{02th}		5.56E+46
J_{0th}		2.51E+48	J_{02th}		1.05E+91
u_{0th}		1.67E+40	u_{02th}		6.97E+82
n_{0th}		1.07E+37	n_{02}		1.05E+111
Λ_{1th}		8.93E-26	Λ_{2th}		5.08E-37

Table 45: Comparative values of the universal constants of gravitational and electric fields obtained by the equations of the corresponding cells of Table 42



(a)



(b)

Figure 88: *Electrions and electron rays*

$$t_1 = Q \frac{G_2}{G} t_2 \quad (515)$$

For consistency of symbols with Section 21.1.2, we set for the gravion energy $E_1 = E_g = E_\omega \equiv \omega$ [apology for the temporary use of multiple symbols for the same quantity in this working manuscript] and for the electrion $E_2 = E_e \equiv \varepsilon$ and write the equations:

$$Q = \frac{m_{2e-e}}{m_{e-e}} = \frac{J_{02th} g_{0th}}{J_{0th} g_{02th}} = \frac{u_{02th} g_{0th}}{u_{0th} g_{02th}} = \frac{n_{02th} E_\varepsilon g_{0th}}{n_{0th} E_\omega g_{02th}} \quad (516)$$

The above is also a direct consequence of Eqs. 189 and 191 ($W = 4cg_0m_e$) for each field and their ratio, since the radius of the linking electron is the same. The radius and real mass of the electron are objectively -in theory- invariant prior to any experimental measurements -per our method. Unlike mainstream theories based on (starting with) measurable quantities, we proceed from certain principles involving given quantities of entities, which we consider preexisting and objective (not subject to our measuring methods) and which are involved in a theory that can presumably forecast certain measurable quantities.

We present the numerical results in the planckion column under electricity of Table 43 based on the numerical values of the planckion column under gravity. We note that the interaction time required for electrions is many orders of magnitude less than the Planck time; the same adverse outcome is for the electrion length. These outcomes cannot be accepted, if nothing can be less than Planck units; the same applies with the ensuing other electric field constants. Hence, they are crossed out in this column. Therefore, the idea that a fraction of the total single planckions mediates the electric field is untenable.

The only way to rectify the above inconsistency is by working backwards an interaction time t_1 from acceptable values of t_2 via Eq. 515. We should have $t_2 \geq t_P$. For the minimum value of Planck time $t_2 = t_P$, we obtain the results in the columns of gravion rays and electrions in the same Table 43. We see that it should be $t_1 = 1.28 \times 10^{-12}$ s. This can be achieved by a long gravion ray made of planckions and having $t_1/t_P = 2.37 \times 10^{31}$ planckion units, say, in the simplest configuration of a straight line chain. The *gravion_length* = $3.83E-04$ m. The latter outcome is a plausible length in the micro-scale. The previously speculated existence of gravion rays has now resulted as a matter of necessity for connecting electricity with gravity. Of course, this is the minimum value for the ray length, which can be longer, if the electrion interaction time is found to be greater. (Note: We have applied the values of $G \equiv G_1 = 6.6740800000E-11$ and $G_2 = 8.9875520000E+09$ in SI units).

By the above approach, we can interplay various constants to obtain a further idea of the order of size among them. For example, if we start with a speculated minimum value of $g_0 = 10^8 \text{ ms}^{-2}$, we obtain the interaction times and gravion-ray lengths along with the other constants in Table 44. We note a “huge” *gravion_length* = $8.99E+08$ m, i.e. of the order of a photon travel distance over a “huge” interaction time of $t_1 = 3$ s. The corresponding electrion $t_2 = 1.27E-31$ s is at the same time much longer than the Planck time. The latter can be achieved by an appropriate group of planckion units making up the electrion. As to the exact configuration, we leave it to particle physics to supply the relevant experimental data, already on file, or by newly designed experiments. We have tentatively shown spiral configurations in Fig. 88(a). We have previously also proposed vortex type configurations, but this question is open for further theoretical and experimental investigations.

To complement the “picture”, we have also compiled a case with intermediate values in Table 45. This case yields a *gravion_length* = 38.3 m and an *electrion_length* = $1.62E-30$ m. The corresponding gravion interaction time $t_1 = 1.28E-07$ s may appear more “reasonable”, but the electrion interaction time $t_2 = 5.39E-39$ s remains by far much shorter than the fastest reported experimental photon absorption times in the femto-scale. It is likely that we have not been able to measure the correct absorption times in the photoelectric or related effects. At any rate, our theory may have placed all things in the correct framework for further research in particle physics.

Below, we add some equations to complement Table 42 with explicit expressions for gravion rays. Let’s assume that there are x planckions per gravion ray. Then, the interaction time is $t_1 \equiv t_{gray} = xt_P$. The gravion ray has a length $\ell_{gray} \equiv \ell_2 = xct_P$ and an energy by the same multiple of the planckion energy $E_1 = E_{gray} = xE_P$. We repeat the basic equations of the table including the parameter x below:

$$\begin{aligned} g_{0th} &= \frac{c}{t_1} = \frac{c}{xt_P} = \frac{c^2}{\ell_2} \\ J_{0th} &= \frac{cg_{0th}^2}{\pi^2 G} = \frac{c^3}{\pi^2 G x^2 t_P^2} = \frac{c^5}{\pi^2 G \ell_2^2} \\ u_{0th} &= \frac{2c^2}{\pi^2 G x^2 t_P^2} = \frac{2c^4}{\pi^2 G \ell_2^2} \end{aligned} \quad (517)$$

$$n_{0th} = \frac{u_{0th}}{E_1} = \frac{2c^2}{\pi^2 G x^3 t_P^2 E_P} = \frac{2c^4}{\pi^2 G \ell_2^2 x E_P}$$

$$A_{1th} = \frac{\pi G}{g_{0th}} = \frac{\pi G x t_P}{c}$$

The corresponding equations for the electric field have a similar form but not identical because the parameter x is replaced an independent parameter y for the total planckions in an electrion generally not necessarily forming a straight line configuration. We apply the above and obtain the results shown in the tables for the given values of x and y . A variation of these parameters has a direct effect on the number density of push particles in both fields to be further discussed below.

We show electrion-rays in Fig. 88(b), which could be handled in a similar fashion as gravion-rays, but this may be unnecessary. It may be that rays of electrions at some regular (repeatable) distance apart may constitute photons with wavelength equal to the repeatable distance, if the number of planckions is related to this distance by the known equation of $\lambda\nu = c$. Such configurations may ultimately be determined by the structure/function of the emitting source (e.g. electrons).

31.2 Analysis and discussion

We have previously distinguished two cases in Fig. 80, where we juxtapose the single gravion (Planckion) number density distribution against mfp , and the photon number density against mfp . Here, in lieu of “photon”, we examine the simpler case of “electrion” as being one organized type of push particle, namely, for the electric field. In a way, it is like a photon composed of single planckions, but its organization is likely to be different on account of the different effects we experience from the interaction of photons with matter; electrions are associated with the static electric field, as distinct from photons associated with the electromagnetic field.

It is interesting to make a comparison of our results with Quantum Electrodynamics (QED): The numerical value of the energy density of planckions in free space for gravity yields $u_0 = 9.39 \times 10^{112} \text{ J/m}^3$. After a brief search, we find that a recent measured value of energy density is $5.3566 \times 10^{-10} \text{ J/m}^3$ (Wikipedia contributors, 2024c), which is said to be smaller than the theoretical value by a factor of $\sim 10^{120}$; this results in a theoretical value of $5.3566 \times 10^{112} \text{ J/m}^3$ being in striking close agreement with our value. This is also very close to the theoretical value of $4.6 \times 10^{113} \text{ J/m}^3$ by Margan (2012) and with further analyses by Oramah (2023) in relation to the cosmological constant problem. Oramah tabulates the density of the expanding universe versus time. Accordingly, the vacuum energy density, after starting at a calculated maximum, it has currently been reduced to a much lower value between $2.183 \times 10^{50} - 1.924 \times 10^{47} \text{ kg/m}^3$ at the age of the universe between 13-14 billion years. Those values converted to energy density are $1.96 \times 10^{67} - 1.73 \times 10^{64} \text{ J/m}^3$, i.e. about half of the order of magnitudes of the calculated maximum values. Tafazoli (2023) has provided a theoretical energy density of $5.18 \times 10^{44} \text{ J/m}^3$.

Given our agreement with the maximum theoretical values by QED, we can also accept that the actual prevailing energy density is much less than the value we found for single planckions in Table 43. We are led to think that the maximum values found are only theoretical ones, but the actual constants have a much lower value. The latter would correspond to lesser values of absorptivities of bodies to provide the prevailing (actually measured) accelerations. We encounter a similar situation in internal fluxes and accelerations as we have done in Sections 8 and 24. The gravion flux inside the heliosphere and inside galaxies should be less than inside the intergalactic space. This is definitely the situation on the surface of planets surrounded by a gaseous atmosphere. Hence, the calculated values here may be the maximum theoretical possible values and not necessarily the prevailing ones at present in the given region of space where we live. This explanation points again to the need for finding ways to measure our constants (at least one of them). A comparison of experiment with the theory will lead us to understand the status and history of the cosmos.

The maximum theoretical g_{0th} value may apply to the situation of contiguous packing of single gravions. That is the maximum energy density of the universe. However, this is an exceptional circumstance, perhaps applicable when a black hole explodes, or even at the maximum black hole density just prior to explosion. The prevailing vacuum energy density should be by far less than that value, and there is not necessarily a contradiction with theory provoking the cosmological problem. For a lesser energy density $u_0 < u_{0theory}$, there corresponds a lesser vacuum acceleration $g_0 < g_{0theory}$ and flux density $J_0 < J_{0theory}$.

Further and beyond the above explanation, we actually found reasons to abandon the seeming agreement with QED of the maximum theoretical values of Table 43. We may advance according to the existence of gravion-rays for gravity, and accordingly of suitable electrions (planckion groups) for electricity. That is, we can establish applicable values of the energy density lesser than the initial maximum theoretical value for

single planckions. By adopting a value near the derived maximum value of $g_0 = 2.35 \times 10^{20} \text{ ms}^{-2}$ from Table 43, we found a radius $7.8 \times 10^{-31} \text{ m}$ for the electron in prior derivations of Section 19.4. The latter radius can be readily accepted as being four orders of magnitude greater than the Planck length. However, values $g_0 > 2.35 \times 10^{26} \text{ ms}^{-2}$ result in radii too close and below the Planck length, which are unacceptable. Hence, we have established a related reason for restricting the range of possible g_0 not above $g_0 = 2.35 \times 10^{20} \text{ ms}^{-2}$. All this also indicates a consistency in our derivations, as it should.

It is also interesting to make a comparison of our results with the energy density found from the field equations of general relativity. Since the cosmological constant provided by GR is used interchangeably with the “vacuum energy” (as being equivalent with each other), we equate the respective energy densities between PG and GR to find if the connection bears some meaning.

For the “energy density of the vacuum state” ρ_{vac} in GR, we have that

$$\rho_{\text{vac}} = \frac{\Lambda_{GR}}{\kappa}, \quad (518)$$

where Λ_{GR} is the *cosmological constant* designated from its standard symbol but here sub-scripted to distinguish it from our same symbol of our constant Λ , while κ is the “*Einstein gravitational constant*” provided by:

$$\kappa = \frac{8\pi G}{c_{ph}^4} \approx 2.07665(5) \times 10^{-43} \text{ N}^{-1}, \quad (519)$$

where c_{ph} is the velocity of photons, so that the energy density from GR is:

$$\rho_{\text{vac}} = \frac{\Lambda_{GR} c_{ph}^4}{8\pi G} \quad (520)$$

The PG energy density given by Eq. 517 equated with above formula yields:

$$u_0(PG) = \frac{2c^4}{\pi^2 G \ell_g^2} = \frac{\Lambda_{GR} c_{ph}^4}{8\pi G} = \rho_{\text{vac}}(GR)$$

$$\Lambda_{GR} = \frac{16}{\pi \ell_g^2} = \frac{5.09}{\ell_g^2} = 1.95 \times 10^{70} \text{ m}^{-2}$$

The above value is by far much higher and inconsistent with the cosmological constant value from the literature, namely, $\Lambda_{GR} = 1.10 \times 10^{-52} \text{ m}^{-2}$ corresponding to the energy density of $5.3566 \times 10^{-10} \text{ J/m}^3$ quoted further above. This is again the same out from PG by 122 orders of magnitude. This comparison might be of interest to workers in GR and QED. In this context, we may also add the relationship below

$$\Lambda \Lambda_{GR} = \frac{16Gg_0}{c_{ph}^4} = \frac{16G}{c_{ph}^3 t_1}$$

It is also interesting that we have found some comparable preliminary results by equating the radii obtained with the Schwarzschild and PG derivations: By applying Eq. 347, we obtain for the required maximum acceleration $g_{02} = 1.4 \times 10^{42} \text{ ms}^{-2}$. This is another indication that we have acquired a legitimate place in related physics investigations.

The discrepancy between theoretical and measured values is well known as “*the cosmological constant problem*”. Our PG values provided in the tables fall in the mid-range of existing expectations. Our approach is totally independent from existing theories and may provide a way for resolving the problem.

The very low value of the measured cosmological constant may be due to the undetectability of gravions. They can only be detected by their generation of gravitational fields, not as directly detectable particles. Gravions pervade all observable matter (hyle) by varying degrees that are calculated via the absorption coefficient k and/or the absorptivity A_R introduced by PG. “Space” is literally filled with gravions but they give the appearance of “vacuum”. The cosmos may be like a “continuum” of extremely fine particles (quanta) of Planck size. The observed sizes of bodies differ by a large range of orders of magnitude all the way down to the Planck length. Within this huge range of space sizes, hyle has an immense number of degrees of freedom to organize itself from the “simple” gravion structure to the most complex formations in the observed and unobserved cosmos. Looking up in the sky through telescopes, we obtain the impression of a vacuum space containing an immense amount of celestial bodies. However, we now understand that there is a continuity among all that there is around us and that the space is not empty but organically connected with what we see. The flicker of lights in the sky is energy (hyle) originating from the seeming vacuum, a hyle that is being in perpetual flow from the smallest to the largest entities and vice versa. The observed bodies are just condensations (much higher densities) of the vacuum gravions.

It may be that “dark matter” from another theory is not detected because it is nothing else but the omnipresent gravions. Actually, we “detect” them all the time, but only as a gravitational force, whilst other types of detector have been built in vain; they are all transparent to gravions. The seemingly dark skies contain a highly dense gravion gas, whilst all the stars, galaxies and all visible formations must constitute a small fraction of the cosmos. It is said that visible matter is only 5% of the total universe and we can agree with a similar statement.

The number density and interaction times are indicative of (pertain to) the quantum nature of the cosmos, while a flow of energy (energy density flux) appears like a continuum (non-quantized) in mainstream physics. PG provides for both by starting with push particles and deriving the “continuous” properties of other theories. It is an integrated theory of both concepts from the outset without singularities and “renormalization” procedures.

Planck’s discovery constitutes a pivotal point in the history of physics: We can use it in PG, and it has been used in QM. However, we provide a greater framework for a quantized union of fields and cosmology. Fatio had much earlier provided the principle for new physics and Planck found a possible push particle for it. However, Newton’s theory took physics in a different direction, whilst other theories took Planck’s discovery further away from the correct path. It seems that PG can bring back all things on the right course.

Now, we note that the electric field energy density, hence pressure, is invariably much greater than the gravitational field pressure. Ordinary bodies constructed on the basis of electricity, i.e. chemistry, would blow out if acted only by a gravitational pressure. We should have an equilibrium in the sum total of all pressures. That means that ordinary objects, planets and stars should be surrounded by an electric field, together with the gravitational field holding and maintaining the integrity of all bodies. This can be achieved either by assuming that electrions permeate the entire universe along with gravions, or they form a cloud of sufficient thickness around bodies in a steady-state flow from inside out. The latter flow may emanate in the case where gravions supply the source for a continuous production of electrions emitted out of ordinary bodies in the surrounding space. In other words, there is a dynamic steady-state of electron flow from a maximum at the surface of objects to a minimal decaying value away in the inter-space region. We can tentatively assign, for example, a layer thickness of about 90 km around the Earth. This is based on the observation of transient luminous events reaching heights of that magnitude; their generation may indicate the spatial extend of the electric fields around planets. In that case, we need to work out an order of magnitude for the mean free path of electrions consistent with maintaining a sufficient thickness layer around bodies. At any rate, this is a temporary speculation for testing, when we can quantify the situation per quoted Kelvin’s teaching.

By a similar reasoning, the mean free paths of the higher strength fields may be confined to much smaller spatial scales within and around molecules and atoms with corresponding field “gases” of push particles diffusing and permeating all intermediate regions all the way from the inside of bodies of all sizes to their surface and beyond; there is an effective thickness of them shrouding the objects in a steady-state flow. By such means, it may be possible to envisage an equilibrium in the sum of all corresponding pressures. If the latter is correct, then we may not have to resort to the presence of all types of field push particles everywhere in the universe. In QED the quantum mechanical calculations provide the sum of contributions from all vacuum modes below an ultraviolet cutoff at the Planck scale, which may be responsible for the extraordinary very high values of energy density. We do not solve the cosmological problem now, but we make an opening for further considerations during subsequent development of PG theory; workers with related expertise may also make a contribution to this aim.

Towards the above aim, an experimental determination of g_0 has been called upon to perform from the outset (per “verification” in the title of this report). We may initially attempt the verification measurements proposed in Section 12. Failing this approach, if g_0 is ultimately too high, then we should do astrophysical observations coupled with a well developed PG theory. We have done the first steps in this report for either eventuality.

Further to the general formulation of field unification theory in Section 30.5, we have provided a possible quantitative connection between gravity and electricity in the hope to make headway towards a similar formulation to include the remaining force fields later. We have envisaged that photons may play a more direct role in nuclear fields. We need to further work out a detailed description of the photon starting with a possible structure of the electrion, which may be the “smallest” size of a primitive photon-like structure. All this must be done in conjunction with models of absorbing and emitting structures, like the MAC and MEC. Combinations of the latter may then take part in higher order structures of other particles.

31.3 All field inter-connection (interaction)

It may be possible to follow the preceding procedure for connecting gravity with electricity also for the weak and strong force fields. We may use the relative strengths among the four fields tabled by Wikipedia

field type	gravity (₀₁)	weak (₀₃)	electricity (₀₂)	strong (₀₄)
particle name	gravions	?	electrions	planckions
published strength	1	1.E+33	1.E+36	1.E+38
adopted strength	1	1.E+28	1.E+31	1.E+33
#planckions x	1.00E+33	1.00E+05	1.00E+02	1.00E+00
$particle_length$	1.62E-02	1.62E-30	1.62E-33	1.62E-35
t_{fth}	5.39E-11	5.39E-39	5.39E-42	5.39E-44
g_{0fth}	5.56E+18	5.56E+46	5.56E+49	5.56E+51
J_{0fth}	1.41E+55	1.05E+94	1.05E+97	1.05E+104
u_{0fth}	9.39E+46	6.97E+82	6.97E+88	6.97E+92
n_{0fth}	1.42E+47	1.05E+111	1.05E+120	1.05E+126
Λ_{fth}	3.77E-29	5.08E-37	5.08E-40	5.08E-42
G_{fth}	6.67E-11	8.99E+09	8.99E+09	8.99E+09

Table 46: Comparative values of universal constants of gravitational, weak, electric and strong field. .

contributors (2024e). We first find this inter-connection between the extremes of strong and gravitational fields and with the intermediate electric force. Last, the weak force may be incorporated in an analogous way. If we set unity for gravity, then the strong force is 10^{38} times stronger and the electromagnetic force is 10^{36} times stronger according to prevailing theories.

Let's use again the symbols g_{01} for gravity, g_{02} for electricity, and g_{04} for the nuclear (strong) field. Then, the ratio g_{02}/g_{01} is given by the inverse ratio of their interaction times:

$$\frac{g_{02}}{g_{01}} = \frac{c/t_2}{c/t_1} = \frac{t_1}{t_2}$$

According to Table 43, the above ratio is $1.28 \times 10^{-12}/5.39 \times 10^{-44} = 2.37 \times 10^{31}$ times stronger, but not 10^{36} times stronger as given by the literature values. This may have to do with the absorptivities of the bodies, a property that is not considered by mainstream theories presumably using ordinary (Newtonian) bodies for gravity. In the latter case, we should have used our Eq. 512 including the absorptivities, so that the five orders of magnitude difference can be accounted for. More precisely, we can use $A_{R2-e} \approx 1$ for the electron and $A_{R-e} \approx 10^{-5}$ being a typical value for Newtonian bodies. In that case, we have a plausible compatibility between our values and the literature ones between these two fields. After all, our values in the tables of the preceding section apply to bodies with $A_{R2-e} \approx 1 \approx A_{R-e}$, as already assumed.

If we extrapolate the same procedure to the strongest (nuclear) field (strong force), we should have $g_{04}/g_{02} \approx 10^2$ based on the literature relative values between these two fields. That is, we should adjust the values in Table 43 by two orders of magnitude. In that case, the strong field should be allotted the shortest possible interaction (Planck) time of $t_4 = t_P = 5.39 \times 10^{-44}$ s, to be followed by $\sim 10^2$ times weaker electric field with $t_2 = 5.39 \times 10^{-42}$ s, to be followed with a gravitational interaction time of $t = 5.39 \times 10^{-9}$ s being $\sim 10^{31}$ times greater than the electric interaction time. The weak field is placed between electricity and gravity in an analogous way. We can see the interaction times and the corresponding field strengths in Table 46.

Therefore, we can adopt the above interaction times for each field and then find the other constants for each field. We have done so and listed the outcomes in the same Table 46. We now add the subscript f ($_f$) for “field” with each constant, like t_{fth} , g_{0fth} etc., collectively denoting, for example, g_{01th} , g_{02th} , g_{03th} and g_{04th} all the characteristic accelerations of the four fields in the first column of the table. In the entire prior report of this work, we have used the symbol g_{02} for electricity, arbitrarily, instead of g_{03} for consistency with the ascending order of strength. That is because we proceed inside our theory by trial-and-error without prejudice from external theories. To avoid extensive editing at present (risking serious errors), we maintain the prior symbolism for the electric field but alerting the reader accordingly; g_{02} could refer to the weak field instead of the electric field in future revisions, but we now use g_{03} for the weak field. After all, there are other intermediate field interactions reported, the examination of which lies beyond a detailed analysis at this stage, while PG may reveal yet another order of previously unidentified fields.

We make an overview of the above approach to see some consequences: The strong field is mediated by single planckions, so that the electric field should be mediated by electrions, each constituted by at least $\approx 10^2$ planckions, if they are configured in a straight line ray. We don't know the configuration of the planckions in the electrion, but they can be many more; we only provisionally take them to be a straight line ray, just for simplicity and comparison, but we can return to this question as needed later. We may apply the same reasoning for the configuration of the push particles mediating the weak field and finally the same straight line configuration of a planckion ray for the gravions of the gravitational field (already done previously). The problem for now is that we do not know the corresponding G values for the weak and strong field, as we know the G_1 and G_2 for gravity and electricity. These constants are required to derive the remaining constants listed in the table below the maximum accelerations for each field. We have used, arbitrarily, $G_4 = G_3 = G_2$ to produce some output for the tabled cells, but we have also crossed them out to indicate that they are arbitrary and possibly incorrect.

The resulting numerical values are interesting. We now obtain a gravion-ray length of 162 mm, which may nicely explain the experience of "inertia" in bodies. This length is relatively long and persists for a relatively long time. If it "binds", or commits the absorption center during the interaction, this might explain the resistance in the change of the kinetic status of a body. We need an external force to change this status, which appears as a resistance to changing the velocity of a given body. Once the velocity is changed and the force withdrawn, a new steady-state of interaction between gravitational field and body is achieved and remains constant unless a new force is applied.

If we may "play" around with various values of G_3 and G_4 , we can adjust the energy density, hence the pressure for each field. Starting with an assumed equality $G_4 = G_3 = G_2$, we note that the corresponding pressures are monotonically decreasing from the strong to the gravitational field. This may be envisaged as partial pressures in a universal push particles gas, as it happens with ordinary gases. The strong field corresponds to a monatomic gas, whilst the other fields correspond to molecular gases with increasing molecular weight towards the gravitational field. The maximum total pressure requires only a slight adjustment of the highest pressure corresponding to u_{04} in summing all the lower partial pressures of the universe; this adjustment is only about two orders of magnitude. We should note that the pressure is not necessarily equal to the energy density. In gravity, the pressure (force component normal to a surface) is given not by $2J_0/c$ per Eq. 16, but by Eqs. 34 and 36. The presented values need further processing to finally arrive at the correct numerical pressures. Also, the G_3 and G_4 probably need to be adjusted to some other values that still invoke a regime of acceptable partial pressures of a total "gas" of push particles.

The above analysis can be very revealing. In Section 21.3.1, we considered the possibility of the nuclear field mediated by the "somions", which having the strongest flux intensity, could supply other weaker fields. We can now identify the somions with the planckions, which we recently introduced according to the developing needs of the theory. We started with gravity as our initial object of investigation and reasonably assumed to be the source of other higher fields, like the electric field. This is in reverse order of hyle flow, if the strong field also supplies intermediate fields.

We intuitively thought that the gravions supply the other fields by creating agglomerations of larger push particles. The larger particles carry more momentum. We have found that this may not be the actual case. Those "larger" particles are not necessarily the reason for mediating stronger fields. The strength of each field is rather determined by the relative interaction times. In other words, it is not the number of planckions constituting each type of push particle, but the interaction time of each agglomerated "particle" as an entirety. In fact, gravions can be the largest agglomeration, but with a configuration yielding the longest interaction time. This raises the question of origin of gravions. This may be during astrophysical explosions. The latter provide the source for an average density flux that generates gravitational fields around bodies. At the same time, the nuclear field is at work continuously as well. That is, there are energy flow loops in the cosmos incessantly at perpetuity.

This major revision of our understanding is important for establishing the interaction (inter-connection) among all fields and their unification thereof. This revision does not change our prior work, except that it re-orders it. The organization of each type of push particle remains to be determined, but for discussion purposes, we have initially introduced the planckion-ray type of configuration. In addition, various vortex types of configuration, helical, etc. have already been proposed and examined. It is now a matter of particle physics and cosmology to take over under the hitherto established framework of our PG theory.

The above ideas appear plausible in a big scheme of a field theory under PG, also indicating compatibility with existing field theories to a good extent. The major difference is that our field theory is placed in a greater framework that will hopefully yield similar results and probably eliminate the impasses of existing theories.

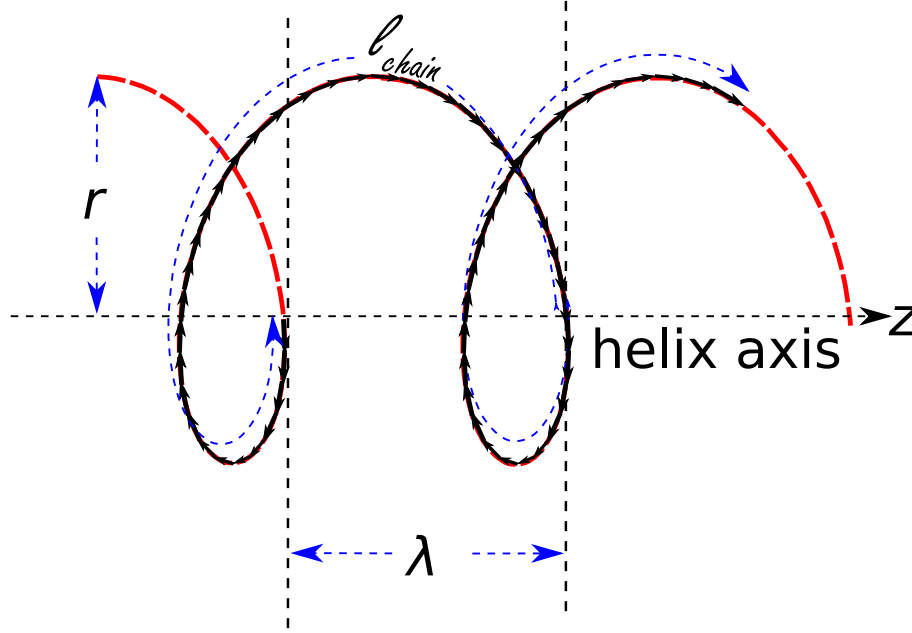


Figure 89: Helical planckion-gravion-electron configuration (black arrows) with chain length ℓ_{chain} moving on a helical path (red line) with radius r and pitch λ .

31.4 Planckion velocity versus electron velocity in the helix model

We refine prior attempts to model the electron, the electron and the photon. We have tentatively proposed that they all have a common structural unit in the form of a helix as depicted in Fig. 88. We think that the photon is a superstructure of the electron and the electron a super structure of the photon and electron. We now pioneer a new understanding arising from modified helical structures of these “particles” in the spirit set out at the outset of Part 3. We attempt an analysis of various possibilities aiming at retaining what eventually can be consistent with all experiments.

31.4.1 Further on the electron and gravion modeling

It is important to note that in Fig. 88 the electron ray is depicted with arrows from each planckion pointing in the direction of travel of the electron ray as a whole along the axis of the helix. This has been necessitated by the attributes that we have assumed in the “gravion” (now planckion) modeling in Section 30.2. If the planckions have a limiting (fixed) velocity, say, equal to the photon velocity (or some other constant value), then their vector of travel must be in the same direction as the vector of electron traveling as a group particle. However, we may have to allow a kind of connection or bond between consecutive planckions forming a chain. This is now depicted in Fig. 89, whereby the planckion vector (arrow) follows the spiral path and tangent to it. In that configuration, the electron ray travels with a lower velocity along the z -axis than the planckion velocity on the helical path. If the electrons mediate the electric field, for which we “know” that its propagation speed is equal to the light speed, then the planckion velocity must assume superluminal speeds along the spiral path (we use the words “speed” and “velocity” interchangeably). The “connection” between consecutive planckions forming the helix may be physical by way of some bond, but it may also be “notional” by way of a predetermined order during emission from a particular source. In either case, we can proceed with the following analysis.

The helix is a space (3D) curve with parametric equations:

$$x = r \cos \psi \quad (521)$$

$$y = r \sin \psi \quad (522)$$

$$z = \zeta \psi \quad (523)$$

where ψ is the angle of rotation of a radial vector expressed in radians, r is the radius of the helix and ζ is a constant providing the helix pitch by $2\pi\zeta$; the range $\psi \rightarrow \psi + 2\pi$ of ψ describes one helical unit (one spiral turn). The length of one helical unit ℓ_{turn} is:

$$\ell_{turn} = 2\pi\sqrt{\zeta^2 + r^2} \quad (524)$$

Now, we propose to investigate the possibility of the helical pitch being identical with the wavelength in a photon/electron:

$$\lambda = 2\pi\zeta$$

We understand that electrions and photons are not identical entities but they may have a characteristic helical pitch/wavelength in common; we can return to this issue later. We must retain the known relationship between wavelength and frequency in a photon, namely:

$$\lambda\nu = c_{ph}$$

yielding the speed of photons c_{ph} . However, in that case, the speed of the chain c (also of planckions) along the helical path must be greater by a factor equal to the ratio of the length of one coil unit over the pitch:

$$\frac{c}{c_{ph}} = \frac{\sqrt{r^2 + \zeta^2}}{\zeta} \quad (525)$$

The possibility of superluminal velocity of the gravion (now planckion) was left open in our prior PG theory, which may be materialized now by the helical configuration of planckions. Hence, the planckion velocity is greater than the photon velocity by:

$$c = \frac{\sqrt{r^2 + \zeta^2}}{\zeta} c_{ph} \quad (526)$$

or

$$c^2 = \left(\frac{r^2}{\zeta^2} + 1\right) c_{ph}^2 = \frac{(\lambda\nu)^2 r^2}{\zeta^2} + c_{ph}^2 = 4\pi^2\nu^2 r^2 + c_{ph}^2$$

Assuming that c is constant and independent of the frequency, then we obtain a relationship between the radius and the frequency by:

$$4\pi^2\nu^2 r^2 = c^2 - c_{ph}^2 = \omega^2 r^2 \quad (527)$$

$$r = \frac{\sqrt{c^2 - c_{ph}^2}}{\omega} \quad (528)$$

using the conventional equation $2\pi\nu = \omega$ for the angular frequency. The helical radius is inversely proportional to the frequency, so that the particle is squeezed laterally at increased frequencies. Let us now see this outcome together with the electron chain length and its projection on the z -axis. The chain length ℓ_{chain} is:

$$\ell_{chain} = [\nu] \ell_P \quad (529)$$

where ℓ_P is the Planck length and $[\nu] = \nu/1\text{Hz}$ is a pure number numerically equal to the frequency. The projection of this chain length on the z axis is obtained via Eq. 525 as:

$$\ell_z = \frac{\zeta}{\sqrt{r^2 + \zeta^2}} [\nu] \ell_P = \frac{c_{ph}}{c} [\nu] \ell_P \quad (530)$$

The above equation provides the longitudinal extent of the particle (photon/electron), so that together with the lateral extent by Eq. 528 we have a geometrical representation of the particle, provided we know the planckion speed c . We proceed to obtain the latter as follows:

We note that the quantity $4\pi^2\nu^2 r^2$ in Eq. 527 is invariant but as yet unknown, because the two velocities are constant. However, this is known at the unitary frequency of 1Hz for a single planckion mass m_P having an energy $E_P = h \cdot 1\text{Hz}$

$$E_P = m_P 4\pi^2 (1\text{Hz})^2 r_1^2 = h \cdot 1\text{Hz}$$

where r_1 designates the radius at the unitary frequency:

$$r_1^2 = \frac{h}{m_P 4\pi^2 \cdot 1\text{Hz}}$$

Then the constant (invariant) term is found to be:

$$4\pi^2\nu^2r^2 = 4\pi^2 \cdot (1\text{Hz})^2 \cdot r_1^2 = \frac{h \cdot 1\text{Hz}}{m_P}$$

where we recognize that the last member of the equation provides the conventional velocity of the photon:

$$4\pi^2\nu^2r^2 = c_{ph}^2 = \omega^2r^2 \quad (531)$$

In that case, we can find the planckion velocity from Eq. 527 as:

$$c = \sqrt{2}c_{ph} \quad (532)$$

whereby the longitudinal velocity and the circumferential velocity of the electrion/photon each being equal to the photon velocity c_{ph} add in quadrature like:

$$c^2 = c_{ph}^2 + c_{ph}^2$$

This is also a direct consequence of the spiral motion of a chain particle, and there must be a 45° angle forward motion. Thus, we have a numerical value for planckion velocity $c = 4.23970560 \times 10^8 \text{ ms}^{-2}$. We think that the total energy is double than that appearing to our experiments, due to presumably the fact that one of these components is carried forward in all transitions and transfers including our to instruments, and goes undetectable. Then, we must also revise the total energy of a photon by a factor of 2, which does not appear as a total in our measurements, because half of this is always carried over internally, while the other half appears as output in our measuring system. This may be seen like the “zero-point” energy of a quantum mechanical system at the ground state, e.g. like the ground state of the quantum harmonic oscillator associated with energy $E = \hbar\omega/2$. We have now arrived at an absolute minimum invariant quantum “grain” of $E_P = h \cdot 1\text{Hz}$, which is already provided in our Table 41 of revised Planck units.

We also note that the number of helical pitches (wavelengths) per unit time is equal to the number of planckions (frequency), so that the helix angular frequency coincides with the photon frequency, i.e. $\psi = \omega t$ and the helix equations can be written as:

$$x = r\cos\psi = r\cos\omega t \quad (533)$$

$$y = r\sin\psi = r\sin\omega t \quad (534)$$

$$z = \zeta\psi = \zeta\omega t = c_{ph}t \quad (535)$$

The helical trajectory is determined (prescribed) during the emission of the relevant particle.

Now, it is interesting to find some numerical values of the radius and the length for various cases. One case to investigate is the visible spectrum, for which we consider the green light in the middle of it. For a frequency $\nu = 5.5 \times 10^{14} \text{ Hz}$ (with $\lambda = 5.45 \times 10^{-7} \text{ m}$), we obtain a helix radius $r = 8.68 \times 10^{-8} \text{ m}$ and a length $\ell_z = 6.29 \times 10^{-21} \text{ m}$ as projected on the z -axis from an electrion with spiral length $\ell_{chain} = 8.89 \times 10^{-21} \text{ m}$. We find a radius (lateral extent) within one order of magnitude of the wavelength of the particle. However, the longitudinal size is by many orders of magnitude shorter than the radius, which results in a transit time along the z -axis equal to $t = \ell_z/c_{ph} = 2.10 \times 10^{-29} \text{ s}$. The chain length lies on an arc subtending and angle ψ_{chain} :

$$\psi_{chain} = 2\pi \frac{\ell_z}{\lambda} \quad (536)$$

yielding for the green light photon $\psi_{chain} = 7.25 \times 10^{-14} \text{ rad}$.

Another worthwhile case is for gamma rays. Specifically, we consider the gamma rays emitted during the “annihilation” in an electron-positron interaction. Each of the two gamma rays produced has a frequency of $\nu = 1.24 \times 10^{20} \text{ Hz}$; the corresponding quantities are: $\lambda = 2.43 \times 10^{-12} \text{ m}$, $r = 3.86 \times 10^{-13} \text{ m}$, $\ell_{chain} = 2.00 \times 10^{-15} \text{ m}$, $\ell_z = 1.41 \times 10^{-15} \text{ m}$, $t = 4.71 \times 10^{-24} \text{ s}$ and $\psi_{chain} = 3.66 \times 10^{-3} \text{ rad}$. In comparison with the green light, this gamma ray is very much elongated along the axis and very much squeezed laterally. However, the longitudinal size still remains much shorter than the radius.

Both of the above numerical examples seem reasonable (plausible) and quite revealing, or at least inspiring: The photons/electrions are relatively short segments of a planckion chain that does not complete one single spiral turn. They are only a small fraction of one coil turn, as determined by Eq. 536. They are almost straight line arc structures tumbling (rotating) along a helical path. This is possible according to the explanation provided in Section 30.3. This possibility for a photon structure can still explain the

photoelectric and related effects. Furthermore, it can still produce the observed interference patterns as expected by a structure characterized by a wavelength. All this now provides a rational understanding of the dual nature of photons. The short chain structures are essentially “particles” propagating along a spiral path, which exhibits the wave properties when projected on an observing screen. This also explains the “single” photon wave interference phenomenon, whereby single photons appear as single specks on a screen, but when they accumulate, they integrate over time to form the apparent wave patterns.

We compile the above examples together with further cases of interest in Table 47. For investigation purposes, we can get an idea of the spatial extent of the one helical turn length given by Eq. 524 and re-written as:

$$\ell_{turn} = 2\pi\sqrt{\frac{\lambda^2}{4\pi^2} + \frac{c_{ph}^2}{\omega^2}} = \sqrt{2}\lambda$$

If this one-turn helical length were to be populated fully by planckions, we would have a frequency of ν_{turn} of a hypothetical photon (particle) with exactly one helical unit. This is found from the total number of planckion lengths in that unit turn by:

$$\nu_{turn} = \frac{\ell_{turn}}{\ell_P} \cdot 1\text{Hz} = \frac{\sqrt{2}\lambda}{\ell_P} \cdot 1\text{Hz} \quad (537)$$

However, in this special case, we must also have that $\lambda = \lambda_{turn}$, which is connected to the frequency via $\lambda_{turn} = c_{ph}/\nu_{turn}$ as:

$$\nu_{turn} = \frac{\sqrt{2}\lambda_{turn} \cdot 1\text{Hz}}{\ell_P} = \frac{\sqrt{2}c_{ph}}{\ell_P\nu_{turn}} \cdot 1\text{Hz} \quad (538)$$

finally yielding:

$$\nu_{turn} = \sqrt{\frac{\sqrt{2}c_{ph}}{\ell_P} \cdot 1\text{Hz}} = 5.12 \times 10^{21} \text{ Hz} \quad (539)$$

The corresponding radius reaches a value of r_{turn} at (per Eq. 531):

$$r_{turn} = \frac{c_{ph}}{2\pi\nu_{turn}} = 9.32 \times 10^{-15} \text{ m}$$

with a corresponding wavelength:

$$\lambda_{turn} = \frac{c_{ph}}{\nu_{turn}} = 5.85 \times 10^{-14} \text{ m}$$

The transit time is $t_{turn} = 1.95 \times 10^{-22} \text{ s}$, $\ell_{chain} = 8.28 \times 10^{-14} \text{ m}$, $\ell_z = 5.85 \times 10^{-14} \text{ m}$ and, of course, $\psi_{turn} = 2\pi \text{ rad}$, i.e. for one turn.

As another reference example (case), we can keep increasing the frequency until a maximum limiting value ν_{max} is reached. Then, the maximum chain length should occur at the minimum wavelength $\lambda_{min} = \ell_P$, for which this maximum possible frequency is:

$$\nu_{max} = c_{ph}/\ell_P$$

The corresponding minimum radius would be (per Eq. 531):

$$r_{min} = \frac{c_{ph}}{2\pi\nu_{max}} = \frac{\ell_P}{2\pi}$$

which should be forbidden on account of it being less than the Planck length. We may make it a condition for the radius to be equal to the Planck length, or maybe better for the diameter to be equal to the Planck length. In the latter case, working backwards, then, we should set

$$2r_{min} = \ell_P \quad (540)$$

so that a revised maximum frequency should be:

$$\nu_{max} = \frac{c_{ph}}{2\pi r_{min}} = \frac{c_{ph}}{\pi\ell_P} = 5.90 \times 10^{42} \text{ Hz} \quad (541)$$

with

$$\lambda_{min} = \pi \ell_P = 5.08 \times 10^{-35} \text{ m}$$

and

$$\ell_{chainmax} = [\nu_{max}] \ell_P = \frac{\nu_{max}}{1\text{Hz}} \ell_P = \frac{c_{ph}}{\pi \ell_P \cdot 1\text{Hz}} \ell_P = \frac{1}{\pi} c_{ph} \cdot 1\text{s} = 9.54 \times 10^7 \text{ m}$$

along with the remaining parameters provided in the same table. Finally, the maximum energy for the above structure would be:

$$E_{max} = h\nu_{max} = 3.91 \times 10^9 \text{ J} \quad (542)$$

which is twice the value of the “Planck energy” tabled by Wikipedia contributors (2024f); this is because we equated the diameter of the helix to the Planck length unit (but we can revise it as we see fit). This maximum length and energy of this helical particle may or may not exist in reality, something to be determined by cosmology, particle physics and theoretical physics. Actually, we further discuss the possibility that this may actually be the gravion for gravity.

An opposite extreme case is to consider a single planckion for a frequency $\nu_{single} = 1 \text{ Hz}$. In the tabulated numerical outcomes, we note that the wavelength (pitch) is numerically equal to the speed of light and its radius a little less than one order of magnitude shorter; that is, the planckion travels one helical turn spanning the same large spatial distances. However, the projected length and transit time of the single planckion along the z -axis are shorter than the Planck length and Planck time, which may not be allowed. In that case, we can revise it with a case where the latter two parameters (ℓ_z and t) are equaled to their Planck units (see bold face numbers in the table), so that, working backwards, we obtain the case named “electron43” in the same table. This particle is like one of the planckions forming the electrion assumed in Table 43 based on the model of Fig. 88, except that we previously assumed (arbitrarily) that the electrion is populated by $y = 10^{10}$ such planckions; in that model, the radius was not constrained and we could assign an arbitrary number of planckions to the electrion. However, it is the interaction time (here transition time $t = t_2$) that determines the strength of the field, whereas the chosen value of y inversely affects only the number density of the particles n_0 (not the g_{02}); this explains the objective difference between these choices of modeling: In the former model of Fig. 88, we did not have the constraints that we have in the last model of Fig. 89 among its parameters.

However, the above single planckion case, when modified to allow for the Planck size restriction, yielded a fractional frequency of $\nu_{single} = 1.4 \text{ Hz}$, which bears doubtful physical meaning, if we also have to have an integral number of planckions. There are two ways to overcome this hurdle, or dilemma: One way is to assume that only more than two planckions are allowed (discounting the “single” planckion case). The other way is to assume that the real Planck length ℓ_{realP} , i.e. the planckion itself is actually longer by

$$\ell_{realP} = \frac{c}{c_{ph}} \ell_P = \sqrt{2} \ell_P \quad (543)$$

where the known (measured) Planck length ℓ_P is only the projection of the real one on the z -axis of propagation. In that case, we can revise the preceding numerical examples by the factor $\sqrt{2}$ that allows the use also of a single planckion on the helical path being projected correctly and compatibly on the axis of propagation (regarding the Planck size limitation). The chain length of the green light and of the gamma rays should then be longer by this factor $\ell_{chain} = \sqrt{2} \ell_P [\nu]$ yielding also a longer projection $\ell_z = [\nu] \ell_P$. Interestingly, the Planck time t_P remains invariable in both of the above ways for resolving this issue. Having discussed this issue, we can continue with the tabulation of further cases even without using the presumed “real” Planck length, because this is not necessary for some other useful conclusions to be arrived at. If we later decide to adopt the “real Planck length”, we can easily update the numerical values in this table by the $\sqrt{2}$ factor.

In continuation for next case, we use the values of the electrion of Table 44 as given for $\ell_z = 3.79 \times 10^{-23} \text{ m}$ and $t = 1.27 \times 10^{-31} \text{ s}$ and find now the interdependent parameters given in Table 47 in the name of “electron44”. For this case, the constrained frequency must be revised to be $3.32 \times 10^{12} \text{ Hz}$ with the same number of planckions as opposed to the arbitrarily assumed $y = 10^{10}$ planckions in the former model of Fig. 88.

We repeat the above adjustment for the electrion of Table 45 providing $\ell_z = 1.62 \times 10^{-30} \text{ m}$ and $t = 5.39 \times 10^{-39} \text{ s}$, and find the corresponding parameters for the “electron45”. The constrained frequency is now $1.41 \times 10^5 \text{ Hz}$ with the same numerical value for the number of planckions as opposed to the assumed $y = 10^5$ planckions in the former model.

For the gravions, we previously assumed a straight line configuration. If we wanted to think that the gravions also exist in a helical formation, then we can repeat the same above adjustments as we did for electrions. We show the outcomes for “gravion43”, “gravion44” and “gravion45” in the same Table 47. We

CASE	ν Hz	λ m	r m	ℓ_{chain} m	ℓ_z m	t s	ψ_{chain} rad
green light	5.50E+14	5.45E-07	8.68E-08	8.89E-21	6.29E-21	2.10E-29	7.25E-14
electron/positron γ	1.24E+20	2.43E-12	3.86E-13	2.00E-15	1.41E-15	4.71E-24	3.66E-03
one turn	5.12E+21	5.85E-14	9.32E-15	8.28E-14	5.85E-14	1.95E-22	6.28E+00
max frequency	5.90E+42	5.08E-35	8.08E-36	9.54E+07	6.75E+07	2.25E-01	8.35E+42
single planckion	1.00E+00	3.00E+08	4.77E+07	1.62E-35	1.14E-35	3.81E-44	2.40E-43
electrion43	1.41E+00	2.12E+08	3.37E+07	2.29E-35	1.62E-35	5.39E-44	4.79E-43
electrion44	3.32E+12	9.03E-05	1.44E-05	5.37E-23	3.79E-23	1.27E-31	2.64E-18
electrion45	1.41E+05	2.12E+03	3.37E+02	2.29E-30	1.62E-30	5.39E-39	4.79E-33
gravion43	3.35E+31	8.95E-24	1.42E-24	5.41E-04	3.83E-04	1.28E-12	2.69E+20
gravion44	7.86E+43	3.81E-36	6.07E-37	1.27E+09	8.99E+08	3.00E+00	1.48E+45
gravion45	3.35E+36	8.95E-29	1.42E-29	5.41E+01	3.83E+01	1.28E-07	2.69E+30

Table 47: Parameters of helical structures for various cases

note that the case of “gravion44” requires a helix radius and pitch (wavelength) much shorter than their Planck units, and hence this case cannot exist if we adopt the present helical model.

31.4.2 Phase velocity versus group velocity

In quantum mechanics, we have a description of the motion of the wave packet. Thereby, we distinguish the speed of the plane wave vs. the speed of a modulating function (envelop). The wave packet describes the dynamics of a particle and it is highly localized. The wave packet is constructed by the superposition of a large number of plane sinusoidal waves. They constructively interfere in a tiny region of space and destructively interfere everywhere else. Solving the Schrödinger equation yields a plane wave solution.

$$\Psi(z, t) = \frac{1}{\sqrt{2\pi}} \int_{-\infty}^{+\infty} \phi(k) e^{i(kz - \omega t)} dk$$

where k is the wave number $k = 2\pi/\lambda$ and ω is the angular frequency. The phase or wave velocity v_p in a non-dispersive medium is given by

$$v_p = \frac{\omega}{k} = \frac{E}{p} = \frac{E}{E/c_{ph}} = c_{ph}$$

which is a mathematical function not yet describing an actual particle. The group velocity v_g is given by

$$v_g = \frac{d\omega}{dk} = \frac{dE}{dp} = \frac{dE}{dE/c_{ph}} = c_{ph}$$

The above is for a photon traveling in vacuum, or in a non-dispersive medium yielding

$$v_p v_g = c_{ph}^2$$

For a relativistic particle

$$E^2 = m_0^2 c_{ph}^4 + p^2 c_{ph}^2$$

and the phase velocity is

$$v_p = \frac{E}{p} = \frac{\gamma m_0 c_{ph}^2}{\gamma m_0 v_g}$$

$$v_p v_g = c_{ph}^2$$

For a relativistic particle, which can never reach the speed of light, the phase velocity is always greater than the group velocity. It is said that “*the phase velocity does not represent anything physical*” and that the wave packet (wave function) is a complex function serving as a solution of the Schrödinger equation. This can best predict how the quantum mechanical system will evolve: The phase velocity does not have a physical nexus with the particle, only the group velocity has a physical connection with the particle. Mathematically, it is said that in a certain case, we can have group and phase velocity being equal in a non-dispersive medium, otherwise “*it can be less, equal, or greater in dispersive media depending on the circumstances*”.

31.4.3 Comparison of models, theories and discussion

It is worthwhile to repeat that, in working out the numerical examples in Table 47, we have been faced with the dilemma where or how to apply the Planck length as an absolute minimum distance of the universe. We opted to identify it with the minimum helical pitch, presumably this being the measurable parameter in our hitherto experiments. That could mean that we measure the projection of the actual minimum length of the planckion on the helical path being $\ell_{Preal} = \sqrt{2}\ell_P$. In this instance, we should adjust all of the parameters of the table by this square root factor accordingly. For now, we need not revise the outcomes of all the associated preceding tables pertaining to the two helical models until we can finally confirm (or feel confident about) the correct model to be used for electrions and gravions. We only assume that the helical structures studied herewith constitute ingredients, or elements, of various super-structures of gravions, electrions, and photons to be worked out later.

It is interesting to note also that the longitudinal transit time of a given particle can be effectively the interaction time discussed and enumerated in Tables 43, 44 and 45. As discussed previously, the interaction times are critical to establish first. The “size” (like frequency, length, radius, etc.) can be derived from the interaction times and, finally, we can work out the number density and flux intensity of various push particles determining the corresponding fields. The field strength is primarily determined by the interaction time and not by the size of the push particle, as a whole, which intuitively was thought to be the case at the outset of our PG theory. On the contrary, we now realize that “bigger” push particles can be associated with weaker strength and lower number density fields. So far, we have only pointed out trends in working out a finalized PG theory.

Actually, the particle with maximum frequency $\nu_{max} = 5.90 \times 10^{42}$ Hz suits our requirements for the gravion. Seeing now that the gravion of Table 44 with $x = 5.56 \times 10^{43}$ planckions is not permitted, the next possible highest frequency ν_{max} (and energy) particle yields a gravitational field with maximum acceleration:

$$g_0 = \frac{c_{ph}}{t_{max}} = 1.33194 \times 10^9 \text{ ms}^{-2} \quad (544)$$

where we used as interaction time $t_2 = t = 2.25 \times 10^{-1}$ s from the table. This may be correct or close to the correct one subject to a correction by factors like π or $\sqrt{2}$. We may start looking for this value by conjecture, as it should be actually measurable by the methods proposed in Section 12. In this case, the corresponding constants for the gravitational field would be: $J_0 = 8.07 \times 10^{35} \text{ J}\cdot\text{m}^{-2}\text{s}^{-1}$, $u_0 = 5.39 \times 10^{27} \text{ J}\cdot\text{m}^{-3}$, $n_0 = 1.38 \times 10^{18} \text{ \#}\cdot\text{m}^{-3}$ and $\Lambda_0 = 1.57 \times 10^{-19} \text{ m}^{-2}$. We wonder if the smallest cross-section (diameter) possessed by this particle can explain its penetrability through ordinary bodies as expected for gravions from the outset of this theory. The cross-section of particles with helical structure is inverse to the number of planckions spanning an entire possible range from the Planck length to planetary and presumably astronomical sizes. We discussed this possibility in the gravion-gravion (now, planckion-planckion) interaction per Section 30.3. An absorption may be expected when the radius is comparable with other particle sizes with which they create a resonance for an interaction to take place. These possibilities are just mentioned at this stage pending further development for a better understanding of the actual situations.

The spiral configuration of electrions proposed now can replace the helical toroidal vortices in Fig. 76 and still explain the “attractive” and “repulsive” forces between electrons and positrons accordingly in the same way. The prior modeling was not binding us from using alternative working models, as it was introduced only as a starting possibility to move forward in the development of our theory. We may still retain the previous model, but the simpler models in Figs. 88 and 89 may be used at least as a precursor to more complex configuration of possibly helical toroidal vortices describing photonic structures. It is important also to note that our modeling explains the spin of photons as being a real physical property. The thrust of this speculative discussion here aims to invite other workers to consider a similar approach for modeling the actual data available in particles physics.

In the above, we have a similarity or connection between electrions and photons, which begs further questions and requirements. We have said that electrions mediate the electric field and that the electrions, if they have a photonic nature must correspond to a very long wavelength, for which we have no experimental measurements. We have no corresponding “atoms” yielding corresponding orbital transitions at such

wavelengths. However, electrons may still generate these push particles via a mechanism already proposed in Section 25. The above helical model may explain a corresponding mechanism of photon generation from electron transitions between orbitals around atoms. The electron/positron structure proposed by Fig. 76, contains sub-units of MAC/MEC with circular planckion chains. The latter can be generated by a mechanism depicted in Fig. 84 together with the gravion (now planckion) attributes. It is then plausible that these internally circular chain structures can be emitted as helical structures during the required shedding of hyle (matter) at lower orbitals in the atomic structure of electrons. In gravity, there is a steady-state exchange of gravions between a two-body-system and the surrounding gravion medium, but there is an emission/absorption of hyle (matter) when the inter-body distance varies; this claimed emission is as yet undetected. Likewise in electricity, there is a steady-state exchange of electrions between a two-body-system (exhibiting charges) and the surrounding electrion medium, but there is (again) an emission/absorption of hyle (matter) when the inter-body distance varies. The latter variation appears here as photons, but gravitational emission/absorption is imperceptible (up to date). The observed photons in electricity can be agglomerations, or configurations, or some forms of organized electrions.

These ideas seem also consistent, to a certain extent, with existing mathematical concepts describing particles, as is summarized in the preceding section for the prevailing photon theory (group and phase velocity, etc.). However, we see no advantage or an overwhelming superiority of the prevailing theory in describing the photon. The latter is an arbitrary mathematical analysis, which is thought to represent reality and physical processes. It is not less arbitrary than our simple mechanical model of a helical structure of planckions. We start with a physical description of a possible system (model) and derive its mathematical representation, which contains similar terms, albeit not identical, with prevailing theory. We have reconfigured the photon in a structure that retains the observed wave nature and measured wavelength. Together with it, we provide the energy of the photon to be again $h\nu$ as required to explain the particle nature of the photons in the photoelectric and related effects. The “dual” nature may have finally been resolved and comprehensively understood.

The customary wavenumber $k = 2\pi/\lambda$ corresponds to our $1/\zeta = 2\pi/\lambda$ for the helix pitch $\lambda = 2\pi\zeta$. A particle may be constructed by a combination of helical structures with numerically neighboring pitches in a given range of values corresponding to the mathematical superposition of waves in a corresponding range of wavenumbers. Looking at the generation of circular motion by gravions (now planckions) in Fig. 86, we can see the increasing angular frequency with decreasing radius. We can visualize a given narrow range of radii forming an annulus. We can then elongate the circular motion to a helical one according to the above model during emission by a “big” particle like an electron. A particle (like a photon/electrion) is thus formed and transmitted with parameters as required by current theories but also with a palpable structure better understood by PG theory. Thus, our model is compatible with quantum mechanics ideas providing, in addition, a tangible basis for understanding what otherwise presents as an abstract mathematical derivation waiting to be given a physical substance. We may be close to achieving this purpose, while we are open to further refinements in order to fit the model with all experimental data in particle physics.

After the above work was completed, a literature survey produced a relevant work by Gauthier (2019). He has reviewed various helical models of the photon proposed in prior works, all of which fundamentally differ from our simplest and independently derived model. However, there is a remarkable coincidence in the form of helical structures, which necessitate an exposition and comparison below.

We quote from Gauthier’s conclusion: “*An internally-superluminal double-helical quantum-mechanically self-entangled oppositely-charged- dipole model of the photon is proposed. It can transform into a relativistic electron and positron, each composed of a superluminal half-photon having a quantitative geometrical continuity with the double- helix photon model. The photon and electron models provide a new way to view the zitterbewegung frequency description of the electron coming from the solution to the Dirac equation for a relativistic electron.*” This model of the photon allows the production of an electron-positron pair by the: “*double-helix composite structure of two mutually circulating oppositely-charged single-helix half- photons that separate during electron-positron pair production and curl up their trajectories to become a quantum vortex electron and a quantum vortex positron pair. A second key feature is that both the double-helix photon model and the quantum vortex electron and positron models are proposed to be internally superluminal by means of a proposed helically-circulating electrically-charged point-like superluminal energy quantum. This internal superluminality is maintained before and after the transformation process, even though the double-helix photon model itself moves forward at light speed and the quantum vortex electron and positron models move forward at sub-light speeds*”. He further states: “*...each spin- $\frac{1}{2}$ half-photon is composed of an electrically charged superluminal energy quantum moving helically at $c\sqrt{2}$ with a forward helical angle of and with a helical radius of $\lambda/2\pi$ and diameter λ/π , where λ is the wavelength of the composite photon model.*”

In Gauthier’s Fig. 1, the photon is depicted as two moving quanta (which are actually point-like) moving

on forward 45-degree helical trajectories. He further provides a detailed derivation of the momentum and spin equations of the helix.

The similarities of Gauthier’s model and ours stop at the description of a generally helical structure of the photon as contained in the above quotations. Apart from that, however, our PG model is fundamentally different from Gauthier’s. He relies on the preexisting concept of “charge” and the thereby electric forces to maintain the traveling helical configuration, whereas this is not necessary according to our theory of charge and the planckion modeling. We maintain that there is no electric “field” driving the internal structure of the photon at this low level of planckion configuration. We maintain that the electric field arises above and outside the electron/electrion/photon structures. The electric field is a consequence of pushing effects of these entities (particles). However, our model might be closer to an earlier idea: “*In 1995 Gauthier [21] (Gauthier, 1996) proposed his first internally superluminal model of the photon, with each photon composed of millions of subquantum helically-moving microvita—hypothetical entities proposed to compose physical particles. This model was transformed by Gauthier [9] into an internally superluminal charged dipole double-helix photon model.*” This “microvita”(*) idea is based on earlier Indian religious theories (with Gauthier having being a yogic monk himself). We then may say that they (their ideas) correspond to our planckions in our current development of PG, however, a concept subsequently denounced by Gauthier. In addition, there is no suggestion of the electric field being mediated by some pushing particles flow. It seems that in his later effort to provide a scientific basis to religious concepts by accepting prevailing physics, he unwittingly re-enforces a religious interpretation of current physics. We stand to differ on all this by our PG theory. We can agree more with the “yin-yang”(**) Chinese concept, as the dialectic counterpart of the union of opposites, etc., which alone does not take us far enough either, until we propose an analogous/appropriate model as is done for the gravion (now planckion) system in our theory earlier.

We have also arrived at a similar proposal of “*curling up*” of helical formations for our planckions in sufficient numbers to create an electron/positron. The “double helix” configuration for photons seems reasonable to create a “neutral” (non-polar) particles; a class of photons may also serve as push particles to mediate attractive fields (without polarity), whereas single helices acting as push particles can explain fields with polarity (positive and negative charge). However, multiple helical structures leading to a helical toroidal configuration for electron/electrion/photon can also generate fields of various kinds. The semi-classical model of a distributed electron charge with helical solenoid geometry proposed by Consa (2018) can be adapted to form an organization of planckions (former gravions) as can be seen in our discussion in 25: “*The notion of quarks may be compatible particles per above: Quarks may be combinations of MECs (MACs) in such a way that we may bridge experimental data with our theory. For this purpose, the electron model proposed may be a model for each quark existing in stable triplets. or having three pairs of MECs in some alternative stable configuration. Furthermore, the display of zitterbewegung at the Compton scale may also be exhibited by modeling around the proposed scheme in Fig. 76, which may also be consistent with certain QED aspects.*” Again, we do not need a separate entity of charge. Both “charge” and “mass” are only mathematical parameters emerging out of the flow of corresponding pushing particles. We have only proposed a variety of possibilities as an incentive to select from by new-comers in PG theory.

In the bigger objective of our work, we welcome Gauthier as a positive contribution in support of a helical structural unit for the photon and much more. We can keep the common ideas while maintaining the bigger framework of a general PG theory. We must also stress that not all particular models and proposals made by us are without fault; we also welcome all criticism and alternative ideas and proposals in support of PG.

(*) “*Microvita are subtle, sub-microscopic living entities that organize energy to create forms, structures and processes in the universe*”. They are supposed to have godly like properties, they are themselves aware,, etc.

(**) From Wikipedia contributors (2024g): “*Yin and yang is a Chinese philosophical concept that describes two opposing but complementary forces that are interconnected and self-perpetuating: Yin: The female, cold, dark, and passive power Yang: The masculine, light, and warm power Yin & Yang: Symbolic Meaning & Connection to Yoga - Yoga ... Yin and yang are core elements of Chinese cosmogony and are seen as influencing health and order in the universe. The balance of yin and yang is essential for harmony and health.*”

31.5 On maximum gravitational acceleration g_0 value, field unification and novel cosmology

The resultant possible value of the maximum acceleration g_0 yielded by Eq. 544 is now the subject of further investigation, which also spurs on to a quantitative field unification.

A new understanding for a possible interconnection between gravitational and electric fields has emerged. By extrapolation, we may also be able to connect all fields including the strong and weak force. We can establish an equivalence between classical “charge” and effective mass with a precise numerical equivalence factor as a result of the push field principle.

We proceed first with a consolidation of a fixed value for g_0 by alternative approaches. All this has been prompted by various novel findings and considerations making a new opening for cosmology.

31.5.1 g_0 from helical gravion

Whereas the helical structure shown in Fig. 89 was initially proposed for the electrion, we now extend it to apply also for the gravion, and possibly for other push particles in various force fields. This is born out by the current investigations.

The maximum gravitational acceleration g_0 depends on the interaction time of the gravion, which, in turn, depends on the interrelated properties of the proposed helical structure: The axial length of the helical chain, depends on the helical length of the gravion ultimately determined by the assumed radius and the concomitant frequency (or wavelength) of the helix. We are initially concerned about the way we calculated the gravion length as being equal to the curved spiral path length, namely, by the product of the frequency times the unit length of the planckion. An assumed straight line length of the planckion taken as $\ell = \ell_P$ actually subtends a helical arc length being longer than the planckion length, if the planckion is thought to lie on the cord and not on the arc. These two lengths are practically equal at sufficiently low frequencies with large radii. However, they become significantly different when the helix radius approaches close to the planckion length ℓ at very high frequencies, particularly close to the limiting maximum possible frequency ν_{max} . For this reason, we have thoroughly examined both cases and we have come to the conclusion that each planckion in the gravion chain should follow along the exact curved helical path and not along the attached cords. In other words, the planckion does not change direction abruptly along the adjacent cords, but the “oscillating” (moving) constituents of the planckion (see model in Figs. 81 and 82) follow the helical path. This is consistent with the principal idea proposed in Section 30.2 for gravion (now planckion) modeling. The planckions (formerly gravions) are tumbling around while they are internally pulsating. This tumbling is not governed by (or associated with) centripetal (or centrifugal) or any other gravitational or other field forces, as they do not yet exist at this fundamental level. All these known forces by various fields evolve at higher levels of physical structures, as all fields are due to pushing entities. At the planckion level, we see only the “trees” and not the “forest”. Thus, we say that the planckions in a gravion chain are tumbling along-and-around a helical path without the need of any preexisting external field forces, while internally its components are pulsating in the general manner described by our model. An internal observer is not aware of the tumbling movement observed only externally. It would not be possible or easy to explain or assign a “zig-zag” movement of each planckion along the cords of our helical configuration. In fact, our results that follow below support exactly the concept of the tumbling motion along the helical path. This also supports the preceding formulations of the helical chain. We now extend and present the same analysis for two cases of an assumed planckion length, namely, for $\ell = \ell_P$ and $\ell = \sqrt{2}\ell_P$. We have already mentioned the possibility that our previous results may need an adjustment by the factor of $\sqrt{2}$, which can be justified by the outcomes obtained.

For convenience, we summarize the equations used in compiling the results for these two cases in Tables 48 and 49.

$$\lambda = 2\pi r$$

$$\nu = \frac{c_{ph}}{2\pi r}$$

$$\ell_{chain} = [\nu] \ell$$

$$\ell_z = \frac{[\nu] \ell}{\sqrt{2}}$$

$$t = \frac{\ell_z}{c}$$

$$\psi_{chain} = 2\pi \frac{\ell_z}{\lambda}$$

$$g_0 = \frac{c_{ph}}{t}$$

These formulae are now used for a range of radii starting from the minimum radius of $r = \ell/2$ followed by multiples of $r = n\ell/2$ with $n = 1, 2, 3...$

We note that in both cases the resulting ℓ_{chain} , ℓ_z , t and g_0 are the same, whilst ν , λ and ψ_{chain} vary by the factor of $\sqrt{2}$, as they all should behave according to the above governing equations. For g_0 being of particular interest, we further note that it increases also by multiples of $n = 1, 2, 3...$. Thus, if an overall g_0 is caused by gravions with a helical configuration, then it could be the result of a series of different length

r	ν , Hz	λ , m	$\ell_{chain,m}$	ℓ_z , m	t , s	ψ_{chain} , rad	g_0 , ms ⁻¹
0.5	5.90E+42	5.08E-35	9.54E+07	6.75E+07	2.25E-01	8.35E+42	1.331943E+09
1	2.95E+42	1.02E-34	4.77E+07	3.37E+07	1.13E-01	2.09E+42	2.663886E+09
1.5	1.97E+42	1.52E-34	3.18E+07	2.25E+07	7.50E-02	9.28E+41	3.995828E+09
2	1.48E+42	2.03E-34	2.39E+07	1.69E+07	5.63E-02	5.22E+41	5.327771E+09
2.5	1.18E+42	2.54E-34	1.91E+07	1.35E+07	4.50E-02	3.34E+41	6.659714E+09
3	9.84E+41	3.05E-34	1.59E+07	1.12E+07	3.75E-02	2.32E+41	7.991657E+09
3.5	8.43E+41	3.55E-34	1.36E+07	9.64E+06	3.22E-02	1.70E+41	9.323600E+09
4	7.38E+41	4.06E-34	1.19E+07	8.43E+06	2.81E-02	1.30E+41	1.065554E+10

Table 48: Graviton parameters versus helix radius with a “curved” planckion length $\ell = \ell_P$ on the helical path

r	ν , Hz	λ , m	$\ell_{chain,m}$	ℓ_z , m	t , s	ψ_{chain} , rad	g_0 , ms ⁻¹
0.5	4.17E+42	7.18E-35	9.54E+07	6.75E+07	2.25E-01	5.90E+42	1.331943E+09
1	2.09E+42	1.44E-34	4.77E+07	3.37E+07	1.13E-01	1.48E+42	2.663886E+09
1.5	1.39E+42	2.15E-34	3.18E+07	2.25E+07	7.50E-02	6.56E+41	3.995828E+09
2	1.04E+42	2.87E-34	2.39E+07	1.69E+07	5.63E-02	3.69E+41	5.327771E+09
2.5	8.35E+41	3.59E-34	1.91E+07	1.35E+07	4.50E-02	2.36E+41	6.659714E+09
3	6.96E+41	4.31E-34	1.59E+07	1.12E+07	3.75E-02	1.64E+41	7.991657E+09
3.5	5.96E+41	5.03E-34	1.36E+07	9.64E+06	3.22E-02	1.20E+41	9.323600E+09
4	5.22E+41	5.74E-34	1.19E+07	8.43E+06	2.81E-02	9.23E+40	1.065554E+10

Table 49: Graviton parameters versus helix radius with a “curved” planckion length $\ell = \sqrt{2}\ell_P$ on the helical path

gravions all contributing to the maximum acceleration, provided only that all of them do exist and all have the required large mean free paths per PG requirements. Nevertheless, a component of g_0 can be accounted for by gravions with the maximum length at the maximum frequency of either $\nu_{max} = 5.90 \times 10^9$ Hz or $\nu_{max} = 4.17 \times 10^9$ Hz both corresponding to the same minimum possible value of g_0 as provided in the tables.

In the ensuing work below, we report independent developments that attribute a special significance to the very first (minimum) value of $g_0 = 1.33194 \times 10^9$ ms⁻² (with maximum length chain) making it the strongest candidate to be the actual creator of the maximum gravitational acceleration of the universe.

31.5.2 g_0 from the physics of Λ

From the outset of this theory, we have derived Eq. 78 also transferred below:

$$G = \frac{1}{\pi} g_0 \Lambda \quad (545)$$

where $\Lambda = k/\rho$, which it is the number of gravion absorption events per unit area density (\equiv mass thickness). We now further analyze this constant and obtain a better insight about its physical meaning.

We explicitly elaborate that:

$$\Lambda = \frac{k}{\rho} = \frac{\frac{\#absorption_events}{unit_length}}{\frac{mass}{unit_volume}} =$$

$$\begin{aligned}
&= \frac{\#absorption_events}{unit_length} \cdot \frac{unit_volume}{mass} = \#absorption_events \cdot \frac{unit_area}{mass} = \\
&\#absorption_events \frac{area}{unit_mass} = \frac{area}{\frac{unit_mass}{\#absorption_events}} = \frac{area}{unit_absorption_event}
\end{aligned}$$

This expression states that Λ is the area (cross-section) of the material per mass of each absorption event. We also explicitly elaborate that:

$$k = \frac{\#absorption_events}{unit_length} = \frac{1}{\frac{unit_length}{\#absorption_events}} = \frac{1}{\frac{length}{unit_absorption_event}} = \frac{1}{\ell_k}$$

where we have now introduced $\ell_k = \frac{length}{unit_absorption_event}$ as the distance over which a graviton is absorbed in any given density body; it is the inverse of k . We note that our theory postulates that each graviton results only in one interaction absorption (as opposed, for example, to an electron propagating through material bodies and undergoing various elastic and inelastic collisions as it gradually slows down). Thus, we understand that k can assume any possible value from well below and to well above unity. Very large values of it indicate that the absorption takes place over very short distances, for example, in white dwarfs, neutron stars and inside electrons. Ordinary Newtonian bodies have a very low value of k meaning that the average collision (absorption) distance ℓ_k is very large. The ℓ_k allows us to eliminate the parameter k , if we always refer to each individual absorption event in all material bodies. In that case, we have an associated absorption volume $(\ell_k \cdot unit_area)$ with a contained mass $(real_mass)_k$. We transfer this understanding to the above explicit description of Λ , which will provide its physical meaning even in a more tangible way:

$$\Lambda = \frac{k}{\rho} = \frac{1}{\frac{(mass)_k}{\ell_k (unit_area)}} = \frac{unit_area}{(mass)_k} = \frac{area}{unit_ (mass)_k}$$

Now, we can assume or envisage that the minimum absorption mass coincides with a Planck unit with Planck dimensions. Then, we can set $\ell_k = \ell_P$, so that $unit_area = \left[\left(\frac{1}{\ell_P} \right)^2 \right] \ell_P^2$ and $(real_mass)_k = \left[\left(\frac{1}{\ell_P} \right)^2 \right] m_P$ (all units being in SI units) and the above derivation reduces to:

$$\Lambda = \frac{\ell_P^2}{m_P} \quad (546)$$

where the bracketed [] quantity is a numerical proportionality factor between Planck and macroscopic units. It seems that we have found the absolute value of Λ for the gravitational field, at least. It is within the provisions of this Part 3 that we accept the available Planck constants to obtain the value of our universal constant Λ in PG. The above formula means that we know the area of the planckion initially being a square of ℓ_P^2 .

We have trialed circular, square and rectangular shapes to calculate the area of the planckion with combinations of lengths $\ell_P/2$, ℓ_P and $\sqrt{2}\ell_P$ with and without π . We found an exceptional agreement with the preceding results by choosing a rectangle with sides $\pi\ell_P$ and $\sqrt{2}\ell_P$. Specifically, we obtain:

$$\Lambda = \frac{\sqrt{2}\pi(1.616255 \times 10^{-35})^2}{7.372497 \times 10^{-51}} = 1.574237 \times 10^{-19} \text{ m}^2/\text{kg} \quad (547)$$

yielding an acceleration of:

$$g_0 = 1.331899 \times 10^9 \text{ ms}^{-2} \quad (548)$$

which is practically equal (up to the forth decimal place) with the value of the first row ($n = 1$) in Table 49 for a spiral graviton with $\ell = \sqrt{2}\ell_P$:

$$g_0 = \frac{c_{ph}}{t_{max}} = 1.331943 \times 10^9 \text{ ms}^{-2} \quad (549)$$

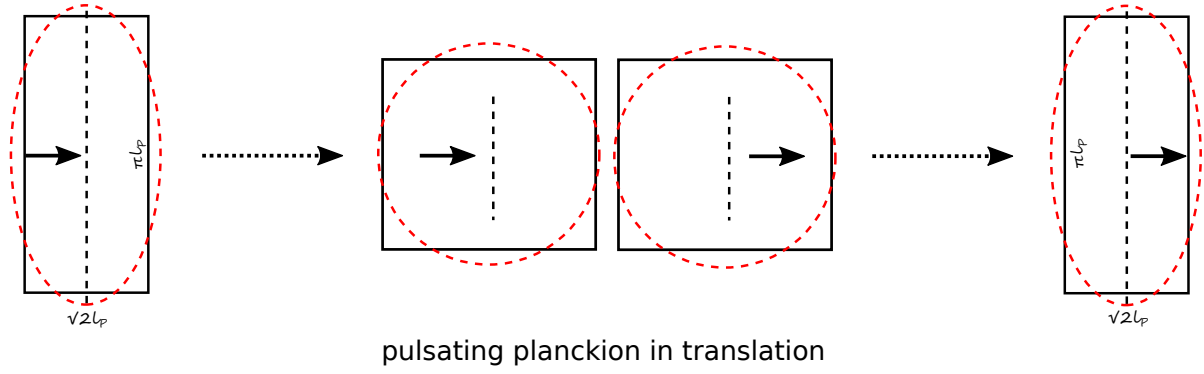


Figure 90: Rectangular shape planckion model pulsating and moving in the direction of pulsation.

This finding, again, is unlikely to be a coincidence. The two derivations are totally independent. The evaluation of Λ has been obtained without any reference to any impacting push particle, like the gravion, in particular. The slight difference may be eliminated in future work by a small refinement of the planckion shape. At present, we are satisfied to visualize a rectangular shape with the above sides. This is also consistent with the concept of a pulsating planckion moving along the direction of the pulsation in accordance with the planckion (formerly gravion) model in Fig. 82. Hence, we may now depict the same model by the scheme in Fig. 90. We have tentatively also “cut the corners” of the rectangle with an ellipsis, but this is to be decided later as we develop our understanding of the actual situation; “curving” (cutting corners) may not be allowed at this fundamental scale, something to bear in mind, as we should only abide by the “rules” we endow to our model of the planckion.

We have arrived at an important understanding of the significance of Λ . It is the cross-sectional area per the most fundamental “mass” in physics, namely, the planckion. We can also better understand the physical significance of the famous universal gravitational constant G now explained by our PG Eq. 545. It is the product of a mass cross-section (provided by a body) multiplied by the universal acceleration g_0 (provided by outer space). This makes perfect sense in deriving the force between bodies as given by Eq. 90. This prompts us to think that it is plausible for Λ to be basically (for starters) the same across all force fields. It may be a true universal constant, literally. For its derivation above, we made no connection to gravity (gravion) or electricity, etc.

However, we can theoretically derive fractional values for Λ by assuming some kind of stacking of a number of planckions above each other presenting the same cross-section but by multiples $n = 1, 2, 3, \dots$ of Planck masses. This situation would result to a subdivision of the Λ by $n = 1, 2, 3, \dots$, which, in turn, would result to multiples of the fundamental value for g_0 for a fixed G exactly as provided in Table 49. This situation would then resurrect the possibility of having to have a series of gravions (per table) with higher g_0 . However, the latter situation is not possible in gravity. This is because the value of Λ provided by Eq. 546 must be uniquely maximum and the force between two bodies is uniquely determined by Eq. 90: Lower values of Λ would require lower values of g_0 (not higher).

Nevertheless, lower values of Λ may be possible for higher strength fields, as we will indeed encounter in special cases. The possibility of stacking a number of planckions inside bodies, which are impacted as a structural unit by a certain type of external push particles (e.g. electrions) may actually exist. A mechanical equivalent for such a situation is given by Newton’s cradle pendulum (Wikipedia contributors, 2025c).

The conclusion is that Eq. 549 is most likely correct and valid based on the compelling convergence of findings by two independent approaches, namely, in this and the preceding sections.

31.5.3 g_0 from field force relationships

If $g_0 = 1.33194 \times 10^9 \text{ ms}^{-2}$ is considered known (given) and, in addition, that it is the outcome from a helical gravion with $\ell = \sqrt{2} \ell_P$ with a maximum frequency of $\nu_{max} = 4.17 \times 10^9 \text{ Hz}$, then it is useful to upgrade Table 46 as shown now in Table 50. This is an interim table of results (like the previous ones), which we need to continue providing as a practical way to demonstrate the progression on field relationships and unification. Otherwise, it would be difficult to convey the development of thought and progress especially needed about novel concepts. This table is based on the possibility for a universal constant value of Λ across all fields, but this will be revised as needed. We will be referring to this table in the ensuing investigation until a subsequent upgrade becomes possible. Noted that these are all theoretical values and there is no need to repeat stating so by the subscript ($_{th}$), whilst the subscript ($_f$) with $f = 1, 2, 3, 4, 5$ is retained to

field type	gravity (01)	weak (03)	electricity (02)	strong (04)	Planck (05)
particle name	gravions	?	electrions	?	planckion
published strength	1.00E+00	1.00E+33	1.00E+36	1.00E+38	4.17E+42
#planckions [ν]	4.17E+42	4.17E+09	4.17E+06	4.17E+04	1.00E+00
<i>particle_length</i>	6.75E+07	6.75E-26	6.75E-29	6.75E-31	1.62E-35
t_f	2.25E-01	2.25E-34	2.25E-37	2.25E-39	5.39E-44
g_{0f}	1.33E+09	1.33E+42	1.33E+45	1.33E+47	5.56E+51
J_{0f}	8.07E+35	8.07E+68	8.07E+71	8.07E+73	3.37E+78
u_{0f}	5.39E+27	5.39E+60	5.39E+63	5.39E+65	2.25E+70
n_{0f}	1.95E+18	1.95E+84	1.95E+90	1.95E+94	3.39E+103
G_f	6.67E-11	6.67E+22	6.67E+25	6.67E+27	2.79E+32
A_f	1.57E-19	1.57E-19	1.57E-19	1.57E-19	1.57E-19

Table 50: Updated comparative values of universal constants for gravitational, weak, electric and strong field applying the published relative strengths between fields with unity strength for gravity with $g_0 = 1.33194E + 09 \text{ ms}^{-2}$. The Planck field has been added as the strongest possible field.

denote any one of the field in each row of the table.

We have up to here used the “published” (in lieu of formerly “adopted”) relative strengths of fields that allow us a quantitative connection between them. Furthermore, we have now added a new field strength in the column under the field name “Planck”. This has emerged by the following considerations.

We start with a highly relevant (and valid) comparison between gravity and static electricity. That is, we can use the known Coulomb (electric) force F_C and simultaneously the Newtonian gravitational force F_N (same as PG force F_{PG}) between two electrons (or an electron and a positron) at any distance r yielding a field strength ratio s :

$$s = \frac{F_C}{F_N} = \frac{\frac{e^2}{4\pi\epsilon_0}/r^2}{Gm_{e-e}^2/r^2} = \frac{\frac{e^2}{4\pi\epsilon_0}}{Gm_{e-e}^2} = 4.1657 \times 10^{42} \quad (550)$$

We immediately note that this value is almost identical to the number of planckions $[\nu] = 4.1749 \times 10^{42}$ in the gravion per Table 50 in conjunction with $\ell = \sqrt{2}\ell_P$ at $r = \ell/2$ with $n = 1$. This numerical outcome is derived quite independently from the previous derivations of the same number. This is an intriguing and extraordinary finding that certainly requires further investigation. Even if one cannot initially exclude some strange coincidence (again?), it can be much more likely that this is governed by an underlying physical structure and mechanism. The slight numerical difference may be explained by the chosen planckion length of $\ell = \sqrt{2}\ell_P$ possibly requiring some second order fine adjustment, as it was also needed in the determination of A . This could be established by the final determination of the planckion model to be adopted for explaining particle physics.

We further note that the number of planckions composing the corresponding push particles in the various fields is inversely proportional to the accepted field strengths. In Table 50, we have plenty of planckions available to construct the electrion chain with 4.17×10^6 units and the “nucleon” (for strong field) with 4.17×10^4 units (planckions). The corresponding times are well above the Planck time, so that we do not have any values in this table breaching the Planck limits.

Consistent with the above relationship between the number of planckions in the push particle chain for each field, we can arrive at an ultimate field with a push particle containing only one planckion. The latter field would have a strength equal to this special number of $[\nu] = 4.1749 \times 10^{42}$. This is how we have been prompted to add the new column for a new field we can call “Plank” field. It remains to be seen if this new field is only theoretical or it exists in reality as well. We subsequently investigate this question in more detail.

We face a new kind of a problem with the “published” field strengths used in the above Table 50. The ratio of strengths between electricity and gravity is taken to be the ratio of $g_{02}/g_{01} = 1.0 \times 10^{36}$. We recognize that the ratio of strengths may not necessarily be the same as the ratio of electrical force over gravitational

force between two bodies, as in the above case between two electrons (positrons). However, in the newly found Planck field, the ratio of strengths of the Planck field over the gravitational field is identical with the ratio of forces of the same fields given that $g_{02}/g_{01} = 4.17 \times 10^{41}$ (see table). This is an initial indication that the Planck field bears at least some relationship with the electric field, or at most the two fields might be identical.

In the latter case, i.e. if this Planck field is identical with the electrical field, we would be forced to reconsider the established (published) relative strengths between all fields. In that case, we might want to adjust the “published” relative strengths for the weak and strong force upwards above the Planck field by 6 orders of magnitude accordingly, i.e. up to 4.1657×10^{44} for the strong field and up to 4.1657×10^{39} for the weak field; this retains the existing relative order of strength for these four fields. However, this would not only seriously upset the published wisdom, but even more importantly, it would require an interaction time for the strong field two orders of magnitude below the limit of Planck time. Therefore, this kind of field strength adjustment cannot be sustained. This provides a contradiction begging for a resolution on account of the actual existence of the force ratio in the two-electron system, namely, the forces ratio of 4.1657×10^{42} by Eq. 550. As a result, we have been forced to accept the Planck field as the strongest possible field (theoretical or real) and place all others below this while retaining their existing relative strengths.

In any case, we have an additional compelling argument that, among the series of theoretical graviton lengths with $n = 1, 2, 3, \dots$ discussed previously, it is only the first one at maximum frequency that is responsible for gravity. That is because the strength ratio s between electrical and gravitational fields is very well determined by objective (existing) measurements in gravity and electricity. If the number of planckions in a push particle is inversely proportional to the strength of the field, then we can only have $[\nu] = 4.1657 \times 10^{42}$ more planckions in the graviton of gravity than the unitary planckion of the Planck field.

At any rate, we defer resolution of the actual strength for each of four or five fields after the following interim and further investigations (under way) later.

31.5.4 Gravitational and electrical properties of proton and electron (positron) from given g_0

Based on the presumed known value for g_0 , we repeat the work in Sections 19.3 and 21 for the properties of the proton and electron/positron and the connection between gravitational and electrical fields. Those sections engaged for a range of unknown values of g_0 , but we are now in a position to re-appraise that work without eliminating it, since it refers to the general case and to which we can always return should the current work under Part 3 provisions be invalidated for some reason. Below, we establish the gravitational properties of proton and electron (positron) followed by their electrical properties and then we work on the quantitative unification between gravity and electricity. For ease of reading and reference, we reproduce the necessary equations as required.

PROTON in gravity: We find the corresponding parameters for proton from Eqs. 145 and 147 given its radius and effective mass; the “charge” radius is used also as the “mass” radius at this stage. The contraction q_{-p} , absorption coefficient k_{-p} and absorptivity A_{R-p} are found in the usual way, except that we now know the value for g_0 and need not compile a table for a range of it. We use the prevailing radius $R_{-p} = 8.414 \times 10^{-16}$ m based on charge collision measurements, and the mass $m_{e-p} = 1.672622 \times 10^{-27}$ kg as its effective mass. Thus, we repeat the needed equations for convenience:

$$g_0 A_{R-p} - \frac{G m_{e-p}}{R_{-p}^2} = 0$$

which we solve for $k_{-p} R_{-p}$ contained in A_{R-p} in order to obtain the contraction factor

$$q_{-p} = \frac{3 A_{R-p}}{4 k_{-p} R_p}$$

and finally, we have the real mas of the proton by

$$m_{-p} = \frac{m_{e-p}}{q_{-p}}$$

The black mass component m_{b-p} is simply

$$m_{b-p} = m_{-p} - m_{e-p} = \frac{m_{e-p}}{q_{-p}} - m_{e-p} = \left(\frac{1}{q_{-p}} - 1 \right) m_{e-p} \quad (551)$$

We compile the numerical outcomes for the proton in Table 51. We find that the contraction factor is very close to unity, which means that the measured (given) effective mass is very close to the real mass.

We have already found that only an extremely small fraction of the real mass is inactive (black), whilst correspondingly the absorptivity is also very greatly lower than unity. All this is based on an adopted (published) radius of the proton, but can be fine tuned by later updates of it. It is important to comprehend the relative magnitudes involved, because they will help us understand the importance of the findings, to which we can arrive from now on.

ELECTRON in gravity: In a series of “exercises” in Section 19.3.2, we assumed that an electron is produced by compressing the proton with constant or variable real mass. We apply the same here, first with constant real mas and arrive at results consistent with experience. These outcomes may then be used to justify the approach used. This method allows us to find the electron properties including its radius.

For constant real mass (i.e. the same for proton and electron), we transfer Eqs. 285 and 286 from the preceding work:

$$\mu = \frac{m_{e-p}}{m_{e-e}} = \frac{q_{-p}}{q_{-e}} = 1836.15267343 \quad (552)$$

where we have canceled the common real mass m and:

$$\mu = \frac{A_{R-p} R_{-p}^2}{A_{R-e} R_{-e}^2} \quad (553)$$

with μ being the known proton-to-electron mass ratio, so that we can find the electron radius as:

$$R_{-e} = \sqrt{\frac{A_{R-p}}{\mu A_{R-e}}} R_{-p} \quad (554)$$

As previously, the contraction factor for the electron is given by:

$$q_{-e} = \frac{q_{-p}}{\mu} = \frac{3A_{R-e}}{4kR_{-e}} \quad (555)$$

yielding the equation

$$\frac{3A_{R-e}}{4kR_{-e}} - \frac{q_{-p}}{\mu} = 0 \quad (556)$$

which we solve first for the product kR_{-e} contained in A_{R-e} and then we find the A_{R-e} . Thus, we find the electron radius by above Eq. 554. We present the results for electron properties in the same Table 51. Like for proton, we find the black (inactive) mass m_{b-e} for the electron (positron) under this particular condition of maintaining a constant real mass $m_{-p} = m_{-e} = m$ by

$$m_{b-e} = m_{-e} - m_{e-e} = \frac{m_{e-e}}{q_{-e}} - m_{e-e} = \left(\frac{1}{q_{-e}} - 1 \right) m_{e-e} \quad (557)$$

Notable is the comparatively large black mass in the electron (positron). We can also find the theoretical limiting radius R_{0-e} by setting $A_{R-e} = 1$ and the small difference between the two radii $R_{-e} - R_{0-e} \equiv \Delta R_{-e}$ due to the small difference of the absorptivity from unity (see also prior Eqs. 283 and 284), but not tabled here for brevity. Since the positron is the counterpart of the electron having the same effective mass, we could imagine the positron as being a compressed proton by the above means, or conversely, the proton as a “blown-up” positron. Please refer to the relevant preceding sections for more information.

If, instead of keeping the same real mass for the electron and proton, we deduct the mass of an emitted neutrino, we can correct the above values, but the difference should very small for the initial practical aims of the current investigation. Actually, the real mass of the electron should be $m_{-p} - m_{-\nu} \pm \Delta m$, where $m_{-\nu}$ is the neutrino mass and Δm is the mass (connected to hyle) exchanged with the surrounding material force fields (gravitational and electrical, and possibly others) as we attempted to incorporate via the fraction $\frac{x}{x+y}$ introduced in Section 19.3.2. and Eq. 552. Then, we should have

$$\frac{m_{e-p}}{m_{e-e}} = \frac{q_{-p} m_{-p}}{q_{-e} (m_{-p} - m_{-\nu} \pm \Delta m)} \quad (558)$$

where we have assumed that the detected neutrino mass has an effective mass equal to its real mass on account of its extremely small size. Then, we obtain the contraction q_{-e} and thereby all other gravitational parameters of the electron in the usual way. We leave this second order of magnitude correction for later work (by us or other contributors), while we first investigate the primary consequences by assuming a constant mass.

GRAVITATIONAL FIELD			
PROTON		ELECTRON	
$k_{-p}R_{-p}$	8.8789143670E-17	$k_{-e}R_{-e}$	1.3771141420E+03
A_{R-p}	1.1838552489E-16	A_{R-e}	9.9999973635E-01
k_{-p}	1.0552548570E-01	k_{-e}	6.4457352862E+27
q_{-p}	1.0000000000E+00	q_{-e}	5.4461702149E-04
m_{-p}	1.6726219230E-27	m_{-e}	1.6726219237E-27
m_{b-p}	1.1138300117E-43	m_{b-e}	1.6717109853E-27
m_{e-p}	1.6726219230E-27	m_{e-e}	9.1093837015E-31
R_{-p}	8.4140000000E-16	R_{-e}	2.1364733127E-25

Table 51: Gravitational properties of proton and electron, all in SI units

ELECTRIC FIELD PROPERTIES OF ELECTRON AND PROTON We proceed further in determining the electron and proton properties relative to the electric field, which is connected with the now given gravitational field of $g_0 = 1.33194 \times 10^9 \text{ ms}^{-2}$. We start with the electron. We transfer the general equations without needing any modifications. Since the real mass m_{-e} of the electron (positron) is taken to be same under both fields (i.e. $m_{2-e} = m_{1-e} \equiv m_{-e}$, we have that:

$$m_{-e} = \frac{m_{e-e}}{q_{-e}} = \frac{m_{2e-e}}{q_{2-e}} \quad (559)$$

or

$$m_{2e-e} = q_{2-e}m_{-e} = \frac{3A_{2R-e}}{4k_{2-e}R_e}m_{-e} \quad (560)$$

The objective radius R_{-e} for the electron (positron) is the same in both fields (i.e. $R_{2-e} = R_{1-e} \equiv R_{-e}$, i.e. without any reference to measurements of it, so that:

$$R_{-e}^2 = \frac{Gm_{e-e}}{A_{R-e}g_0} = \frac{G_2m_{2e-e}}{A_{2R-e}g_{02}} \quad (561)$$

In the usual way, the constitutional equation for the electric field g_{02} is:

$$A_{2R-e}g_{02} - \frac{G_2m_{2e-e}}{R_{-e}^2} = 0$$

where the effective mass m_{2e-e} can be taken from Eq. 557, and the equation to solve becomes:

$$A_{2R-e}g_{02} - \frac{3A_{2R-e}}{4k_{2-e}R_{-e}} \frac{G_2}{R_{-e}^2} m_{-e} = 0$$

or

$$A_{2R-e} \left(g_{02} - \frac{3}{4k_{2-e}R_{-e}} \frac{G_2}{R_{-e}^2} m_{-e} \right) = 0 \quad (562)$$

In the usual way, we find first the unknown product $k_{2-e}R_{-e}$ contained in A_{2R-e} , which is originally set to be:

$$A_{2R-e} = 1 - \frac{1}{2(k_{2-e}R_{-e})^2} + \frac{\exp(-2k_{2-e}R_{-e}) \cdot (2k_{2-e}R_{-e} + 1)}{2(k_{2-e}R_{-e})^2}$$

and then we obtain q_{2-e} and m_{2e-e} , and the black mass $m_{2b-e} = m_{-e} - m_{2e-e}$ in the usual way. All these are in terms of an initially unknown G_2 (universal electrical constant) of the electric field. The latter was set in Section 21.1.2 by arbitrarily assuming a 1:1 numerical equivalence between electrical charge measured in Coulomb and gravitational mass measured in kg.

For an equivalence between charge and mass to exist, we must satisfy also the equation between electric force F_C and gravitational force F_{PG} as:

ELECTRIC FIELD (Planck field with $G_2 = 8.2514882444 \times 10^{25}$)			
PROTON		ELECTRON	
$k_{2-p}R_{-p}$	2.6293887088E-23	$k_{2-e}R_{-e}$	4.0781656714E-04
A_{2R-p}	3.5058516117E-23	A_{2R-e}	5.4358914467E-04
k_{2-p}	3.1250162928E-08	k_{2-e}	1.9088306169E+21
q_{2-p}	1.0000000000E+00	q_{2-e}	9.9969420409E-01
m_{2-p}	1.6726219230E-27	m_{2-e}	1.6726219237E-27
m_{2b-p}	3.2984798988E-50	m_{2b-e}	5.1148094478E-31
m_{2e-p}	1.6726219230E-27	m_{2e-e}	1.6721104427E-27
R_{-p}	8.4140000000E-16	f	1.0436492502E-08
		J_{02}	1.1382866115E+85
		J_{2aR}	1.9438930599E+82

Table 52: Electrical properties of proton and electron in the electric field applying G_2 , all in SI units

$$F_C = G_{2C} \frac{e^2}{r^2} = G_2 \frac{m_{2e-e}^2}{r^2} = F_{PG}$$

where G_{2C} is the same as previously in Eq. 336, namely:

$$G_{2C} = \frac{1}{4\pi\epsilon_0} = 8.987552 \times 10^9 m^3 kg^{-1} s^{-2} \quad (563)$$

Thus, we must satisfy the condition that

$$G_2 m_{2e-e}^2 = G_{2C} e^2 \quad (564)$$

or to solve:

$$G_2 m_{2e-e}^2(G_2) - G_{2C} e^2 = 0 \quad (565)$$

The above equation together with Eq. 562 establish the interdependence among all the unknown electrical properties, for which we can have a solution. The effective mass is parametrized as a function of G_2 , i.e. as $m_{2e-e}(G_2)$ (or vice versa) to help us solve the equations graphically, or numerically, since we have no explicit function between these parameters. To solve this system of equations, we need to know the maximum acceleration g_{02} for the electric field. [Important: $m_{2e-e}^2(G_2)$ means $[m_{2e-e}(G_2)]^2$]

However, when we trialed the value of $g_{02} = 1.33 \times 10^{45} \text{ ms}^{-2}$ from Table 50, we could not find a real solution for G_2 at all. Instead, we found a cut-off point for g_{02} , above which there are two real values of G_2 that satisfy the system of equations. Furthermore, we found that, out of the two values thus found, only one of them can adequately satisfy the conditions (properties) expected for the electric field, and that is when we apply the maximum possible acceleration provided by the Planck field, namely, when we use $g_{02} = g_{0P} = 5.56 \times 10^{51} \text{ ms}^{-2}$.

We used our standard Python program for numerical equation solving, which has yielded the below two values:

$$G_2 = 8.2514882444 \times 10^{25} m^3 kg^{-1} s^{-2} \quad (566)$$

and

$$G_P = 2.7924827978 \times 10^{32} m^3 kg^{-1} s^{-2} \quad (567)$$

We investigate first the consequences of the first value G_2 leaving the second value G_P to follow next. This allows us to digest some initial findings and to highlight the salient findings, whilst the second solution (G_P) points to additional novel findings requiring special consideration.

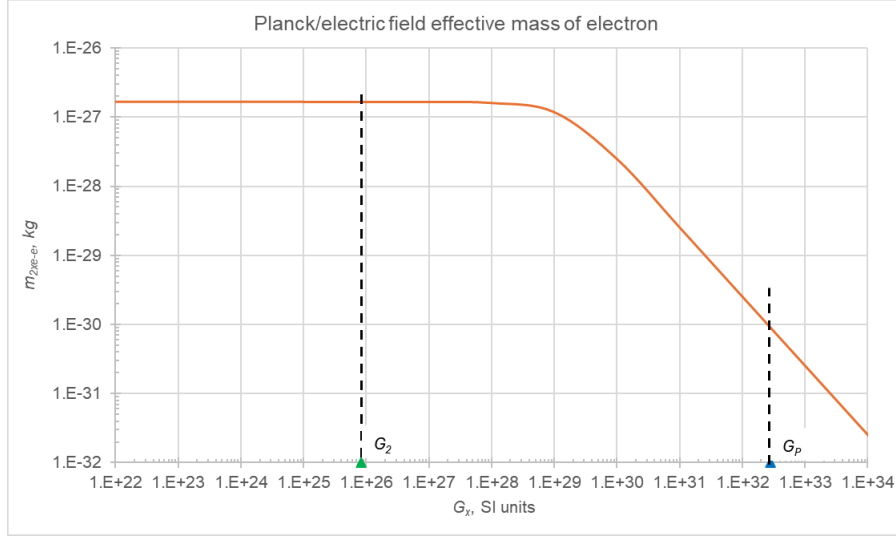


Figure 91: Variation of electrical mass m_{2e-e} of the electron vs. theoretical variation of the universal electric al constant G_{2x} , all in SI units.

Applying G_2 : Thus, based on G_2 , we have finally computed the properties of the electron provided in Table 52 and assigned under the electric field.

Lastly, we need to see the corresponding properties of the proton as determined by the electric field with G_2 . We compute the proton via the same equations used for gravity, but applying the new values of $g_{02} = 5.56072636271391 \times 10^{51} \text{ ms}^{-2}$ and $G_2 = 8.2514882444 \times 10^{25} \text{ m}^3\text{kg}^{-1}\text{s}^{-2}$ in lieu of the low values of g_0 and G used for gravity. The results are added in the same Table 52.

We obtain a better appreciation of the above findings by also plotting the electrical mass m_{2e-e} against G_2 as shown by the graph in Fig. 91. This mass appears constant over a very wide range of values of G_2 , but actually it varies extremely slowly as a second order of magnitude variation around the actual value provided in Table 52. This is what we would expect from a very high value of a g_{02} strength field. We know that for a given (fixed) spherical real mass, the effective mass increases with increasing g_{02} approaching a final value equal to the real mass. Considering the real electron mass m_{-e} , it should be almost entirely activated to an electrical mass at $g_{02} = 5.56 \times 10^{51} \text{ ms}^{-2}$, i.e. $m_{2e-e} \approx m_{-e}$. At the other end, the much lower gravitational value of $g_0 = 1.331943 \times 10^9 \text{ ms}^{-2}$ results in a saturated gravitational effective mass being equal to the measured (known) mass of the electron, i.e. $m_{e-e} = 9.1093837 \times 10^{-31} \text{ kg}$. In other words, the electrical field operates at the low extreme on the sigmoid like shape of the absorptivity in Fig. 3, whilst the gravitational field operates at the high extreme of this curve at (near) maximum absorptivity.

We supplement our understanding by further plotting the first term $G_2 m_{2e-e}^2$ in Eq. 565 against G_2 together with the second fixed (and known) term $G_{2C}e^2$ of the equation as shown in Fig. 92. Each of these terms (quantities) is the product of force times the square of the distance between two electrons (positrons). For convenience in the presentation, let us refer to them as “*force_strength*” measured in Nm^2 . We note that the variable *force_strength* has a maximum, while it is crossed at two points by the fixed Coulomb *force_strength* $G_{2C}e^2$. The two points provide to the two values of G_2 and G_P already found by the numerical solution of our equations.

It is the seemingly constant electrical mass that has created a perception of a constant (fixed) value of the charge of the electron. However, this is because the measured value corresponds to the “lone” electrical mass like we have found for the gravitational lone mass. At distances of atomic radii, the electrons are relatively very far from the nucleus rendering it in a “lone” status, but in reality the electrical mass varies with distance. We have already discussed the new understanding of the Millikan and Fletcher experiment and the nature of “electricity” in Section 21.3; will return to this topic later.

SALIENT FINDINGS

Electron radius: We highlight one important outcome that we have now obtained, i.e. the radius of the electron is:

$$R_{-e} = 2.1364733127 \times 10^{-25} \text{ m} \quad (568)$$

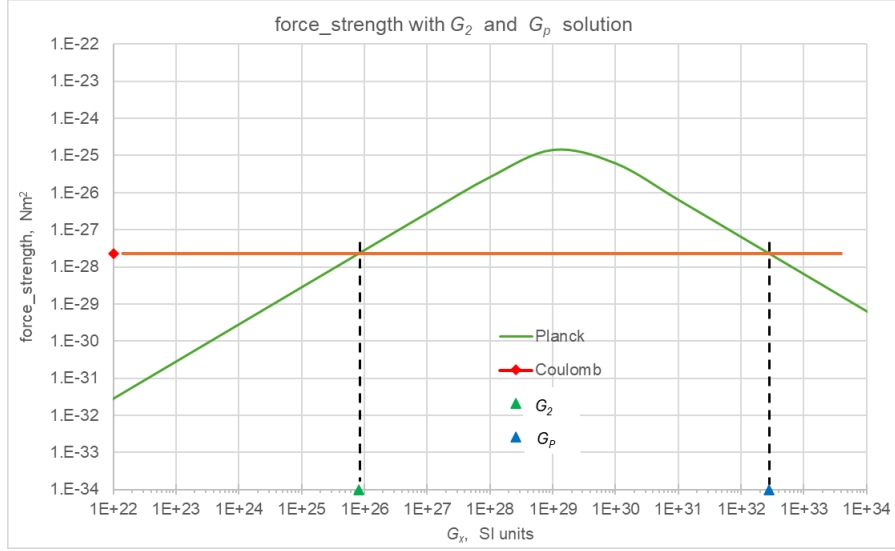


Figure 92: Variable force_strength (PG) and fixed force_strength (Coulomb) against variable G_x with solutions G_2 and G_P for Planck field.

Electrical mass: The absorptivity and contraction factors in the gravitational field clearly indicate that the gravitational mass m_{e-e} of the proton is essentially nearly all of the real mass being activated as effective mass, i.e. a very small amount remains inactivated in the black fraction of real mass. However, from the same parameters of the electron, it is clear that most of the real mass is inactive (remains black) with an effective mass practically close to the limiting value allowed for this strength of gravity at the given radius and real mass. This is a saturation value of effective mass corresponding to the high (extreme) level on the sigmoid like shape of the absorptivity curve (see early Fig. 3). However, the absorptivity and contraction factors in the electric field indicate that the electrical mass of the electron m_{2e-e} should be practically equal to its entire real mass being activated and effective. That is, it should almost be identical to the gravitational mass of the proton. All this is better understood

The above analysis is further supported by the electrical properties of the proton shown in the table. We see that the electrical masses of the proton and electron are $m_{2e-p} \approx m_{2e-e}$ as expected by the known equality of the classical charge between proton and electron. In addition, the electrical and gravitational mass of the proton are equal within ten decimal places presented in the table, so that we can write an extended equation like:

$$m_{e-p} = m_{2e-p} \approx m_{2e-e} \quad (569)$$

The approximately equal sign can arise from not considering the emission of a neutrino and other possible exchange of energy with the surrounding fields in Eq. 552, which is based on constant real mass between proton and electron. On this basis, we can summarize the above findings by restating the above equation in the form of a theorem that:

THEOREM: *The electrical mass of the electron is practically equal to the gravitational mass of the proton.*

We maintain the “*practically equal*” expression, because even if we introduce the exact real mass in our equations, the gravitational mass and the electrical mass of the electron may always differ by an extremely minute amount owing to the asymptotic nature of the corresponding absorptivities. This minute difference may not be measurable experimentally, as it is practically the case to date. On the latter proviso, we have used the “equal” sign in Eq. 569 above.

Given the above theorem, we can work out again an expected and more accurate value of G_2 working backwards from Eq. 564, but now setting (by theorem) $m_{2e-e} = m_{e-p}$:

$$G_2 = \frac{G_2 C e^2}{m_{e-p}^2}$$

yielding the value:

$$G_2 = 8.2464424800 \times 10^{25} \text{ m}^3 \text{ kg}^{-1} \text{ s}^{-2} \quad (570)$$

All this leads us to establish an actual equivalence between the charge of classical electricity and electrical mass in our PG theory below.

Charge to mass equivalence: In Section 21.1.2, we set the charge expressed in Coulombs numerically equal to mass expressed in kg by:

$$mass = 1 \cdot [charge] \text{ kg}$$

which we must now modify by introducing an appropriate conversion factor f_c (instead of unity) in order to accommodate the new value of G_2 and corresponding conversion of units.

$$mass = f_c \cdot charge$$

This means that for the electron (positron), we can write:

$$m_{2e-e} = f_c e \quad (571)$$

and from Eq. 565, we obtain

$$G_2 m_{2e-e}^2 = G_{2C} e^2 = G_2 f_c^2 e^2 \quad (572)$$

yielding

$$f_c = \sqrt{\frac{G_{2C}}{G_2}} = 1.0439684911 \times 10^{-8} \text{ kg/Cb} \quad (573)$$

where we used the derived value for G_2 from Eq. 570. This varies slightly, if we use the computed value for G_2 from Eq. 566 as:

$$f_c \approx 1.0436492502 \times 10^{-8} \text{ kg/Cb}$$

Given the above relationships, we have a corollary liaising the well known quantities of quotient Q (charge-to-mass ratio for electron) and proton-to-electron mass ratio as:

$$Q = \frac{e}{m} = \frac{m_{2e-e}/f}{m_{e-e}} = \frac{m_{e-p}}{f m_{e-e}} = \frac{\mu}{f} \quad (574)$$

We can indeed verify that:

$$\mu = f_c Q = 1836.1526727 \quad (575)$$

using the theorem of equivalence. Using the computed values, we find a slightly different figure, as expected, by:

$$\mu \approx f_c Q = 1835.5911854$$

Note: For subsequent work, we should distinguish between the two values provided for the same G_2 constant. One is referred to as “computed,” based on solving Eq. 562, while the other referred to as “calculated” is obtained by straightforward calculation based on Theorem 570.

31.5.5 Interim Discussion

We have conducted a series of investigations, all of which have resulted in inter-related and self consistent results.

They have culminated with a derivation (explanation) of the long awaited the value of the proton-to-electron mass ratio μ . We have provided the fundamental work, upon which we can finally derive the same μ based on the actual structures of the proton and electron. It should be appreciated that our derivation is independently produced. Although we used the basis that the proton and electron have the same real mass, this condition is not sufficient for the outcome we have produced. The other condition is the value of g_{02} used for the planckion field, which has yielded the electrical masses for both the proton and electron needed to

obtain Eq. 574. Any lower value of g_{02} starts compromising the electrical masses and the dependent charge-mass equivalence found. For example, the value of the “electric field” $g_{02} = 1.33 \times 10^{45} \text{ ms}^{-2}$ assumed in Table 50 cannot yield the necessary electrical masses and the corollary Eq. 574. Furthermore, the planckion field parameters were produced not arbitrarily, but as a result of preceding consistent investigation. We may say that the near equation of real masses between the proton and electron is vindicated by an independent series of findings.

Prior to the derivation of μ , we found a value for the radius of the electron, which may be an ultimate one subject only to second order corrections. This is a novel outcome, actually contrary to established theory that the electron has no real diameter.

Prior to above, we found a value for the universal constant Λ by self-contained means of examining its physical significance. Then, we can better appreciate the physical meaning of the long established bigG for gravity. That is, we have $G = \Lambda g_0 / \pi$, which makes very good sense by connecting the nature of a given body via Λ with the surrounding field medium of push particles via g_0 . Over and above this understanding, the two values G_2 and G_P for the Planck field having the maximum possible $g_{0P} = 5.56 \times 10^{51} \text{ ms}^{-2}$ correspond to $\Lambda_2 = 4.66 \times 10^{-26} \text{ m}^2 \text{ kg}^{-1}$ and $\Lambda_P = 1.57 \times 10^{-19} \text{ m}^2 \text{ kg}^{-1}$. The Λ_P is already given in Table 50, which is the maximum possible and same for all fields with $\Lambda_P = \Lambda$. However, the value for Λ_2 is a novel one and less than Λ_P , as it should. The latter points to a special structure of the absorbing electrical mass with a stacking of planckions as predicted in Section 31.5.2. For this reason, we need to continue with a separate report about a novel situation, while we digest the preceding new outcomes.

Prior to that, we found the value of g_0 for the gravitational field based on the helical structure of gravions. The latter helical structure has been the initiating point to subsequent derivations, which points to a possible explanation of the consistency of all the above outcomes. It seems that they are all interconnected via the geometry of the helical structure and the planckion attributes we have used.

In examining the numerical values in the tables for the proton and electron, it should be appreciated that we have rounded them off to the tenth decimal place. This is done for practical restrictions in the available table space. It does not indicate the actual or expected precision for each property. For example, the value of $q_{2-p} = 1.0000000000$ has been computed to be a little less than unity, but the difference is rounded-off by the decimal place used. We provide enough precision for comparison by readers who might wish to reproduce our theory and results.

It is fascinating to discover that the number $s = 4.1657 \times 10^{42}$ obtained from the humble derivation of the ratio of electric over gravitational forces between two electrons (see Eq. 550) connects the weakest push field of gravity with the strongest push field of planckions. This number happens to be the number of planckions in the longest possible helical chain acting as push particle for gravity, whilst a single planckion acts as push particle of the strongest possible field (the Planck field). The two fields seem to interact in an analogous way to a cradle pendulum. The energy of this particle (gravion) is directly connected via a factor of $\sqrt{2}$ with the known “Plank energy” in the literature. At the same time, we find that the maximum acceleration of our Planck field being $g_{0P} = 5.56 \times 10^{51} \text{ ms}^{-2}$ is exactly what has been tabled as the “Planck acceleration” in the literature (Wikipedia contributors, 2024f). At the same time, these numbers are connected with our universal “constant” Λ , a material characteristic, and all are connected with the gravitational bigG. We have extended our discoveries with establishing corresponding bigG_x’s for the other push fields, whilst they are inter-connected in a similar fashion. We now better understand the significance of G , actually being the product of two other more fundamental constants of nature as in the equation $G = \Lambda g_0 / \pi$. All these discoveries/successes have been made possible only by applying the push principle for every force field together with a structural connectivity among all these. We have proposed and successfully tested the helical structure of planckions, where this structure seems to yield results compatible and in agreement with existing experience. We envisage that more composite structures are made out these fundamental helices, like multi-stranded helices, vortices and possibly other. Thus, the agreement of the above quoted figures points to a good purpose for the development and adoption of push field theory. We can now confidently claim that our theory stands on solid ground and it warrants the participation of the wider scientific community.

We are continuing the development of PG with success. We only pause here, while preparing further reporting in continuation to all above and more.

31.5.6 Further on electrical properties of proton and electron

We continue from where we left off the investigation of solving the equations of the electric field.

Applying G_P : We should also investigate the consequences of applying the second value G_P , obtained in solving the equations for the Planck field. Our initial focus was on the first value, as it appeared to provide a plausible relationship between Q , μ , and f , together with a possible explanation (or mechanism) for the

PLANCK FIELD with $G_P \equiv G_5 = 2.78636084797137 \times 10^{32}$ SI units			
PROTON		ELECTRON	
$k_{5-p}R_{-p}$	8.8789143670E-17	$k_{5-e}R_{-e}$	1.3771141425E+03
A_{5R-p}	1.1838552489E-16	A_{5R-e}	9.9999973635E-01
k_{5-p}	1.0552548570E-01	k_{5-e}	6.4457352888E+27
q_{5-p}	1.0000000000E+00	q_{5-e}	5.4461702127E-04
m_{5-p}	1.6726219230E-27	m_{5-e}	1.6726219237E-27
m_{5b-p}	1.1138300117E-43	m_{5b-e}	1.6717109853E-27
m_{5e-p}	1.6726219230E-27	m_{5e-e}	9.1093836978E-31
		J_{05}	3.3709060407E+78
		J_{5aR}	1.0590010861E+79

Table 53: “Electrical” ($_{5e-}$) properties of proton and electron in the Planck field applying $G_P \equiv G_5$, with $g_{05} = 5.56072636271391 \times 10^{51}$, all in SI units.

attractive and repulsive properties known for electrons and positrons (or charges). By contrast, applying G_P to this field does not yield a similar explanation for electrical properties.

The computation instead produces "electrical" – or, more precisely, Planck-related – properties for the proton and electron, as listed in Table 53. Until the outcomes of the Planck field are more clearly sorted, we may continue to use the term "electrical" for this case as well. Interestingly, the "electrical" mass of the electron is found to be approximately equal to its gravitational mass ($m_{2e-e} \approx m_{e-e}$), and likewise the "electrical" mass of the proton is approximately equal to its gravitational mass ($m_{2e-p} \approx m_{e-p}$).

For the electron, however, such an outcome contradicts Eq. 569 and the associated equivalence theorem. In this case, the electron interacting with the Planck field does not exhibit the expected "charge" properties under the effective "electrical" mass m_{2e-e} . Moreover, the charge–mass equivalence (Eq. 571) and the μ -derivation (Eq. 575) are no longer applicable.

These results, along with earlier findings concerning the electron’s behavior under G_2 and G_P , suggest two possible interpretations:

1. Only one of these cases can physically exist, while the other is excluded.
2. The particle we identify as the "electron" may exist in two distinct states: one behaving as a charge, and another behaving as a "normal" particle with a gravitational-like (rather than electrical) effective mass.

At this point, no firm conclusion can be drawn. Instead, we are gathering fragments of understanding – pieces of a larger puzzle – expecting that the forward investigation will provide the missing links needed to form a coherent and plausible determination.

31.5.7 Updating the field unification table

We update Table 50 with the upgraded results presented in Table 54. The column under the Planck field is subdivided into two columns, containing parameters that differ depending on the two distinct “G” values, namely, G_2 and G_P .

The corresponding functions have been summarized in Table 42, as they apply separately to each field. Both G_2 and G_P are associated with push particles, and each case is carefully reviewed as we continue to build our understanding.

This update allows us to:

1. Differentiate the parameters associated with G_2 and G_P .
2. Apply the corresponding functions consistently for each field.
3. Review the behavior of push particles under each case to improve our understanding of the Planck field.

Further, we note that in the previous Table 50, under the “electricity” column, we have $G_2 = 6.56 \times 10^{25}$ SI units, which is surprisingly of the same order and close to the value $G_2 = 8.25 \times 10^{25}$ SI units derived for the Planck field. This prompted us to investigate this as an interim “x” field independently, using the latter value (from the Planck field) as its G_x .

This requires upgrading (or tweaking) its former maximum acceleration value to $g_{02} = 1.65 \times 10^{45} \text{ ms}^{-2}$, with a corresponding field strength factor of 1.24×10^{36} (slightly above the “published” strength value). All

field type	gravity (01)	weak (03)	x (02)	strong (04)	Planck (05)	
particle name	gravions	y-ions	x-ions	z-ions	G_2	G_P
adopted strength	1.00E+00	1.00E+33	1.24E+36	1.00E+38	4.17E+42	
#planckions $[\nu]$	4.17E+42	4.17E+09	3.38E+06	4.17E+04	1.00E+00	
<i>particle_length</i>	6.75E+07	6.75E-26	5.46E-29	6.75E-31	1.62E-35	
t_f	2.25E-01	2.25E-34	1.82E-37	2.25E-39	5.39E-44	
g_{0f}	1.33E+09	1.33E+42	1.65E+45	1.33E+47	5.56E+51	
J_{0f}	8.07E+35	8.07E+68	9.98E+71	8.07E+73	1.14E+85	3.37E+78
u_{0f}	5.39E+27	5.39E+60	6.66E+63	5.39E+65	7.60E+76	2.25E+70
n_{0f}	1.95E+18	1.95E+84	2.97E+90	1.95E+94	1.15E+110	3.39E+103
G_f	6.67E-11	6.67E+22	8.25E+25	6.67E+27	8.25E+25	2.79E+32
A_f	1.57E-19	1.57E-19	1.57E-19	1.57E-19	4.66E-26	1.57E-19
L_{fmd}	8.01E-07	8.01E-29	6.95E-31	3.72E-32	2.06E-37	3.09E-35

Table 54: Upgraded comparative values of universal constants for gravitational, weak, x, strong and Planck fields. The Planck field acts on two separate types of absorbing/emitting body (electron or positron) with separate push particles acting either as electrions or planckions

other parameters have been adjusted accordingly, as shown in the new table under the column labeled as the “x” field. The change of name is necessitated by the finding that this field also does not yield the expected behavior of the electric field, as we will show shortly.

Nevertheless, we have undertaken this investigation in case it represents another type of existing field (or not), or it might be somehow modified to satisfy the requirements for electricity, as we can actually do later. We may also need to update the “weak” and “strong” fields in follow up investigations. For this reason, we have maintained the same tentative values for the weak and strong fields in their respective columns. For lack of names, we have called the corresponding push particles “y-ions” and “z-ions” until further work is done later.

If this x-field exists, then its push particles, “x-ions,” are (for now) assumed to consist of helical arcs populated with $[\nu_x] = 3.38 \times 10^6$ planckions. We have used a similar assumption (albeit arbitrary) for all fields, namely, that their push particles have the helical structure introduced in Fig. 89. We will revise this proposal as we review each field separately and establish their requirements.

It should be noted that the value of $G_P = 2.78636084797137 \times 10^{32} \text{ m}^3\text{kg}^{-1}\text{s}^{-2}$ (as given in Table 53) is provided on the basis of a constant Λ as for all fields; it slightly differs from the computed $G_P = 2.7924827978 \times 10^{32} \text{ m}^3\text{kg}^{-1}\text{s}^{-2}$ (see Eq. 567) found by solving Eq. 562.

We will return again with another updating of the unification table after we investigate some emerging issues and after we can derive the electric field based on more solid arguments.

Note on subscripts: We use the subscript (2) for solving Eq. 562, where “2” indicates the “second” field as opposed to the “first” gravitational field. This “second” field (2) can be any of the fields f in Table 54. To ensure backwards compatibility with previous reports, the absence of a subscript implies the subscript (1), which has been reserved for the gravitational field.

However, we also reserve and use the subscript (2) to denote the electric field, because we have done so in all preceding reports and because we intend to maintain this convention for the electric field until we can establish firm conclusions about the existence of each of the tabled fields. In other words, Eq. 562 serves in the investigation of all fields without changing its subscript index, since it retains the same form for all fields.

In later revisions of the report, we may use the subscript (f) in the equation to denote and solve for every field with $f = 1, 2, 3, 4, 5$, while the reader may gather enough patience to see this work through. Temporarily, we maintain two sub-columns for the Planck field (5) in Table 54, corresponding to the G_2 and G_P solutions, but we intend to revise this again as we proceed with our investigation.

Note on masses in different fields: Based on the above and further findings, we refresh the meaning of “mass”: The subscript (2) in the symbol of mass should again indicate the “second” mass due to the “second” field (as opposed to the “first” gravitational field) in solving Eq. 562. This “second” mass (2) can be generated by any of the fields in Table 54. Actually, we use the corresponding subscript (f) in various tables with the numerical properties of proton and electron,

If the push principle generally applies to all fields (as we contend that it does), then we must assume a different mass type for each field. For spherical bodies and particles with a given radius, Eq. 561 can be generalized to apply between the gravitational field and field (f) as follows:

$$R^2 = \frac{Gm_e}{A_R g_0} = \frac{G_f m_{fe}}{A_f R g_{0f}} \quad (576)$$

Applying $G_f = \Lambda_f g_{0f} / \pi$, the above becomes:

$$R^2 = \frac{\Lambda m_e}{A_R} = \frac{\Lambda_f m_{fe}}{A_f R} \quad (577)$$

By our latest understanding, it may be that Λ is constant across all fields, except for the electric field. For fields with constant (and known) Λ , the above reduces to:

$$\frac{m_e}{A_R} = \frac{m_{fe}}{A_f R} \quad (578)$$

This means that the corresponding masses are equal if the absorptivities are also equal. We have found near equality for these properties of the electron in the Planck field with G_P and in the gravitational field. Because generally the absorptivity of a body depends on the respective field, and it is different for each field, so the masses are not generally equal. However, they are nearly equal among all fields except for the electrical field. This near equality will become apparent as we progress with the study of each field.

Furthermore, we have established that the absorptivity A_R for spherical particles with radius R corresponds to a mass, not only across fields but also across kinetic states within a field, resulting in a variety of masses as provided in Table 31. The concept of “mass” should be considered appropriately at the fundamental and higher levels. We should critically investigate how the various types of mass of a given body behave in different fields, both quantitatively and qualitatively.

For example, we cannot apply the above mass equations “as are” to particles with helical structures, to planckions, etc. We have applied them to the case of proton and electron, the latter found to have a radius of $R_{-e} = 2.13 \times 10^{-25}$ m. While this is extremely small relative to other known particles, it remains greatly larger than the Planck length (by ten orders of magnitude); this leaves considerable “room” for various other particle structures in between, before they become spherical by accruing hyle from the surrounding fields.

To supplement the above relationships in the case of unequal Λ , specifically for the electrical mass, we have:

$$g_{02} = \frac{G_2}{\Lambda_{2-e}} = \frac{G_P}{\Lambda_{P-e}} = g_{0P}$$

and Eq. 577 yields:

$$\begin{aligned} \frac{\Lambda_{2-e} m_{2e-e}}{A_{2R-e}} &= \frac{\Lambda_{P-e} m_{Pe-e}}{A_{PR-e}} \\ \frac{G_2 m_{2e-e}}{A_{2R-e}} &= \frac{G_P m_{Pe-e}}{A_{PR-e}} \\ \frac{G_P}{G_2} &= \frac{m_{2e-e} A_{PR-e}}{m_{Pe-e} A_{2R-e}} = \mu \frac{A_{PR-e}}{A_{2R-e}} \end{aligned} \quad (579)$$

If we substitute the values taken from the relevant tables of the parameters for the proton and electron, we find that the first member of the above equation yields $G_P/G_2 = 3.3818388184 \times 10^6$ (computed), which is practically the same as the second member of the equation yielding 3.3818385480×10^6 with values taken also from the tables.

In addition, we have $\mu^2 = 3.3714566373 \times 10^6$ from original (raw) value and $[\nu_2] = 3.3788637069 \times 10^6$ from Table 54 under the x-field column. Thus, we have:

$$\mu^2 \approx \frac{G_P}{G_2} \approx [\nu_2] \quad (580)$$

By combining the above results, we also obtain:

$$\mu \approx \frac{m_{2e-e}}{m_{Pe-e}} = \frac{A_{PR-e}}{A_{2R-e}} \quad (581)$$

The latter equation confirms the equivalence between effective mass and absorptivity, and supports the use of absorptivity in a general kinetic theory of push fields, as we attempted for the gravitational field in Section 23.

In Section 21.1.1, we investigated the case where the electrical and gravitational masses for the electron are equal and derived Eq. 325, with a value of $G_2 = 2.7803909099 \times 10^{32} \text{ m}^3\text{kg}^{-1}\text{s}^{-2}$, which is practically equal to G_P currently computed and also used in Table 54. Since the masses in different fields (not including the electric field) are not exactly equal, we may use symbols \lesssim , or \gtrsim with proper definition. They may mean a “little less” or a “little greater” in reference to a given property across different fields. Usually, this amounts to some decimal places difference as a quantity (property, mass, etc.) rides on the corresponding asymptotic branch of the curve in Fig. 3.

Furthermore, we investigated the case of unequal mass (see Section 21.1.2), yielding yet another value for G_2 , but associated with a different charge–mass equivalence equation. Our current work has revealed that both cases (i.e., of equal and unequal masses) are possible, corresponding to the presently found G_2 and G_P .

31.5.8 On field strength ranking

Now, we have used the published (established) relative “strength” between fields in Table 54, while also adding the new Planck field. This has prompted us to rethink the basis and meaning of field strengths. It is not clear (to this author) whether they are based on force, on energy considerations, or something else entirely. A cursory search provides the following understanding:

It is stated that “*electromagnetism at 1/137 is still way more powerful than gravity at 6×10^{-39}* ”. Also: “*How much stronger is static electricity than gravity? The units for q are coulombs, which is equal to 6.3×10^{18} electrons. Gravity is 6×10^{-39} orders of magnitude weaker than electricity.*” This indicates that the relative strengths are only indicative.

We further quote from the same source (Stack Exchange): “*I often see and hear people claiming that “the gravitational force is much weaker than the electromagnetic force”. Usually, they justify it by comparing the universal gravity constant to Coulomb’s constant. But obviously, such comparison is meaningless, as they differ in dimensions. I’ll make myself clear: of course you can say it is true for electron-electron interaction, but I’m talking about whether they can be compared fundamentally somehow in any area of physics*”. Also, from same source: “*Yes, they can. Both interactions can be modeled using perturbative quantum field theory, where their strength is parametrized by a dimensionless coupling constant*”. “*Electromagnetic repulsion between two electrons can be written as a power series in α , the fine structure constant, which is dimensionless and has a value of roughly 1/137*” Also: “*The precise value of αG depends somewhat on which particle you’re comparing, since ultimately it’s the square of the ratio of the particle’s mass to the Planck mass. However, for fundamental particles, this ratio does not vary by more than ten orders of magnitude, which still places αG far smaller than a no matter which fundamental particle you choose to compare*”. Further: “*You may not be able to compare the constants directly, but you can compare the resulting forces. For instance, when you put two electrons 1m apart, you can calculate their gravitational attraction and their electrostatic repulsion*”... and more. All this, again, shows that there is no general agreement about how to quantitatively compare gravity with electricity. However, it seems that we can overcome and resolve this issue via our push field theory by the following analysis.

We have obtained our results with a new understanding, especially with the possible existence of the Planck field. We explore possible situations below, with more to discuss later.

First, it is compelling to undertake experimental work to measure the actual value of g_0 . Pending this work, we have arrived at the theoretical value of $g_0 = 1.33 \times 10^9 \text{ ms}^{-2}$. The energy of the graviton is

$$E_g = [\nu_{\max}] E_P = 2.77 \times 10^9 \text{ J} \quad (582)$$

where we use interchangeably $[\nu_1] = [\nu_{\max}]$. The above is an upgrade from Eq. 542, now with a new ν_{\max} . The new value compares very well with the published “Planck energy” given by Wikipedia contributors (2024) as $E_g = 1.9561 \times 10^9 \text{ J}$. In fact, they differ by the now familiar factor of $\sqrt{2}$, which is explained by our choice of the Planck length.

Thus, we have excellent agreement of figures between our results and the published maximum energy (the Planck energy), as expected by both approaches using the minimum possible wavelength (i.e., the Planck length). However, the interpretation of the relevant physical quantities differs. We have not understood

what the published “Planck energy” represents in reality, but we have a rational interpretation under our PG theory by identifying this energy with the gravion energy.

This is the highest energy achievable by the proposed helical structures of push particles. We now realize that this highest energy relates to the weakest force field, namely, the gravitational field. Thus, gravity has the weakest strength by way of force despite the most energetic particle that mediates it (actually, as re-interpreted later in Section 31.10.5). The very low “strength” of this field corresponds to a very long interaction time.

At the other extreme, the planckion has the least energy together with the shortest interaction time, i.e., the Planck time. It is important to recognize that the rate of energy delivery during interaction is the same for both gravion and planckion, while the total energy is proportional to the total interaction time. The gravitational and Planck forces are at opposite extremes, while the “strong” and “weak” fields may have intermediate push particle energies, also intermediate “strengths,” ordered between gravity and the Planck field. These observations will be qualified and elucidated as we derive more information from subsequent development.

We could rank all the fields according to the energy of their mediating push particles, but also by their maximum acceleration in reverse order. If gravity (weakest strength) has the most energetic particle, and the Planck field (strongest) has the least energetic particle (with a Planck energy E_P per our adopted Planck units in Table 41), then the other three field push particles should rank according to their energy levels as:

$$E_{gravity} >>> E_{weak} >> E_{x-field} >> E_{strong} >> E_{Planck} \quad (583)$$

Correspondingly, by way of maximum acceleration (or force), the ranking should be:

$$g_{gravity} <<< g_{weak} << g_{x-field} << g_{strong} << g_{Planck} \quad (584)$$

where we have explicitly expressed the subscripts to readily recognize the proposed explanation or concept. We interpret our notation as $g_{gravity} \equiv g_{01} \equiv g_0$ (gravions), $g_{weak} \equiv g_{03}$ (y-ions), $g_{x-field} \equiv g_{0x}$ (x-ions), $g_{strong} \equiv g_{04}$ (z-ions, or nuclions but not “nucleons”), and $g_{Planck} \equiv g_{05}$ (electrions and planckions), though we can reassign the notation and nomenclature once a final working situation is established. This ranking is based on Table 54 until we upgrade it.

Our early notation of subscripts was assigned in the order of development of the theory, without anticipating what we would subsequently find. This development has proceeded intuitively, without preconceptions or prejudice, as we explored the unknown. Thus, we will reassign the electric field to the x-field column with a proper modification a little later. For now, we retain the published strength position of electricity under the x-field, anticipating a revision shortly. As mentioned, we proceed step-wise to ensure the progress is clearly understood.

The above exposition presents two different (albeit equivalent) ways to rank relative strength: either based on relative force level or on relative energy level among various push particles. Furthermore, looking at Table 54, we might also choose to rank based on relative interaction times, maximum acceleration, number of planckions in the push particles, particle length for each field, energy density, etc.

However, much of this is based on the arbitrary assumption that push particles in each field have the helical structures we have devised in Fig. 89. This assumption is made to help us start the investigation, and it has yielded some plausible outcomes. Nevertheless, it will be modified if alternative structures of these particles are found for good reasons.

On this note, we pause this topic until after we consider the mean free path of push particles, their mean distance between closest neighbors in various fields, and the mean separation time of absorption events by different size bodies.

31.6 Mean free path and mean distance between nearest neighbors in various fields

We might be getting an insight about the mean free path of gravions that is required to generate the gravitational field by the following considerations, as we can also derive the mean distance between nearest neighbors further on. These are critical requirements to establish a push field theory, a reason for which they were assumed axiomatically at the outset. If we could independently establish these requirements based on other more obvious or acceptable principles or findings, then we can adjust the exposition of our theory accordingly.

31.6.1 Mean free path:

The conventional equation for the Planck length is:

$$\ell_P^2 = \frac{\hbar G}{c^3} \quad (585)$$

We can replace the \hbar and G constants with our PG ones. In the previous version, we inadvertently copied the derivation incorrectly from the work sheet, but the end result is the same, i.e. the correct one. Below, we repeat the derivation with more detailed interim steps, to elucidate the mishap:

$$\begin{aligned} \ell_P^2 &= \frac{\hbar G}{c^3} = \frac{E_P J_0 \Lambda^2}{2\pi \cdot 1\text{Hz} \cdot c^4} = \frac{E_P J_0 k^2}{2\pi \cdot 1\text{Hz} \cdot \rho^2 c^4} = \frac{E_P J_0 k^2}{2\pi \cdot 1\text{Hz} \cdot u_0^2} = \frac{E_P k^2}{4\pi u_0^2} \frac{2J_0}{c} \cdot 1\text{sec} = \\ &= \frac{E_P k^2}{4\pi u_0^2} u_0 c \cdot 1\text{sec} = \frac{E_P k^2}{4\pi u_0} \cdot 1\text{sec} \cdot c = \frac{k^2 E_P^2}{4\pi u_0} \cdot L_c = \frac{k^2 L_c}{4\pi n_0} \end{aligned}$$

where L_c is the distance of photons traveled for 1 second, i.e. a distance equal to the numerical value of the velocity of light. We also used $u_0 = \rho c^2$ and $2J_0/c = u_0$. From the above, we find also the absorption factor k by:

$$k^2 = 4\pi n_0 \frac{\ell_P^2}{L_c} \quad (586)$$

The above was derived prior to new addition on the interrelation among G , g_0 and Λ . Now, for Λ we used:

$$\begin{aligned} \Lambda &= \frac{\pi \ell_P^2}{m_P} = \frac{\pi \ell_P^2}{E_P/c^2} = \frac{\pi \ell_P^2 c^2}{\hbar \cdot 1\text{Hz}} = \frac{\ell_P^2 c^2}{\hbar \cdot 1\text{Hz}} = \pi \frac{G}{g_0} = \pi \frac{G}{c/t_g} \\ &= \frac{\ell_P^2 c^2}{\hbar \cdot 1\text{Hz}} = \pi \frac{G}{c/t_g} \\ &= \frac{\ell_P^2 c^3}{\pi G \hbar \cdot 1\text{Hz} \cdot t_g} = 1 \\ \ell_P^2 &= \frac{\pi G \hbar \cdot 1\text{Hz} \cdot t_g}{c^3} = \frac{G \hbar}{c^3} (1\text{Hz} \cdot t_g \pi) = \frac{\hbar G}{c^3} (1\text{Hz} \cdot t_g) \end{aligned}$$

Hence

$$\pi \cdot 1\text{Hz} \cdot t_g = 1$$

$$t_g = \frac{1}{\pi \cdot 1\text{Hz}} = 0.3183$$

which divided by $\sqrt{2}$ yields

$$t_{g-\text{adjusted}} = \frac{1}{\pi \sqrt{2} \cdot 1\text{Hz}} = 0.225$$

exactly per value used shortly above for Eq. 544.!!!!

From a known absorption factor k of “free” space, we obtain the mean free path (mfp) L_{mfp} of gravions, but probably also of other push particles of various fields. Starting with gravity, we have assumed that the mfp is long enough to allow “attraction” (i.e. pushing together) at least among the Sun and planets. In fact, this is our principle #1 at the outset of PG theory. If we can now (or later) derive an equation for this quantity, then we can simplify the reliance of the theory by stating that this is derivable from other principles, like those concerning the planckions (formerly gravions) (see Section 30). We make such an attempt below by way of investigation, because we cannot be satisfied by the outcomes so far. We include various approaches in order to facilitate further work on this issue. We do so for gravity and the newly emerged Planck field.

For the gravitational field, we earlier set the value of $n_0 = 1.42 \times 10^{47} \text{ \#}/\text{m}^3$ from Table 46 for gravions (gravity) and obtained $k = 1.25 \times 10^{-15} \text{ m}^{-1}$. This means that there is about one absorption (here collision) event for every $\sim 10^{15} \text{ m}$. This is $\sim 10^4 \text{ a.u.}$ (astronomical units). If we repeat the same calculation by use of the latest value of $n_0 = 1.95 \times 10^{18} \text{ \#}/\text{m}^3$ derived from the latest value of $g_0 = 1.33 \times 10^9 \text{ ms}^{-2}$ per Eq. 544, we find $k = 4.62 \times 10^{-30} \text{ m}^{-1}$, which corresponds to about 15 orders of magnitude longer

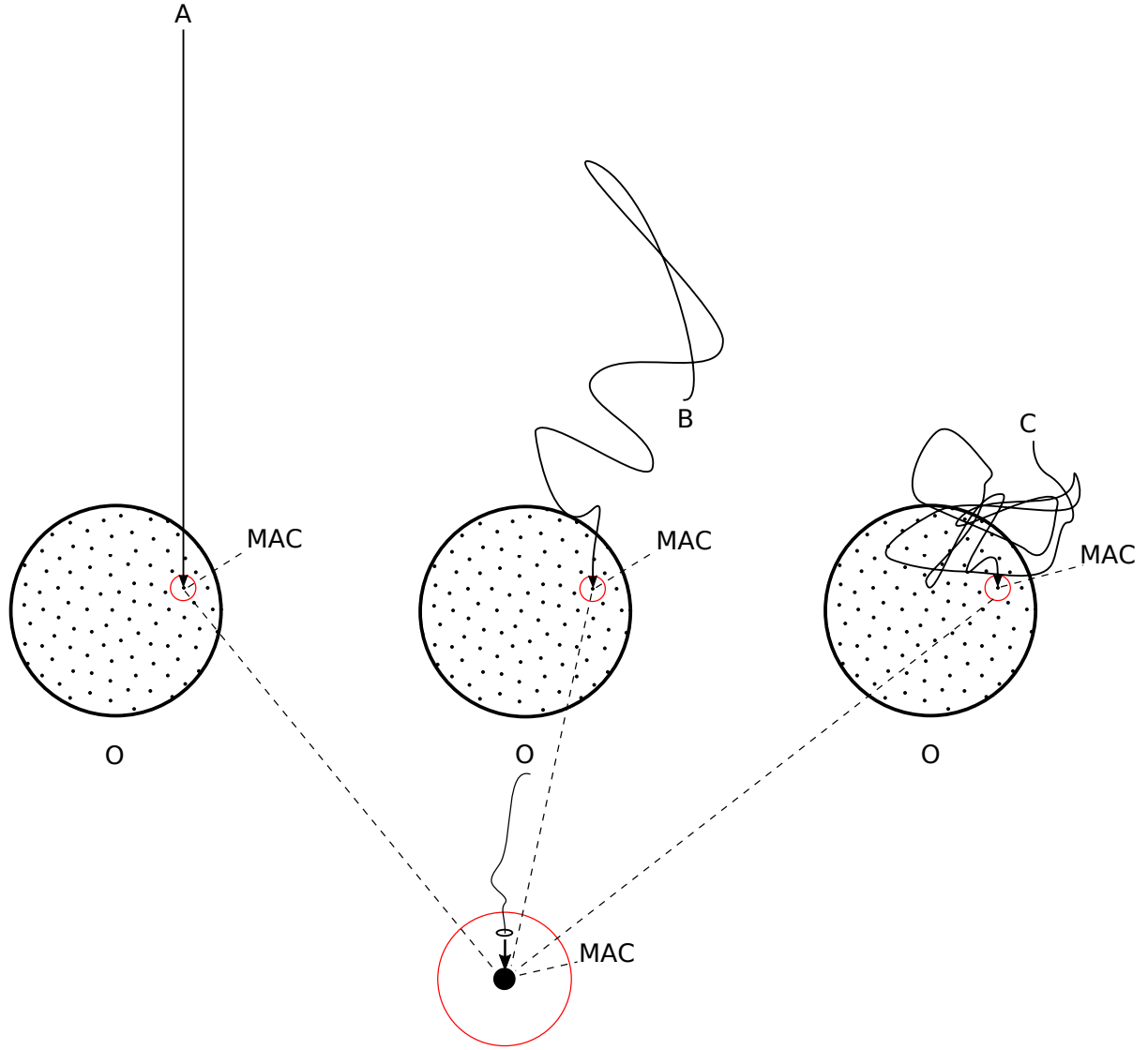


Figure 93: Gravion configurations

distance per absorption event. These numbers are interesting, because they may be the mean free paths of gravions. They range from interplanetary to interstellar distances, as anticipated from the outset of our PG theory. They are enough to make all the planets of the solar system “attract” each other, and beyond. ~~However, we need to finally establish the correct g_0 value.~~ Below, we continue by considering the value of $g_0 = 1.33 \times 10^9 \text{ ms}^{-2}$ as established.

Therefore, the above formula of Eq. 586 may provide the mean free path L_{mfp} of push particles by its inverse value as:

$$L_{mfp} = \frac{1}{k} = \sqrt{\frac{L_c}{4\pi n_0 \ell_P^2}} \quad (587)$$

If we take $n_0 = 1.94719 \times 10^{18} \text{ particles/m}^3$ from Table 54, we find $L_{mfp} = 2.17 \times 10^{29} \text{ m}$. This value is larger than the size of the known universe, taken as 93 billion light years ($= 8.79 \times 10^{26} \text{ m}$) across. The latter value of L_{mfp} might be unacceptably large, in which case we would have to revise our ideas about “cosmic weather” conditions mentioned in several parts of the theory.

We initially require, or at least expect, a mean free path in the range between a minimum on the order of the heliosphere size (about 150 a.u.) and a maximum smaller than a typical galaxy (say, around 100000 light years). Let us therefore assume that we need to have:

$$\sim 2 \times 10^{13} < L_{mfp} << \sim 1 \times 10^{21} \text{ m} \quad (588)$$

The reason we set a lower limit is to allow the generation of “attractive” forces inside the heliosphere. The reason we set the upper limit is to preserve the “cosmic weather” effect of the gravion gas, which could potentially explain the spiral rotation properties of galaxies. Thus, a lower limit is necessary, but the upper one may be relaxed without affecting PG theory as a whole.

The derived value of $L_{mfp} = 2.17 \times 10^{29}$ m clearly falls outside the proposed range. This discrepancy might arise from the special shape of the gravion, which has been conceived as a very long helical chain requiring special consideration in regard to inter-gravion collisions. It may be that lateral interactions are extremely rare, or even forbidden, under a final accepted planckion–gravion model (see Section 30.3).

The gravion appears to be a peculiar particle, for which we need to establish a consistent physical configuration based on the attributes already provided for the planckion (formerly gravion) in Section 30, together with some additional (or modified) features as required to ensure an integrated physical existence.

For now, we may adjust its overall configuration. Given its relatively long length, it does not necessarily have to exist in a straight line, but instead may adopt a squiggly configuration, as illustrated in Fig. 93. This could be conceived as analogous, in a limited way, to a molecular polymer chain. The planckions move along a spiral path forming a globule due to statistical fluctuations; we do not call for an analogous elastic force as in rubber.

We may envisage gravion chains occupying minimal space in a squiggly configuration, while still maintaining a “linear forward” motion of planckions along the spiral path in the local axis direction. As the planckions tumble within the helical chain, the macroscopic gravion chain itself may assume an overall minimal-space configuration, i.e., of much smaller extent than the straight line extent.

This idea is not essential for the continuation of PG theory. If found unconvincing, it need not be adopted. It is presented here primarily because it connects with other arguments and possible solutions, which will be examined later. Actually, it will help us understand a fragmented form of the gravion while retaining its overall interaction and integration times.

Returning to the diagrams in the figure, we illustrate the same body O (planet, star, electron) containing minimum absorption centers (MAC). The same absorption center (shown in a red circle) can be struck by different gravions with different overall configurations, except that in every case the leading head points in the same direction. It is this leading head that initiates and governs the entire interaction process, while the trailing tail follows through the same entry point and direction.

No external forces (fields) are required to produce this situation. The reason is that the curvatures of the squiggly helix are extremely small compared with the curvature of the tightly wound helical path of very small radius. Thus, the macroscopic squiggly configuration does not interfere with the motion of planckions along the helix. Consequently, a striking gravion produces the same outcome regardless of its overall “macroscopic” shape.

The above conceptualizations are subject to modification and refinement as we gradually progress toward a deeper understanding of the structure of hyle, beginning with the planckion, as introduced in the model of the gravion (now planckion) in Section 30. If needed, we can endow that model with an additional property that permits the formation of planckion chains, namely, a mechanism (or bond) that connects adjacent units.

To complement this investigation, we borrow the formula of mean free path for an ordinary gas. In this case, the well-established general scattering theory gives the mean free path as

$$L_{mfp} = \frac{1}{\sigma n_0} \quad (589)$$

where σ is the scattering cross-section of the particles. In a gravion gas, this quantity is presently unknown and must somehow be determined.

We begin with two extreme estimates:

(a) $\sigma \approx \ell_P^2$, corresponding to the order of magnitude of the area of the leading head of the traveling helical chain. This yields $L_{mfp} = 1.97 \times 10^{51}$ m, i.e. an even larger value than that obtained previously.

(b) A rectangular area with sides (*helix_diameter* \times *helix_length*), i.e. $\sigma = \sqrt{2} \ell_P \times 6.75 \times 10^7 = 1.54 \times 10^{-27}$ m². This gives $L_{mfp} = 3.33 \times 10^8$ m, which is too small to satisfy the condition for L_{mfp} in Eq. 588.

Therefore, we still need to establish a verifiable formula for the actual gravion mean free path.

In conclusion, the issue of the mean free path for gravions remains unresolved by any of the above attempts. Nevertheless, these estimates may serve as a useful starting guide for subsequent investigations of this problem.

Mean free path in Planck field: We repeat the same investigation for the mean free path of planckions in the Planck field. To ensure that the push principle applies in this field, we require a general guiding range of mean free paths within:

$$\sim 1 \times 10^{-34} \rightarrow \sim 1 \times 10^{-25} < L_{5mfp} << \sim 1 \times 10^{-25} \rightarrow \sim 1 \times 10^{-14} \text{ m} \quad (590)$$

The lower limit is taken to lie between the Planck length and the electron radius, while the upper limit lies between the electron radius and the size of the largest known nucleus, i.e., of uranium. These ranges are intended to encompass particle sizes that are shaped by the push forces of planckions, which bring together smaller fragments of hyle toward a roughly spherical shape.

As before, this range serves only as an initial guide and may be adjusted as the theory develops. In fact, the upper limit is particularly critical for establishing the relationship between the Planck field and the strong field in connection with nuclear structure and nucleons, as we will discuss later.

Now, applying Eq. 587, we obtain a mean free path $L_{5mfp} = 5.19 \times 10^{-14} \text{ m}$ using $n_0 = 3.39 \times 10^{103} \text{ \#}/\text{m}^3$ (under G_P) from Table 54 (we also find $k_5 = 1.93 \times 10^{13} \text{ m}^{-1}$). [Note: We use the subscripts (P) and (5) interchangeably].

This is encouraging, as it lies slightly above the upper limit of the range in condition 590, which is sufficient to maintain the nucleus of atoms as a compact unit from its constituent nucleons. In fact, it exceeds even the size of the largest nucleus, uranium, at approximately $1.5 \times 10^{-15} \text{ m}$.

This result requires further analysis and development within push field theory, and a dedicated report on “nuclear physics” is currently under preparation.

Applying Eq. 587 again, with $n_0 = 1.15 \times 10^{110} \text{ \#}/\text{m}^3$ (under G_2) from Table 54, we obtain $L_{2mfp} = 2.82 \times 10^{-17} \text{ m}$.

The acceptability of this value will be determined by the forthcoming interpretation of electrions (associated with G_2) and their expected mean free path.

We should also examine the outcomes using the remaining formula previously applied for gravions. Applying Eq. 589, we obtain

$$L_{2mfp} = 3.34 \times 10^{-41} \text{ m using } n_{02} = 1.15 \times 10^{110} \text{ under } G_2 \text{ from Table 54, and}$$

$$L_{5mfp} = 1.13 \times 10^{-34} \text{ m using } n_{05} = 3.39 \times 10^{103} \text{ under } G_P; \text{ in both cases, } \sigma = \ell_P^2.$$

As evident, these values are far too small to meet the required range, with the first being even smaller than the Planck length. This suggests that the formula may not be applicable in this context.

We conclude that Eq. 587 may be a suitable candidate for estimating the mean free path, whereas Eq. 589 appears unsuitable.

Current theories on nuclear structure have faced a similar issue, as noted by Wikipedia contributors (2025b) that “*The effective mean free path of a nucleon in nuclear matter must be somewhat larger than the nuclear dimensions in order to allow the use of the independent particle model. This requirement seems to be in contradiction to the assumptions made in the theory ... We are facing here one of the fundamental problems of nuclear structure physics which has yet to be solved.*”

—John Markus Blatt and Victor Weisskopf, *Theoretical nuclear physics* (1952)”

31.6.2 Mean distance between nearest neighbors:

Another important quantity to consider is the *mean distance* (L_{md}) between nearest neighbors, defined analogously to ordinary gases as:

$$L_{md} = \frac{1}{n_0^{1/3}} \quad (591)$$

This is a straightforward classical derivation for any gas, and it should also apply to distinguishable push particles used in our theory. Since we can derive the number density of push particles for each field, we have included an additional row in Table 54, listing the value of L_{fmd} for each field (f). We next evaluate this for gravions and planckions.

Gravions: For gravions, this distance is $L_{1md} = 8.01 \times 10^{-7} \text{ m}$. To obtain a sense of relative magnitude, we have $L_{md} = 1.56 \times 10^{-7} \text{ m}$ for an ordinary gas at 1 Pa and 273 K. This comparison illustrates the extent of “dilution” or “vacuum” associated with gravions.

We have not added a row for the mean free paths in Table 54, since we have not yet obtained a reliable derivation for it. In general, we would expect that $L_{mfp} \gg L_{md}$ for the actual values of these parameters. We should not be influenced by our ordinary experience of gases when considering the properties and behavior of an entirely different world situation. Thus, we must adjust our models accordingly.

Planckions: The corresponding mean distance of nearest neighbors for planckions are $L_{2md} = 2.06 \times 10^{-37}$ m when using the G_2 value, and $L_{5md} = 3.096 \times 10^{-35}$ m when using the G_P value. The former result is problematic, because it is less than the Planck length, which is the reason we have crossed out the figures under the column of G_2 in Table 54. The second value is just under double the Planck length and would be acceptable in principle. This problem will be overcome in the following section while deriving the electric field.

The great inequality $L_{5mfp} \gg L_{5md}$ (associated with G_P) could be explained by the fact that planckions are not simple spherical objects as in classical diffusion theory. Instead, they are active pulsating entities, always moving forward in addition to their random collisions. Whilst relatively densely packed, they appear (or must be) very “slippery”, behaving like superconducting entities that traverse much longer distances than their mean distance of nearest neighbors.

We should think in terms of planckion (formerly gravion) interactions described in Section 30.3; these may be accepted as they are, or modified accordingly to suit anticipated experimental outcomes. We will gradually address these issues through further work.

31.7 Deriving the electric field from the Planck field

The problem of the forbidden value $L_{2md} = 2.06 \times 10^{-37}$ m under G_2 in the Planck field arises from the increased value of number density over and above the number density of planckions if they were in a most compact state with separation equal to the Planck size. The increased field number density under G_2 is found from the application of Eq. $J_{02} = \frac{cg_{02}^2}{\pi^2 G}$ in Table 42. This equation implies a direct nexus between the field properties and the body properties with an associated body acceleration via G_2 . The flux intensity is also expressed by its equivalent $J_{02} = \frac{cg_{02}}{\pi \Lambda}$ (see Eq. 65), which allows us to fix the parameter Λ among various fields instead of the field being dependent on G .

At the outset, we introduced the universal constant Λ to replace G via $G = \Lambda g_0 / \pi$. We had no means to measure either Λ or g_0 , so we assumed a range of values for g_0 and, from the known G , we could find Λ in a corresponding range. This did not mean that the gravitational universal constant G by itself has a primary function (role, or mechanism) in the physics of nature. It means that this is actually accessible for measurement by us (via Newton’s law), from which we can derive the objectively existing flux J_0 of push particles.

For this class of fields (like for gravity), the flux is externally imposed on the absorbing bodies and not the other way around. Thus, the field flux exists primarily and independently outside of bodies. They all appear “attractive” fields associated with absorbing bodies. This is in opposition to the understanding of the hitherto prevailing theories, namely, that gravity (for example) is generated by a “mass” (or body) by “bending the space” around it. We steadfastly disagree with this concept, as our PG theory has shown that gravitational bodies play a secondary but necessary role in shaping the surrounding flux of push particles.

However, we have found at least one exception to the above type of field so far. The exception regards the charged particles actually generating the electrical field, as it is explained (or posited) in Section 21 on push electricity and in Section 25 on electron modeling. Based on this, we can explain the inconsistent result of nearest neighbors in the table under G_2 .

The double solution of Eq. (562) can refer to two separate push particle fields associated with the electron but both having the same value of g_{02} in their equation. The mathematical equation involved makes no reference to or demand on the nature of respective push particles, other than to their same interaction time t_2 and t_5 .

According to our electrical theory, we require “electrions” consisting of right-handed and left-handed helical toroidal vortices. In addition, we now require a maximum acceleration of $g_{02} = 5.56 \times 10^{51} \text{ ms}^{-2}$ for it, i.e. the same as for the Planck field with (under) G_P . We can have the latter requirement with a different type of push particles, if the different push particles have somehow the same interaction time.

This is obtained if $[\nu_2]$ planckions are not configured in the proposed helix but, instead, in a planar (mono-layer) ring rotating in the right- or left-hand sense and propagating along the axis of the ring as shown in Fig. 94. In that case, we have equal interaction times $t_2 = t_P \equiv t_5$ and equal maximum accelerations $g_{02} = g_P \equiv g_{05} = 5.56 \times 10^{51} \text{ ms}^{-2}$ between two separate fields of push particles with different G_2 and G_5 . This configuration of a mono-layer ring is a subset of the helical toroidal vortices in Fig. 76, i.e. simpler but consistent with the prior requirement.

We start with the simplest (logical) proposition of a closed ring to allow some initial calculations and make some headway forward, but with possible equivalent configurations left for later work, if needed: Any variant configuration of this group of $[\nu_2]$ planckions arranged on a plane with the same interaction time (as of single planckions) fulfills the requirement.

Examples of variant formations are: an open arc with a bigger radius, a plane coil configuration, or concentric rings all having the shortest interaction time t_P . The ring configuration in Fig. 94 does not necessitate the existence of a bond between adjacent planckions, because they can be formations of planckions created and emitted by the electron on account of its structural conditions. Nevertheless, we by no means exclude some kind of “bond” in the ring or in the helix configurations if required to explain particle physics experiments. Furthermore, we do not exclude a few additional layers on additional planes so as to form 3-dimensional toroidal vortices per Fig. 76; the quantitative consequence of this will be a small adjustment of the interaction time t_2 and g_{02} value by small factor while retaining the order of magnitude of all electrical properties and the relative strength of the electric field. For simplicity, we retain the revised concept in Fig. 94, while we envisage the electrions emitted in a similar way to the rings of air shot out of vortex cannons.

The field generated by electrons (positrons) via emission of the above electrions has a maximum particle flux at the surface of the emitting electron (positron) according to our initial proposal (see Fig. 49). Further details and consequences of this type of field have already been elaborated in the preceding relevant sections on push electricity.

We also need to take into account the envisaged mathematical proposal for elastically back-scattered push particles according to Section 28. The latter theoretical possibility may take place in the bulk of the electron or at its surface, an issue to be resolved as we develop the theory.

Accordingly, we must also consider the general description of masses and fields in Section 22, from where we quote that

“... Until we find the correct quantitative relationships, the latter particles behave like a black-hole with respect to gravions and either (a) like a white hole or (b) like a bright hole with respect to electrions...”.

Therefore, we need to continue work on the origin of the electric field with a rigorous mathematical derivation of the acceleration as we did with gravity.

We worked out the absorption of gravitational flux intensity at the surface of a sphere with radius R by Eq. 188. This provides the absorbed density flux per unit area of the sphere from all directions inside a hemispherical solid angle, i.e., by integrating from $\varphi_0 = 0$ to $\varphi_0 = \pi/2$ and obtaining for the Planck field:

$$J_{5aR} = \pi J_{05} A_{5R}$$

If we move away from the surface at a distance r from the center of the sphere, we obtain the corresponding flux absorption J_{5ar} by integrating from $\varphi_0 = 0$ to $\varphi_0 < \pi/2$ and given by:

$$J_{5ar} = \pi J_{05} A_{5R} \frac{R_{-e}^2}{r^2} \quad (592)$$

We have changed the subscripts, including the numeral (5), so as to apply the same equations to the field of planckions.

The total energy rate W_{5ar} that would be crossing the entire spherical surface at r but is absorbed (only) by the spherical body is found by multiplying with the entire surface area as:

$$W_{5ar} = 4\pi r^2 J_{5ar} = 4\pi^2 J_{05} A_{5R} R_{-e}^2$$

which is a constant (as it should) at any distance; this is because any absorption is due to the body enclosed by the surface, which is fixed. It is similar to Gauss’s law $\Phi = 4\pi q$ for electrical flux Φ around a charge q . The difference is subtle but important for our understanding of the background reality.

The quantity J_{5ar} is the deficit of flux from the real background flux J_0 , so that the variation of real (actual) flux $J(r)$ around an absorbing body is given by:

$$J_5(r) = \pi J_{05} - \pi J_{05} A_{5R} \frac{R_{-e}^2}{r^2} = \pi J_{05} \left(1 - A_{5R} \frac{R_{-e}^2}{r^2} \right) \quad (593)$$

where πJ_{05} is the integrated (total) flux flowing perpendicularly from the outside and through any spherical surface element in the absence of any absorbing body in the neighborhood, i.e., in free space. We remind that we defined at the outset J_0 to represent only the flux from one side of a surface element so that $2J_0 = 0$ from two opposite directions in free space.

The above Eq. 593 describes a monotonically increasing flux from a finite minimum value at the surface of a spherical body to very long distance reaching a saturation value. We can apply the above equations for the electron in the Planck field as depicted schematically in Fig. 95(a) with subscripts provided for this field.

Since we have $A_{5R-e} = 0.99999973732$ (i.e., very close to unity) from Table 53, there is a total absorption very close to the surface over a very thin layer dx . At the surrounding maximum acceleration g_{05} , the incident

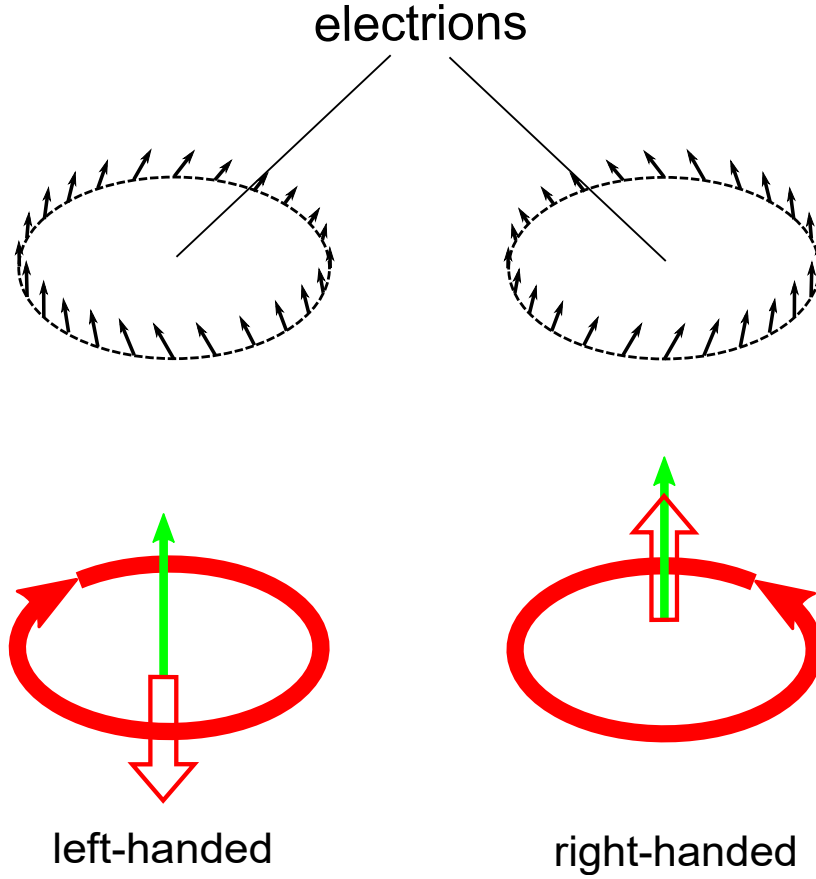


Figure 94: Revised electron model with mono-layer right-handed and left-handed circular planckions replacing the prior helical toroidal vortices.

flux normal to the surface element dS is the above derived quantity J_{5aR} after integrating all the incident planckions from all directions shown by the dashed green lines inside the electron.

We can repeat the above procedure for the electric field with g_{02} , J_{02} , G_2 and J_{2aR} . We now have $A_{2R-e} = 5.4378029778 \times 10^{-4}$ (i.e., a very small but finite value) indicating very little absorption. Depicting this field in Fig. 95(b), the primary push particle flux is located inside the electron surface boundary, in lieu of the general case of being located in the external free space. We can use the same traces as previously from all directions shown by the same dashed green lines inside the electron, which, however, here belong to another push particle class, namely, the electrions. Then, the integration yields the same formula as with the external flux.

Thus, we change the subscripts accordingly and write:

$$J_{2aR} = \pi J_{02} A_{2R}$$

for the flux of “would be absorbed electrions not arriving at the surface of the electron”. However, the preceding phrase in quotation marks is now immediately reversed by stating that this flux is emitted rather than absorbed. This is a key reversal of the role played by the electrical mass of the electron. In other words, that fraction of flux is actually arriving at the surface from within in order to be emitted by the electron externally. In addition, it is crucial to state that the prevailing "background" electron flux J_{02} exists only inside the boundary of the electron! We will further discuss the physics of this situation shortly, but let's clear the validity of the mathematical equations first. Suffice it to say that this internal flux is analogous to the electromotive force in a battery with an internal resistance producing an "electrical pressure" that drives a current in the external electrical circuit.

Therefore, we should change the subscript (a) to (e) as J_{2eR} denoting emitted flux in lieu of absorbed flux. We now have a function of electron emission with a value $J_2(R)$ at R in lieu of the previously incoming flux of planckions given by $J_5(R)$.

Henceforth, the electrions travel in the outside (“free”) space with a decreasing value inversely proportional to the square of distance.

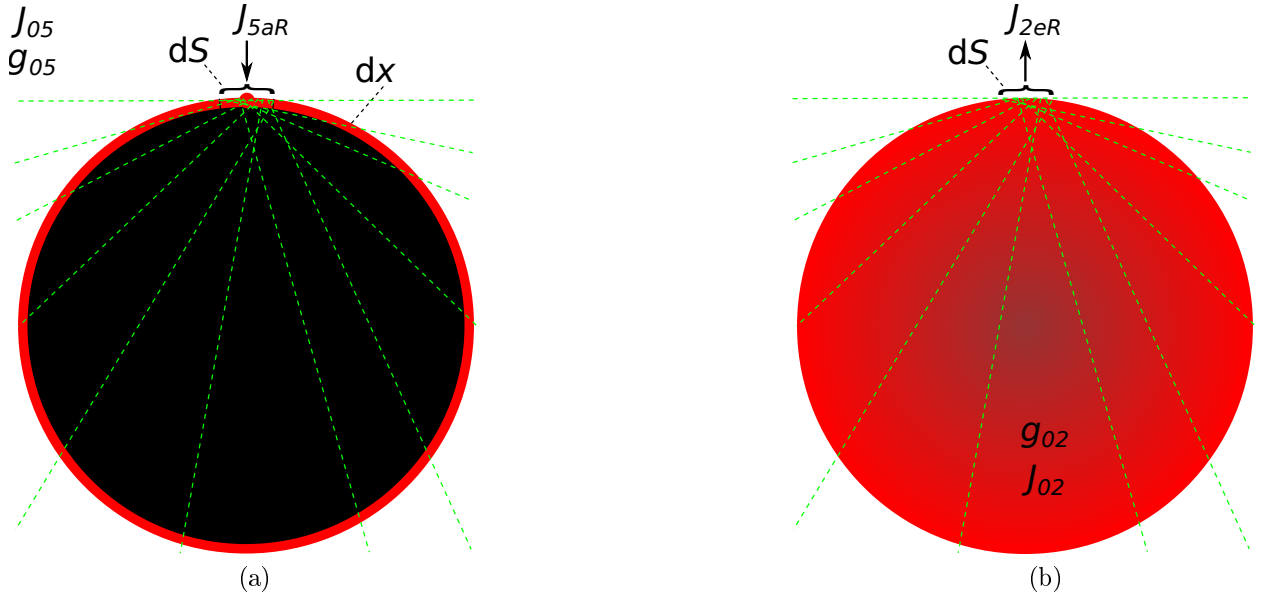


Figure 95: Integrating (a) the external planckion (somion) flux and (b) the internal electron flux, absorbed by the electron; dashed traces of planckion and electrons cross the surface element dS yielding corresponding fluxes J_{5aR} and J_{2aR}

$$J_2(r) = \pi J_{02} A_{2R} \frac{R_{-e}^2}{r^2} \quad (594)$$

Strictly speaking, the “absorptivity” denoted by A_2 is actually an “*emissivity*” for the electron and the electric field, and we should change the symbol for it, or redefine it. For now, we defer this change to take place along with many other symbol changes required by the newly generated concepts in our theory.

The total energy rate crossing an entire spherical surface at r is W_{2r} and is found by multiplying by the entire surface area as

$$W_{2r} = 4\pi^2 J_{02} A_{2R} R_{-e}^2$$

which is a constant (as it should); this is because the electron emits a fixed flux of electrons without any further “sinks” or “sources” in the surrounding space. It is similar to Gauss’s law $\Phi = 4\pi q$ for electrical flux Φ around a charge q , which still applies for a collection of electrons, but with an enclosing surface not intersecting through individual electrons; that is because the electrical mass (equivalent to charge) is distributed in a special way (by our derivation) inside the electron not obeying Gauss’s law.

Discussion and analysis: According to our electricity theory, the electrons must have a source feeding the electrons, out of which the electrons are emitted. For that source, we posited the existence of a “somion” ς field of particles, which, interacting with the electrons, generate electrons (secondary push particles) that mediate the electric field.

We can now say that this role is provided by the Planck field, i.e. the somions must be identified with planckions. In that sense, the planckions of the fifth field ($_{05}$) are not electrons, but the strongest and densest push particles in free space compacting and creating electrons and positrons, and presumably other “elementary” (classical) particles of higher and lower size order. The latter applies to all particles that have a size smaller than the mean free path of the somions. The electron, in particular, achieves very small radius, as we have computed.

We will use the words “somion” and “planckion” interchangeably until we are in a position to rationalize the terminology in a consistent way.

In the original proposal, we designated the somion flux intensity by J_{03} , but the reader should appreciate the developmental need to re-designate the same by the Planck J_{05} flux intensity.

The electrons are surrounded by a force field with an associated universal field constant $G_5 \equiv G_P$. For this value, Eq. 562 yields the Planck properties of the electron given in Table 53.

At the same time, the electrons are also “surrounded internally” by a force field with an associated universal field constant G_2 , which is intimately connected with A_2 of the electrons, but different and much less than A . There should be no inconsistency that the same particle (electron) presents two different

reactions via its two different values of Λ : one refers to absorption of planckions (somions), while the other refers to emission of electrions. We said “surrounded internally” to stress our transition from the usually external fields around particles to the special case of an internal particle field that has been responsible for the centuries long perception of the existence of “charge” as something of a unique entity. The internal field of the electron creates the electrical mass of the electron, which relates to the classical charge via our equivalence mass-charge Eq. 571.

It is quite rational that the structure of the electron is such that it reacts and generates two different outcomes to two different push particles as follows:

The somions (planckions) accrue one by one during their absorption and are subsequently emitted from the electron in groups of electrions once they reach a critical condition within the electron structure. This condition may be likened to the intermittent mechanical motion of the “drinking bird” toy (Wikipedia contributors, 2025a). In that toy, material intermittently accumulates until a critical point is reached, at which the accrued liquid tips over and leaks out.

In an analogous manner, planckions accrue inside the electron until the necessary amount is reached, at which point they are emitted as an electrion. The electrions are emitted as organized subgroups inside the electron, each containing a number of $[\nu_2]$ somions.

Thus, we can explain the dual function of the electron as both an absorber of somions and an emitter of electrions, exactly as we have always envisaged it to be. We initially argued for this type of process under the second law of thermodynamics in Section 15.8, to explain away the alleged violation of it by the re-emission of gravions via a different type of particles. All fields liaise among themselves to ensure a continuous flow of hyle without “friction”.

This burdens us with the task of finding a structure that explains this behavior. The dual function of the electron is a response to the different nature of push particles (somions and electrions). The absorption of gravions by bodies envisaged in preceding reports also takes place via electrons; thus the gravions provide an additional source of planckions via a gradual supply of planckions in their gravion chain. The latter takes place over a much longer interaction time inside a much lower density of gravions, i.e. the relative contribution to hyle accrual in the electron by gravions is greatly lesser than by somions: quantitatively, they should be insignificant, but here we have an explanation of the long-standing query about the “huge” amount of energy deposited by gravions inside planets, presumably melting away in seconds. In this regards, we have maintained that the energy flow of gravions takes place sub-atomically decoupled from the ordinary heat at atomic and molecular level.

We examine in more detail the relative importance of interactions along with associated time scales in a follow-up section.

The nearest neighbors distance problem of electrions solved: From the known g_{02} and G_2 we obtain $\Lambda_2 = \frac{\pi G_2}{g_{02}}$, electrion flux $J_{02} = \frac{cg_{02}}{\pi \Lambda_2}$ and energy density $u_0 = 2J_{02}/c$. Then the electrion number density crossed out under G_2 in Table 54 can be restored to acceptable values by dividing the energy density by $[\nu_2]$. The electrion number density is given by $n_{02} = \frac{u_{02}}{[\nu_2] E_P}$, i.e. much less than the previous unacceptable value. As a result, we can rectify the mean distance of nearest neighbors to an unacceptable value of $L_{2md} = 3.09 \times 10^{-35}$ m, actually the same as the somion L_{5md} . The difference between the two corresponds only to the different distribution of electrions vs. somions in their respective domains. We update this datum along with other newly obtained data in Table 61.

The electrions have a maximum concentration inside the electron, whilst the somions have a maximum concentration “far away from bodies”, a steady-state value prevailing and pervading the “vacuum” space everywhere with a universal Planck field constant G_5 . The universal electrical constant G_2 remains also invariant everywhere in the same way as the universal gravitational G is maintained constant inside and outside of bodies (see Section 24.1).

We already have from classical electricity for the Coulomb force the constant $G_{2C} = \frac{1}{4\pi\epsilon_0}$ (per Eq. 563) being invariable via the vacuum permittivity ϵ_0 (in conjunction with the use of electric charge measured in Coulomb). We have only modified this by our charge-mass equivalence to the new value G_2 in conjunction with the electrical mass measured in kg. At the atom and inter-atom distances, we must be dealing with an average electrion flux intensity being consistent with measurements at this level; at very close proximity with the electron and positron, the situation varies intensely, whilst we have no experimental access at such a close range.

PEAK FIELD with $G_{peak} = 1.5174305772 \times 10^{29}$ SI units			
PROTON		ELECTRON	
$k_{peak-p}R-p$	4.8353881239E-20	$k_{peak-e}R-e$	7.4996571596E-01
$A_{peakR-p}$	6.4471841652E-20	$A_{peakR-e}$	6.0694037684E-01
k_{peak-p}	5.7468363726E-05	k_{peak-e}	3.5102976082E+24
q_{peak-p}	1.0000000000E+00	q_{peak-e}	6.0696812261E-01
m_{peak-p}	1.6726219230E-27	m_{peak-e}	1.6726219237E-27
$m_{peakb-p}$	6.0658321367E-47	$m_{peakb-e}$	6.5739373483E-28
$m_{peake-p}$	1.6726219230E-27	$m_{peake-e}$	1.0152281888E-27
		J_{0peak}	6.1897794568E+81
		J_{peakaR}	1.1802420343E+82

Table 55: Properties of proton and electron in the “peak” field with $g_0 = g_{05}$

31.8 Deriving all fields

Having progressed with the investigation of the electric field, we now advance the study of the remaining fields—particularly the strong and weak fields—based on our underlying principles. This means producing push fields with strengths as close as possible to their expected values in the literature. It will then be up to other investigators to assess whether our theoretical findings agree with experimental data.

We also update and extend the previous Figs. 92 and 91, now expanded by Figs. 96 and 97, which incorporate the latest results of our analysis. In both graphs the horizontal axis is designated as G_f , representing the variable field parameter “ G ” used in solving the equations. This procedure yields corresponding (discrete) values of G for known push-fields with $f = 1, 2, 3, 4, 5$, and potentially other, as-yet-unknown, fields within the full theoretical range shown.

The force-strength curve of the Planck field establishes an upper limit for the field strength of all possible fields. There exists a family of force-strength curves that intersect the Coulomb force-strength horizontal line at two points, but none of these satisfy all the known properties of the electric field, except the upper limiting one.

The Planck-field curve itself exhibits a “peak” point at $G_{peak} = 1.5174305772 \times 10^{29}$ SI units (using $g_{05} = 5.56 \times 10^{51} \text{ ms}^{-2}$). This point is of interest because it might represent the strong field. However, its ratio $\frac{G_{peak}}{G_2} = 1.84 \times 10^3$ is about one order of magnitude higher than the anticipated relative strength of the strong field compared to the electric field. The resulting properties for the proton and electron are provided in Table 55, which show that this “field” does not qualify to be the electric field as obtained with G_2 in Table 52 (updated using the same precision of figures as currently presented with all other tables).

Additionally, there exists a unique curve tangent to the Coulomb line, touching it at a single point. This occurs when $g_{0tangent} \equiv g_{0t} = 8.1189495 \times 10^{48} \text{ ms}^{-2}$ and $G_{tangent} \equiv G_t = 2.6386912141 \times 10^{26}$ SI units. We have included this curve in Fig. 96. The corresponding curve for its “electrical” mass (m_{2e-e}) is shown in Fig. 97, and the related properties for the proton and electron are given in Table 56. While this “field” also does not produce the desired properties of the electric field (as obtained with G_2), it remains of interest because its strength ratio $\frac{G_t}{G_2} = 3.20$ is higher (albeit modestly) than that of the electric field, but still much lower than the expected strong field by two orders of magnitude less.

We will shortly proceed to resolve the strong and weak fields numerically using the above candidate G -values, but other values as well by resorting and including the balance of all flux intensities around an electron, namely, the field fluxes J_{0f} and the normal-at-electron fluxes $J_{faR} = \pi J_{0f} A_{fR}$ for each candidate scenario. The ultimate aim is to arrive at a would be “final” unifying table beyond previous Table 54.

Field ranges: Furthermore, we investigate the general variation of *force_strength* by fixing $\Lambda_f = \Lambda$, i.e. setting all fields to the same value as for the gravitational field. Then, $\Lambda_5 = \Lambda = \pi G/g_0$, with which we obtain $g_{05} = \pi G_5/\Lambda_5 = G_5/(G/g_0)$ for Eq. 562, which now becomes dependent on Λ in the expression as:

TANGENT FIELD with $G_t = 2.6386912141 \times 10^{26}$ SI units			
PROTON		ELECTRON	
$k_{t-p}R_{-p}$	5.7589427835E-20	$k_{t-e}R_{-e}$	8.9320847408E-01
A_{tR-p}	7.6785903780E-20	A_{tR-e}	6.6589673542E-01
k_{t-p}	6.8444768047E-05	k_{t-e}	4.1807612047E+24
q_{t-p}	1.0000000000E+00	q_{t-e}	5.5913324387E-01
m_{t-p}	1.6726219230E-27	m_{t-e}	1.6726219237E-27
m_{tb-p}	7.2244004647E-47	m_{tb-e}	7.3740340173E-28
m_{te-p}	1.6726219230E-27	m_{te-e}	9.3521852195E-28
		J_{0t}	7.5880828962E+78
		J_{taR}	1.5874089521E+79

Table 56: Properties of proton and electron in the “tangent” field with $g_0 = 8.1189495000 \times 10^{48} \text{ ms}^{-2}$

$$A_{2R-e} \left(\frac{\pi}{\Lambda} - \frac{3}{4k_{2-e}R_{-e}} \frac{1}{R_{-e}^2} m_{-e} \right) = 0 \quad (595)$$

We replace “ g_{02} ” in the equation with g_{05} for solution. The above equation is solved to first find the unknown product $k_{2-e}R_{-e}$ and then k_{2-e} , from which all other parameters are calculated including the effective mass $m_{2e-e} = 9.1093836978 \times 10^{-31} \text{ kg}$. This is a fixed amount, practically equal to (and slightly less than) the gravitational mass of the electron. For this condition, the *force_strength* function $f(G_f) = G_f m_{2e-e}^2$ is plotted in Fig. 96 as a straight line on logarithmic scales (labeled A). This line crosses the parallel line of $G_2 C^2$ (Coulomb *force_strength*) slightly before the point $(G_5, f(G_5))$, where the second solution of G_5 was found for the Planck field by applying the original Eq. 562. The difference is not distinguishable on the graph.

This straight line provides the locus of all possible values of G_f across all fields using a fixed Λ , namely, the maximum possible value provided by Eq. 546. In that case, all field G_f s are proportional only to their corresponding maximum accelerations g_{0fs} , as in $G_f = \Lambda g_{0f} / \pi$. We have used $g_{01} \equiv g_0 = 1.33194279663676 \times 10^9 \text{ ms}^{-2}$ and $G_1 \equiv G = 6.67408 \times 10^{-11} \text{ m}^3 \text{kg}^{-1} \text{s}^{-2}$ for generating this line.

It should be noted that the value of $G_5 = 2.78636084797137 \times 10^{32} \text{ m}^3 \text{kg}^{-1} \text{s}^{-2}$ (calculated and given in Table 54) is provided on the basis of a constant Λ for all fields. It slightly differs from the computed $G_5 = 2.7924827978 \times 10^{32} \text{ m}^3 \text{kg}^{-1} \text{s}^{-2}$ (see Eq. 567). This is a necessary theoretical difference, which we have called the difference between “calculated” and “computed” values. This difference presumably arises from the assumption of constant real mass in Eq. 559 between a proton-electron (positron) transformation. We should repeat that this “transformation” is arbitrary for the time being, but it will be considered again by our theory of the nucleus later. For now, we can explain the difference by a missing small amount of mass (hyle) in the electron, which, if added, would raise the computed values resulting in a vanishing difference between the two values of G_5 (see also Eq. 558).

For completeness, we backtrack to investigate the variation of *force_strength* by fixing $\Lambda_f = \Lambda_2$, i.e. all fields to the same value as $\Lambda_2 = \pi G_2 / g_{02}$ found for the electric field. Then, Eq. 562 reduces to

$$A_{2R-e} \left(\frac{\pi}{\Lambda_2} - \frac{3}{4k_{2-e}R_{-e}} \frac{1}{R_{-e}^2} m_{-e} \right) = 0 \quad (596)$$

We used $g_{02} = 5.56072636271391 \times 10^{51} \text{ ms}^{-2}$ and $G_2 = 8.2514882444 \times 10^{25} \text{ m}^3 \text{kg}^{-1} \text{s}^{-2}$ to obtain Λ_2 for the above equation. Similarly, we find the fixed effective mass $m_{2e-e} = 1.6721105758 \times 10^{-27} \text{ kg}$ (slightly less than the gravitational mass of the proton but slightly more than the electrical mass of the electron).

Similarly, we plot the function $f(G_f) = G_f m_{2e-e}^2$ resulting in the straight line labeled Λ_2 in Fig. 96. This straight line crosses the parallel line of $G_2 C^2$ (Coulomb *force_strength*) slightly before the “computed” point $(G_2, f(G_2))$, i.e., where the first solution of G_2 was found for the Planck field by applying the original Eq. 562. The difference is not distinguishable on the graph. The important lesson we learn here is that this is a theoretical asymptote to all force-strength curves of all possible fields. They all converge on this asymptote as we move towards low values of G_f . This asymptote sets a lower limit for all Λ s.

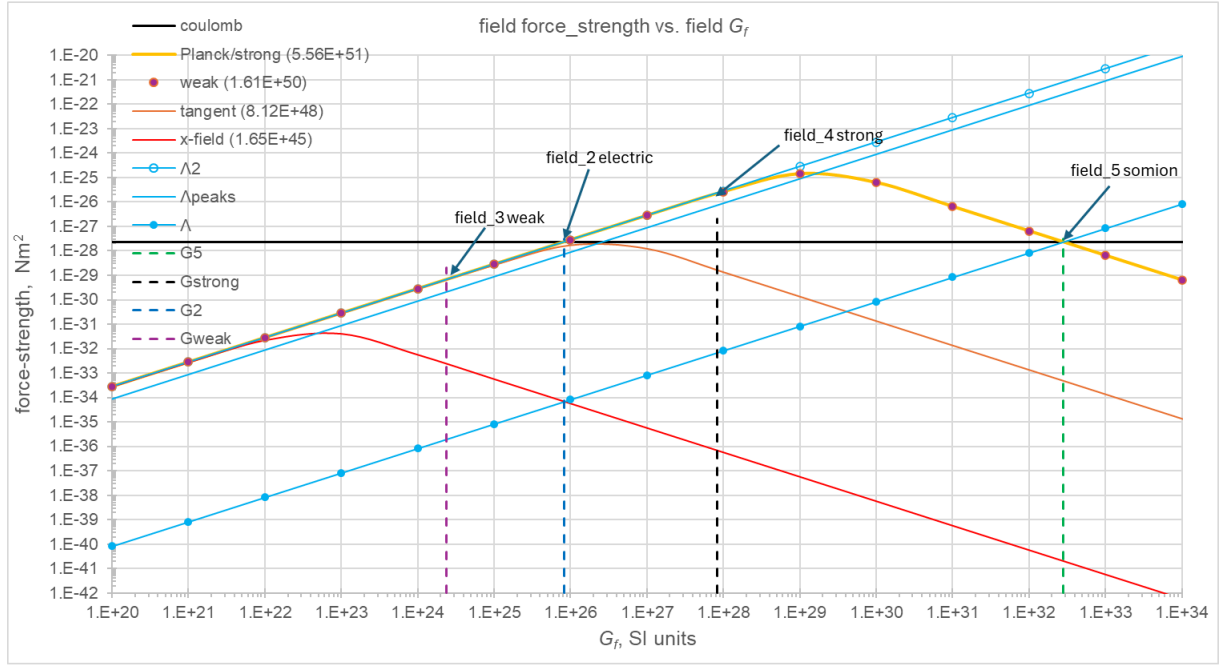


Figure 96: Plank field *force_strength* (curve) crossing with Coulomb *force_strength* (line) at two points G_2 and G_p ; x-field *force_strength* (curve); all-field *force_strength* straight lines with fixed Λ_{max} and Λ_2

The corresponding variation of effective masses are included in Fig. 97. Since they are fixed values at m_{2e-e} , they appear as parallel lines and are indistinguishable on the graph from the provided points of gravitational masses of the proton and electron.

To illustrate the order of magnitude of variation of the effective mass m_{2e-e} along what appears to be a “constant” (parallel) line—together with the subsequent rapid change—we present the actual numerical values in a snapshot of the Excel sheet, formatted in text mode to allow the display of an extended part of the mantissa variation, in Fig. 98.

To reproduce the numbers in this figure, use $g_0 = 1.33241092444440e9$, $g_{02} = 5.56072636271391e51$, $R_{-p} = 8.414e-16$, $m_{e-p} = 1.672621923e-27$, $m_{e-e} = 9.109383701500000e-31$, $G = 6.67408e-11$, $G_2 = 8.2514906793e20$, $G_{2C} = 8.9875520000e9$, $e = 1.6021766340e-19$, all in SI units as input in a Python program to compute all related electron and proton parameters with precision set via `mp.dps = 190`. [Note: The value of $g_0 = 1.33241092444440e9$ was inadvertently used in the Python program in previous versions, which has been replaced by the intended value of $g_0 = 1.33194279663676e9$ as from this version, but one needs to use the above values in order to reproduce the figures in the snapshot provided].

As a result of the above analysis, we conclude that the force-strength of all fields is constrained between the two straight lines described earlier, each having fixed y -intercepts and a slope equal to unity on a logarithmic scale. Strictly speaking, the “computed” Λ_2 asymptote would be shifted slightly upwards (or leftwards) if we used the “calculated” G_2 value, which would then represent the asymptote of the correctly “computed” force-strength curve when the small “missing” mass in the electron transformation is accounted for.

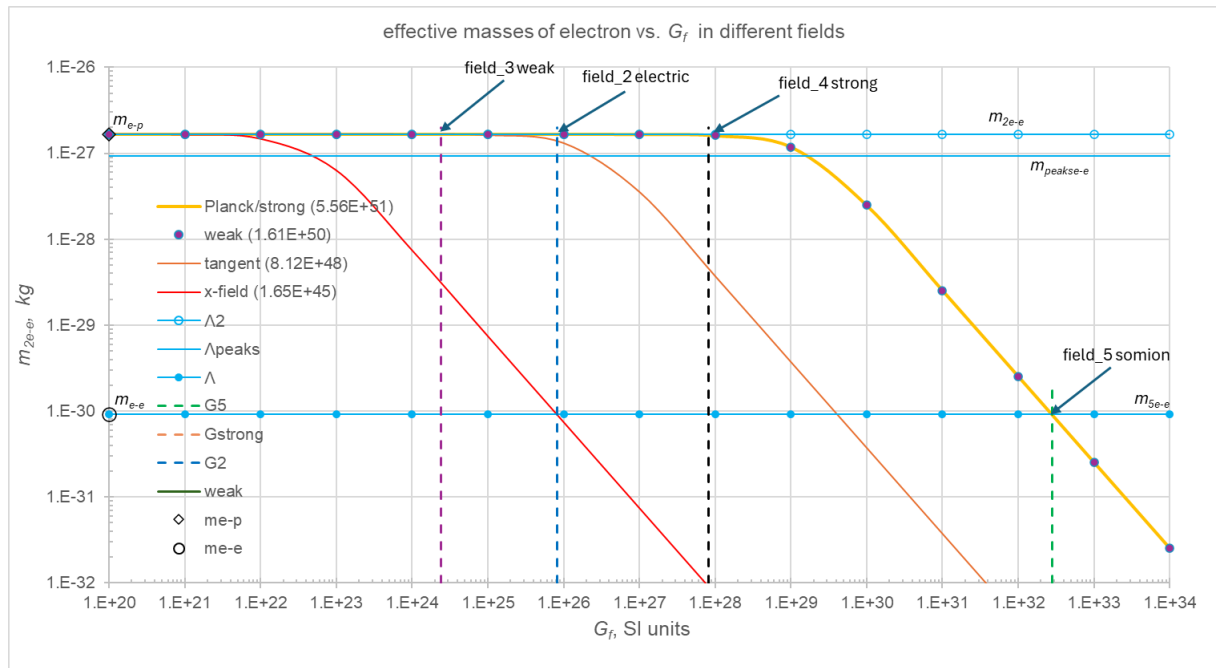
Similarly, the effective mass of the electron is constrained between the two parallel lines shown in the corresponding figure, for which the same remarks apply regarding the difference between “computed” and “calculated” values. This small difference may be important in understanding the physics involved in its origin.

Quantitatively, the two straight lines constrain the fields in a range with Λ_f values lying between:

$$4.66 \times 10^{-26} < \Lambda_f < 1.57 \times 10^{-19} \quad (597)$$

Consistent with the above finding, we also find that there is a straight line on logarithmic scales analogous to the preceding ones, and crossing the Planck curve at its peak point. For this line we have the constant Λ_{peaks} :

$$\Lambda_{peaks} = \frac{\pi G_{peaks}}{g_{05}} = 4.6589170953 \times 10^{-26} \text{ m}^2 \text{ kg}^{-1}$$



X-FIELD with $G_x = 8.25148824441899 \times 10^{25}$ SI units			
PROTON		ELECTRON	
$k_{x-p}R_{-p}$	8.8843471231E-17	$k_{x-e}R_{-e}$	1.3779567597E+03
A_{xR-p}	1.1845796164E-16	A_{xR-e}	9.9999973667E-01
k_{x-p}	1.0559005376E-01	k_{x-e}	6.4496792516E+27
q_{x-p}	1.0000000000E+00	q_{x-e}	5.4428398950E-04
m_{x-p}	1.6726219230E-27	m_{x-e}	1.6726219237E-27
m_{xb-p}	1.1145115327E-43	m_{xb-e}	1.6717115423E-27
m_{xe-p}	1.6726219230E-27	m_{xe-e}	9.1038133354E-31
		J_{0x}	9.9703448022E+71
		J_{xaR}	3.1322760474E+72

Table 57: Properties of proton and electron in the “x-field” field with $g_0 = 1.6457383878 \times 10^{45} \text{ ms}^{-2}$

We note graphically that it crosses the peak point of the force-strength curve of every possible field. The analogous parallel line for this case is also drawn in Fig. 97 for the effective masses.

Since the x-field still mentioned in Table 54 has played a transitory role in the understanding and development of fields, we supplement with its properties of the electron and proton in Table 57; it might help in the better understanding and analysis of this work.

Finally, we invoke also the “note on subscripts” used for fields and masses stated in Section 31.5.7 to avoid possible confusion in the above expressions.

31.8.1 Flux intensity balance, strong and weak fields

A new issue arises from the exiting electric flux intensity $J_{02} = 1.1382866115 \times 10^{85} \text{ Js}^{-1} \text{ m}^{-2}$ (Table 52), which is vastly greater than the entering Planck (somion) flux $J_{05} = 3.3709060407 \times 10^{78} \text{ Js}^{-1} \text{ m}^{-2}$ (Table 53).

To maintain steady-state energy balance in an electron, the total incoming and outgoing energy fluxes must cancel. The gravitational field is many orders of magnitude smaller and can be neglected at this stage, leaving the electric, Planck, strong and weak fields as the dominant contributors. Only the electric field flux is emitted from the electron, while all other fluxes are absorbed. Having worked out quantitatively all properties for various fields, we have added two more rows for J_{0f} and J_{faR} in their tables, and compare them as follows.

The absorbed flux from the Planck field at the electron surface is $J_{5aR} = \pi J_{05} A_{5R} = 1.0590010861 \times 10^{79} \text{ Js}^{-1} \text{ m}^{-2}$, with $A_{5R} \approx 1$ (Table 53). The exiting (emitted) electric flux is $J_{2aR} = \pi J_{02} A_{2R} = 1.9438930599 \times 10^{82} \text{ Js}^{-1} \text{ m}^{-2}$ (Table 52).

This leaves a large imbalance of fluxes.

At steady state, the local energy-flux balance for the electron should read schematically:

$$\pi J_{05} A_{5R} + (\text{other in-fluxes}) = \pi J_{02} A_{2R} \quad (598)$$

That is, if all of our derivations are correct, then this excess flux in the electron must originate from the other external fields. We note that the value of J_{2aR} lies nearly halfway on a logarithmic scale between J_{05} and J_{02} . Also, the peak of the force-strength curve in Fig. 96 lies halfway between G_2 and G_5 . As stated, this curve is the locus of all fields with a fixed g_{05} at various G_f values. We have already found good applications at G_2 and G_5 , while the value G_{peak} , at the peak of the curve has been already considered to be of special interest in the preceding section.

The pair (g_{05}, G_{peak}) defines a new field, for which we readily find:

$$J_{0peak} = 6.1897794568 \times 10^{81} \text{ Jm}^{-2} \text{ s}^{-1}.$$

The absorbed fraction normal to the surface is then:

$$J_{0peakaR} = \pi J_{0peak} A_{peakR-e} = 1.1802420343 \times 10^{82} \text{ Jm}^{-2} \text{ s}^{-1},$$

STRONG FIELD with $G_4 = 8.2464424800 \times 10^{27}$ SI units			
PROTON		ELECTRON	
$k_{4-p}R_{-p}$	2.6277808442E-21	$k_{4-e}R_{-e}$	4.0756718833E-02
A_{4R-p}	3.5037077922E-21	A_{4R-e}	5.2716684353E-02
k_{4-p}	3.1231053532E-06	k_{4-e}	1.9076633717E+23
q_{4-p}	1.0000000000E+00	q_{4-e}	9.7008577718E-01
m_{4-p}	1.6726219230E-27	m_{4-e}	1.6726219237E-27
m_{4b-p}	3.2964628866E-48	m_{4b-e}	5.0035184920E-29
m_{4e-p}	1.6726219230E-27	m_{4e-e}	1.6225867388E-27
		J_{04}	1.1389833418E+83
		J_{4aR-e}	1.8863198387E+82

Table 58: Properties of proton and electron in the strong field with $g_{04} = g_{05}$

with computed $A_{peakR-e} = 0.60694037684$ per Table 55. Adding this to the Planck input gives:

$$J_{\text{input-aR}} = 1.1802420343 \times 10^{82} + 1.0590010861 \times 10^{79} = 1.1813010354 \times 10^{82}.$$

This may be considered close enough to the missing term in Eq. 598. The outstanding difference is:

$$\pi J_{0?} A_{?R} = 1.9438930599 \times 10^{82} - 1.1813010354 \times 10^{82} = 7.6259202450 \times 10^{81},$$

which should be coming from another field, subscripted with a question mark (?). This amount is reasonable and can potentially be contributed by the as-yet unaccounted weak field.

Therefore, if this “peak” field exists, then we have potentially accounted for the discrepancy in the balance of fluxes arriving at and exiting the electron. We might even claim that this field coincides with the nuclear field. We have computed the usual properties for this field as we can see in Table 55. In fact, if our calculations are correct, this can be the nuclear field, for which we are preparing a separate report.

The expected $G_{strong} \equiv G_4 = 6.67 \times 10^{27}$ SI units, based on the published field-strength factor of $\sim 10^{38}$, is clearly less than the G_{peak} value by a factor $G_{peak}/G_4 = 22.736$, which is not too far out from the indicative expected value, but may not be accepted by prevailing requirements. However, it is presented for consideration by nuclear or other physicists for acceptance or not.

Based on the above, we can work out the remaining properties of the weak field and thereby elucidate its physics. We have now found that the three fields — electric, strong and Planck — share the same known maximum acceleration, $g_{02} = g_{0peak} = g_{05}$, with the corresponding values (found) for G_2, G_{peak} and G_5 . We also know G and g_0 for the gravitational field, so we can use these quantities to compute the remaining parameters of each field in a next updated table after Table 54.

Alternative strong and weak field parameters: We should emphasize that the preceding method of establishing the strong field, while leaving the weak field still undetermined, is a heuristic approach based only on our independent theoretical findings. We can use the same approach to find an alternative set of possible values for both the weak and strong fields while satisfying even better the flux intensity balance equation.

For this purpose, we now provide two additional rows with the field flux J_{0f} and the normal at the electron flux $J_{faR} = \pi J_{0f} A_{fR}$ in the tables for each presented case. so that we can check the best outcome with respect to flux balance combined with expected field strength. The columns for the proton are left blank to continue later with more work and analysis.

We can derive the properties of the strong and weak fields by accepting their expected strengths. Thus, we accept two orders of magnitude above the electric field with $G_4 = 8.2464424800 \times 10^{27}$ SI units, **for the strong field**. We match it with a maximum acceleration $g_{04} = g_{05}$; the latter choice is arbitrary but is a first logical choice. The numerical outcomes are compiled in Table 58.

For the weak field, after a previous rectification and trial, at present we adopt the last pair of values: $G_3 = 2.3997147617 \times 10^{24}$ SI units and $g_{03} = 1.6067643946 \times 10^{50}$ SI units, **which also yielded improved agreement in the total flux balance; we can see** that the sum of input fluxes $J_{5ar} + J_{4ar} + J_{3ar} = 1.9435472566 \times 10^{82}$

WEAK FIELD with $G_3 = 2.3997147617 \times 10^{24}$ SI unitsS			
PROTON		ELECTRON	
$k_{3-p}R_{-p}$	2.6464363706E-23	$k_{3-e}R_{-e}$	4.1046064898E-04
A_{3R-p}	3.5285818275E-23	A_{3R-e}	5.4711242424E-04
k_{weak-p}	3.1452773599E-08	k_{3-e}	1.9212065348E+21
q_{3-p}	1.0000000000E+00	q_{3-e}	9.9969222189E-01
m_{3-p}	1.6726219230E-27	m_{3-e}	1.6726219237E-27
m_{3b-p}	3.3198656185E-50	m_{3b-e}	5.1479640953E-31
m_{3e-p}	1.6726219230E-27	m_{3e-e}	1.6721071273E-27
J_{03}	3.2678772365E+83	J_{03}	3.2678772365E+83
J_{3aR-p}	3.6225617650E+61	J_{3aR-e}	5.6168416834E+80

Table 59: Properties of proton and electron in the [weak](#) field with $g_{03} = 1.6067643946 \times 10^{50}$

ELECTRIC FIELD with $G_2 = 8.24644248003 \times 10^{25}$			
PROTON		ELECTRON	
$k_{2-p}R_{-p}$	2.6277808442E-23	$k_{2-e}R_{-e}$	4.0756718833E-04
A_{2R-p}	3.5037077922E-23	A_{2R-e}	5.4325684287E-04
k_{2-p}	3.1231053532E-08	k_{2-e}	1.9076633717E+21
q_{2-p}	1.0000000000E+00	q_{2-e}	9.9969439104E-01
m_{2-p}	1.6726219230E-27	m_{2-e}	1.6726219237E-27
m_{2b-p}	3.2964628866E-50	m_{2b-e}	5.1116824343E-31
m_{2e-p}	1.6726219230E-27	m_{2e-e}	1.6721107554E-27
		J_{02}	1.1389833418E+85
		J_{2aR-e}	1.9438934234E+82

Table 60: Electrical properties of proton and electron in the electric field applying calculated G_2 , all in SI units

$\text{Jm}^{-2}\text{s}^{-1}$ compares very well with the electrical output flux $J_{2aR} = 1.9438934234 \times 10^{82} \text{ Jm}^{-2}\text{s}^{-1}$. The latter value is taken from the present Table 60 based on the “calculated” G_2 instead of the “computed” G_2 used in the earlier Table 52, i.e. for consistency in the electrical properties applied through the analysis.

We will discuss again the tentative parameters of both the weak and strong fields derived so far in a forthcoming section on nuclear physics.

It would be futile to persist in finding an exact balance of flux intensities at this stage of our development, since the published field strength values are approximate in addition that we have adopted a heuristic approach. We should be satisfied at least that we have demonstrated the possibility of making our theory work consistently with existing ideas of field strengths, etc.

Given that the maximum acceleration and interaction time of the “peak” field, or the strong field as proposed above are the same as in the Plank field, their push particles must also lie on a plane, like the in the electric field.

Current updating of field unification table: If we can finally have the equation $g_{02} = g_{0peak} = g_{05}$, the interaction time for these three fields is the minimum possible and equal to the Planck time. Hence, neither the interaction time nor the maximum acceleration can be used for ranking the strength of fields as we did in Section 31.5.8. That leaves the energy of the push particle in each field that could be used for ranking in reverse order, provided the preceding theory about it can be verified. However, even the graviton composition will be reappraised shortly.

field type (f)	gravity ($_1$)	weak ($_3$) test	electricity ($_2$)	strong ($_4$) test	Planck ($_5$)
particle name	gravions	y-ions	electrions	z-ions	planckions
g_{0f}	1.33E+09	1.61E+50	5.56E+51	5.56E+51	5.56E+51
G_f	6.67E-11	2.40E+24	8.25E+25	8.25E+27	2.79E+32
strength, s_f	1.00E+00	3.60E+34	1.24E+36	1.24E+38	4.17E+42
#planckions, $[\nu_f]$	4.17E+42	1.16E+08	3.38E+06	3.38E+04	1.00E+00
t_f	2.25E-01	1.87E-42	5.39E-44	5.39E-44	5.39E-44
ℓ_f	6.75E+07	5.59E-34	1.62E-35	1.62E-35	1.62E-35
J_{0f}	8.07E+35	3.27E+83	1.14E+85	1.14E+83	3.37E+78
u_{0f}	5.39E+27	2.18E+75	7.59E+76	7.60E+74	2.25E+70
n_{0f}	1.95E+18	2.83E+100	3.39E+103	3.39E+103	3.39E+103
A_f	1.57E-19	4.69E-26	4.66E-26	4.66E-24	1.57E-19
L_{fmd}	8.01E-07	3.28E-34	3.09E-35	3.09E-35	3.09E-35

Table 61: Comparative values of universal constants for gravitational, weak, electric, strong and Planck fields

The number of planckions $[\nu_f]$ in the push particle of each field was previously determined from the helical length, which was inversely proportional to the field strength G_f . Since the helical configuration has now been replaced by a planar planckion configuration, we can only use the field strength G_f to determine $[\nu_f]$, again assuming an inverse proportionality.

As a result, we are left with G_f as the best indicator of field strength. It combines the overall effect of field-body interaction in its product

$$G_f = \frac{\Lambda_f g_{0f}}{\pi}.$$

It serves as a measure of the force exhibited in this interaction. While G is a constant, it applies only within the gravitational field and is not a universal constant throughout the universe. Each field f has its own characteristic G_f , which can be used to rank the relative field strengths.

Furthermore, G is accessible and measurable—raising the important question of how to access or measure the corresponding G_f values, which have now theoretically emerged from our push field theory.

The final updated results are presented in Table 61, which supersedes Table 54. The corrected Planck column under G_2 has been reassigned to the former x-field column, now reserved for the electric field as in prior tables. These revised values satisfy the requirements of the electric field while retaining the values of G_2 and $g_{05} = g_{02}$. Furthermore, they yield the correct Coulomb force (Coulomb force-strength) and electrical mass, as represented in Figs. 96 and 97.

In addition, we have rearranged the order of the rows so that those containing the starting values of g_f and G_f appear at the top, since all other properties are derived from these given quantities.

The strength of all fields is in general agreement with the literature. In addition, we have now introduced the new (fifth) Planck field. It remains to be determined whether this field corresponds to some as-yet-unrecognized experimental data or whether it will prompt a new line of investigation. However, adjustments for the weak field remain to be found in conformity with flux intensity balance requirement.

Finally, to assist the reader in reproducing or verifying our results—and to avoid possible confusion with similar but evolving tables—we also provide an updated Table 62, which contains the exact equations (formulas) used to generate the preceding numerical table.

31.9 Further field analysis

In the graphs of the previous Figs. 96 and 97, the force-strength and mass curves were labeled with the names of the corresponding fields. This labeling was originally based on the presumption that each field

field type ($_{0f}$)	gravity ($_{01}$)	weak ($_{03}$)	electricity ($_{02}$)	strong ($_{04}$)	Planck ($_{05}$)
particle name	gravions	y-ions	electrions	z-ions	planckions
g_{0f}	g_{01}	g_{03}	g_{02}	g_{04}	g_{05}
G_f	G	G_3	G_2	G_4	G_5
strength, s_f	$s_1 = \frac{G}{G} = 1$	$s_3 = \frac{G_3}{G}$	$s_2 = \frac{G_2}{G}$	$s_4 = \frac{G_4}{G}$	$s_5 = \frac{G_5}{G}$
#planckions, $[\nu_f]$	$[\nu_1] = \frac{s_5}{s_1}$	$[\nu_3] = \frac{s_5}{s_3}$	$[\nu_2] = \frac{s_5}{s_2}$	$[\nu_4] = \frac{s_5}{s_4}$	$[\nu_5] = \frac{s_5}{s_5}$
t_f	$t_1 = \frac{c}{g_{01}}$	$t_3 = \frac{c}{g_{03}}$	$t_2 = \frac{c}{g_{02}}$	$t_4 = \frac{c}{g_{04}}$	$t_5 = \frac{c}{g_{05}}$
ℓ_f	$\ell_1 = ct_1$	$\ell_3 = ct_3$	$\ell_2 = ct_2$	$\ell_4 = ct_4$	$\ell_5 = ct_5$
J_{0f}	$J_{01} = \frac{cg_{01}^2}{\pi^2 G}$	$J_{03} = \frac{cg_{03}^2}{\pi^2 G_3}$	$J_{02} = \frac{cg_{02}^2}{\pi^2 G_2}$	$J_{04} = \frac{cg_{04}^2}{\pi^2 G_4}$	$J_{05} = \frac{cg_{05}^2}{\pi^2 G_5}$
u_{0f}	$u_{01} = \frac{2J_{01}}{c}$	$u_{03} = \frac{2J_{03}}{c}$	$u_{02} = \frac{2J_{02}}{c}$	$u_{04} = \frac{2J_{04}}{c}$	$u_{05} = \frac{2J_{05}}{c}$
n_{0f}	$n_{01} = \frac{u_{01}}{[\nu_1] E_P}$	$n_{03} = \frac{u_{03}}{[\nu_3] E_P}$	$n_{02} = \frac{u_{02}}{[\nu_2] E_P}$	$n_{04} = \frac{u_{04}}{[\nu_4] E_P}$	$n_{05} = \frac{u_{05}}{[\nu_5] E_P}$
Λ_f	$\Lambda_1 = \frac{\pi G}{g_{01}}$	$\Lambda_3 = \frac{\pi G_3}{g_{03}}$	$\Lambda_2 = \frac{\pi G_2}{g_{02}}$	$\Lambda_4 = \frac{\pi G_4}{g_{04}}$	$\Lambda_5 = \frac{\pi G_5}{g_{05}}$
L_{mdf}	$L_{md1} = \frac{1}{n_{01}^{1/3}}$	$L_{md3} = \frac{1}{n_{03}^{1/3}}$	$L_{md2} = \frac{1}{n_{02}^{1/3}}$	$L_{md4} = \frac{1}{n_{04}^{1/3}}$	$L_{md5} = \frac{1}{n_{05}^{1/3}}$

Table 62: Updated formulas used to produce the numerical values of the preceding Table 61

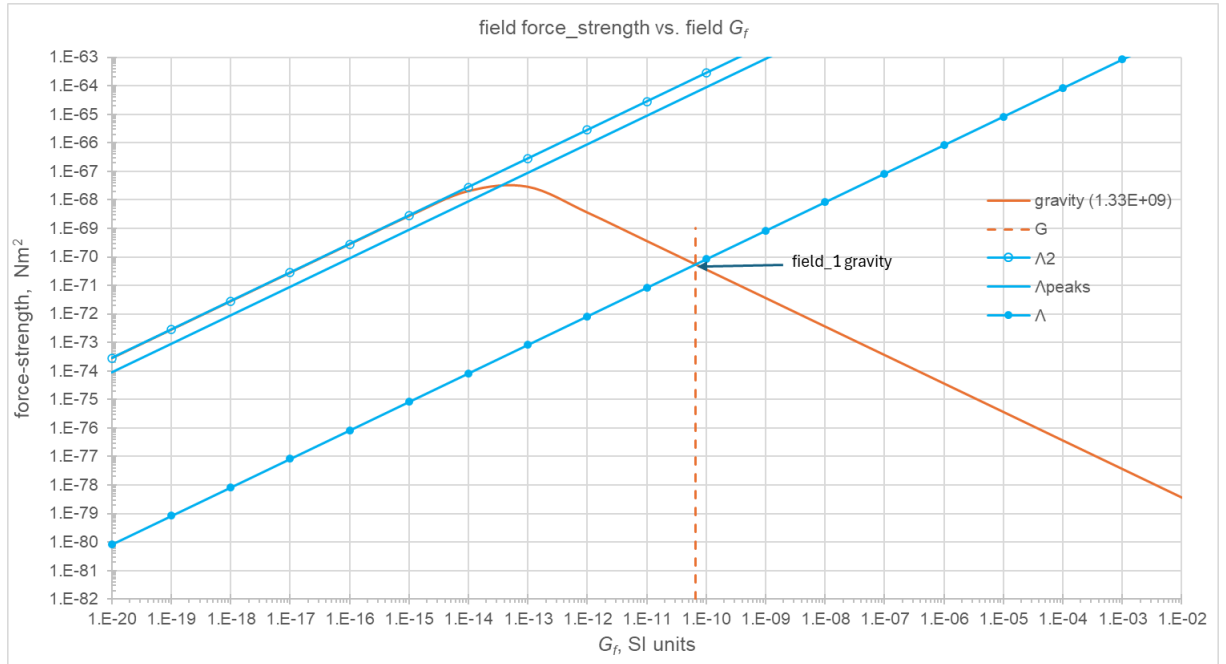


Figure 99: Force-strength variation against G_f for gravity

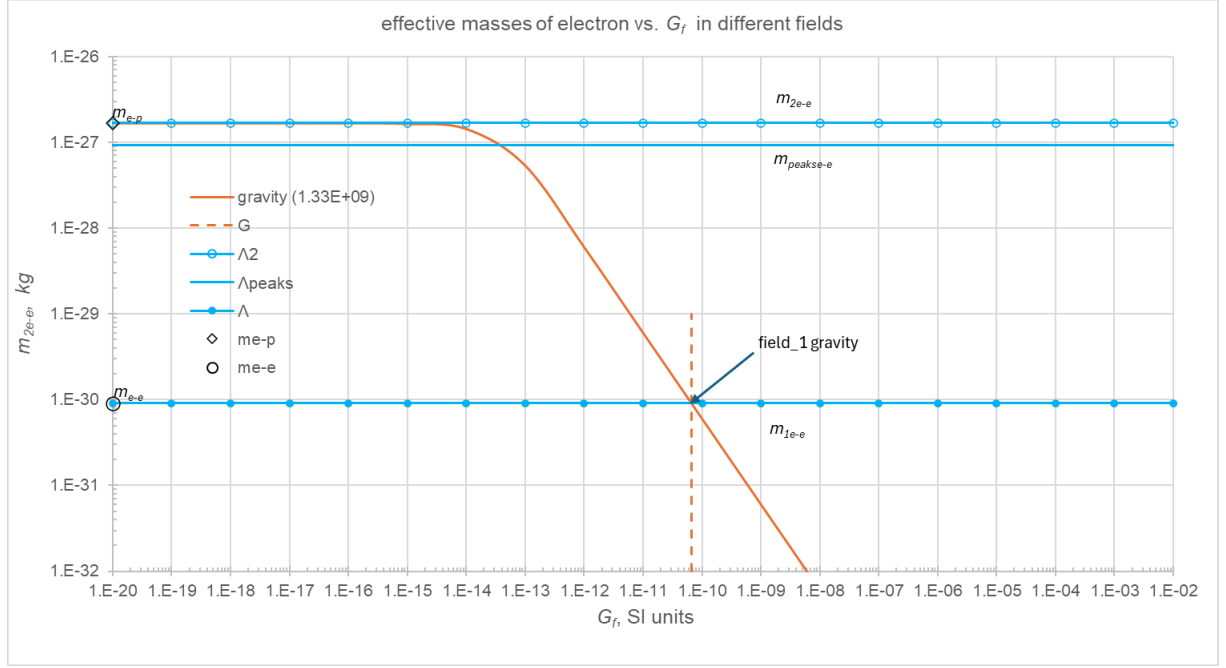


Figure 100: Force-strength variation against G_f for gravity

f is characterized by its own unique value of maximum acceleration g_{0f} . However, it was later found that different fields may share the same maximum acceleration while differing in G_f (or Λ_f).

In other words, each field is now characterized by a pair (g_{0f}, G_f) , or equivalently by a pair (g_{0f}, Λ_f) , given the relationship $\pi G_f = \Lambda_f g_{0f}$. This clarification is now explicitly shown by indicating the points that define the gravitational, weak, electric, strong, and somion fields as *field_1*, *field_2*, *field_3*, *field_4*, and *field_5*, respectively.

The gravitational field was not previously included because it is positioned many orders of magnitude lower on the G_f axis, and its omission allowed for greater clarity in the displayed graphs. We now supplement the corresponding plots for force-strength and effective mass (m_{2e-e}) in Figs. 99 and 100. These graphs were generated by setting $g_{02} = g_{01} \equiv g_0$ and $G_2 = G_1 \equiv G$ for solving Eq. 562.

For clarity, we have now added in parentheses the actual value of g_{0f} used, next to the field-name labels, in Fig. 100 and other related preceding figures.

The various data presented in the above figures and tables, such as Table 60, were obtained sequentially in a single computation run for each given (fixed) value of g_{0f} , while varying G_f over a wide range of values. Thus, all quantities can be compiled into an Excel worksheet for further processing, such as plotting and comparison. This approach enables the observation of the relative variations among all computed parameters of the electron (or positron) and proton, which aids in understanding the underlying physics and in determining the actual fields objectively involved among the theoretical “possibilities” presented. Once we decide on a possible value of G_f for a given field, we repeat the computation to determine the unique properties corresponding to the chosen pair (g_{0f}, Λ_f) . The electric and Planck field were determined from the intersection of the Coulomb force-strength line at two points with the force-strength curve at g_{05} value, while for the gravitational field we have the existing G (or Λ) and the derived g_0 . The remaining weak and strong fields are yet to be established quantitatively under the push field theory under development.

Following the above procedure, it is useful to plot some of these computed properties against the variation of Λ_f within its expected range provided by expression 597. Accordingly, the force-strength variation is plotted in Fig. 101, encompassing all five fields.

We note in Fig. 101 that the peak of force-strength occurs at a common value of Λ_f for all cases, as expected from the straight line graphs in Fig. 96, which are parallel to the asymptote at the minimum value of Λ_f . The difference is that we now resolve the previously “infinite” parallel lines of constant Λ_f , which lay between the “peak straight line” and the asymptote and were indistinguishable in the earlier graphical presentation toward low values of G_f . These lines are now distinguishable along the vertical axis of force-strength. The five fields are represented by the intersection points of the respective Λ_f value for each field f with the corresponding g_{0f} curve.

Following again the same procedure, the absorptivity, contraction factors and effective mass are shown in Fig. 102a, b, c, d, e and f. Each property is plotted twice on different scales, namely, on log-log and

on linear-log scales. This approach reproduces the expected “sigmoid” shape often discussed previously but not visible on log-log scales. This distinction is important to bear in mind to avoid misunderstanding the varying nature of each property. Specifically, there is a slow variation in the Newtonian regime, another slow variation in the “saturation” absorption regime, and a transient range in between—visible on the linear-log scales—which corresponds to a short inflection region on the log-log scales.

All of the above three properties are plotted against Λ_f with points (markers) obtained by the said single computation run with incremental steps of G_f . We note that for each property, all the points fall on a common curve. This behavior is expected from the known relationships in gravity, which also apply across all fields. For convenience, we restate the key relationships, now introducing the subscript (f) to denote applicability across fields:

All of the above three properties are plotted against Λ_f using data points (markers) obtained from the said single computation run with incremental steps of G_f . For each property, all the points fall on a common curve. This behavior is expected from the known relationships in gravity, which also apply across all fields. For convenience, we restate the key relationships, now introducing the subscript (f) to denote applicability across fields:

$$A_{fR-e} = 1 - \frac{1}{2(k_{f-e}R_{-e})^2} + \frac{\exp(-2k_{f-e}R_{-e}) \cdot (2k_{f-e}R_{-e} + 1)}{2(k_{f-e}R_{-e})^2} \quad (599)$$

$$q_{f-e} = \frac{m_{fe-e}}{m_{-e}} = \frac{3A_{fR-e}}{4k_{f-e}R_{-e}} \quad (600)$$

$$m_{fe-e} = q_{f-e}m_{-e} \quad (601)$$

All the above quantities depend on the product $k_{f-e}R_{-e}$, which is proportional to Λ_f :

$$\Lambda_f = \frac{k_{f-e}}{\rho_{-e}} = \frac{k_{f-e}}{\frac{4}{3}\pi R_e^3} = \frac{4\pi R_e^2}{3m_{-e}} k_{f-e}R_e$$

$$k_{f-e}R_e = \Lambda_f \frac{3m_{-e}}{4\pi R_e^2} \quad (602)$$

This means that the above quantities (and many others) are invariant functions of Λ_f (or $k_{f-e}R_{-e}$), provided that the electron radius and real mass remain invariant and, hopefully, retain the values we have determined so far.

We plot the above functions as a line labeled “function,” together with the same relationships presented as data points in Fig. 102a, b, c, d, e and f, all of which fall along the line as expected.

The field analysis is now paused and will be continued later under a broader framework on quantum push field theory in Section 32, as we must first investigate additional aspects of space, time, and quantum mechanics.

31.10 Space, time and quantum mechanics: Interaction, integration and mean separation times vs. body size

We undertake an investigation into the various time constants involved in push field theory. We have already mentioned the interaction and integration times in PG, but we also need a third important time concept, to which we will refer as the mean separation time between particle absorption events. We aim to find the relationship among all these time constants in conjunction with the corresponding body size.

31.10.1 Interaction time

We define the interaction time (of a gravion, electrion, etc.) as the duration of the absorption process of a given pushing particle by a given body. For a gravion, we denote this as t_g or t_1 , and similarly as t_f for other field- f particles with $f = 1, 2, 3, 4, 5$. The interaction time is finite, although extremely short. We assume that the shortest possible interaction time is that of a planckion, equal to the Planck time $t_P = 5.391247 \times 10^{-44}$ s. Longer interaction times may arise through sequential absorption of consecutively

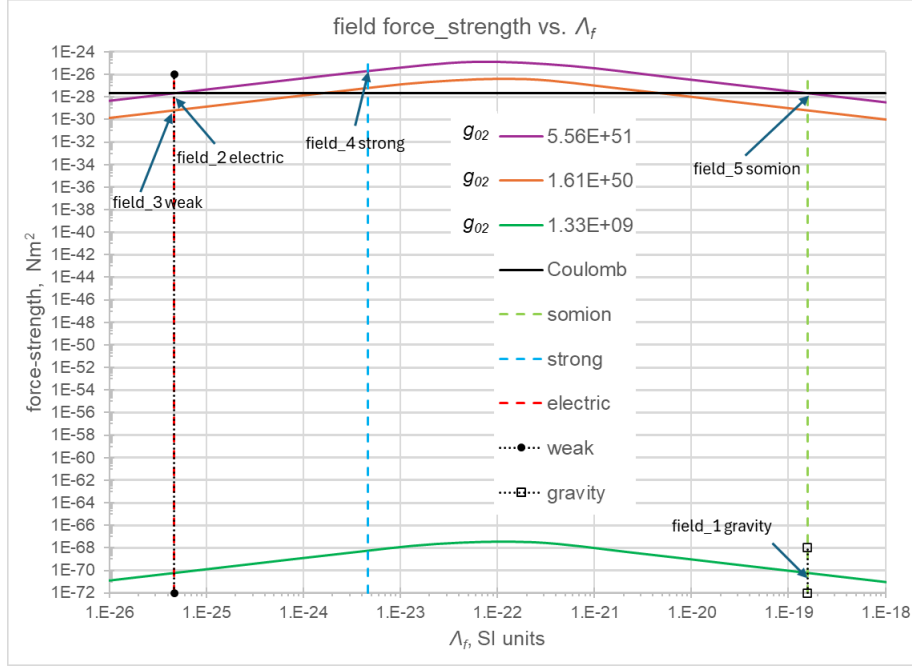


Figure 101: Fields force-strength variation against Λ_f

arriving planckions of a push particle. We initially assume this possibility without specifying whether adjacent planckions are physically linked (or bonded) together, or whether they arrive sufficiently close in time due to preceding production/emission processes. This question is left open for future treatment within the appropriate modeling framework.

In previous work, we initially considered the interaction time to be approximately equal to the integration time. However, this is not generally the case, and a more detailed theory of the integration time is developed in the following section.

31.10.2 Integration time

The integration time (of a gravion, electron, etc.) is the duration of time necessary to reach a steady state (equilibrium) situation in any physical system or process. We have already briefly touched upon this subject early on by Eq. 195. This means that, over and above the interaction time, we have to wait until an equilibrium is established with relation to the generation of the effective mass in a given body. This time is a natural duration dependent on the size (or geometry, in general) of the body. The larger the body size, the longer this time constant is.

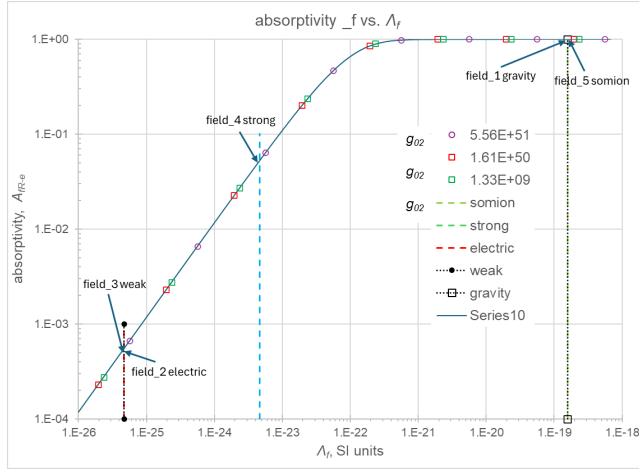
This is an objective physical process or mechanism integrating the effects of absorption of all pushing particles by a given body to reach equilibrium. The observation itself (by humans) may introduce a superimposed time constant that is characteristic of the measuring equipment. We initially assume that our instrument does not affect the measurement, as we first wish to establish the objective reality theoretically. Later, we may apply known theories of measurement, fluctuations, and signal-to-noise ratio in experimental systems. For now, we only discuss the simplest of relevant ideas from scratch as needed to understand our particular issues.

The characteristic time needed for a physical process to come close to its steady-state condition is usually designated with τ , which we can also use from now on. This must be very short in our theory of push fields for small particles and generally Newtonian bodies, but increases with size and density of bodies. It is superimposed with the relevant interaction time to yield an effective integration time τ_f for each field $f = 1, 2, 3, 4, 5$ that we are now investigating. We should generally have that $\tau_f > t_f$.

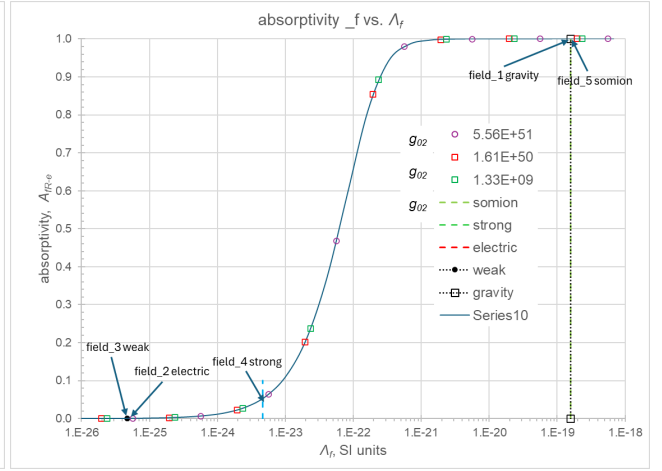
[Note: As stated repeatedly, we have an outstanding issue with the numerous novel terms and quantities introduced by our new theory, often not anticipated; this issue may be sorted out later on a rationalized basis, once we have sufficiently established a self-contained theory.]

By way of illustration, we can see the importance of the integration time in the case of internal versus external physical properties already analyzed in Section 24.1. This case also explains how we should view the number density (and energy density) for each of the fields we have been investigating.

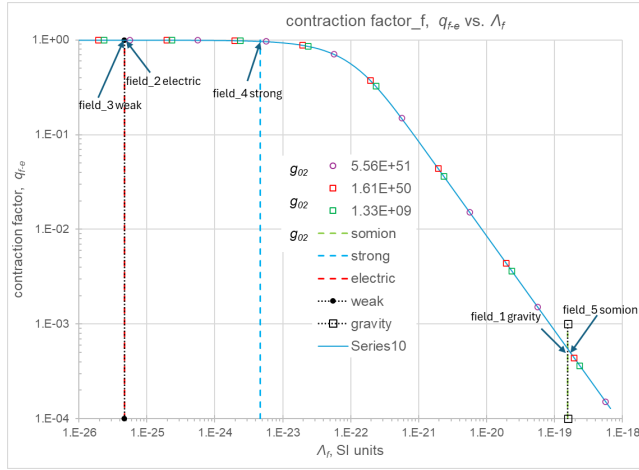
Thus, we have the variation of internal (i) maximum acceleration g_{0Xi} by Eq. 441. We rewrite it as a



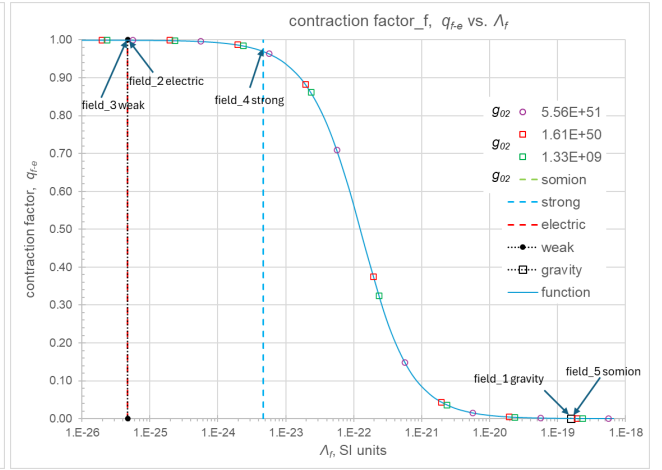
a



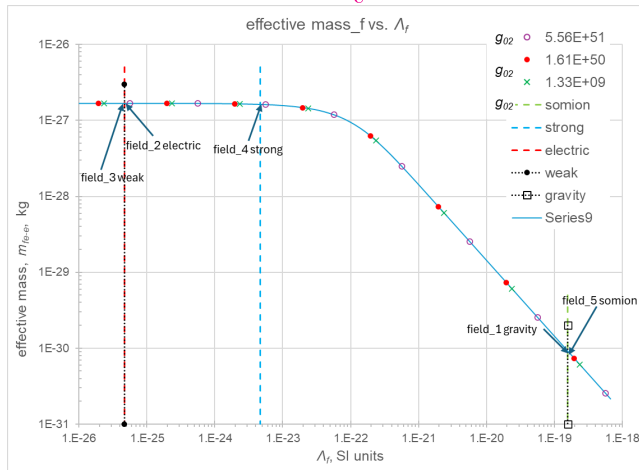
b



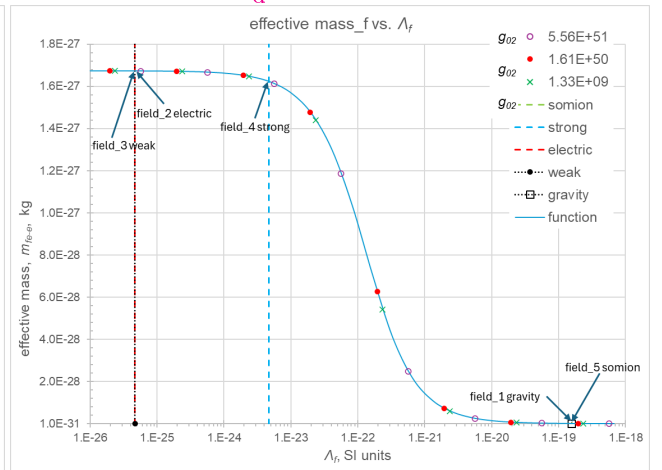
c



d



e



f

Figure 102: Electron (positron) field properties vs. Λ_f : (a) field force-strength, (b) effective mass_2, (c) absorptivity and (d) contraction factor

function of the external g_0 as:

$$g_{0Xi} = \frac{f_{gXi}}{\pi A_{R_{Xi}}} g_0 \quad (603)$$

With reference to the definition of variables in Fig. 67, the internal maximum acceleration is plotted in Fig. 73a, where we see that it further depends on the internal shielding radius R_{Xi} and coefficient k , which is linked with the density of a given body.

$$\begin{aligned} \frac{c}{t_{Xi}} &= g_{0Xi} = \frac{f_{gXi}}{\pi A_{R_{Xi}}} \frac{c}{t_g} \\ t_g &= \frac{f_{gXi}}{\pi A_{R_{Xi}}} t_{Xi} \\ t_{Xi} &= \frac{\pi A_{R_{Xi}}}{f_{gXi}} t_g \end{aligned}$$

The number density for the external vacuum is given by

$$n_0 = \frac{2g_0}{\pi E_g \Lambda}$$

For the internal vacuum, it is:

$$\begin{aligned} n_{0Xi} &= \frac{2g_{0Xi}}{\pi E_g \Lambda} \\ \frac{n_{0Xi}}{n_0} &= \frac{g_{0Xi}}{g_0} \\ n_{0X} &= \frac{2g_{0Xi}}{\pi E_g \Lambda} = \frac{2}{\pi E_g \Lambda} \frac{f_{gXi}}{\pi A_{R_{Xi}}} g_0 \end{aligned}$$

where we have Λ being the same in both regimes, as we should, according to our latest understanding of its physical meaning.

We have $\tau_f \approx t_f$ for relatively “small” size particles, where the steady state is achieved fast relative to the interaction time.

We should check if this (low acceleration) relates to Chae (2023) work on the breakdown of the Newton–Einstein standard gravity at low acceleration in internal dynamics of wide binary stars.

In conclusion, we should include (apply) the integration time rather than the interaction time for determining the maximum acceleration of each field, like:

$$g_{0f} = \frac{c}{\tau_f} \quad (604)$$

For gravity in particular, if we can verify that the graviton interaction time t_1 is independently due to the maximum length of the proposed helical chain of planckions, then $\tau_1 \geq t_1$.

31.10.3 Mean separation time

A new concept of time interval is required by our push field theory. That is the time interval between two consecutive absorption events for any given body (macroscopic, or particle). Specifically, we define a mean separation time interval T_f between absorption events of push particles for each field $f = 1, 2, 3, 4, 5$. Since each absorption event has a duration of its own, i.e. the interaction time t_f , we define the mean separation time as being between time moments at the same corresponding phase of the absorption process, for example, at the arrival moment between two consecutive events.

To assist in understanding this concept, we present three possible combinations (cases) of interaction times between two consecutively arriving particles in Fig. 103:

Case A1 shows two particles with an interaction time t_f each arriving with a separation time $T_f > t_f$. This leaves a remaining time interval t_{fb} , the *black time interval*, during which the impacted body undergoes no further action at all, until the next particle arrives.

Case A2 shows two particles with an interaction time t_f each arriving with a separation time $T_f = t_f$. This leaves no resting time (i.e., $t_{fb} = 0$) for the impacted body as one particle takes over immediately from

the preceding particle's action; this case may be rare, but we will need it in connection with the theory of graviton; it is a transition case between the previous case and the next.

Case A3 shows two particles with an interaction time t_f each arriving with a separation time $T_f < t_f$; that is, there is an overlap of interactions between consecutive particles.

We can find T_f as follows: The particle number rate of absorption w_f is obtained by dividing the energy rate of absorption W_f by the individual push particle energy:

$$\frac{\text{\#particles}}{\text{unit-time}} \equiv w_1 = \frac{W_f}{E_f} = \frac{4cg_0m_{fe}}{E_f} \quad (605)$$

The inverse of the above quantity yields the desired mean separation time:

$$T_1 = \frac{E_f}{W_f} = \frac{E_f}{4cg_0m_{fe}} \quad (606)$$

The mean separation time (or interval) defined above can be exceedingly small for a large body, like a planet or star; nevertheless, it exists objectively, even if it is much less than the Planck time. This is because we consider independent events (i.e., the starting of each absorption process), which can take place at time moments not connected with each other. These events may *approach* "practical simultaneity" (by our experience), but they can always be distinguished by some infinitesimal time interval (T_f) for large enough bodies, no matter how small this time interval can become. For a large body like a planet, this time is unimaginably small and much smaller than any interaction or integration time and even much less than the Planck time.

At the other extreme, the interval T_f defined above can be very large for a very small body, like an electron, as we will show shortly. As we consider smaller and smaller absorbing bodies, T_f gradually increases, approaching the Planck time at $T_f = t_P$, then the interaction time at $T_f = t_f$ and then becoming exceedingly large for exceedingly small particles or entities. In the latter situation, the force on the particle and its motion will be intermittent. This will correspond to an intermittent gravitational event, electrical event, Planck event, and so on, according to the force field considered in connection with the given body.

The relative extent of all three times t_f , τ_f and T_f are conceptualized on the absolute time scale in Fig. 103B. Consistent with our findings so far, we show the interaction times for the Planck and electric fields being equal to the Planck time t_P . The weak, strong, and gravitational interaction times are depicted only in relative positions (arbitrarily) on the time scale. The integration time for gravity is shown as $\tau_1 > t_1$ for illustration purposes, but the exact integration times for each field and particle (body) are left for future work.

The importance of the above time intervals in relation to particle or body size will become evident in the ensuing investigation. We will run numerical examples on different size bodies to obtain an idea of the magnitudes involved, in particular for this new quantity, the mean separation time T_f .

Let us concentrate first on gravity and the consequences of having separated absorption events between consecutive gravitons. We consider the case whereby the interaction time is much shorter than the mean separation time, i.e. $t_1 \ll T_1$. Each graviton absorption creates an effective gravitational mass around the point of absorption. For the duration of T_1 , the entire remaining body stays inactivated, i.e. according to our PG theory it has a black mass presenting no resistance to motion. It is literally inert (passive), having no classical "inertia." Hence, the entire body will be moving in the direction commanded by the incident graviton at the start by a burst of acceleration during t_1 and then moving at constant speed of light during the remaining black time. Since $t_1 \ll T_1$, the particle will be displaced by a distance practically equal to cT_1 for the duration of T_1 . At the next graviton incidence, this process will be repeated and the body will be pushed in a new direction of motion superimposed on the previous motion.

In other words, the body is subjected to a continual intermittent and random motion over a much longer time interval. If we add up all the motions over the longer time interval, we will observe a tendency towards an *average* location in space. If the body is in the vicinity of another body, then we will additionally observe that there is a net number of absorption events coming from the opposite side (free side) in relation to the neighboring body. Hence, in addition to the average location, we will observe a preferred directional motion towards the other body. If we try to prevent this net motion, say by a physical constraint like a spring, then we will observe a finite extension of the spring measuring the force exerted on the body under consideration. Depending on the bandwidth of our recording equipment (or its time constant), the position will appear more or less well defined or blurred, but we can ignore the effects of our equipment in this analysis.

Here, we have described another situation, where interaction and integration times are different, in addition to the preceding situation of a decreased number density inside a very dense body. Actually, we can even envisage (Gedanken case) a cavity in a macroscopic body with very high density (or size), whereby

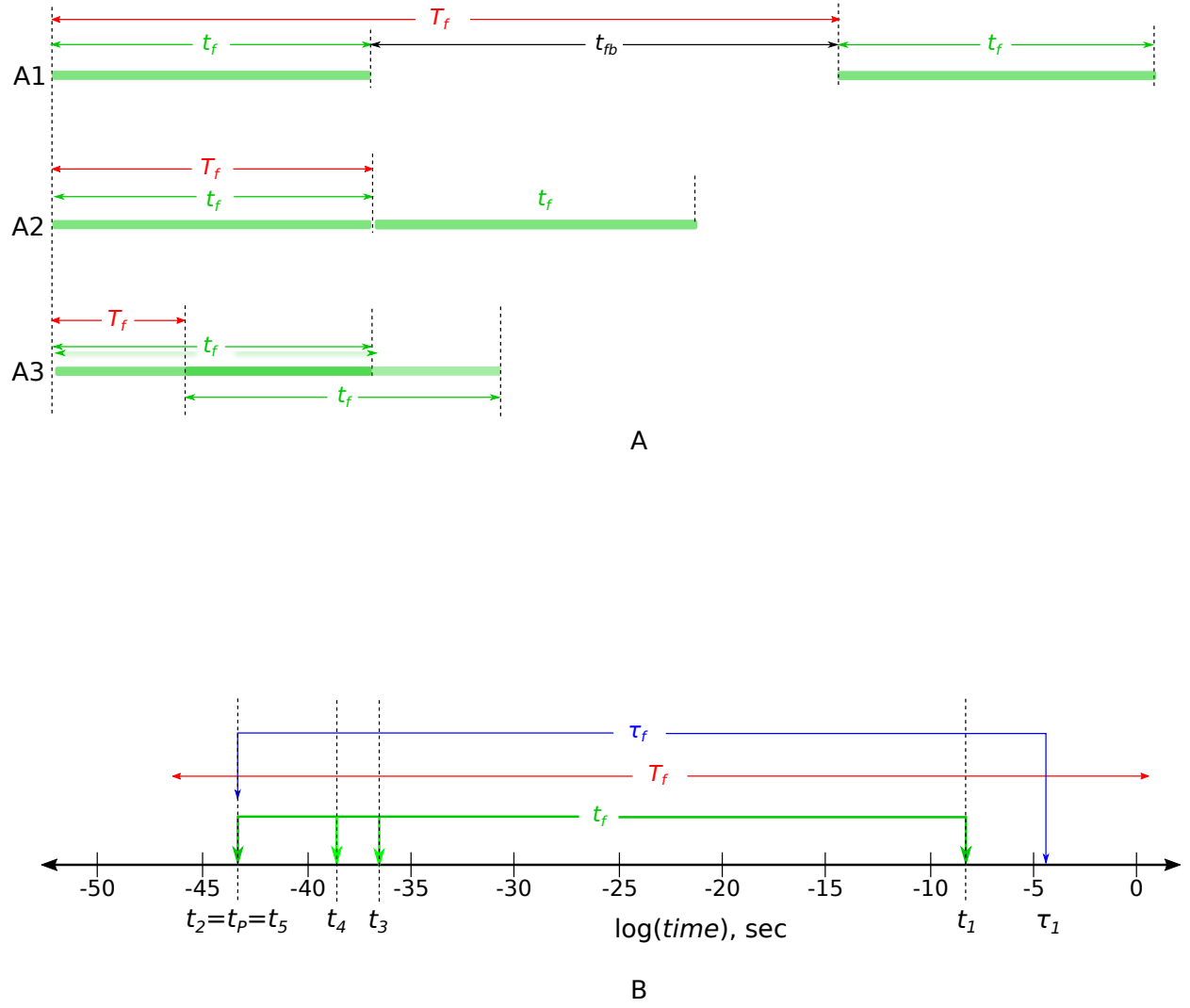


Figure 103: A: Relationship between interaction time t_f and mean separation time T_f ; B: Relative time intervals t_f , T_f , Planck time t_P and integration time τ_f on the absolute time scale

the flux intensity is extremely low, resulting in intermittent motion of bodies inside the cavity. Hence, Eq. 604 should be generally applicable, but for ordinary (Newtonian) situations we could apply $\tau_1 \approx t_1$.

We propose that this intermittency may be the cause of quantum mechanics at very small sizes. This would open a novel approach to all physics and cosmology, but we need to examine the veracity of our theory also by the following emerging problem and its resolution. It would be an irony if we can confirm the generation of quantum mechanics by gravity, namely, by gravitational action of push particles, when it is broadly declared that gravity is not compatible with quantum mechanics.

31.10.4 Problem of gravion absorption by electron

We can find the gravion particle number rate of absorption w_1 by an electron from Eq. 605 with gravion energy rate of absorption W_1 and gravion energy $E_g \equiv E_1$:

$$w_1 = \frac{W_1}{E_1} = \frac{4cg_0m_{e-e}}{E_1} = \frac{4cg_0m_{e-e}}{[\nu_1]E_P} \quad (607)$$

where $[\nu_1]$ is the number of planckions in the gravion and m_{e-e} the electron gravitational mass.

The numerical output above gives a particle absorption rate of $w_1 = 5.26 \times 10^{-22} \# \text{ gravions s}^{-1}$. This is extremely small (far below unity) and, for a single electron, would imply an essentially vanishing effective gravitational activation by gravions.

Also, the inverse of the above equation yields the mean separation time:

$$T_1 = \frac{E_1}{W_1} = \frac{[\nu_1]E_P}{4cg_0m_{e-e}} \quad (608)$$

which gives a value of

$$T_1 = 1.90 \times 10^{21} \text{ s.}$$

For context, this is many orders of magnitude larger than the age of the Universe ($\approx 1.38 \times 10^{10}$ years). Therefore, with the present numbers, gravion absorption events for a single electron would be effectively non-occurring on any physical timescale relevant to experiments or astrophysics.

The source of this discrepancy is immediately apparent: the extremely high gravion energy E_1 assumed in the model of Fig. 89 combined with the fixed planckion (formerly gravion) length (Figs. 81 and 82) leads to an unphysical result. This impasse invalidates calculations that relied on the previous value $g_0 = 1.33 \times 10^9 \text{ ms}^{-2}$.

One naive resolution would be to arbitrarily increase g_0 to obtain sensible values for the electron, but a more satisfactory approach will be proposed below to restore consistency with the hitherto theory.

31.10.5 Decomposition of gravion into helical segments with minimum pitch and radius

The problem identified above stems from the extremely high gravion energy

$$E_1 = [\nu_1]E_P,$$

which arises due to the very large number of planckions arranged on a single helix with minimum pitch and maximum frequency, as adopted previously.

This difficulty can be overcome if the continuous helical chain is broken into smaller segments, each containing a much smaller number of planckions on average. In this way, we retain the pitch and radius of the helix, but avoid the excessively long, continuous chain illustrated in Fig. 93.

To proceed, we should first investigate the possible mechanisms involved in generating the helical chain. Previously, we had not attempted this, and the value of $[\nu_1]$ planckions in a continuous chain was adopted only because it yielded a consistent derivation of g_0 with other independent methods (see Section 31.5). We are now compelled to explore this mechanism in detail below.

In Section 30.3, we posited that circular motion originates from the interaction of two planckions (formerly gravions). We now extend this idea by opening the circle into a helix, considering combined forward and circular motion.

We have discussed the relative contributions of rotational and linear energy. It is therefore logical to consider the accumulation of single helical segments up to an average number ξ of planckions, forming a continuous chain with axial length

$$\ell_z = \xi \ell_P.$$

These segments can then move independently in all directions as push particles for gravity. In this scenario, the interaction time $t_{1\xi}$ for these much shorter particles would be significantly reduced:

$$t_{1\xi} = \frac{\ell_z}{c} = \frac{\xi \ell_P}{c} \ll \frac{[\nu_1] \ell_P}{c}.$$

This would result in a much higher value for g_0 if the shorter segments were to replace the long gravion, which is clearly undesirable. However, we can still recover the desired value for g_0 if we assume that the gravitational steady state is not reached during the shorter interaction time $t_{1\xi}$, but only after integrating all absorption events up to the previously considered and accepted interaction time t_1 .

In other words, the minimum possible gravitational *integration* time is constrained, or determined by the bigger scope of a body, and remains at the prior value

$$\tau_1 \approx t_1.$$

Under this assumption, we can preserve the desired value of g_0 via the general Eq. 604. This is consistent with the inequality between integration time and interaction time, namely

$$\tau_1 \gg t_{1\xi}.$$

By the above decomposition of the gravion, the number of segments m is given by:

$$m = \frac{[\nu_1]}{\xi}.$$

The energy per segment is

$$E_\xi = \xi E_P.$$

The total integrated energy for the m segments is then:

$$E_1 = m \cdot \xi E_P = \sum_i^m E_{\xi i} = [\nu_1] E_P,$$

where $E_{\xi i} = \xi E_P$ is a constant term, purposefully indexed for insertion in the summation symbol \sum_i^m to emphasize the present decomposition of the gravion in lieu of the previous continuous chain that resulted in relationship 583. The separate (independent) push particles arriving from different random directions are “summed”, yielding again the same number of planckions as in the continuous chain (previously shown as a product but with no substantial difference between the two).

The important point is that we end up with the same gravion energy E_1 , the same $[\nu_1]$, and the same t_1 ; the latter can be similarly expressed as the sum:

$$t_1 = m \cdot t_{1\xi} = \sum_i^m t_{1\xi i}$$

Also, the previous interaction time now becomes an initial integration time, both being numerically equal but physically different. As a result, they generate the same g_0 value, which we have also obtained by other independent methods (see expression by 549).

The total integration time for a body is finally dependent on the body’s nature and position in space.

In other words, the gravion is a collection of push particles arriving from all directions continuously, one after another, as shown by case A2 in Fig. 103. Their pushing effects are integrated over the time $\tau_1 \approx t_1$, where $t_1 = 2.25 \times 10^{-1}$ s.

We can calculate the effective mass $m_{e\text{-gravion}}$ created inside any given body by such a collective “single” gravion from as follows:

$$W_{1\text{-gravion}} = \frac{E_e}{t_1} = cg_0 m_{e\text{-gravion}}$$

where we omitted the factor 4 if we use only the effective energy E_e and not the total absorbed energy E (see the 3+1 mass scheme in Section 29.4.1). Then we get:

$$m_{e\text{-gravion}} = \frac{W_{1\text{-gravion}}}{cg_0} \quad (609)$$

where $W_{1\text{-gravion}}$ is the rate of energy delivered by the gravion, which is E_P/t_P , so that we obtain:

$$m_{e\text{-gravion}} = \frac{E_P}{cg_0 t_P} = 3.07794 \times 10^{-8} \text{ kg} \quad (610)$$

The above effective mass divided by $[\nu_1]$ gives a mass equal to the planckion mass:

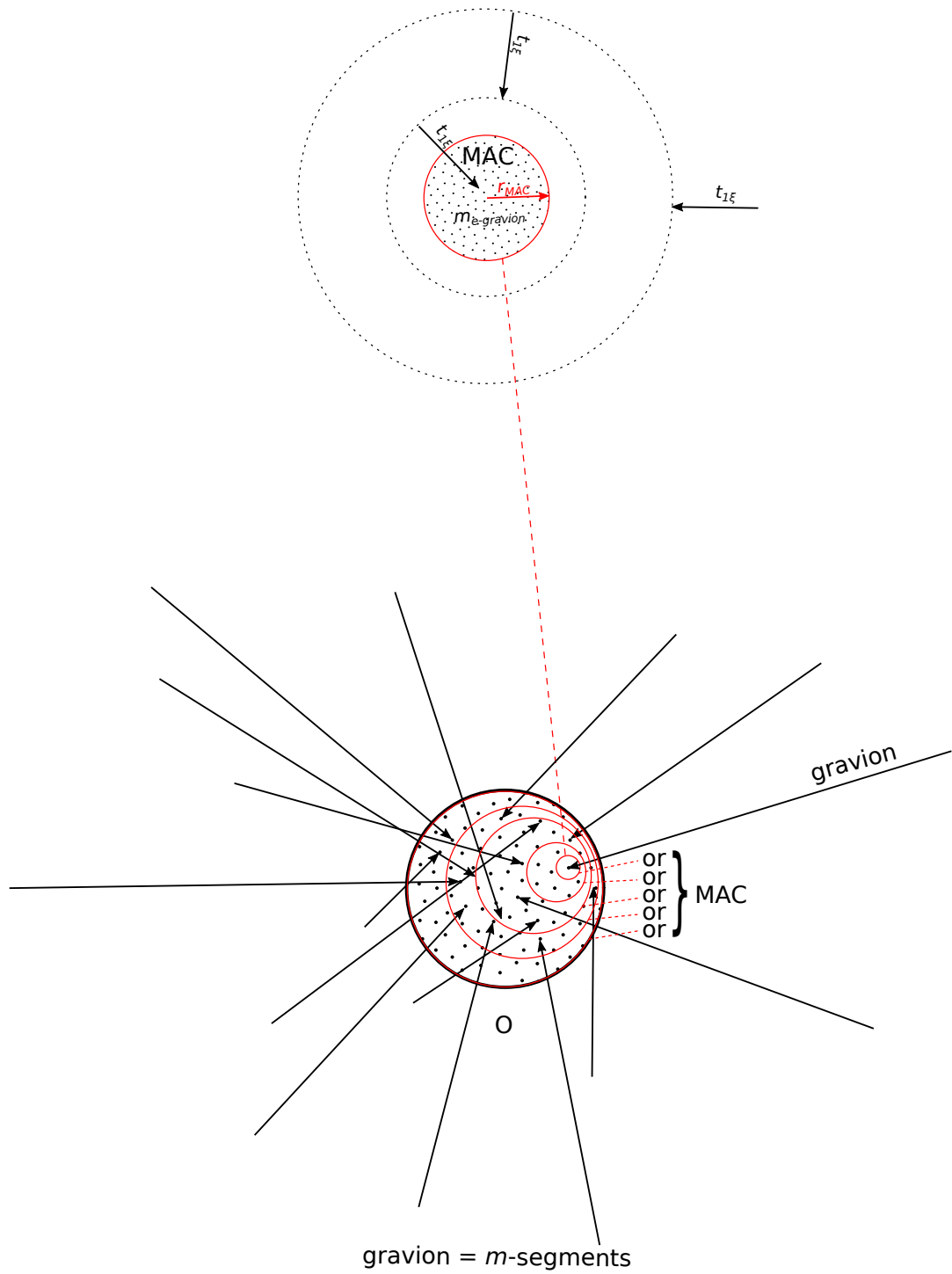


Figure 104: Segmented gravion arriving at minimum absorption center (MAC); Ontegrated gravions arriving at larger body O

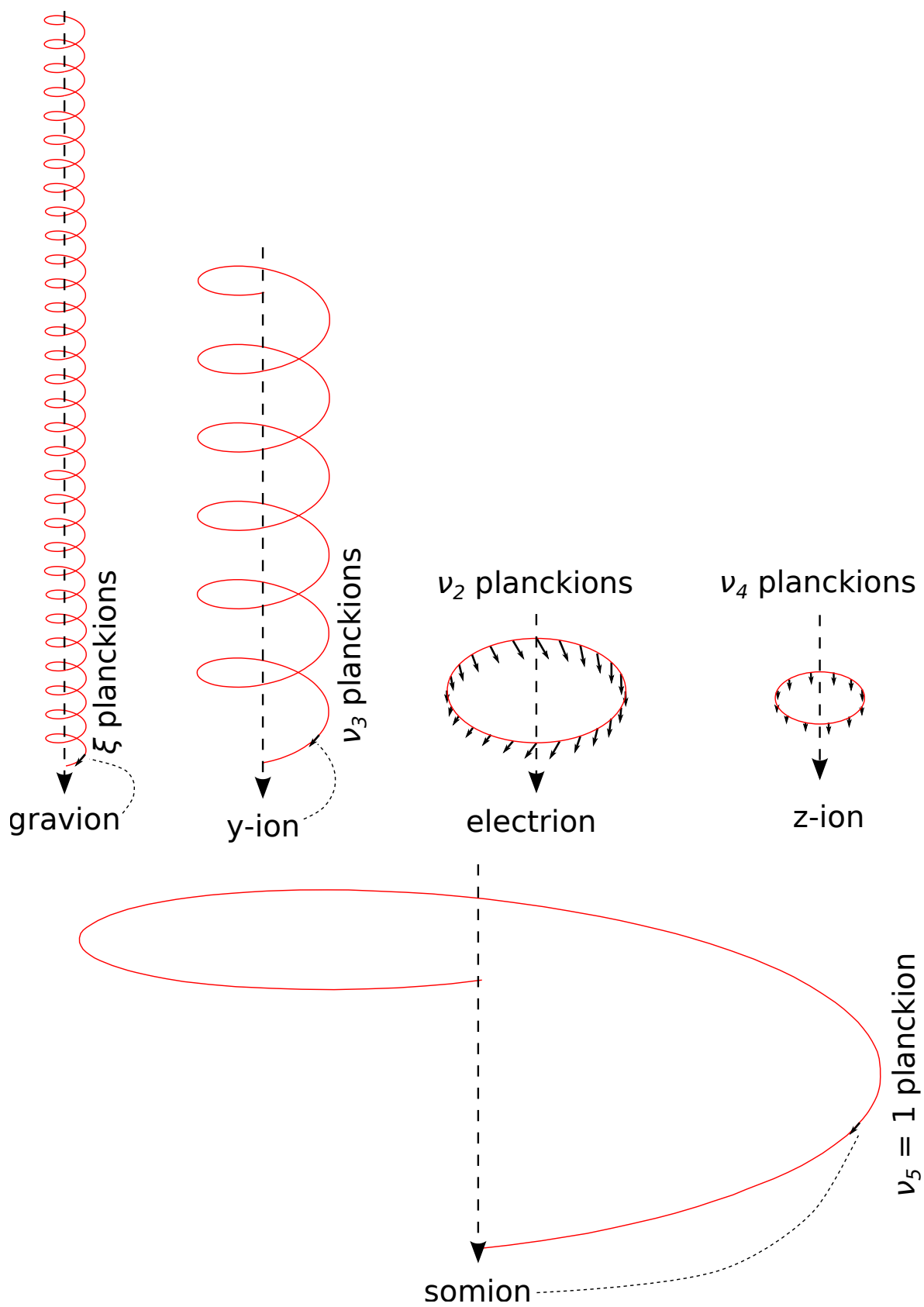


Figure 105: Planckion species in the Planck field

$$m_{e\text{-planckion}} = \frac{m_{e\text{-gravion}}}{[\nu_1]} = 7.372496 \times 10^{-51} \text{ kg}$$

The above numerical results are not trivial or tautological. They indicate that the planckion (and gravion) generates an effective mass in the absorbing body as calculated above. We do not know how an effective mass could arise or even if it exists within the planckion (or gravion) itself; we have previously discussed this issue in Section 29.

We may describe the planckion as having an inherent (intrinsic) “mass” that manifests as effective mass only in the absorbing body, as what we can be certain of is the effect observed in the absorbing body. Attributes may be assigned to the planckion itself, as initiated in Section 30.1.

We have extensively discussed the concept of mass in Section 29 and throughout this work. What we achieve now is a confirmation of those results. In fact, the above value of $m_{e\text{-gravion}}$ differs only by a factor of $\sqrt{2}$ from the accepted “Planck mass” as tabulated by Wikipedia contributors (2024); we previously found the same for the published “Planck energy”. We now provide a physical explanation and practical use for these quantities.

We can visually describe the gravion in Fig. 104. For a very small effective mass (like that of an electron, not shown here), there are not enough gravion ξ -segments to complete a “whole” gravion (case A1 of Fig. 103 applies). As the size of the particle increases, we reach a cross-over point where case A2 applies: the gravion segments arrive one after another continuously, on average, as depicted at the top of Fig. 104. This corresponds to the minimal effective mass $m_{e\text{-gravion}}$ per Eq. 609, with the value given in Eq. 610. This is required for the absorption of one gravion, which is what we have conceived as a MAC and graphically shown at the top of Fig. 104.

We now understand that this relatively high mass is distributed inside a larger mass body O , as illustrated at the bottom of Fig. 104. The gravitational MAC is not what was initially conceived as a minimal contiguous amount of organized hyle. It is rather a collection of absorption centers for ξ -segments distributed inside a body. This distribution has a volume with an effective radius r_{MAC} , which is variable throughout the body; it ranges from a minimal radius r_{MACmin} required to have one whole gravion absorbed up to the full size of the absorbing body with radius r_O :

$$r_{MACmin} \leq r_{MAC} \leq r_O$$

The above relationship is illustrated at the bottom of the figure by different red circles each representing alternative (or, or, or,...) extents of a MAC inside the body O . To create the gravitational force (acceleration), the body needs to accumulate (integrate) sufficient MACs over a time interval τ . If the body has the minimal radius r_{MACmin} , then $\tau = t_1$, otherwise $\tau > t_1$. The latter inequality may be very small for ordinary Newtonian bodies, but it becomes larger with body mass increase, like stars, white dwarfs, etc. The quantitative relationships are left for future research, as we only laid the foundations on which future work must be done.

The decomposition of the gravion resolves the impasse regarding the values of w_1 and T_1 for an electron, with the revised equations now becoming:

$$w_1 = \frac{W_1}{E_\xi} = \frac{4cg_0m_{e-e}}{\xi E_P} \quad (611)$$

$$T_1 = \frac{E_\xi}{W_1} = \frac{\xi E_P}{4cg_0m_{e-e}} \quad (612)$$

With $\xi \ll [\nu_1]$, we can obtain acceptable outcomes for the electron. For instance, with $\xi = 10^{12}$, we get $w_1 = 2.20 \times 10^9$ particles/s and $T_1 = 4.55 \times 10^{-10}$ s, which are plausible and overcome the previous problem. More numerical examples are provided later in combination with other results.

We summarize the revised concept of gravions along with the push particles of the other fields in Fig. 105. The gravion is represented now by the ξ _segment populated by ξ planckions, which retain the smallest pitch and radius as previously adopted for gravion.

The other fields retain the number of planckions in their push particles as given in the last Table 61. For the electric field, we have $[\nu_2] = 3.38 \times 10^6$ planckions arranged on a ring configuration with spin. For the presumed strong field, we have $[\nu_4] = 3.38 \times 10^4$ planckions arranged also on a ring (smaller) configuration but without spin. For the Planck field, $[\nu_5] = 1$ planckion moves on a helical trajectory with the largest radius and pitch. Meanwhile, for the weak field $[\nu_3] = 3.38 \times 10^9$ planckions remain in helical configuration until further investigation is undertaken for it.

At this point, we are seeking further evidence in support of the above integration requirement, in alignment with our previous work. This is a legitimate approach, as it does not violate any of our established

principles, while we remain attentive to reasons that might justify or falsify this condition in subsequent developmental work.

The above arguments are presented with the intention of subjecting them to further testing and validation in the ensuing analysis. As long as the revised graviton model remains internally consistent with the overall theory and is plausible—and hopefully consistent with experimental evidence—there should be no issue. In fact, we have begun producing such outcomes, some of which are presented in the current report, with additional results to follow in future reports.

One advantage of the revised graviton model is that the parameter ξ (or equivalently m) can be adjusted to yield plausible values for w_1 and T_1 for the electron. At the same time, ξ regulates the number density of the segmented graviton particles, from n_0 to $n_{0\xi}$.

The revised $n_{0\xi}$ can then be used in Eq. 587 to determine the mean free path of gravitons, a quantity that is crucial for the theory. In this way, ξ provides substantial leverage in calculating key parameters and plays a fundamental role in the structure of particles such as the electron, positron, proton, neutron, and even atoms. Moreover, ξ can be chosen to yield expected quantum mechanical outcomes, further linking the push particle framework to observed physical phenomena.

The prospect of a distributed gravitational MAC actually simplifies and unifies a general push field theory. It appears that a genuine, organized, contiguous MAC exists at the electron (and positron) level, which accommodates all push particle fields. This MAC may ultimately prove to be the fundamental converter of all absorbed push particles into electrions. Other particles, such as the proton and neutron, may possess a direct nexus with the electron, but this remains to be determined in subsequent analysis. We shall examine this idea further as we progress.

31.10.6 Uncertainty Principle vs. Certainty Condition

Important insights emerge from the new concept of the mean separation time T_f between arriving push particles in each field. Multiplying both sides of Eq. 612 by the associated effective mass of a body, we obtain:

$$T_f m_{fe} = \frac{E_f m_{fe}}{4c g_0 m_{fe}} = \frac{E_f}{4c g_0} = \frac{t_f E_f}{4c^2} = \text{constant} \quad (613)$$

If we consider only the effective energy in the body, the factor 4 can be omitted, giving:

$$T_f m_{fe} c^2 = t_f E_f,$$

where the associated body effective energy is given as $E_{fe} = m_{fe} c^2$. Hence:

$$\boxed{T_f E_{fe} = t_f E_f = \text{constant}} \quad (614)$$

The first term represents a product of the inversely varying T_f and E_{fe} for a body, while the second term is constant for any given field:

$$t_f E_f = \frac{c}{g_{0f}} [\nu_f] E_P = c \frac{[\nu_f]}{g_{0f}} h \cdot 1\text{Hz} = c \frac{h \nu_f}{g_{0f}}$$

where $t_f = \frac{c}{g_{0f}}$ and $E_f = [\nu_f] E_P$, which changes for each field by the factor $\frac{\nu_f}{g_{0f}}$.

For the Planck field, we have:

$$T_5 E_{5e} = c \frac{\nu_5}{g_{05}} h = 3.5722780818 \times 10^{-77} \text{ J}\cdot\text{s} = \text{constant} \quad (615)$$

For the gravitational field, we have:

$$T_1 E_{1e} = 6.2264013255 \times 10^8 \text{ J}\cdot\text{s} = \text{constant} \quad (616)$$

The above value differs numerically by a factor of π from the “Planck energy” of 1.9561×10^9 J provided in the Planck units table by Wikipedia contributors (2024f).

Equivalently, Eq. 614 is re-written as:

$$\frac{T_f}{t_f} E_{fe} = E_f = [\nu_f] (h \cdot 1\text{Hz}) = h\nu_f \quad (617)$$

and further as:

$$\frac{T_f}{t_f} \frac{E_{fe}}{\nu_f} = h \quad (618)$$

which resembles the Heisenberg uncertainty principle $\Delta E \Delta t \geq h$. However, the two describe different physics. Our expression relates a definite effective energy to a definite mean separation time in any given body, regardless of its size, whereas Heisenberg relates an uncertain energy spread over an uncertain time interval via an inequality (indeterministic).

In contrast, our relation is deterministic: it provides a fundamental law connecting the actual entities T_f and m_{fe} (or E_{fe}) in any body, independent of size. Furthermore, we can have $T_f \ll t_P$ (less than the Planck time), resulting in an all-encompassing time scale, while the body energy is adjusted to obey the certainty Eq. 614.

With the above realization, we may also prefer to express Eq. 614 by:

$$T_f E_{fe} = t_f \nu_f h = \text{f-field-constant} \quad (619)$$

For the gravitational field, in particular, further work is required to incorporate the m ξ -planckion segments in the gravion, which could assist in a more inclusive interpretation of our findings in absolute terms and in terms of the Heisenberg principle if there is a connection.

For consistency in checking out numerical outcomes across various derivations, we can re-insert the omitted factor 4 in the above expression to have:

$$T_f E_{fe} = \frac{1}{4} t_f \nu_f h = \text{f-field-constant} \quad (620)$$

31.10.7 Gravity vs. Quantum Mechanics

We define Δx as the distance traveled, $\Delta x \approx cT_{1\xi} \approx ct_{1\xi b}$, in the case where $t_{1\xi} \ll T_{1\xi}$ so that the electron moves with constant speed c during the black time interval $t_{1\xi b}$ shown in case A1 of Fig. 103. PG presents this new possibility of the electron having no classical inertial mass during the interval $t_{1\xi b}$, when it moves with constant speed of light until it is struck by the next gravion segment and changes direction, repeating the process.

The integration of all Δx in time τ_1 results in an apparent scattered (diffused) average position. This may be characterized by a normal distribution with standard deviation σ , measuring the spread of location from the mean position. We provide a visualization of this effect in Fig. 106.

In this figure we depict three bodies: a steel sphere with a radius of 1 m, a proton, and an electron at a distance r from the center of a planet. The dimensions are drawn far outside correct proportions in a “gedanken” situation. Each body is suspended from a spring, the extension of which measures the weights, or forces F_1 , F_2 , and F_3 exerted by a net flow of gravion segments due to the presence of the planet. Only the smallest particles undergo intermittent motion Δx between arriving gravions segments.

In Fig. 107 we illustrate the relative interaction times of gravions, electrions, and somions (drawn not to scale). The latter two push particles form an adsorption-like layer analogous to the Helmholtz layer in chemistry. Being extremely thin, this layer may move along with the electron without changing the kinetic status of the electron. The somions serve the role of compacting the electron together into a particle entity without producing a net force that dynamically moves the electron. By contrast, the gravions and electrions do act dynamically and move the electron if there is a net flow of them in a particular direction, thereby producing a net gravitational or electric force. The latter effect is a consequence of their relative mean free paths being much longer than the somion mean free path.

Statistically significant, only the gravion segments can cause a scatter in the motion of the electron, owing to their relatively “rare” rate of incidence when compared to the very short time scales of somions and electrions (see numerical examples below). Overall, we may consider the electron as a passive object being

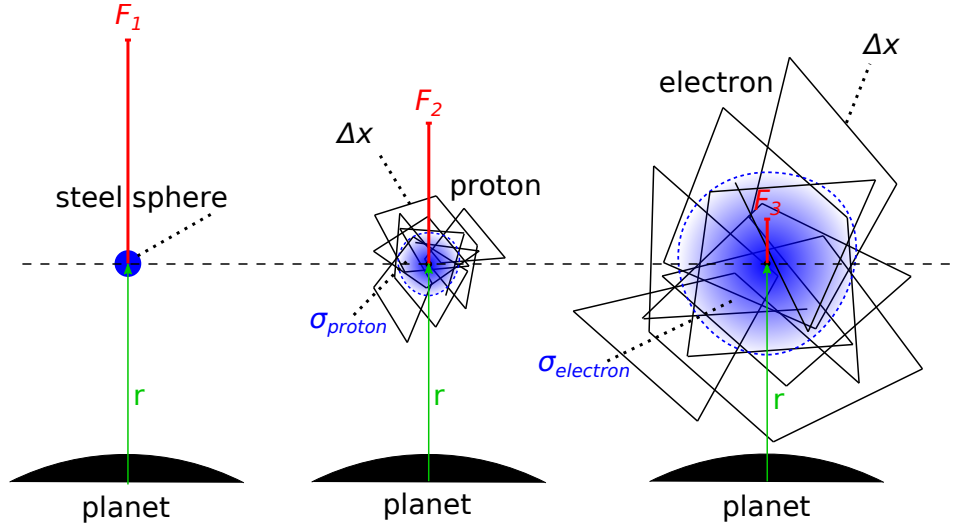


Figure 106: Relative body size motion and location: A steel sphere, a proton and an electron are suspended from a spring measuring their weights F_1 , F_2 and F_3 in the presence of a planet. Push particles create intermittent motion Δx for the smallest particles with a dispersion σ but without any measurable effect on the steel sphere.

struck by random gravion segments at discrete time intervals. The separation of gravion segment incidences by a time $T_{1\xi} \gg t_{1\xi}$ ensures that the electron has practically no effective gravitational mass until the next gravion segment transfers its momentum to the newly created effective mass in the electron. The newly created effective mass in the electron must be equal to a presumed gravion segment mass $m_{e\xi}$ (as discussed for $m_{e-gravion}$). During the interaction time, the electron acquires the speed of the impacting segment, which is the speed of light. This reasoning is fundamental and consistent with all our preceding PG theory about “mass” and should present no difficulty in being accepted.

However, a main problem now emerging is how the somion medium reacts to the electron’s motion in the interval $T_{1\xi}$. Does it present a resistance to electron motion by way of drag, or not?

The question of drag persists with any push field theory, and we have attempted to address it in various ways before. The basic question is: if drag is present, how large is it, and to what extent does it affect our theory?

Because drag presumably exists, to argue that we cannot have any PG theory in the first place is not valid. If that were the case, we should not have started to develop our theory at all. In fact, this is one of the main reasons PG has been ignored for too long.

However, PG has already provided numerous reasons for its validity *a posteriori*. We made this premise at the outset, and we have no reason to abandon this work on the “drag” issue now.

It is neither illogical nor invalid to claim that (a) the planckion drag may be absent, or (b) it is so small that it does not affect our findings. Until the opposition can calculate and prove that drag must exist to such an extent that it necessarily invalidates PG theory, we feel confident to continue with this work. We therefore proceed below by considering both cases (a) and (b).

With or without resistance by the somion field, further work is required on the statistics that would determine an effective standard deviation of Δx that can be consistent with experiment and with valid quantum mechanical computations. To assist our understanding, we present numerical examples for various typical bodies along with their new properties in the current context.

Preliminary calculations: By way of numerical examples, we present the variation of gravion properties and their interaction with the electron by selecting different values of ξ for possible fragmentation. The results are provided in Table 63. We chose values of ξ in the range $1 < \xi < 4.17 \times 10^{42}$ to provide an idea of the trend between the two extremes, together with some intermediate values likely to prevail.

The gravion parameters in the field are listed first: ξ , m , $t_{1\xi}$, $n_{0\xi}$ and L_{mfp} . The gravity index ($_1$) is replaced with the segmented gravion index ($_{1\xi}$) for all quantities.

We find the corresponding number of segments m per decomposed gravion, from which we obtain an increased number density $n_{0\xi}$. We note that the new particle density is $n_{0\xi} < 8.13 \times 10^{60}$, which is still many orders of magnitude below the Planck field with $n_{05} = 3.39 \times 10^{103}$ particles/m³ (see Table 61). The segmented gravions therefore behave like a very dilute gas with relatively low partial pressure inside the

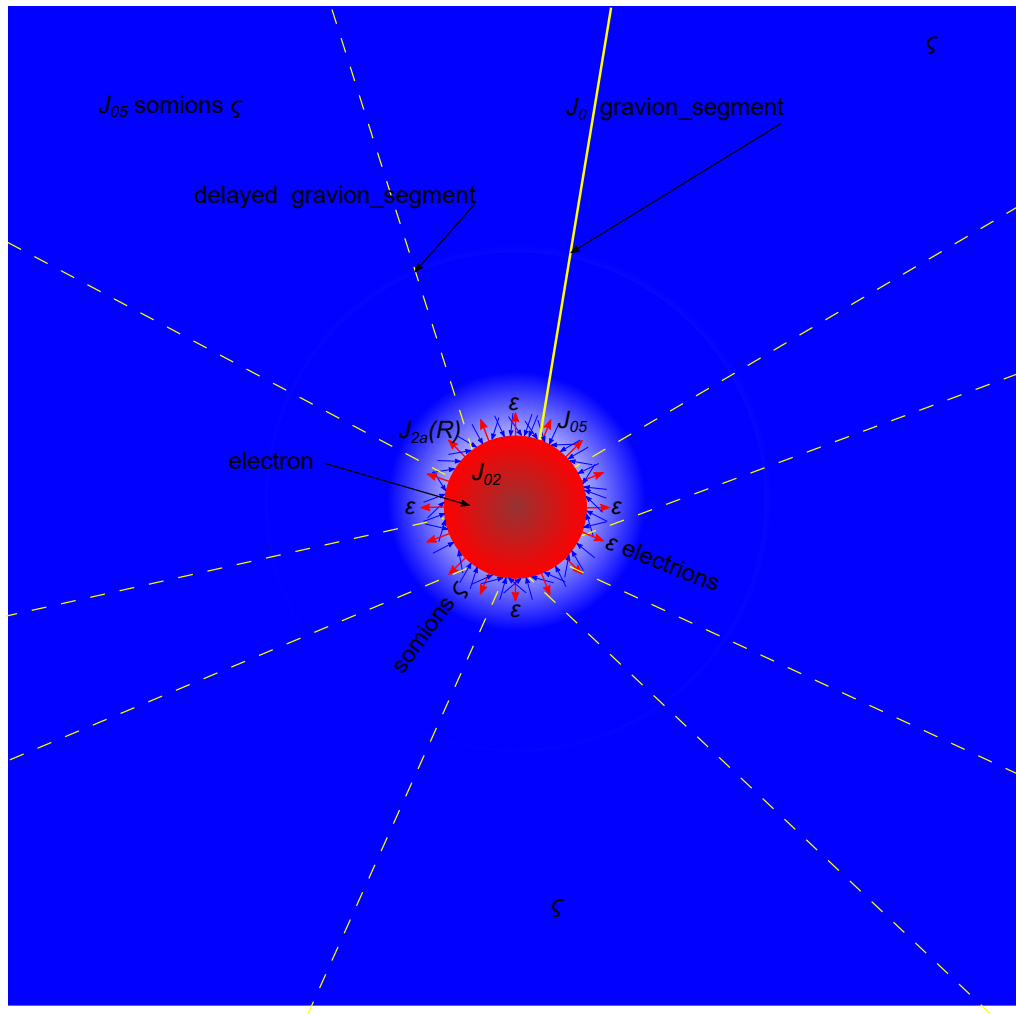


Figure 107: Electron and relative mean separation times indicated by the length of lines for gravion segments, and arrows for electrons ε and somions ζ ; dashed lines indicate delayed arrivals of gravion segments

graviton parameters					electron graviton interaction		
ξ	m	$t_{1\xi}$, s	$n_{0\xi}$, #m ⁻³	L_{mfp} , m	$w_{1\xi}$, #s ⁻¹	$T_{1\xi}$, s	Δx , m
1	4.17E+42	5.39E-44	8.13E+60	1.06E+08	2.20E+21	4.55E-22	1.37E-13
1.00E+03	4.17E+39	5.39E-41	8.13E+57	3.35E+09	2.20E+18	4.55E-19	1.37E-10
1.00E+05	4.17E+37	5.39E-39	8.13E+55	3.35E+10	2.20E+16	4.55E-17	1.37E-08
1.00E+07	4.17E+35	5.39E-37	8.13E+53	3.35E+11	2.20E+14	4.55E-15	1.37E-06
1.00E+09	4.17E+33	5.39E-35	8.13E+51	3.35E+12	2.20E+12	4.55E-13	1.37E-04
1.00E+11	4.17E+31	5.39E-33	8.13E+49	3.35E+13	2.20E+10	4.55E-11	1.37E-02
1.00E+13	4.17E+29	5.39E-31	8.13E+47	3.35E+14	2.20E+08	4.55E-09	1.37E+00
4.17E+42	1.00E+00	2.25E-01	1.95E+18	2.17E+29	5.26E-22	1.90E+21	5.70E+29

Table 63: Graviton parameters vs number of planckions in the graviton ξ ; corresponding electron-graviton interaction parameters

planckion gas.

We then consider the electron interaction and calculate the number rate $w_{1\xi}$ of impacting segments, together with their mean separation time $T_{1\xi}$. In the final column of the table, we present the electron scatter Δx between consecutive impacts, which is an important new concept.

For the mean free path, we applied Eq. 587. To satisfy the range given by 588, we would need $\xi > 1.00 \times 10^{11}$, producing $\Delta x > 1.37 \times 10^{-2}$ m, which is too large to be consistent with the electron “uncertainty” or expected σ range of Δx spread.

We have raised doubts about the applicability of the mean free path formula to elongated graviton-type particles. It is more likely that one of the shorter values of Δx corresponds to the desired mean free path. For example, we have an atom-sized $\Delta x = 1.37 \times 10^{-10}$ m with $\xi = 1000$ and $L_{mfp} = 3.35 \times 10^9$ m, which is too short for the range 588.

Actually, we need to consider the statistics of Δx and establish the standard deviation σ , for which to add another column in Table 63. Then we can have a better correlation with L_{mfp} and presumably determine the correct value ξ . The table contains only preliminary examples of the possibility to correlate PG findings with particle physics data and quantum mechanics.

Let us further consider the magnitudes of the mean separation times $T_{1\xi}$ for the electron, proton, a macroscopic steel sphere (with radius 1 m), the Earth, and the Sun in the gravitational field. We use the case with $\xi = 1000$, and present the results in Table 64. For completeness, we have also added the electric and somatic fields for the electron and proton.

The electron ring configuration has $\nu_2 = 3.38 \times 10^6$ planckions, while the somion has $\nu_5 = 1$ planckion.

We can appreciate the huge variation of these parameters with body size. In particular, we note the extremely short mean separation times involved with macroscopic bodies, planets, and stars; these are far below the Planck time, and yet they should exist, though implying an imperceptible effect to measure.

The electron and proton have plausible values of $T_{1\xi}$, i.e. very short but still many orders of magnitude greater than the Planck time. In the electric field, we used the electrical mass of the electron and proton, which, being the same, yield identical values for w_2 and T_2 . Otherwise, we use their gravitational mass.

Conclusion: The above exposition provides a strong indication that gravity and quantum mechanics are intimately connected. Gravity causes quantum mechanics. Quantum mechanics is the process or mode via which push particles are absorbed by bodies of all sizes, resulting in the observed gravitational field around them.

field →		gravitational		electric		somatic	
body ↓	mass, kg	$w_1, \#s^{-1}$	$T_{1\xi}, s$	$w_2, \#s^{-1}$	T_2, s	$w_5, \#s^{-1}$	T_5, s
electron	9.11E-31 1.67E-27	2.20E+18	4.55E-19	4.98E+60	2.01E-61	9.17E+63	1.09E-64
proton	1.67E-27 1.67E-27	4.03E+21	2.48E-22	4.98E+60	2.01E-61	1.68E+67	5.94E-68
steel sphere	3.14E+04	7.57E+52	1.32E-53				
Earth	5.97E+24	1.44E+73	6.95E-74				
Sun	1.99E+30	4.79E+78	2.09E-79				

Table 64: Mean separation times and incidence number rate of push particles on various bodies in various fields

31.10.8 Discussion

Subsequent work has confirmed the coexistence of a Planck field with a highest value of G_P (G_5) and an electric field ($_2$) having a lower G_2 but the same maximum acceleration, namely, $g_{02} = g_{05}$. The corresponding field strengths and properties confirm the establishment of the electric field with the expected properties. The electrions are emitted from “charged” particles such as electrons, positrons, and protons, exhibiting the corresponding expected behavior, as forecast in the introductory Section 21 on push electricity.

All four fields have thus been restored in the expected order, with the addition of a fifth one, the Planck field. All fields—subject to further study of the strong and weak fields—are “attractive,” in the sense that their push particles are absorbed, with the exception of the electric field, which is repulsive due to its electrion emission.

In Table 61, we note that the emitted flux intensity of the electric field is much higher than the maximum flux intensity of the Planck field. This imbalance has been accounted for by establishing the electric field as an emitter of electrions by charged particles and the other fields providing input fluxes that can offset the output. In essence, the charged particles are regions where the universe bounces back into much larger absorbing bodies (ordinary objects, stars, white dwarfs, neutron stars, etc.) until some of the latter reach limiting conditions and explode to replenish the accrued hyle into a perpetual cycle of hyle flow.

The mean free path of push particles in each field is a critical subject, which we have only now begun to explore. We must approach it with an open mind regarding possible “unusual” behavior. For instance, if “free space” or “vacuum” is the domain of the Planck field, how are we to understand the transmission of particles and bodies—ranging from push particles to photons, electrons, nuclei, ordinary bodies, planets, and stars—through this medium?

This is not a problem arising only in our PG/PF theory, because the exact same question holds for current theories of “vacuum” or “zero-point energy”. We may suggest that the said energy corresponds to the Planck field, characterized by the flow of the finest possible discrete particles in the known universe. Some theories refer to this medium as “aether,” or by other equivalent terms.

Suffice it here to reference a recent understanding, namely, that a body moving in “free” space will eventually come to a halt (see <https://www.youtube.com/watch?v=lcjdwSY2AzM>). This then provides an answer to the previously raised question of somion drag. With or without it, we should not be discouraged from pursuing further work along the hitherto advances that have been achieved.

A new subject that has emerged is the *mean separation time* and the *rate of particle incidence* on bodies of all sizes. This development has led us to reappraise the structure of the gravion. While the helical structure is retained, it is now conceived as being broken down into much smaller segments, each with the same smallest pitch and radius as before. For convenience, we may need to coin a short name for this refinement, such as “*fundamental helicity*”. This modification is further supported by a clearer understanding of the

distinction between interaction time and the greater integration time required, particularly in the case of the gravitational field.

The group of segmented gravions retains the same interaction time, as a whole, as the previous long gravion, but it also possesses an integration time determined by the size of the body or the surrounding flux intensity. More specifically, the gravion is defined as follows:

- (i) It is a collection of helical segments characterized by the fundamental helicity.
- (ii) The segments are populated with an average number ξ of planckions (to be determined).
- (iii) The segments have an average interaction time $t_{1\xi}$, with $T_{1\xi} = t_{1\xi}$. That is, the segments arrive consecutively, one after another (on average), to complete the action of one gravion, provided the absorbing body is large enough to allow the complete gravion to arrive (see case A2 in Fig. 103)..

However, if the absorbing body is relatively small, like an electron, then only a small fraction of the gravion-segment group will arrive randomly and separately, as in case A1 of Fig. 103. The body size (m_e) and $T_{1\xi}$ vary according to Eqs. 614 or 620.

We can be confident in the revised configuration of the gravion, primarily due to the requirement of preserving the value of g_0 , which was independently derived through various physical considerations in Section 31.5 and shown to be both reasonable and plausible. Nevertheless, it is now even more imperative to confirm g_0 experimentally, as such confirmation would greatly facilitate the further development of the theory within verifiable limits.

Fig. 104 may also assist in visualizing the long-established concept of “inertia”. We propose that classical inertia arises from the persistence of gravion segments during their interaction, which resists changes in the kinetic state of bodies. The gravion segments may be envisaged as “strings” that hold a body in a given kinetic condition. This perspective renews the question of whether the planckions within the gravion segments are “bonded” or otherwise linked among themselves, or whether the absorbing body itself is engaged with the gravion absorption process in such a way that it resists a change in kinetic state.

Eqs. 613 (mass–time) and 614 (energy–time) establish an *exact certainty* between the paired variables, a relation that deserves a new designation. More importantly, this is a transparent and physically meaningful relationship in which every parameter is well defined and free from the alternative interpretations of the Heisenberg Principle advanced by different schools of thought. In particular, Eq. 614 expresses a direct and natural connection between the effective gravitational energy (or mass) of a body—arising from the absorption of gravions in the gravitational field—and the mean separation time of the corresponding absorption events.

The presence of the somion field is essential for maintaining the integrity of the electron as a stable particle entity, while the gravitational and electric forces act to move it within their respective range of action, which is the mean free path of their mediating push particles. The relatively “sparse” incidence of gravion segments gives rise to the random—yet confined—localization of the electron, whereas the electric force dominates in guiding its motion along specific trajectories inside matter, such as around the nucleus of an atom or between two charged plates. This framework provides a plausible explanation for the perceived electron “clouds,” or orbitals, in atoms.

Gravity appears to be responsible for the random motion of very small particles such as electrons. Gravion momentum is transferred randomly to such particles, which are distributed over a much wider volume, effectively acting as a distributed gravitational MAC. These particles are held around an average location by forces provided by other fields, such as the electric and strong fields. These forces act in lieu of the hypothetical (gedanken) mechanical springs illustrated in Fig. 106 (top). The integration of forces on all these “elementary” particles is then averaged out, giving rise to the observed phenomenon of gravity.

We can now avoid anthropocentric or metaphysical interpretations of nature. Based on the PG theory of gravity, we are able to describe phenomena consistently across all scales of time and size in a well-understood way. We thus reach the conclusion that gravity can be responsible for the widely accepted “uncertainty” in the position of an electron and analogous small particles. It is an irony that gravity and quantum mechanics now appear to be intimately related and complementary, rather than mutually exclusive. In this framework, gravity causes quantum mechanics. Both are naturally integrated, not incompatible.

We have now advanced a theory of fields interconnected via a fifth field, the Planck field. Concrete values have been derived for the gravitational, electric, and Planck field properties, possibly for the strong and weak field as well. In this way, we have essentially integrated all fields via the planckion, a common denominator.

Our theory may provide a way to decipher the fundamental difference between fermions and bosons—for instance, explaining why bosons can share the same quantum numbers and occupy the same space, while fermions cannot. This could lead to a deeper understanding of widely adopted empirical rules, such as the Pauli exclusion principle.

If we can ultimately construct all matter and interactions from planckions, then quantum mechanics and its associated “rules” should be reducible to more fundamental structures and processes, some of which we

have only just begun to uncover. Conversely, these established rules may be deduced from a smaller, more elementary set of principles governing the planckion itself. In this way, we may arrive at simpler yet plausible explanations for many of the “strange” phenomena that are not easily understood within existing theoretical frameworks.

The present work is again paused while preparing further developments for the next version of the report. As an open-source endeavor, it will greatly welcome contributions by other researchers.

31.11 All field unification

Based on the preceding developments, it is now possible to formulate a unification of all fields by identifying a common underlying denominator, namely the planckion. This idea has served as both the aspiration and guiding principle from the outset of this work. If all physical fields are to be unified, it is natural to expect that they share a common material basis. If this basis is quantized, then there must exist a common quantum among all fields—a quantum of substance, or hyle. The planckion represents this quantum.

The planckion is in perpetual flow among all manifestations of hyle. Its behavior is governed by a set of fundamental rules that remain invariant as it transitions among fields and bodies. Owing to this invariance, the flow of planckions must obey strict continuity: there can be no “sinks” or “springs,” and no creation or annihilation of hyle. This expresses the grand conservation law of nature within the push-field framework.

Beginning with gravity, it was proposed that the flow of gravions provides the physical basis for the emergence of force, acceleration, mass, and observable gravitational phenomena. The same principle was subsequently applied to electricity and then extended to the strong and weak fields. Each field can therefore be described in terms of flowing push particles endowed with field-specific characteristics. Nevertheless, every push particle ultimately reduces to the same common quantum of hyle—the planckion.

With this understanding, it is now possible to formalize the basic equations governing flux intensities for each field and to establish the relationships that unify them.

31.11.1 Field flux intensities

Before proceeding to investigate nuclear physics in the following sections, it is necessary to expand and consolidate the earlier work on field flux intensities introduced in Section ???. An expanded summary of the definitions and relationships among the symbols describing field flux intensities is therefore presented below.

Definition of basis quantities The symbol J_{0f} represents the *field flux intensity*, that is, the fixed flow of energy carried by push-particles of field f per unit time and per unit area from all directions from one side of a surface element at any point in free space. This flux is modified in the presence of hyle (matter)—specifically, bodies that absorb push particles of various kinds. In particular, for the electron (or positron) ($-e$) and proton ($-p$), we define the following components of flux intensities.

J_{faR-e} : is the flux absorbed at any point on the surface of electron from all incoming directions, which is the energy of push particles absorbed per unit time per unit surface area of the electron. This relates to the field flux intensity by:

$$J_{faR-e} = \pi A_{fR-e} J_{0f} \quad (621)$$

where A_{fR-e} is the absorptivity of the electron (or positron) in the field f .

The same symbol is shared and used for the positron being identical with the electron except for their associated electrons having opposite spinning sense; the initial letter “p” of the positron precludes it for use in the symbol, because the same letter “p” is reserved and used for the proton.

Hence, J_{faR-p} refers to proton, with the implied understanding that $R = R_{-p}$ for proton and $R = R_{-e}$ for electron and positron in the respective subscripts of their symbols. Thus, for proton:

$$J_{faR-p} = \pi A_{fR-p} J_{0f} \quad (622)$$

where A_{fR-p} is the absorptivity of the proton in the field f .

Flux at a distance At any point in space located a distance r from the center of a particle (electron/positron or proton), the absorbed flux intensity is expressed by $J_{fa-e}(r)$ or $J_{fa-p}(r)$, respectively for the electron (positron) and proton. The presence of the subscript “a” (for “absorbed”) indicates that the symbol represents the total absorbed energy per unit time per unit area normal to the direction between the point of observation and the particle center. The flux is integrated over the solid angle subtended by the particle.

When the “a” subscript is omitted, as in $J_{f-e}(r)$ and $J_{f-p}(r)$, the expressions denote the field flux towards the particle, at that point, that is not absorbed by the particle including the part of the flux that skirts around the particle in the free space; in other words, it is the total non-absorbed flux integrated in the hemisphere on the side containing the particle. That is, they describe the free energy flux per unit time per unit area normal to the line joining the observation point and the particle center. To be clear:

$$J_{fa-e}(r) + J_{f-e}(r) = J_{0f}, \quad J_{fa-p}(r) + J_{f-p}(r) = J_{0f}$$

Thus, by definition of Eqs. 621 and 622,

$$J_{fa-e}(R_{-e}) \equiv J_{faR-e}, \quad J_{fa-p}(R_{-p}) \equiv J_{faR-p}.$$

Finally, we apply the square of distance decrease of flux away from the particle surface at distance r from the center of the respective particle; based on the workings in Section 31.7, we have:

$$J_{fa-e}(r) = \pi J_{0f} A_{fR-e} \frac{R_{-e}^2}{r^2}, \quad J_{fa-p}(r) = \pi J_{0f} A_{fR-p} \frac{R_{-p}^2}{r^2}, \quad f \neq 2 \quad (623)$$

$$J_{f-e}(r) = \pi J_{0f} \left(1 - A_{fR-e} \frac{R_{-e}^2}{r^2} \right), \quad J_{f-p}(r) = \pi J_{0f} \left(1 - A_{fR-p} \frac{R_{-p}^2}{r^2} \right), \quad f \neq 2 \quad (624)$$

Both of these Eqs. 623 and 624 apply to all fields other than the electric field ($f \neq 2$), because J_{02} is thought to be *internal* to the particle. In the electric field, there is an emission (in lieu of absorption) of electrions by the electron (positron) and proton. The flux of electrions runs in the opposite direction to all other absorbed push particles. If the absorbed flux is assigned the positive sign, then the electric flux has the negative sign (or vice-versa). In this case, we might as well call the A_{2R-e} “emissivity” and replace it with the symbol E_{R-e} , where there is no ambiguity if the number $f = 2$ is omitted from the subscript, since there is no other field with an emissivity of push particles (so the theory goes). In that case, Eq. 623 for electricity can be written as

$$J_{2-e}(r) = -\pi J_{02} E_{R-e} \frac{R_{-e}^2}{r^2}, \quad J_{2-p}(r) = -\pi J_{02} E_{R-p} \frac{R_{-p}^2}{r^2} \quad (625)$$

where $E_{R-e} \equiv A_{2R-e}$, $E_{R-p} \equiv A_{2R-p}$ and $r \geq R_{-e}$, $r \geq R_{-p}$. This understanding applies retrospectively to all references to the absorptivity in the electric field together with its prior and future use of the symbol A_{2R-e} .

As mentioned previously, there is an outstanding issue with terminology in push field theory, because it is in continual evolution creating novel situations that require the introduction of new terms and symbols or the revision of previously introduced ones. Once the theory is firmly consolidated to a satisfactory level, then we can rationalize the entire terminology for consistency and purpose.

In summary: These expressions demonstrate the inverse-square dependence of absorbed and total flux intensities with respect to distance r , consistent with the general push-field principle. The coefficients A_{fR-e} and A_{fR-p} , also E_{R-e} and E_{R-p} represent the dimensionless field absorption factors for each particle. The parameter J_{0f} characterizes the free-space flux of the particular field f , except for the electric field where J_{02} is internal to the electron (positron) and proton. They form an interim mathematical foundation for subsequent analysis and development shortly.

Precursor of electric field In the earlier development of the electric field theory, it was postulated that a precursor maximum flux intensity J_{02} exists *inside* electric particles (electron, positron, and proton), from which electrions are emitted. This assumption was initially introduced as a mathematical necessity, without requiring a physical mechanism. It was implicitly expected that a suitable physical justification could emerge later, provided numerical results remained consistent with the broader evolution of the theory.

A tentative explanation was suggested that the somions and gravions absorbed were a source of J_{02} behaving as an internal source feeding the electrion production by the electron. Having subsequently considered further contributions by the strong and weak fields, we can re-appraise the overall situation as follows.

The J_{0f} is generally a uniform physical entity everywhere when it is considered alone without the presence of a physical body. However, when it is absorbed or emitted by a specific body, it is the fraction $J_{faR-e} = \pi A_{fR-e} J_{0f}$ that achieves specific quantitative and qualitative significance. We may say that J_{0f} is a precursor to J_{faR-e} connected with a body (here, electron) of radius R_{-e} and absorptivity A_{fR-e} . It so happens that each of the four fields $f = 1, 3, 4, 5$ has its own flux intensity except for the electric field. The latter in its existence outside the electron does not have its own dedicated, uniform and independent field like each of the other fields. Instead, it has an *effective* precursor field flux J_{02} internal to the particle (electron, positron and proton) created in consequence of the absorption of all the other field fluxes. It is the other four fields, which converge and conflate by the structure of the electron to produce electrions with a flux $J_{eR-e} = -\pi E_{R-e} J_{02}$ flowing out of and normal to the particle surface.

Whether this effective J_{02} is physically present locally (like an internal layer) or distributed somehow inside the electron, or it is rather a mathematical intermediary quantity calculating the out-flowing flux does not invalidate the mathematical formulation of this term in the balance of the overall flux in-and-out of the electron (positron). The physical existence or not will be established as we gradually determine the structure of the electron in order to accommodate the mathematical requirements in the balance of all fluxes. In any case, all the electrions produced appear straight at the surface of the electron (positron, or proton). The factor E_{R-e} on its own describes an actual physical property of the relevant body; this is an actual emissivity playing a corresponding role to the absorptivity of the other fields by the same body. This emissivity is provided by the equation:

$$-\pi E_{R-e} J_{02} = \pi A_{4R-e} J_{04} + \pi A_{5R-e} J_{05} + \pi A_{3R-e} J_{03} + \pi A_{1R-e} J_{01}.$$

The body symbols for electron (positron) ($-e$) and proton ($-p$) have now been omitted altogether, because the same equation applies for all three bodies alike. The J_{02} enters as a mathematical factor to satisfy the above equation and arises from the combined action of all the absorptivities in the right hand side of the equation. The question on its physical existence (on its own) in a physical space can be deferred for later consideration. The symbols g_{02} , J_{02} and $J_{eR-e} \equiv J_{2eR}$ for the electron can be seen again in Fig. 95b.

The terms on the right-hand side are arranged in descending order of relative field strength:

$$J_{4aR-e} \gg J_{5aR-e} \gg J_{3aR-e} \gg J_{1aR-e}. \quad (626)$$

It can be said that the internal supply J_{02} is formed from accumulated hyle originating from external fluxes J_{05} , J_{04} , J_{03} , and J_{01} . The numerical values can always be adjusted to balance the incoming and outgoing fluxes for a particle. In an attempt to achieve this, it became apparent that the strong-field flux J_{4aR-e} played by far the dominant role in balancing the electric flux J_{eR-e} .

In other words, the flux intensity of the strong field can simply be taken nearly equal to the flux intensity of the electric field, but slightly less so that together with the incoming fluxes of all the other fields to yield an output electric flux as already computed. J_{04} can be numerically adjusted to ensure the proper balance of all field fluxes. Thus, we propose:

$$J_{04} \lesssim J_{02}. \quad (627)$$

where the symbol \lesssim signifies *slightly less than*. In effect, we have already done so with the numerical example provided for the strong field before. This envisages that strong-field push particles (z-ions) are first absorbed in the bulk of the body producing an “attractive” force between bodies and then are emitted as electrions in all directions producing a repulsive force between bodies. The said bodies (electron, positron and proton) are in effect converters of all absorbed push particles, of which z-ions are predominant, to electrions.

A further implication is that strong-field push particles must consist not only of nearly the same number density but also of nearly the same number of planckions per particle arranged in a ring-shaped configuration of nearly same size as electrions, and depicted in Fig. 94, but without spin; these strong-field push particles correspond to the neutral (i.e. without spin) ring structure shown in Fig. 105. In effect, the z-ion should have $[\nu_4] \lesssim [\nu_2]$ planckions and $r_4 \lesssim r_2$ but with no associated spin.

With this revision, both the conceptual structure and the mathematical formulation of the theory become substantially simpler. The next step is to revise the unification tables and recalculate the numerical values, thereby preparing a streamlined transition to the forthcoming chapter on nuclear physics.

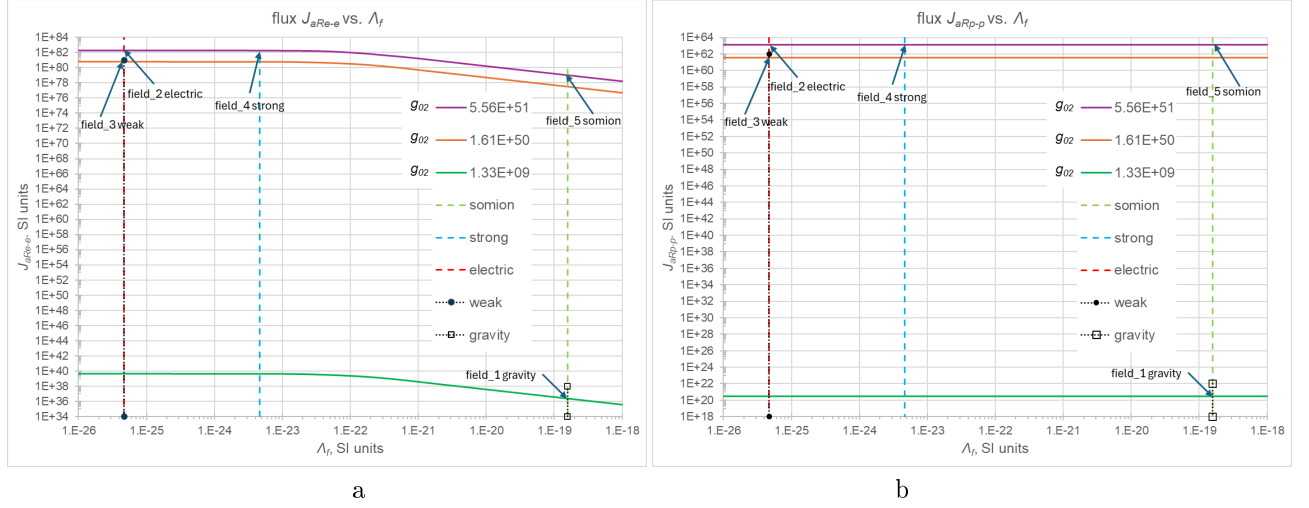


Figure 108: Electron (positron) and proton field fluxes vs. Λ_f

Results The theoretical variation of absorbed and emitted fluxes as functions of Λ_f is shown in Fig. 108a&b. The five fields are indicated by single points on each graph, at which the parameter Λ obtains its actual value.

Numerical values of the flux intensities for each field are summarized in in Table 65. The table has the same format as the field unification tables like the preceding Table 61. It provides the various flux intensities in columns starting with the defining values of Λ_f and g_{0f} (or G_f and g_{0f}) in the top rows of the table.

Analysis and further consideration of these results will be undertaken as needed during development of the theory. They are presented at this point also should the reader wish to use them for their understanding of the preceding work but also for their possible application outside this report. Suffice it to say that numerical equation among several parameters are only apparent in the table permitting only some decimal places, but the reader should reproduce the same figures to establish very small differences by using a high precision worksheet.

Other theoretical derivations From Eq. 580

$$\frac{G_P}{G_2} = \mu^2$$

$$\frac{G_P/g_{05}}{G_2/g_{02}} = \frac{\Lambda_5}{\Lambda_2} = \frac{\nu_2}{\nu_5} = [\nu_2] = \mu^2$$

$$\mu = \frac{m_{e-p}}{m_{e-e}} = \frac{q_{-p}m_{-p}}{q_{-e}m_{-e}} = \frac{\frac{3A_{R-p}}{4k_{-p}R_{-p}}}{\frac{3A_{R-e}}{4k_{-e}R_{-e}}}$$

$$\mu = \frac{m_{e-p}}{m_{e-e}} = \frac{m_{2e-e}}{m_{e-e}} = \frac{q_{2-e}m_{-p}}{q_{-e}m_{-e}} = \frac{\frac{3A_{2R-e}}{4k_{2-e}R_{-e}}}{\frac{3A_{R-e}}{4k_{-e}R_{-e}}} = \frac{A_{2R-e}k_{-e}R_{-e}}{A_{R-e}k_{2-e}R_{-e}} = \frac{A_{2R-e}\Lambda_1}{A_{R-e}\Lambda_2}$$

Also from Eq. 581 we re-write as

$$\mu \approx \frac{m_{2e-e}}{m_{5e-e}} = \frac{A_{5R-e}}{A_{2R-e}} = \frac{J_{5aR-e}/J_{05}}{J_{2aR-e}/J_{02}} = \frac{J_{5aR-e}J_{02}}{J_{2aR-e}J_{05}} = \frac{1}{\mu}\mu^2 \quad (628)$$

$$\mu_1 = \frac{m_{fe-p}}{m_{fe-e}} = \frac{Gg_0A_{fR-p}R_{-p}^2}{Gg_0A_{fR-e}R_{-e}^2} = \frac{A_{fR-p}R_{-p}^2}{A_{fR-e}R_{-e}^2} = \frac{\pi J_{f0}}{\pi J_{f0}} \frac{A_{fR-p}R_{-p}^2}{A_{fR-e}R_{-e}^2} = \frac{J_{faR-p}R_{-p}^2}{J_{faR-e}R_{-e}^2}$$

field type ($_{0f}$)	gravity ($_1$)	weak ($_3$) test	electricity ($_2$)	strong ($_4$) test	Planck ($_5$)
	GRAVITY	WEAK	ELECTRIC	STRONG	PLANCK
Λ_f	1.57363E-19	4.69199E-26	4.65892E-26	4.65892E-24	1.57418E-19
g_{0f}	1.33241E+09	1.60676E+50	5.56073E+51	5.56073E+51	5.56073E+51
G_f	6.67408E-11	2.39971E+24	8.24644E+25	8.24644E+27	2.78636E+32
J_{0f}	8.07990E+35	3.26788E+83	1.13898E+85	1.13898E+83	3.37091E+78
J_{faR-e}	2.53837E+36	5.61684E+80	1.94389E+82	1.88632E+82	1.05900E+79
$J_{fa-e}(R_{-p})$	1.63661E+17	3.62145E+61	1.25332E+63	1.21620E+63	6.82789E+59
$J_{f-e}(R_{-p})$	2.53838E+36	1.02663E+84	3.57822E+85	3.57822E+83	1.05900E+79
J_{faR-p}	3.00401E+20	3.62256E+61	1.25370E+63	1.25370E+63	1.25370E+63
$J_{f-p}(R_{-p})$	2.53838E+36	1.02663E+84	3.57822E+85	3.57822E+83	1.05900E+79
$\frac{J_{f-e}(R_{-p})}{J_{faR-e}}$	1.00000E+00	1.82778E+03	1.84075E+03	1.89693E+01	1.00000E+00
$\frac{J_{faR-p}}{J_{fa-e}(R_{-p})}$	1.83551E+03	1.00031E+00	1.00031E+00	1.03084E+00	1.83615E+03
$m_{fe-e} - m_{e-e}$	3.20160E-34	1.67120E-27	1.67120E-27	1.62168E-27	-3.68839E-40
$\mu_f = \frac{m_{fe-p}}{m_{fe-e}}$	1.83551E+03	1.00031E+00	1.00031E+00	1.03084E+00	1.83615E+03

Table 65: Comparative values of universal constants for gravitational, weak, electric, strong and Planck fields [Note: the updated blue figures differ imperceptibly only in a few cells at the precision shown and much less at higher precision, without affecting the arguments presented in the theory]

31.11.2 More on terminology

Further terminological issues arise not only from the evolving nature of the present report, but also from inherited conventions in the broader physics literature. These require explicit clarification to avoid ambiguity.

We introduce the quantity *force-strength*, defined as the product of the force $F(r)$ between two spherical bodies and the square of their separation distance r ,

$$\text{force} - \text{strength} \equiv F(r)r^2$$

In the gravitational field this quantity is given by

$$F(r)r^2 = GM_e \equiv \mu$$

where μ is commonly referred to as the standard gravitational parameter.

To avoid confusion with the proton-to-electron mass ratio, which is also conventionally denoted by μ , we explicitly distinguish the gravitational standard parameter by the notation μ_{sp} , as introduced in Eq. 320. By analogy, we use μ_{2sp} for the standard electric-field parameter in 321, and more generally μ_{fsp} for the corresponding parameter of any field f .

Within this notation, the standard gravitational parameter μ_{sp} coincides with the value of force-strength at a fixed value of the universal gravitational constant G , as represented on the theoretical graph in Fig. 99 for gravity. Correspondingly, within the Push Gravity framework, one may define field-specific constants G_f for each field interaction f , yielding a standard field- f parameter at particular reference points on the graphs shown in Figs. 96 and 101.

Regarding the proton-to-electron mass ratio μ , this can be further differentiated for each field with μ_f as provided in Table 65.

Care should therefore be exercised when interpreting the symbol μ , whose meaning depends on context. The notational conventions adopted here provide a consistent framework while a broader rationalization of symbols and terminology across the developing PG theory is ongoing.

32 Towards a quantum push field theory (QPFT)

In Section 19, we began developing the idea of a “Quantum Push Gravity (QPG)” theory. At that early stage, it was thought that the gravion might represent the fundamental quantum responsible for mediating the gravitational interaction. Before proceeding further, it is important to clarify what we mean by the term “quantum.”

In physics, the word *quantum* usually denotes the smallest possible discrete unit of any physical quantity that can exist or be exchanged. We can retain this conventional meaning, provided we allow that a “quantum” might itself be composed of even smaller entities, which could take part in deeper, or lower-level, sub-processes. In other words, we can think of a hierarchy of quanta, where each level may, in principle, be subdivided further—until a final limit is reached beyond which no further subdivision is possible.

We identify this ultimate limit with the *planckion*, the smallest and most fundamental quantum of nature. All other previously known quanta—such as photons (for light), electrons, electrions (for electric interactions), and gravions (for gravity)—may then be regarded as composite structures made up of planckions.

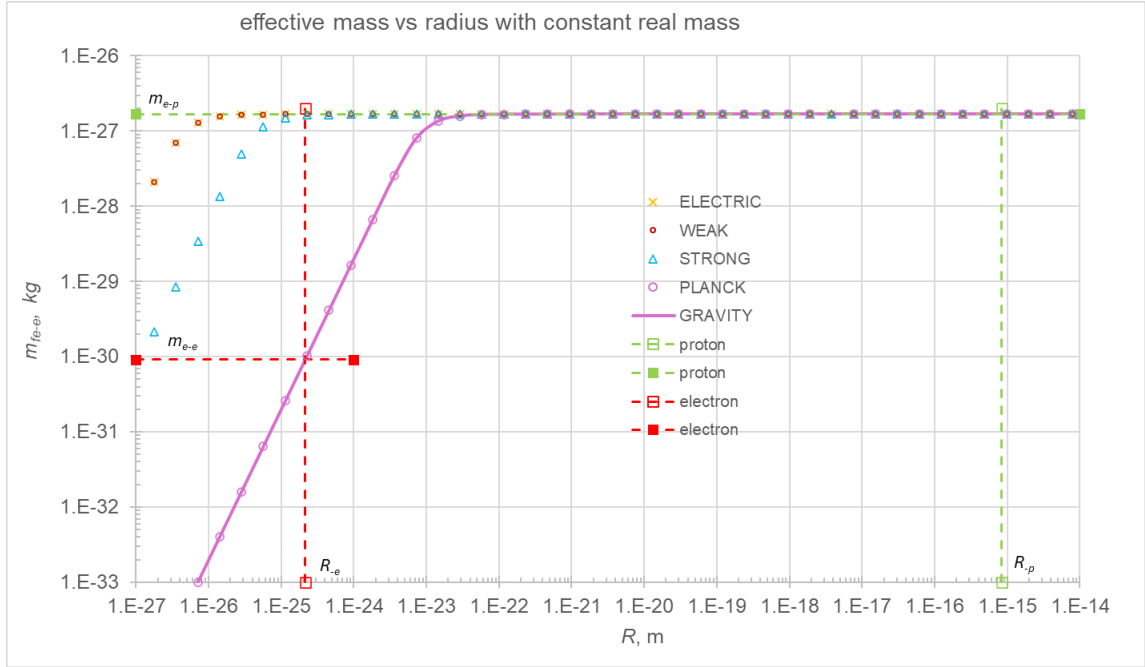
Originally, the gravion was considered to be the smallest possible quantum, since gravity is the weakest of all interactions. However, further reasoning suggests that even the gravion should have an internal structure composed of smaller constituents—the planckions. This leads to the realization that the *Planck field*, corresponding to the strongest of all fields, is the one that is absolutely quantized—that is, fundamentally mediated by planckions.

Having clarified this broader meaning of the term “quantum”, which now includes both fundamental (planckions) and composite (such as photons or gravions) quantized entities, we can proceed to extend the *push principle* to a general *Quantum Push Field Theory* (QPFT).

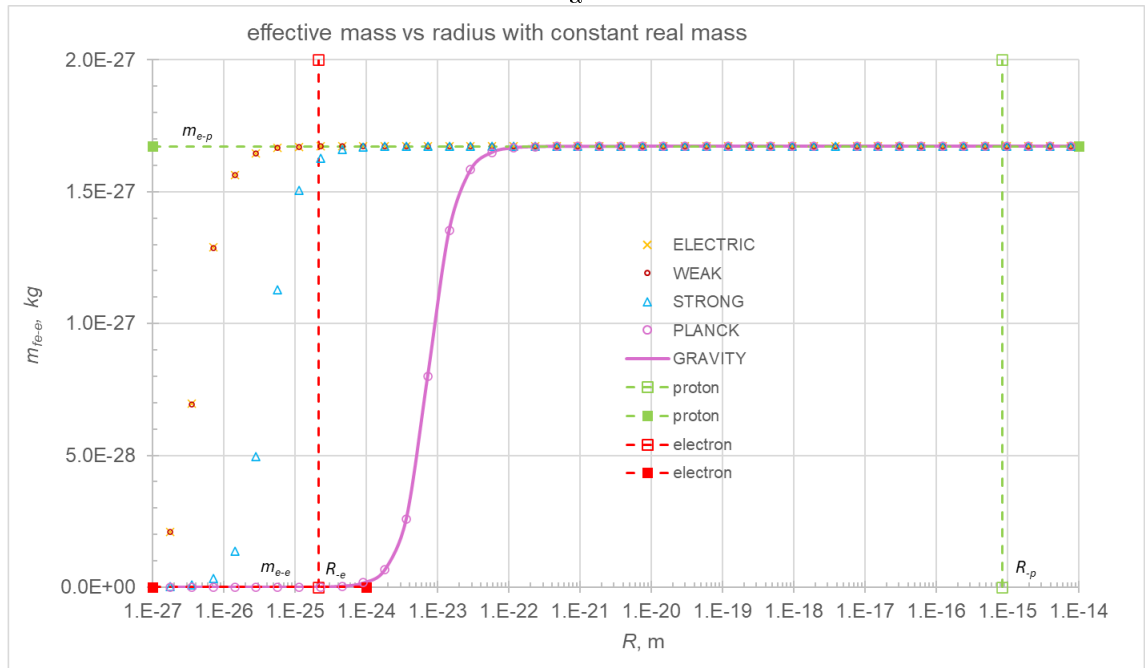
In subsequent development of QPFT, this new framework will be explored by examining specific quantitative relationships within and between various force fields, providing deeper insight into how the push principle might unify them at the quantum level.

32.1 Effective-mass variation at constant real mass

From earlier considerations, we have already examined the behavior of the gravitational field—specifically, acceleration—when a sphere shrinks while maintaining constant mass (see Section 9.1). We now investigate



a



b

Figure 109: Effective mass variation against radius with constant real mass

what happens to the effective mass of a sphere with the dimensions of a proton that contracts while its real mass remains constant.

Plotting this variation against Λ_f (or $k_{f-e}R_{-e}$) in Fig. 102e&f combines the joint effects of k_{f-e} and R_{-e} . We now decouple these two parameters to examine the variation of effective mass m_e specifically with respect to radius R , assuming that the real mass m is invariant. This follows directly from

$$m_e = qm = \frac{3A_R}{4kR}m,$$

together with Eq. 602 (see also early Eq. 102):

$$k = \Lambda \frac{3m}{4\pi R^3} = \frac{3Gm}{4g_0 R^3}.$$

Thus, the functional dependence $m_e = f(R)$ is plotted in Fig. 109, using log–log axes in (a) and linear–log axes in (b). This dependence is shown for each of the five fields by setting the appropriate values of Λ_f , or the pair (g_{0f}, G_f) for each field f .

The graphs indicate that the effective mass decreases monotonically without limit as the radius approaches zero, yet reaches asymptotically a “saturation” value beyond a transition region as the radius increases. This behavior is clearly visible in the linear–log plot, where zero mass is approached asymptotically with a familiar sigmoid-like trend. On the log–log plot, the same trend appears as a straight line descending indefinitely toward zero effective mass, with an inflection “point” marking the transition from a nearly constant effective mass at high radius values.

The variations of effective mass in the Planck and gravitational fields are practically indistinguishable (albeit not identical). The same close correspondence appears for the electric and weak fields, whereas the strong field behaves distinctly from all others. The quantitative behavior for the strong and weak fields remains tentative, depending (and pending) on the parameter choices made in Section 31.8.1, while the gravitational, electric, and Planck fields may be considered well determined so far.

It is important to note that the inflection (transition) points of effective mass in the electric and weak fields fall clearly below the computed electron radius, while for the strong field the transition lies below but near the electron radius. This suggests that such transitions are purely theoretical, if the electron indeed possesses a definite radius—namely, the one previously calculated. Specifically for the electric field, this implies that the electrical mass is practically invariant in reality. This is consistent with the empirical observation that the electron “charge” is constant in a quantum, since we have established that the electrical mass (in our framework) and the conventional charge are equivalent.

However, in both the gravitational and Planck fields, the effective-mass transition occurs clearly between the electron and proton radii. This represents a real case of two distinct effective masses for the same real mass, corresponding respectively to the proton and electron. At the same time, the proton exhibits practically the same effective mass in both fields (though not exactly identical); similarly, the electron exhibits practically the same effective mass in both fields (again, not exactly identical).

These findings mark a clear departure from Newtonian physics, under which mass is invariant regardless of its spatial distribution. In contrast, the push-field framework predicts an effective mass that is associated with the surrounding acceleration field. The magnitude of this effect is governed by the spatial distribution of real mass (*hyle*, or matter), which produces self-shadowing and thereby modulates the active (effective) mass associated with each field. Nevertheless, the inverse-square law of distance remains valid.

The conventional charge (interpreted as electrical mass) appears invariant in practice—hence the observed “quantization of charge”—but in fact, even this invariance is only approximate, with variations too small for current instruments to detect.

This new physics also provides a resolution to the long-standing Zeno’s Paradox (Wikipedia contributors, 2025e). According to the paradox, “*it is impossible to traverse an infinite number of things in a finite time*”, or equivalently, “*that which is in locomotion must arrive at the half-way stage before it arrives at the goal.*” The infinite dichotomy of halving the distance between an arrow and its target is a conceptual abstraction rather than a manifestation of physical reality. As the arrow approaches a Planck-length separation from the target, continuous subdivision ceases to have meaning; the arrow must undergo a discrete transition to its destination without traversing the remaining midpoint. Nevertheless, Zeno’s conception retains profound significance, providing valuable insight into the fundamental nature of space and time within the further development of PG.

With reference to the Quantum Zeno effect (Wikipedia contributors, 2025d), the Copenhagen interpretation of quantum mechanics is idealist not, materialist. Application of it to the Zeno paradox is absurd, claiming that *observing* the arrow at the start, it collapses its quantum state at the start and it doesn’t move!!! Its counterpart of the quantum anti-Zeno effect, where frequent measurements can instead accelerate the

decay of a quantum system, depending on the measurement intervals and dynamics, is also absurd. This is due to a blurring between idealism and materialism. An understanding of these issues under a quantum push field theory should clarify these misconceptions once and for all.

Therefore, the push-field framework implies quantization not only through the discrete nature of the mediating push particles, but also through the inherently quantized structure of the bodies that interact with them.

These concepts will be further elucidated by applying the theory to the electron–proton system. In the following sections, we examine various numerical calculations using the electron and proton parameters established so far, to determine whether the theory can achieve internal consistency. The calculations involve the electron radius, surface area, and volume, in conjunction with the planckion and associated mass.

32.2 Electron surface area

If the electron radius shown in Fig. 109 represents the (near) minimum possible radius resulting from the (near) maximum packing order of planckions, then we should be able to derive consistent relationships from this electron state that align with other independently obtained results.

Gravions and planckions are expected to be absorbed at, or very near, the electron surface. Therefore, the outermost layer of the electron should consist of activated planckions, the collective contribution of which determines the known effective mass of the electron. Each incident planckion should activate a surface area per planckion equal to Λ , according to Eq. 546. Hence, the total activated mass on the entire surface is given by:

$$m_{\text{surface-e}} = \frac{4\pi R_{-e}^2}{\Lambda} = 3.6423542930 \times 10^{-30} \text{ kg}$$

This value is notably close to four times the known effective mass of the electron:

$$m_{e-e} = \frac{4\pi R_{-e}^2}{4\Lambda} = 9.1058857325 \times 10^{-31} \text{ kg}$$

which is consistent with the experimentally known value of $9.1093837015 \times 10^{-31} \text{ kg}$.

This outcome aligns well with the 3+1 mass scheme described in Section 29.4.1, which proposes that three of the absorbed push particles cancel out in terms of force, leaving the fourth to account for the activated effective mass—thus producing the factor of four in the energy–mass equivalence. While this mechanism was originally derived for gravions, it appears that the same principle may apply to planckions as well.

Even if the proposed 3+1 mass scheme is not the underlying explanation, the factor of four remains significant and must be accounted for by other means. It generally implies that only one quarter of the electron’s surface area—statistically, on average—contributes effectively to the observable mass of the electron. In any case, the derivation above provides a consistent result that matches the expected effective gravitational and/or somatic (Planck-field-induced) mass of the electron.

The gravitational absorption constant for the electron is:

$$k_{-e} = 6.4468679035 \times 10^{27} \text{ m}^{-1}$$

which is very close to the somatic (Planck field) value:

$$k_{5-e} = 6.4491337378 \times 10^{27} \text{ m}^{-1}.$$

The inverse of either of these gives the depth corresponding to one planckion absorption (or mean free path inside the electron). As found in Section 18.2, the *total absorption layer* (TAL) concept for dense bodies can be extended here, treating the electron as a miniature black hole relative to the gravitational and Planck fields. Thus, for the electron:

$$\text{TAL}_{-e} = \frac{1}{k_{5-e}} = 1.5505958485 \times 10^{-28} \text{ m}.$$

This distance is considerably larger than the Planck length, over which absorption was originally assumed to occur—that is, across the top layer of planckions. However, this is not inconsistent, because in reality absorption is a statistical process occurring randomly over a greater depth that effectively encompasses more *hyle* than a single planckion (see Section 24.2). In other words, each surface planckion is accompanied by additional “matter” with which it interacts (the absorption center), thereby generating the absorption event.

The corresponding fractional thickness of this layer relative to the electron radius is:

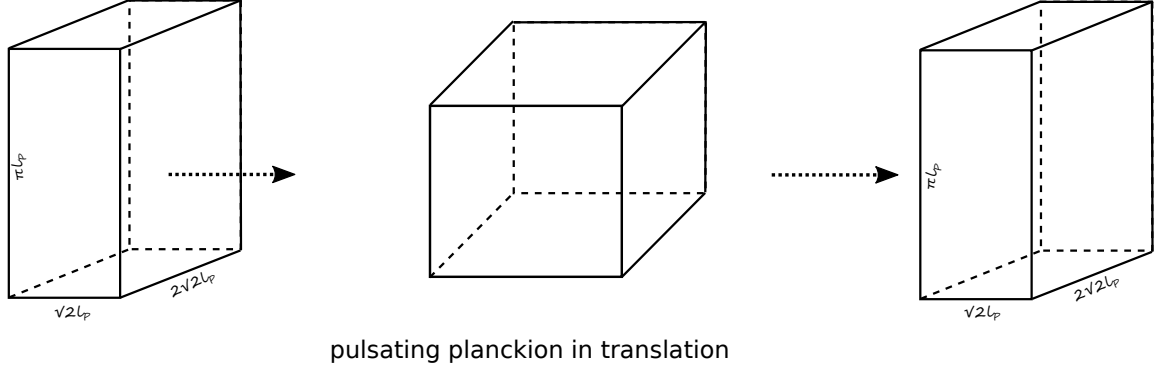


Figure 110: Three dimensional representation of the planckion model pulsating and moving in the direction of pulsation.

$$\frac{\text{TAL}_{-e}}{R_{-e}} = \frac{1}{k_{5-e}R_{-e}} = 7.259 \times 10^{-4} = 0.07259\%.$$

This is a very small fraction, which may conveniently represent the total absorption layer (TAL) on the electron's surface and is consistent with the conceptual depiction shown in Fig. 95a.

These derivations may later assist in determining the internal structure of the electron, which should conform to the numerical relationships derived above. It is also noteworthy that the absorption thickness is of the same order of magnitude as the chain length of planckions within the circumference of a single *electron*. Specifically, the number of planckions in the electron is 3.38×10^6 (see Table 61), while the absorption layer corresponds to:

$$\frac{\text{TAL}_e}{\ell_P} = 9.59 \times 10^6 \text{ Planck lengths.}$$

The graviton, electron and planckion may be organically inter-related in various absorption and emission processes to bear in mind during future work. These insights will be valuable in subsequent efforts to elucidate the detailed structure of the electron.

32.3 Electron volume

We can derive further consistent relationships by considering the electron state as a (nearly) maximally packed configuration of planckions, now incorporating their volumetric relationships. This is prompted by the fact that the electrical mass occupies the entire volume as depicted in Fig. 95b.

To begin, we must establish a third dimension for the planckion beyond the two dimensions used in the model of Fig. 90. These two dimensions were previously chosen as $\sqrt{2}\ell_P$ and $\pi\ell_P$, satisfying the conditions set in Section 31.5.2 for aligning the theoretical values of g_0 and Λ . Consequently, we obtained the effective cross-section $\sigma_{\text{planckion}}$ for the planckion:

$$\sigma_{\text{planckion}} = \pi\ell_P \times \sqrt{2}\ell_P = 1.1606055241 \times 10^{-69} \text{ m}^2,$$

associated with the Planck mass m_P , as given in Table 41. A three dimensional model is now depicted in Fig. 110 with a third dimension added.

We have found that if the “thickness” or third dimension of the planckion is taken equal to $2\sqrt{2}\ell_P$, we can produce the following outcomes.

The volume of the planckion becomes:

$$V_{\text{planckion}} = 4\pi\ell_P^3,$$

resulting in the total number of planckions within the electron:

$$[\nu_{\text{electron}}] = \frac{\frac{4}{3}\pi R_{-e}^3}{4\pi\ell_P^3} = 7.6950704614 \times 10^{29}.$$

The total real (hyle) mass of the electron is therefore:

$$m_{-e} = [\nu_{\text{electron}}] m_P = 5.6731886383 \times 10^{-21} \text{ kg.}$$

If all the above planckions are grouped into electrions inside the electron, the total number of electrions becomes:

$$[\text{electrions}] = \frac{[\nu_{\text{electron}}]}{[\nu_2]} = \frac{7.6950704614 \times 10^{29}}{3.3767969404 \times 10^6} = 2.2788075793 \times 10^{23},$$

where $[\nu_2]$ is the number of planckions per electron. If we assign an effective mass m_P to each electrion (equal to the Planck mass), the total effective mass of the electron becomes:

$$m_{\text{total}-e} = [\text{electrions}] m_P = 1.6790224360 \times 10^{-27} \text{ kg,}$$

which is remarkably close to the independently computed electrical mass of the electron, $m_{2e-e} = 1.6721105758 \times 10^{-27} \text{ kg}$. This agreement would be highly significant if accompanied by a physically plausible interpretation.

Interpretation One interpretation may be based on the “Newton’s cradle” pendulum analogy already discussed in Section 31.5.2. Each electrion *inside* the electron has the Planck mass m_P , implying that only one out of the $[\nu_2]$ planckions is activated at any given time, while the remaining planckions constitute dormant or “black” mass (hyle). Equivalently, an effective mass of m_P (or equivalent energy) is distributed over a chain of $[\nu_2]$ planckions; this is not enough to make the electrion “spring” out of the electron yet.

This mechanism can also be visualized as an intermittent mechanical process similar to the “drinking bird” toy (Wikipedia contributors, 2025a). A single electrion chain inside the electron remains dormant while it gradually accumulates planckions until the entire chain is activated; upon reaching a critical state, it is emitted as an electron outside the electron. In other words, there is a periodic accumulation of hyle reaching a threshold, after which the stored hyle is released as an electrion in accordance with the derivation of the electric field theory in Section 31.7. This process was initially framed under the second law of thermodynamics in Section 15.8.

Criticism The preceding interpretation, while internally consistent, faces challenges when compared with empirical evidence—particularly regarding the electron–positron annihilation process. This process yields two gamma-ray photons whose combined energy is equivalent to the rest-mass energy of the two particles initially at rest.

If the real mass of the electron (or positron) were indeed much greater than its known effective mass, the resulting gamma rays should possess correspondingly higher energy. In that case, we would observe a clear violation of the conservation of energy law by converting a much higher amount of mass to photon energy. This would imply that our theoretical understanding of the meaning of various masses has been fundamentally flawed.

We address this apparent contradiction by proposing that the dormant component—*black mass*—remains inactive during annihilation. This component may be transferred, partly or wholly, into surrounding fields as push particles or retained within the photons as an inert form of hyle. Because it lacks classical inertia, such transfer proceeds undetected, maintaining the known conservation of mass–energy. We have previously argued that undetectable exchanges of hyle between bodies and surrounding fields may occur frequently without violating the conservation of total hyle and the known conservation laws.

Although this explanation may at first appear ad hoc, it gains plausibility once the nature of black mass is reconsidered. Black mass is not devoid of energy or motion; it merely behaves as such relative to the gravitational field that generates measurable gravitational mass. The known fact that photons exhibit gravitational interaction implies that they are affected by gravions—the absorption of which activates part of the photon while leaving the remainder inactive as black mass. The photon itself has yet to be investigated in this framework, though it may contain helical structural units as suggested in Fig. 89. It remains the task of particle-physics researchers to develop a photon model compatible with the push-field interpretation of the electron–positron annihilation process.

In particle-physics experiments, the measurable quantity corresponds to the *gravitational mass*, mediated by gravions. These gravions have relatively long interaction times, during which much faster processes can occur without exhibiting measurable gravitational effects. Hence, such rapid processes remain undetected as mass or energy transformations. The observed equality between the effective mass of the electron–positron system and the combined mass of the emitted gamma rays can therefore be understood as a consequence

of the gravions' long interaction time, which effectively preserves gravitational mass before and after the annihilation event.

This concept is illustrated schematically in Figs. 104 and 107, showing that gravion interactions occur over much longer mean duration than those involving electrions or somions. Such persistence allows the gravitational mass to appear invariant during transient high-energy processes.

The entrenched notion of classical inertia introduces strong conceptual bias in our understanding of mass and energy, hindering acceptance of the push-field framework. Conventional physics presumes that mass necessarily entails observable inertia and measurable energy, whereas in the push-field model, part of the total hyle may exist in an inert, non-interacting state relative to gravions or gravity.

To further elucidate this perspective, the interrelations among space, time, and mass must be expanded as introduced in Section 31.10. That framework provides a basis for understanding how black mass maintains theoretical and experimental consistency within push-field physics.

Clarification on geometry and mass concepts The geometrical model of the planckion in Fig. 110 does not imply its actual shape. We may, for instance, represent a circular area by a square with side $\sqrt{\pi}R$, giving the equivalent circle area πR^2 . If such a model helps our understanding of outcomes arising from an as-yet unknown true shape, it is acceptable as a working representation. If all other results remain consistent, an investigation into the actual nature of the planckion can be deferred for future research. Meanwhile, this model yields satisfactory and consistent results with the general description of the electron.

It is essential to distinguish among various meanings of “mass.” Both gravitational and electrical masses are expressed in kilograms, yet they participate in distinct physical processes: the gravitational mass relates to gravions, while the electrical mass relates to electrions. The common denominator is that both gravions and electrions are push particles mediating forces distinguishable only by magnitude and measured in the same physical units. However, mass itself is not a substantial entity like hyle (matter); rather, it emerges through various interactions and may correspond to various amounts of hyle.

The energy $m_e c^2$ corresponds to gravitational mass, while $m_{2e} c^2$ corresponds to electrical mass. Thus, gravitational and electrical energy must be distinguished within the push-field theory. A portion of electrical energy can transform into gravitational energy when manifested as mechanical work—such as in a rocket propelled by chemical reaction—yet most electrical energy propagates into the electric field undetected by current instruments. An early illustration of hyle flow between fields was shown in Figs. 50 and 51 in Section 22.

Both “mass” and “energy” are conceptual quantities introduced through Newtonian mechanics, and their conventional conservation laws apply to a limited portion of hyle. A much larger portion of hyle continually circulates undetected throughout the universe. If the planckion represents the smallest invariant quantum of hyle, then planckions perpetually flow among bodies and push particles in an ongoing universal process, of which only partial effects are observable.

For a detailed discussion of this concept, see also Sections 24 and 24.2 . In essence, mass originated as a mathematical construct in Newton’s law of gravity and subsequently became ubiquitous in physics. We are now compelled to reassess its meaning and consider its role within this new physical framework. Even if the present electron model ultimately proves inadequate, future researchers should strive to develop an alternative model consistent with the push-field principle. Collaboration across the broader scientific community will be essential for this progress. We hope that the present work serves as an initial step toward a viable new framework for fundamental physics.

In summary, we should not attempt to deduce the nature of the universe solely from measurable phenomena. Instead, we must model the hidden processes in a way that remains consistent with all observable evidence, recognizing that observable energy and mass reflect only a small fraction of the total hyle flux permeating physical reality.

Specifically, the demonstrated consistency of the electron’s volumetric relationships reinforces the view that the electron behaves as a white-hole-like entity radiating electrical energy. This phenomenon has historically appeared as a distinct property called “charge.” However, this notion requires reappraisal and reinterpretation under the simpler and more unified system proposed by the push-field theory. This will be assisted by a more detailed examination of the balance of various field flux intensities next.

32.4 Nuclear physics

(Under preparation)

Part Four (4)

This final Part was originally meant to discuss matters pertaining to all preceding parts. However, this has not been practical to do in full yet, while pending much re-arrangement of discussion on various topics among all Parts. Also, the theory is continually evolving, which makes it also necessary to re-arrange the content of each part, and transfer of Sections. We now realize that any attempt to effect those re-arrangements would be futile, or even detrimental. This is because we learn new things, so that editing the entire work before some final conclusions are reached, or before some experimental verification of the theory, could become not only burdensome but also problematic. It seems that it is more instructive for new readers to follow the various versions as they have appeared in chronological order rather than reading the latest version by itself not fully organized. Luckily, this is possible to do, because new material of each version is typed in a different color font.

33 General discussion

CAVEAT: Throughout this report, no claim is made or implied that PG theory will ultimately prevail, other than the assertive wish to be put to the test by objective means and not by means of another incomplete or erroneous theory. It does not specifically state that the theory of relativity is invalid other than it may be expanded and improved, although later advances indicate that GR itself is an approximate theory and may need re-appraisal. The report is supplied as an open source publication with no financial or employment strings attached prior, during or after publication. It is motivated purely by a scientific urge of the author to overcome his ignorance on outstanding questions in physics during his free time outside life's mundane tasks. By obtaining a new set of derivations for a hitherto ostracized push gravity, it was felt compelling to share the novel findings publicly. It would be a great personal satisfaction, if the scientific community could engage in some way towards verification (i.e. testing) and further elaboration of PG. In particular, should the veracity of PG become proven, it would be to the greatest benefit of science, whilst, otherwise, the author will be content to feel that it was at least “*a good try with some novel work*”, but without the need for exorcisms.

By the same token, we expect a reciprocal caveat to apply from the scientific community with respect to our findings. What would happen if, in the course of this development, it is found or deduced that some fundamental tenets of mainstream science are broken? For example, we already found that the equivalence principle is an approximation in a certain realm of the universe and generally invalid elsewhere. We found that it is invalid with very dense bodies both at macroscopic and elementary particle levels; Kajari *et al.* (2010) have reported on this possibility on the inertial and gravitational mass in quantum mechanics. Likewise, we have proposed that we be free from the uncertainty principle at sub-quantum mechanical level, as the only way to progress with our push particle theory. We think that we have gained good ground there. We fully accept, endorse and adopt the great achievements of QM but only in its specific range of applicability. In fact, we have recently come across a report on possible violation of the uncertainty principle with experimentally direct observation of deterministic macroscopic entanglement (Kotler *et al.*, 2021). Furthermore, the Standard Model seems inadequate, whilst a general field unification theory seems to have founded in Section 30.5.

Therefore, we anticipate reciprocal respect and attention from those who may have built a professional career on the validity established theories. We welcome constructive criticism of our findings from an objective and independent point of view, not based on authority alone.

Subject to the above caveats, it is now (as of version 4, after the first publication) decided to release some discussion in relation to important topics such as the gravitational law, expanding universe, galaxies, perpetual motion universe and philosophy, which were omitted from the first version. They could constitute topics for further advances in PG later, but are provided only briefly on a tentative basis at present. This may at least help avoid unwarranted criticism based on some issues not yet addressed, even briefly, with the understanding that the following discussion does not reflect on the validity of a working PG per se. Even so, it is with some trepidation that the ideas are presented below. Some specific technical proposals may prove to be totally incorrect, whilst existing or new controversies can be dealt with by the relevant experts.

An interesting exposition of push gravity is presented by Thomas (2014). This provides a good philosophical basis of the concept of push/shadow gravity and a motive for further investigation. However, the positive aspects of PG should not be diminished by possible failure of certain specific interpretations of important issues. For example, the referenced gravitons are thought to be a kind of strings as proposed therein, which may or may not be proven correct, so that PG should not be bound by such specific technical claims. The Allais effect is attributed to some sort of “lensing” mechanism of the gravitons around the Moon,

but we have showed that the effect can be readily interpreted and even measured by the PG derivations in Part 1. These and other speculative technical interpretations, if found incorrect, should by no means reflect on PG in general. We have now tried to create an alternative paradigm of PG by building the mathematics on a set of postulates in order to arrive at the established laws of physics and beyond. One fundamental difference from all prior PG theories is that the graviton absorption need not be weak and linear, but must be exponential in accordance with established laws of absorption theory.

The present author's main expertise lies outside the fields directly pertaining to this report. As a result, Part 2, in particular, may not be as authoritative as it should be, whilst Part 1 could be seen as an attempt to produce and report new data and evidence in support of a long standing hypothesis to explain gravity. It is hoped that others may use and apply the latter findings in a better way, or as they see fit. In this context, the primary aim would have been achieved, namely, to place PG within the mainstream of physics. For the latter, it would be an even greater achievement, if work is undertaken to test the veracity of the present findings within the programs of various institutions and organizations. Should an affirmative finding be achieved, then PG could immediately find its rightful place in science. At any rate, the present author should be excused for possible "collateral" errors, whilst attention to the novel disclosures may not diminish. It is in this context that we discuss some ideas necessitated for expanding the general PG theory.

After initially writing the above introductory discussion, there has been a long development with numerous examples of application, proposed experiments and tentative explanations of outstanding issues in physics, and much more. Whether some or most of them are correct or not, valid or not, they all together strongly indicate that PG is not just Fatio's idea already discarded a long time ago. It is a novel basis on which physics can be written in several of its diverse disciplines and contends to be included by contemporary science.

33.1 Expanding universe

We already canvassed the various possibilities of mean free path (mfp) of gravitons in Part 1. The case of an infinite mfp would result in a universal "attractive" force regardless of distance, pretty much the same as would be expected by Newton's gravitational law. However, such a system would beg to explain how gravitons interact with matter but never between themselves, i.e. how they have an affinity with matter but not with each other. As a result, it is more plausible to accept and consider a finite mfp, which also implies that gravitons would behave like a gas in the vast universe.

The idea of push gravity occurred to this author during work on gas flows in an environmental scanning electron microscope (ESEM) (Danilatos, 1997) using the direct simulation Monte Carlo (DSMC) method (Bird, 1995). The latter method made possible the study of gaseous flows under specific conditions (e.g. novel differential pumping stages by Danilatos (2012)). It was tested and confirmed the idea of two spherical bodies being "attracted" to each other, when the mean free path of gaseous molecules was much greater than the diameter of the spheres, while absorption to any degree was also present. It was then thought that the same might happen, if planets and stars are immersed in a medium with particles having mean free paths much greater than the size of the celestial bodies. That would then be the cause of gravitational acceleration and force to start with. For distances much greater than the mfp, no "attraction" force is generated, while the celestial bodies will float around and more:

The implication of this would go much further, if we consider the analogy between a real (familiar) gas and the universe gas (or graviton gas), as follows: Dust particles in a real gas under the above condition of mfp would appear to attract each other (at close range), while also, if the overall gas is set free to expand, the dust particles would expand in unison with the surrounding gas. Likewise, the stars, planets and celestial bodies are like dust particles attracting each other at relatively short distances (relative to mfp), but move apart from each other as a whole, when the distances become far greater than the mfp of the gravitons behaving like an expanding gas. We may then say that PG is consistent with an expanding universe and consistent with the conclusions of the theory of a big bounce or bang, but not with the theory itself (based on different premises). The visual picture of a starry night through a high resolution telescope conveys the impression of a dusty space, which might be more than a coincidence to treat it like an expanding dusty gas. In proposing such a model, the observed accelerated expansion rate of the universe might correspond to the initial (or close to it) accelerated rate of expansion of a gas, which, however, eventually reaches supersonic and hypersonic speeds, after which it expands at a constant rate (with terminology taken from the dynamics of an expanding gas, as through an aperture). The initial gaseous expansion may be taken like the inflation period of current Big Bang theories (and vice-versa). Therefore, if this model is correct, our universe exists still at an initial (or near initial) expanding rate state, provided that the proposed revision of existing measurements still indicate an accelerated expansion. Finally, if this model were to be accepted, dark energy (repulsion) of current theories might have a tangible explanation too via PG. Terminology is again important to avoid

confusion. If the expanding gravion gas is responsible for pushing galaxies apart (not “attracting” them), then we might as well call this type of field “negative push gravity” (NPG), consistent with “dark energy”.

Prior to all this, we take for granted that redshift can only be explained by an expanding universe and that we understand the nature of light and its propagation: We take for granted also that the Michelson-Morley experiment can only be interpreted by the exclusion of aether, while we are unclear about the wave-particle duality principle and the double slit paradox. It seems that we may have to revisit all these experiments and phenomena anew under PG.

None of the above should be less plausible than various other hypotheses already on record to explain the observed expanding rate of the universe, like: A dark energy inherent in the fabric of space itself, or the quintessence field that expands space at changing rates, or a phantom energy, and so on and so forth. In any event, the said applications of PG in this area are only on a tentative basis, which should be adjusted as new data and information are compiled on any of these controversial topics.

In a separate article, the universe expansion itself is queried (Danilatos, 2024). The possibility of the Big Bang being an artifact is briefly investigated. This is because the distance, size and mass have to be re-appraised on a fundamentally different basis per Section 18.3. In addition, the remotest visible celestial bodies happen also to be the most massive, while the majority of smaller bodies are not visible at the same distance and are screened out of consideration. In that case, the redshift can be dominated by gravitational redshift, which does not provide a recessional velocity. The same objects can have an approaching velocity, the blueshift of which, however, is overwhelmed by the redshift of immense gravity of those largest visible bodies at ever increasing distances. The Hubble constant loses its purported meaning. Therefore, universe expansion and the Big Bang theory can be man-made artifacts.

Overall, an expanding universe is not incompatible with push gravity, but we must first take into consideration the proposed revision of astronomical and astrophysical measurements. Afterwards, if we still find that the universe is expanding, then our theory is capable of explaining it as well. We may still have to resort to a kind of Big Bang, which could also be accommodated by our PG theory.

33.2 Galaxies

Let us next consider the case where the mean free path is, say, several times the size of our heliosphere. The gravitational law derived in Part One will gradually degenerate and cease to apply at longer distances. The generated field will continue to generate a push for a significant transition region, after which stars will float around as previously described. Thus, there is a transition region corresponding to the transition region from free molecule flow to continuum flow in gas dynamics.

The galactic spiral shapes resemble closely to the spirals of weather storm clouds on Earth seen from space. This might be more than a coincidence, as it might provide a classically intuitive explanation for galaxies. The spiral storm formations are caused by pressure gradients in the Earth’s atmosphere in conjunction with Coriolis forces. They belong to an atmospheric barometric low (bad weather), but a similar weather pattern is formed with a barometric high (good weather) circling in the opposite direction. We should then examine the possibility of galactic formations created by the gravion pressure gradients (barometric high) in conjunction with an as yet unknown cause for circular motion. The gravion gas beyond the galaxy in the greater universe may have its own “weather” patterns. The stars in galaxies may correspond to the condensed water droplets in clouds. They are stormy regions of a more general cosmic weather system. Galaxies have high concentrations of gravions at their center creating gravion pressure gradients toward the periphery. Macroscopic gravion pressure may play a major part in galaxy formation. This suggestion could be consistent with a “mock-gravity”-like of the creation not only of the chemical elements but also of the condensation of matter into galaxies (Gamow, 1949; Hogan, 1989; Wang & Field, 1989; Field, 1971). Gamow proposed that such a “mock gravity” could have played a role in galaxy formation after the Big Bang. Although there has been much controversy over such theories, it is envisaged now that the new PG could help re-appraise all these theories by incorporating them under a bigger framework for a new understanding of cosmic motion beyond the “local” gravitational fields.

PG then might provide a good explanation why galaxies rotate faster than the existing laws of physics predict, and the motion of vast clusters of galaxies in the universe. We are presented with an opportunity to consider ideas that are still possible and rule out others completely. Thus, one more anomaly may be readily accounted for by PG.

Furthermore, PG very nicely removes the singularities (infinities) of current theories, as the maximum force that can be generated is limited by the upper boundary of push gravion flux density. There is an asymptotic approach to this limit by an increase in mass or density of mass. The forces transmit at the speed of gravions, which can be the speed of light.

Galaxies are generally considered to date to be gravitationally bound systems of stars and not weather-like systems, as we propose now, so that the above ideas are totally out of established beliefs. Dark matter has

been used to explain the galaxy rotational anomaly. However, if dark matter and dark energy have been invented to fill the shortcomings of other theories, PG may also be entitled for expansion (development) at long distances as well. For it might be ultimately easier to comprehend and apply weather-like systems in the cosmos than imaginary forces acting at vast distances.

Modified Newtonian dynamics (MOND) has been promoted to account for observed properties of galaxies. It is an alternative to the hypothesis of dark matter, but it still seems insufficient to account for all observable data. All of these theories are based on the idea that gravity is inherently generated by mass, whereas PG is a theory of an emerging gravity by an external source surrounding massive bodies (i.e. the gravions), like mass is also an emerging property of hyle but not the source of gravity.

These and other anomalies reported, like by extra massive hydrogen clouds and extra energetic photons, should be also re-examined in the light of a general PG theory for possible explanations.

Fulton (2022) “*proposes a model refinement for the Newtonian Law of Universal Gravitation to correctly apply the Law at the extremely large scales of galaxies*”. He uses a heuristic model of “*Diffusion Gravity*” to derive a modified Newtonian equation of force at galactic scales. The theory is akin to Fatio’s principle and ours albeit not identically. In view of this approach in the derivation of the relevant equations, we should also attempt to apply our method to derive the force for an agglomeration of stars, white dwarfs, neutron stars and black holes (etc.) as expected to be distributed in a typical spiral galaxy. Like we apply the equation of absorption of gravions by a single homogeneous sphere, as well as for concentric spheres with different densities, we can generalize our approach for a galactic system of spheres to derive the galactic equation of force. This should give a correct outcome on the assumption that the mean free path of gravions is much greater than the size of the galaxy. Otherwise, if the mean free path is much less than the size of the galaxy, then we can expect the cosmic weather storm-like pattern per preceding speculation. Prospective workers interested in this approach may like to produce this outcome for the further development of PG.

Our method may also explain the “*Breakdown of the Newton–Einstein Standard Gravity at Low Acceleration in Internal Dynamics of Wide Binary Stars*” (Chae, 2023)

33.3 Perpetual motion of universe

The biggest challenge of PG is to understand and explain the recycling of the gravions in the universe overall. Our proposed model suggests that they are transformed successively to various types of push particles with a correspondingly smaller mean free path until they diffuse out back into space without an obvious direct trace to us yet, but somehow finding their way by accretion back into exploding massive stars, dwarfs, neutron stars and black holes. By such means, the universe must be regenerated and overall frictionless in contrast to a forecast thermodynamic thermal death of the cosmos. The idea of a static universe recycling itself has been advocated before among others by Edwards (2007), who adopts yet another approach to PG. His model seems much more complex in an attempt to base it on (or use) existing theories, whereas our model of PG is being built from simple principles in the simplest possible terms. Then we try to see if it is consistent with existing data and theories. However, his central thesis might apply at least in some aspect. The central thesis of his model is an inter-conversion of photon and graviton energy, whereby the gravitons cumulatively establish a quantum lattice connecting all masses. “*Photons incident on the filaments of this lattice impart energy to the gravitons, while at the same time losing a portion of their original energy. This loss of energy corresponds in the model to the cosmological redshift in a static universe*”. Whilst the perpetual motion machine is readily rejected by thermodynamics, we may not say the same for the universe overall or parts thereof. Otherwise, the universe would come to a grinding halt, from which we would still require an exit without resorting to god; the Big Bang is only shifting the perpetual motion to a more distant past. Nothing should prevent the existence of frictionless regions in the universe, albeit extremely small and “invisible” to our instruments as yet.

If the entire universe existed in the form of a gravion gas only, we might say that the second law of thermodynamics has had its sway (has prevailed), i.e. to which everything has succumbed. However, the fluctuation theorem is also universally applicable and operates by way of another **law** for undoing the second law in no uncertain terms. This fact is often, or mostly overlooked in science. Fluctuation results in order and creation, whilst the second law results in disorder and destruction. It may be that quantitatively the amount of gravions constitutes an overwhelming majority of mass over and above the visible mass of the universe. Nevertheless, both laws coexist intent on undoing each other’s work. This is exactly a manifestation of another overriding universal law, namely, that of the coexistence of opposites. A one-sided view of things can lead to error and impasse, whereupon we should be spurred on to find the missing (overlooked) side of things.

The above is consistent with the thinking of the universe as continuously and continually recycling itself and appearing in different forms of matter and energy, all of which is spun from a common entity that pervades all that we can experience.

33.4 Philosophy of physics and theory of everything

To say that the human mind cannot conceive the most intricate workings of nature (when a particular theory becomes complex and unintelligible), may also be a cowardice preventing us from moving forward. Skepticism inevitably leads to religion and to the end of science. This author subscribes to the school of thought that humans can and will ultimately comprehend nature and in the simplest of terms.

There is now an opportunity and a need to disassemble certain ideas about rest mass, gravitational mass, inertial mass and relativistic mass under existing theories and re-assemble them under the platform of PG and the newly found concepts of effective and real mass.

Could the limiting speed of light for all material bodies be explained and not postulated? Could it be that, by matter organization from gravion level up, nothing can be pushed faster than gravions?

If there is a unifying theory of everything, would there be a unifying common denominator? What is it that would unify them? A common particle? Some common entity and what is its nature? If mass and energy are equivalent, and if energy can appear in different forms but always conserved, we should be able to reduce all those forms to a common denominator. That common denominator may be the gravions at different levels of organization. The latter possibility has been investigated in Section 30.

Overall, nothing is invariable in the cosmos, but universal constants appear under “local” provisos and conditions, which are only recurring over the entire cosmos.

The universe consists of particles distributed over a wide range of mean free paths that allow auto-sorting of particles and bodies with the end result of a self-assembling universe like a DNA. Self-assembly and self-organization are general prevailing processes triggered by random fluctuations. In support of the above exposition, Nobel Prize winner Prigogine (1977) has described a theory of self-organization in non-equilibrium systems from dissipative structures to order through fluctuations. Furthermore, *“it has been argued by some that all emergent order in the universe from galaxies, solar systems, planets, weather, complex chemistry, evolutionary biology to even consciousness, technology and civilizations are themselves examples of thermodynamic dissipative systems; nature having naturally selected these structures to accelerate entropy flow within the universe to an ever-increasing degree”* (Gleick, 1998; Wikipedia contributors, 2021). Allahverdyan & Nieuwenhuizen (2000) showed the feasibility of extracting zero-point energy for useful work from a single bath, without contradicting the laws of thermodynamics. Even before quantum theory, Nikola Tesla claimed that useful energy could be obtained from an all-pervasive aether. Last, we have also proposed an explanation of the fly-by acceleration, which can now be seen also as extraction of energy from the surrounding gravions (see Section 14.3). *“The Big Bang never happened”* according to Lerner (Wikipedia contributors, 2024d), who also adopts an eternal universe. Order emerges from chaos, as we also see that the second law of thermodynamics is no obstacle to PG. As we move away from equilibrium (per fluctuation theorem) order can spontaneously emerge.

Ordinary matter is the decomposition of black holes and re-assembly to form elementary and/or other particles, which may still incorporate tiny black matter (holes) with their layered TALs. Conversely, black holes may also be the decomposition and “precipitation” or “distillation” of ordinary matter to corresponding massive bodies with black mass.

We now put forward the hypothesis that all particles are held together by the pressure of push particles. Different particles may be formed by different types or fractions of push particles, a topic that has been taken up in recent versions of this report. Rotational and spin motion has now been introduced as a consequence of the gravion properties (see Section 30, and which dominates at the fundamental level of hyle organization.

In attempting to conceptualize the deeper meaning and application of the second law of thermodynamics together with the re-emission of gravion energy, we may have come to a better understanding of quantum mechanics too. In quantum mechanics, anything that is possible to happen can happen governed by the probabilities of that situation. The latter provides a probabilistic relational description of the states of particles but not the origin or an explanation why quantum particles move about incessantly in certain patterns (e.g. electron orbitals). By analogy, general relativity provides an accurate relational explanation of various parameters but it does not provide a hint about how and why gravity exists, or why the spacetime around a mass is bent and warped. PG via an incessant gravion flow may provide the basis for understanding both quantum mechanics and relativity at the same time. The ever flowing gravions pass through various levels of material organizations via quantitative accumulations leading to qualitative transformations from level to level. The universal relationship between quantity and quality can be seen at all levels of organization of matter, starting from the smallest quantum mechanical states, to chemical and mechanical systems of ordinary sizes, and all the way up to white dwarfs, neutron stars and black holes. Actually, the smallest of entities may not even be subject to quantum mechanical rules, if quantum mechanics has so far described an “intermediate” level of the universe. Quantum mechanics may be simply a macroscopic description of other underlying processes, like pressure and temperature are macroscopic statistical properties of a gas. Likewise, those other underlying of quantum mechanics processes may be ultimately the simplest ones waiting for us

to discover.

A perpetual motion of matter/energy can rightfully belong to the universe as a whole, a principle which has been attributed to Heraclitus (Wikipedia contributors, 2019a). All these ideas eventually lead to the need to understand the nature of gravions and its interactions with matter and with themselves.

34 Conclusion

An attempt has been made to modify and advance the old principle of push gravity theory to a stage where gravity may be seen from a totally novel perspective. It constitutes a daring step, because it challenges and potentially provokes a re-consideration of long standing ideas and principles. This has already required a daunting determination especially as it comes from a non-established expert in the field of gravity.

The basic new element is the use of a gravity particle absorption coefficient that is not limited only to very low values as in prior PG theories. The consequences of that can be dramatic.

The theory of PG has now been brought to a stage ready for verification with several proposed tests and methods. Should these tests yield a positive outcome, they could provide explanation to many outstanding issues in science. Otherwise, the test may prove insufficient pending further instrument refinements. Alternatively, if one produces sufficient evidence to reject PG once and for all, that would compel science to concentrate on other pathways, as it does, even more. At any rate, it should be appreciated that the proposed tests are inexpensive at least in relative terms for many organization to engage.

In summary, new work provides sufficient evidence for a genuine re-appraisal of push gravity. A novel quantitative theory has been advanced on the basis of a set of primary principles (postulates), from which the derivation of classical acceleration and force by stationary massive bodies in the steady state is possible. In contrast to prior conceptions, it is shown that the absorption of gravity particles by matter need not be extremely weak and linear, in order to derive and explain the observed classical laws of gravity. Any value of the absorption coefficient by a uniform spherical mass produces a gravitational field obeying the inverse square of distance law. The gravitational constant (big G), is itself a function of the ratio of the absorption coefficient over the density of matter. The latter ratio now becomes the new universal constant of the cosmos, whilst G can vary in different regions of the universe. The measured mass of planets and stars is only an effective or apparent mass actually smaller than the real mass due to a self-shadowing or shielding effect of the absorption of gravitational particles. Any given body has an effective mass that appears quantitatively different depending on its spatial distribution including orientation. We now find that Newton's gravitational law uses only the apparent (or effective) masses with a potentially variant G , but the inverse square distance relationship is preserved in the cosmos. The radiant flux of energetic particles being uniform over a region of space creates a maximum acceleration of gravity for all material bodies in that region, so that any further mass accretion over a certain upper limit does not create additional acceleration; this limit is reached when practically all gravitational particles are absorbed (saturation state) by the massive body above a saturation mass. The latter limit should be measurable, for which some tentative situations and experiments are proposed for prospective experiments and tests. The internal field of a spherical mass and the external field of a two layered sphere have been derived. The gravitational parameters inside a hollow spherical shell and their relationship to the corresponding external properties have also been found. The superposition principle of gravity fields has been reformulated and the Allais effect explained. The equivalence principle can now be properly understood and explained in a way that the principle per se becomes redundant. We can now better understand the meaning of matter (better, hyle), inertia and mass. ~~For moving bodies, the established relationships from special and general relativity may continue to operate within the gravitational fields created by push particles, but may need to be adapted and re-aligned within the greater framework of push gravity principles operating at any distance.~~

An attempt is made to overcome the main remaining objection of presumed catastrophic thermal accretion of absorbed particles. A further attempt is made also for the push-gravity principles to explain the vastly higher intensity gravitational fields of white dwarfs, neutron stars and black holes. It is proposed that the field of white dwarf stars is created also by push particles but of a different kind, namely, by those responsible for mediating the electric field. In the same way, the field of neutron stars is created by yet a third kind of push particles, namely, those responsible for mediating the nuclear field. In general, various types of push particles may exist with different energy ~~(or mass)~~ having different mean free paths as they traverse different concentrations of masses (black holes, neutron stars, dwarfs, stars, planets, ordinary masses, atoms, nuclei, protons and all the known or unknown sub-nuclear particles). The invariable principle of momentum transfer (push) by particles directly relating to their absorption rate by the various concentrations (density) of masses could be the basis and the starting principle for a prospective unification theory of everything. The first part of this report, if verified, should create the basis for new physics across many fields of physical science. Pending such a verification, we may also work towards the development of a general PG including

a theory of the dynamics of the observed motion of celestial bodies.

If there is a “theory of everything”, then gravions could provide an underlying mechanism not only in gravity but also in quantum mechanics. Gravions may be responsible for both the gravitational fields and the associated masses being nothing else than effective masses. It may be that we can make one step closer to a better philosophical understanding of the cosmos, if we can grasp the nature of the gravion, perhaps, as being the embodiment of the coexistence of opposites in a perpetual flow of the universe.

The above concepts are consistent with and further supported by the latest developments on energy and mass in Section 29. Mass is not a static quantity, nor is it an invariant according to prevailing theories. Mass is the outcome of the energy rate of absorption by material bodies. If this energy rate of absorption ceased for a while, there would be no mass, but there would be organized hyle. Mass is the manifestation of the flow of something else (hyle). Flow is a time rate process. Mass is not an entity to hold and behold. Power and mass appear concurrently in an equation involving a time derivative of energy (see Eq.469). The conventional equation $E = mc^2$ is an integral for a hypothetical static situation, it is a human conception. It is like filling a bucket of water under a running tap, whereby we have a start and finish time for filling the bucket. However, nature proceeds inexorably at its own rate. Any blocks to its flow is temporary and transient often resulting in a change of form of hyle. Learning to think in terms of motion and change seems the correct method for understanding the cosmos. Static entities, like photographic images, alone can lead to an impasse.

35 REVIEW

The present report has not been submitted to a conventional scientific journal for peer review. This decision should not be interpreted as an attempt to avoid critical scrutiny. Rather, it reflects the current scope, format, and developmental status of the work.

The material presented here does not yet conform to the structural or thematic requirements of a journal article. It remains incomplete in several respects, with multiple open questions intentionally left unresolved while the theoretical framework continues to develop. Substantial rewriting, consolidation, and reorganization will ultimately be required before the work can be reduced to publishable components appropriate for specialist journals. Moreover, the report spans a broad range of topics—from particle-scale structure to gravitation, astrophysics, and cosmology—making it unsuitable, in its present form, for submission to any single disciplinary venue. It is evolving toward a monograph-length treatment rather than a standard research paper.

While formal peer review plays an essential role in maintaining scientific standards within established fields, its application at this exploratory stage—particularly through a small number of narrowly specialized referees—could constrain rather than assist the development of a deliberately cross-disciplinary framework. The present objective is to document the full conceptual trajectory of the theory, including intermediate steps, revisions, and abandoned paths, in a manner that would not be feasible within the conventions of journal publication.

For these reasons, dissemination via Zenodo has been adopted as the most appropriate interim platform. Zenodo provides versioned publication, persistent digital object identifiers (DOIs), and long-term archival stability, making it well suited for a work of this nature. The ability to release successive versions allows the theory to evolve transparently while maintaining a permanent scholarly record of its development.

The report is also intended as a potential platform for constructive external engagement. Contributions, critiques, or extensions from other researchers—particularly those working in related or complementary areas—are welcome. Such material may appear either as independent publications or as addenda incorporated into future versions of this report, subject to editorial integration and consistency of terminology. Final decisions regarding inclusion rest with the present author, to preserve coherence and readability within the overarching framework.

Readers who wish to consult the author’s broader publication record or professional background are directed to the list of publications available at [<http://www.danilatos.com/publications.htm>].

APPENDIX

A Gravitoids

Let us be reminded that a prolate spheroid is a surface of revolution obtained by rotating an ellipse about its major axis, whereas an oblate spheroid is obtained by rotating about its minor axis. It is well known

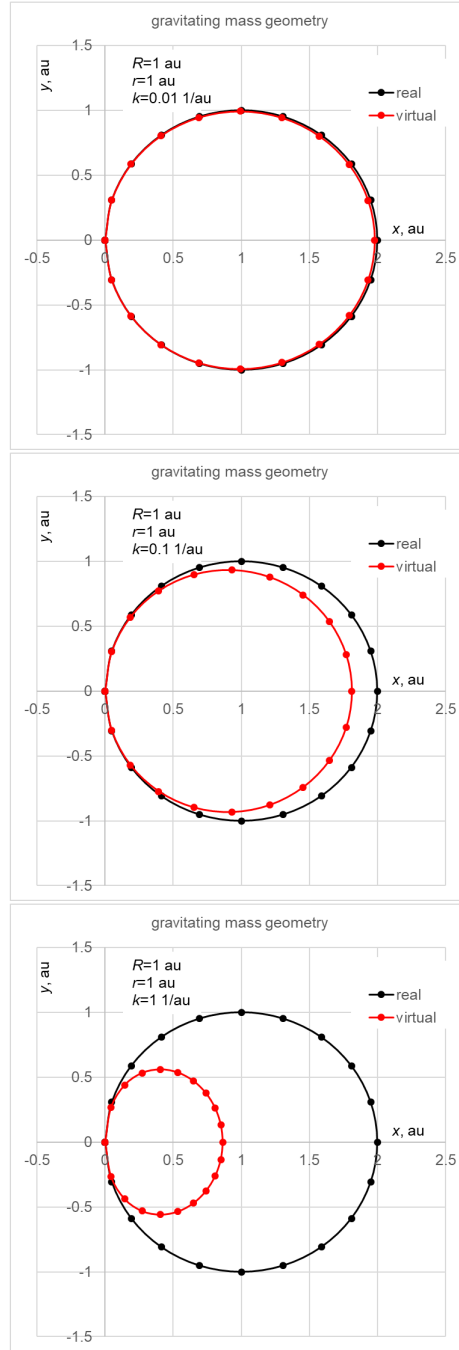


Figure 111: *Real sphere in black, gravitoid (virtual) shape in red for three values of k and $r = R = 1$.*

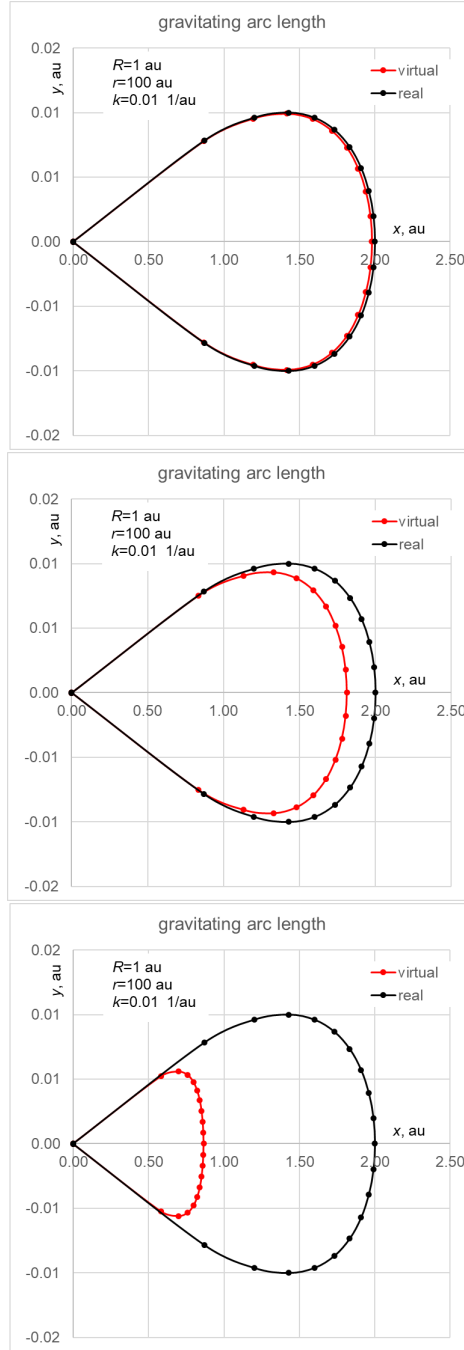


Figure 112: Arc length for real sphere in black and gravitoid (virtual) in red for three values of k at $n_R = 100$.

that spheroids acting as gravitational bodies would produce precession or regression of the elliptical orbit of a planet around it. This arises by the gravitational force being slightly greater or lesser than the inverse of the square of the distance. In other words, it is the distance (not the mass) responsible for these phenomena (here, we are not referring to the relativistic cause of the extra Mercurial precession). It is interesting to examine and clarify what happens with PG theory in this connection via the following observations.

Now, by virtue of Eq. 43, the self-shadowing effect produces a gravitational force (acceleration) less than the value expected from simple Newtonian attraction by a sphere. By increasing k with all else constant, the force increases in proportion to it (or the density) by Newtonian mechanics, but to a lesser degree by PG theory, on account of the exponential decrease along a chord (straight line) of the sphere in Fig. 2. That is, the Newtonian length that would produce an attractive force effectively contracts (shrinks) to produce the correct force. Each elemental component is then equivalent to having a lesser length at a given density, whilst in reality there is additional mass for the remainder of the length of the chord. This becomes, in effect, a virtual mass distributed inside a spheroid-like shape. It may initially look like an oblate spheroid, but it has a peculiar shape dependent on the distance OP and k . For a sufficiently long distance OP (i.e. r), the lines u are nearly parallel (very small angles φ), whilst as we approach the surface at point C, the same lines radiate at large angles φ , and the shape becomes more like a compressed egg along its axis while being inflated at right angles. We can see these and other effects by plotting the corresponding lengths and shapes quantitatively for two positions of the point O, namely, at the surface of the sphere and at a relatively long distance of $n_R = 100$.

On the surface of the sphere, we show pairs of the chord lengths and body shapes between Newtonian and virtual PG cases for three different values of k , in Fig. 111. To clarify, because point O lies on the surface of the sphere, any distance from the fixed point O to any other point on the surface defines the chord length, via which we also plot the sphere. Thus, these graphs show simultaneously both the chords and volumes of revolution corresponding to the real sphere and virtual shape yielded by PG. As expected, for $k < 0.01$, PG shapes become gradually indistinguishable from Newton. Otherwise, the difference increases significantly.

Next, we plot the virtual chord lengths for a sphere with unity radius from a distance $r = 100$ units. Planet Mercury approximately has this distance from the Sun at its aphelion. We consider again three values for $k = 0.01$, $k = 0.1$ and $k = 1$ in Fig. 112 together with the same **real** chord lengths of the same sphere (in black). We have used the same Eqs. 17 and 52.

Finally, we can visualize the corresponding virtual shapes of the sphere (here, like the Sun) from the same distance of 100 sphere radii (as from Mercury) with the same corresponding values of k in Fig. 113. This is obtained by adding the PG chord length by 52 to the corresponding u_1 provided by Eq. 21, i.e. we use the virtual end points of u_{e2} in PG given by Eq. 53.

The above spheroid-like shapes are bounded by the red lines together with overlapping black lines on the left. We note that a shallow dimple appears on the far side, the depth of which increases as we further increase k , effectively producing a *dimpled spheroid-like* shape.

As previously noted, the real shapes (and sizes) of a sphere effectively act as some peculiar virtual shapes, fictitious and invisible, for which we may collectively use (coin) the new term *gravitoids*. Their mass may be used with linear absorption as in Newton's law to yield the force as predicted by PG.

Below, we also present the analytical expressions already used to plot these gravitoids in Fig. 6 and discussed in Section 6.4. We follow the steps in finding the volume of a sphere to illustrate the point of deviation (departure) between the two approaches:

$$\begin{aligned}
 V_{sphere} &= \int_0^{\varphi_0} \int_{u_1}^{u_2} 2\pi \sin \varphi d\varphi \cdot u^2 du = \frac{2\pi}{3} \int_0^{\varphi_0} [\sin \varphi d\varphi \cdot u^3]_{u_1}^{u_2} \\
 &= \frac{2\pi r^3}{3} \int_0^{\varphi_0} \sin \varphi d\varphi \left[\left(\cos \varphi + \sqrt{a^2 - \sin^2 \varphi} \right)^3 - \left(\cos \varphi - \sqrt{a^2 - \sin^2 \varphi} \right)^3 \right] \quad (629)
 \end{aligned}$$

and by using the limits in Eqs. 21 and 22, it finally yields the expected result:

$$V_{sphere} = \frac{2\pi r^3}{3} \left[-2 \cos \varphi (\cos^2 \varphi + a^2 - 1)^{3/2} \right]_0^{\varphi_0} = \frac{4\pi R^3}{3} \quad (630)$$

Similarly, starting from the same elementary volume equation

$$V_{gravitoid} = \int_0^{\varphi_0} \int_{u_1}^{u_2} 2\pi \sin \varphi d\varphi \cdot u^2 du = \frac{2\pi}{3} \int_0^{\varphi_0} [\sin \varphi d\varphi \cdot u^3]_{u_1}^{u_2} \quad (631)$$

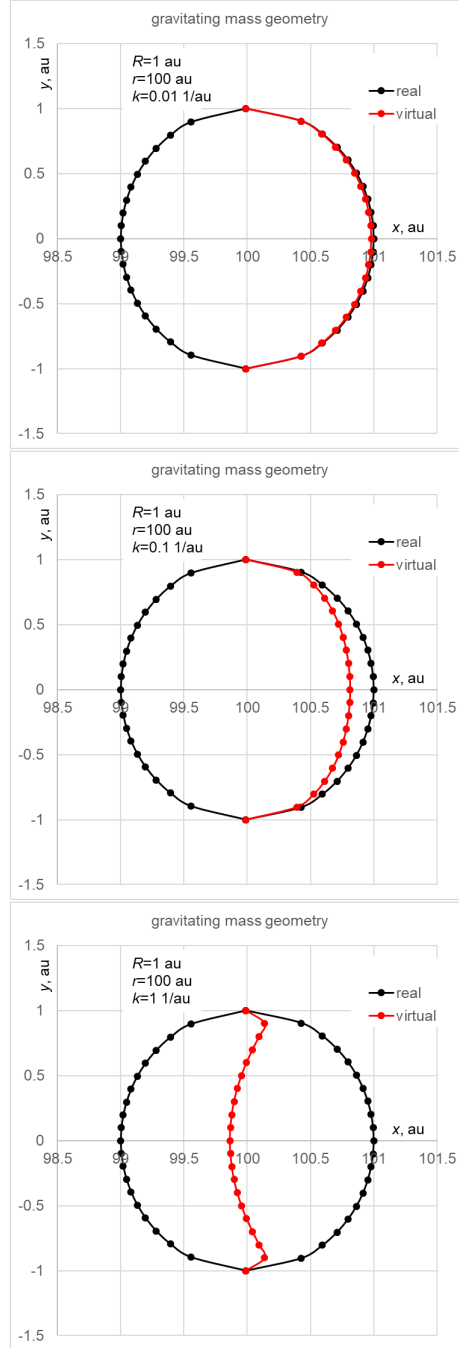
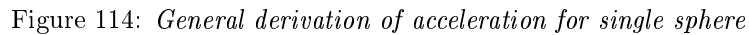


Figure 113: *Real sphere in black, gravitoids (virtual) shape in red (together with black left of red line) for three values of k and $n_R = 100$.*


$$V_{gravitoid} = \frac{2\pi}{3} \int_0^{\varphi_0} \sin \varphi d\varphi.$$

$$\left[\left(r \left(\cos \varphi - \sqrt{a^2 - \sin^2 \varphi} \right) + \frac{1}{k} - \frac{1}{k} \exp \left(-2kr \sqrt{a^2 - \sin^2 \varphi} \right) \right)^3 - \left(r \left(\cos \varphi - \sqrt{a^2 - \sin^2 \varphi} \right) \right)^3 \right] \quad (632)$$

We note that the effective volume generally lies above the gravitoid, as it should, because it is further away from the gravitoid relative to the reference point O. If they both contain the same real density matter, then both yield the correct value of acceleration by applying Newton's equation. We further note that the gravitoid volume (effective mass) increases, as we move away from the gravitating mass (e.g. compare the obvious corresponding sizes provided by Figs. 111 and 113). However, this does not affect the inverse of r^2 dependency, because this effective mass increase is compensated by the integration to a lower upper limit of angle (i.e. over a smaller angle range). For a possible precession to be generated, we need to consider the time effects also in PG as in the corresponding GR theory.

We have initially derived the absorption fraction of gravions at a point outside a sphere based on its axial symmetry around the line joining the point with the center of the sphere. However, we can also generally

derive the same fraction by considering a Cartesian reference frame of x, y, z axes for later use in non-axially symmetric systems. We integrate the graviton absorption by revolving an elementary solid angle around each of the x, y, z axes to yield three components of absorption corresponding to the classical vector of acceleration. For simplicity, here we consider only a sphere intersecting one coordinate plane of symmetry along its diameter, but the derivation can be expanded for any location of the test point located outside the sphere; points inside the sphere are considered during the two sphere “bulk” formulation.

With reference to Fig. 114, the plane of symmetry intersecting the sphere is the yOz and we define and use the following notations of constants and parameters:

$$y_0 = OY = ZP.$$

$$z_0 = OZ = YP.$$

$$r = OP.$$

$$\varphi_z = \angle ZOB \text{ is the zenith angle of rotation around axis } z.$$

$$\theta_z = \text{is the azimuth angle of rotation around axis } z.$$

$$\varphi = \angle ZOP, \text{ the angle of axis of rotation with OP.}$$

$$a = \frac{R}{r} \equiv \sin \varphi_0 \text{ with } \varphi_0 \text{ (subtended angle by the sphere) used in the limit of integration.}$$

$$u_A = OA.$$

$$u_B = OB.$$

$$\psi = \angle POB = \psi(\varphi_z, \theta_z) \text{ varies with } \theta_z \text{ during rotation.}$$

The length (chord) AB is obtained by the intersection of the straight line u with the surface of the sphere, for which we need to solve the analytical equations for u :

$$x^2 + (y - y_0)^2 + (z - z_0)^2 = R^2 \quad (633)$$

$$y = u \sin \varphi_z \cos \theta_z \quad x = u \sin \varphi_z \sin \theta_z \quad z = u \cos \varphi_z \quad (634)$$

yielding:

$$u_A = y_0 \sin \varphi_z \cos \theta_z + z_0 \cos \varphi_z - \sqrt{(y_0 \sin \varphi_z \cos \theta_z + z_0 \cos \varphi_z)^2 - (r^2 - R^2)} \quad (635)$$

$$u_B = y_0 \sin \varphi_z \cos \theta_z + z_0 \cos \varphi_z + \sqrt{(y_0 \sin \varphi_z \cos \theta_z + z_0 \cos \varphi_z)^2 - (r^2 - R^2)} \quad (636)$$

$$(AB)_z = 2\sqrt{(y_0 \sin \varphi_z \cos \theta_z + z_0 \cos \varphi_z)^2 - (r^2 - R^2)} \quad (637)$$

$$(AB)_z = 2\sqrt{OM(\varphi_z, \theta_z)^2 - (r^2 - R^2)} \quad (638)$$

$$(AB)_z = 2r\sqrt{a^2 - \sin^2 \psi} \quad (639)$$

Now, the operand under the square root must be positive, which sets the limits of azimuth angle as a function of zenith angle by solving the equation:

$$(y_0 \sin \varphi_z \cos \theta_z + z_0 \cos \varphi_z)^2 - (r^2 - R^2) = 0 \quad (640)$$

$$y_0 \sin \varphi_z \cos \theta_z + z_0 \cos \varphi_z = \pm \sqrt{(r^2 - R^2)} \quad (641)$$

$$\theta_z = \arccos \left(\frac{-z_0 \cos \varphi_z + \sqrt{(r^2 - R^2)}}{y_0 \sin \varphi_z} \right) \quad (642)$$

where we use the positive root sign because $OM = y_0 \sin \varphi_z \cos \theta_z + z_0 \cos \varphi_z$ must be positive and, when $OM=ON$, it becomes tangent at the limits:

$$\theta_{z1} = -\arccos \left(\frac{-z_0 \cos \varphi_z + \sqrt{(r^2 - R^2)}}{y_0 \sin \varphi_z} \right)$$

$$\theta_{z2} = \arccos \left(\frac{-z_0 \cos \varphi_z + \sqrt{(r^2 - R^2)}}{y_0 \sin \varphi_z} \right)$$

$$\varphi_{z1} = \varphi - \text{asin}(a)$$

$$\varphi_{z2} = \varphi + \text{asin}(a)$$

With the chord length AB found, the absorption fraction for the z -axis is given by the double integral:

$$f_{gz} = \int_{\varphi_{z1}}^{\varphi_{z2}} \int_{\theta_{z1}}^{\theta_{z2}} (1 - \exp(-k(AB)_z)) \sin \varphi_z \cos \varphi_z d\varphi_z \quad (643)$$

Similarly, we follow the same steps for the y axis by interchanging the corresponding parameters and notations and adding $\pi/2$ to φ_z as follows:

$$(AB)_y = 2\sqrt{(z_0 \sin \varphi_y \cos \theta_y + y_0 \cos \varphi_y)^2 - (r^2 - R^2)} \quad (644)$$

with limits:

$$\theta_{y1} = -\text{acos} \left(\frac{-y_0 \cos \varphi_y + \sqrt{(r^2 - R^2)}}{z_0 \sin \varphi_y} \right)$$

$$\theta_{y2} = \text{acos} \left(\frac{-y_0 \cos \varphi_y + \sqrt{(r^2 - R^2)}}{z_0 \sin \varphi_y} \right)$$

$$\varphi_{y1} = \varphi - \text{asin}(a)$$

$$\varphi_{y2} = \varphi + \text{asin}(a)$$

with which we obtain the integration around y axis for the absorption component f_{gy} , so that the total absorption fraction is $f_g = \sqrt{f_{gz}^2 + f_{gy}^2}$. Noted $(AB)_z = (AB)_y = AB$. The above equations are valid while the sphere does not cross any axis. In the case when it crosses one axis (let's say the z axis), there are two consecutive sub-ranges of the angles with limits:

First:

$$\theta_{z11} = -\pi$$

$$\theta_{z21} = \pi$$

$$\varphi_{z11} = 0$$

$$\varphi_{z21} = \varphi - \text{asin}(a)$$

Second:

$$\theta_{z12} = -\text{acos} \left(\frac{-y_0 \cos \varphi_y + \sqrt{(r^2 - R^2)}}{z_0 \sin \varphi_y} \right)$$

$$\theta_{z22} = \text{acos} \left(\frac{-y_0 \cos \varphi_y + \sqrt{(r^2 - R^2)}}{z_0 \sin \varphi_y} \right)$$

$$\varphi_{z22} = \varphi - \text{asin}(a)$$

$$\varphi_{z22} = \varphi + \text{asin}(a)$$

with which we obtain two sub-components for this axis to be added as $f_{gz} = f_{gz1} + f_{gz2}$

We repeat the same when the sphere crosses the other axis. Likewise, when the sphere crosses both axes. For negative values of $-\varphi$, we replace with positive φ , whilst for $\varphi > \pi/2$ we replace φ with $\pi - \varphi$.

B.1 Alternative formulation for the normal component

Beyond the general formulations above, the normal component of acceleration can be deduced with an alternative simpler way: The component of absorption around the normal axis y can be found concurrently during rotation around z axis inside the same solid angle used for axis z . As we rotate around the fixed z axis, we can project and find the component of the chord AB on the fixed y -axis by multiplying with azimuth $\cos \theta_z$ times zenith $\sin \varphi_z$, so the normal component is:

$$f_{gy} = \int_{\varphi_{z1}}^{\varphi_{z2}} \int_{\theta_{z1}}^{\theta_{z2}} (1 - \exp(-kAB)) \cos \theta_z \sin^2 \varphi_z d\varphi_z \quad (645)$$

The two components f_{gz} and f_{gy} must subsequently themselves be projected on the line OP to obtain the required total absorption fraction, namely:

$$f_g = f_{gz} \cos \varphi + f_{gy} \sin \varphi$$

We can re-write all above in a combined expression as:

$$f_g = \int_{\varphi_{z1}}^{\varphi_{z2}} \int_{\theta_{z1}}^{\theta_{z2}} (1 - \exp(-kAB)) (\sin \varphi_z \cos \varphi_z \cos \varphi + \cos \theta_z \sin^2 \varphi_z \sin \varphi) d\varphi_z \quad (646)$$

Although we have already described the field around the axis of symmetry at the outset of PG theory with the simplest equations, the above formulations are more than a theoretical exercise, because they are needed in more complex mass distributions like the two-sphere problem examined later.

Further theoretical processing and analysis of the above derivations can be done separately, but the above can be used immediately as “raw” material for numerical integration to obtain some early results without further ado.

C Force between two spherical masses - bulk method

For the formulation of the problem of force between two material spheres, we have used two different methods. One method involves the points (elements) inside the bulk of one sphere followed by integration over the entire bulk of the sphere. The other method involves the points (elements) on the surface of one sphere and integration over the entire surface of the sphere. The outcomes are equivalent (equal) since traces of gravions passing through any point inside the bulk of a sphere must also cross the surface of the sphere and vice-versa. The bulk method involves four integrals and takes far longer integration times with numerical methods. The second method has its own complexity, but it involves three integrals requiring much shorter integration times.

With reference to Fig. 115, we define and use the following notations of constants and parameters: We have sphere_1 (*sphere*₁) and sphere_2 (*sphere*₂) with corresponding radii $R_1 = P_1N$ and $R_2 = P_2M$, and with uniform material densities and hence uniform absorption coefficients k_1 and k_2 ; the distance between the centers of the spheres is $P_1P_2 = r$. We choose a random point O inside sphere_2 forming an angle $\angle OP_1P_2 = \varphi_2$ with corresponding differential semi-angle $d\varphi_2$ and maximum subtended angle $\angle P_2P_1S = \varphi_{20}$. From point O, we define the direction u along OP_1 , around which we draw a random solid angle Ω_1 with semi-angle $\angle P_1OB_1 = \varphi_1$ with corresponding differential angle $d\varphi_1$ and maximum subtended angle $\angle P_1ON = \varphi_{10}$. The solid angle Ω_1 is enveloped by line u' , which crosses sphere_1 at points A₁ and B₁, and sphere_2 at points A₂ and B₂; we will also need the points A and B, at which the axis u crosses the sphere_2. Normal to the axis u is the axis ν with a third axis y (not shown) normal to the plane of $u\nu$, thus defining the coordinate system (νuy). Another coordinate system (xzy') is rotated around y' by the angle φ_2 with the axis z aligned with the two centers P_1 and P_2 and y' normal to the plane xz , i.e. parallel to y .

Point O is at a distance u from the center P_1 , i.e. $OP_1 = u$, and the usual parameters are:

$$a_1(u) = R_1/u = \sin \varphi_{10} \quad (647)$$

$$a_2 = R_2/r = \sin \varphi_{20} \quad (648)$$

$$P_1B = u_1(\varphi_2) = r \cos \varphi_2 - r \sqrt{(a^2 - \sin^2 \varphi_2)} \quad (649)$$

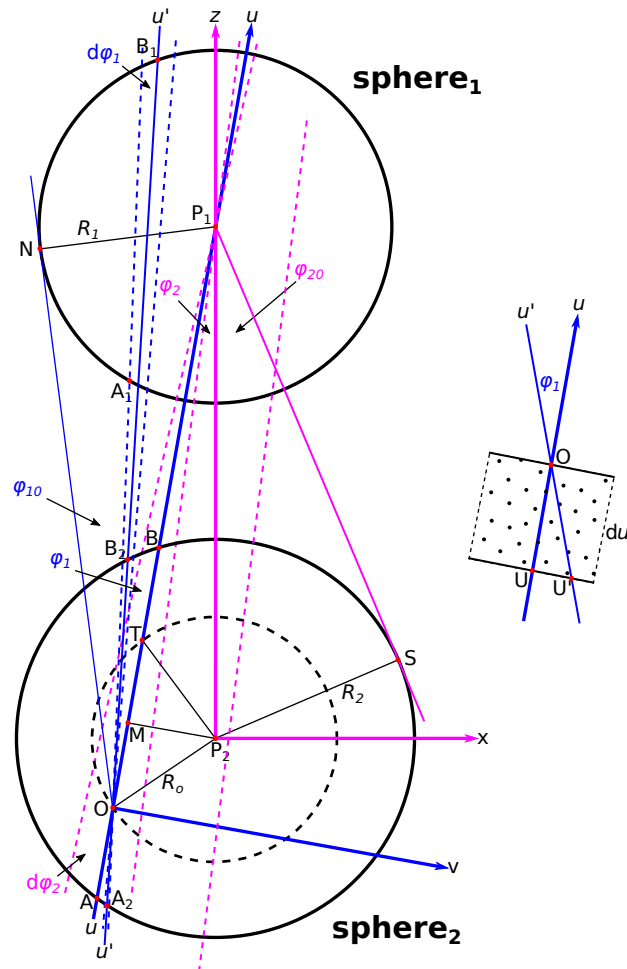


Figure 115: *Diagram for the derivation of the force exerted between two spherical masses with different diameters and different but uniform densities*

$$P_1 A = u_2(\varphi_2) = r \cos \varphi_2 + r \sqrt{(a^2 - \sin^2 \varphi_2)} \quad (650)$$

The normal from P_2 to u crosses AB at mid point M, so that we obtain for the segments:

$$OM(u, \varphi_2) = u - r \cos \varphi_2 \quad (651)$$

$$MP_2(\varphi_2) = r \sin \varphi_2 \quad (652)$$

The length $A_1 B_1$ is derived per Eq. 17 again as:

$$A_1 B_1(\theta, \varphi_1, u) = 2u \sqrt{a_1^2 - \sin^2 \varphi_1} \quad (653)$$

which is independent of (being constant with) the azimuth angle of rotation around axis u ; we introduce the azimuth because we further require to know the chord lengths OB_2 and OA_2 , which vary by rotating the line u' around the axis u at constant angle φ_1 ; the azimuth angle of rotation θ is not shown for simplicity of drawing. We derive the latter chords by solving the equations of sphere_2 and line u' per analytical geometry as follows:

$$y^2 + (\nu - MP_2)^2 + (u - OM)^2 = R_2^2 \quad (654)$$

$$\nu = (OB_2) \sin \varphi_1 \cos \theta \quad y = (OB_2) \sin \varphi_1 \sin \theta \quad u = (OB_2) \cos \varphi_1 \quad (655)$$

The simultaneous solution of above equations gives the required lengths

$$OA_2(\theta, \varphi_1, u, \varphi_2) = MP_2 \sin \varphi_1 \cos \theta + OM \cos \varphi_1 - \sqrt{(MP_2 \sin \varphi_1 \cos \theta + OM \cos \varphi_1)^2 + R_2^2 - OM^2 - MP_2^2} \quad (656)$$

$$OB_2(\theta, \varphi_1, u, \varphi_2) = MP_2 \sin \varphi_1 \cos \theta + OM \cos \varphi_1 + \sqrt{(MP_2 \sin \varphi_1 \cos \theta + OM \cos \varphi_1)^2 + R_2^2 - OM^2 - MP_2^2} \quad (657)$$

where it is important to take the absolute value of the above lengths (when they are negative) in the exponent of the exponential factor used to derive the graviton absorption below.

The general strategy is briefly as follows: We consider all graviton flows in all possible directions at every given point and vectorially sum the flows (forces) over all points inside the sphere. The components of flow in the direction $P_1 P_2$ are responsible for the force, whilst those perpendicular (normal) to that direction contribute no force between the spheres. We first group all the components of flow in the direction of axis u and all the components in the normal direction of axis v , and then project the two outcomes in the direction of z defined by the centers of the two spheres, whilst all components in the normal direction x vanish. In the latter stage, the useful absorption fraction $f_g(O)$ at point O is the absorption $f_g(O)_z$ in direction (projection) z derived from the absorption $f_g(O)_u$ in direction u plus the absorption $f_g(O)_v$ in direction v as follows:

$$f_g(O) \equiv f_g(O)_z = f_g(O)_u \cos \varphi_2 + f_g(O)_v \sin \varphi_2 \quad (658)$$

This will be used in a final integration to find the force F by:

$$F = 2\pi \frac{J}{c} \int_0^{\varphi_{20}} \left(\int_B^A f_g(O) u^2 k_2 du \right) \sin \varphi_2 \cos \varphi_2 d\varphi_2 \quad (659)$$

The above provides only a general idea of what we better explain and clarify with detailed steps next.

C.1 u -axis

There are two components of graviton absorption by integration around this axis, namely, those crossing both spheres by joint traces and those crossing only sphere_2.

C.1.1 Joint crossing (*variable_{uj}*)

Gravions passing through point O and crossing both spheres (“jointly”) along the line B₁A₁B₂OA₂ undergo exponential absorption before they arrive at point O, the difference of which multiplied by the usual product $\sin \varphi_1 \cos \varphi_1$ yields the absorption component along the u axis:

$$f_{g-uj}(\theta, \varphi_1, u, \varphi_2) = [\exp(-|k_2 OA_2|) - \exp(-k_1 A_1 B_1 - k_2 OB_2)] \sin \varphi_1 \cos \varphi_1 \quad (660)$$

which we integrate around the axis over the full azimuth angle θ and over the zenith angle φ_1 within the subtended solid angle by sphere₁ at the given angle φ_2 of the axis with P₁P₂ and the given distance u of O from P₁:

$$F_{uj}(u, \varphi_2) = \int_0^{\text{asin}(a_1(u))} \int_{-\pi}^{\pi} f_{g-uj}(\theta, \varphi_1, u, \varphi_2) d\theta d\varphi_1 \quad (661)$$

The subscripts $_{uj}$ stand for u axis (direction) and “joint” traces. The above integrated gravion component exerts a pressure J_0/c on an elementary thin material segment disposed normal to the axis of rotation (u), so that the product of the pressure with the area of the element times the absorption coefficient k_2 of material sphere₂ over the elementary thickness du produces an elementary force at point O. We may omit the constant factor J_0/c from the interim formulations until we obtain the end result for the absorption factor. Now, we need to multiply by the area $u^2 d\Omega_2$, where $d\Omega_2$ is the elementary solid angle subtended by the surface element at the center P₁ times $k_2 du$ to allow for the absorption along du generating an elementary force:

$$d^2 S_{uj}(u, \varphi_2) = F_{uj}(u, \varphi_2) u^2 k_2 du d\Omega_2 \quad (662)$$

It is noteworthy at this point that the above factor has acquired the dimensions of an area being an elementary surface (S) after initially being a pure number. From the above, we find the total absorption along the length of chord A₂B₂

$$dS_{uj}(\varphi_2) = \left[\int_{u_1(\varphi_2)}^{u_2(\varphi_2)} F_{uj}(u, \varphi_2) u^2 k_2 du \right] d\Omega_2 \quad (663)$$

Here and in following derivations, when we use an elementary solid angle $d\Omega$, we replace it either with $d\Omega = \sin \varphi d\varphi$ in an asymmetrical rotation by involving the azimuth angle, or with the elementary annular solid angle $d\Omega = 2\pi \sin \varphi$ being the integral around a rotational symmetry without use of the azimuth angle. We do this without explicitly stating it. Thus, and by projecting the above force on P₁P₂ by $\cos \varphi_2$, we finally integrate over the entire bulk of sphere 2 by

$$S_{uj} = \int_0^{\text{asin}(a_2)} dS_{uj}(\varphi_2) \cdot 2\pi \sin \varphi_2 \cos \varphi_2 d\varphi_2 \quad (664)$$

C.1.2 Single crossing (*variable_{us}*)

For traces of gravions crossing only sphere₂, to which we refer with the term “single” or “lone” (with subscript _s), the corresponding integrand of the innermost integral is a little simpler by:

$$f_{g-us}(\theta, \varphi_1, u, \varphi_2) = [\exp(-|k_2 OA_2|) - \exp(-k_2 OB_2)] \sin \varphi_1 \cos \varphi_1 \quad (665)$$

We repeat the same steps except that we integrate with respect to zenith angle from φ_{10} (i.e. $\text{asin}(a_1(u))$) to $\pi/2$, so that by changing the notation of “j” to “s”, we get:

$$F_{us}(u, \varphi_2) = \int_{\text{asin}(a_1(u))}^{\pi/2} \int_{-\pi}^{\pi} f_{g-us}(\theta, \varphi_1, u, \varphi_2) d\theta d\varphi_1 \quad (666)$$

and finally

$$S_{us} = \int_0^{\text{asin}(a_2)} dS_{us}(\varphi_2) \cdot 2\pi \sin \varphi_2 \cos \varphi_2 d\varphi_2 \quad (667)$$

We find that the terms for “single” absorption are not needed for the final force derivation, because they cancel out exerting a null force. However, we consider the steps involved not only for completeness, but also because we need to follow the corresponding steps during derivation of mass or energy in subsequent sections.

C.2 ν -axis

Again, there are two kinds of components of graviton absorption by integration around this axis, namely, those crossing both spheres by joint traces and those crossing only sphere_2. The latter “single” crossings contain two subgroups, namely, those in the complementary angle to the joint zenith angle (i.e. outside the joint zenith angle up to $\pi/2$) and those in the supplementary joint azimuth angle within the joint zenith angle (i.e. outside the joint azimuth angle $2\pi - \text{joint_azimuth}$ angle). We explain this in the following three steps.

C.2.1 joint crossing (*variable $_{\nu j}$*)

The notation of angles (θ, φ_1) could have been designated as (θ_u, φ_{1u}) for the u -axis and as $(\theta_\nu, \varphi_{1\nu})$ for the ν -axis, because the angles with reference to the normal axis ν are different, but there is no ambiguity to retain the same notation with both axes noting that the range of integration angles are different, for which special care is required to avoid possible errors; by use of the correct integration limits, we do not need to change notation of azimuth and zenith angles.

Now, $A_1 B_1$ is found by a different expression:

If *operand* $= (u \sin \varphi_1 \cos \theta)^2 + R_1^2 - u^2 > 0$ then

$$A_1 B_1 \equiv A_1 B_{1\nu j}(\theta, \varphi_1, u) = 2\sqrt{\text{operand}} \quad (668)$$

From the condition of a positive operand above, we obtain the range of angles:

$$\begin{aligned} \theta_1 &= -\text{acos}\left(\sqrt{u^2 - R_1^2}/(u \sin \varphi_1)\right) \\ \theta_2 &= +\text{acos}\left(\sqrt{u^2 - R_1^2}/(u \sin \varphi_1)\right) \\ \varphi_{11} &= \pi/2 - \text{asin}(a_1(u)) \\ \varphi_{12} &= \pi/2 + \text{asin}(a_1(u)) \end{aligned}$$

The above limits ensure that the integration contains only joint traces. Note that φ_1 must cover the range on either side from $\pi/2$. The lengths OA_2 and OB_2 are given by the same Eqs. 656 and 657 provided we apply the above (correct) range of angles. Then, we follow the same steps changing the notation of u with ν accordingly:

$$f_{\nu j}(\theta, \varphi_1, u, \varphi_2) = [\exp(-|k_2 OA_2|) - \exp(-k_1 A_1 B_1 - k_2 OB_2)] \sin \varphi_1 \cos \varphi_1 \quad (669)$$

finally obtaining:

$$S_{\nu j} = \int_0^{\text{asin}(a_2)} dS_{\nu j}(\varphi_2) \cdot 2\pi \sin \varphi_2 \cos \varphi_2 d\varphi_2 \quad (670)$$

C.2.2 Single (or lone) crossing

There are two terms for “single” (lone) crossing traces to derive in ν -direction:

(i) ν -axis single complementary - (*variable $_{\nu s-c}$*) This term arises in the zenith angle range $0 \rightarrow \pi/2 - \text{asin}(a_1(u))$ (being the complement of the joint zenith angle), with corresponding full azimuth angle range $-\pi \rightarrow +\pi$. We follow the same steps leading to the final integral:

$$S_{\nu s-c} = \int_0^{\text{asin}(a_2)} dS_{\nu s-c}(\varphi_2) \cdot 2\pi \sin \varphi_2 \cos \varphi_2 d\varphi_2 \quad (671)$$

(ii) **ν -axis single supplement** (*variable $_{\nu s-s}$*) This term arises in half of the joint zenith angle range $\varphi_{11} \rightarrow \varphi_{12}$ (below) with corresponding partial (i.e. supplementary) azimuth angle range $\theta_1 \rightarrow \theta_2$ (i.e. outside the “joint” crossings), where

$$\begin{aligned}\theta_1 &= \text{acos}\left(\sqrt{u^2 - R_1^2}/(u \sin \varphi_1)\right) \\ \theta_2 &= 2\pi - \text{acos}\left(\sqrt{u^2 - R_1^2}/(u \sin \varphi_1)\right) \\ \varphi_{11} &= \pi/2 - \text{asin}(a_1(u)) \\ \varphi_{12} &= \pi/2\end{aligned}$$

It should be noted that, while the zenith range is actually between $\pi/2 - \text{asin}(a_1(u)) \rightarrow \pi/2 + \text{asin}(a_1(u))$, we use only half of this range to avoid a second pass of the same single crossing in the second semi-range $\pi/2 + \text{asin}(a_1(u))$ of the zenith angle.

The above limits ensure that the integration contains only “single” chords in the function of absorption along the given line u' . We follow again the same steps yielding the other additional component now indexed with “ $_{\nu s-s}$ ”

$$S_{\nu s-s} = \int_0^{\text{asin}(a_2)} dS_{\nu s-s}(\varphi_2) \cdot 2\pi \sin \varphi_2 \cos \varphi_2 d\varphi_2 \quad (672)$$

C.3 Summation of terms

In the general case above, we have formulated five terms initially to be summed for the total force between the two spheres. These terms are all components projected along the line joining the spheres, so that we must take their algebraic sum. Each derivation provides a positive number for each component. However, the configuration of Fig. 115 is such that all terms of the ν -axis are pointing in the negative direction and hence they must enter with a negative sign in the sum for the total S_F :

$$S_F = S_{uj} + S_{us} - S_{\nu j} - S_{\nu s-c} - S_{\nu s-s} \quad (673)$$

As already mentioned, the sum of all “single” terms vanishes, because $S_{us} = S_{\nu s-c} + S_{\nu s-s}$, leaving only the joint components:

$$S_F = S_{uj} - S_{\nu j} \quad (674)$$

The latter is to be finally multiplied by J_o/c to yield the force.

C.4 Alternative joint ν -axis component along with joint u -axis (combination) (*variable $_{uvj}$*)

Similar to the alternative derivation by Eq. B.1, it is possible also to account for the joint component arising from the ν -axis. This is facilitated first because all “single” components of force contribute a null effect. Therefore, if only the “joint” components are important for the force derivation, then we need to find the ν -axis joint component in the same range of limits of integration along (concurrently) with u -axis joint component. With this approach, the equations for the lengths A_1B_1 , OA_2 and OB_2 are all the same in both cases. To account for the ν -component while revolving around the u -axis, we use the factors $\cos \theta \sin^2 \varphi_1$ (corresponding to $\cos \theta_z \sin^2 \varphi_z$ in Eq. 645) in the first double integral followed by the same steps, namely:

$$f_{uvj}(\theta, \varphi_1, u, \varphi_2) = [\exp(-|k_2 OA_2|) - \exp(-k_1 A_1 B_1 - k_2 OB_2)] \cos \theta \sin^2 \varphi_1 \quad (675)$$

$$F_{uvj}(u, \varphi_2) = \int_0^{\text{asin}(a_1(u))} \int_{-\pi}^{\pi} f_{uvj}(\theta, \varphi_1, u, \varphi_2) d\theta d\varphi_1 \quad (676)$$

then we form the third integral in the usual way by

$$d^2 S_{uvj}(u, \varphi_2) = F_{uvj}(u, \varphi_2) u^2 k_2 du d\Omega_2 \quad (677)$$

$$dS_{uvj}(\varphi_2) = \left[\int_{u_1(\varphi_2)}^{u_2(\varphi_2)} F_{uvj}(u, \varphi_2) u^2 k_2 du \right] d\Omega_2 \quad (678)$$

Since $d\Omega_2 = 2\pi \sin \varphi_2$ and projecting on P_1P_2 , however, now by $\sin \varphi_2$, we finally integrate over the entire bulk of sphere 2 by

$$S_{uvj} = \int_0^{\text{asin}(a_2)} dS_{uvj}(\varphi_2) \cdot 2\pi \sin^2 \varphi_2 d\varphi_2 \quad (679)$$

Thus, we can write as an alternative formulation of the total force factor:

$$S_F = S_{uj} - S_{uvj} \quad (680)$$

which again multiplied by the pressure J_0/c yields the total force between the two spheres.

C.5 Quadruple integral

We have conducted numerical integration of all of the above formulations and have confirmed the expected equivalent results with all cases within the set integration tolerance. The starting formulations may be thought of as the “raw” constituting equations of PG theory. They can be further worked out. They are amenable to further theoretical analysis and processing, which can be done separately. For now, we can summarize with a general quadruple integration of all the above by taking advantage of the common integration limits when using the alternative ν -axis joint component as follows:

$$S_F = 2\pi k_2 \int_0^{\varphi_{20}} \left\{ \sin \varphi_2 \cos \varphi_2 \int_{u_1}^{u_2} \left[\left(\int_0^{\varphi_{10}} \int_{-\pi}^{\pi} f_u() d\theta d\varphi_1 \right) u^2 \right] du \right. \\ \left. - \sin^2 \varphi_2 \int_{u_1}^{u_2} \left[\left(\int_0^{\varphi_{10}} \int_{-\pi}^{\pi} f_v() dx dy \right) u^2 \right] du \right\} d\varphi_2 \quad (681)$$

where

$$f_u() = [\exp(-|k_2 O A_2|) - \exp(-k_1 A_1 B_1 - k_2 O B_2)] \sin \varphi_1 \cos \varphi_1 \quad (682)$$

$$f_v() = [\exp(-|k_2 O A_2|) - \exp(-k_1 A_1 B_1 - k_2 O B_2)] \cos \theta \sin^2 \varphi_1 \quad (683)$$

By re-writing we get

$$S_F = 2\pi k_2 \int_0^{\varphi_{20}} \int_{u_1}^{u_2} \int_0^{\varphi_{10}} \int_{-\pi}^{\pi} [f_u() \sin \varphi_2 \cos \varphi_2 - f_v() \sin^2 \varphi_2] u^2 \cdot d\theta d\varphi_1 du d\varphi_2 \quad (684)$$

or

$$S_F = 2\pi k_2 \int_0^{\varphi_{20}} \int_{u_1}^{u_2} \int_0^{\varphi_{10}} \int_{-\pi}^{\pi} f() [\sin \varphi_1 \cos \varphi_1 \sin \varphi_2 \cos \varphi_2 - \cos \theta \sin^2 \varphi_1 \sin^2 \varphi_2] u^2 \cdot d\theta d\varphi_1 du d\varphi_2 \quad (685)$$

where

$$f() = \exp(-|k_2 O A_2|) - \exp(-k_1 A_1 B_1 - k_2 O B_2) \quad (686)$$

with integration limits and chord lengths or segments as provided during the preceding detailed derivations.

We have also performed a numerical integration of the above and found consistency with all other other part term computations. With every computation, we have normalized by the factor $(\pi^2 A_1 A_2)/r^2$ where

$$A_1 = \left[R_1^2 - \frac{1}{2k_1^2} + \frac{\exp(-2k_1 R_1)(2k_1 R_1 + 1)}{2k_1^2} \right] \quad (687)$$

$$A_2 = \left[R_2^2 - \frac{1}{2k_2^2} + \frac{\exp(-2k_2 R_2)(2k_2 R_2 + 1)}{2k_2^2} \right] \quad (688)$$

as used with the original “reverse engineering” derivation by Eq. 90. The normalization has invariably resulted in unity within the prescribed tolerance of the integrals. Having said that, the original (“raw”) derivations of the various terms of absorption (like “single” and “joint”) are also needed to study the physics and underlying mechanisms of force and mass or energy not otherwise directly obvious from the end Eq. 90. This is done in the theory of the main body of this report in Section 16.

D Effective Mass or Energy for one and two spherical masses - bulk method

In this section, we formulate the problem of finding the gravion absorption rate by one (single) or two interacting spheres. Since we have also established that we can deduce the corresponding effective mass or energy from the gravion absorption rate per Sections 15.7 and 16, we can compare the expressions of mass or energy with the expressions of force.

D.1 General case for two spheres

The mas or energy, being a scalar, can be derived from summing (integrating) the absorption rate of gravions by the elementary volume around points O inside the bulk of the sphere. This is done first by summing, instead of subtracting, the two terms of Eq. 660 corresponding to the absorption lengths along the direction u' on either side of point O, so that the absorption factor f_{a-} is:

$$f_{a-uj}(\theta, \varphi_1, u, \varphi_2) = [\exp(-|k_2 OA_2|) + \exp(-k_1 A_1 B_1 - k_2 OB_2)] \sin \varphi_1 \quad (689)$$

without the factor $\cos \varphi_1$, which was necessary to obtain the projection of gravion flow along the direction u . We conduct the double integration by setting:

$$M_{uj}(u, \varphi_2) = \int_0^{\text{asin}(a_1(u))} \int_{-\pi}^{\pi} f_{a-uj}(\theta, \varphi_1, u, \varphi_2) d\theta d\varphi_1 \quad (690)$$

Then, we come to the third integral and account for the gravions absorbed by the elementary material slice facing in the direction u . The gravions absorbed by the elementary thickness $du = OU$ (see inset in Fig. 115) is actually proportional to the elementary length $OU' = du / \cos \varphi_1$, which must also be multiplied by the same $\cos \varphi_1$ to account for the cosine law reduction (oblique incidence) of the arriving gravions; the net result is that the absorption is proportional to the elementary thickness du times k_2 times the elementary area $u^2 d\Omega_2$, as with the force:

$$d^2 S_{a-uj}(u, \varphi_2) = M_{uj}(u, \varphi_2) u^2 k_2 du d\Omega_2 \quad (691)$$

from which we correspondingly obtain the absorption along the length of chord $A_2 B_2$

$$dS_{a-uj}(\varphi_2) = \left[\int_{u_1(\varphi_2)}^{u_2(\varphi_2)} M_{uj}(u, \varphi_2) u^2 k_2 du \right] d\Omega_2 \quad (692)$$

Now, we again have $d\Omega_2 = 2\pi \sin \varphi_2$, but there is no reason to project the scalar quantity of absorbed gravions on $P_1 P_2$ to obtain the last integration over the entire bulk of sphere_2, so that we finally obtain

$$S_{a-uj} = \int_0^{\text{asin}(a_2)} dS_{a-uj}(\varphi_2) \cdot 2\pi \sin \varphi_2 d\varphi_2 \quad (693)$$

We must further add the absorption by the “single” sphere term in the remaining zenith angle from $\text{asin}(a_1(u))$ to $\pi/2$. Here, the absorption factor f_{a-} is a simpler expression:

$$f_{a-us}(x, y, u, \varphi_2) = [\exp(-|k_2 OA_2|) + \exp(-k_2 OB_2)] \sin \varphi_1 \quad (694)$$

as the gravions trace only the chord $A_2 B_2$ of sphere_2, and

$$M_{us}(u, \varphi_2) = \int_{\text{asin}(a_1(u))}^{\pi/2} \int_{-\pi}^{\pi} f_{a-us}(\theta, \varphi_1, u, \varphi_2) d\theta d\varphi_1 \quad (695)$$

We do the third and fourth integral in the same way by replacing “j” with “s”, so that finally we have

$$S_{a-us} = \int_0^{\text{asin}(a_2)} dS_{a-us}(\varphi_2) \cdot 2\pi \sin \varphi_2 d\varphi_2 \quad (696)$$

The total graviton absorption rate is then the sum of the above two terms:

$$S_a = S_{a-uj} + S_{a-us} \quad (697)$$

The latter is again a characteristic area, the product of which with J_0 , i.e. $S_a J_0$, yields the total graviton rate of absorption by sphere_2. Equivalently, we also obtain the effective mass by $\frac{S_a}{4\pi\Lambda}$.

D.2 Single sphere

We have used and confirmed the following two alternative bulk method formulations for graviton absorption rate by a single sphere over and above the method already provided in Section 15.7.

D.2.1 Single sphere general

For a single sphere, say sphere_2, we can apply the preceding Eq. 696 by setting $\text{asin}(a_1(u)) = 0$, i.e. by initially integrating over the entire zenith angle ($0 < \varphi_1 < \pi/2$), i.e. by vanishing sphere_1 with $R_1 = 0$ at any arbitrary distance r :

$$M_{us-full}(u, \varphi_2) = \int_0^{\pi/2} \int_{-\pi}^{\pi} f_{a-us}(\theta, \varphi_1, u, \varphi_2) d\theta d\varphi_1 \quad (698)$$

Then, we follow with the same third and fourth integrals. The final integral is similar to Eq. 696 but for the full zenith angle (in the above integral):

$$S_{a-us-full} = \int_0^{\text{asin}(a_2)} dS_{a-us}(\varphi_2) \cdot 2\pi \sin \varphi_2 d\varphi_2 \quad (699)$$

D.2.2 Single sphere bulk alternative

With reference to Fig. 7 used to find the internal acceleration, we can derive a simple formulation for the graviton absorption rate as follows:

We now add the scalar terms of absorption to obtain the absorption factor at point O (prior $R_X = R_O$ here):

$$f_{aO} = 2\pi \sin \varphi d\varphi \cdot \left[\exp \left(-k\sqrt{R^2 - (R_O \sin \varphi)^2} + kR_O \cos \varphi \right) + \exp \left(-k\sqrt{R^2 - (R_O \sin \varphi)^2} - kR_O \cos \varphi \right) \right] \quad (700)$$

We integrate to find the absorption from all the traces radiating out from this point:

$$M_{aO} = \int_0^{\pi/2} 2\pi \sin \varphi d\varphi \cdot \left[\exp \left(-k\sqrt{R^2 - (R_O \sin \varphi)^2} + kR_O \cos \varphi \right) + \exp \left(-k\sqrt{R^2 - (R_O \sin \varphi)^2} - kR_O \cos \varphi \right) \right] \quad (701)$$

This is the same for all points on the internal spherical surface with radius R_O , so that the spherical shell with thickness dR_O absorbs $M_{aO} \cdot 4\pi R_O^2 \cdot kdR_O$, from which we sum (integrate) for the total bulk of the sphere by:

$$S_a = \int_0^R M_{aO} \cdot 4\pi k R_O^2 dR_O = 4\pi^2 R^2 A_R \quad (702)$$

Since

$$\frac{dS_a}{dR_O} = M_{aO} \cdot 4\pi k R_O^2$$

$$kM_{aO} = \frac{dS_a}{dR_O} \frac{1}{4\pi R_O^2} \quad (703)$$

we can readily recognize that the product kM_{aO} is a per unit volume characteristic area at point O, the product of which by $\frac{1}{4\pi\Lambda}$ yields the effective mass per unit volume at that point, i.e. the point effective density $\rho_{e-point}$.

D.3 Net loss of absorption rate between two spheres - bulk method

There is an important quantity arising by the difference of the absorption rate of one sphere in the presence of another from the absorption rate it has, when it is alone (without the absence of other bodies in the neighborhood). In this difference, there is a common term $f_{a-us}(x, y, u, \varphi_2)$ in the interval from $\text{asin}(a_1(u))$ to $\pi/2$ of the zenith angle, leaving only the difference between the “single” and “joint” terms in the common zenith interval from 0 to $\text{asin}(a_1(u))$:

$$f_{a-netloss}() = f_{a-us}() - f_{a-uj}() = [\exp(-|k_2OA_2|) - \exp(-k_1A_1B_1 - k_2OB_2)] \sin \varphi_1 \quad (704)$$

which is identical to the force term in Eq. 660 except for the $\cos \varphi_1$ that was necessitated to project the graviton flow on the axis joining the centers of the two spheres. We use the term “net” loss to distinguish it from the generally present (current) steady-state absorption in any or both spheres. The net loss is not “current”, i.e. it represents a loss of gravitons that is not present absorption in any of the spheres, but which was present prior to the interaction between the two spheres and now has gone “missing”. We will return to this net loss and the common mathematical factor again, when we consider the “surface” derivations of graviton absorption.

E Effective Mass or Energy for one and two spherical masses - surface method

The “bulk” method for the force and effective mass appeared to be the logical or standard way to start with. It provides good insight on the various fractions of graviton absorption and their possible inter-relationships, whilst it forms a basis for further elaboration. However, it presents a practical disadvantage by the long computation times, if we opt to follow this method. Fortunately, there is also an alternative method by expanding the approach used in Section 15.7 for a single sphere. We have thus developed the “surface” method with one less integration and much faster computation time, but subject to considerable complexity in defining the integration ranges as we move around the surface of one sphere relative to the other. We explain this method in detail below.

E.1 General case for two spheres

With reference to Fig. 116, we have sphere_1 and sphere_2, for which we designate certain variables and relationships needed for the intended formulations. The three tangents from the sphere centers, namely, P_2D and P_2W and P_1L together with the two mutual tangents IS and KT cross the surface of sphere_2 at points G , S , L , T , E and F signaling a transition of the angle $\omega = \angle qP_2z$ from $0 \rightarrow \omega_G \rightarrow \omega_S \rightarrow \omega_L \rightarrow \omega_T \rightarrow \omega_E \rightarrow \pi$. Concomitant with these lines and points, we need the following lengths and relationships:

$$\begin{aligned} r &= P_1P_2, & r_1 &= P_1N, & r_2 &= P_2N, & r_3 &= P_2M \\ R_1 &= P_1K, & R_2 &= P_2T, & \frac{R_2}{r_2} &= \frac{R_1}{r_1} \\ r_1 + r_2 &= r, & r_1 &= \frac{R_1}{R_1 + R_2}r, & r_2 &= \frac{R_2}{R_1 + R_2}r, & r_3 &= \frac{R_2}{R_2 - R_1}r \\ \omega_G &= \angle P_1P_2D = \text{asin} \varphi_{01} \\ \omega_S &= \text{acos} \left(\frac{R_2}{r_2} \right) = \text{acos} \left(\frac{R_1 + R_2}{r} \right) \\ \omega_L &= \text{acos} \left(\frac{R_2}{r} \right) \\ \omega_T &= \text{acos} \left(\frac{R_2}{r_3} \right) = \text{acos} \left(\frac{R_2 - R_1}{r} \right) \end{aligned}$$

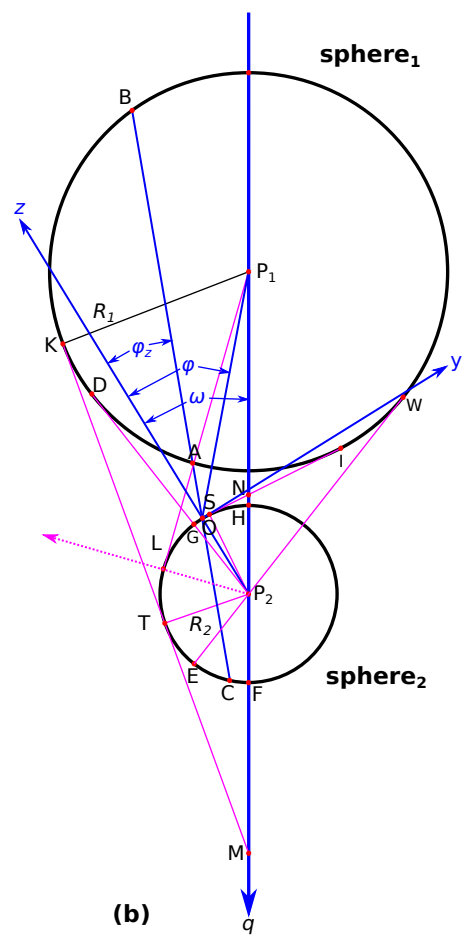
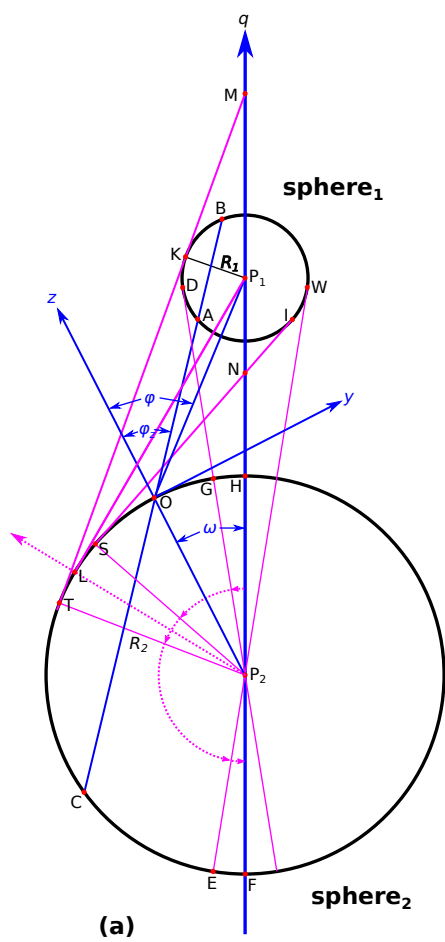


Figure 116: *Surface method for the formulation of the energy absorption rate.*

We consider all points O on the surface of this sphere and all the traces of gravions through this point crossing this sphere alone or both spheres. The line from the center of sphere_2 to point O on the surface constitutes the axis z of revolution, around which we calculate the first two integrals with respect to azimuth angle θ and zenith angle $\varphi_z = \angle zOB$. For this moving coordinate system with origin O, we further require the distance d of center P_1 and angle φ of OP_1 with axis z , which are easily found to be:

$$d = OP_1 = \sqrt{r^2 + R_2^2 - 2rR_2 \cos \omega}.$$

$$\varphi = \angle P_1Oz = \omega + \arcsin\left(\frac{R_2}{d} \sin \omega\right).$$

We further require the usual limiting angles subtended by each sphere as:

$$a = \frac{R_1}{d}, \quad a_{01} = \frac{R_1}{r} = \sin \varphi_{01}, \quad a_{02} = \frac{R_2}{r} = \sin \varphi_{02}$$

Now, with such a configuration, there is always (at all zenith angles) a chord OC of sphere_2 with every trace through this point (even with one vanishing length), whilst only within the subtended solid angle by sphere_1 there are traces crossing sphere_1 along the chords AB. The length of these corresponding chords are:

$$OC = 2R_2 |\cos \varphi_z|, \text{ which always enters as a positive number in the exponential factor of absorption and}$$

$$(AB)_z = 2\sqrt{(y_0 \sin \varphi_z \cos \theta_z + z_0 \cos \varphi_z)^2 - (d^2 - R_1^2)},$$

where $z_0 = d \cos \varphi$ and $y_0 = d \sin \varphi$, as we have found in Appendix B.

Next, we proceed to find the two fractions of absorption (“single” or “joint”) by this sphere by first establishing the integrand for absorption around axis P_2z . Since there is an axis of symmetry defined by the centers of the two spheres (P_1P_2), the situation must be the same for all points on the surface annulus around this axis at angle ω . Thus, we can find the absorption rate for the elementary surface annulus and then integrate with respect to ω in the interval $0 < \omega < \pi$. For the surface element at point O, we note that sphere_2 is always located entirely on one side of the plane of the element. However, sphere_1 changes location relative to the said surface element plane in ways that it can be (i) entirely on one side of the plane, or the other, i.e. on the same side as, or the alternate side from sphere_2, or (ii) the plane crosses sphere_1. In the latter case, sphere_1 can be crossed either above or below its “equator”, i.e. sphere_1 lies more than half above the horizon or more than half below the horizon of sphere_2, or (iii) the axis of rotation P_2z crosses sphere_1. The latter is also important to bear in mind, when we obtain the double integral of gravion absorption with respect to zenith and azimuth angles. During integration, we must either avoid doubling up the same absorption traces, or we must consistently do so and then divide by 2 (necessary to avoid dubious errors). Depending on how we decide to formulate the problem, we can finish up with 4, 5 or 6 absorption terms, the situation also depending on the relative size, configuration and distance of the spheres. Thus, for the “joint” absorption we require 4 terms, or 5 terms when the distance is very short, whilst 6 terms are used for the “single” absorption. The details of this are better explained inside the Python code used during numerical integration, which is planned for uploading in the near future. For consistency and to avoid confusion, let us consider sphere_2 the one, for which we wish to find its absorption as affected by the other sphere_1.

It is helpful to clarify again that ω_G is the semi-angle subtended by sphere_1 with $\omega_G = \arcsin(a_{01})$, when the z -axis becomes tangent to sphere_1; ω_S is at the point where the normal axis y (i.e. the horizon plane of sphere 2) first becomes tangent to sphere_1, ω_L is at the point where the horizon plane crosses the center of sphere_1, ω_T is at the point where the horizon plane becomes again tangent with sphere_1, ω_E is where the z -axis becomes again tangent with sphere_1 and $\omega_F = \pi$. This subdivision is necessitated in order to apply the rules and limits of integration for a single sphere (sphere_1) as described in Appendix B regarding the various positions of sphere_1 relative to the frame of reference with origin at O. However, sphere_2 always being on one side of (“below” or “above”) the tangent plane, the rule is straightforward with absorption chords OC always radiating from point O. The need to distinguish the six intervals of angle ω arises from the changing integration limits of the first double integral. Thus, we integrate separately in each of these intervals and then sum all the results. In summing all the latter integrals, we should note that each chord is traced twice (once from each of its ends), so that we must divide the final result by a factor 2. Alternatively, we can take care to include only those terms (four or five terms), which exhaust all chords once, namely, by avoiding to integrate over the zenith angle below the horizon of sphere 2; then we should not divide by the factor 2, whilst it saves us dealing with unnecessary terms and speeds up the computation work. In the latter case, again care should be taken for the “single” traces not to cross the other sphere either above or below the horizon.

Further, it is important to note that, while the integration ranges of ω are for the most of distance r as depicted by Fig. 116(a), the situation is different at close enough distance depending on the given set of radii R_1 and R_2 and their relative location with regard to which sphere is under examination. For example, in the first diagram 116(a), point G lies between H and S, whilst in the second diagram Fig. 116(b), point

S lies between points G and H. This cross-over of points S and G occurs as we decrease the distance so that $\omega_G = \omega_S = \varphi_{01}$. Then $\text{acos}\left(\frac{R_1 + R_2}{r}\right) = \text{asin}\left(\frac{R_1}{r}\right)$, $\frac{R_1 + R_2}{r} = \sqrt{1 - \left(\frac{R_1}{r}\right)^2}$ and:

$$r_S = \sqrt{(R_1 + R_2)^2 + R_1^2} \quad (705)$$

It is also possible sometimes to have a cross-over of the corresponding points T and E, when $\omega_T = \omega_E = \pi - \varphi_{01}$. Then $\text{acos}\left(\frac{|R_1 - R_2|}{r}\right) = \text{asin}\frac{R_1}{r}$, $\frac{R_2 - R_1}{r} < \sqrt{1 - \left(\frac{R_1}{r}\right)^2}$ and:

$$r_T = \sqrt{(R_1 - R_2)^2 + R_1^2} \quad (706)$$

No diagram is shown for the latter condition here, but it can be easily envisaged. The latter characteristic situation can arise only when one of the spheres is sufficiently smaller than the other, whilst the two spheres do not merge (overlap). In summary, care should be taken to establish when and if the distance r is in the ranges:

$$r \leq r_T \leq r \leq r_S \leq r \quad (707)$$

in order to correctly define the corresponding ranges of ω with correct integration limits of the double integral.

As with the bulk method, we consider the two fractions of absorbed gravions, i.e. (a) along lines jointly crossing both spheres and (b) along lines singly crossing the sphere under investigation (let's say sphere_2).

For the joint absorption, in all traces of gravions through point O in the figure, we have $1 - \exp(-k_2 OC)$ absorbed from the side (direction) of sphere_2 and $\exp(-k_1 AB) - \exp(-k_1 AB)\exp(-k_2 OC)$ from the side (direction) of sphere_1. Their sum yields the integrand as a function of the azimuth and zenith angle by

$$f_{a-zj}(\theta_z, \varphi_z, \omega) = (1 - \exp(-k_2 OC))(1 + \exp(-k_1 AB)) \sin \varphi_z \cos \varphi_z \quad (708)$$

where the factor $\cos \varphi_z$ is again introduced to allow for the oblique incidence of gravions relative to the sphere surface element. However, it is not canceled out now as it was for the gravions absorbed by the elementary material slice $du = OU$ (see inset in Fig. 115), because we use the integrated absorption through the entire chord length OC already containing the same factor in its exponential (not like the elementary length $OU' = du / \cos \varphi_1$). The distinction is subtle, but underlies an important mechanism: Both involve an elementary surface attached to an elementary mass slice in the bulk method but to the entire massive chord in the surface method. This saves us from the integration along this chord, which is a significant advantage of the "surface" method. Since the above integrand is not rotationally symmetric around the variable axis z , we must integrate with respect to the interdependent azimuth and the zenith angle to obtain the intermediate factor

$$M_{a-zj}(\omega) = \int_{\varphi_1}^{\varphi_2} \int_{\theta_1}^{\theta_2} f_{a-zj}(\theta_z, \varphi_z, \omega) d\theta_z d\varphi_z \quad (709)$$

It is important to obtain the limits of integration such that all traces fall inside the subtended solid angle by sphere_1 (see Appendix B). The above result is rotationally symmetric about the line joining the centers of the spheres and hence we multiply times the elementary annular surface $2\pi \sin \omega R_2^2 d\omega$ and integrate within each of the above defined ω intervals between points H, G, S, L, T and E, the limits denoted by ω_1 and ω_2 in the final integration for each term:

$$S_{a-j} = \int_{\omega_1}^{\omega_2} M_{a-zj}(\omega) \cdot 2\pi \sin \omega R_2^2 d\omega \quad (710)$$

It should be noted that the absorption factor given by Eq. 708 remains the same in all intervals of ω , because the absorption along chord OC is the same from whichever end we look at (as can be easily verified).

For single absorption, we follow the same steps: The absorption in each direction of the trace through point O is $(1 - \exp(-k_2 OC))$, and the starting integrand is the simplest by

$$f_{a-zs}(\theta_z, \varphi_z, \omega) = 2(1 - \exp(-k_2 OC)) \sin \varphi_z \cos \varphi_z \quad (711)$$

so that the first double integral gives:

$$M_{a-zs}(\omega) = \int_{\varphi_1}^{\varphi_2} \int_{\theta_1}^{\theta_2} f_{a-zs}(\theta_z, \varphi_z, \omega) d\theta_z d\varphi_z \quad (712)$$

Here, the limits of integration are the supplementary angle of the limits used for the azimuth (i.e. $2\pi - \theta_{joint}$) in joint absorption and the complementary angles used for the zenith ($0 \rightarrow \varphi_1$) and/or ($\varphi \rightarrow \pi/2$) of the joint absorption (in one or two parts). Extra care should be taken that the gravion trace does not cross sphere_1 in either direction as we rotate the trace. The final integral is similar by:

$$S_{a-s} = \int_{\omega_1}^{\omega_2} M_{a-zs}(\omega) \cdot 2\pi \sin \omega R_2^2 d\omega \quad (713)$$

While the distance r between the two spheres is fixed and not explicitly seen in the integrands above, it is clear that the two absorption fractions are a function of distance, and we could also use the subscript r as we do in Section 16. The characteristic total surface factor S_a is the sum of the above:

$$S_a = S_{a-j} + S_{a-s} \quad (714)$$

The gravion absorption rate is the product $S_a J_0$ and the corresponding effective mass $\frac{S_a}{4\pi\Lambda}$

E.2 Net loss of absorption rate between two spheres - surface method

Like in Appendix D.3, we can derive the same net loss of absorption rate $f_{a-netloss}$ using the surface method. Again, we find the difference of the absorption rate of one sphere in the presence of another from the absorption rate it has when it is alone (in the absence of other bodies in the neighborhood). This is obtained from the difference of Eqs. 711 and 708 :

$$f_{a-netloss} = f_{a-zs}(\theta_z, \varphi_z, \omega) - f_{a-zj}(\theta_z, \varphi_z, \omega) = (1 - \exp(-k_2 OC)) (1 - \exp(-k_1 AB)) \sin \varphi_z \cos \varphi_z \quad (715)$$

in the common integration solid angle subtended by sphere_1, outside of which the terms of single absorption cancel out. Thus, we form the double integral:

$$M_{a-netloss}(\omega) = \int_{\varphi_1}^{\varphi_2} \int_{\theta_1}^{\theta_2} f_{a-netloss} d\theta_z d\varphi_z \quad (716)$$

The final integral yields a characteristic net-loss-surface-quantity $S_{a-netloss}$

$$S_{a-netloss} = \int_{\omega_1}^{\omega_2} M_{a-netloss}(\omega) \cdot 2\pi \sin \omega R_2^2 d\omega \quad (717)$$

We repeat the clarification as previously: We use the term “net” loss to distinguish it from the generally current (present) absorption in any or both spheres. This loss is not a “current” absorption loss, i.e. it represents a loss of gravions that is not present in any of the spheres at the given distance, but which was present prior to the interaction (at very long distance) between the two spheres but now gone “missing”.

F Force between two spherical masses - surface method

We can derive the total force exerted on sphere_2 by summing (integrating) all the forces exerted along all the chords traced by gravions in all possible directions through the point O on the surface. The “lone” or “single” crossings cancel out leaving only the “joint” ones. For any given chord OC, there is a force component from the direction that is free from (out of the way of) sphere_1 and caused by the absorption fraction $1 - \exp(-k_2 OC)$. The other component in the opposite direction arises from the arriving diminished intensity of absorption by a factor $\exp(-k_1 AB)$ after passing through sphere_1, while it traverses chord OC; The gravion absorption by this second beam of gravions is then $\exp(-k_1 AB) - \exp(-k_1 AB)\exp(-k_2 OC)$. The net force is the difference of the second from the first with a net force factor $(1 - \exp(-k_2 OC))(1 - \exp(-k_1 AB))$. To prepare the integrand for integration around axis z , we should multiply by the usual product of $\sin \varphi_z$ (to account for the

elementary solid angle around the chord) and by $\cos \varphi_z$ to account for the per unit area oblique incidence with regard to absorption per se at that point. However, this is incomplete until we multiply again by $\cos \varphi_z$ to project that absorption flow on the axis z . Thus, the integrand for this component of force around this axis is given by:

$$f_{g-z}(\theta_z, \varphi_z, \omega) = (1 - \exp(-k_2 OC))(1 - \exp(-k_1 AB)) \sin \varphi_z \cos^2 \varphi_z \quad (718)$$

with first double integration around this axis taken inside the solid angle subtended by sphere_1:

$$F_z(\omega) = \int_{\varphi_1}^{\varphi_2} \int_{\theta_1}^{\theta_2} f_{g-z}(\theta_z, \varphi_z, \omega) d\theta_z d\varphi_z \quad (719)$$

yielding the intermediate force factor per unit area on the surface at this point O. We multiply times the elementary annular surface at angle ω by $2\pi \sin \omega R_2^2$ as preciously, but we must also multiply by $\cos \omega$ to project this component of force on the line joining the centers of the two spheres. The above yields a characteristic surface area, which finally integrated is S_F :

$$S_{Fz} = \int_{\omega_1}^{\omega_2} F_z(\omega) \cdot 2\pi \sin \omega \cos \omega R_2^2 d\omega \quad (720)$$

Last, we must repeat the same steps for the normal component of force around y axis. It is easier (less complicated) to use the alternative method as per Appendix C.4. That is, we deduce the y component concurrently with the revolution used for integrating around z axis by using the same (common) limits of integration (see also Eq. 645). We again need to multiply Eq. 715 by the azimuth and zenith product $\cos \theta_z \sin \varphi_z$ as in:

$$f_{g-y}(\theta_z, \varphi_z, \omega) = (1 - \exp(-k_2 OC))(1 - \exp(-k_1 AB)) \cos \theta_z \sin^2 \varphi_z \cos \varphi_z \quad (721)$$

and follow by the next two steps:

$$F_y(\omega) = \int_{\varphi_1}^{\varphi_2} \int_{\theta_1}^{\theta_2} f_{g-y}(\theta_z, \varphi_z, \omega) d\theta_z d\varphi_z \quad (722)$$

$$S_{Fy} = \int_{\omega_1}^{\omega_2} F_y(\omega) \cdot 2\pi \sin^2 \omega R_2^2 d\omega \quad (723)$$

noting that we used $\sin \omega$ to project this component on the line joining the centers, and the usual $2\pi \sin \omega$ for the elementary annular angle.

The algebraic sum $S_{Fz} + S_{Fy}$ yields a component of the total force for each interval $\omega_1 \rightarrow \omega_2$ prescribed for the angle ω , so that the final grand total S_F is the sum from all these intervals. Again, the total force acted upon sphere_2 by sphere_1 is given by the product $\frac{J_0}{c} S_F$. In the steady state considered by this report, this force is the same for both spheres (see also the symmetry of the force factor above).

Attention is drawn again (like with the bulk method) to the common factor presenting itself in the corresponding Eqs. 715, 718 and 721 between net loss and net force, which are discussed in the main body of the report in Section 16.

Whilst further theoretical processing and analysis of all of the above derivations can be done separately, we have used them to obtain some immediate results with numerical integration with simple Python codes and a good laptop computer. Computation time can be a practical problem with the “bulk” method, but this depends on each case. The “surface” method is the fastest that has allowed us to accumulate a significant amount of results. Computation time has been greatly reduced also by parallel running of codes in a multi-core CPU computer, i.e. separate codes are executed concurrently for the various terms involved in the mass and force derivations. Key cases have been run with both “bulk” and “surface” formulations yielding identical results within the integration tolerances set, which has provided further reassurance that no errors are involved with the derivation of equations or the computer codes. The “personal” codes used are now available in the public domain separately. They have been edited with sufficient commentary and symbols consistent with (matching) the presented theory; this is necessary to make it readily understood and applicable by the general user. This task can also be better undertaken by expert computer programmers, who may prefer to develop a dedicated integrator for the fundamental needs of PG. As a reference example,

the computer specifications used at present are: x64based PC, MS Windows 7 Home Premium, Processor: Intel(R) Core(TM) 3612QM CPU @2.10 GHz up to 3.0 GHz with turbo boost, 4-Core, 8-Logical Processors, 8 GB RAM. The codes can be found in <https://doi.org/10.5281/zenodo.7951860> with file named **PYTHON CODES for PUSH GRAVITY**.

References

- Adâmuți, I. A. (1982) The screen effect of the earth in the TETG. *Il Nuovo Cimento C* **5**(2), 189–208. doi:10.1007/BF02509010.
- Aidelsburger, M., Kirchner, F. O., Krausz, F. & Baum, P. (2010) Single-electron pulses for ultrafast diffraction. *Proceedings of the National Academy of Sciences* **107**(46), 19714–19719. ISSN 1091-6490. doi: 10.1073/pnas.1010165107.
- Akiyama, K. et al. (2019) First m87 event horizon telescope results. i. the shadow of the supermassive black hole. *Astrophys. J. Lett.* **875**, L1. doi:10.3847/2041-8213/ab0ec7.
- Akiyama, K. et al. (2022) First sagittarius a* event horizon telescope results. i. the shadow of the supermassive black hole. *Astrophys. J. Lett.* **930**, L12. doi:10.3847/2041-8213/ac6674.
- Allahverdyan, A. E. & Nieuwenhuizen, Th. M.. (2000) Extraction of work from a single thermal bath in the quantum regime. *Physical Review Letters* **85**(9), 1799–1802.
- Bannikova, E. Yu., Kontorovich, V. M. & Poslavsky, S. A. (2016) Helicity of a toroidal vortex with swirl. *Journal of Experimental and Theoretical Physics* **122**(4), 769–775. doi:10.1134/s1063776116040026.
- Bialy, S. & Loeb, A. (2018) Could solar radiation pressure explain Oumuamua’s peculiar acceleration? *The Astrophysical Journal Letters* **868**:L1, 1–5. doi:<https://doi.org/10.3847/2041-8213/aaeda8>.
- Bird, G.A. (1995) *Molecular Gas Dynamics and the Direct Simulation of Gas Flows*. Oxford University Press, New York.
- Bulgac, A., Luo, Y.-L., Magierski, P., Roche, K. J. & Yu, Y. (2011) Real-time dynamics of quantized vortices in a unitary fermi superfluid. *Science* **332**(6035), 1288–1291. doi:10.1126/science.1201968.
- Bulgac, Aurel, Forbes, Michael McNeil, Kelley, Michelle M., Roche, Kenneth J. & Wlazłowski, Gabriel (2014) Quantized superfluid vortex rings in the unitary fermi gas. *Physical Review Letters* **112**(2). doi: 10.1103/physrevlett.112.025301.
- Carroll, Sean M. (2004) *Spacetime and Geometry: An Introduction to General Relativity*. Addison-Wesley, San Francisco.
- Catto, G. (2014) Newtonian derivation of gravitational redshift. *European Journal of Theoretical Physics* **11**, 21–30.
- Chae, Kyu-Hyun (2023) Breakdown of the newton–einstein standard gravity at low acceleration in internal dynamics of wide binary stars. *The Astrophysical Journal* **952**(2), 128. ISSN 1538-4357. doi:10.3847/1538-4357/ace101.
- Chappel, J.M., Iqbal, A. & Abbott, D. (2012) The gravitational field of a cube. *arXiv:1206.3857v1 [physics.class-ph]*.
- Consa, O (2018) Helical solenoid model of the electron. *Progress in Physics* **14**, 80–89.
- Danilatos, G.D. (1997) *In-Situ Microscopy in Materials Research*, chap. 2. Environmental Scanning Electron Microscopy, pp. 14–44. Kluwer Academic Publishers, Boston/Dordrecht/London.
- Danilatos, G.D. (2012) Velocity and ejector-jet assisted differential pumping: Novel design stages for environmental SEM. *Micron* **43**, 600–611.
- Danilatos, Gerasimos (2024) Is the big bang an artifact? doi:10.5281/ZENODO.11401298. URL <https://doi.org/10.5281/zenodo.11401298>.
- Danilatos, Gerasimos (2025) The massive black hole bias: A potential origin for the cosmological redshift-distance relation without universal expansion. doi:10.5281/ZENODO.17855884. URL <https://doi.org/10.5281/zenodo.18012085>.

- Darwin, G.H. (1905) The analogy between lesage's theory of gravitation and the repulsion of light. *Proceedings of the Royal Society of London. Series A, Containing Papers of a Mathematical and Physical Character* **76**(511), 387–410. ISSN 2053-9150. doi:10.1098/rspa.1905.0042.
- de Duillier, Nicolas Fatio (1929) *De la cause de la pesanteur*. Drei Untersuchungen zur Geschichte der Mathematik, in: Schriften der Strassburger Wissenschaftlichen Gesellschaft in Heidelberg, 10:(19-66). URL https://fr.wikisource.org/wiki/De_la_cause_de_la_pesanteur#.
- Dehmelt, HG (1989) Experiments with an isolated subatomic particle at rest URL <https://www.nobelprize.org/uploads/2018/06/dehmelt-lecture.pdf>.
- Dibrov, A. (2011) Unified model of shadow-gravity and the exploding electron. *Apeiron* **18**, 43–83.
- Donnelly, Russell J. (1991) *Quantized vortices in helium II*. Cambridge University Press. ISBN 0521324009.
- Edwards, R. M. (2007) Photon-graviton recycling as cause of gravitation. *Apeiron* **14**(3), 214–233.
- Falconer, Isobel (2019) Vortices and atoms in the maxwellian era. *Philosophical Transactions of the Royal Society A: Mathematical, Physical and Engineering Sciences* **377**(2158), 20180451. doi:10.1098/rsta.2018.0451.
- Fedi, Marco (2016) A superfluid Theory of Everything? URL <https://hal.archives-ouvertes.fr/hal-01312579>. Working paper or preprint.
- Fedosin, Sergey (2015a) The graviton field as the source of mass and gravitational force in the modernized Le Sage model. *Physical Science International Journal* **8**, 1–18. ISSN 2348-0130. doi:10.9734/psij/2015/22197.
- Fedosin, Sergey G. (2017) The substantial model of the photon. *J Fundam Appl Sci.* **9**, 411–467. ISSN 1112-9867. doi:10.4314/jfas.v9i1.25.
- Fedosin, Sergey G. (2021) On the structure of the force field in electro gravitational vacuum doi:10.5281/zenodo.4515206.
- Fedosin, S.G. (2012) The radius of the proton in the self-consistent model. *Hadronic Journal* **35**, 349–363.
- Fedosin, S.G. (2015b) The force vacuum field as an alternative to the ether and quantumvacuum. *WSEAS Transactions on Applied and Theoretical Mechanics* **10**, 31–38.
- Fedosin, S.G. (2018) The charged component of the vacuum field as the source of electric force in the modernized Le Sage model. *Journal of Fundamental and Applied Sciences* **8**(3), 971. ISSN 1112-9867. doi:10.4314/jfas.v8i3.18.
- Feyerabend, Paul (2010) *Against Method*. Verso Books. ISBN 1844674428. URL https://www.ebook.de/de/product/9026002/paul_feyerabend_against_method.html.
- Field, G.B. (1971) Instability and waves driven by radiation in interstellar space and in cosmological models. *The Astrophysical Journal* **165**, 29–40. doi:10.1086/150873.
- Freedman, W.L. (2024) New JWST results the current tension in Ho signaling new physics. *American Physical Society Meeting* .
- Fulton, DH (2022) Diffusion gravity (11) the newtonian law of gravitation at galactic scale doi:10.13140/RG.2.2.29557.65764.
- Gagnebin, B (1949) De la cause de la pesanteur. Mémoire de Nicolas Fatio de Duillier présenté à la Royal Society le 26 février 1690. *The Royal Society* **6**(2), 125–160. doi:https://doi.org/10.1098/rsnr.1949.0017.
- Gallemí, A., Rocuzzo, S. M., Stringari, S. & Recati, A. (2020) Quantized vortices in dipolar supersolid bose-einstein-condensed gases. *Physical Review A* **102**(2), 023322. doi:10.1103/physreva.102.023322.
- Gamow, G. (1949) On relativistic cosmology. *Reviews of Modern Physics* **21**(3), 367–373. doi:10.1103/RevModPhys.21.367.
- Gauthier, RF (1996) Microvita: A new approach to matter, life and health. *Biomedical and LifePhysics ed D N Ghista (Braunschweig/Wiesbaden: Friedr. Vieweg I& SohnVerlagsgesellschaft mbH)* pp. 347–58. URL <https://richardgauthier.academia.edu/research>.

- Gauthier, Richard (2019) Quantum-entangled superluminal double-helix photon produces a relativistic superluminal quantum-vortex zitterbewegung electron and positron. *Journal of Physics: Conference Series* **1251**(1), 012016. ISSN 1742-6596. doi:10.1088/1742-6596/1251/1/012016.
- Giacintucci, S., Markevitch, M., Johnston-Hollitt, M., Wik, 5 Q. D. R., Wang, H. S. & Clarke, T. E. (2020) Discovery of a giant radio fossil in the ophiuchus galaxy cluster. *arXiv:2002.01291 [astro-ph.GA]* .
- Giulietti, Marika, Gandolfi, Giovanni, Massardi, Marcella, Behiri, Meriem & Lapi, Andrea (2024) Observing dusty star-forming galaxies at the cosmic noon through gravitational lensing: Perspectives from new-generation telescopes. *Galaxies* **12**(2), 9. ISSN 2075-4434. doi:10.3390/galaxies12020009.
- Gleick, J. (1998) *Chaos: Making a New Science*. Vintage. ISBN 9780749386061. URL https://www.ebook.de/de/product/3307050/james_gleick_chaos.html.
- Gottumukkala, R, Barrufet, L, Oesch, P A, Weibel, A, Allen, N, Alcalde Pampliega, B, Nelson, E J, Williams, C C, Brammer, G, Fudamoto, Y, González, V, Heintz, K E, Illingworth, G, Magee, D, Naidu, R P, Shuntov, M, Stefanon, M, Toft, S, Valentino, F & Xiao, M (2024) Unveiling the hidden universe with jwst: the contribution of dust-obscured galaxies to the stellar mass function at $z = 3-8$. *Monthly Notices of the Royal Astronomical Society* **530**(1), 966–983. ISSN 1365-2966. doi:10.1093/mnras/stae754.
- Grangier, P, Roger, G & Aspect, A (1986) Experimental evidence for a photon anticorrelation effect on a beam splitter: A new light on single-photon interferences. *Europhysics Letters (EPL)* **1**(4), 173–179. ISSN 1286-4854. doi:10.1209/0295-5075/1/4/004.
- Hogan, C.J. (1989) Mock gravity and cosmic structure. *The Astrophysical Journal* **340**(1-10). doi:10.1086/167371.
- Hunt, A.J. (2019) New atomic model from the spectra of hydrogen, helium, beryllium, boron, carbon, and deuterium and their ions. *American Based Research Journal* ISSN 2304-7151. doi:10.5281/ZENODO.3456955.
- Kajari, E., Harshman, N.L., Rasel, E.M., Stenholm, S., Sussmann, G. & Schleich, W.P. (2010) Inertial and gravitational mass in quantum mechanics. *arXiv* doi:10.1007/s00340-010-4085-8. URL <https://arxiv.org/abs/1006.1988>.
- Kelvin, Lord (1867) On vortex atoms. *Proc. Royal Society of Edinburgh* **VI**, 94–105.
- Klaus, Lauritz, Bland, Thomas, Poli, Elena, Politi, Claudia, Lamporesi, Giacomo, Casotti, Eva, Bisset, Russell N., Mark, Manfred J. & Ferlaino, Francesca (2022) Observation of vortices and vortex stripes in a dipolar condensate. *Nature Physics* **18**(12), 1453–1458. doi:10.1038/s41567-022-01793-8.
- Kokorev, Vasily, Jin, Shuowen, Gomez-Guijarro, Carlos, Magdis, Georgios E., Valentino, Francesco, Lee, Minju M., Daddi, Emanuele, Liu, Daizhong, Sargent, Mark T., Trebitsch, Maxime & Weaver, John R. (2023) Dust giant: Extended and clumpy star-formation in a massive dusty galaxy at $z = 1.38$. *Astronomy and Astrophysics* **677**, A172. ISSN 1432-0746. doi:10.1051/0004-6361/202346937.
- Kotler, Shlomi, Peterson, Gabriel A., Shojaee, Ezad, Lecocq, Florent, Cical, Katarina, Kwiatkowski, Alex, Geller, Shawn, Glancy, Scott, Knill, Emanuel, Simmonds, Raymond W., Aumentado, José & Teufel, John D. (2021) Direct observation of deterministic macroscopic entanglement. *Science* **372**(6542), 622–625. doi:10.1126/science.abf2998.
- Labbe, Ivo, van Dokkum, Pieter, Nelson, Erica, Bezanson, Rachel, Suess, Katherine A., Leja, Joel, Brammer, Gabriel, Whitaker, Katherine, Mathews, Elijah, Stefanon, Mauro & Wang, Bingjie (2023) A population of red candidate massive galaxies 600 Myr after the Big Bang. *Nature* **616**(7956), 266–269. ISSN 1476-4687. doi:10.1038/s41586-023-05786-2.
- Lagoudakis, K. G., Wouters, M., Richard, M., Baas, A., Carusotto, I., André, R., Dang, Le Si & Deveaud-Plédran, B. (2008) Quantized vortices in an exciton–polariton condensate. *Nature Physics* **4**(9), 706–710. doi:10.1038/nphys1051.
- Lahres, Stefan (2023a) Effects of different interaction mechanisms between hypothetical gravions and matter on push gravity theories doi:10.5281/ZENODO.8176256.
- Lahres, Stefan (2023b) What if the basic force "gravity" is basically repulsive? *SMuK-2023* URL <https://www.dpg-verhandlungen.de/year/2023/conference/smuK/part/gr/session/8/contribution/4>.

- Liu, Haisheng (2010) On new phenomena of photon from modified double slit experiment doi:10.48550/ARXIV.1007.5323.
- Liu, Haisheng (2011) On new phenomena of photon from modified double slit experiment. In *AIP Conference Proceedings*, no. 1327 in 400.
- Llanes-Estrada, Felipe J. & Navardo, Gaspar Moreno (2012) CUBIC NEUTRONS. *Modern Physics Letters A* **27(06)**, 1250033. doi:10.1142/S0217732312500332.
- Lomas, Robert (1999) *The Man Who Invented the Twentieth Century*. Headline Book Publishing. ISBN 0747275882.
- Lorenzen, B. (2017) The cause of the allais effect solved. *International Journal of Astronomy and Astrophysics* **7**, 69–90.
- Loureiro, A, Cuceu, A, Abdalla, FiB., Moraes, B, Whiteway, L, McLeod, M, Balan, ST., Lahav, O, Benoit-Lévy, A, Manera, M & et al. (2019) Upper bound of neutrino masses from combined cosmological observations and particle physics experiments. *Physical Review Letters* **123(8)**. ISSN 1079-7114. doi: 10.1103/physrevlett.123.081301. URL <http://dx.doi.org/10.1103/PhysRevLett.123.081301>.
- Margan, Erik (2012) Estimating the vacuum energy density - an overview of possible scenarios. *Josef Stefan Institute, Slovenia* URL https://www-f9.ijs.si/~margan/Articles/vacuum_energy_density.pdf.
- Meis, Constantin (2020) Quantum vacuum gravitation and cosmology. the electromagnetic nature of gravitation and matter-antimatter antigravity. doi:10.5281/ZENODO.5815000.
- Meis, Constantin (2022) The electromagnetic nature of gravitation and matter-antimatter antigravity. surmise on quantum vacuum gravitation and cosmology. *Journal of Modern Physics* **13(06)**, 949–968. doi: 10.4236/jmp.2022.136054.
- Meis, Constantin (2025) Photocosmos, is the universe made of light? photons, particles, gravitation from the electromagnetic vacuum. *Journal of High Energy Physics, Gravitation and Cosmology* **11(02)**, 209–223. ISSN 2380-4335. doi:10.4236/jhepgc.2025.112017.
- Michaud, André (2024) Critical analysis of the origins of heisenberg’s uncertainty principle. *Journal of Modern Physics* **15(06)**, 765–795. ISSN 2153-120X. doi:10.4236/jmp.2024.156034.
- Michell, John (1784) On the means of discovering the distance, magnitude,. *Philosophical Transactions of the Royal Society of London* pp. 35–57.
- Naidu, Rohan P., Oesch, Pascal A., Dokkum, Pieter van, Nelson, Erica J., Suess, Katherine A., Brammer, Gabriel, Whitaker, Katherine E., Illingworth, Garth, Bouwens, Rychard, Tacchella, Sandro, Matthee, Jorjyt, Allen, Natalie, Bezanson, Rachel, Conroy, Charlie, Labbe, Ivo, Leja, Joel, Leonova, Ecaterina, Magee, Dan, Price, Sedona H., Setton, David J., Strait, Victoria, Stefanon, Mauro, Toft, Sune, Weaver, John R. & Weibel, Andrea (2022) Two remarkably luminous galaxy candidates at $z = 10-12$ revealed by jwst. *The Astrophysical Journal Letters* **940(1)**, L14. ISSN 2041-8213. doi:10.3847/2041-8213/ac9b22.
- Netz, Reviel (2007) *The Archimedes codex : revealing the secrets of the world’s greatest palimpsest*. Weidenfeld & Nicolson, London. ISBN 9780297645474.
- Okun, R.F. (2006) The concept of mass in the Einstein year. *arXiv* doi:10.1142/9789812772657_0001. URL <https://arxiv.org/abs/hep-ph/0602037v1>.
- Oramah, Kevin (2023) Mass of the universe from quarks: A plausible solution to the cosmological constant problem. *Journal of Modern Physics* **14(12)**, 1672–1692. ISSN 2153-120X. doi:10.4236/jmp.2023.1412098.
- Panarella, E. (1987) *Nonlinear Behaviour of Light at Very Low Intensities: The “Photon Clump” Model*, pp. 105–167. Springer US. ISBN 9781468453867. doi:10.1007/978-1-4684-5386-7_8.
- Panarella, Emilio (2005) Single photons have not been detected: the alternative photon clump model. In Chandrasekhar Roychoudhuri & Katherine Creath, eds., *The Nature of Light: What Is a Photon?* SPIE. ISSN 0277-786X. doi:10.1117/12.637651.
- Papathanasiou, KS & Papathanasiou, MK (2020) *Proton and Electron as Cyclones Formulation of a Theory of Everything*. ISBN 978–960–8257–77–1.

- Parson, A.L (1915) A magneton theory of the structure of the atom. *Smithsonian Miscellaneous Collections* **65(11)**, 1–86.
- Pines, David & Alpar, M. Ali (1985) Superfluidity in neutron stars. *Nature* **316(6023)**, 27–32. doi:10.1038/316027a0.
- Poincaré, H. (1908) La dynamique de l' électron. *Revue Gen. Sci. Pures Appl.* **19**, 386–402.
- Prasad, Narasimha & Roychoudhuri, Chandrasekhar (2009) Exploring divisibility and summability of “photon” wave packets in nonlinear optical phenomena. In Chandrasekhar Roychoudhuri, Al F. Kracklauer & Andrei Yu. Khrennikov, eds., *The Nature of Light: What are Photons? III*. SPIE. ISSN 0277-786X. doi:10.1117/12.828557.
- Prigogine, N.G. (1977) *Self-organization in Nonequilibrium Systems: From Dissipative Structures to Order Through Fluctuations*. Wiley-Blackwell. ISBN ISBN 978-0471024019.
- Rankine, William John Macquorn (1855) LVII. on the hypothesis of molecular vortices, or centrifugal theory of elasticity, and its connexion with the theory of heat. *The London, Edinburgh, and Dublin Philosophical Magazine and Journal of Science* **10(68)**, 411–420. doi:10.1080/14786445508642001.
- Richard, L.S. (1962) Two-photon photoelectric effect. *Physical Review* **128(5)**, 2225–2229.
- Riess, Adam G., Anand, Gagandeep S., Yuan, Wenlong, Casertano, Stefano, Dolphin, Andrew, Macri, Lucas M., Breuval, Louise, Scolnic, Dan, Perrin, Marshall & Anderson, Richard I. (2024) JWST observations reject unrecognized crowding of Cepheid photometry as an explanation for the Hubble tension at 8sigma confidence. *The Astrophysical Journal Letters* **962(1)**, L17. ISSN 2041-8213. doi: 10.3847/2041-8213/ad1ddd.
- Roychoudhuri, Chandrasekhar & Tirfessa, Negussie (2006) Do we count indivisible photons or discrete quantum events experienced by detectors? In Wolfgang Becker, ed., *SPIE Proceedings*. SPIE. ISSN 0277-786X. doi:10.1117/12.691832.
- Simaciu, I. (2006) Contribution to the development of the theory with absorption of gravitational interaction. *BULETINUL Universitatii Petrol - Gaze din Ploiesti* **Vol. LVIII(1)**, 73–80.
- Stein, Robert, van Velzen, Sjoert, Kowalski, Marek, Franckowiak, Anna, Gezari, Suvi, Miller-Jones, James C. A., Frederick, Sara, Sfaradi, Itai, Bietenholz, Michael F., Horesh, Assaf, Fender, Rob, Garrappa, Simone, Ahumada, Tomás, Andreoni, Igor, Belicki, Justin, Bellm, Eric C., Böttcher, Markus, Brinell, Valery, Burruss, Rick, Cenko, S. Bradley, Coughlin, Michael W., Cunningham, Virginia, Drake, Andrew, Farrar, Glennys R., Feeney, Michael, Foley, Ryan J., Gal-Yam, Avishay, Golkhou, V. Zach, Goobar, Ariel, Graham, Matthew J., Hammerstein, Erica, Helou, George, Hung, Tiara, Kasliwal, Mansi M., Kilpatrick, Charles D., Kong, Albert K. H., Kupfer, Thomas, Laher, Russ R., Mahabal, Ashish A., Masci, Frank J., Necker, Jannis, Nordin, Jakob, Perley, Daniel A., Rigault, Mickael, Reusch, Simeon, Rodriguez, Hector, Rojas-Bravo, César, Rusholme, Ben, Shupe, David L., Singer, Leo P., Sollerman, Jesper, Soumagnac, Maayane T., Stern, Daniel, Taggart, Kirsty, van Santen, Jakob, Ward, Charlotte, Woudt, Patrick & Yao, Yuhang (2021) A tidal disruption event coincident with a high-energy neutrino. *Nature Astronomy* doi:10.1038/s41550-020-01295-8.
- Sukhorukov, NV (2017-2020) Electron radius in the macroneutrino model of the electron using the orbital conception of elementary particles URL <https://sites.google.com/site/snvspace22/science/electronradius>.
- Tafazoli, Siamak (2023) Calculation of the vacuum energy density using zeta function regularization. In *The 2nd Electronic Conference on Universe*, vol. 61 of *ECU 2023*, p. 31. MDPI. doi:10.3390/ecu2023-14053.
- Thomas, C.M. (2014) Graviton theory of everything. <http://astronomy-links.net/GToE.html> .
- Touboul, Pierre, Métris, Gilles, Rodrigues, Manuel, André, Yves, Baghi, Quentin, Bergé, Joel, Boulanger, Damien, Bremer, Stefanie, Chhun, Ratana, Christophe, Bruno, Cipolla, Valerio, Damour, Thibault, Danto, Pascale, Dittus, Hansjoerg, Fayet, Pierre, Foulon, Bernard, Guidotti, Pierre-Yves, Hardy, Emilie, Huynh, Phuong-Anh, Lämmerzahl, Claus, Lebat, Vincent, Liorzou, Françoise, List, Meike, Panet, Isabelle, Pires, Sandrine, Pouilloux, Benjamin, Prieur, Pascal, Reynaud, Serge, Rievers, Benny, Robert, Alain, Selig, Hanns, Serron, Laura, Sumner, Timothy & Visser, Pieter (2019) Space test of the equivalence principle: first results of the MICROSCOPE mission **36(22)**, 225006. doi:10.1088/1361-6382/ab4707.

- Vayenas, CG & Grigoriou, D (2020) Mass generation via gravitational confinement of relativistic neutrinos. *arXiv:2001.09760 [physics.gen-ph]* URL <https://arxiv.org/abs/2001.09760>.
- Vayenas, CG, Tsousis, D & Grigoriou, D (2020) Computation of the masses, energies and internal pressures of hadrons, mesons and bosons via the rotating lepton model. *Physica A: Statistical Mechanics and its Applications* **545**, 123679. ISSN 0378-4371. doi:<https://doi.org/10.1016/j.physa.2019.123679>. URL <http://www.sciencedirect.com/science/article/pii/S0378437119320515>.
- Wang, B. & Field, G.B. (1989) Galaxy formation by mock gravity with dust. *The Astrophysical Journal* **346**, 2–11. doi:10.1086/167981.
- Watkins, T (2020a) Estimates of the mass densities of up and down quarks and estimates of the outer radii of the small, medium and large up and down quarks URL <https://www.sjsu.edu/faculty/watkins/quarkmasses.htm>.
- Watkins, T (2020b) A sensible model for the confinement and asymptotic freedom of quarks URL <https://www.sjsu.edu/faculty/watkins/quarkconfine2.htm>.
- Wikipedia contributors (2018) Le sage's theory of gravitation — Wikipedia, the free encyclopedia. URL https://en.wikipedia.org/w/index.php?title=Le_Sage%27s_theory_of_gravitation&oldid=867302622. [Online; accessed 14-December-2018].
- Wikipedia contributors (2019a) Heraclitus — Wikipedia, the free encyclopedia. URL <https://en.wikipedia.org/w/index.php?title=Heraclitus&oldid=918062946>. [Online; accessed 30-September-2019].
- Wikipedia contributors (2019b) Le sage's theory of gravitation — Wikipedia, the free encyclopedia. URL https://en.wikipedia.org/w/index.php?title=Le_Sage%27s_theory_of_gravitation&oldid=914070602. [Online; accessed 22-July-2023].
- Wikipedia contributors (2019c) Neutron star — Wikipedia, the free encyclopedia. URL https://en.wikipedia.org/w/index.php?title=Neutron_star&oldid=914385779. [Online; accessed 9-September-2019].
- Wikipedia contributors (2019d) Quantum fluctuation — Wikipedia, the free encyclopedia. URL https://en.wikipedia.org/w/index.php?title=Quantum_fluctuation&oldid=908783886. [Online; accessed 6-September-2019].
- Wikipedia contributors (2019e) Radioactive decay — Wikipedia, the free encyclopedia. URL https://en.wikipedia.org/w/index.php?title=Radioactive_decay&oldid=912368878. [Online; accessed 6-September-2019].
- Wikipedia contributors (2019f) Urca process — Wikipedia, the free encyclopedia. URL https://en.wikipedia.org/w/index.php?title=Urca_process&oldid=913174313. [Online; accessed 9-September-2019].
- Wikipedia contributors (2019g) White dwarf — Wikipedia, the free encyclopedia. URL https://en.wikipedia.org/w/index.php?title=White_dwarf&oldid=913789261. [Online; accessed 9-September-2019].
- Wikipedia contributors (2021) Zero-point energy — Wikipedia, the free encyclopedia URL https://en.wikipedia.org/w/index.php?title=Zero-point_energy&oldid=1004926536. [Online; accessed 5-February-2021].
- Wikipedia contributors (2022) Hyle — Wikipedia, the free encyclopedia. URL <https://en.wikipedia.org/w/index.php?title=Hyle&oldid=1078144578>. [Online; accessed 22-March-2022].
- Wikipedia contributors (2023) Physics beyond the standard model — Wikipedia, the free encyclopedia. URL https://en.wikipedia.org/w/index.php?title=Physics_beyond_the_Standard_Model&oldid=1181844389. [Online; accessed 1-February-2024].
- Wikipedia contributors (2024a) Alternatives to general relativity — Wikipedia, the free encyclopedia. URL https://en.wikipedia.org/w/index.php?title=Alternatives_to_general_relativity&oldid=1205746044. [Online; accessed 7-May-2024].

- Wikipedia contributors (2024b) Cosmic microwave background — Wikipedia, the free encyclopedia. URL https://en.wikipedia.org/w/index.php?title=Cosmic_microwave_background&oldid=1221641058. [Online; accessed 3-May-2024].
- Wikipedia contributors (2024c) Cosmological constant — Wikipedia, the free encyclopedia. URL https://en.wikipedia.org/w/index.php?title=Cosmological_constant&oldid=1245577480. [Online; accessed 15-September-2024].
- Wikipedia contributors (2024d) Eric lerner — Wikipedia, the free encyclopedia. URL https://en.wikipedia.org/w/index.php?title=Eric_Lerner&oldid=1220543144. [Online; accessed 7-May-2024].
- Wikipedia contributors (2024e) Fundamental interaction — Wikipedia, the free encyclopedia. URL https://en.wikipedia.org/w/index.php?title=Fundamental_interaction&oldid=1245722694. [Online; accessed 11-October-2024].
- Wikipedia contributors (2024f) Planck units — Wikipedia, the free encyclopedia. URL https://en.wikipedia.org/w/index.php?title=Planck_units&oldid=1204830067. [Online; accessed 16-February-2024].
- Wikipedia contributors (2024g) Yin and yang — Wikipedia, the free encyclopedia. URL https://en.wikipedia.org/w/index.php?title=Yin_and_yang&oldid=1259399978. [Online; accessed 21-December-2024].
- Wikipedia contributors (2025a) Drinking bird — Wikipedia, the free encyclopedia. https://en.wikipedia.org/w/index.php?title=Drinking_bird&oldid=1300294752. [Online; accessed 2-August-2025].
- Wikipedia contributors (2025b) Mean free path — Wikipedia, the free encyclopedia. https://en.wikipedia.org/w/index.php?title=Mean_free_path&oldid=1301635977. [Online; accessed 8-August-2025].
- Wikipedia contributors (2025c) Newton's cradle — Wikipedia, the free encyclopedia. URL https://en.wikipedia.org/w/index.php?title=Newton%27s_cradle&oldid=1313889114. [Online; accessed 2-November-2025].
- Wikipedia contributors (2025d) Quantum zeno effect — Wikipedia, the free encyclopedia. URL https://en.wikipedia.org/w/index.php?title=Quantum_Zeno_effect&oldid=1314831181. [Online; accessed 16-November-2025].
- Wikipedia contributors (2025e) Zeno's paradoxes — Wikipedia, the free encyclopedia. URL https://en.wikipedia.org/w/index.php?title=Zeno%27s_paradoxes&oldid=1315747767. [Online; accessed 24-October-2025].
- Williams, James G., Boggs, Dale H. & Currie, Douglas G. (2022) Next-generation laser ranging at lunar geophysical network and commercial lander payload service sites. *The Planetary Science Journal* **3**(6), 136. ISSN 2632-3338. doi:10.3847/psj/ac6c25.
- Xu, Zhenglong (2021) The size and shape of a single photon. *OALib* **08**(02), 1–22. ISSN 2333-9705. doi:10.4236/oalib.1107179.
- Zhang, Mingyue, Müller, Jürgen, Biskupek, Liliane & Singh, Vishwa Vijay (2022) Characteristics of differential lunar laser ranging. *Astronomy & Astrophysics* **659**, A148. ISSN 1432-0746. doi:10.1051/0004-6361/202142841.
- Zumberge, Mark A., Ander, Mark E., Lautzenhiser, Ted V., Parker, Robert L., Aiken, Carlos L. V., Gorman, Michael R., Nieto, Michael Martin, Cooper, A. Paul R., Ferguson, John F., Fisher, Elizabeth, Greer, James, Hammer, Phil, Hansen, B. Lyle, McMechan, George A., Sasagawa, Glenn S., Sidles, Cyndi, Stevenson, J. Mark & Wirtz, Jim (1990) The greenland gravitational constant experiment. *Journal of Geophysical Research* **95**(B10), 15483. doi:10.1029/jb095ib10p15483.